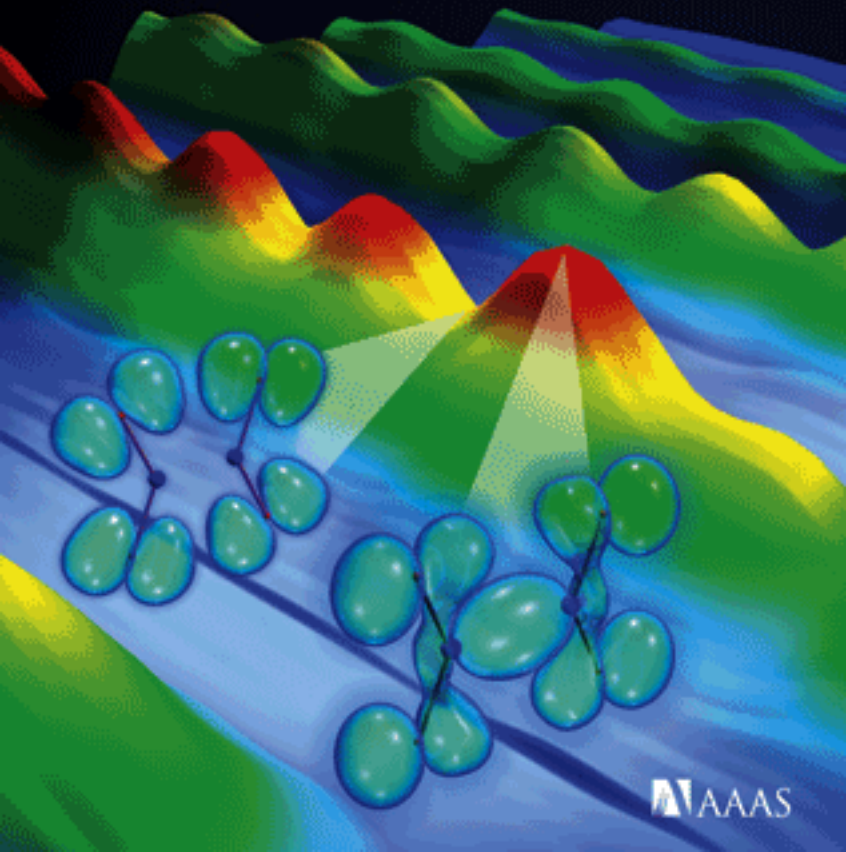
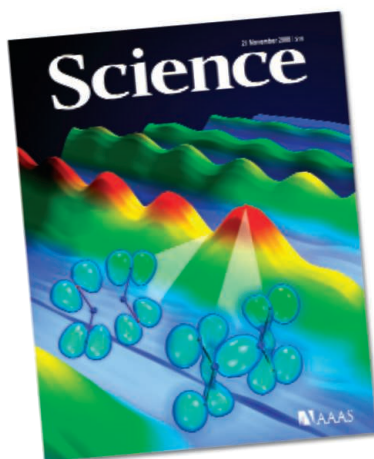


21 November 2008 | \$10

# Science





## COVER

X-rays emerge with varying intensity (red/green wave) as an electron is pulled out of and then pushed back into a vibrating  $N_2O_4$  molecule by an intense laser field. The pattern reveals real-time dynamic changes in electronic spatial configurations, or orbitals, at the compressed (left blue orbital) and stretched (right blue orbital) limits of the vibration cycle. See page 1207.

*Image: Greg Kuebler, JILA/University of Colorado*

## DEPARTMENTS

- 1157 *Science Online*
- 1159 *This Week in Science*
- 1164 *Editors' Choice*
- 1166 *Contact Science*
- 1169 *Random Samples*
- 1171 *Newsmakers*
- 1263 *New Products*
- 1268 *Science Careers*

## EDITORIAL

- 1163 *Opening Japan Up to the World*  
by Kiyoshi Kurokawa

## NEWS OF THE WEEK

- U.S. Visa Delays on the Rise, Scientists Abroad Report 1172
- Excess Particles From Space May Hint at Dark Matter 1173
- Malaria Drugs, the Coca-Cola Way 1174
- Study Shows How Degraded Surroundings Can 1175  
Degrade Behavior

>> *Science Express Report by K. Keizer et al.*

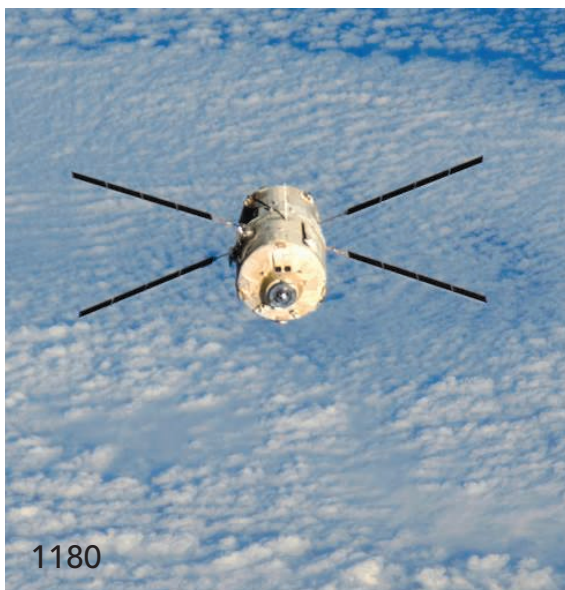
## SCIENCESCOPE 1175

- The New Groove in Science Aid: South-South Initiatives 1176
- Cast of 1000 Proteins Shines in Movies of Cancer Cells 1176

>> *Science Express Research Article by A. A. Cohen et al.*

## NEWS FOCUS

- World Oil Crunch Looming? 1178
- Cloudy Future for Europe's Space Plans 1180
- Last Stand for the Body Snatcher of the Himalayas? 1182
- Reaching for the Stars in Romania 1183  
At Home in Bucharest, for Better and for Worse



1180

## LETTERS

- Looking Beyond Head Trauma *D. T. Okuda* 1186
- Fostering a Culture of Responsible Lab Conduct  
*A. M. Peiffer, P. J. Laurienti, C. E. Hugenschmidt*
- The Path Forward for DNA Data  
*P. Boddington et al.*
- Priorities Come with the Career *C. Bolon*
- STEM Education Crisis: Overblown? *A. Deprieto*
- Changes to NIH Grant System May Backfire *P. D. Karp et al.*
- Listening to the Ocean's Heartbeat *E. S. Poloczanska et al.*
- Legislation Leaves Common Sense Behind *H. Scarbro*

## CORRECTIONS AND CLARIFICATIONS 1188

## BOOKS ET AL.

- The Scientific Life* A Moral History of a Late Modern Vocation *S. Shapin, reviewed by T. F. Gieryn* 1189
- Tomorrow's Table* Organic Farming, Genetics, and the Future of Food *P. C. Ronald and R. W. Adamchak, reviewed by M. Tester* 1190
- The Termosphere Gallery* 1191

## POLICY FORUM

- A Force for Peace in the Middle East 1192  
*M. Greene*

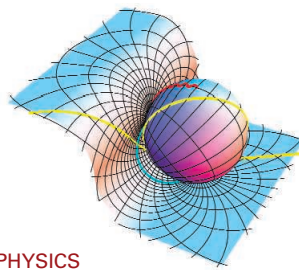
## PERSPECTIVES

- Gamma Rays and Neutron Stars 1193  
*G. F. Bignami* >> *Reports p. 1218 and 1221*
- Interrogating Molecules 1194  
*G. Doumy and L. F. DiMauro*  
>> *Research Article p. 1207; Report p. 1232*
- Brain Wnts for Blood Vessels 1195  
*E. Lammert* >> *Report p. 1247*
- Coming Soon to a Library Near You? 1196  
*J. Wouters*
- The Weight of the World Is Quantum Chromodynamics 1198  
*A. S. Kronfeld* >> *Report p. 1224*
- Rogue Insect Immunity 1199  
*D. S. Schneider and M. C. Chambers* >> *Report p. 1257*



1191

CONTENTS continued >>



## SCIENCE EXPRESS

[www.scienceexpress.org](http://www.scienceexpress.org)

### SOCIOLOGY

#### The Spreading of Disorder

K. Keizer, S. Lindenberg, L. Steg

Upon observing signs of social disorder (such as littering or graffiti), individuals are more likely to disobey a variety of social rules, including prohibitions against theft.

>> *News story* p. 1175

10.1126/science.1161405

### CELL BIOLOGY

#### Dynamic Proteomics of Individual Cancer Cells in Response to a Drug

A. A. Cohen et al.

Cells that escape death from a chemotherapy drug express a different array of proteins from genetically identical ones that died, which may help to inform cancer therapeutics.

>> *News story* p. 1176

10.1126/science.1160165

### PHYSICS

#### Broadband Invisibility by Non-Euclidean Cloaking

U. Leonhardt and T. Tyc

In theory, materials with a negative refractive index deployed in a curved, non-Euclidean space can provide a route to cloaking and invisibility across a range of wavelengths.

10.1126/science.1166332

### CHEMISTRY

#### Real-Time DNA Sequencing from Single Polymerase Molecules

J. Eid et al.

Arrays of narrow waveguides can record the action of a DNA polymerase stepping along a primer template, potentially providing a way to sequence DNA molecules.

>> *Science Podcast*

10.1126/science.1162986

## REVIEW

### PSYCHOLOGY

#### The Psychology of Transcending the Here and Now 1201

N. Liberman and Y. Trope

## BREVIA

### ECOLOGY

#### Fossil Pollen as a Guide to Conservation in the Galápagos 1206

J. F. N. van Leeuwen et al.

Fossil pollen shows that six plant species in the Galápagos, presumed to be invasive, had actually been native to the islands for thousands of years before human colonization. >> *Science Podcast*

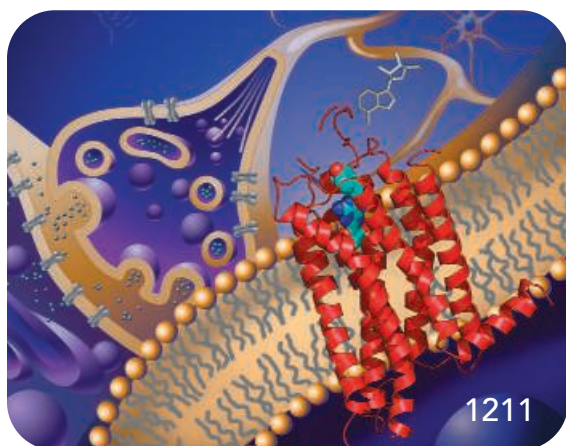
## RESEARCH ARTICLES

### CHEMISTRY

#### Time-Resolved Dynamics in N<sub>2</sub>O<sub>4</sub> Probed Using High Harmonic Generation 1207

W. Li et al.

Electrons can be ejected from multiple orbitals of N<sub>2</sub>O<sub>4</sub> by exploiting different stages in its excited vibrations, yielding an attosecond light probe of molecular dynamics. >> *Perspective* p. 1194



## RESEARCH ARTICLES CONTINUED...

### BIOCHEMISTRY

#### The 2.6 Angstrom Crystal Structure of a Human A<sub>2A</sub> 1211

Adenosine Receptor Bound to an Antagonist

V.-P. Jaakola et al.

The ligand binding pocket of the caffeine-binding human adenosine receptor has a different position and orientation than that of other G protein-linked receptors.

## REPORTS

### ASTRONOMY

#### The Fermi Gamma-Ray Space Telescope Discovers the Pulsar in the Young Galactic Supernova Remnant CTA 1 1218

A. A. Abdo et al.

The Fermi Space Telescope has detected a gamma-ray pulsar associated with a young supernova remnant, implying that such stars may be unidentified gamma-ray sources.

>> *Perspective* p. 1193

### ASTRONOMY

#### Observation of Pulsed $\gamma$ -Rays Above 25 GeV from the Crab Pulsar with MAGIC 1221

The MAGIC Collaboration

The MAGIC telescope has detected higher-energy, pulsed gamma rays from the Crab pulsar and a threshold suggesting that they are emitted from the outer magnetosphere.

>> *Perspective* p. 1193

### PHYSICS

#### Ab Initio Determination of Light Hadron Masses 1224

S. Dürr et al.

A quantum electrodynamics model that includes a full representation of quarks and their electromagnetic interactions accurately determines the masses of neutrons and protons.

>> *Perspective* p. 1198

CONTENTS continued >>





1198 &amp; 1224

## REPORTS CONTINUED...

## PHYSICS

## 4D Imaging of Transient Structures and Morphologies in Ultrafast Electron Microscopy 1227

*B. Barwick et al.*

Imaging with single electrons can track structural dynamics of gold and graphite in real space with femtosecond temporal resolution and angstrom spatial resolution.

## CHEMISTRY

High Harmonic Generation from Multiple Orbitals in N<sub>2</sub> 1232*B. K. McFarland et al.*

Electron ejection from multiple N<sub>2</sub> orbitals, controlled by the molecule's orientation relative to a laser, produces attosecond light spectra that can reveal molecular dynamics.

>> *Perspective p. 1194*

## PLANETARY SCIENCE

## Radar Sounding Evidence for Buried Glaciers in the Southern Mid-Latitudes of Mars 1235

*J. W. Holt et al.*

Radar data from the Mars Reconnaissance Orbiter show that a series of lobate landforms at low latitudes are composed primarily of massive ice covered by debris.

## EVOLUTION

## Variation in Evolutionary Patterns Across the Geographic Range of a Fossil Bivalve 1238

*M. Grey, J. W. Haggart, P. L. Smith*

Within a fossil bivalve genus, evolution tended to occur as a random walk at the highest latitudes and to be in stasis mode in deep marine environments.

## EVOLUTION

## Selfish Genetic Elements Promote Polyandry in a Fly 1241

*T. A. R. Price et al.*

Genes that confer a deleterious sex ratio in *Drosophila* also decrease male fertility and promote repetitive mating in females, providing a possible explanation of polyandry.

## CELL BIOLOGY

## Regulation of Microtubule Dynamics by Reaction Cascades Around Chromosomes 1243

*C. A. Athale et al.*

A reaction-diffusion model involving regulatory molecules and a microtubule-stabilizing phosphoprotein predicts the spatial distribution of microtubules during cell division.



ADVANCING SCIENCE. SERVING SOCIETY

**SCIENCE** (ISSN 0036-8075) is published weekly on Friday, except the last week in December, by the American Association for the Advancement of Science, 1200 New York Avenue, NW, Washington, DC 20005. Periodicals Mail postage (publication No. 484460) paid at Washington, DC, and additional mailing offices. Copyright © 2008 by the American Association for the Advancement of Science. The title **SCIENCE** is a registered trademark of the AAAS. Domestic individual membership and subscription (51 issues): \$144 (\$74 allocated to subscription). Domestic institutional subscription (51 issues): \$770; Foreign postage extra: Mexico, Caribbean (surface mail) \$55; other countries (air assist delivery) \$85. First class, airmail, student, and emeritus rates on request. Canadian rates with GST available upon request, GST #1254 88122. Publications Mail Agreement Number 1069624. **SCIENCE** is printed on 30 percent post-consumer recycled paper. **Printed in the U.S.A.**

**Change of address:** Allow 4 weeks, giving old and new addresses and 8-digit account number. **Postmaster:** Send change of address to AAAS, P.O. Box 96178, Washington, DC 20090-6178. **Single-copy sales:** \$10.00 current issue, \$15.00 back issue prepaid includes surface postage; bulk rates on request. **Authorization to photocopy** material for internal or personal use under circumstances not falling within the fair use provisions of the Copyright Act is granted by AAAS to libraries and other users registered with the Copyright Clearance Center (CCC) Transactional Reporting Service, provided that \$20.00 per article is paid directly to CCC, 222 Rosewood Drive, Danvers, MA 01923. *Science* is indexed in the *Reader's Guide to Periodical Literature* and in several specialized indexes.

## DEVELOPMENTAL BIOLOGY

## Canonical Wnt Signaling Regulates Organ-Specific Assembly and Differentiation of CNS Vasculature 1247

*J. M. Stenman et al.*

In mice, two specialized ligands for a key developmental signaling pathway are produced by neuroepithelial cells and direct endothelial cells to form the blood-brain barrier. >> *Perspective p. 1195*

## MEDICINE

Regulation of Pancreatic  $\beta$  Cell Mass by Neuronal Signals from the Liver 1250*J. Imai et al.*

In obese mice, fat tissue stimulates proliferation of insulin-producing pancreatic cells via a neural relay through the liver, contributing to symptoms of metabolic syndrome.

## ECOLOGY

## Control of Toxic Marine Dinoflagellate Blooms by Serial Parasitic Killers 1254

*A. Chambouvet, P. Morin, D. Marie, L. Guillou*

As successive populations of protists have caused summer red tides in France, each has been killed off by a distinct, persistent parasite, establishing a self-regulating ecosystem.

## IMMUNOLOGY

## Antimicrobial Defense and Persistent Infection in Insects 1257

*E. R. Haine, Y. Moret, M. T. Siva-Jothy, J. Rolff*

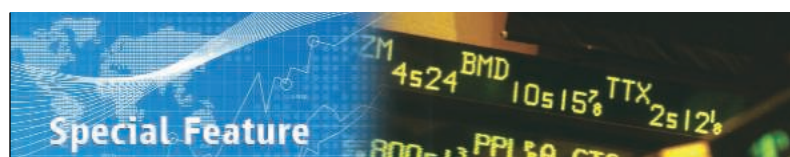
Flies fight some infections by quickly engulfing bacteria in phagocytic cells then deploying antimicrobial peptides, a system that avoids bacterial resistance. >> *Perspective p. 1199*

## SOCIOLOGY

## Multi-University Research Teams: Shifting Impact, Geography, and Stratification in Science 1259

*B. F. Jones, S. Wuchty, B. Uzzi*

Over the past 30 years, scientific papers have become increasingly likely to be written by teams of authors from more than one of a small number of elite universities.



## Scientists as Financial Analysts

Finance's Quant(um) Mechanics 1264

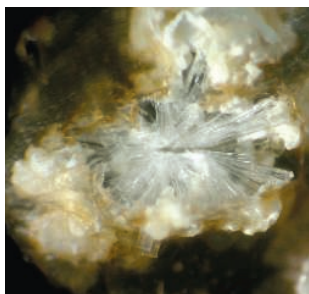
Analyzing Scientific Investments 1266

>> See *Science Careers* section p. 1157or go to [www.sciencedcareers.org](http://www.sciencedcareers.org); *Science Podcast*

Printed on  
30% post-consumer  
recycled paper.

CONTENTS continued &gt;&gt;





A clue to the past.

## SCIENCE NOW

[www.sciencenow.org](http://www.sciencenow.org)

HIGHLIGHTS FROM OUR DAILY NEWS COVERAGE

### Earth's Minerals Evolved, Too

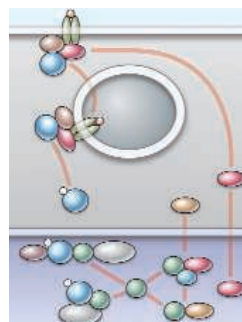
Life and rocks have changed in concert.

### Tumor Secrets Written in Blood

Cancer cells release telltale traces into the bloodstream.

### Prehistoric Family Values

Archaeologists find what may be the oldest examples of a nuclear family.



Regulating TGF- $\beta$  signaling from the nucleus.

## SCIENCE SIGNALING

[www.sciencesignaling.org](http://www.sciencesignaling.org)

THE SIGNAL TRANSDUCTION KNOWLEDGE ENVIRONMENT

### EDITORIAL GUIDE: Focus Issue—An Expanding World for TGF- $\beta$ Signaling

*N. R. Gough*

With new modes of regulation and new functions for members of the pathway, TGF- $\beta$  breaks the canonical barrier.

### PERSPECTIVE: Holding Their Own—The Noncanonical Roles of Smad Proteins

*L. L. Hoover and S. W. Kubalak*

There are TGF- $\beta$ -independent regulatory mechanisms and functions of Smads.

### PERSPECTIVE: PCTA—A New Player in TGF- $\beta$ Signaling

*F. Liu*

The distribution of promyelocytic leukemia protein between the nucleus and cytoplasm controls Smad activation.

### FORUM: Highlights from a TGF- $\beta$ Workshop

*N. R. Gough*

In addition to talks emphasizing the role of TGF- $\beta$  in cancer, many speakers shared memories of Anita Roberts, scientist mentor, colleague, and friend.

### NETWATCH: Cell Biology Promotion

Find an array of images, animations, and slides for teaching cell biology and signal transduction; in Educator Sites.

### NETWATCH: Pfam

Explore the structures and functions of thousands of protein domain families; in Protein Databases.



Careers for scientists as financial analysts.

## SCIENCE CAREERS

[www.sciencereers.org/career\\_development](http://www.sciencereers.org/career_development)

FREE CAREER RESOURCES FOR SCIENTISTS

### Special Feature: Scientists as Financial Analysts

*A. Kotok*

Despite today's headlines, it might be a good time to plan for a career as a financial analyst.

### Science Careers Podcast: Scientists as Quants

*C. Wald*

Financial systems executive Lee Maclin explains why scientists often succeed as quantitative analysts.

>> See *Scientists as Financial Analysts* feature p. 1264

## SCIENCE PODCAST

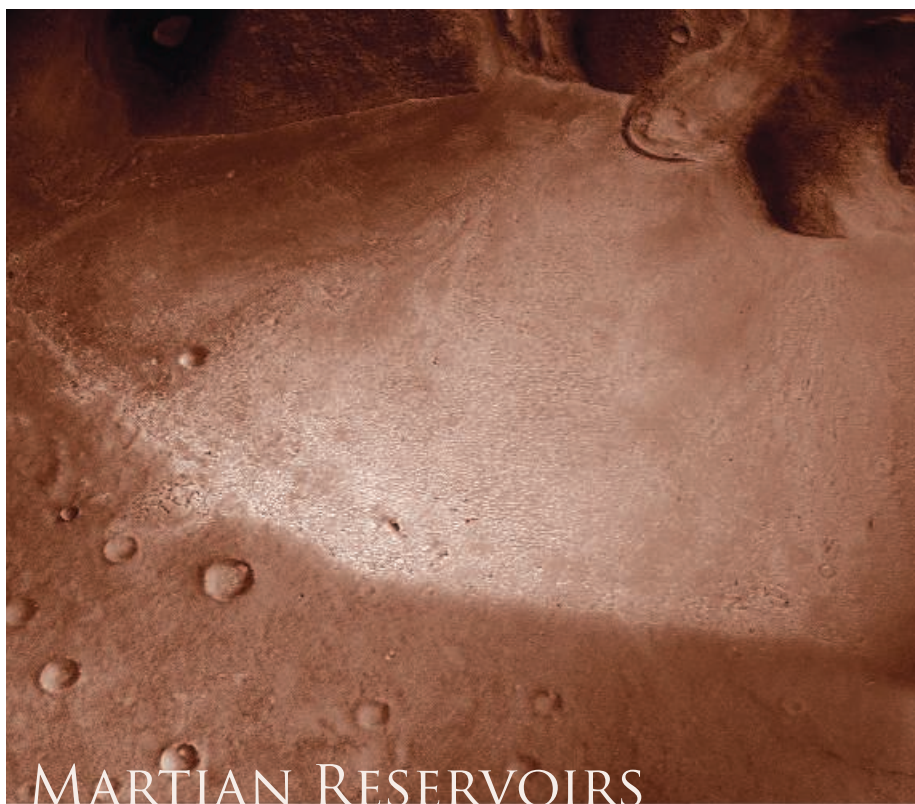
[www.sciencemag.org/multimedia/podcast](http://www.sciencemag.org/multimedia/podcast)

FREE WEEKLY SHOW

Download the 21 November *Science* Podcast to hear about classifying native and non-native Galápagos plant species, speeding up DNA sequencing, scientists as financial analysts, and more.



Separate individual or institutional subscriptions to these products may be required for full-text access.



## MARTIAN RESERVOIRS

Most of the visible water on Mars is locked up in its polar caps. There have been hints and evidence of some water flow at lower latitudes, but evidence for large reservoirs has been lacking. A series of large lobate landforms have been identified in several mid-latitude areas, and one hypothesis is that these may be covered glaciers or ice-filled rock piles. **Holt *et al.*** (p. 1235) have used the radar on the Mars Reconnaissance Orbiter to probe two of these deposits. The regions are indeed made predominantly of water ice covered with recent debris that probably formed during a previous climatic episode when Mars's orbit was more inclined. If these two deposits are representative, these landforms contain the largest volume of Martian water outside the poles.

## Visions from Afar

Events distant in time and objects distant in space are processed in psychologically similar ways. **Liberman and Trope** (p. 1201) review the evidence describing commonalities among faraway objects, far-in-the-future events, and imagined (versus real) happenings. How do the various kinds of distance induce these events or objects to become more strongly associated with each other, as in the phrase "long ago, in a faraway place"? More distal objects are represented in terms of more abstract characteristics, which leads to grouping distant objects into fewer and more general categories than objects closer in time or space. In everyday life, forming high-level or abstract constructions that incorporate perceptions and beliefs may

increase the value of future events and facilitate self-control and the delay of gratification.

## Massive Stars and MAGIC Crab Nebula

Energetic pulsars may produce gamma rays. Gamma rays have been observed emanating from several locations, but many specific sources remain unidentified (see the Perspective by **Bignami**). **Abdo *et al.*** (p. 1218, published online 16 October) report that the recently launched Fermi Gamma-Ray Space Telescope has detected a gamma-ray pulsar and tied the emissions to a neutron star. Many other

unidentified gamma-ray sources may have a similar origin, implying a greater number of massive stars than thought. The Crab pulsar is a neutron star remaining following a supernova in 1054. Gamma rays from it have been observed from space to energies of about 5 GeV. Ground-based observations have failed to detect pulsed emissions at energies above their usual minimum threshold of about 60 GeV. The threshold of the MAGIC Cherenkov telescope has now been lowered to 25 GeV, and **The MAGIC Collaboration** (p. 1221, published online 16 October) has been able to detect pulsed emissions from the Crab pulsar. The emissions were observed at a flux lower than expected from extrapolation of the lower energy data, which challenges models for the location and source of the emission in the outer parts of the neutron star.

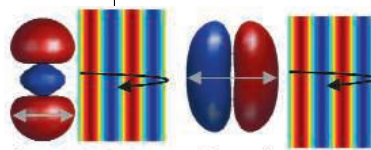
## GPCR Structural Diversity

G protein-coupled receptors (GPCRs) respond to diverse extracellular signals to activate different signaling pathways. They are important pharmacological targets, but, so far, structural information that might aid drug design is limited to the rhodopsin and adrenergic receptors, and determinants of ligand binding specificity among different GPCRs are unclear. Now **Jaakola *et al.*** (p. 1211, published online 2 October) report the structure of the human A<sub>2A</sub> adenosine receptor, a receptor that is blocked by caffeine, in complex with an antagonist. The binding pocket is distinct from that in the rhodopsin and adrenergic receptors, suggesting that, rather than a conserved binding pocket with specific amino acid side chains determining specificity, the GPCR binding pocket itself can vary in position and orientation.

## Light from Below

A strong oscillating laser field can pull electrons from the outer layer of an atom or molecule and then send them careening back, releasing high-energy photons upon collision. This process underlies recent techniques for generating the shortest light

pulses, with durations below 10<sup>-15</sup> second. Two studies now show that more tightly bound electrons



can also undergo this ricochet process in strong fields (see the Perspective by **Doumy and DiMauro**). **Li *et al.*** (p. 1207; published online

*Continued on page 1161*

Continued from page 1159

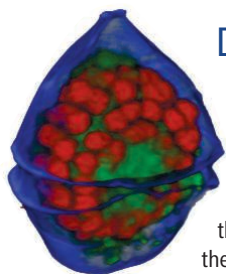
30 October) observed distinct emission intensities at different stages in the vibrational period of a vibrating  $N_2O_4$  molecule. Similarly, **McFarland *et al.*** (p. 1232, published online 30 October) found distinct spectral signatures depending on the spatial orientation of  $N_2$  molecules relative to the polarization of the applied laser field. In both cases, the results are attributed to involvement of electrons in both the highest and second-highest energy-occupied orbitals. The findings open the door to wide-ranging probes of electronic coupling to molecular vibrations and rotations on time scales previously too fast to monitor.

## Promoting Polyandry

Females of almost all animals mate with more than one male, but the evolutionary drivers of this behavior, known as polyandry, remain enigmatic. **Price *et al.*** (p. 1241) show that selfish genetic elements, which affect male fertility in sperm relative to those lacking such elements, are associated with increased rates of remating. These data document the potential impact of selfish genetic elements within populations and provide a general explanation for the evolution of polyandry.

## Modeling Subcellular Morphogenesis

Within cells during mitosis, the subcellular architecture, particularly the arrangement of cellular microtubules, is substantially remodeled to promote the faithful segregation of chromosomes to daughter cells. **Athale *et al.*** (p. 1243, published online 23 October) report how enzymatic networks self-organize around chromosomes to affect the symmetry of the stochastic dynamics of microtubules nucleated by centrosomes in an open cell cytoplasm (frog egg extracts). A theoretical model shows how a true reaction diffusion mechanism can generate complex steady-state patterns of microtubules from enzymatic reactions. The coupling of a stochastic system (microtubule dynamics) and a deterministic regulatory gradient may thus provide a generic mechanism for subcellular morphogenesis.



## Dinospore Control

Harmful algal blooms, or red tides, are of increasing concern in warm coastal waters polluted by nitrogen runoff from agricultural land. The blooms are commonly produced by dinoflagellate protozoans, some species of which can produce dangerous toxins and are a major problem for the shellfish industry. During the 1980s, red tides swept the estuaries of northern France, but in the past decade these have largely disappeared. **Chambouvet *et al.*** (p. 1254) have been monitoring the algal succession in one of these estuaries and observed that during each summer, waves of different dinoflagellate species are successively knocked out by waves of distinct and highly specific parasitic species. Phylogenetic analysis indicated that these host and parasite associations have been established only in the past decade in these estuaries, but now persist in the environment throughout the year and help to suppress the formation of the toxic blooms.

## Wnts and the Brain Vasculature

Whereas all tissues in our bodies share a vasculature, different organs display distinct modes of vascularization during development, and the vessels that form are not alike. For example, blood vessels in the brain form a tight seal, the blood-brain barrier, enabling normal brain function but also restricting access of potentially therapeutic drugs. Now **Stenman *et al.*** (p. 1247; see the Perspective by **Lammert**) provide in vivo evidence that neural Wnt-signals, *Wnt7a* and *Wnt7b*, promote both the formation and differentiation of central nervous system vasculature by direct signaling to endothelial cells through a canonical Wnt pathway.

## A Drive Along the Metabolic Information Highway

Metabolic regulation in mammals requires communication between multiple organs and tissues. Studying mouse models, **Imai *et al.*** (p. 1250) found that obesity stimulates pancreatic  $\beta$  cell proliferation through a neural-mediated relay of metabolic signals from the liver to the pancreas. Obesity-induced activation of extracellular regulated kinase (ERK) signaling in the liver was identified as a key component of this metabolic relay. In mouse models of insulin-deficient (type 1) diabetes, liver-specific activation of ERK signaling resulted in an increase in  $\beta$  cell mass and normalization of serum glucose levels. Thus, interorgan metabolic communication systems may serve as valuable therapeutic targets for diabetes.

CREDIT: CHAMBOUVET/UPMC, CNRS

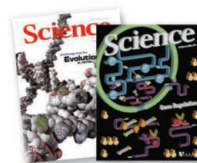
# Plug-In



## Let *Science* feed your mind with new multimedia features

Connect to *Science*'s multimedia features with videos, webinars, podcasts, RSS feeds, blogs, interactive posters, and more. Log on, click in and get your mind plugged into *Science*.

[sciencemag.org/multimedia](http://sciencemag.org/multimedia)



Discover more with *Science*.







Kiyoshi Kurokawa is a professor at the National Graduate Institute for Policy Studies in Tokyo and was Special Advisor to the Cabinet of Japan from 2006 to 2008.

## Opening Japan Up to the World

WITH A GLOBAL FINANCIAL CRISIS AT HAND, IT IS CLEAR THAT MAJOR CHANGE IS NEEDED among leading nations. For Japan, this comes at a time when two prime ministers have left office in barely 2 years, and support for the new prime minister, Taro Aso, is weak less than 2 months after he took up office. Perhaps the public, sensing the need for change, is pessimistic about the possibilities, given that Japan has been so resistant to change over the past decade.

Clearly, today's global competition demands entrepreneurs with distinct out-of-the-box talents. The flattening global market is also driving the need for diversity and collaboration, essential for the kind of open innovation that creates new markets. Like other nations, Japan's investments in science, technology, and innovation are crucial to its economic growth. Universities play a key role in nurturing future talents and leaders in every sector of society. Therefore, government support for academic science is vitally important. However, in Japan, such investment by the government often fails to nurture the potential of these individuals. This is partly due to an insular, hierarchical, and male-dominated system that still prevails in every sector of Japanese society, including academic institutions.

Meanwhile, many universities in other countries have become more open to the world, thereby becoming cores of the global community. They are creating programs that attract students from around the world and address global challenges in areas such as health, energy, climate change, and the environment. The international student-faculty-alumni network that these efforts forge is a powerful tool that is crucial for any nation's future success. In contrast, only a few universities in Japan are truly international: At Ritsumeikan Asia Pacific University, 50% of the undergraduate students are international and half of the courses are given in English; Akita International University, a typical small liberal arts college, has 40% international students, with most courses taught in English.

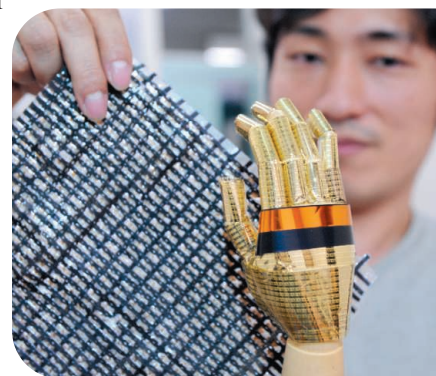
Leading universities outside of Japan aim to attract not only the world's most promising students but also the best faculty and academic leadership, be it dean, provost, or president. Some invite outstanding women to lead them: the University of Cambridge, Massachusetts Institute of Technology, Princeton University, and Harvard University, to name a few. Among approximately 80 national universities in Japan, only one has a woman at the top (Ochanomizu University, a women's university). Among Japan's private universities and colleges, the situation is not much different. Inviting someone from the outside to a top academic position is still exceptional, as it is in Japan's business sector.

But change is imminent. In 2009, the Japanese government will launch new programs in science and technology that join universities and research institutes in Japan with those in Africa. The program moves beyond simply inviting graduate students from Africa to Japan; it will promote joint bilateral research projects involving faculty and students.

Also, the Ministry of Education has submitted a budget beginning in fiscal year 2009 for an unusually ambitious program that increases opportunities for students to go abroad for a year as part of an exchange. The number of Japanese students who go abroad, even to universities in the United States, has fallen rapidly over the past few years (from 46,000 to 35,000). Reasons for this decline are unclear, but it comes at a time when meeting the future challenges in any country requires a circulation of human capital and resources that supports a vibrant international exchange of ideas and talents. The newly proposed exchange programs target 30 leading universities and aim to have at least 10% of all students study abroad within the next 5 years. The budget also requires that these universities offer many courses in English, which will hopefully attract non-Japanese students and faculty.

It is critical to approve this 2009 budget request because it will ultimately keep Japan economically robust and competitive. Otherwise, I fear that my country will become closed off from an increasingly interconnected global community, turning Japan back 150 years in its history to a time before Commodore Matthew Perry opened Japan to the world.

— Kiyoshi Kurokawa





## ECOLOGY

### Harmonious Agriculture

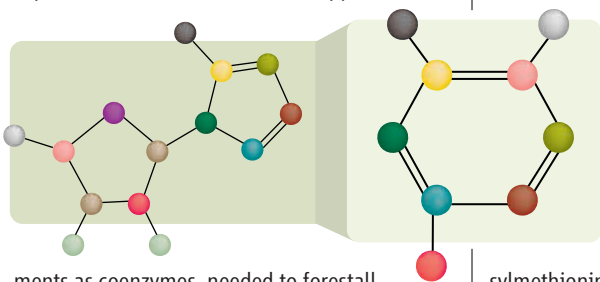
Long-term or large-scale agriculture is generally associated with substantial losses of biodiversity, yet there is increasing evidence that these losses can be mitigated by appropriate management practices at the landscape scale. Ranganathan *et al.* show that cultivation of arecanut palm in the Western Ghats region of southern India has not displaced the great majority (90%) of the native forest bird species such as the Malabar grey hornbill. Several factors underlie this favorable outcome: intercropping with other woody species, which creates structural complexity; and proximity to native forest, which is used as a source of mulch. Although similar effects have been observed in other tropical agroecosystems over the short term, the arecanut system has been operating in the Western Ghats for at least 2000 years. Hence, it may offer valuable lessons for the harmonizing of tropical agriculture (including biofuel crops) and conservation in the long run. — AMS

*Proc. Natl. Acad. Sci. U.S.A.* **105**, 10.1073/pnas.0808874105 (2008).

## BIOCHEMISTRY

### Out of Thin Air

In the pre-iPod era, eating a bowl of cold cereal at breakfast offered the opportunity for a detailed reading of the cereal box, on which the uncommon words niacin, thiamin, and riboflavin appeared. Years later, much more reading had explained the role of these trace supple-



ments as coenzymes, needed to forestall the exotic diseases of beriberi and pellagra. Thiamin, also known as vitamin B<sub>1</sub>, is an invaluable aid in carbohydrate metabolism, specifically during chemical transformations of  $\alpha$ -keto compounds. It contains two heterocyclic rings, a thiazole and a pyrimidine; the biosynthesis of the former is well understood; not so for the latter.

Chatterjee *et al.* establish by means of biochemical and structural analyses that the *Caulobacter crescentus* enzyme ThiC catalyzes the conversion of 5-aminoimidazole ribonucleotide (AIR) into 4-amino-5-hydroxymethyl-2-methylpyrimidine phosphate (HMP-P), which is

then coupled to the thiazole moiety to give thiamine monophosphate. What makes this reaction more than another bit of esoterica is the intricate rearrangement of AIR atoms effected by ThiC. Of the five carbon atoms in the ribose portion of AIR, C2' (red) is used to methylate C2 (blue) of the imidazole ring, and C4' (pink), with C5' still attached, is inserted in between C4

(olive) and C5 (yellow) of the imidazole ring, expanding it into a pyrimidine. How this is accomplished is not entirely clear, but these authors, as Martinez-Gomez and Downs have achieved recently for *Salmonella enterica* ThiC, show via *in vitro* reconstitution that a bound [4Fe-4S] cluster and the co-substrate S-adenosylmethionine participate in what bears the hall-

marks of a radical-based mechanism. — GJC

*Nat. Chem. Biol.* **4**, 10.1038/nchembio.121 (2008); *Biochemistry* **47**, 9054 (2008).

## EVOLUTION

### Fishing for Worms

The earthworm *Allolobophora chlorotica* has two color morphs: pink and green. The facts that these morphs are found in different habitats and crosses between them are sterile have suggested that they represent distinct species. King *et al.* have examined two mitochondrial

genes of *A. chlorotica* and eight other worms in the United Kingdom. They found that four of the worms, including *A. chlorotica*, displayed relatively high levels of diversity in the pair of mitochondrial genes. Furthermore, polymorphism markers showed similar divergence for *A. chlorotica*, where five deeply divergent clades were identified—three clades corresponding to the pink morphotype and two to the green. The relationships among these clades suggest that *A. chlorotica*, along with three of the other British earthworms, is actually a group of cryptic species as opposed to a single species with phenotypic diversity. — LMZ

*Mol. Ecol.* **17**, 4684 (2008).

## CHEMISTRY

### Tubular Templates

The hydrophobic surfaces of dispersed carbon nanotubes can attract a diverse range of small molecules from a surrounding solution, which in turn interact with one another to form loose assemblies. Thauvin *et al.* capitalized on this templating behavior by preparing lipids with a photoactive diacetylene group inserted between the polar head and lipophilic tail. After arranging around a nanotube, these lipids could be irradiated in the ultraviolet to rigidify their connections to one another through polymerization (which selectively linked neighboring diacetylenes without inducing covalent attachment to the nanotube surface). Elec-

trophoresis then liberated a batch of uniformly sized assemblies from the nanotube templates, which the authors characterized by transmission electron microscopy and light-scattering measurements. With a polar exterior and a hydrophobic interior hollowed out where the nanotube previously resided, these assemblies proved effective at solubilizing hydrophobic pigments, inhibiting full-ene aggregation, and stabilizing membrane proteins in an aqueous environment. Analysis of their detailed morphology remains underway. — JSY

*Nat. Nanotechnol.* 10.1038/nnano.2008.318 (2008).

## GEOLOGY

## Breaking Early and Often

In 1857, a major earthquake ruptured the central part of the San Andreas fault from near Parkfield in the Carrizo Plain southward to just northeast of Los Angeles (a distance of about 300 km). Surface slip was up to 9 m. Excavations along this break have revealed evidence of several earlier major earthquakes; accurate dating of these events provides an indication of how frequent and regular such major quakes might be. Akciz *et al.* provide a series of new dates on a section through the fault at Bidart Fan, in the Carrizo Plain, that revise the history of previous quakes. Four previous events are recognized and resolved here, dating from about 1310. The intervals between the quakes range from as short as about 80 years to as long as 200 years; the average recurrence interval is 137 years. This interval is shorter than previously thought and now longer than the time since the 1857 quake. Although the revised dates imply a more regular rupture of the fault, it is not yet clear if the previous major quakes were like that in 1857, or even greater, or ruptured to the north, rather than the south. — BH

Four previous events are recognized and resolved here, dating from about 1310. The intervals between the quakes range from as short as about 80 years to as long as 200 years; the average recurrence interval is 137 years. This interval is shorter than previously thought and now longer than the time since the 1857 quake. Although the revised dates imply a more regular rupture of the fault, it is not yet clear if the previous major quakes were like that in 1857, or even greater, or ruptured to the north, rather than the south. — BH



Although the revised dates imply a more regular rupture of the fault, it is not yet clear if the previous major quakes were like that in 1857, or even greater, or ruptured to the north, rather than the south. — BH

*J. Geophys. Res.* 10.1029/2007JB005285 (2008).

## BIOMEDICINE

## Helpful Bystanders

Although transformed cells can grow in artificial culture medium on plastic plates, in the body they thrive in very different surroundings. Individual cells are thought to become tumorigenic independently of their local environment, by acquiring genetic and epigenetic changes, although their

neighbors may permit and possibly even nourish the growth of transformed cells. Indeed, tumorigenic cells have been shown to secrete signals that induce changes in the surrounding tissues.

Yang *et al.* show that in neurofibromatosis type 1 (NF1), a genetic disease that predisposes individuals to tumors such as neurofibromas, the premalignant cells and the cells that form the microenvironment cooperate to promote tumorigenesis. Neurofibromas form from malignant Schwann cells and are associated with peripheral nerves, which are infiltrated by inflammatory mast cells that are derived from the bone marrow. The disease is caused by germline mutations in the *NF1* tumor suppressor gene; however, biallelic loss only in the Schwann cells is not sufficient for tumor progression. Instead, the authors find that a heterozygous *Nf1* mutation in the nonmalignant infiltrating mast cells is necessary for neurofibroma formation. By blocking mast cell release from the bone marrow, they could delay disease progression. This work upgrades the role of the microenvironment from being permissive for tumorigenesis to being causative. Whether this phenomenon is limited to familial disorders or can also contribute to the development of sporadic tumors remains to be seen. — HP\*

*Cell* 135, 437 (2008).

## MOLECULAR BIOLOGY

## Acting at a Distance

Unfolded proteins are dangerous to the cell; exposing hydrophobic amino acid side chains will promote nonspecific aggregation and interfere with intracellular processes. Chaperones are proteins that assist in the folding and unfolding of other proteins. They are found in all organisms, and among their number are the so-called heat shock proteins (Hsps),

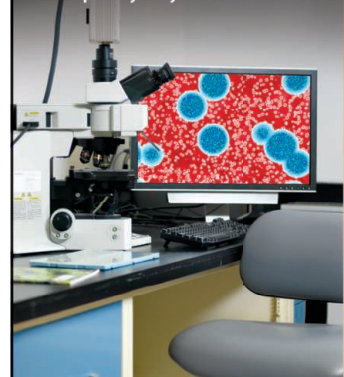
which combat heat-induced stress. In *Escherichia coli*, the heat shock transcription factor  $\sigma^{32}$  regulates heat-shock gene expression, and it is in turn regulated by Hsps: DnaK (the prokaryote equivalent of Hsp70) and the co-chaperone DnaJ.

Rodriguez *et al.* show that DnaK and DnaJ bind independently to distinct domains of  $\sigma^{32}$  in its native, folded state. The DnaK binding site would normally be occluded on  $\sigma^{32}$  that is bound to RNA polymerase, suggesting that DnaJ binds  $\sigma^{32}$  first. The binding of DnaJ destabilizes  $\sigma^{32}$  at a site in the vicinity of the DnaK binding site, favoring the rapid binding of DnaK once  $\sigma^{32}$  is released from RNA polymerase. Hsp70 systems in general may act in a similar manner: promoting disassembly and folding of aggregated substrate proteins by altering their conformations from a distance. — GR

*Mol. Cell* 32, 347 (2008).

Visit our enhanced website!

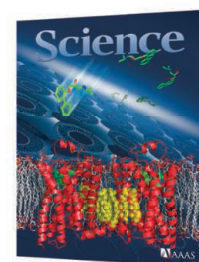
**Science Careers**  
is the window that  
displays your vision.



Revealing your vision to employers is our job. Whether you're seeking a career in academia, industry, or advancement in your chosen field, *Science Careers* is your window to a limitless future.

## Improved Website Features:

- » New design for easier navigation
- » More relevant job search results
- » Automated tools for a more effective search



Your Future Awaits.

**Science Careers**

From the journal *Science*



ScienceCareers.org



1200 New York Avenue, NW  
Washington, DC 20005

Editorial: 202-326-6550, FAX 202-289-7562

News: 202-326-6581, FAX 202-371-9227

Bateman House, 82-88 Hills Road  
Cambridge, UK CB2 1LQ

+44 (0) 1223 326500, FAX +44 (0) 1223 326501

**SUBSCRIPTION SERVICES** For change of address, missing issues, new orders and renewals, and payment questions: 866-434-AAAS (2227) or 202-326-6417, FAX 202-842-1065. Mailing addresses: AAAS, P.O. Box 96178, Washington, DC 20090-6178 or AAAS Member Services, 1200 New York Avenue, NW, Washington, DC 20005

**INSTITUTIONAL SITE LICENSES** please call 202-326-6755 for any questions or information

**REPRINTS:** Author Inquiries 800-635-7181

Commercial Inquiries 803-359-4578

202-326-7074, FAX 202-682-0816

**MEMBER BENEFITS** AAAS/Barnes&Noble.com bookstore www.aaas.org/bn; AAAS Online Store www.apisource.com/aaas/ code MKB6; AAAS Travels: Betchart Expeditions 800-252-4910; Apple Store www.apple/epstore/aaas; Bank of America MasterCard 1-800-833-6262 priority code FAA3YU; Cold Spring Harbor Laboratory Press Publications www.cshlpress.com/affiliates/aaas.htm; GEICO Auto Insurance www.geico.com/landingpage/go51.htm?logo=17624; Hertz 800-654-2200 CDP#343457; Office Depot www.officedepot.com/portalLogin.do; Seabury & Smith Life Insurance 800-424-9883; Subaru VIP Program 202-326-6417; VIP Moving Services www.vipmayflower.com/domestic/index.html; Other Benefits: AAAS Member Services 202-326-6417 or www.aaasmember.org.

science\_editors@aaas.org (for general editorial queries)

science\_letters@aaas.org (for queries about letters)

science\_reviews@aaas.org (for returning manuscript reviews)

science\_bookrevs@aaas.org (for book review queries)

Published by the American Association for the Advancement of Science (AAAS), *Science* serves its readers as a forum for the presentation and discussion of important issues related to the advancement of science, including the presentation of minority or conflicting points of view, rather than by publishing only material on which a consensus has been reached. Accordingly, all articles published in *Science*—including editorials, news and comment, and book reviews—are signed and reflect the individual views of the authors and not official positions of view adopted by AAAS or the institutions with which the authors are affiliated.

AAAS was founded in 1848 and incorporated in 1874. Its mission is to advance science, engineering, and innovation throughout the world for the benefit of all people. The goals of the association are to: enhance communication among scientists, engineers, and the public; promote and defend the integrity of science and its use; strengthen support for the science and technology enterprise; provide a voice for science on societal issues; promote the responsible use of science in public policy; strengthen and diversify the science and technology workforce; foster education in science and technology for everyone; increase public engagement with science and technology; and advance international cooperation in science.

## INFORMATION FOR AUTHORS

See pages 634 and 635 of the 1 February 2008 issue or access www.sciencemag.org/about/authors

EDITOR-IN-CHIEF **Bruce Alberts**

EXECUTIVE EDITOR **Monica M. Bradford**

DEPUTY EDITORS

**R. Brooks Hanson, Barbara R. Jasny,**  
**Katrina L. Kelnor**

NEWS EDITOR

**Colin Norman**

**EDITORIAL SUPERVISOR** SENIOR EDITOR Phillip D. Szuroni; **SENIOR EDITOR/ PERSPECTIVES** Lisa D. Chong; **SENIOR EDITORS** Gilbert J. Chin, Pamela J. Hines, Paula A. Kiberstis (Boston), Marc S. Lavine (Toronto), Beverly A. Purnell, L. Bryan Ray, Guy Riddihough, H. Jesse Smith, Valda Vinson; **ASSOCIATE EDITORS** Kristen L. Mueller, Jake S. Yeston, Laura M. Zahn; **ONLINE EDITOR** Stewart Wells; **ASSOCIATE ONLINE EDITORS** Robert Frederick, Tara S. Marathe; **WEB CONTENT DEVELOPER** Martyn Green; **BOOK REVIEW EDITOR** Sherman J. Suter; **ASSOCIATE LETTERS EDITOR** Jennifer Sills; **EDITORIAL MANAGER** Cara Tate; **SENIOR COPY EDITORS** Jeffrey E. Cook, Cynthia Howe, Harry Jach, Barbara P. Ordway, Trista Wagoner; **COPY EDITORS** Chris Filiatreau, Lauren Kmeck; **EDITORIAL COORDINATORS** Carolyn Kyle, Beverly Shields; **PUBLICATIONS ASSISTANTS** Ramatoulaye Diop, Joi S. Granger, Jeffrey Hearn, Lisa Johnson, Scott Miller, Jerry Richardson, Jennifer A. Seibert, Brian White, Anita Wyne; **EDITORIAL ASSISTANTS** Carlos L. Durham, Emily Guise, Patricia M. Moore; **EXECUTIVE ASSISTANT** Sylvia S. Kihara; **ADMINISTRATIVE SUPPORT** Maryrose Madrid

**NEWS DEPUTY NEWS EDITORS** Robert Coontz, Elizabeth Marshall, Jeffrey Mervis, Leslie Roberts; **CONTRIBUTING EDITORS** Elizabeth Culotta, Polly Shulman; **NEWS WRITERS** Yudhijit Bhattacharjee, Adrian Cho, Jennifer Couzin, David Grimm, Constance Holden, Jocelyn Kaiser, Richard A. Kerr, Eli Kintisch, Andrew Lawler (New England), Greg Miller, Elizabeth Pennisi, Robert F. Service (Pacific NW), Erik Stokstad; **INTERN** Rachel Zerkowitz; **CONTRIBUTING CORRESPONDENTS** Jon Cohen (San Diego, CA), Daniel Ferber, Ann Gibbons, Robert Koenig, Milt Lisch, Charles C. Mann, Virginia Morell, Evelyn Strauss, Gary Taubes; **COPY EDITORS** Linda B. Felaco, Melvin Gatling, Melissa Raimondi; **ADMINISTRATIVE SUPPORT** Scherraine Mack, Fannie Groom; **BUREAU** New England: 207-549-7755, San Diego, CA: 760-942-3252, FAX 760-942-4979, Pacific Northwest: 503-963-1940

**PRODUCTION DIRECTOR** James Landry; **SENIOR MANAGER** Wendy K. Shank; **ASSISTANT MANAGER** Rebecca Doshi; **SENIOR SPECIALISTS** Steve Forrester, Chris Redwood; **SPECIALIST** Anthony Rosen; **PREFLIGHT DIRECTOR** David M. Tompkins; **MANAGER** Marcus Spiegler

**ART DIRECTOR** Yael Kats; **ASSOCIATE ART DIRECTOR** Laura Creveling; **ILLUSTRATORS** Chris Bickel, Katharine Sutfitt; **SENIOR ART ASSOCIATES** Holly Bishop, Preston Huey, Nayomi Kevitiyagala; **ART ASSOCIATE** Jessica Newfield; **PHOTO EDITOR** Leslie Blizard

## SCIENCE INTERNATIONAL

**EUROPE** (science@science-int.co.uk) **EDITORIAL: INTERNATIONAL MANAGING EDITOR** Andrew M. Sugden; **SENIOR EDITOR/PERSPECTIVES** Julia Fahrenkamp-Uppenbrink; **SENIOR EDITORS** Caroline Ash, Stella M. Hurtle, Ian S. Osborne, Peter Senior; **ASSOCIATE EDITOR** Maria Cruz; **EDITORIAL SUPPORT** Deborah Dennison, Rachel Roberts, Alice Whaley; **ADMINISTRATIVE SUPPORT** John Cannell, Janet Clements; **NEWS: EUROPE NEWS EDITOR** John Travis; **DEPUTY NEWS EDITOR** Daniel Clery; **CONTRIBUTING CORRESPONDENTS** Michael Balter (Paris), John Bohannon (Vienna), Martin Enserink (Amsterdam and Paris), Gretchen Vogel (Berlin); **INTERN** Sara Coelho

**ASIA** Japan Office: Asca Corporation, Eiko Ishioka, Fusako Tamura, 1-8-13, Hirano-cho, Chuo-ku, Osaka-shi, Osaka, 541-0046 Japan; +81 (0) 6 2602 6272, FAX +81 (0) 6 2602 6271; asca@os.gulf.or.jp; **ASIA NEWS EDITOR** Richard Stone (Beijing: rstone@aaas.org); **CONTRIBUTING CORRESPONDENTS** Dennis Normile (Japan: +81 (0) 3 3391 0630, FAX +81 (0) 3 5936 3531; dnormile@gol.com); Hao Xin (China: +86 (0) 10 6307 4439 or 6307 3676, FAX +86 (0) 10 6307 4358; cindyhao@gmail.com); Pallava Bagla (South Asia: +91 (0) 11 2271 2896; pbagla@vsnl.com)

EXECUTIVE PUBLISHER **Alan I. Leshner**

PUBLISHER **Beth Rosner**

**FULFILLMENT SYSTEMS AND OPERATIONS** (membership@aaas.org); **DIRECTOR** Waylon Butler; **SENIOR SYSTEMS ANALYST** Jonny Blaker; **CUSTOMER SERVICE SUPERVISOR** Pat Butler; **SPECIALISTS** Latoya Casteel, LaVonda Crawford, Vicki Linton, April Marshall; **DATA ENTRY SUPERVISOR** Cynthia Johnson; **SPECIALISTS** Eintou Bowden, Tarrika Hill, William Jones

**BUSINESS OPERATIONS AND ADMINISTRATION DIRECTOR** Deborah Rivera-Wienhold; **ASSISTANT DIRECTOR, BUSINESS OPERATIONS** Randy Yi; **MANAGER, BUSINESS ANALYSIS** Michael LoBue; **MANAGER, BUSINESS OPERATIONS** Jessica Tierney; **FINANCIAL ANALYSTS** Priti Pamnani, Celeste Troxler; **RIGHTS AND PERMISSIONS: ADMINISTRATOR** Emilie Davis; **ASSOCIATE** Elizabeth Sandler; **MARKETING DIRECTOR** John Meyers; **MARKETING MANAGER** Allison Pritchard; **MARKETING ASSOCIATES** Aimee Aponte, Alison Chandler, Mary Ellen Crowley, Marcia Leach, Julianne Wielga, Wendy Wise; **INTERNATIONAL MARKETING MANAGER** Wendy Sturley; **MARKETING EXECUTIVE** Jennifer Reeves; **MARKETING/MEMBER SERVICES EXECUTIVE** Linda Rusk; **DIRECTOR, SITE LICENSING** Tom Ryan; **DIRECTOR, CORPORATE RELATIONS** Eileen Bernadette Moran; **PUBLISHER RELATIONS, RESOURCES SPECIALIST** Kiki Forsythe; **SENIOR PUBLISHER RELATIONS SPECIALIST** Catherine Holland; **PUBLISHER RELATIONS, EAST COAST** Phillip Smith; **PUBLISHER RELATIONS, WEST COAST** Philip Tsolakidis; **FULFILLMENT SUPERVISOR** Iquo Edim; **ELECTRONIC MEDIA: MANAGER** Lizabeth Harman; **PROJECT MANAGER** Trista Snyder; **ASSISTANT MANAGER** Lisa Stanford; **SENIOR PRODUCTION SPECIALISTS** Christopher Coleman, Walter Jones; **PRODUCTION SPECIALISTS** Nichele Johnston, Kimberly Oster

**ADVERTISING DIRECTOR, WORLDWIDE AD SALES** Bill Moran

**PRODUCT** (science\_advertising@aaas.org); **MIDWEST/WEST COAST/W. CANADA** Rick Bongiovanni: 330-405-7080, FAX 330-405-7081; **EAST COAST** E. Canada Laurie Faraday: 508-747-9395, FAX 617-507-8189; **UK/EUROPE/ASIA** Roger Gonçalves: TEL/FAX +41 43 234 1358; **JAPAN** Masuyoshi Yoshikawa: +81 (0) 3 3235 5961, FAX +81 (0) 3 3235 5852; **SENIOR TRAFFIC ASSOCIATE** Deandra Simms

**COMMERCIAL EDITOR** Sean Sanders: 202-326-6430

**PROJECT DIRECTOR, OUTREACH** Brianna Blaser

**CLASSIFIED** (advertise@sciencemag.org); **US: RECRUITMENT SALES MANAGER** Ian King: 202-326-6528, FAX 202-289-6742; **INSIDE SALES MANAGER: MIDWEST/CANADA** Daryl Anderson: 202-326-6543; **INSIDE SALES REPRESENTATIVE** Karen Foote: 202-326-6740; **KEY ACCOUNT MANAGER** Joribah Able; **NORTHEAST** Alexis Fleming: 202-326-6578; **SOUTHEAST** Tina Burks: 202-326-6577; **WEST** Nicholas Hintzbide: 202-326-6533; **SALES COORDINATORS** Erika Foad, Rohan Edmondson, Shirley Young; **INTERNATIONAL: SALES MANAGER** Tracy Holmes: +44 (0) 1223 326525, FAX +44 (0) 1223 326532; **SALES** Susan Kharraz, Dan Pennington, Alex Palmer; **SALES ASSISTANT** Louise Moore; **JAPAN** Masuyoshi Yoshikawa: +81 (0) 3 3235 5961, FAX +81 (0) 3 3235 5852; **ADVERTISING PRODUCTION OPERATIONS MANAGER** Deborah Tompkins; **SENIOR PRODUCTION SPECIALIST/GRAPHIC DESIGNER** Amy Hardcastle; **SENIOR PRODUCTION SPECIALIST** Robert Buck; **SENIOR TRAFFIC ASSOCIATE** Christine Hall; **PUBLICATIONS ASSISTANT** Mary Lagnaoui

**AAAS BOARD OF DIRECTORS** RETIRING PRESIDENT, CHAIR David Baltimore; PRESIDENT James J. McCarthy; PRESIDENT-ELECT Peter C. Agre; TREASURER David E. Shaw; CHIEF EXECUTIVE OFFICER Alan I. Leshner; BOARD LYNN W. Enquist, Susan M. Fitzpatrick, Alice Galt, Linda P. B. Katchi, Nancy Knowlton, Cherry A. Murray, Thomas D. Pollard, Thomas A. Woolsey



ADVANCING SCIENCE, SERVING SOCIETY

## SENIOR EDITORIAL BOARD

**John I. Brauman**, Chair, Stanford Univ.  
**Richard Losick**, Harvard Univ.  
**Robert May**, Univ. of Oxford  
**Marcia McClurt**, Monterey Bay Aquarium Research Inst.  
**Linda Partridge**, Univ. College London  
**Vera C. Rubin**, Carnegie Institution  
**Christopher R. Somerville**, Univ. of California, Berkeley

## BOARD OF REVIEWING EDITORS

**Joanna Aizenberg**, Harvard Univ.  
**R. McNeill Alexander**, Leeds Univ.  
**David Altshuler**, Broad Institute  
**Arturo Alvarez-Buylla**, Univ. of California, San Francisco  
**Richard Amasino**, Univ. of Wisconsin, Madison  
**Angelika Amon**, MIT  
**Meinrat O. Andreae**, Max Planck Inst., Mainz  
**Kristi S. Anseth**, Univ. of Colorado  
**John A. Bargh**, Yale Univ.  
**Cornelia I. Bargmann**, Rockefeller Univ.  
**Ben Barres**, Stanford Medical School  
**Marisa Bartolomei**, Univ. of Penn. School of Med.  
**Ray H. Baughman**, Univ. of Texas, Dallas  
**Stephen J. Benkovic**, Penn State Univ.  
**Michael J. Bevan**, Univ. of Washington  
**Ton Bisseling**, Wageningen Univ.  
**Mina Bissell**, Lawrence Berkeley National Lab  
**Peter Bork**, EMBL  
**Dianna Bowles**, Univ. of York  
**Robert W. Boyd**, Univ. of Rochester  
**Paul M. Brakefield**, Leiden Univ.  
**Dennis Bray**, Univ. of Cambridge  
**Stephen Buratowski**, Harvard Medical School  
**Joseph A. Burns**, Cornell Univ.  
**William P. Buttz**, Population Reference Bureau  
**Peter Carmeliet**, Univ. of Leuven, VIB  
**Gerbrand Ceder**, MIT  
**Mildred Cho**, Stanford Univ.  
**David Clapham**, Children's Hospital, Boston  
**David Clary**, Oxford University  
**J. M. Claverie**, CNRS, Marseille

**Jonathan D. Cohen**, Princeton Univ.  
**Stephen M. Cohen**, Temasek Life Sciences Lab, Singapore  
**Robert H. Crabtree**, Yale Univ.  
**F. Fleming Crim**, Univ. of Wisconsin  
**William Cumberlan**, Univ. of California, Los Angeles  
**Gerhard O. Daley**, Children's Hospital, Boston  
**Jeff L. Dangl**, Univ. of North Carolina  
**Stanislav Dehaene**, Collège de France  
**Edward DeLong**, MIT  
**Emmanouil T. Dermizakis**, Wellcome Trust Sanger Inst.  
**Robert Desimone**, MIT  
**Dennis Discher**, Univ. of Pennsylvania  
**Scott C. Doney**, Woods Hole Oceanographic Inst.  
**Peter J. Donovan**, Univ. of California, Irvine  
**W. Ford Doolittle**, Dalhousie Univ.  
**Jennifer A. Doudna**, Univ. of California, Berkeley  
**Julian Downward**, Cancer Research UK  
**Denis Duboule**, Univ. of Geneva/EPFL Lausanne  
**Christopher Dye**, WHO  
**Richard Ellis**, Cal Tech  
**Gerhard Ertl**, Fritz-Haber-Institut, Berlin  
**Douglas H. Erwin**, Smithsonian Institution  
**Mark Estelle**, Indiana Univ.  
**Barry Everitt**, Univ. of Cambridge  
**Paul G. Falkowski**, Rutgers Univ.  
**Ernst Fehr**, Univ. of Zurich  
**Ton Fenchel**, Univ. of Copenhagen  
**Alain Fischer**, INSERM  
**Scott E. Fraser**, Cal Tech  
**Chris D. Frith**, Univ. College London  
**Wulfram Gerstner**, EPFL Lausanne  
**Charles Godfrey**, Univ. of Oxford  
**Diane Griffin**, Johns Hopkins Bloomberg School of Public Health  
**Christian Haas**, Ludwig Maximilians Univ.  
**Niels Hansen**, Technical Univ. of Denmark  
**Dennis L. Hartmann**, Univ. of Washington  
**Chris Hawkesworth**, Univ. of Bristol  
**Martin Heimann**, Max Planck Inst., Jena  
**James A. Hendler**, Rensselaer Polytechnic Inst.  
**Ray Hilborn**, Univ. of Washington  
**Ove Hoegh-Guldberg**, Univ. of Queensland  
**Ronald R. Hoy**, Cornell Univ.  
**Olli Ikkala**, Helsinki Univ. of Technology  
**Meyer B. Jackson**, Univ. of Wisconsin Med. School

**Stephen Jackson**, Univ. of Cambridge  
**Steven Jacobsen**, Univ. of California, Los Angeles  
**Peter Jonas**, Universität Freiburg  
**Barbara B. Kahn**, Harvard Medical School  
**Daniel Kahne**, Harvard Univ.  
**Gerd Karsenty**, Columbia Univ. College of P&S  
**Bernhard Keimer**, Max Planck Inst., Stuttgart  
**Elizabeth A. Kelloff**, Univ. of Missouri, St. Louis  
**Alan B. Krueger**, Princeton Univ.  
**Lee Kump**, Penn State Univ.  
**Mitchell A. Lazar**, Univ. of Pennsylvania  
**Virginia Lee**, Univ. of Pennsylvania  
**Norman L. Letvin**, Beth Israel Deaconess Medical Center  
**Lois Lindvall**, Univ. Hospital, Lund  
**John Lis**, Cornell Univ.  
**Richard Losick**, Harvard Univ.  
**Ke Lu**, Chinese Acad. of Sciences  
**Andrew P. MacKenzie**, Univ. of St. Andrews  
**Raul Madariaga**, Ecole Normale Supérieure, Paris  
**Anne Maquarrie**, Univ. of St. Andrews  
**Virginia Miller**, Washington Univ.  
**Yasushi Miyashita**, Univ. of Tokyo  
**Richard Morris**, Univ. of Edinburgh  
**Edward Moser**, Norwegian Univ. of Science and Technology  
**Naoto Nagaosa**, Univ. of Tokyo  
**James Nelson**, Stanford Univ. School of Med.  
**Timothy W. Nilsen**, Case Western Reserve Univ.  
**Roeland Nolte**, Univ. of Nijmegen  
**Helen Nowotny**, European Research Advisory Board  
**Eric N. Olson**, Univ. of Texas, SW  
**Elin O'Shea**, Harvard Univ.  
**Erin Ostrom**, Indiana Univ.  
**Jonathan T. Overpeck**, Univ. of Arizona  
**John Pendry**, Imperial College  
**Philippe Poulin**, CNRS  
**Molly Power**, Univ. of California, Berkeley  
**Marty Przeworski**, Univ. of Chicago  
**Colin J. Read**, Univ. of Sheffield  
**Les Real**, Emory Univ.  
**David Renfrew**, Univ. of Cambridge  
**Trevor Robbins**, Univ. of Cambridge  
**Barbara A. Romanowicz**, Univ. of California, Berkeley  
**Edward M. Rubin**, Lawrence Berkeley National Lab  
**Jürgen Sandkühler**, Medical Univ. of Vienna  
**David S. Schimel**, National Center for Atmospheric Research

**David W. Schindler**, Univ. of Alberta  
**Georg Schulz**, Albert-Ludwigs-Universität  
**Paul Schulze-Lefert**, Max Planck Inst., Cologne  
**Christine Seidman**, Harvard Medical School  
**Terrence J. Sejnowski**, The Salk Institute  
**David Sibley**, Washington Univ.  
**Montgomery Slatkin**, Univ. of California, Berkeley  
**George Somero**, Stanford Univ.  
**Joan Steitz**, Yale Univ.  
**Elisbeth Stern**, ETH Zürich  
**Jerome Strauss**, Virginia Commonwealth Univ.  
**Glen Telling**, Univ. of Kentucky  
**Marc Tessier-Lavigne**, Genentech  
**Jurg Tschopp**, Univ. of Lausanne  
**Michiel van der Klis**, Astronomical Inst. of Amsterdam  
**Derek van der Kooy**, Univ. of Toronto  
**Bert Vogelstein**, Johns Hopkins Univ.  
**Ulrich H. von Andrian**, Harvard Medical School  
**Bruce D. Walker**, Harvard Medical School  
**Christopher A. Walsh**, Harvard Medical School  
**Graham Warren**, Yale Univ. School of Med.  
**Colin Watts**, Univ. of Dundee  
**Detlef Weigel**, Max Planck Inst., Tübingen  
**Jonathan Weisman**, Univ. of California, San Francisco  
**Ellen D. Williams**, Univ. of Maryland  
**Ian A. Wilson**, The Scripps Res. Inst.  
**Jerry Workman**, Stowers Inst. for Medical Research  
**John R. Yates III**, The Scripps Res. Inst.  
**Jan Zaenen**, Leiden Univ.  
**Martin Zatz**, NIMH, NIH  
**Huda Zoghbi**, Baylor College of Medicine  
**Marta Zubir**, MIT

## BOOK REVIEW BOARD

**John Aldrich**, Duke Univ.  
**David Bloom**, Harvard Univ.  
**Angela Creager**, Princeton Univ.  
**Richard Swedger**, Univ. of Chicago  
**Ed Wasserman**, DuPont  
**Lewis Wolpert**, Univ. College London

## Big Chill

Political pressure on sex-related research drove some scientists to “self-censorship,” a researcher at Rutgers University in Piscataway, New Jersey, reports.

In 2003, some members of the U.S. Congress tried to rescind funding for several National Institutes of Health (NIH)–funded projects dealing with various aspects of sexual behavior. A conservative Christian group called the Traditional Values Coalition followed up with a list of 250 sex-related grants, which NIH dutifully reviewed.

Although all remained funded, observers worried about the “chilling effect” on research. So sociologist Joanna Kempner asked the 157 principal investigators how they were affected. Eighty-two filled out a written survey. In items answered by 76 respondents, 54 felt the controversy had a chilling effect on research, and 60 felt funding decisions were getting more political during the Bush Administration. Nonetheless, 60 agreed that “no amount of political controversy could dissuade me from conducting HIV- or sex-related research,” Kempner reported last week online in *PLoS Medicine*. To cope with the scrutiny, half of the researchers said they had resorted to camouflage, purging their abstracts of dicey terms such as “gay,” “bisexual,” “homophobia,” and “needle exchange” to foil key-word searches on NIH’s grants database. One interviewee even changed the euphemism “sex workers” to “women at risk.” But 24% of the respondents said they had shifted the content of their research, and one reported being driven out of research altogether.

## Silicon Seminar Room

Don’t tell the graduate student who is sweating to get his or her first paper accepted, but publication is only the beginning. Next come the critical discussions during which scientists pore over a paper’s methods, dissect its conclusions, and plumb its implications. The goal of the Web site BioMed Critical Commentary ([bmcc.org/home.php](http://bmcc.org/home.php)) is to ensure that these discussions, which are often confined to journal clubs or seminar rooms, reach a broader audience.

Edited by cancer geneticist Scott Kern of Johns Hopkins University School of Medicine in Baltimore, Maryland, the site lets researchers submit brief commentaries on any paper in PubMed. Commentaries are not limited to recent papers but may rehash historical gems by luminaries such as Gregor Mendel and



## A Family Affair

A Stone Age grave (above) has yielded what scientists say is the oldest molecular genetic evidence yet of a “classic nuclear family.” Known as Grave 99, it’s one of four multiple burials discovered 3 years ago near Eulau, Germany, that are casting new light on the people who lived in northern Europe some 4600 years ago.

The grave held the bones of a man, a woman, and two boys, presumably killed in a raid, as they were buried at the same time. The boys shared the woman’s mtDNA haplogroup and the man’s Y haplogroup, indicating that they were a family, researchers led by geneticist Wolfgang Haak of the University of Adelaide in Australia report online this week in the *Proceedings of the National Academy of Sciences*.

The scientists also found evidence that the men in the graves sought wives from outside communities. Analysis of strontium isotopes in tooth enamel—levels of which vary depending on where people spent their early years—showed that only the men and children were locals.



Louis Pasteur. So far, the work that’s attracted the most page views is an influential 1971 article by Alfred Knudson asserting that the eye cancer retinoblastoma stems from two mutations.

Commentary contributors have to provide their contact information, but comments can run anonymously.



## Slow’s the Way to Go

Real-life turtles might never outrace hares, but they can claim green credentials for energy efficiency.

Biologists Peter Zani and Rodger Kram of the University of Colorado, Boulder, trained 18 ornate box turtles to walk on a

treadmill and measured their oxygen consumption. After 141 trials in which the turtles trudged along at a little over 4 meters an hour, the scientists concluded that their “cost of transport”—an index of the power needed to move an animal’s body mass—is about half of what would be expected for reptiles of their size.

Turtles owe their efficiency to their peculiar skeletons, Zani says. The top shell keeps the shoulder in place, and the plastron (bottom shell) helps hold in the gut, so energy is saved from these tasks. Sluggishness helps, too. “Fast muscle is very expensive,” says Zani, whose paper is in last week’s *Journal of Experimental Biology*.

Biomechanicist Roland Ennos of the University of Manchester in the U.K. calls the work “fascinating.” He says that with their short legs and constraining shell, turtles “have a lurching gait which should be energetically expensive.” Most researchers concentrate on the mechanical aspects of locomotion, he adds, but this result suggests that for walking animals, “muscle efficiency is more important.”



## Pathways Into Science

**TURNING AROUND.** Craig Ulrich was studying biology at the University of Washington, Seattle, in 2004 when he shot a friend after a night of partying. Instead of graduating from college and going to medical school, he spent 4 years in a state prison after being convicted of manslaughter. But now Ulrich has his life back on track, thanks in part to his interest in science.

While serving his time, Ulrich studied how to improve the efficiency of the prison's composting system. The corrections center now generates half as much food waste and produces 5000 kg of organic fertilizer a year for its gardens.

His work caught the attention of Nalini Nadkarni, an ecologist at The Evergreen State College in Olympia, Washington,

who had worked with other inmates to investigate sustainable cultivation of certain mosses harvested illegally for use in flower arrangements. Earlier this year, the pair published a paper in *Environment, Development and Sustainability* on the advantages of enlisting inmates in research, and in August, Ulrich gave a talk at the annual meeting of the Ecological Society of America. "I walked in a prisoner and walked out a scientist," he told his audience. Ulrich is now a graduate student in biochemistry at the University of Nevada, Reno.



## Three Q's >>

Last week, a group of adventurers and scientists set off from the Philippines in two traditional Polynesian catamarans on a 6-month, 6000-km voyage to trace the migrations of the ancient Lapita people, possible ancestors of several Pacific Islander groups. **Keith Dobney**, 48, a noted animal-domestication expert at Durham University in the United Kingdom, plans to join them en route to the outer Solomon Islands.

**Q: Is this a serious research trip or a publicity stunt?**

It is clearly both. The organizers are famous boat builders and designers, although the trip will probably not be a faithful reconstruction of Lapita dispersals. Yet, they wanted scientists aboard to do real research.

**Q: What do you hope to learn?**

During our many island stops, my Durham colleague Greger Larson and I will be collecting feather and hair samples from chickens, pigs, and dogs for genetic analysis. They represent the original ancestors of animals from the mainland and will tell us a lot about the dispersal and domestication of these species.

**Q: Have you ever gone on a long voyage by boat?**

Never in my entire life. I'm absolutely petrified!

## ON CAMPUS

**A HARD STAND.** A biochemistry professor at the University of California, Irvine, has been disciplined for refusing to undergo state-mandated training on sexual harassment. Alexander McPherson, who says participating in such training would cast aspersions on his character, can no longer supervise the two researchers in his lab—both men. The university is enforcing a 2004 California law that requires all state employees in managerial positions at large businesses to receive the training—typically a 2-hour session—once every 2 years. McPherson thinks the mandatory attendance is ineffective and impinges on academic freedom. "Once you gain tenure, you're supposed to be protected against various sorts of social, political, and even scientific pressures," he says.



The matter is far from settled. Last week, McPherson skipped another training session, a move that he says could cost him his job. University officials would not say what action, if any, they plan to take next.

## IN BRIEF

**Ronald Daniels**, a Canadian-born legal scholar who is provost of the University of Pennsylvania, will become the next president of Johns Hopkins University in Baltimore, Maryland. He succeeds William Brody, who is taking the helm of the Salk Institute for Biological Studies in San Diego, California, in March 2009 (*Science*, 24 October, p. 511). Daniels worked as dean of the University of Toronto before moving to the University of Pennsylvania in 2005.

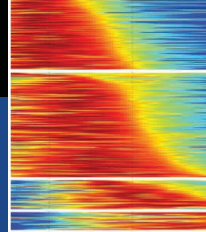
A postdoctoral researcher at the University of California, San Francisco, was arrested last week for attempting to poison a labmate by adding chemicals to her drinking water.

**Benchun Liu**, who works in the urology department, told the labmate—technician Mei Cao—that he intended to kill her. She drank the water but was unharmed. According to the *San Francisco Chronicle*, Liu told police that he had been "stressed out" lately.



Using the market  
to treat malaria

1174

Protein dynamics  
in cancer cells

1176

## TECHNICAL EXCHANGES

## U.S. Visa Delays on the Rise, Scientists Abroad Report

**BEIJING**—Huang Yanyi was looking forward to the 11th Chinese-American Kavli Frontiers of Science Symposium, held last month in Irvine, California. He had organized a session on microfluids and planned to huddle with collaborators from the Georgia Institute of Technology in Atlanta. But Huang never made it out of China. Although the materials scientist at Peking University applied for a U.S. visa in early July, the visa was not issued until 7 October—3 days after the symposium wrapped up. “It’s very frustrating,” says Huang, who recently completed postdoctoral stints at the California Institute of Technology in Pasadena and Stanford University in Palo Alto, California. “My American colleagues joke that maybe we should look for a ‘neutral zone,’ like Europe, for our future meetings.”

It may not be long before that dark humor becomes reality. The Chinese scientist Huang lined up to speak at his session also failed to get a visa in time; the chair of his session, who got his visa the day before he was due to fly, agreed to stand in for the speaker. All told, visa woes prevented 11 Chinese from attending the symposium. In a similar case in August, the leader of China’s delegation to the General Assembly of the International Union of Radio Science in Chicago, Illinois, did not get a visa in time to attend and present his country’s proposal to host the next assembly.

All were snared by a recent slowdown in the processing of U.S. visas for foreign scientists. Procedures instituted after the 11 September 2001 attacks require the U.S. Department of Homeland Security, CIA, FBI, and other agencies to vet most scientists from countries whose citizens must obtain visas to enter the United States. In 2003, visa delays prompted scientific societies to warn of an erosion of U.S. competitiveness if top foreign talent were to eschew travel to the United States. By last year, U.S. security agencies had managed to whittle average visa-processing time for scientists from 7 weeks to 3 weeks. It has since climbed back up to 8 weeks. “We are quite



**Grounded.** Huang Yanyi was one of 11 Chinese scientists who failed to get a visa in time for a symposium last month in California.

concerned about the possibility of seeing all the ground we made lost,” says Amy Scott, assistant vice president for federal relations at the Association of American Universities in Washington, D.C.

Visa-processing delays are not the only complaint. U.S. managers say it is harder than ever to secure H-1B visas for foreign researchers they wish to employ in the United States. “It is nearly impossible to bring in the best people in the world and build a company without spending a huge amount of time and money to get these people to the States,” says biomedical engineer and entrepreneur Jonathan Rothberg, who founded 454 Life Sciences and several other biotech start-ups. Reaching out to U.S. legislators has done little good, Rothberg says. “They see it as a zero-sum game, where we are hiring ‘one less qualified American.’”

Meanwhile, the visa delays, observers say, have worsened since last summer. “It’s driving everyone crazy,” says an official at the U.S. Embassy in Beijing. “It obviously

damages our S&T relationship with China.” The embassy has a channel to intervene in high-profile cases, which it used earlier this year to expedite review of a visa application from Jiang Mianheng, vice president for high-tech research at the Chinese Academy of Sciences and son of the former president of China, Jiang Zemin. “We can use this channel only in exceptional cases,” says the embassy official. A recurring problem is seemingly arbitrary visa denials. According to a State Department official authorized to speak on background, visa rejections are rare and, for reasons he declined to elaborate on, tend to target scientists in aeronautics and aviation.

The renewed concerns have prompted a fresh look at how to streamline the Security Advisory Opinion (SAO) process. Parts of this bureaucratic machine date to the Cold War. For example, the decades-old Technology Alert List allows consular officials to flag visa applications from students and scientists in disciplines in which the U.S. government is determined to restrict sensitive information. The list—described in congressional testimony in 2003 as 15 critical fields—is now classified; in the past, it included biotechnology, chemistry, and robotics. “Maybe the only field that doesn’t raise a red flag is pure mathematics,” says the State Department official.

The State Department introduced a layer of complexity in 1998 with its Visas Mantis Program, aimed at thwarting the leakage of S&T secrets. Under Mantis, consular or Homeland Security officials can reject a visa application if they have “reasonable grounds” to believe an applicant’s proposed activities will “violate or evade any law prohibiting the export from the United States of goods, technology, or sensitive information.” Mantis cases comprise about 10% of SAO cases. Then in 2002, the State Department launched Visas Condor, which lists 25 countries, including China, India, and Russia, from which visa applicants who meet certain classified criteria receive special scrutiny.

The post-9/11 change with the biggest impact on visa processing time, says the State Department official, is a requirement that each reviewing agency give a thumbs-up, no matter how long a review takes. Before 9/11, a visa would be granted if no agency objected within 10 days. The official says that agencies simply don’t have the staff to make much ▶

CREDIT: COURTESY OF HUANG YANYI

headway on the visa backlog.

One remedy would be for security agencies to hire more reviewers. Experts also argue that agencies could speed up the process by relying more on the judgment of the U.S. scientific community. For instance, some researchers would like to see an executive order stipulating that if a scientific body or university supports an application, a decision to grant or deny a visa must be made within 30 days. Advocates say this approach might

also rely on qualified U.S. scientists to vouch for the credibility of the work of foreign experts. They argue that researchers who build a reputation in the scientific community are unlikely to trash that and become a terrorist or spy. A U.S. National Research Council panel is expected to recommend a vouching system in a report due out in several weeks on how U.S. security controls are impeding the flow of scientific information.

An expert vouching system “might speed

things up to some degree,” says Albert Teich, director of science and policy programs at AAAS (*Science's* publisher). But he warns that reviewing agencies would still have a good deal of responsibility to weigh whether granting a visa presents a security risk. He and others will be watching whether President-elect Barack Obama addresses concerns about the visa issue through an executive order early in his Administration.

—RICHARD STONE

With reporting by Chen Xi.

## ASTROPARTICLE PHYSICS

# Excess Particles From Space May Hint at Dark Matter

An unexpected abundance of high-energy electrons from space could be evidence of particles of dark matter—the weighty and mysterious stuff whose gravity holds the galaxies together. The observation is the second in 4 months that suggests a link between cosmic rays and dark matter. But if the sightings really do point to dark matter, then physicists may have to revise their ideas about what the stuff is.

The latest result comes from the Advanced Thin Ionization Calorimeter (ATIC), a NASA-funded balloon-borne particle detector that circled the South Pole. “If it is true, it’s fantastic,” says Lars Bergström, a theoretical astroparticle physicist at Stockholm University in Sweden.

Using data collected in 2000 and 2002, ATIC researchers observed about 210 electrons and positrons with energies between 300 billion and 800 billion electron volts (GeV), they report this week in *Nature*. That was about 70 more than they expected by extrapolating from lower energies. The excess could be born of the collisions of dark-matter particles, says ATIC team leader John Wefel, an astrophysicist at Louisiana State University, Baton Rouge. According to leading theories, when two dark-matter particles collide, they should annihilate each other and produce either an electron and a positron or some other particle-antiparticle pair.

The excess could also be produced by a nearby pulsar or other astrophysical beast that accelerates particles in some unexpected way. But “so far we have not been able to find anything out there that’s able to do this,” Wefel says. Moreover, the excess abruptly disappears at energies above 800 GeV. That detail

might point toward dark matter, as the mass of the colliding dark-matter particles would limit the energy of electrons and positrons, Bergström explains.

Another cosmic-ray observation also hints at dark matter. In August, researchers with the orbiting PAMELA (Payload for Anti-matter Matter Exploration and Light-Nuclei Astrophysics) experiment reported that at energies between 10 GeV and 100 GeV, the ratio of positrons to the sum of electrons and positrons begins to climb. Ordinarily, electrons from space should far outnumber positrons. But dark-matter annihilations should produce equal numbers of electrons and positrons, causing the ratio to rise, as PAMELA observed. The PAMELA and ATIC data are “completely compatible,” says Marco Cirelli of the Institute of Theoretical Physics of the French Atomic Energy Commission in Saclay, France. “PAMELA is seeing the start of the rise [in electron-positron pairs], and ATIC is seeing the whole bump,” he says.

Ironically, if ATIC and PAMELA are detecting dark matter, then theorists may have to rethink a favorite idea. Many believe that dark-matter particles might be the lightest particles predicted by supersymmetry, which posits a heavier “superpartner” for every known type of particle. But colliding particles of supersymmetric dark matter ought to produce a lot of proton-antiproton pairs. Unless the supersymmetric particles are heavier than



**Going up?** Researchers prepare ATIC to be hauled aloft by a balloon. The particle detector may have spotted signs of dark matter.

generally expected, PAMELA should also see the ratio of antiprotons to protons increase at energies above 10 GeV, which it doesn’t.

Moreover, annihilating supersymmetric particles won’t directly produce electron-positron pairs, but it will make other particles that decay into the electron and proton. That should smooth over the sharp drop-off ATIC sees. “If this is dark matter, it is not the standard dark matter,” Cirelli says.

Clarity may come soon. NASA’s Fermi Gamma-Ray Space Telescope, launched in June, will look for photons produced by dark-matter annihilations. If ATIC and PAMELA are seeing a real signal, then Fermi should see one, too.

—ADRIAN CHO



## GLOBAL HEALTH

# Malaria Drugs, the Coca-Cola Way

Most parents would buy the most effective drug they could afford to save their child's life. But it's not so simple if you are poor and living in Africa, where the local drugstore stocks a bewildering array of medicines, ranging in price from a few dimes to \$10, usually with no information about which work and which don't. There's a good chance you would choose a cheap treatment—and that it would turn out to be totally ineffective.

That, in a nutshell, is the problem with a new generation of malaria drugs called artemisinin-based combination therapies (ACTs). Although cheap by Western standards, they're expensive to the world's poorest, and in the private sector where most Africans buy their drugs, they face stiff competition. But on 7 November, the Board of the Global Fund to Fight AIDS, Tuberculosis and Malaria voted to adopt a new financing system aimed at bringing the best drugs to stores at rock-bottom prices—by letting the market do the work. “From an economics point of view, it's going to be an incredibly exciting experiment,” says Barry Bloom, dean of the Harvard School of Public Health in Boston.

ACTs combine a drug derived from *Artemisia annua*, a plant used in Chinese medicine for centuries, with a second malaria drug to make it harder for the malaria parasite to develop resistance. Highly effective, ACTs have revived hope that the enormous burden of malaria can be slashed, but their rollout has been slow and difficult (*Science*, 26 October 2007, p. 560). The Global Fund, the World Bank, and others provide subsidies to poor countries that buy the drugs for their public health systems, but more than half of patients in Africa get their drugs from private outlets. Those drugstores often don't carry ACTs, however, and if they do, they're much more expensive than old, ineffective drugs like chloroquine, counterfeit drugs, and artemisinin monotherapies. (Drug resistance to artemisinin-based drugs—already emerging in Southeast Asia—is a huge worry, which is why global health leaders discourage the use of monotherapies.) A recent study by the Medicines for Malaria Venture and the Ugandan Ministry of Health shows just how expensive and difficult ACTs are to obtain in

the private sector (see table).

In 2004, a U.S. National Academies' Institute of Medicine (IOM) panel chaired by retired economist and Nobel laureate Kenneth Arrow proposed a solution. Pharmaceutical wholesalers in poor countries should be able to buy ACTs straight from the manufacturer for pennies instead of dollars, the panel said;

## ACCESS TO MALARIA DRUGS IN UGANDA

- » 174 different formulations and strengths of often outdated drugs for sale
- » Fewer than 14% of private drug outlets sell ACTs
- » ACTs are up to 60 times more expensive than other drugs

donors would pay the difference directly to the manufacturer. That way, the drugs could be traded down the supply chain and be sold in even the smallest village at the same price or for less than the undesirable drugs—which would, with any luck, be pushed off the market. “For years, we've been saying in public health: If only we knew how Coca-Cola gets its cans into the most remote African villages, we could do the same for drugs,” says health economist Ramanan Laxminarayan of Resources for the Future in Washington, D.C., who sat on the IOM panel. “Well, this is how they do it—by relying on the market.”



**Take your pick.** A street vendor in Niger—one of 11 countries targeted for the new program—has a huge variety of drugs for sale, including many for malaria.

Still, the idea is untested in global health, says Oliver Sabot, director of the Clinton Foundation Malaria Control Team. Some worry that, instead of passing the benefit on to patients, intermediaries will pocket most of the subsidy. Some also contend it's better to expand access to the public health system than to subsidize the chaotic private sector. For those and other reasons, the U.S. government has opposed the plan so far. “This is an expensive proposition,” says Bernard Nahlen, deputy coordinator of the U.S. President's Malaria Initiative. “We'd better have good evidence that it will work.”

Some evidence came earlier this year from a small-scale trial in Tanzania run by the Clinton Foundation. Wholesalers were sold the locally preferred ACT, arthemeter-lumefantrine, for about \$0.12 per treatment course and were allowed to sell it in two rural districts. Researchers interviewed customers coming out of shops and audited stores' inventories and sales data. The number of patients who came home with an ACT shot up from 1% to 44% in 4 months, and patients paid the same average price or even less for ACTs than for older drugs. Nahlen calls the results “encouraging” but adds, “You can't extrapolate from two districts in Tanzania to the entire world.”

Many organizations, including the World Bank and even the Global Fund, were initially skeptical, says Laxminarayan, but they have come on board. In 2007, Roll Back Malaria, an international partnership of governments, organizations, and companies, threw its weight behind the idea, which is now called the Affordable Medicines Facility for malaria (AMFm). And in New Delhi on 7 November, the Global Fund's board approved a plan to host and manage AMFm, starting with a 2-year pilot project in 10 African countries and in Cambodia. (The United States, whose delegation was divided on the issue, ended up abstaining.)

So far, the U.K. government has pledged \$60 million of the projected \$350 million needed for the pilot. The board of UNITAID, an international fund that raises money from taxes on airline tickets, is expected to approve a large contribution on 25 November. (Both the Global Fund and UNITAID declined to comment for this story pending that decision.)

Arrow, 87, who knew next to nothing about malaria before 2004 but has become quite the expert, says he's “very happy” that his panel's idea is becoming reality. “I'm only disappointed that it took so long.”

—MARTIN ENSERINK

CREDITS: (DATA SOURCE) MEDICINES FOR MALARIA VENTURE AND MINISTRY OF HEALTH, UGANDA; (PHOTO) M. ENSERINK/SCIENCE





**Antisocial cues.** People are much more likely to litter a graffiti-adorned alley than one in which the walls are clean.

## CRIMINOLOGY

# Study Shows How Degraded Surroundings Can Degrade Behavior

If you're walking by a wall covered with graffiti, are you also more likely to litter? The Broken Window Theory, crystallized in a 1982 article in *The Atlantic* by political scientist James Q. Wilson and criminologist George L. Kelling, posits that the environment has a significant effect on whether people engage in antisocial behavior. But there's been little empirical research on just how "broken windows" lead to social disorder and crime—until now.

In a series of cleverly designed experiments reported in a paper published online by *Science* this week ([www.sciencemag.org/cgi/content/abstract/1161405](http://www.sciencemag.org/cgi/content/abstract/1161405)), researchers at the University of Groningen in the Netherlands found that if people see one norm or rule being violated (such as graffiti or a vehicle parked illegally), they're more likely to violate others—such as littering, or even stealing.

In one setup, for example, the experimenters attached useless fliers to the handles of bicycles parked in an alley that had a sign on the wall forbidding graffiti. There was no trash can in the alley. The experimenters covertly watched how many people tossed the fliers on the pavement or put them on another bike rather than pocketing them for disposal. On another day, they set up the same condition in the same place, except with graffiti on the wall.

The results were striking: When there was no graffiti, a third of 77 cyclists tossed the flier away. But more than two-thirds littered after the graffiti was applied. In another experiment involving a €5 note left sticking out of a mailbox, 13% of subjects pocketed it when the mailbox was in a clean environment, compared with 23% when there was trash around.

Auditory cues can also set the scene for disorder. Four out of five cyclists littered their fliers when they could hear illegal firecrackers being set off, whereas barely half did so when it was quiet.

Kelling commends the experiments as "very tidy." He says that most earlier studies "dealt with correlation rather than causality" but that there is growing evidence for the broken window effect. A Harvard University study, reported earlier this year, found that scrupulous "situational prevention" in troubled neighborhoods in Lowell, Massachusetts—in particular, added policing and cleanup—was more effective than social services or law enforcement in maintaining order.

The study demonstrates that disorder in the environment has a generalized effect, says social psychologist Robert Cialdini of Arizona State University, Tempe. That finding suggests government agencies can expect a big payoff from what he calls "relatively minor efforts, let's say, to keep the streets clean."

Cialdini says his research has found that people's pro-social behavior can be calibrated to quite a fine degree and is shaped not only by what they see but also by what they believe to be true. For example, many hotel bathrooms have signs advising visitors that reusing their towels is good for the environment. On any given day, he says, about 38% of guests will reuse their towels. But the percentage rises to one-half if guests are told that a majority of the hotel's guests reuse their towels. "And if we say, 'The majority of guests in this room' reuse towels, we get even more [participation]," says Cialdini.

—CONSTANCE HOLDEN

## Obama Transition: Agencies, Meet Microscope

President-elect Barack Obama's transition team has announced the officials who will review federal agencies for the new Administration. Prominent among the hundreds of names is that of Nobelist Mario Molina of the University of California, San Diego (UCSD), who along with former White House science and technology official Thomas Kalil will head the review of the White House Office of Science and Technology Policy. "You get someone like Mario who knows science and has some experience working with governments—that's a good choice," says Mark Thiemens, a colleague of Molina's at UCSD. Molina has served on the President's Council of Advisors on Science and Technology under Bill Clinton and runs an institute devoted to energy and the environment in Mexico City.

One reviewer for the U.S. Department of Health and Human Services, parent agency for the National Institutes of Health, is former NIH Director Harold Varmus, who headed Obama's scientific advisory group. That group shaped the candidate's stances on issues such as a proposed doubling of basic research over 10 years, lifting the limitations on stem cell research, and funding comprehensive sex education. Space lobbyist Lori Garver, who has helped author Obama's space policy, will review NASA along with former NASA policy chief Alan Ladwig and space advocate George Whitesides.

—ELI KINTISCH

## E Pluribus Unum

Hoping to broaden its reach, the Howard Hughes Medical Institute (HHMI) has launched a program to solve specific scientific challenges using collaborative teams. The \$10-million-a-year, 4-year pilot recognizes that "certain scientific problems couldn't be attacked by a single laboratory," says HHMI Vice President and Chief Scientific Officer Jack Dixon, in contrast to the charity's usual approach of funding "people, not projects." HHMI also wants to reach scientists who are not Hughes investigators, he says.

The eight "collaborative innovation awards" were chosen from 62 applications and are funded at roughly \$700,000 to \$1.4 million a year, Dixon says. One project links an HHMI biochemist with an ant researcher to study whether changes in gene activity that don't involve DNA mutations affect aging. In 2 years, HHMI's advisers will decide whether to expand the program.

—JOCELYN KAISER

## DEVELOPING WORLD

## The New Groove in Science Aid: South-South Initiatives

**MEXICO CITY**—When 42 elite scientists from the developing world founded their own academy 25 years ago, they aimed to help close the divide between the research capabilities of the northern and southern hemispheres. Today, that community, the 871-member Academy of Sciences for the Developing World (known as TWAS after its original name, the Third World Academy of Sciences), is also focused on another divide: the widening gap between the South's scientific haves and have-nots.

While research in about 80 struggling countries in Africa and elsewhere has lagged, it has advanced dramatically in several of the South's largest nations—led by China, India, and Brazil. That gap sparked a lively debate at TWAS's 25th anniversary meeting here about the academy's programs and the responsibilities of the top developing countries.

"The growth of science and technology in the developing world has been as uneven as it is impressive," says mathematician Jacob Palis, president of TWAS and the Brazilian Academy of Sciences. He wants TWAS to

expand its grants and fellowship programs and bolster initiatives to help young scientists.

Others contend that big science projects are also needed. Physicist Mambillikalathil G. K. Menon, a TWAS founder who advises India's Space Research Organization, is calling for projects funded by developing nations that might parallel Europe-wide ventures such as the European Space Agency and CERN. He also suggested that the South's prosperous countries should mentor far more scientists in Africa and other less-developed countries. "We should undertake some major scientific activities," Menon says.

One such regional effort seems likely to succeed, says Moneef R. Zou'bi, director general of the Islamic World Academy of Sciences: the Synchrotron-light for Experimental Science and Applications in the Middle East (SESAME). It brings together scientists from 10 Middle Eastern countries to conduct experiments at a relocated German synchrotron that will start operating next year in Jordan. Other researchers, arguing that big science is not yet

feasible in most of Africa, want to build better research networks to link scientists from poorer nations to strong labs in the emerging South economies.

C. N. R. Rao, a past TWAS president who led the Jawaharlal Nehru Center for Advanced Scientific Research in Bangalore, India, says small African nations need basic assistance to build their research capacity. It's the kind of support India received a quarter-century ago, Rao says, and is now giving back. India, China, and Brazil have joined with TWAS to run a South-South fellowship program for 250 Ph.D. students and postdocs.

Tieniu Tan, deputy secretary general of the Chinese Academy of Sciences (CAS) and director of China's National Laboratory of Pattern Recognition, says China is expanding fellowship programs and sharing technology and data in the developing world. "We feel obliged to do this because we are the largest developing country," he says.

African postdocs praise the Chinese fellowship program but say that returning to their home countries—with expertise but limited equipment and grant money—can be a shock. "It is great to train at a good institute, but the training and equipment I had in China was not matched when I returned home," says S. Idowu Ola, a Nigerian reproductive

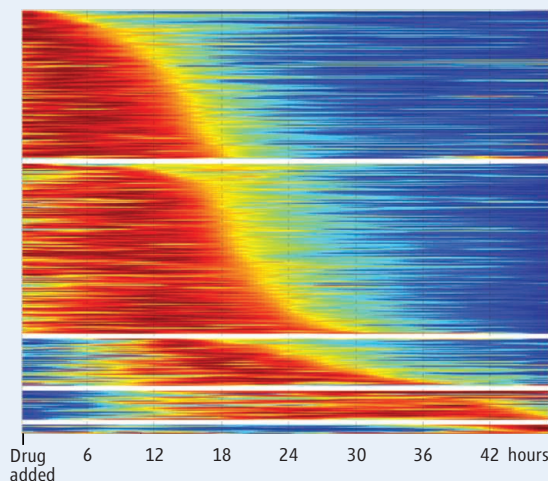
## SYSTEMS BIOLOGY

## Cast of 1000 Proteins Shines in Movies of Cancer Cells

Like the instruments of an orchestra, the thousands of proteins inside a living cell sometimes individually surge into prominence, blend in with each other, or fade to a whisper. Biologists have not had an effective way to eavesdrop on this full protein symphony—but now they're a step closer. Systems biologists led by Uri Alon of the Weizmann Institute of Science in Rehovot, Israel, describe online in *Science* this week ([www.sciencemag.org/cgi/content/abstract/1160165](http://www.sciencemag.org/cgi/content/abstract/1160165)) how fluorescent markers and a time-lapse microscope have allowed them an unprecedented view of the fluctuating locations and levels of about 1000 proteins in individual human cancer cells.

Leroy Hood, president and co-founder of the Institute for Systems Biology in Seattle, Washington, calls the new work "pioneering," pointing to the number of proteins Alon's group followed and how precisely their abundance and whereabouts were tracked. "I think it will be a milestone paper," he says. The new technique should help drug developers as

well as basic cell biologists, notes Alon. In their study, for example, his group fingered two proteins that may help explain why some lung tumors resist a well-known cancer drug.



**Protein symphony.** Each horizontal line shows the level of a specific protein (redder is higher, bluer is lower) as cells respond to a cancer drug.

Existing ways to monitor multiple proteins in a cell include gene expression arrays, which detect RNA from transcribed genes, and mass spectrometry, which measures protein levels.

But both methods entail crushing large numbers of cells, collecting the cytoplasmic juice, and analyzing it. Results reflect an average across many cells.

To develop a new way to gauge protein dynamics, Alon's group relied on fluorescent proteins plucked from jellyfish and other organisms that biologists commonly use these days to tag proteins in cells. Researchers typically fuse the gene for a fluorescent protein to the gene for a single protein of interest and add the construct back into a cell's DNA.

Instead of creating tagged proteins one by one, however, Alon's team took a more global approach. They infected lung cancer

CREDIT: A. COHEN ET AL., SCIENCE



**Lab boost.** Expansion of South-South scientific cooperation might help research at labs across Africa, like this one in Tunisia.



physiologist who was a postdoc at the CAS Institute of Zoology in Beijing. Eventually, with some help from TWAS and the International Foundation for Science, he set up an animal reproduction lab at Obafemi Awolowo University in Ile-Ife, Nigeria.

Both South Africa and Nigeria, two of the continent's strongest nations, now offer programs to train other African students and

young scientists. "We are fully committed to South-South cooperation in S&T," says South Africa's science minister, Mosibudi Mangena, noting that his country already hosts three "flagship centers" to train African students in advanced math, biosciences, and laser technology. "But political support is absolutely crucial for South-South cooperation."

—ROBERT KOENIG

cells with a retrovirus ferrying the DNA for a yellow fluorescent protein. In each cell, the retrovirus integrated its payload at a random place, often within one of the cell's 20,000 or so genes that encode a protein. Voilà: a cell with a fluorescently marked protein. The researchers ultimately isolated individual cells with 1020 different, randomly tagged proteins.

Then it was time to make movies. Working with an automated microscope that could record the fluorescence of 12 cell colonies at a time, each one with a different protein tagged, the researchers gave each group of cells a dose of the common cancer drug camptothecin and watched what happened over the next 48 hours. The drug kills cancer cells by gumming up an enzyme called topoisomerase-1 (TOP1) that the cells need to unwind DNA and copy it or transcribe it into the RNA instructions for making proteins.

Not surprisingly, in TOP1-tagged cells, levels of the enzyme dropped soon after the drug was introduced. In cells tagged for other proteins, sometimes a protein's level rose, but more often it fell after the drug treatment. Some tagged proteins faded from the cell's

nucleus and appeared in the cytoplasm or made another translocation that could further explain camptothecin's mechanism of action.

The big surprise was the fate of cells tagged with two particular proteins. After exposure to the cancer drug, these cell colonies each split into two sets of cells with differing characteristics. In one, the concentration of the tagged protein rose, and the cells survived. In the remaining cells of the colony, the protein's level slumped, and the cells later self-destructed. Understanding the role these two proteins play in cell survival could suggest a new strategy for overcoming a tumor's resistance to camptothecin, Hood says.

The technique developed by Alon's team could be "an amazing tool for working out drug mechanisms," says computational biologist Joseph Lehar of CombinatoRx, a company in Boston that tests pairs of known drugs to see if they work better than one alone.

Alon acknowledges that with 5000 to 10,000 proteins being produced by cells at any one time, his team is far from observing a complete picture of protein dynamics. Still, "1000 is pretty impressive," says Boston University systems biologist James Collins.

—JOCELYN KAISER

## INSERM in Flux?

The French government plans to adopt proposals for a major overhaul of the life sciences, presented last week by a panel led by the U.S. National Institutes of Health's former director Elias Zerhouni. The group recommends ending the current fragmentation of biomedical research by setting up a strong, unified agency to fund biomedical research.

In its review of the French National Institute for Health and Medical Research (INSERM), it takes aim at the entire life sciences effort. The report said that "striking" fragmentation has led to "unnecessary turf battles" and "inordinate amounts of time" being spent on paperwork. Recommendations include rewarding good researchers better and streamlining peer review. Unions are expected to object to deep reforms, but French Prime Minister François Fillon has asked research minister Valérie Pécresse to set up a panel to implement the recommendations.

—MARTIN ENSERINK

## Stretching Out LHC Repairs

Repairs to the Large Hadron Collider (LHC) at CERN near Geneva, Switzerland, could take longer than anticipated. LHC project director Lyn Evans told *Science* last week that the work, costing an estimated \$13 million or more, could extend beyond the previously announced target of May 2009. At least 20 of the facility's 10,000 superconducting magnets suffered electrical damage 9 days after the 27-kilometer collider was unveiled on 10 September. Repairs began 2 weeks ago.

—YUDHIJIT BHATTACHARJEE

## Gene Tests Under Scrutiny

Australia may soon get its own direct-to-consumer genetic testing business, but the company is heading into choppy waters. Lumigenix, based in Sydney, aims for a commercial launch early next year. But it could run afoul of the national Therapeutic Goods Administration (TGA), which a spokesperson says could ban the test kits with legislation being drafted now. CEO Romain Bonjean says Lumigenix is taking a cautious approach to wording on promotional material for the service: "We've been communicating at length [with TGA] to understand what we can and can't do." But Ron Trent, chair of the Human Genetics Advisory Committee of Australia's National Health and Medical Research Council, says "it's hard to make sense of some of these tests unless you're a statistician. ... When it comes to genes for serious medical conditions, direct-to-consumer testing shouldn't be allowed."

—ELIZABETH FINKEL

# World Oil Crunch Looming?

Even those who believe there's plenty of oil left in the ground to meet rising demand are warning that the final crisis could come uncomfortably soon

Breathing a sigh of relief as the price of gasoline plummets toward \$2 a gallon and maybe beyond? Thinking \$100-a-barrel oil was just a passing inconvenience? Think again.

The fall in oil prices will likely be short-lived, say those in the know. Although price spikes and drops may recur for years, says economist Fatih Birol, “we think the era of cheap oil is over.” He and colleagues at the Paris-based International Energy Agency (IEA) just released their *World Energy Outlook 2008*. IEA analysts see enough oil still in the ground to satisfy ever-rising demand for decades to come—assuming the price continues to rise. But they aren’t at all sure that the Middle Eastern government-owned oil companies sitting on most of the remaining oil will be pumping it fast enough a decade or two from now to meet the unbri- dled demands of the rest of world.

Already, countries outside oil-rich OPEC (the Organization of the Petroleum Exporting Countries) seem unable to increase production further, even with the enticement of high prices. IEA’s *World Energy Outlook* sees that plateau of non-OPEC oil production continuing, putting the burden on a reluctant OPEC to make up the shortfall, if it can.

“It’s getting harder and harder to find an optimist” on the outlook for

the world oil supply, says Beijing-based petroleum analyst Michael Rodgers of PFC Energy, a consulting company. Indeed, the IEA report as well as one coming from the U.S. Department of Energy’s Energy Information Administration (EIA, confusingly enough) see hints that the world’s oil production could plateau sometime about 2030 if the demand for oil continues to rise. Unless oil-consuming countries enact crash programs to slash demand, analysts say, 2030 could bring on a permanent global oil crunch that will make the recent squeeze look like a picnic.

## Stagnation close to home

It took 140 years for the world to consume its first trillion barrels of oil, notes oil infor-

mation analyst Richard Nehring of Nehring Associates in Colorado Springs, Colorado. Now, if long-running trends continue, the world will demand its next trillion barrels within just 30 years. Some oil analysts working from their best estimate of how much oil remains in the ground—dubbed “peakists”—see world production reaching its limits in the next few years or a decade and then declining.

Signs of strain may already be emerging. Outside OPEC, oil production has not risen since 2004, even as prices soared. IEA sees no recovery in this non-OPEC production from conventional oil fields. Moreover, it projects that the plateau in conventional oil will turn into a decrease beginning in the middle of the next decade, accelerating through to 2030. Only the growth of production from expensive unconventional sources, such as mining tarry sands in Canada, will keep total non-OPEC production from falling during the next 20 years, according to IEA.

“Non-OPEC conventional production is definitely at a peak or plateau,” says Rodgers. “That’s starting to make people nervous. It’s not what even pessimistic people anticipated.” Three years ago, analysts in and out of the industry predicted that

**Soon the norm?** Gas-sipping vehicles would be de rigueur if OPEC doesn’t come through with more oil.



CREDITS (TOP TO BOTTOM): CHARLIE REID/AP; IVAN ALVARADO/REUTERS



◀ **Don't stop.** Kansas will have to squeeze out more oil just to help keep non-OPEC production steady.

projects under way or planned would dramatically boost world production during the second half of the decade, sending prices back down (*Science*, 18 November 2005, p. 1106). Only in the 2010s would non-OPEC producers—who had boosted their output 35% in 25 years—falter and level off their production, analysts thought. That predicted plateau may be here already. “Despite all the work,” says Rodgers, “we can’t grow non-OPEC.”

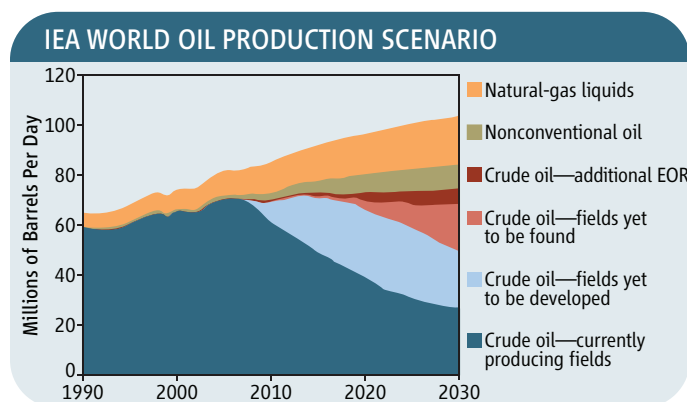
### That sinking feeling

A big part of any problem with slaking the world's thirst for oil, according to IEA's report ([www.iea.org/Textbase/npsum/WEO2008SUM.pdf](http://www.iea.org/Textbase/npsum/WEO2008SUM.pdf)), is the rapid decline of production from fields past their prime. Any new field produces increasing volumes of oil each year as more and more wells are drilled, but production eventually peaks and, in time, begins to decline. IEA studied 800 fields around the world that had already passed their peak production to see how fast they are declining—a rather rapid 6.7% decline per year, it turns out. And that rate could increase to 8.6% by 2030, IEA says, as the industry turns more and more from waning giant onshore fields to smaller fields and offshore fields, both of which decline faster after peaking.

The decline rate “is a major challenge in itself,” says Birol. “We have found that if we want to stand still—that is, continue producing 85 million barrels per day—for the next 22 years, we need new production of 45 million barrels per day to compensate for the decline. That means four Saudi Arabias.” Add on a demand increase of the sort seen the past couple of decades—equivalent to another two Saudi Arabias—and the world will have to work that much harder to meet rising demand, Birol says.

Even given the extra effort, IEA in its “reference scenario” of future world oil production (see figure) has the world production of conventional crude leveling off early in the next decade. Only a considerable increase in unconventional oil and natural-gas liquids—an oil-like byproduct of natural-gas extraction—keeps world production rising to 2030. With non-OPEC conventional production in this scenario leveling out and then falling, “this time [the effort] needs to come from the national oil companies,” says Birol.

Those are the government-owned companies with the biggest reserves of oil in the ground, principally the OPEC countries of the Middle East. “This aspect is more uncertain,” Birol adds. In the past, IEA and its U.S. equivalent, EIA, have assumed that OPEC could and would make up for any shortfall in non-OPEC production. But this year, IEA's *World Energy Outlook* warns that although there's enough oil in the ground to meet growing demand through 2030, there “remains a real risk” that oil companies—OPEC's in particular—will soon fail to invest enough in exploration and production efforts. That could precipitate a calamitous oil crunch as early as the middle of the next decade, the report says. “There can be no guarantee that [oil resources] will be exploited quickly enough” to meet expected demand, the report says.



**It'll work, if ...** In this scenario from IEA, the world's rising demand for fluid fuels will be met by growing unconventional oil and natural-gas liquids production, but only if OPEC expands its production of crude oil.

### Less encouraging still

In its first look ever beyond 2030, the U.S. EIA is finding even less support for a rosy oil scenario than IEA is. Its report is yet to be released, but EIA's Glen Sweetnam of the Washington, D.C., offices outlined preliminary results at an EIA conference in April ([www.eia.doe.gov/conf\\_pdfs/Monday/Sweetnam\\_eia.pdf](http://www.eia.doe.gov/conf_pdfs/Monday/Sweetnam_eia.pdf)). Moving beyond their usual approach of simply depending on OPEC to make up any shortfall, EIA analysts considered four factors that bear on how much oil of all sorts—conventional, natural gas liquids, and unconventional—gets produced: demand (high, intermediate, and low scenarios), how much oil was in the ground to start, what fraction of that oil will ever be extracted (some always remains no matter how great the effort), and OPEC's willingness and ability to respond to increasing demand.

Things look fine right through the rest of the century if, starting now, the whole world

severely curbs its appetite for oil, the EIA analysis suggests. In this low-demand scenario, the lingering demand for oil could be met even if the nondemand factors were unfavorable.

Still on the optimistic side, if demand were to continue rising as before and level off starting in 2030—say, in response to crash programs to increase efficiency and develop alternatives—demand could be met into the second half of the century even if a single factor were unfavorable, with one exception. If OPEC does not increase its production beyond its current 34 million barrels per day, world production will plateau within a few years, reminiscent of the potential crisis IEA sees in the middle of the next decade. Most ominously, EIA's high-demand scenario—higher demand to 2030, then business-as-usual increases in demand thereafter—“may be difficult to meet even with favorable supply assumptions,” said Sweetnam. Unbridled consumption does not seem to be an option.

### A hard place

The energy agencies “have done a good job of describing the fix we're in,” says energy analyst David Greene of Oak Ridge National Laboratory in Knoxville, Tennessee. “They're recognizing that the non-OPEC world won't be able to increase production much if at all. The IEA correctly points out the massive investment required” to meet any increase in demand. In fact, it's not clear to Greene or other analysts that OPEC has any inten-

tion of upping production to keep the price of oil relatively low, which would not be in its self-interest. Better to keep more oil in the ground, pinching supply, and sell that oil later at a higher price. And some OPEC countries, such as Iran and Iraq, may not be capable of making the required investment, even though they have the oil.

The United States can help itself, Greene notes, but it's going to be tough. Insulating the economy from the worst oil price effects “takes a long time, 10 to 15 years. You have to do just about everything you can think of,” from further improving the efficiency of cars and light trucks to bringing on biofuels to producing more oil in the United States. “You have to have a comprehensive structure and a measurable goal. We don't have that now. I just hope the Obama Administration doesn't look at the [current] price of oil and shove the problem to the back burner.”

—RICHARD A. KERR

**Please recycle.** ESA wants to make its one-shot automated transfer vehicle (ATV) into a reusable craft.

SPACE

## Cloudy Future for Europe's Space Plans

A string of successful missions had the European Space Agency riding high and making ambitious plans, but the worldwide financial downturn may bring it back to Earth

Doing science in space is, above all, expensive, so space researchers often find their careers hanging on the decisions of government ministers rather than grants committees. In Europe, the pinnacle of this nail-biting process happens roughly every 3 years when the European Space Agency (ESA) convenes a meeting of politicians from its member states to agree on budgets and approve new programs.

With the dark cloud of a global economic crisis overhead—Germany, for example, last week confirmed that it was in a recession—ministers will gather in The Hague, the Netherlands, next week for the latest such meeting. The air of uncertainty leading into this gathering contrasts starkly with the last, which was held in Berlin in 2005, when ESA got almost everything it asked for (*Science*, 16 December 2005, p. 1749). This time round, governments are tightening their belts, and the run-up to The Hague conference has seen wrangling over funding for even well-established ESA programs. “Earlier in the year, it looked like this meeting would be straightforward. Now it looks to be a very crucial and very tricky one,” says space scientist Mark Sims of the University of Leicester in the United Kingdom. “Economic times are difficult.”

In contrast to NASA, whose budget is set by the U.S. Congress every year, ESA works on a roughly 3-year cycle. This gives projects added stability, if approved, but it also means that a lot rides on each ministerial budget meeting. Getting 18 different governments, with differing priorities, to agree on something can be like herding cats. “Germany and Spain are the most ambitious at the moment and want bigger roles. Other countries are retrenching,” says Mike Healy, head of earth

observation, navigation, and science with the aerospace company EADS Astrium.

The wildcard in the pack is Italy, which contributed generously in 2005 but has since had a change of government and consequently a new chief for the Italian Space Agency, industrialist Enrico Saggese. Apparently following a shift in emphasis ordered by Italian Prime Minister Silvio Berlusconi, Saggese has so far emphasized national space projects, and it looks as though he will not have a lot of new money to put on the table in The Hague.

Italy's and other nations' reluctance to increase their contributions to ESA means that next week's negotiations will be tense. At risk will be some high-profile future missions, including ExoMars, an ambitious mission to the surface of the Red Planet, and Kopernikus, an effort to turn environmental monitoring into an operational service. “Ministerials sometimes bring surprises, both pleasant and unpleasant ones,” says Sims. “We all cross our fingers and hope our missions will survive.”

### Costly options

In recent years, ESA's stock has risen as the agency has completed a series of high-profile science missions, such as planet mappers Mars Express and Venus Express, the Huygens lander on Titan, the Rosetta comet chaser, and space telescopes Integral and XMM-Newton. All were funded through ESA's science program, one of the agency's mandatory programs to which each ESA member must contribute in line with its gross domestic product. Because all 18 member states have to agree to the program's total budget, large increases are rare. At the 2005 meeting, officials were pleased to get annual increases of 2.5%, just above inflation, after years of flat funding. “We've had a small growth in purchasing power,” says ESA Science Director David Southwood.

With inflation now above 4%, next week ESA will ask for 3.5% yearly increases in the science program's €396 million annual funding, which, if as expected the recession forces inflation down, should give some wiggle room. “The issue for me is how fast we can introduce the new missions selected earlier

this year for further study,” says Southwood. These include a mission to the outer planets, an x-ray observatory, and the first space-based gravitational-wave interferometer. Southwood is expecting a tough debate next week. “The battle is between the majority who are happy to go along with [the increase], and one or two who feel they can't afford it.”

Yet the fighting may be even fiercer over ESA's optional programs, to which member nations can contribute as much, or as little, as they like. In deep trouble is the



**Copy charges.** ESA members are happy to pay for environmental monitoring Sentinels, but not the backup craft.

CREDITS (TOP TO BOTTOM): NASA; ESA/P. CARRIL



ExoMars mission. Part of the Aurora program to send a series of probes to Mars and possibly the moon, followed by crewed missions, ExoMars was well-supported in 2005 and given a budget of €650 million. Since then, researchers have kept adding new capabilities, and ExoMars's costs have snowballed. In spring 2007, a program committee gave the ExoMars team approval to move ahead with an expanded mission, including an orbiter, a static base station, and a rover with a drill to get samples from below the surface. Cost estimates are now at about €1.2 billion, and managers figured that ministers, enthusiastic in 2005, would pony up again in The Hague.

They figured wrong. Italy, for one, will pay no more than the €250 million to €300 million it agreed to 3 years ago in Berlin (40% of the original project), Saggese told the International Astronautical Congress in September. Although other nations, including the United Kingdom, want to increase their contributions, these fall well short of the €1.2 billion needed. "We're not going to get that much, but we could reach €1 billion," says Southwood, who, in a shuffling of portfolios, took over the robotic parts of Aurora a few months ago. Healy says some states want to keep the budget at €800 million and scrap the rover, a decision that could cause the United Kingdom to pull out. "Potentially, it could all collapse," says Sims, "but the implications of not continuing with Aurora would be pretty severe for ESA and Europe."

ESA's current plan is to delay ExoMars's launch from 2013 to the next window in 2016 to get some breathing space to reconfigure the mission. Next week, ESA will ask member states to indicate their level of funding for ExoMars, and the mission's managers will spend the next year talking with potential partners, such as NASA and the Russian Space Agency, about sharing costs. Sims thinks that teaming up with the United States could work well. NASA is already planning a rover mission for 2016. Together, the two agencies could launch a series of Mars probes culminating in a joint sample-return mission the following decade. "It could be quite a good marriage of capabilities," he says.

Storm clouds are also gathering over Kopernikus (formerly GMES), the environmental monitoring program. Kopernikus is one of two large collaborations between ESA and the European Union (E.U.). It aims to provide operational data on Earth, the oceans, and the atmosphere for government

agencies, businesses, and other users. ESA's role is to provide the hardware: the ground infrastructure for processing data and delivering it to users, and a series of five spacecraft, dubbed Sentinels, each with different sensors. Sentinel-1, for example, provides all-weather radar imaging, whereas Sentinel-2 will produce multispectral images like the U.S. earth-monitoring satellite Landsat, and Sentinel-3 will monitor land and sea-surface conditions with a radar altimeter and temperature and color sensors.

ESA is looking for €850 million in funding from 2009 to 2018 to continue construction of the first four Sentinels, with launches beginning about 2011, and to make Kopernikus an operational system. But a spat has broken out over who pays for what. Each of the Sentinels will be followed by a duplicate, or b-unit, put in place to ensure continuity of data. "We need a certain budget from countries that paid for a-units to make b-units," says ESA earth observation chief Volker Liebig. But some countries

to the station. At the moment, each ATV is discarded after delivering its cargo, but ESA wants to give it a reentry capability to return material to Earth. Support for ISS varies among member states; the United Kingdom, for example, takes no part in human space flight. "This will be a challenging issue," says David Parker, head of space at the U.K.'s Science and Technology Facilities Council. "Some want funding to go up, some down."

There is also likely to be a new round of discussion about astronaut-carrying spacecraft. ESA has long struggled with this topic: A planned minishuttle called Hermes was canceled in 1993, and the 2005 Berlin meeting nixed a plan to develop a shuttle called Clipper with Russia. As a result, ESA astronauts must hitch a ride on the U.S. shuttle or Soyuz. Next week, ministers will consider another ESA-Russian proposal, this time for a capsule that looks similar to Orion, NASA's shuttle replacement. But EADS Astrium will also present a rival plan for a crewed vehicle based on an evolution of the ATV and lofted with Europe's Ariane V rocket. Decisions are unlikely at this meeting, but ministers may approve seed money.

### In with the new?

Several entirely new programs will also be put to the ministers in The Hague. One is a climate change initiative that will demand no new spacecraft but will involve recalibrating archival data so that they can be compared with newly acquired data from the latest satellites. That project, whose

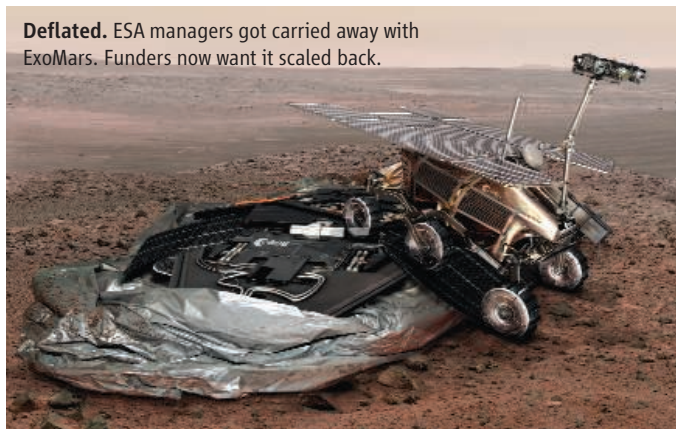
budget from 2009 to 2014 would be €170 million, will "build on what we have ... to create [a] long time series of essential climate variables," says Liebig. "It's not a trivial task to calculate these data sets," he adds.

Another plan calls for €50 million between 2009 and 2011 to investigate a space situational awareness system: a network of telescopes that will track all current and decommissioned satellites, space debris, and near-Earth objects and monitor space weather to give Europe warning of any threats to its satellites or ground infrastructure. At the moment, Europe must rely on warnings from other space agencies. ESA now feels it's time to take on that responsibility itself.

While researchers keep their fingers crossed, the negotiators will be trying to get the best possible roster of programs with the money available. Says Parker: "That's the genius of Europe: finding compromises."

—DANIEL CLERY

**Deflated.** ESA managers got carried away with ExoMars. Funders now want it scaled back.



don't want to pay up, arguing that the customer, i.e., the E.U., should pay for them. There are precedents: For each new generation of European weather satellites, ESA makes the prototype and EUMETSAT pays for the rest. "Most member states are concerned about the funding of b-units," says Healy.

As *Science* went to press before The Hague meeting, Liebig said that he was still "in full negotiation" with member states looking for a compromise. "I'm optimistic we won't be undersubscribed. [The environment] is still high on the [political] agenda," he says.

The extent of ESA's partnership with NASA on the International Space Station (ISS) is also up for discussion next week. ESA's Columbus laboratory module was delivered to ISS earlier this year (*Science*, 30 November 2007, p. 1374), and ESA wants more funding for microgravity research there and to upgrade the automated transfer vehicle (ATV) it has already built for delivering cargo

## MYCOLOGY

# Last Stand for the Body Snatcher Of the Himalayas?

The caterpillar-hijacking fungus *Cordyceps sinensis* is touted as a natural Viagra. But overharvesting has put the peculiar parasite's back against the wall

**KUNMING, CHINA**—Some people kill for it. Others risk their lives for it. To many, it's the creepiest thing they've ever seen. It is *Cordyceps sinensis*, a parasitic fungus that consumes its host, ghost moth caterpillars, from inside out as they hibernate in alpine meadows in the Himalayas and on the Tibetan Plateau. But one of nature's more curious creatures is in trouble: Surveys by the Chinese Academy of Sciences' Xishuangbanna Tropical Botanical Garden (XTBG) in Yunnan Province have discovered that the range of *C. sinensis* is shrinking fast. "It's disappearing before our eyes," says XTBG entomologist Yang Da-Rong.

The fungus is in this predicament because it's one of the hottest commodities around. There are nearly 400 known species of *Cordyceps*, mostly in Asia, including 68 in China, but *C. sinensis* is prized above all others as a treatment for everything from impotence to cancer. Also called *aweto* or *yarchagumba*, *C. sinensis* caught the fancy of Western herbalists in 1993, when Chinese track coach Ma Junren claimed that *Cordyceps*-based concoctions boosted the stamina of his record-setting runners. "What makes it fascinating is all the unproven hype," says Nigel Hywel-Jones, a mycologist at the National Center for Genetic Engineering and Biotechnology in Bangkok.

Hype or no, huge demand coupled with dwindling supplies—China's harvest was about 100 tons in each of the past 3 years, less than 10% of the hauls 20 years ago—pushed top-grade *C. sinensis* to \$60,000 per kilogram last year. (Prices have receded to under \$10,000 per

kilo.) Cultivation is a dream: *C. sinensis* grows poorly in the lab. "A few labs claim to have commercially available isolates for mass production," says Hywel-Jones. But he suspects that they are not *C. sinensis*.

Hywel-Jones got the urge to sample *C. sinensis* on his first survey in Bhutan in 2002. "I had heard it was a natural Viagra," he says. He took a bite—"It tastes fine, a bit nutty"—then joked to a male colleague, Tshitila, that he needed a woman. "There were none around, so I sprinted after a yak saying, 'That will do.'" But at 4300 meters above sea level, Hywel-Jones passed out from lack of oxygen. "When I came round, Tshitila was standing over me laughing and telling me that it doesn't work that quick."

Every year in late spring, villagers in search of "Himalayan Viagra" fan out across Tibet and surrounding swaths of southwestern China, Bhutan, India, and Nepal. Yang estimates that more than 1 million people forage for *C. sinensis* on the Tibetan Plateau alone. "Only the elderly and children stay home," says XTBG's Peng Yan-Qiong. Collectors crouch on hands and knees in search of "summer grass winter worm," brownish fruit bodies a few centimeters long that are hard to discern from alpine vegetation. In a couple of months, says Yang, a skilled collector can earn \$2000—more than most Chinese villagers earn in a year.

Tragedy comes with the turf. In July 2007, a gun battle between rival villages over access to prime *C. sinensis* habitat in Sichuan Province's Garze Tibetan Autonomous Prefecture left eight people dead, according to news reports. That followed an episode several weeks earlier, when collectors in Nepal were stranded in the mountains by a late-season blizzard. By the time the army arrived, dozens had perished.

Against this backdrop, a 23-person-strong

XTBG team set out to assess how the species is holding up. On Yang's first survey 25 years ago, he recalls, *C. sinensis* was so cheap that he could trade a bag of salt for a bag of the fungus. These days, locals see the scientists as competition: "Villagers don't like us to collect *aweto*," says Yang. But his team persisted, and in 47 excursions over the past two summers they documented what Yang calls a "shocking" decline: Prime habitat starts 500 meters higher than it did 20 years ago, translating to a 70% to 97% decline in *C. sinensis* biomass.

Meanwhile, the harvesting hordes are punishing the fragile land. "They destroy the soil and trample vegetation," Yang says. As a result, he says, each year some 3.5 square kilometers of grassland are "turned into desert." That, in turn, is degrading a vital watershed where many of China's major rivers originate, including the Yangtze and Yellow.

If *C. sinensis* dies out, it may take a few biological secrets to the grave. Its life cycle is a fungal version of the movie *Invasion of the Body Snatchers*. In late summer, the fruit bodies disperse spores, just as ghost moth larvae are shedding their skin. "That's when larvae are vulnerable," says Yang, who estimates that up to 12% of ghost moth larvae become infected. "But we don't understand the infection mechanism."

Infected larvae, which live in the soil, fall under the spell of the fungus, which steers the caterpillars to park vertically near the surface, head up. As *C. sinensis* consumes its victim, its fruit body slowly pushes up out of the head and by early spring emerges from the soil. Ghoulish as it sounds, Yang views the *Cordyceps*-moth relationship as "coevolutionary," in that the fungus may keep moth populations at sustainable levels.

To protect *C. sinensis*, Yang suggests a number of measures, including a law that would mandate a kind of crop rotation: harvesting the fungus from some areas while leaving others unmolested for a few years to give habitat time to recover. Yang's team is also taking a Johnny Appleseed approach, dispersing moth eggs in *C. sinensis* habitat.

If these remedies fail, *C. sinensis* may make its last stand high in the Himalayas, in areas even the most industrious or foolhardy of fungus hunters cannot reach.

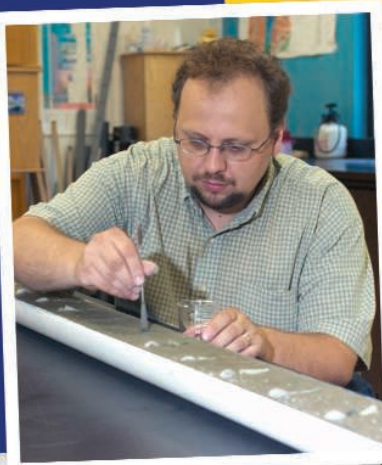
—RICHARD STONE

**Prize parasite.** Scientists searching for *C. sinensis* in Tibet.



CREDITS: COURTESY OF YANG DA-RONG





## SCIENCE IN ROMANIA

## Reaching for the Stars in Romania

A small association of Romanian scientists, many of them working abroad, is fed up with the slow pace of reforms in their country. And politicians are paying attention

**BUCHAREST**—As the sun was setting, scientists flocked to Victoria palace, a massive 1930s complex in Romania's capital and the headquarters of the country's prime minister. Among them were hundreds of Romanian scientists working abroad, flown in for the occasion. Sipping Romanian wine, the expats chatted with local researchers, hatching ideas for collaborations or, who knows, quietly pondering a return to their homeland.

Prime Minister Călin Popescu-Tăriceanu extolled the country's scientific talent. U.S. Ambassador Nicholas Taubman offered words of praise while encouraging further reforms in science and education. The message of the evening—part of a 3-day meeting on "The Romanian Scientific Diaspora"—was upbeat: Almost 20 years after the fall of communism, Romanian science was on the right path—its future as bright as the floodlights bathing the palace's façade.

But to some Romanian scientists—especially the younger generation and the majority who work abroad—the positive tone was a bit of a façade itself. Look behind it, they say, and you'll find a nepotistic old guard that controls research funding, an unfair peer-review process, abysmal starting salaries for young talent, and a lack of recognition for scientific excellence. "Despite all the rhetoric, there's little progress," says Liviu Giosan, a Romanian marine geologist at the Woods Hole Oceanographic Institution in Massachusetts.

The discontent has found a voice in Ad Astra, an association of Romanian scientists that Giosan co-founded in 2000. With fewer than 60 members so far—entry criteria are strict—Ad Astra seems almost laughably small. But thanks to its Web site that more than 800 registered nonmembers frequently visit, high-profile spokespeople, and a series of well-publicized policy studies it ran, Ad Astra is "one of the most successful nongovernmental organizations in Romania," boasts Daniel Funeriu, a chemist at the Technical University in Munich, Germany.

Other members, including Giosan, are more skeptical about Ad Astra's impact. But nobody denies that the group has captured politicians' attention. In 2006, when Romanian President Traian Băsescu assembled a panel to map out the future of science and education, four of its 12 members came from Ad Astra's ranks. "I don't always agree with Ad Astra, but I want to talk with them," Anton Anton, Romania's minister of education, research and youth, told *Science* recently. "They're a strong, clear, and independent voice."

### Out of Ceaușescu's shadow

Both Romania's particular brand of communism and the tumultuous transition to democracy have left their marks on the country's sci-

**Watchdogs.** Ad Astra, which is critically following Romanian science policy, was founded by Liviu Giosan (left) and Răzvan Florian.

ence. Nicolae Ceaușescu, who ruled the country for 24 years until 1989, had a keen interest in certain scientific fields, such as nuclear physics and chemistry, that could help achieve his dreams of national self-reliance. But he neglected biology, except for a few prestige projects (see sidebar, p. 1184), and banned psychology, a field he deemed unnecessary in a socialist paradise. Research funding was generally tight, especially during the 1980s, when Ceaușescu's decision to pay off the national debt plunged the country into poverty.

Because Ceaușescu had kept a particularly tight lid on emigration, the brain drain seen in many Eastern European countries after the fall of the Iron Curtain in 1989 became a hemorrhage in Romania. "Everybody wanted to leave, and now they finally could," says cell biologist Nicanor Moldovan, who left to do a postdoc in the United States in 1995. "It was like an elastic band that suddenly snapped." The exodus robbed the country of a generation of its top scientific talent. The official number of scientists in Romania is about 30,000, but the country now has an estimated 16,000 researchers abroad.

Giosan decided he had to leave in 1990, when, as a student and a senate member of the University of Bucharest, he took part in political demonstrations that were brutally repressed by miners, called in by then-president Ion Iliescu. He got out 3 years later and started his graduate studies at the State University of New York, Stony Brook. But in 2000,

*"Despite all the rhetoric, there's little progress."*

—LIVIU GIOSAN, WHOI

after attending a science policy meeting in Bucharest, he realized he hadn't turned his back on the country for good. The conference, organized by other young scientists from the diaspora, was supported by his former teacher, mineralogist Emil Constantinescu, who had been elected the country's president in 1996.

Soon after the meeting, Giosan met Răzvan Florian, a computational neuroscientist from the northern city of Cluj-Napoca who had worked at the Pierre and Marie Curie University (Paris VI) in Paris and the Xerox Palo Alto Research Center in California. Florian, a computer whiz, helped Giosan put together an "online community" where Romanian scientists could debate policy, post documents, and share experiences. Its name was derived from Seneca's quote, "*Per aspera ad astra*," or "Through hardship to the stars." "That's how I envisioned the battle ahead," Giosan says.



**Family affair.** Maya Simionescu, with husband, Nicolae, and Nobelist George Palade (center) in the 1970s—and today, with a bust of her husband at the institute they founded.

facility run by Nicolae and Maya Simionescu, a scientist couple that had previously worked at top labs in the United States.

Then came the Christmas revolution of 1989. Ceaușescu didn't survive; ICBP did. Today, its top floors offer an excellent view of the dictator's Hollywood-esque creation.



## At Home in Bucharest, for Better and for Worse

In the late 1980s, one of the darkest periods in Romania's history, the future of one of the country's flagship research centers hung by a thread. In downtown Bucharest, communist dictator Nicolae Ceaușescu was erecting his "House of the People," a gigantic government building for which a large part of the historic city had been flattened. To expand a park surrounding the building, Ceaușescu had also set his sights on demolishing the Institute of Cellular Biology and Pathology (ICBP), a modern research

her as stifling reforms in Romanian science.

During a recent meeting at her institute, Simionescu took some time out in her giant office to discuss her scientific adventure, which spans almost half a century. She and her husband—she was his student in Bucharest first—spent the 1970s working at Rockefeller University in New York City and at Yale University with Romanian Nobel laureate George Palade, who died last month at age 95. "We loved life in the U.S., and the working con-

The story could be emblematic for Maya Simionescu, who colleagues say is a survivor herself. She replaced her husband as ICBP director when he died in 1995, and today, at 71, she is a heroine and an icon of Romanian science, says Marilena Lupu, who took a job at the institute in 2007 after completing a post-doc in the United States. The lab has remained one of a few "islands of excellence" in a sea of rather mediocre research, says cell biologist Octavian Voiculescu of University College London. But not everyone is a fan; Simionescu's tough leadership style has driven some lab members away, and some see

In 2002, the duo set up an association by the same name. To be voted in, aspiring members must have a Ph.D. or be Ph.D. students, have at least one paper in an international journal, and offer a statement about what they hope to bring to Ad Astra.

### More money

Financially, the position of Romanian science has greatly improved since Ad Astra's birth—but the group had little to do with that. To meet the conditions for membership in the European Union (E.U.), Romania hiked public spending on research from a paltry 0.2% of its gross domestic product (GDP) in 2004 to 0.6% this year. The figure is slated to grow to 1% in 2010. The country's GDP itself has been growing fast as well since 2001, and E.U. membership has brought access to so-called structural funds, some of which are used for science. In a few short years, many scientists say, money stopped being the problem.

But many other concerns remain. Compared with countries such as the Czech Republic and Hungary, Romania hasn't been nearly as successful in reforming its science system, says Giosan. Due to the massive brain drain, power has remained in the hands of communist-era scientists whose productivity is low.

Many publish only in the hundreds of Romanian journals, whose circulation is often limited and whose main goal seems to be puffing up authors' resumé, Florian says. According to an Ad Astra analysis, only about one in three scientists in Romania has ever published in an international journal.

Persuading young scientists to stay and replace the old guard is tough. Although veteran scientists now earn salaries comparable to those in Western Europe, starting Ph.D. students can get paid as little as €300 per month. That makes recruitment very difficult, says Ștefana Petrescu, who heads the Institute for Biochemistry in Bucharest. Romania has also been faring poorly in E.U. competitions. For instance, it didn't win a single one of the prestigious new grants—300 for beginning researchers and 275 for more established scientists—awarded in 2007 and 2008 by the European Research Council.

Ad Astra's biggest complaint is that the way Romania distributes its growing science budget—through grants disbursed by the National Authority for Scientific Research (ANCS) and its subagencies—is flawed. Many reviewers have no knowledge of the topics they're supposed to judge, says Florian, who says the government should enlist foreign

experts. "You may propose a project in quark-gluon plasmas, but the reviewer may know little about nuclear physics and write that plasma problems were solved 20 years ago," says Nicolae Zamfir, who returned from the United States in 2005 to become director general of Romania's National Institute of Physics and Nuclear Engineering.

Ad Astra has fought back by lobbying and debating online—and by studying and documenting the problems. Florian became a part-time scientometrist who meticulously keeps score of the country's achievements. In 2006, he published a "white book" showing that entire national institutes in Romania produce little more than some small research groups abroad. Ad Astra's national university ranking, modeled on the global index published by Shanghai Jiao Tong University in China, shook up the academic pecking order and revealed that many universities are scientific lightweights.

### A little patience

To many young Romanian scientists, the wave of activism was a breath of fresh air—even an inspiration. Veterinary scientist Marilena Lupu says she wanted to come back to Romania after working in the United States for 3



ditions were great," Simionescu recalls after lighting a long, thin cigarette and ordering coffee. "But we always felt we could make a bigger contribution here." So they persuaded the Romanian government to build a brand-new lab for them. ICBP opened in 1979.

Just how well-connected the Simionescus were at the time is under dispute. Some assert that Ceaușescu was personally interested in repatriating the high-profile couple, and Nicanor Moldovan, who worked at the lab for 13 years and is now at Ohio State University, Columbus, says they seemed to have "some form of access to the higher political hierarchy," up to Ceaușescu and his chemist wife, Elena. But Simionescu says she and her husband remained "apolitical" and insists that a reception at the Romanian embassy in Washington, D.C., in the early 1970s was the only time she met Ceaușescu. Other officials, such as the health minister, championed their cause, she says, as did Palade.

Whatever the backstory, it didn't take the Simionescus long to create "a unique place in Eastern Europe," Moldovan says. Focusing on the cardiovascular system—in particular the cell biology and biochemistry of the vascular endothelium—they introduced to Romania new techniques, such as electron microscopy, and new habits, such as working long hours and publishing in international journals; they obtained Fulbright scholarships and visas to send young scientists to the West and flew in Palade and other top scientists to discuss research in Bucharest. "Working with the Simionescus was a passport to the best labs and scientists in the world," Moldovan says.

In the 1980s, however, Ceaușescu's economic policies plunged the country into hardship. Funding for the lab dried up, the government ordered the lights out after 5 p.m. to save electricity, and there was often no heating during the winter. It also became increasingly difficult to get visas to go abroad, says Simionescu. Grants from the U.S. National Institutes of Health—a rare honor for a foreign institute—kept the lab afloat.

The 1989 revolution ended the immediate threat to ICBP, but it also

triggered the departure of more than a third of the staff, many of them looking for a better life outside Romania. Lingering tensions over the Simionescus' controlling management style may have hastened the exodus, some researchers say. The duo had little patience for dissent and created a personality cult, says one former ICBP scientist who asked not to be identified because he worries it might hurt his career. "People wrote songs and poetry about the Simionescus," the researcher says. Moldovan confirms that the lab was run "like an autocracy"—although to him, it felt more like a family at the time.

For Maya Simionescu, the post-revolution defection was a blow. "I had trained so many of those people, taught them everything—they were like my children," she says. The revolution did offer new opportunities, however, such as a chance to hire fresh, young people with new skills—computers had just begun to alter how biology research was done—engage in collaborations with foreign labs, and receive E.U. funds.

After her husband didn't wake up one Monday morning in 1995—a heart attack—she named the institute after him and took on the directorship. "I wasn't sure I could do it. We had always done everything together," she says. Opinions on her tenure since then are divided. Moldovan says he "has nothing but the greatest admiration." But Mircea Mică, a former science minister, says Simionescu has become a conservative force herself, for instance, by blocking his attempts to reform the Romanian Academy of Sciences, of which she was the vice president for 8 years.

Simionescu has no plans to leave. She recently received some €14 million in E.U. "structural funds" to renovate ICBP's aging building and buy new equipment. She is moving into stem cells. "Maybe in a couple of years," she says, "I will find a new director, and I will become honorary director, if that is helpful." Then she pulls a rose from a nearby vase, lays it gently on the pedestal of a large bronze bust of her husband, and walks back to her meeting.

—M.E.

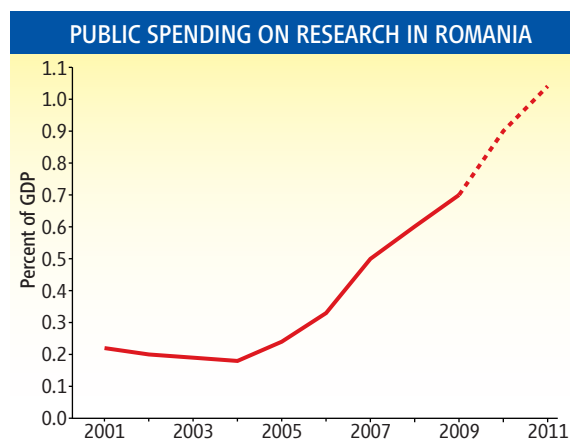
years but was worried about the scientific climate; she took the plunge after discovering that she wasn't the only one who wanted to improve the research system.

But not many have followed her—perhaps a sign of how much improvement is still needed. So far, about 30 expat researchers have taken advantage of national and European "reintegration grants." Still, the government is listening to Ad Astra and other critics, says Anton, the science and education minister, who took that job last month after 4 years as the president of ANCS. "I want the young people to be happy," Anton says.

Acknowledging problems in the grant-review system, Anton says that the government has already raised the bar for reviewers. He would like to hire foreign reviewers as well, but that has proven impossible, he says; expat researchers don't have time, and the number of proposals is vast. Anton urges a little more patience with the older generation of scientists, however. They were educated when publishing in Western journals was discouraged, and now

they're told that only international papers count—"that's a pretty big change," he says.

Some Ad Astra members say they can see the group's work beginning to pay off. The presidential advisory committee, chaired by



**Booming budget.** Romanian science spending has risen fast and the increases are projected to continue, but the way grants are distributed has come under fire.

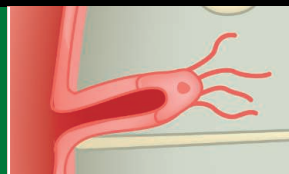
psychologist and former education and science minister Mircea Mică—another Ad Astra member—has raised awareness of the problems, says Technical University's Funeriu. All nine major parties participating in the 30

November parliamentary elections have committed to new investment and reforms in science and education. Other scientists say that the government has been serious about reforms, and Petrescu credits Anton for "being very open and reform-minded."

Ad Astra's founders are perhaps least impressed about what the group has achieved. Florian agrees that widespread media attention to his studies has made the public familiar with the problems, and science administrators are more prone to use reform-minded language. But he doesn't see much real change at universities and labs. He has been successful himself, however. Together with a colleague, he set up a small institute for cognitive and neural science in Cluj-Napoca, which managed to bag a research grant. (Sometimes the system does work, he concedes.)

Giosan returns to his homeland annually to study the Danube delta, a key area for environmental research. "The country is still very close to my heart," he says—but he's been unable to get Romanian funding, and he can't envision himself moving back anytime soon. Despite Ad Astra's best efforts, Giosan still sees primarily hardship for Romanian science—and few stars in sight.

—MARTIN ENSERINK



## LETTERS

edited by Jennifer Sills

### Looking Beyond Head Trauma

RECENT SCIENTIFIC INTEREST HAS FOCUSED ON THE STUDY OF TRAUMATIC ENCEPHALOPATHY ("The battered brain," *Random Samples*, 3 October, p. 23). However, the current hypothesis that the neuropathological findings are the direct result of the cumulative effects of head trauma warrants further investigation.



Although plausible biological mechanisms exist to support the causal relationship

between repeated head injuries and chronic traumatic encephalopathy (CTE), researchers should also strongly consider the influence of confounding variables and effect modifiers beyond trauma. These include the long-term biological effects of potential concomitant exposures associated with athletes at risk: frequent attempts at cutting weight, radical dietary regimens, and exposure to and abuse of performance-enhancing drugs (i.e., anabolic steroids) and illicit substances, as well as over-the-counter and prescription medication mega-dosing. Without accurate clinical historical data involving exposures, the accuracy of any conclusions made from the pathological study of these athletes may be extremely limited in yielding useful data.

Continued clinical surveillance, noninvasive in vivo brain imaging, and basic science inquiries are needed to further comprehend the underlying biology of the relationship between head trauma and CTE. These data, along with the acquired pathological tissues, will help to clarify pathological mechanisms and improve preventive recommendations to deter injury.

**DARIN T. OKUDA**

Department of Neurology, Multiple Sclerosis Center, University of California, San Francisco, San Francisco, CA 94117, USA.  
E-mail: [darin.okuda@ucsf.edu](mailto:darin.okuda@ucsf.edu)

### Fostering a Culture of Responsible Lab Conduct

THERE IS MUCH DEBATE AND RESEARCH devoted to determining the best practice for teaching responsible conduct of research (RCR) to trainees as federally required (1, 2). The majority of institutional programs require trainees (i.e., graduate students and postdoctoral fellows) to attend instruction isolated from the laboratory. However, laboratory behavior is our field's "hidden curriculum," and the principal

investigator and senior laboratory staff represent the professional role models that trainees see on a daily basis, whether good or bad (3).

At Wake Forest, over the past 3 years, we have implemented a program of 15-minute discussions that takes place after our weekly journal club. This amounts to about 11 to 12 hours of training per year. Each laboratory member takes a turn selecting a topic, many of which are also being discussed among scientists, policy-makers, and taxpayers. All laboratory personnel attend, and discussions include a variety of viewpoints as well as

discourse on the policies for best practices within the laboratory.

We believe that by moving the ethical discussion into the laboratory environment and empowering individual scientists at all seniority levels to actively participate in expanding their own awareness of RCR issues facing research and science policy, we can change the culture of the laboratory itself for the better.

**ANN M. PEIFFER,\* PAUL J. LAURIENTI,  
CHRISTINA E. HUGENSCHMIDT**

Department of Radiology, Wake Forest University School of Medicine, Winston-Salem, NC 27157, USA.

\*To whom correspondence should be addressed. E-mail: [apeiffer@wfbmc.edu](mailto:apeiffer@wfbmc.edu)

#### References

1. M. S. Anderson *et al.*, *Acad. Med.* **82**, 853 (2007).
2. E. Heitman, C. H. Olsen, L. Anestidou, R. E. Bulger, *Acad. Med.* **82**, 838 (2007).
3. K. Fryer-Edwards, *Am. J. Bioeth.* **2**, 58 (2002).

### The Path Forward for DNA Data

THE POSSIBILITY THAT INDIVIDUALS MAY BE identifiable in pools of DNA data appears to have come as a surprise to researchers and funding bodies (News of the Week, "Whole-genome data not anonymous, challenging assumptions," J. Couzin, 5 September, p. 1278) (1). But these concerns could have been foreseen by those directing open-access policies, especially given the rapid and unpredictable pace of technological change in genomics research. Such foresight might have obviated the need to precipitously remove genomic data from public access. This development indicates that the full ethical, social, and legal implications of open-access policies require more consideration, with appropriate attention to possible developments in technological capabilities.

What has worked well here is the vigilance of the researchers involved who had the foresight to contact the NIH early on about their concerns. Such ethical troubleshooting frequently occurs as scientists on the ground become alert to new possibilities, and in this situation funders have responded in a timely way.

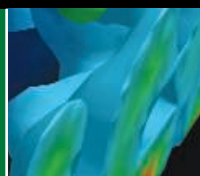
CREDIT: JUPITER IMAGES





Assessing the  
condition of paper

1196



Weighty calculations

1198

Some scientists have remarked that dangers have been exaggerated and withdrawal of data may be premature (2). But sequence data will still be accessible online, provided an application to the relevant body is made. The 1-month lag time predicted by Wellcome and the NIH is not long and could be concurrent with other approvals. Moreover, even a few months is not an excessive delay, if it protects the privacy of an individual, given that a privacy breach could have important ramifications.

This matters for science, too. But it is not just scientists' concerns that should be addressed; it is potential concerns of individuals participating in research projects and the maintenance of public trust. If it really transpires that fears are exaggerated, then open access could be resumed.

**PAULA BODDINGTON,\* NAOMI HAWKINS, CATHERINE HEENEY, JANTINA DE VRIES, JANE KAYE**

The Ethox Centre, Oxford University, Badenoch Building, Old Road Campus, Headington, Oxford OX3 7LF, UK.

\*To whom correspondence should be addressed. E-mail: paula.boddington@ethox.ox.ac.uk

#### References

1. N. Homer *et al.*, *PLoS Genet.* **4**, e1000167 (2008).
2. N. Gilbert, *Nat. News*, 10.1038/news.2008.1083 (2008).

## Priorities Come with the Career

N. R. AUGUSTINE'S EDITORIAL ("SCIENCE," 19 September, p. 1605) vainly tried to compare physicians and lawyers with scientists and engineers.

Physicians and lawyers are economic professionals; they can independently earn a living—i.e., they can choose self-employment to avoid dependence on grants or other employers. Most scientists and engineers are vocational professionals—they cannot independently earn a living outside of the system. This dichotomy results in different priorities. Because they are motivated to protect their jobs and avoid competition, scientists and engineers are less likely to spend political effort on research infrastructure or to strongly support education expansion.

**CRAIG BOLON**

Electronic Health Records Corporation, 275 Grove Street, South, Newton, MA 02466, USA. E-mail: cbolon@ehrcorp.net

## STEM Education Crisis: Overblown?

IN HIS EDITORIAL "SCIENCE" (19 SEPTEMBER, p. 1605), N. R. Augustine claimed that there is a crisis in science and technology education in the United States. However, there is evidence that the crisis is overblown.

In May, *Science* reported that one of the crucial statistics in *The Gathering Storm*, the report Augustine cited, was incorrect (1). The report claimed that "there were almost twice as many U.S. physics bachelor's degrees awarded in 1956 [pre-Sputnik] than in 2004." In fact, according to the *Science* story, "U.S. colleges and universities awarded 72% more undergraduate physics degrees in 2004 than in 1956—4965 versus 2883."

Recently, *Inside Higher Ed* (2) quoted Michael S. Teitelbaum, a demographer at the Alfred P. Sloan Foundation, who said that concerns about science education seem to surface every 10 years but that the shortfalls have so far failed to materialize.

I have a few suggestions for esteemed business leaders like Augustine: Stop outsourcing jobs overseas. Pay engineers and scientists more, hire those who might not perfectly match every job requirement, and invest in training and educating new hires.

**ANDREW DEPRISTO**

Wayland, MA 01778, USA. E-mail: adepristo@yahoo.com

#### References

1. Y. Bhattacharjee, Ed., *Science* **320**, 857 (2008).
2. A. Guess, "Challenging conventional wisdom on STEM supply," *Inside Higher Ed* (17 September 2008); [www.insidehighered.com/news/2008/09/17/pcast](http://www.insidehighered.com/news/2008/09/17/pcast).

## Letters to the Editor

Letters (~300 words) discuss material published in *Science* in the previous 3 months or issues of general interest. They can be submitted through the Web ([www.submit2science.org](http://www.submit2science.org)) or by regular mail (1200 New York Ave., NW, Washington, DC 20005, USA). Letters are not acknowledged upon receipt, nor are authors generally consulted before publication. Whether published in full or in part, letters are subject to editing for clarity and space.

## Changes to NIH Grant System May Backfire

ALTHOUGH WE APPRECIATE THE MANY CHALLENGES facing the current NIH grant system and applaud attempts at reform, we believe that several of the changes planned (*News of the Week*, "Changes in peer review target young scientists, heavyweights," J. Kaiser, 13 June, p. 1404) will cause more harm than good.

The proposal to change the length of the R01 application from 25 to 12 pages, with a directive to emphasize potential impacts of the research rather than methodology, will have detrimental consequences for research. This extremely short application length will make it very difficult for reviewers to evaluate the qualifications of the investigator, the technical approach proposed, and the preliminary work that supports the proposed approach. It will be particularly difficult to evaluate team science, large high-throughput projects, and large interdisciplinary projects, including genomics projects, research resources, clinical trials, and bioinformatics databases that accelerate the work of entire scientific communities. Multidisciplinary projects will also suffer because of the inability to explain concepts from multiple disciplines to reviewers. Grant funding will hinge on the applicant's ability to make flashy promises rather than to demonstrate technical excellence. We recommend a length limit of 20 pages, which would decrease the burdens of preparation and review, and represent a much smaller likelihood of hurting science. Another possibility would be to make application length proportional to budget requested.

Forcing reviewer service for scientists who are principal investigators of three or more grants is also an issue. Three panels per year for 4 years (or even 6 years, as proposed), with a huge number of reviews on each panel, is too heavy a load. We propose requiring all investigators to serve on review panels if needed. This way, each investigator would review three times the number of grant proposals they submit (based on three reviews per submitted proposal), and would serve on no more than two panels per year.

Another proposal that could have negative effects is the requirement that any investigator whose yearly funding would exceed \$1 million provide reason for additional funds. It should be up to the review panel to decide whether an investigator can deliver great science given the technical merits of their application, their past track

record, and the other demands on their time.

This area is far too complex to be resolved by legislating a single cap or major barrier on funding, or by declaring that everyone must be equal. Considerations must be made for different investigator abilities and variability among scientific fields. Budgets should be defined by project needs, risk level, and potential payoffs, not by political limitations.

PETER D. KARP,<sup>1\*</sup> GAVIN SHERLOCK,<sup>2</sup>  
JOHN A. GERLT,<sup>3</sup> IDA SIM,<sup>4</sup> IAN PAULSEN,<sup>5</sup>  
PATRICIA C. BABBITT,<sup>6</sup> KEITH LADEROUTE,<sup>1</sup>  
LAWRENCE HUNTER,<sup>7</sup> PAUL STERNBERG,<sup>8</sup>  
JOHN WOOLEY,<sup>9</sup> PHILIP E. BOURNE<sup>10</sup>

<sup>1</sup>AI Center, SRI International, Menlo Park, CA 94025, USA.

<sup>2</sup>Department of Genetics, Stanford University, Stanford, CA

94305, USA. <sup>3</sup>Department of Biochemistry, University of

Illinois, Urbana-Champaign, Urbana, IL 61801, USA.

<sup>4</sup>Department of Medicine, University of California, San

Francisco, CA 94143, USA. <sup>5</sup>Department of Chemistry and

Biomolecular Sciences, Macquarie University, Sydney, NSW

2109, Australia. <sup>6</sup>Department of Biopharmaceutical

Sciences, University of California, San Francisco, CA

94134, USA. <sup>7</sup>Center for Computational Pharmacology,

University of Colorado, Denver, CO 80262, USA. <sup>8</sup>Division

of Biology, California Institute of Technology, Pasadena, CA

91125, USA. <sup>9</sup>Associate Vice Chancellor for Research,

University of California, San Diego, La Jolla, CA 92093,

USA. <sup>10</sup>Skaggs School of Pharmacy and Pharmaceutical

Sciences, University of California, San Diego, La Jolla, CA

92093-0743, USA.

\*To whom correspondence should be addressed. E-mail:  
pkarp@ai.sri.com

## Listening to the Ocean's Heartbeat

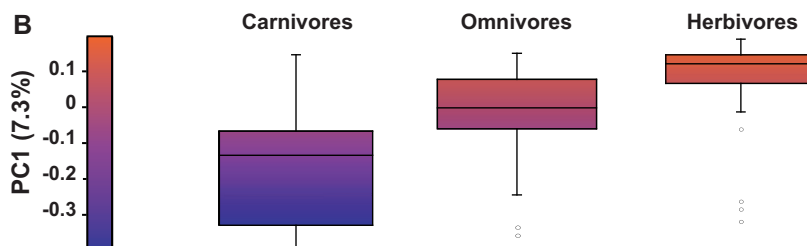
IT IS WITH GREAT INTEREST THAT WE READ the Policy Forum by R. J. Scholes *et al.* ("Toward a global biodiversity observing system," 22 August, p. 1044). Certainly a global network is required to observe and help understand changes in biodiversity. Scholes *et al.* suggest "[t]here is no general shortage of biodiversity data." While this may be true for terrestrial systems, it is not the case for many marine ecosystems, as we noted in our 6 June Policy Forum (1).

We need a multinational observing network for marine organisms. Fortunately, the basis for such an observing system already exists in the Global Ocean Observing System (GOOS), endorsed by the Intergovernmental Oceanographic Commission (IOC) in 1991, but it is focused on physical and chemical monitoring. GOOS is now moving toward biological observations with the initiation of the Ocean Tracking Network, but a comprehensive biological observing system does not yet exist. Only now has technology progressed to the point where we can conceive of a global biological observing system, equal to and comple-

## CORRECTIONS AND CLARIFICATIONS

**News Focus:** "You say you want a revolution" by H. Xin (31 October, p. 664). The article stated that China's premier Zhao Ziyang in 1985 told scientists to "go up hills and pick peaches." While the saying appeared in a speech by Zhao, he attributed the phrase to then-General Secretary of the Chinese Communist Party Central Committee Hu Yaobang.

**Reports:** "Evolution of mammals and their gut microbes" by R. E. Ley *et al.* (20 June, p. 1647). A corrected Fig. 3B is provided here. The caption should read, "Box plots (box and whisker) display the following: median (horizontal line dissecting box), upper and lower quartiles (top and bottom box edges), highest and lowest data values that fall within 1.5 times the interquartile distance from the box edges (lines extending to "whiskers"), and data outliers outside of this range (circles)." The line representing the median in the herbivore box was missing from the original.



menting the existing physical-chemical observing system. Such a vision will ensure that we not only feel the physical pulse of the global ocean, but listen to its biological heartbeat.

ELVIRA S. POLOCZANSKA<sup>1\*</sup>  
AND ANTHONY J. RICHARDSON<sup>1,2</sup>

<sup>1</sup>Climate Adaptation Flagship, Commonwealth Scientific and Industrial Research Organisation (CSIRO), Marine and Atmospheric Research, GPO Box 1538, Hobart, TAS 7001, Australia. <sup>2</sup>Department of Mathematics, University of Queensland, St Lucia, QLD 4072, Australia.

\*To whom correspondence should be addressed. E-mail:  
elvira.poloczanska@csiro.au

### Reference

1. A. J. Richardson, E. S. Poloczanska, *Science* **320**, 1294 (2008).

## Legislation Leaves Common Sense Behind

"WE DEMONSTRATE THAT NEARLY ALL elementary schools in California will fail to meet the [Adequate Yearly Progress] requirements for proficiency by 2014." So say M. J. Bryant *et al.* in their 26 September Education Forum ("School performance will fail to meet legislated benchmarks," p. 1781). This is also true for the other states. For example, a 2005 study (1) of the five Great Lakes states says that "nearly every school in the Great Lakes states is threatened to fail the Adequate Yearly Progress (AYP) requirements." Why does failure seem inevitable?

The main reason is the lofty goal of the No Child Left Behind (NCLB) Act: "All children will be proficient in communication arts and mathematics by 2014." The act

further states that this includes the subgroups of White, Black, Hispanic, American Indian, Asian and Pacific Islanders, Free/Reduced Lunch, Limited English Proficiency, and Special Education. The goal ignores everything that psychologists and educators know about individual differences in learning abilities. These abilities fall on a bell curve, and you cannot repeal this fact of nature by legislation.

Furthermore, after thousands of experimental programs aimed at raising all children to some level of achievement, no one has done it. The Bush Administration spent \$6 billion on the Reading First program (2), a model to show schools how to improve reading skills. Yet according to a recently released evaluation by the Department of Education (3), the children in the program read no better than those who were not in it. We simply do not know how to make all children proficient in reading and math. Some programs bring modest gains, but no more. We have not found the secret of Garrison Keillor's mythical town of Lake Wobegon, where all of the children are above average.

HAROLD SCARBRO

Scarbro Educational Consulting, Inc., 5057 Cedar Lawn Way, Las Vegas, NV 89130, USA. E-mail: harold@scarbro.com

### References

1. E. W. Wiley, W. J. Mathis, D. R. Garcia, *The Impact of the Adequate Yearly Progress Requirement of the Federal "No Child Left Behind" Act on Schools in the Great Lakes Region* (The Great Lakes Center for Education Research & Practice, 2005); [www.greatlakescenter.org](http://www.greatlakescenter.org).
2. E. Shaps, "Missing in action: The non-role of research in policy and practice," *Education Week*, 5 November 2008.
3. G. Toppo, "Study: Bush's Reading First program ineffective," *USA Today*, 2 March 2008; [www.usatoday.com/news/education/2008-05-01-reading-first\\_n.htm](http://www.usatoday.com/news/education/2008-05-01-reading-first_n.htm).



## HISTORY OF SCIENCE

## Who Scientists Are Now

Thomas F. Gieryn

**T**he *Scientific Life* is a history of science not quite like any other. To be sure, Newton, Einstein, and even James D. Watson and Richard Feynman get bit parts.

But the stars are people like C. E. Kenneth Mees (who directed the research labs at Eastman Kodak), Charles F. ("Boss") Kettering (his counterpart at General Motors), a chorus of entrepreneurial scientists not as famous as the iconic Craig Venter or Kary Mullis, and venture capitalists who move out from behind the scenes. Harvard historian Steven

Shapin needs such players to tell a story of the scientific life that is not anchored in research universities and does not revolve around Nobel Prize-worthy discoveries. His ambition is to show that although the rise of "big" industrial science bracketing World War II and the frenzy of Genentech and Cetus in the 1980s represent profound changes in the world of research and innovation, there are persistent continuities reaching back to Newton. None is more consequential than the enduring necessity of reckoning the credibility of knowledge via personal judgments about the virtues and character of the knower.

Shapin has written a "moral history," no matter how awkward that might first seem as the subtitle for a book on "the way we live now." His history reverses the analytic telescope. Instead of looking back at the 17th century and its so-called "scientific revolution" [Shapin has written influential books on that period (1–3)], he looks from early modern to late modern science in a way that instructively complicates familiar understandings of this passage. For example, some suspect that the scientific life was once a "calling" but is now an impersonal "job," stripped of what Max Weber called its enchanting, value-relevant, and charismatic qualities in favor of bureaucratic and instrumental rationalities. That view ignores the realities of industrial science at mid-20th century, when "institutional life came *personified*" in managers like Mees or Kettering, whose success depended on their

"moral authority" and on cultivating "social relations of familiarity."

Another common view is that scientists were once set apart from *hoi polloi* by virtue of distinctive skills and a civic responsibility to use them for esteemed ends. Now, the story goes, labs are populated by interchangeable researchers and Organization Men who are just like ordinary folk, and their occasional achievement of great things is not due to genius or goodness but to scientific management and strategic planning. But this assumption of the "moral equivalence" of scientists is undone by a look at venture capitalists struggling to discern the unique scientist who just might have the next fortune-making widget and (possibly more important) who possesses a personal character worthy of the investor's trust and confidence.

What makes this a moral history? Shapin writes about virtues and vices associated with the scientific life—such as trust, integrity, independence of mind, commitment to social betterment, cooper-

**The Scientific Life**  
A Moral History of a  
Late Modern Vocation

by Steven Shapin

University of Chicago  
Press, Chicago, 2008.  
486 pp. \$29, £15.  
ISBN 9780226750248.



**Manager and his forms.** C. E. Kenneth Mees and research and daily report forms used at the Eastman Kodak Research Laboratory.

ativeness, openness, or (to shift registers) avarice, egoism, and geekiness—and how these moral judgments are refracted through the changing organizational conditions in which scientists work. He is impatient with cultural commentators and academic social theorists who align virtue only with a "pure science" ideal and university-based inquiry and who often treat industrial and entrepreneurial science (or science done in big teams at state facilities) as corruptions of what makes science and scientists "good." Shapin wants to describe the scientific life rather than celebrate or deplore it, and he dives into quotidian realities of practically minded workers in the trenches by examining how-to manuals of research managers from the 1930s and by interviewing entrepreneurial scientists active today.

His findings will shake up what many have long believed about academic, industrial, and entrepreneurial research. At times, however, Shapin exaggerates both the liabilities of the university and the seductions of the corporation or marketplace. *Academe* comes off as resource starved, a place where scientists are distracted by teaching and endless committees and where the need to refresh

one's grants speeds up the treadmill as it forces research agendas to align themselves with mandates of funding agencies. Science in the corporate world comes off as endlessly challenging opportunities to put knowledge to use in the service of humanity, to publish one's research and sustain professional visibility, and to work on the hottest problems with an ever-changing cast of interdisciplinary colleagues—with no worries about how the next

instrument will be paid for. These narratives are never found so neatly in Shapin's interviews, which are full of ambivalence and misgivings. He resists the temptation to substitute one oversimplification for another, but he is up against a century of writings that have had it the other way around. The business end of science has been vilified and the ivory tower (or at least its imagined form) worshipped, but surely reality is somewhere in between.

But why should we believe the contrary Shapin? The author's credibility does not depend on his own moral virtue but on a method for rescuing historical reality from the supposed fog of theory and ideology. He excoriates sociologist Robert K. Merton

The reviewer is at the Department of Sociology, Indiana University, Bloomington, IN 47405, USA. E-mail: gieryn@indiana.edu

for misrecognizing scientists in industry as merely instances of “role strain,” a result of Merton’s slavish commitment to functional theories that declare the values of science and those of the market to be inherently incompatible. Shapin distrusts theory and, for that matter, sociological methods that are not grounded in up-close “naturalistic” attention to the radically unstable and contingent particulars visible most accurately (he believes) in the words and actions of scientific insiders as they make practical everyday decisions. In his discussion of venture capitalists and entrepreneurial scientists, Shapin makes no use of sophisticated network analyses of who hooks up with whom, probably because those rely on statistical analyses and seek wider patterns underneath the surface heterogeneities of everyday practical life. The words of Mees and Kettering (or later scientific entrepreneurs) become for him privileged windows on the real story by virtue of their practical-mindedness and distance from academic theorizing or ideological enthusiasms. But surely they too had axes to grind and ledger books to balance, and if theorists suffer from a “metonymic bias,” those in the trenches have their own “abridgments of the social realities they purport to describe.”

What makes Shapin’s attention to industrial and entrepreneurial research so compelling is how different today’s technoscience looks when contrasted with histories in which pure science in universities becomes the gold standard. In these other sites of science, Shapin finds the paradox that gives the book its spring. Research managers at Bell Labs or General Electric judge scientists not only on their impressive credentials and technical skills but also by their personal dispositions for working well in large, variegated, transient, and loosely organized teams. Venture capitalists must, in the face of massive uncertainties about whether an invention will yield profits, rely on character judgments about the personal trustworthiness and dedication of this particular scientist or engineer, who may differ little from a thousand others in terms of bench skills or academic achievements. *The Scientific Life* provokes us to discard worn-out understandings that science outside universities is necessarily aberrant and that the credibility of scientific knowledge no longer depends upon moral judgments about the experts who make reality claims. In that task, the book succeeds masterfully.

#### References

1. S. Shapin, S. Schaffer, *Leviathan and the Air Pump: Hobbes, Boyle, and the Experimental Life* (Princeton Univ. Press, Princeton, NJ, 1985); reviewed by T. L. Hankins, *Science* **232**, 1040 (1986).
2. S. Shapin, *A Social History of Truth: Civility and Science in Seventeenth Century England* (Univ. Chicago Press, Chicago, 1994); reviewed by P. Forman, *Science* **269**, 707 (1995).
3. S. Shapin, *The Scientific Revolution* (Univ. Chicago Press, Chicago, 1996); reviewed by D. C. Lindberg, *Science* **274**, 1148 (1996).
4. C. E. K. Mees, *The Organization of Industrial Scientific Research* (McGraw-Hill, New York, 1920).

10.1126/science.1166262

## AGRICULTURE

# Organic and GM—Why Not?

Mark Tester

**T**he organic movement’s opposition to genetically modified (GM) crops is causing it to miss an opportunity. Like agriculture across the planet, organic farming needs all the technological help it can get to be both sustainable and high-yielding. As with many recent innovations, GM technologies provide myriad possibilities for reducing the impacts of agriculture on the environment and the need for chemical inputs to maintain yield. But from the start, the organic movement rejected the use of GM crops. Genetic engineering is a technology, and like so many technologies, its benefits, costs, and risks depend on how it is used. A comparison with nuclear technology is not unfair: most of us benefit from medical applications of nuclear technologies, while many of us have major concerns with the large stockpiles of nuclear weapons that still threaten the planet. So, the risks of GM depend on the genes being put into the plants, not on the technology per se. Yet the numerous potential applications of GM to reduce chemical inputs to agriculture are flatly rejected by most organic farmers.

In *Tomorrow’s Table*, we now have the positive aspects of both organic and GM approaches discussed logically and clearly. The delightfully constructive book was written by a talented wife-and-husband team: Pamela Ronald, a very successful plant geneticist at the University of California, Davis, and Raoul Adamchak, an organic farmer who



**To increase harvests and efficiency.** The authors propose that combining genetic engineering with organic farming offers the best path to sustainable food production.

teaches at the same university. The authors are eminently qualified to present authoritative descriptions of their respective disciplines, which they do in a readable and accurate manner. But the noteworthy aspect of the book is the way they then marry their separate fields to argue logically for the use of GM technologies to improve organic agriculture. As Gordon Conway (a former president of the Rockefeller Foundation) comments in his foreword, “The marriage is long overdue.”

The authors describe the possibilities for GM to assist organic agriculture with examples drawn from their own and others’ research. Pest control is a particular focus. Ronald was centrally involved in the genetic engineering of flood-tolerance in rice (*1*). She describes lucidly how this would enable farmers to flood a paddy field in which the rice

has been established, thus killing the weeds that inevitably afflict the crop but not the rice itself. When the water is subsequently lowered, the rice has a head start on any weeds that eventually emerge, which provides a simple, cheap, and clearly organic method for weed control. How can the organic movement turn its back on such opportunities?

**Tomorrow’s Table**  
Organic Farming,  
Genetics, and the  
Future of Food

by Pamela C. Ronald and  
Raoul W. Adamchak

Oxford University Press,  
New York, 2008. 226 pp.  
\$29.95, £17.99.  
ISBN 9780195301755.

The reviewer is at the Australian Centre for Plant Functional Genomics and University of Adelaide, Australia. E-mail: mark.testers@acpfg.com.au



The false dichotomy that has been constructed between GM crops and organic farming can be illustrated with numerous similar examples. Another discussed by the authors is *Bacillus thuringiensis* (*Bt*) toxin, which has been successfully commercialized by Monsanto. These small insecticidal proteins, synthesized by widespread soil bacteria, can be applied in an almost unregulated way by organic farmers. This has been done for many decades. Yet when genetic engineering is used to place the gene encoding the *Bt* toxin in a plant's genome, the resulting GM plants are vilified by the very people willing to spray the product encoded by this same gene over otherwise similar plants. The organic movement's sustained rejection of this current application of GM appears increasingly illogical as evidence continues to accumulate that it does reduce pesticide use. In fact, this reduction is the principal reason farmers pay more for the biotech seeds—their lowered expenditures on pesticides are saving them money.

The authors marshal many additional examples to support their thesis that GM technologies and organic agriculture are quite compatible. Their discussion of these two topics exposes the complexity of the biological systems in which the issues surrounding them have to be addressed. This highlights the superficial nature of much of the GM debate, in which both sides make oversimplifications that support unnecessarily polarized standpoints. The biology is more complex. Unlike most protagonists, Ronald and Adamchak do not crudely lump together every GM crop as though they are all the same. That oversimplification blurs the issues (2, 3) to the detriment of fruitful consideration of topics that are increasingly important in a world in which we need to produce more food, fiber, and fuels in the face of global environmental change. In contrast, the authors calmly argue something that makes perfect sense to me, but their book will be controversial.

All proponents of organic agriculture, especially the noisier ones such as Prince Charles, should read *Tomorrow's Table*. Ronald and Adamchak's clear, rational approach is refreshing, and the balance they present is sorely needed in our increasingly polarized world. In addition, plant scientists—who have the privilege of greater knowledge than most in this area and who therefore have a responsibility

to share their understanding with a wider audience—will find the book provides useful information and arguments to help them when doing their next “science in the pub” talk.

#### References

1. K. Xu *et al.*, *Nature* **442**, 705 (2006).
2. M. Tester, *Nature* **402**, 575 (1999).
3. M. Tester, *New Phytol.* **149**, 9 (2001).

10.1126/science.1165961

## EXHIBITIONS: ART

### Global Perspectives

You wouldn't necessarily think of the Black Hills of South Dakota as the place to find innovations in communicating mathematics through art. However, the small town of Spearfish offers visitors an extraordinary gallery owned by a man who has devoted his life to capturing the total visual world. Painter Dick Termes creates Termespheres, pictures on globes that provide what Termes calls a sixfold perspective.

As he describes them, “What you are seeing when you look at a Termesphere painting is an inside-out view of a total physical world around you

on the outside surface of the hanging and rotating sphere. If you were on the inside of the sphere this painted image around you would seem normal, but I make you read it from the outside.”

The gallery itself is a wooden geodesic dome. Walking inside feels like floating in space past planets that capture pieces of different realities. Among the many works on view are a spherical model of Shakespeare's Globe Theatre, a surreal portrayal of the senses “not so much outside as within ourselves,” and a cityscape based on a rhombic dodecahedron. Optical illusions abound, and the viewer's perspective seems to snap from inside to outside the scenes.

Termes has exhibited his spheres in one-man and group shows, and they also appear in the permanent collections of art and science museums, mathematics departments, local governments, and corporations. For example, Science Centre Singapore includes Termes's *Life in a Fish Bowl in The Mind's Eye*, an exhibition on optical illusions. *Human Cage*, acquired by the Glasgow Science Centre, also presents an illusion. Are you, the observer, looking at birds in a cage? Or are you in the cage itself, surrounded by strange birds and animals? Your perspective shifts as you look at the sphere.

One of the artist's creations became part of the 100th birthday celebration for M. C. Escher in 1998. Termes took the famous picture of Escher holding a mirror ball and flipped it around: The 36-inch-diameter sphere creates the illusion that one is standing inside of Escher's mirror ball, looking out at his room. According to George Escher, Termes's recreation of the room is faithful (even to the lack of a door in the attic room, as that was hidden in the floor).

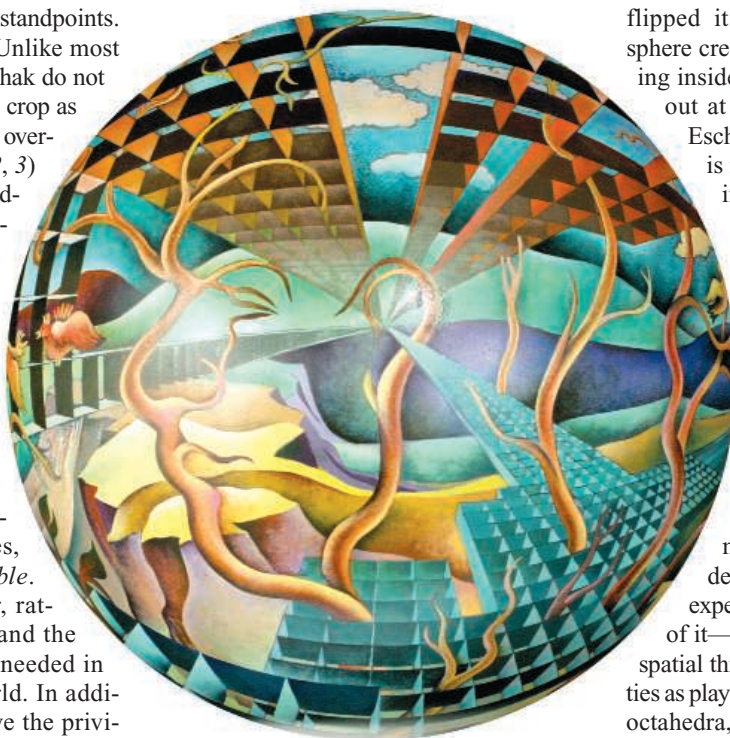
Currently Termes divides his time between creating designs on the surfaces of transparent spheres and developing a traveling display called “Up, Down, and All Around: Geometry in Your Visual World.” That exhibit (sponsored by the Hands-On Partnership for Science, Literature, and Art in South Dakota) primarily targets middle-school students, but children of any level are expected to be able to get something out of it—especially in terms of developing spatial thinking skills. Through such activities as playing with mobius strips and building octahedra, students should be turned on by and to both math and art.

—Barbara Jasny

10.1126/science.1167366

#### The Termesphere Gallery

1920 Christensen Drive,  
Spearfish, SD 57783, USA.  
[www.termespheres.com](http://www.termespheres.com)



*The Six Senses.*

## POLICY

# A Force for Peace in the Middle East

Michael Greene

One characteristic of the Middle East region, and especially the area occupied by Israel, Jordan, and the Palestine Authority, is the small geographic area and the high degree of interdependence among the populations in matters of resources and the environment. A major toxic spill or natural disaster in any of the territories could affect them all almost simultaneously and would require close coordination of remedial action. Yet, direct communication is limited essentially to government officials and members of a few professions. Because of the international nature of science, the scientific, engineering, and medical communities have the necessary international channels, technical capability, and, in a sense, the political dispensation to meet and communicate with their counterparts throughout the region. However, this type of communication is routine only among a few institutions in and around Jerusalem.

At a meeting of the science academies of Israel, Jordan, Palestine, and the United States in Washington in 2002, convened in part in response to the events of 9/11/2001, Hani Mulki, at that time secretary general of the Jordan Higher Council for Science and Technology and, subsequently, foreign minister and Jordanian ambassador to Egypt, offered a resolution for discussion. He argued that scientific cooperation should not be a by-product of the peace process; it should be a driving force for peace. When the situation is most critical, scientists and engineers must make the greatest efforts to work together. His resolution was adopted by acclamation (1).

During the activities surrounding the Oslo Peace Process, scientists were easily recruited to participate in committees to discuss such topics as water and the environment. The question is how, in the absence of a formal peace process, regional scientific cooperation might be encouraged and lead to general progress toward peace.

There are grant programs active in the region, such as the MERC program sponsored by USAID (2), which supports research collaboration among Israelis and Moslem neighbors, and IPSO, the Israeli-Palestinian

Science Organization, which makes research grants available to collaborating Israelis and Palestinians (3). There is no doubt that they have helped to increase scientific cooperation. But such programs do not necessarily make a lasting contribution to overall peace in the region. Cooperation tends to end when grant funds are exhausted, and individual successes often lead to overseas employment and a loss to the region.

I believe that the most effective approach for the donor community is the creation and support of scientific associations and institutions that are based within the region, like IPSO, and are specifically focused on regional cooperation. There are many programs currently operating, some well-established and some new, and the following examples are intended mainly to define the genre. During the Cold War, the Soviet and U.S. National Academies of Sciences held joint meetings without direct government participation on arms control issues (4). Today the Association of Middle East and United States National Academies of Science has been formed to further scientific cooperation (5). The individual national academies of Israel, Jordan, and Palestine in the Association are independent organizations, but the Association brings them together in joint projects dealing with common problems.

This Association has recently proposed the creation of a Middle East Food and Nutrition Board. Regional conferences on common nutrition and health problems are not infrequent in the region, but the concerted actions needed to eliminate disease and malnutrition are rare. In the United States, the Food and Nutrition Board of the Institute of Medicine has the stature and experience to identify such problems and propose solutions to the government and the country. It produces the report on Dietary Reference Intakes that is used as a standard reference for food labeling, fortification of foods, government nutrition assistance programs, and guidance to individuals. A similar body under the Middle East Association could propose standards for foods that are traded commercially in the region and help to combat micronutrient deficiencies and anemia.

Another model that could be effective in the Middle East is the dedicated technical

Support of regional scientific institutions or associations may make a difference.

institution in which regional governments participate. A prototype is IIASA, the International Institute for Applied Systems Analysis, which was supported during the Cold War by both the USSR and the United States as a place where scientists could confer. SESAME, the synchrotron radiation source for regional physics experiments being established in Jordan, could offer similar venues, as could the King Hussein Cancer Center, in which several countries participate.

Examples of possible regional efforts include: a Middle East Association for the Advancement of Science; a Web portal for students and researchers to exchange information on local problems, such as nutrition, renewable energy, agriculture, and water resources; a network of excellent technical universities such as those created in Africa and Latin America by the "Millennium Science Initiative" supported by the World Bank and others (6); multinational research centers for focused study on issues like the Dead Sea or the desert environment; and an industrial incubator that would attract Israeli-Arab partnerships.

An advantage of such models is that the organization or institution is permanently dedicated to continuing the cooperation among the participating countries. If and when the original donors withdraw, there likely will be a concerted effort to find support from other sources, which ultimately might be the governments of the region. Short of the facility earning a profit, joint support of the governments is the closest we can come to peaceful cooperation and sustainability.

## References

1. Report of the Meeting on Interacademy Cooperation for Long-Term Regional Stability, National Academy of Sciences, Washington, DC, 17 and 18 January 2002, unpublished.
2. Middle East Regional Cooperation (MERC) Program, U.S. Agency for International Development (USAID), [www.usaid.gov/our\\_work/merc/program\\_description.html](http://www.usaid.gov/our_work/merc/program_description.html)
3. J. Bohannon, *Science* **312**, 352 (2006).
4. R. Jeanloz, A. Harrington, *APS News* **14**(8), 6 (2005); [www.aps.org/publications/apsnews/200508/international.cfm](http://www.aps.org/publications/apsnews/200508/international.cfm).
5. *Scientific Cooperation in the Middle East: Current Status and Future Prospects*, [www7.nationalacademies.org/dsc/Middle\\_East\\_Cooperation.html](http://www7.nationalacademies.org/dsc/Middle_East_Cooperation.html).
6. Institute for Advanced Study, Science Initiative Group, <http://sites.ias.edu/sig/msi>.

Policy and Global Affairs Division, the National Academies, Washington, DC 20418, USA. E-mail: [mgreene@nas.edu](mailto:mgreene@nas.edu)

10.1126/science.1166978



## ASTRONOMY

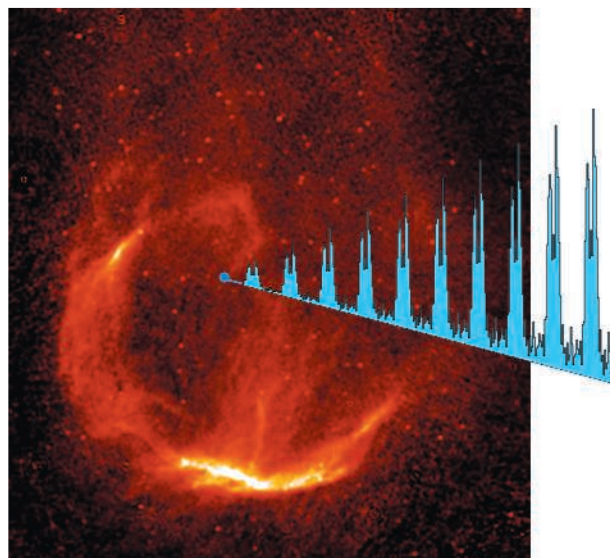
## Gamma Rays and Neutron Stars

Giovanni F. Bignami

Only Galileo was quicker. After discovering the satellites of Jupiter on 10 January 1610 in Padua, he wrote up his results in elegant Latin, personally did the artwork, allowed time for refereeing (by the Inquisition) and for printing (by hand), and had the *Sidereus Nuncius* hit the streets, or the canals, of Venice on 10 March. The NASA-led, international GLAST mission, now called the Fermi Observatory, was launched on 11 June 2008, deployed flawlessly into orbit, started taking in gamma rays from the sky and routing them through an impressive data-crunching machine, allowed time for a minimum of thinking, and just 4 months later, its first important result was reported online [Abdo *et al.*, see p. 1218 of this issue (1)]. Even Galileo would have been impressed, and so should we: Here is a new way of doing science, right on the eve of the International Year of Astronomy.

As Abdo *et al.* report, the Fermi Observatory has—for the first time in gamma-ray astronomy—discovered a rotating neutron star purely through its gamma-ray emission: Fewer than 1000 photons, collected over 2 months, are shown to have a convincing periodicity of about a third of a second. The star is not seen to emit at all at radio and optical wavelengths, and the weak x-ray emissions from the star are not pulsed. In short, Fermi has found a pure gamma-ray star, a “gamstar,” or, if you will, the second Geminga (2). Only, it took 20 years (from 1973 to 1993) to understand the unidentified gamma-ray source that we had called Geminga, and which until today, was the only known rotating gamma-ray neutron star invisible in radio.

The new gamstar, as yet unnamed, is close to the center of CTA1, a diffuse remnant of a supernova that exploded about 10,000 years ago (see the figure). The gamstar’s age, estimated by the slowing of its rotation, is consistent with its being the hard-core remnant of that explosion. A nice, coherent association—if a little déjà vu: It brings to mind the Vela pulsar and the diffuse emission surrounding it, remnants of a supernova explosion that took place around the time of the CTA1 supernova. However, the Vela pulsar is much closer to us



**A new gamstar.** The CTA1 supernova remnant has a well-formed radio shell, with a diameter of about 1.5°. Close to its center, the Fermi gamstar (blue dot) discovered by Abdo *et al.* (1) emits trains of pulsed gamma radiation.

and could be observed at the dawn of gamma-ray astronomy in 1975 (3), using radio data to clock the sparse gamma-ray photons. In fact, scientists continued to find gamma-ray pulsars using radio data, with the remarkable, if laborious, exception of Geminga. Fermi’s little brother, the Italian gamma-ray mission AGILE, has just found another Vela-like gamma-and-radio pulsar (4), the sixth of its kind.

Herein lies the importance of the Fermi gamstar discovery: From now on, given half-decent photon statistics, no radio data will be required for finding pulsating gamma-ray sources. Known gamstars, now numbering two, are not only here to stay but are likely to quickly increase in number.

A third one may already be coming up: a previously discovered gamma-ray source officially called 3EG J18335+5918, which Jules Halpern (co-discoverer of Geminga) has called the “next Geminga.” This gamma-ray source lacks a radio counterpart, but otherwise has all the markings of a neutron star. AGILE has now found interesting time variability for the source (5). CTA1 ended up being the real “next Geminga,” but this one may be next in line.

Many more Geminga-like gamstars may soon be discovered by Fermi (and AGILE) by looking at the position of unidentified gamma-ray objects (UGOs), which represent the

Satellite and ground observations provide new insights into gamma-ray emissions from neutron stars.

majority of known gamma-ray sources in our Galaxy. Interpreting UGOs as gamstars would provide a natural explanation for the quarter-of-a-century UGO mystery: Gamstars are simply pulsars that emit gamma rays in a fan beam geometrically different from the radio one, which may well exist but does not intercept the Earth. Gamstars would then be neutron stars with a somewhat different physics (and geometry) from that of the gamma-and-radio pulsars (like Vela and the Crab), for which both beams sweep the Earth.

But neutron stars and gamma rays seem to have even more in common. On page 1221 of this issue, The

MAGIC Collaboration (6) shows that the Crab pulsar—our prototype of the well-behaved neutron star, known to judiciously emit pulsed radiation from radio photons to gigaelectron volt (GeV) gamma rays—reaches its peak emission energy at 25 GeV and quickly fades afterwards. This is a brilliant result of the MAGIC Collaboration, who lowered the energy threshold of their ground-based telescope to around 25 GeV and for the first time detected pulsed gamma rays from the Crab at that energy.

Detecting 25 GeV gamma rays from the ground requires careful discrimination between signal and noise. By doing so, the authors bridged the decade-long gap between ground- and space-based gamma-ray astrophysics, because the upper energy limit of Fermi photons will be close to 20 GeV. Since the 1970s, gamma-ray energies detected from the Crab have increased from tens of MeV (7) to several GeV (8, 9), and now 25 GeV from MAGIC—an increase by an energy decade per calendar decade.

The MAGIC data show that even young neutron stars, like the Crab, less than 1000 years old, have their limitations in producing higher and higher energy photons. Above 25 GeV, MAGIC sees a sharp cut-off in the Crab spectrum. This has immediate implications for neutron star physics, because it discrimi-

Istituto Universitario Studi Superiori, IUSS, Viale Lungo Ticino Sforza 56, Pavia, 27100 Italy. E-mail: giovanni.bignami@gmail.com

nates between models that have competed, unchecked, for decades. Models in which gamma rays are produced near the outer gap of pulsar magnetosphere, far from the neutron star surface, appear best suited to explain the MAGIC data.

To prove theoreticians wrong or right is but a small satisfaction to the observer, who strives to see the unseen. Galileo and Fermi,

who excelled both in theory and observations, would have loved to explore the new horizons opened up by gamma rays and neutron stars working together to teach us something new.

#### References

1. A. A. Abdo *et al.*, *Science* **322**, 1218 (2008); published online 16 October 2008 (10.1126/science.1165572).
2. G. F. Bignami, P. A. Caraveo, *Annu. Rev. Astron. Astrophys.* **34**, 331 (1996).
3. D. J. Thompson *et al.*, *Astrophys. J.* **200**, L79 (1975).

4. J. Halpern *et al.*, *Astrophys. J.*, in press; <http://arxiv.org/abs/0810.0008>.
5. A. Bulgarelli *et al.*, *Astron. Astrophys.* **489**, L17 (2008).
6. The MAGIC Collaboration, *Science* **322**, 1221 (2008); published online 16 October 2008 (10.1126/science.1164718).
7. D. Kniffen *et al.*, *Nature* **251**, 397 (1974).
8. R. D. Wills *et al.*, *Nature* **296**, 723 (1982).
9. P. L. Nolan *et al.*, *Astrophys. J.* **409**, 697 (1993).

10.1126/science.1166967

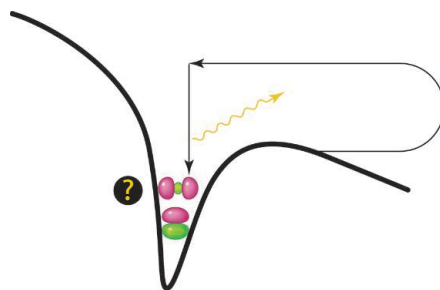
## CHEMISTRY

# Interrogating Molecules

Gilles Doumy and Louis F. DiMauro

The study of chemical reactions in real time (1) has been a major success of lasers capable of generating light pulses shorter than several tens of femtoseconds ( $1 \text{ fs} = 10^{-15} \text{ s}$ ). Facilitated by the discovery of the strong-field phenomenon of high harmonic generation (HHG) (2, 3), these pulses now promise to let us observe the electron dynamics inside an atom or a molecule, which occur over an even shorter time scale: tens of attoseconds ( $1 \text{ as} = 10^{-18} \text{ s}$ ). On pages 1232 and 1207 in this issue, McFarland *et al.* (4) and Li *et al.* (5) show how it is possible to use HHG selectively for probing different molecular orbitals, thus meeting a necessary condition for studying the internal dynamics of complex molecular systems.

To understand the complex interplays at work in the two studies, consider what happens to an atom or a molecule subjected to an intense laser field with a magnitude comparable to that of the Coulomb field that binds the electrons to the nucleus. Such conditions ("strong-field physics") are readily accessible with, for example, femtosecond-based titanium-sapphire laser systems. Most of the relevant physics can be explained by a simple three-step model (6, 7) (see the figure). First, the laser field suppresses the potential barrier, thereby allowing quantum tunneling to free the electron from the nucleus. Second, the freed electron is accelerated by the laser field and is either completely ionized or, after approximately one-half of an optical cycle, is accelerated back toward the parent ion. Third, the returning field-accelerated electron may recombine with the parent ion and emit a very short (attosecond duration) burst of soft x-rays. Because this process



**Three-step model.** An electron can tunnel out of the suppressed potential barrier and come back accelerated by the field. It can recombine to emit x-ray photons. It is now possible to select which molecular orbital is involved in this process.

occurs every half optical cycle, the signature of this emitted radiation is a spectral comb of odd-order high harmonics of the fundamental field frequency.

Since the discovery of this process, most studies have concentrated on improving such properties of HHG as bandwidth, number of photons, and duration of the attosecond bursts. However, it became apparent that those properties were extremely dependent on the specific target, typically dense gas jets, used for the generation. Thus, HHG not only provides a unique opportunity to study laser-matter interactions in the strong-field regime, but can also be used as a probe of the generating system itself. Furthermore, the sensitivity of the process to variations faster than an optical cycle provides a probe of unmatched temporal resolution.

The dependence on the generating medium is particularly important for molecules, because molecular symmetry and rotational-vibrational dynamics make for richer physics (8). An important demonstration with nitrogen ( $\text{N}_2$ ) as the generating medium introduced a new method that allowed for the tomographic reconstruction of the molecular

orbital involved in the HHG process (9). By measuring the HHG spectrum from the  $\text{N}_2$  molecules as a function of the angle between the laser polarization and the molecular axis, the static highest occupied molecular orbital (HOMO) describing the original electronic state involved in the HHG process was reconstructed. However, realizing the full potential of HHG tomography in the time domain requires a probe of the multiple orbitals involved in the dynamics. The two studies in this issue directly address this challenge by showing that HHG is indeed capable of providing information on different orbitals, provided that one "interrogates" the system in the correct way: By modifying the "configuration" of the molecule (orientation or bond length), HHG preferentially involves either the HOMO or the orbital immediately below it, called HOMO-1.

McFarland *et al.* investigated the HHG emission of different harmonic orders for  $\text{N}_2$  molecules. The molecular alignment was controlled by another lower-intensity short-pulsed laser that induced alignment along its polarization axis (10). The alignment of the molecular axis relative to the polarization of the HHG generating field (e.g., perpendicular or parallel) can then be controlled by adjusting the delay between the two laser pulses. When measured as a function of this delay, the highest-order harmonics displayed a peculiar behavior: a decreased signal when parallel, and an increased signal when orthogonal. They explained this behavior by involving HHG from the HOMO-1 on top of the expected generation from the HOMO.

Li *et al.* approached the problem differently by studying HHG from  $\text{NO}_2$  dimers. The weak N-N bond was first nonresonantly excited by an ultrashort pulse. By introducing a variable delayed HHG generating pulse, they studied the influence of the bond length

Department of Physics, Ohio State University, Columbus, OH 43210, USA. E-mail: gdoumy@mps.ohio-state.edu; dimauro@mps.ohio-state.edu



on the HHG process in real time. They found that emission was suppressed as the bond length reached its minimum value, while ionization yields were unchanged. The role of the HOMO-1 state was established through comparison to quantum chemistry *ab initio* calculations showing that (i) the HOMO-1 ionization is favored when the bond is compressed, (ii) the total ionization rates do not appreciably change with bond length, and (iii) the HOMO-1 symmetry greatly reduces the recombination probability, making it a “dark state” for HHG emission; that is, it does not emit harmonics, or it does so with much lower efficiency.

These new studies can provide particular insight into the electronic processes within molecules. Tackling the complex problems involved in molecular dynamics relies criti-

cally on very good modeling. The measurements can then be used to identify the most probable mechanism. They effectively open a whole new class of experiments, in which the system (molecule) is “prepared” so that HHG is probing a specific orbital. In the papers described here, the molecules were either aligned or excited selectively, but this will become more difficult as the molecule grows in size and complexity. However, solutions for avoiding alignment have already been suggested. For instance, the recollision angle can be controlled by using elliptically polarized light in the driving field (11) or a two-color field (12). These two studies, along with recent advances in single-cycle interactions (13), are developing the essential tools for probing attosecond dynamics in complex molecules.

## References

1. A. Zewail, *J. Phys. Chem. A* **104**, 5660 (2000).
2. X. F. Li, A. L'Huillier, M. Ferray, L. A. Lompre, G. Mainfray, *Phys. Rev. A* **39**, 5751 (1989).
3. A. McPherson *et al.*, *J. Opt. Soc. Am. B* **4**, 595 (1987).
4. B. K. McFarland, J. P. Farrell, P. H. Bucksbaum, M. Gühr, *Science* **322**, 1232 (2008); published online 30 October 2008 (10.1126/science.1162780).
5. W. Li *et al.*, *Science* **322**, 1207 (2008); published online 30 October 2008 (10.1126/science.1163077).
6. K. J. Schafer, B. Yang, L. F. DiMauro, K. C. Kulander, *Phys. Rev. Lett.* **70**, 1599 (1993).
7. P. B. Corkum, *Phys. Rev. Lett.* **71**, 1994 (1993).
8. T. Kanai, S. Minemoto, H. Sakai, *Nature* **435**, 470 (2005).
9. J. Itatani *et al.*, *Nature* **432**, 867 (2004).
10. H. Stapelfeldt, T. Seideman, *Rev. Mod. Phys.* **75**, 543 (2003).
11. Y. Mairesse *et al.*, *New J. Phys.* **10**, 025015 (2008).
12. M. Kitzler, X. Xie, S. Roither, A. Scrinzi, A. Baltuska, *New J. Phys.* **10**, 025029 (2008).
13. E. Goulielmakis *et al.*, *Science* **320**, 1614 (2008).

10.1126/science.1166078

## DEVELOPMENTAL BIOLOGY

# Brain Wnts for Blood Vessels

Eckhard Lammert

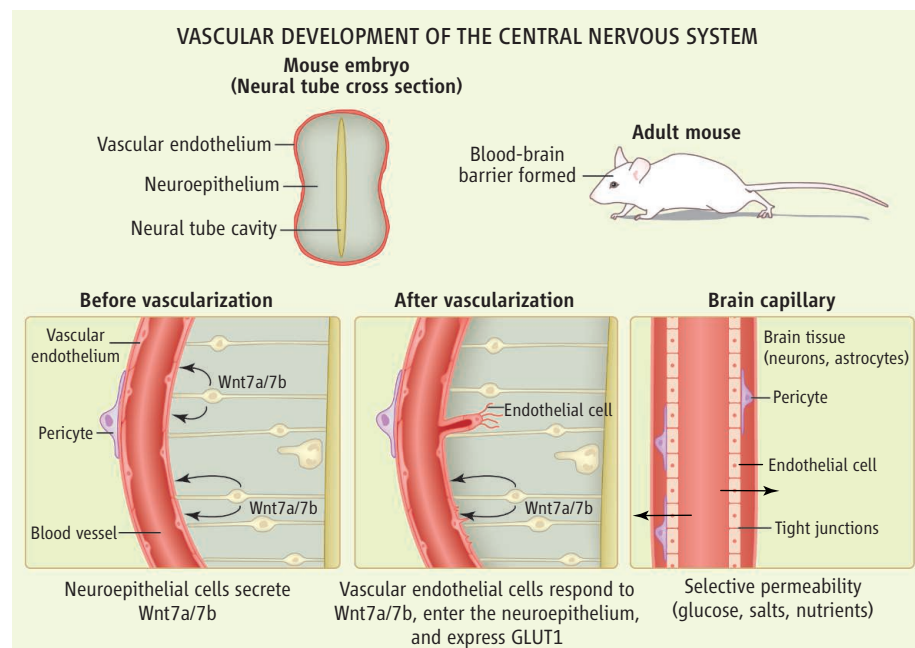
The human brain constitutes 2% of the total body weight, but receives 16% of the cardiac output and accounts for nearly 25% of the oxygen consumed by the body (1). The brain and spinal cord form the central nervous system, which, in keeping with its role as the control center of the organism, requires protection as well as sustained energy supply, both of which are provided by a specialized system of blood vessels. On page 1247 of this issue, Stenman *et al.* (2) show that secreted proteins of the Wnt family of growth factors promote vasculature formation in the central nervous system of the mouse embryo, thereby initiating development of the blood-brain barrier, a critical interface that restricts the passage of solutes between the bloodstream and neural tissue. Similarly, Liebner *et al.* report that Wnt signaling is required and sufficient for initiating blood-brain barrier formation in vascular endothelial cells of mice (3).

The vasculature of the mammalian central nervous system arises during embryogenesis through a process called angiogenesis, in which preexisting blood vessels grow from the outside into the inside of the neural tube (the precursor to the central nervous system) (4). In most parts of the brain, the blood vessels are

impermeable to hydrophilic substances and, therefore, protect the brain from toxic and infectious agents present within the blood—a feature referred to as the blood-brain barrier

Development of the blood-brain barrier in mammals starts in the embryo, through specific molecules that induce vascular development in the neural tube.

(5). To ensure that nutrients can pass through the blood-brain barrier to nourish the neural tissue, endothelial cells express nutrient transporters, such as the glucose transporter-



**Vascularization of the nervous system.** The formation of blood vessels in the mouse neural tube is initiated by Wnt7a and Wnt7b that are secreted by neuroepithelial cells. Vascular endothelial cells that surround the neural tube respond to these signals and enter the neuroepithelium, forming a vascular plexus. These vascular endothelial cells also start to express the glucose transporter GLUT-1. Unknown signals from the blood vessels inhibit GLUT-1 expression in the neuroepithelium. Wnt expression continues to promote formation of the intraneural vascular plexus and initiation of a protective blood-brain barrier.

Institute of Animal Physiology, Heinrich-Heine-University, D-40225 Düsseldorf, Germany. E-mail: lammert@uni-duesseldorf.de

GLUT-1 for D-glucose. Heterozygous mutations in the gene encoding GLUT-1 are associated with neurological and developmental symptoms, showing that glucose uptake is essential for human brain development and function (6).

To date, few growth factors have been shown to be involved in formation of the central nervous system vasculature and blood-brain barrier. Stenman *et al.* report that large areas of the neuroepithelium in the developing neural tube express the growth factors Wnt7a and Wnt7b (see the figure). Wnt proteins regulate various aspects of cell behavior, including tissue patterning and morphogenesis, as well as cell differentiation and proliferation. In humans and mice, 19 different genes encode Wnt proteins and 10 genes code for Frizzled proteins, the receptors for Wnts (7). Using mouse genetics, Stenman *et al.* show that Wnt7a and Wnt7b are required for vascularization and initiation of a blood-brain barrier in the developing central nervous system. The authors show that in the absence of these Wnts, the central nervous system displays reduced and abnormal vascular sprouting, severe vascular leakage, and lack of GLUT-1 expression in the developing blood vessels.

Wnts induce different intracellular events downstream of the Frizzled receptors they activate. These events are grouped into canonical and noncanonical Wnt signaling pathways (7). Canonical Wnt signaling stabilizes the protein  $\beta$ -catenin, which translocates into the nucleus and interacts with LEF/TCF transcription factors to activate Wnt target genes (8, 9). In line with canonical Wnt signaling, Stenman *et al.* observed  $\beta$ -catenin-activated gene expression, as well as LEF1 expression, in endothelial cells in the neural tube in the mouse embryo. Moreover, the authors show that deletion of  $\beta$ -catenin results in vascular defects similar to the ones observed in mouse embryos when Wnt7a and Wnt7b genes are deleted. By contrast, deletion of  $\beta$ -catenin in the neuroepithelial cells in the neural tube does not result in vascularization defects, showing that autocrine canonical Wnt signaling in the neuroepithelium is not required for central nervous system vascularization.

Taken together with the findings of Liebner *et al.* (3), who show that Wnts induce features of a blood-brain barrier in cultured mouse endothelial cells via  $\beta$ -catenin, Stenman *et al.* demonstrate that the neuroepithelium signals to the vascular endothelium through canonical Wnt signaling to induce a central nervous system-specific vascular system.

Previous studies proposed that mutual signaling between organs and endothelial cells of blood vessels results in structural and func-

tional coupling between organs and their respective vascular beds (10). Stenman *et al.* show that similar signaling events shape the vascularized central nervous system. The authors demonstrate that neuroepithelial cells induce GLUT-1 expression in the vascular endothelium via Wnt7a and Wnt7b, and that the endothelial cells in turn inhibit GLUT-1 expression in the neuroepithelium. A physiological explanation for this switch in GLUT-1 expression from neurons to endothelial cells could be that the blood vessels reduce the neuronal demand for facilitated glucose transport, but themselves require GLUT-1 for facilitating glucose passage from blood to neurons (11).

In general, organs harbor blood vessels with tissue-specific features (12). For example, most endocrine glands contain permeable blood capillaries to facilitate release of hormones into the bloodstream, and the liver sinusoidal endothelial cells are fenestrated to facilitate lipoprotein exchange between blood and liver. By contrast, the capillary bed is not fenestrated and is tightly sealed in most parts

of the central nervous system. Because each vascular bed contributes to organ function, the Wnt7a and Wnt7b signaling pathways identified by Stenman *et al.* may harbor valuable drug targets for specifically manipulating the cerebral vasculature and brain function in several human diseases.

#### References

1. K. J. Tracey, C. N. Metz, in *Endothelial Biomedicine*, W. C. Aird, Ed. (Cambridge Univ. Press, New York, 2007), chap. 124.
2. J. M. Stenman *et al.*, *Science* **322**, 1247 (2008).
3. S. Liebner *et al.*, *J. Cell Biol.* **183**, 409 (2008).
4. P. Carmeliet, *Nature* **438**, 932 (2005).
5. B. Engelhardt, *Cell Tissue Res.* **314**, 119 (2003).
6. J. Klepper, T. Voit, *Eur. J. Pediatr.* **161**, 295 (2002).
7. N. L. Parmalee, J. Kitajewski, *Curr. Drug Targets* **9**, 558 (2008).
8. T. Grigoryan, P. Wend, A. Klaus, W. Birchmeier, *Genes Dev.* **22**, 2308 (2008).
9. A. J. Mikels, R. Nusse, *Oncogene* **25**, 7461 (2006).
10. G. Nikolova, E. Lammert, *Cell Tissue Res.* **314**, 33 (2003).
11. R. Dermietzel, D. Krause, M. Kremer, C. Wang, B. Stevenson, *Dev. Dyn.* **193**, 152 (1992).
12. E. Lammert, in *Endothelial Biomedicine*, W. C. Aird, Ed. (Cambridge Univ. Press, New York, 2007), chap. 22.

10.1126/science.1167451

#### CHEMISTRY

## Coming Soon to a Library Near You?

Jan Wouters

Conservation efforts will be aided by a tool that facilitates surveys of the condition of paper in libraries, archives, and museums.

Many paper objects produced in the West in the 19th and 20th centuries are deteriorating rapidly. Their longer-term conservation requires a full understanding of chemical degradation mechanisms and of how they can be slowed down. Paper condition assessments carried out by staff in libraries, archives, and museums are indispensable for the rapid and effective screening of massive collections and to prioritize subsequent conservation efforts. A newly developed analytical protocol for rapid noninvasive paper condition assessments (1, 2) should facilitate the performance of such condition surveys of paper collections and may also contribute to the dating of paper objects.

Paper conservation science is a relatively young field. In contrast, paper conservation practice has a long history and has long been regarded and executed as a craft with its associated secrets and empiricisms. Whereas

progress in conservation science may have a rapid impact on evaluating the condition of paper, its implementation in practical paper conservation processes tends to proceed at a much slower pace.

However, time is running out and the economic, political, and social challenges are enormous. Paper condition surveys in libraries reveal an average of 30% of objects in poor condition, needing urgent intervention to prevent irreversible loss, and another 30% to reach that poor condition by the end of this century. All those papers are subject to physical, biological, and chemical degradation, induced by manipulations, climate, and the composition of the paper and of materials added to it. This is especially true for Western paper produced from the beginning of the 19th century, when demands for paper became much higher than traditional sources could provide, to the end of the 20th century, when more durable acid-free paper began to be produced.

Nowadays, staff involved in the care of collections routinely use risk assessment

The Getty Conservation Institute, Neerbroek 54, 2070 Zwijndrecht, Belgium. E-mail: jan.j.wouters@telenet.be



procedures and conservation measures to reduce paper degradation through manipulation, to monitor noxious museum environments (3), and to identify and remedy biological degradation of paper (4). Recent research has also yielded new procedures for characterizing the chemical degradation of paper and its attenuation, as well as conservation processes. However, these procedures still need critical verification and further development before finding widespread application in practical conservation (5).

prone to oxidative breakdown than the formerly acid ones, several groups have attempted to stabilize paper by combining deacidification treatment with the addition of antioxidants in one single conservation action. Antioxidants used include calcium phytate (8), magnesium phytate (9), and potassium halides (10).

Major advances in assessing the condition of paper and the efficacy of a conservation treatment have also been made. Approaches include solid-phase microextraction, fol-

evaluation to analyze paper condition (1) (chemometrics is the mathematical-statistical treatment of chemical data). They analyzed more than 170 historical papers both with standard methods and with the infrared approach. Parameters covered included lignin and aluminum content, pH, degree of cellulose polymerization, and ash content, measured on papers ranging from the 17th to the 21st centuries.

All these parameters provide information about the condition and durability of the paper: Lignin and aluminum (through the use of alum in paper production) are two of the most crucial products for explaining the rapid decay of 19th- and 20th-century papers; pH measurements reveal potential acid-catalyzed hydrolysis of cellulose and help to assess the effectiveness of deacidification treatments; the degree of polymerization of cellulose is a direct measure for the paper's mechanical strength; and ash content relates to the use of inorganic fillers, the chemical nature of which has changed over time.

The determination of these crucial parameters in a single analytical protocol on microsamples, with good correlations between parameter values determined with established standard methods and those retrieved from the infrared spectra, has never been achieved before. To allow easy and efficient implementation of the protocol by staff in libraries, archives, and museums, researchers have recently developed a portable near-infrared instrument (weighing less than 10 kg), which allows noncontact measurements on flat objects of any size in less than a second, together with software covering survey modes at the level of single items, at random, and of the total paper collection (2).

Once validated, this portable instrument will be a revolutionary step forward in the assessment of the paper condition in libraries, archives, and museums at any survey level. Its use will contribute to better prioritization before conservation and to a more efficient use of resources, for example, when deciding between remedial conservation and restoration (15) and digitization of brittle paper (16). Last but not least, the infrared spectra reflect the integrated effect of all natural aging processes that occurred during the paper's lifetime and that changed the structures, ratios, and interactions of materials present in the paper; this signature may help to date paper objects.

#### References

1. T. Trafela *et al.*, *Anal. Chem.* **79**, 6319 (2007).
2. M. Strlič *et al.*, in *Preprints of the 15th Triennial Conference of ICOM-CC*, J. Bridgland, Managing Ed. (Allied Publishers, New Delhi, India, 2008), pp. 293–300.



**Toward nondestructive paper condition surveys.** What is the condition of books in libraries such as the Old Library at Trinity College in Dublin? Chemometrics of infrared data (1), collected noninvasively from paper artifacts with a portable instrument linked to user-friendly software (2), may soon become an indispensable facet of investigations into the past manufacture and aging, the present condition, and the conservation of paper artifacts.

Since the 1990s, national and international research programs have contributed substantially to a better understanding of paper degradation and to the development of new paper conservation treatments. For example, laser cleaning—a technique that has been used successfully in other fields of cultural heritage conservation—offers high spatial resolution and allows remote handling. It thus has obvious advantages, especially for the treatment of precious single documents. However, it is still reluctantly implemented in paper conservation practice because of justified fears of irreversible damage (6).

Another method uses nanosized particles of magnesium or calcium hydroxide in volatile alcohols with low surface tension (representing high surface reactivity and narrow size distribution) for the deacidification of paper. This method can be readily implemented in mass treatments (7). However, paper is also damaged by iron gall ink, which simultaneously oxidizes and acidifies the paper. Because deacidified papers are more

lowed by capillary gas chromatography and mass spectrometric characterization of volatile organic compounds emitted by paper through aging (11); the performance of paper acidity measurements at the micrometer scale (12); and the use of chemiluminescence to evaluate photodegradation of deacidified papers (13). However, most condition evaluation measurements still require direct contact between the paper document and the measuring probe (for example, in pH measurements with a surface pH electrode); in most cases, samples up to several square millimeters in size must be taken. When dealing with precious historic documents, sampling must be avoided as much as possible, and alterations induced by in situ measurements—even by those which are called “nondestructive” in confusing terminology (14)—must be anticipated and limited.

A paper published in 2007 overcomes many of these limitations. Trafela *et al.* combined infrared spectroscopy (used in the reflectance mode) with chemometric data

3. C. M. Grzywacz, *Monitoring for Gaseous Pollutants in Museum Environments* (Getty Publications, Los Angeles, CA, 2006).
4. F. Fliedler, C. Capderou, *Sauvegarde des Collections du Patrimoine* (CNRS Editions, Paris, 1999).
5. M. Strlič, J. Kolar, Eds., *Ageing and Stabilisation of Paper* (National and University Library, Ljubljana, 2005).
6. W. Kautek et al., *Proc. SPIE* **4402**, 130 (2001).
7. P. Baglioni, R. Giorgi, *Soft Matter* **2**, 293 (2006).
8. J. G. Neevel, *Restaurator* **16**, 143 (1995).
9. J. Kolar et al., *e-PS* **4**, 19 (2007).
10. J. Malesič et al., *e-PS* **2**, 13 (2005).
11. T. Doering, *Altes Papier—Neue Techniken, Zerstörungsfreie Untersuchungen von Papier mit Festphasenmikroextraktion (SPME)* (Berliner Wissenschafts-Verlag, Berlin, 2007).
12. M. Strlič et al., *e-PS* **1**, 35 (2004).
13. M. Strlič et al., in *Ageing and Stabilisation of Paper*, M. Strlič, J. Kolar, Eds. (National and University Library, Ljubljana, 2005), pp. 133–148.
14. J. Wouters, *Chem. Int.* **30**, 4 (2008).
15. International Council of Museums—Committee for Conservation (ICOM-CC), *Terminology to Characterize the Conservation of Tangible Cultural Heritage* (2008); [www.icom-cc.icom.museum](http://www.icom-cc.icom.museum).
16. J. Levin, J. Druzik, *Conservation, the Getty Conserv. Inst. Newsl.* **22**(3), 10 (2007).

10.1126/science.1164991

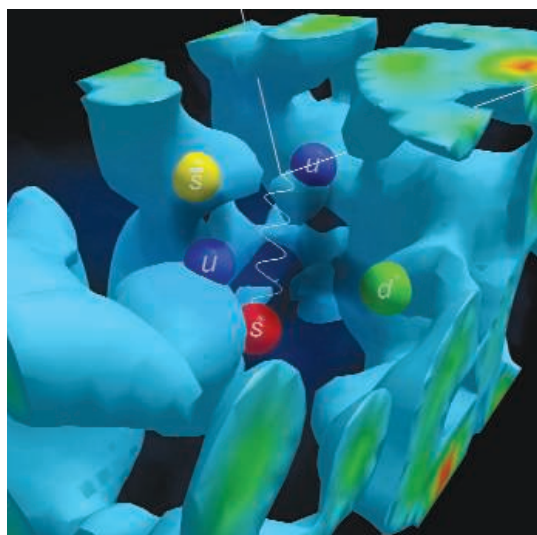
## PHYSICS

# The Weight of the World Is Quantum Chromodynamics

Andreas S. Kronfeld

The reason for excitement surrounding the start-up of the Large Hadron Collider (LHC) in Geneva, Switzerland, has often been conveyed to the general public as the quest for the origin of mass—which is true but incomplete. Almost all of the mass (or weight) of the world we live in comes from atomic nuclei, which are composed of neutrons and protons (collectively called “nucleons”). Nucleons, in turn, are composed of particles called quarks and gluons, and physicists have long believed that the nucleon’s mass comes from the complicated way in which gluons bind the quarks to each other, according to the laws of quantum chromodynamics (QCD). A challenge since the introduction of QCD (1–3) has been to carry out an *ab initio* calculation of the nucleon’s mass. On page 1224 of this issue, Dürr et al. (4) report the first such calculation that incorporates all of the needed physics, controls the numerical approximations, and presents a thorough error budget. Because these accurate calculations agree with laboratory measurements, we now know, rather than just believe, that the source of mass of everyday matter is QCD.

The key tool enabling this advance is lattice gauge theory (5), a formulation of QCD and similar quantum field theories that replaces space-time with a four-dimensional lattice. To picture the lattice, think of a crystal with cubic symmetry evolving in discrete time steps. Lattice gauge theory has theoretical and computational advantages. The watershed theoretical result of QCD is the weakening at short distances of the coupling between quarks and gluons, called asymptotic freedom (2, 3). The flip side is the strengthening of the



**The busy world of the QCD vacuum.** The interior of a hadron, such as the proton or neutron, is not static. Gluons fluctuate in a collective fashion, illustrated by the red-orange-yellow-green-blue fluid. Sometimes the gluon field produces extra quark-antiquark pairs; here, a proton ( $uud$ ) has fluctuated into a  $\Lambda$  hyperon ( $uds$ ) and a kaon ( $\bar{s}u$ ). Animations of these phenomena are available at (7).

coupling at large distances, which is responsible for confining quarks and gluons inside one of the broad class of particles called hadrons.

Confinement emerges naturally in lattice gauge theory at strong coupling (5). The lattice also reduces everything we would want to calculate to integrals that, in principle, can be evaluated numerically on a computer. Thus, 30 years ago a challenge was set: Use numerical computations to connect strongly coupled lattice gauge theory with weakly coupled asymptotic freedom, thereby recovering the hadron masses of our world, with continuous space and time.

The first numerical efforts (6) showed this approach to be sound, but as the subject developed, two major obstacles arose, both

connected to physics and to computation. The first obstacle is describing the “vacuum.” In classical physics, the vacuum has nothing in it (by definition), but in quantum field theories, such as QCD, the vacuum contains “virtual particles” that flit in and out of existence. In particular, the QCD vacuum is a jumble of gluons and quark-antiquark pairs, so to compute accurately in lattice QCD, many snapshots of the vacuum are needed.

The second obstacle is the extremely high amount of computation needed to incorporate the influence of the quark-antiquark pairs on the gluon vacuum. The obstacle heightens for small quark masses, and the masses of the up and down quarks are very small. An illustration of the vacuum and the quark-antiquark pairs is shown in the figure. The fluid material is a scientifically accurate snapshot, sometimes

called the QCD lava lamp, of a typical gluon field drawn from a lattice-QCD computation (7). Three of the quarks (up + up + down, or  $uud$  for short) could constitute the proton, but a strange quark ( $s$ ) and strange ( $\bar{s}$ ) antiquark have popped out of the vacuum: The proton has fluctuated into a  $\Lambda$  hyperon ( $uds$ ) and a kaon ( $\bar{s}u$ ).

To make progress despite limited computing power, 20 years’ worth of lattice QCD calculations were carried out omitting the extra quark-antiquark pairs. The computation of the nucleon’s mass passed some technical milestones (8, 9) but was still unsatisfactory. As well as demonstrating the validity of strongly coupled QCD, we want to compute properties of hadrons *ab initio*, to help

Theoretical Physics Group, Fermi National Accelerator Laboratory, Batavia, IL 60510, USA. E-mail: ask@fnal.gov



interpret experiments in particle and in nuclear physics. Without the quark-antiquark pairs, it is impossible to quantify the associated uncertainty.

A breakthrough came 5 years ago, with the first wide-ranging calculations incorporating the back-reaction of up, down, and strange quark pairs (10, 11). This work used a mathematical representation of quarks that is relatively fast to implement computationally (12), and these methods enjoyed several noteworthy successes, such as predicting some then-unmeasured hadron properties (13). This formulation is, however, not well suited to the nucleon, and so a principal task for lattice QCD remained unfinished.

Dürr *et al.* use a more transparent formulation of quarks that is well suited to the nucleon and other baryons (hadrons composed of three quarks). They compute the masses of eight baryons and four mesons (hadrons composed of one quark and one antiquark). Three of these masses are used to fix the three free parameters of QCD. The other nine agree extremely well with measured values, in most cases with total uncertainty below 4%.

For example, the nucleon mass is computed to be  $936 \pm 25 \pm 22 \text{ MeV}/c^2$  compared with  $939 \text{ MeV}/c^2$  for the neutron, where  $c$  is the speed of light and the reported errors are the statistical and systematic uncertainties, respectively. The final result comes after careful extrapolation to zero lattice spacing and to quark masses as small as those of up and down (the two lightest quarks, with masses below 6

$\text{MeV}/c^2$ ). The latter extrapolation may not be needed in the future. Last July, a Japanese collaboration announced a set of lattice-QCD calculations (14) of the nucleon and other hadron masses with quark masses as small as those of up and down.

These developments are serendipitously connected to the work honored by this year's Nobel Prize in physics. The lightest hadron—the pion—has a mass much smaller than the others. Before QCD, Nambu (15) proposed that this feature could be understood as a consequence of the spontaneous breaking of chiral symmetry (16). In QCD, it has been believed, the spontaneous breaking of this symmetry by the vacuum predominates over an explicit breaking that is small, because the up and down quarks' masses are so small. Lattice QCD (4, 10, 11, 13, 14) simulates and, we see now, validates these dynamical ideas in the computer. Moreover, this success puts us in a position to aid and abet the understanding of the role of quark flavor (17), including asymmetries in the laws of matter and antimatter (18), for which Kobayashi and Maskawa received their share of the Nobel Prize.

Dürr *et al.* start with QCD's defining equations and present a persuasive, complete, and direct demonstration that QCD generates the mass of the nucleon and of several other hadrons. These calculations teach us that even if the quark masses vanished, the nucleon mass would not change much, a phenomenon sometimes called “mass without mass” (19, 20). It then raises the question of the origin of

the tiny up and down quark masses. The way nature generates these masses, and the even tinier electron mass, is the subject of the LHC, where physicists will explore whether the responsible mechanism is the Higgs boson or something more spectacular.

#### References and Notes

1. H. Fritzsch, M. Gell-Mann, H. Leutwyler, *Phys. Lett. B* **47**, 365 (1973).
2. D. J. Gross, F. Wilczek, *Phys. Rev. Lett.* **30**, 1343 (1973).
3. H. D. Politzer, *Phys. Rev. Lett.* **30**, 1346 (1973).
4. S. Dürr *et al.*, *Science* **322**, 1224 (2008).
5. K. G. Wilson, *Phys. Rev.* **10**, 2445 (1974).
6. M. Creutz, *Phys. Rev. Lett.* **45**, 313 (1980).
7. D. Leinweber, “Visualizations of Quantum Chromodynamics ([www.physics.adelaide.edu.au/theory/staff/leinweber/VisualQCD/Nobel](http://www.physics.adelaide.edu.au/theory/staff/leinweber/VisualQCD/Nobel)).
8. F. Butler, H. Chen, J. Sexton, A. Vaccarino, D. Weingarten, *Nucl. Phys. B* **430**, 179 (1994).
9. A. Ali Khan *et al.* (CP-PACS Collaboration), *Phys. Rev. D* **65**, 054505 (2002).
10. C. T. H. Davies *et al.* (HPQCD, MILC, and Fermilab Lattice Collaborations), *Phys. Rev. Lett.* **92**, 022001 (2004).
11. C. Aubin *et al.* (MILC Collaboration), *Phys. Rev. D* **70**, 094505 (2004).
12. C. Bernard *et al.* (MILC Collaboration), *Phys. Rev. D* **64**, 054506 (2001).
13. A. S. Kronfeld, *J. Phys. Conf. Ser.* **46**, 147 (2006).
14. S. Aoki *et al.* (PACS-CS Collaboration), <http://arXiv.org/abs/0807.1661> (2008).
15. Y. Nambu, *Phys. Rev. Lett.* **4**, 380 (1960).
16. J. Goldstone, *Nuovo Cim.* **19**, 154 (1961).
17. N. Cabibbo, *Phys. Rev. Lett.* **10**, 531 (1963).
18. M. Kobayashi, T. Maskawa, *Prog. Theor. Phys.* **49**, 652 (1973).
19. F. Wilczek, *Phys. Today* **52**, 11 (November 1999).
20. F. Wilczek, *Phys. Today* **53**, 13 (January 2000).
21. Fermilab is operated by Fermi Research Alliance LLC, under Contract DE-AC02-07CH11359 with the U.S. Department of Energy.

10.1126/science.1166844

## MICROBIOLOGY

# Rogue Insect Immunity

David S. Schneider and Moria C. Chambers

Two recent studies have quietly and subversively broken the models we've used to describe insect immunity. Impressively, they've accomplished this by using gross observational studies rather than mechanistic approaches. On page 1257 in this issue, Haine *et al.* (1) suggest that what we've considered the central pillar of insect immunity—antimicrobial peptides—may perform a “mopping up” role in clearing pathogens. Hedges *et al.* (2) show that heritable epigenetic properties can have as large an impact on insect immunity as any genetically encoded

pathway yet tested. Both studies teach us important lessons about the way a host organism interacts with microbes and may have immediate practical applications.

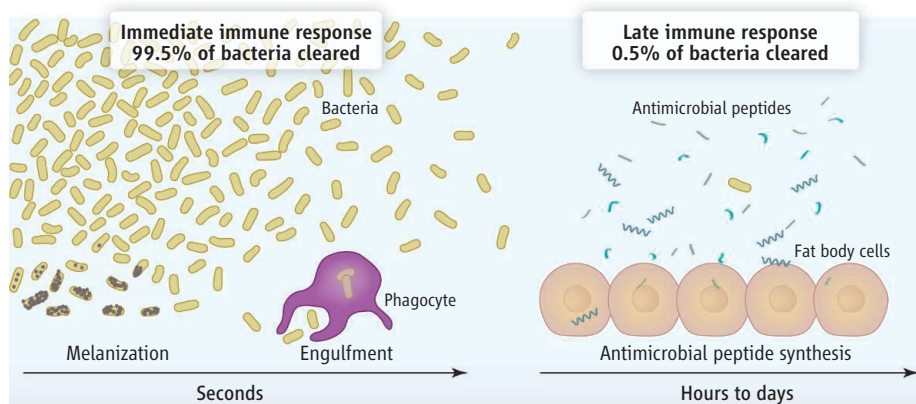
We often study host-pathogen interactions in insects to model human infections. A good illustration of this approach was the discovery that the immune-activated signaling pathway mediated by the Toll receptor in the fly *Drosophila melanogaster* is partially conserved by a family of Toll-like receptors in humans (3, 4). This is now a cornerstone of the field, and much of the recent work in insects has involved further dissection of the molecular details of the Toll pathway and the related Immune deficiency (Imd) pathway (5). When activated by microbes, these two pathways

Insects use a variety of strategies to fight pathogens at different stages of infection, which may guide antimicrobial development for human use.

induce the massive production of antimicrobial peptides by host cells, and the loss of signaling that is caused by mutations in pathway components deeply compromises the fly's immune response (6).

Haine *et al.* show that the vast majority of bacteria are cleared from an insect before antimicrobial peptides are produced. In the mealworm beetle, *Tenebrio molitor*, immediate-acting immune responses, such as engulfment of bacteria by phagocytes (specialized immune cells) and melanization (in which bacteria are killed by reactive oxygen) likely do most of the heavy lifting when it comes to clearing microbes; more than 99.5% of injected bacteria are cleared from beetles, in the first hour of infection, before

Department of Microbiology and Immunology, Stanford University, CA 94305-5124, USA. E-mail: dschneider@stanford.edu



**Clearing and mopping up.** The majority of bacteria that infect an insect are cleared by immediate-acting immune responses, whereas the late-acting antimicrobial peptide immune response targets the few bacteria that are resistant to the early response.

any antimicrobial peptides are detectable. The authors hypothesize that the inducible antimicrobial peptide system removes residual microbes that are selected for resistance to the first wave of immune effectors.

The importance of this finding is that it provides a new logic for the order of immune events. The immediate-acting immune response followed by inducible antimicrobials in insects resembles the events that send a patient to the doctor—the patient's immune system fails to clear some microbes and the doctor gives them antimicrobials to cure the infection.

This two-step approach to immunity works well for insects, but in the clinic, resistance is an inevitable outcome of antibiotic use. What is different between these two systems? In insects, we observe pairs of constitutive responses and subsequent “mopping up” antimicrobials that have been selected through evolution. By contrast, the drugs we use in the clinic are chosen because they are cheap, immediately effective, and cause few side effects, not because they prevent further resistance. Another possible difference is that insects produce dozens of antimicrobial peptides at once to fight infections, whereas a patient might be given one or two antibiotics. It may be difficult for microbes to evolve resistance to a large panel of antimicrobials. Haine *et al.* found that even though antimicrobial peptides are produced, and bacterial levels are knocked down about ten thousandfold, the beetles don't clear the infections over the 2 week course of the experiment. This is a different outcome from what we demand of our doctors—a complete cure. That bacteria remain in infected bugs suggests that antimicrobial peptides aren't just bacteriocidal. They may be functioning at low concentrations to alter the physiology of the bacteria and reduce pathology.

The founding principle of *Drosophila* immunogenetics is that genetically identical

flies have similar immune responses. Hedges *et al.* found that flies carrying a common bacterial endosymbiont, *Wolbachia*, had increased resistance to two insect viruses when compared to genetically identical flies lacking *Wolbachia*. Consider the following: When either the Toll or Imd pathway is disrupted through mutation, pathogens can kill mutant flies 10 times as fast as their wild-type parents. The loss of *Wolbachia* produces a similar phenotype during viral infections. This is terrifying; few, if any, insect immunology studies report the *Wolbachia* status of their flies (7). Apart from the obvious question, “How does this work?” the finding of Hedges *et al.* raises other questions: Does the presence of *Wolbachia* affect the ability of the fly to fight other infections (bacterial, fungal, parasitoid, or protozoan)? Is *Wolbachia* the only member of the native microbiota that has this effect? Recent work with herpesvirus in mice demonstrates a protective effect of persistent viral infection on subsequent bacterial infections. Together, the studies by Haine *et al.* and Hedges *et al.* promote the broad theme that our native microbes are symbionts that shape our immune response (8).

Even without knowing the mechanisms underlying these immune processes, it is easy to imagine their ecological impact. *Wolbachia* is transmitted maternally, through the germ line (9). *Wolbachia* could provide a fitness advantage to flies in the field if these flies face viral infections, providing a mechanism to drive *Wolbachia* into a naïve population.

What would happen if *Wolbachia* affects an economically important insect, like honeybees, the way it affects flies? If bees that normally harbor *Wolbachia* were cured of their infections, the epidemiological picture in the field would be hard to work out from scratch. We would find that bees lost one minor microbe and that many infectious agents could then produce stronger or different dis-

eases than were seen in the past. This could be confusing because our methods are optimized for identifying infectious diseases caused by the presence of single pathogens.

One might guess that an insect would be safe from having its microbiota altered. Honeybees are an exception, however, because we've been dosing commercial colonies of bees with antibiotics for decades (10). Before the rise of colony collapse disorder, one of the most important honeybee diseases was American foulbrood, caused by the bacterium *Bacillus larvae*. To deal with this threat, many beekeepers prophylactically treat their hives with tetracycline derivatives—the same antibiotics used to cure flies of *Wolbachia*. If these treatments cured queen bees, then all hives descending from these queens would also be *Wolbachia* free, because the microbe is transmitted maternally. A *Wolbachia*-virus sensitivity experiment may have already been performed on honeybees nationwide and may change the way bees interact with previously characterized pathogens.

The beauty of the studies by Haine *et al.* and by Hedges *et al.* is that they take simple observations and step beyond direct mechanistic questions like, “What does it take to turn on this immune pathway?” and lead us into new territory. In the past, our justification for studying insect immunity was that the molecular mechanisms of signaling were evolutionarily conserved and it is faster to work in systems where you can do rapid genetic screens. This new work shows how studying the progression of disease in insects can teach us the logic behind the structure of the immune response and promises to teach us how to avoid the evolution of drug resistance. The studies highlight the notion that our body is an ecosystem and that our microbiota are an essential part of our immune system.

## References

1. E. R. Haine, Y. Moret, M. T. Siva-Jothy, J. Rolff, *Science* **322**, 1257 (2008).
2. L. M. Hedges, J. C. Brownlie, S. L. O'Neill, K. N. Johnson, *Science* **322**, 702 (2008).
3. B. Lemaitre, E. Nicolas, L. Michaut, J. Reichhart, J. Hoffmann, *Cell* **86**, 973 (1996).
4. R. Medzhitov, P. Preston-Hurlburt, C. A. Janeway Jr., *Nature* **388**, 394 (1997).
5. M. M. Shirasu-Hiza, D. S. Schneider, *Cell. Microbiol.* **9**, 2775 (2007).
6. M. S. Dionne, D. S. Schneider, *Dis. Model. Mech.* **1**, 43 (2008).
7. M. E. Clark, C. L. Anderson, J. Cande, T. L. Karr, *Genetics* **170**, 1667 (2005).
8. E. S. Barton *et al.*, *Nature* **447**, 326 (2007).
9. L. R. Serbus, C. Casper-Lindley, F. Landmann, W. Sullivan, *Annu. Rev. Genet.* **42**, 683 (2008).
10. J. D. Evans, *J. Invertebr. Pathol.* **83**, 46 (2003).

10.1126/science.1167450



CORRECTED 13 MARCH 2009; SEE LAST PAGE

# The Psychology of Transcending the Here and Now

Nira Liberman<sup>1</sup> and Yaacov Trope<sup>2</sup>

People directly experience only themselves here and now but often consider, evaluate, and plan situations that are removed in time or space, that pertain to others' experiences, and that are hypothetical rather than real. People thus transcend the present and mentally traverse temporal distance, spatial distance, social distance, and hypotheticality. We argue that this is made possible by the human capacity for abstract processing of information. We review research showing that there is considerable similarity in the way people mentally traverse different distances, that the process of abstraction underlies traversing different distances, and that this process guides the way people predict, evaluate, and plan near and distant situations.

Our experiences of the world are limited to the self, here and now, yet people, events, and situations that are beyond our immediate experience populate our mind. We plan for the future, remember the past, think about remote locations, take others' perspective, and consider alternatives to reality. In each case, we transcend the present to consider psychologically distant objects. An object is psychologically distant from us to the extent that it is remote in time (future or past) or in space; refers to experiences of others (e.g., relatives, acquaintances, or strangers); and unlikely to occur. But how do we transcend the present, evaluate, and make decisions with respect to psychologically distant objects? And how does increasing distance from objects affect the way we respond to these objects?

The question of how people transcend the present and respond to increasingly more distant objects is central to behavioral and social sciences, because both collective and personal human development is associated with traversing increasingly greater distances. The turning points of human evolution include developing tools, which required planning for the future; making function-specific tools, which required constructing hypothetical alternative scenarios of future events; developing language, which enabled forming larger and more complex social groups and relations; and domestication of animals and plants, which required an extended temporal perspective (1). Human history is associated with expanding horizons—traversing greater spatial distances (e.g., discovering new continents, space travel); forming larger social groups (families versus cities versus states versus global institutions); planning and investing in the more distant future; and reaching farther back into the

past. Human development in the first years of life involves acquiring the ability to plan for the more distant future, to consider possibilities that are not present, and to consider the perspective of more distant people [from self-centeredness to acknowledging others, from immediate social environment to larger social groups (2)].

Although evolution, history, and child development have different time scales, we propose that the expanding horizons that all of them entail require and are enabled by the human capacity for abstract mental representation. This hypothesis is based on Construal Level Theory (CLT) of psychological distance (3, 4), which links psychological distance from objects to the mental construal of those objects. In the following, we explain what we mean by mental construal and how it relates to traversing psychological distances. We then describe research findings demonstrating that there is considerable commonality in the way people traverse different dimensions of psychological distance; that similar mental construal processes underlie traversing different distance dimensions; and that these construal processes guide the way people predict, evaluate, and plan psychologically near and distant situations.

Any event or object can be represented at different levels of construal. Lower-level construals are concrete, relatively unstructured, and contextualized representations that include subordinate and incidental features of events. Higher-level construals are abstract, schematic, and decontextualized representations that extract the gist from



Musée des Beaux Arts

by W. H. Auden

About suffering they were never wrong,  
The Old Masters; how well, they understood  
Its human position; how it takes place  
While someone else is eating or opening a window or just walking dully along;  
....

In Bruegel's Icarus, for instance: how everything turns away  
Quite leisurely from the disaster; the ploughman may  
Have heard the splash, the forsaken cry,  
But for him it was not an important failure; the sun shone  
As it had to on the white legs disappearing into the green  
Water, and the expensive delicate ship that must have seen  
Something amazing, a boy falling out of the sky,  
had somewhere to get to and sailed calmly on.

**Fig. 1.** Bruegel the Elder's *Landscape with the Fall of Icarus* represents an intriguing mixture of high-level, abstract features, and low-level, concrete features.

<sup>1</sup>Department of Psychology, Tel Aviv University, Post Office Box 39040, Tel Aviv 69978, Israel. <sup>2</sup>Department of Psychology, New York University, 6 Washington Place, New York, NY 10003, USA.

\*To whom correspondence should be addressed. E-mail: niralib@post.tau.ac.il or yaacov.trope@nyu.edu

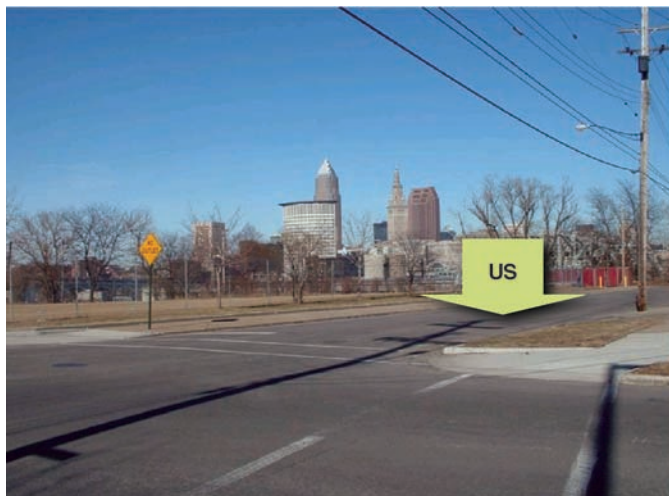


**Fig. 2.** Two examples of incongruent visual stimuli: a word denoting social proximity, “us,” located far from the observer, and a word denoting social remoteness, “them,” located near the observer. Because spatial distance is associated with temporal distance, social distance, and hypo-

theticality, participants are slower to indicate the location of the arrow and to identify the word on it with incongruent stimuli than with congruent stimuli [“us” located near the observer and “them” located far from the observer (6)].

the available information. They emphasize superordinate, core features of events and omit incidental features that may vary without significantly changing the meaning of events. Consider, for example, children playing basketball in the backyard. A lower-level construal of this activity might include such details as the children’s age, the color of the ball, and the temperature outside. A higher-level construal of the same activity might simply be “having fun.” The higher-level construal disregards the unique features of the event and entails an implicit decision about which features are central to the event and which are peripheral. For example, the omitted feature “basketball” could have been replaced with a jumping rope, but “having fun” would still apply. Given a different context or goal, however (e.g., “practicing basketball”), the same feature could become central and, therefore, included in a high-level construal. Regardless of the particular construal chosen, construing objects at higher-levels involves omitting features that are perceived as secondary and variable and retaining those aspects that are essential and invariant from the perspective of that high-level construct. At the same time, abstraction links the object to a more general set of objects and adds a new meaning that is not part of its more concrete, lower-level construal (e.g., “having fun” emphasizes the positive valence of “playing basketball outside” and connects it to such activities as “partying.”) Bruegel the Elder’s *Landscape with the Fall of Icarus* and its interpretation in Auden’s poem (Fig. 1) illustrate the tension between central and secondary aspects of a situation. In this painting, the ploughman witnesses the fall of Icarus. However, as he is immersed in the details of his immediate chore, he is oblivious to the significance of the event.

Objects that are more distant on any dimension will be represented at a more abstract, higher

level of construal, because higher-level construals capture those features of objects that remain relatively invariant with increasing distance, and thus enable prediction across distance. Well in advance, the children in our example may have known that they will have fun, but they could not know that they will play basketball outside, possibly because they did not know how cold it would be or whether a ball would be available. Similarly, high-level features tend to change less than low-level features across social distance—most people have fun from time to time, but only specific social groups would play basketball outside.

Construals may also affect perceived distance. Construing an object at a higher level connects it to other objects that span a wider range in time, space, social perspectives, and hypothetical situations and, therefore, brings to mind more distal times, places, people, and alternatives. For example, “having fun” relative to “playing basketball outside” would bring to mind experiences that span wider time and space and pertain to more diverse individuals and to more yet-unexperienced, hypothetical events.

In sum, different dimensions of psychological distance—spatial, temporal, social, and hypotheticality—correspond to different ways in which objects or events can be removed from the self, and farther removed objects are construed at a higher (more abstract) level. Three hypotheses follow from this analysis. (i) As the various dimensions map onto a more fundamental sense of psychological distance, they should be interrelated. (ii) All of the distances should similarly affect and be affected by the level of construal. People would think more abstractly about distant than about near objects, and more abstract construals would lead them to think of more distant objects. (iii) The various distances would have similar effects on prediction, evalu-

ation, and action. We now discuss research bearing on each of these hypotheses.

### The Interrelations Among Psychological Distance Dimensions

Try to complete the sentence “A long time ago, in a \_\_\_\_ place.” The tendency to complete it with “far away” rather than with “nearby” reflects not only a literary convention but also an automatic tendency of the human mind. Indeed, people use spatial metaphors to represent time in everyday language and reasoning (5). More generally, if psychological distance is reflected in different dimensions, then these dimensions should be mentally associated. Remote locations should bring to mind the distant rather than the near future, other people rather than oneself, and unlikely rather than likely events. Initial support for this hypothesis comes from a set of studies (6) in which participants viewed landscape photographs containing an arrow that was pointing to either a proximal or a distal point on the landscape. Each arrow contained a word denoting either psychological proximity (e.g., tomorrow, we, sure) or psychological remoteness (e.g., year, others, maybe) (Fig. 2). Participants had to respond by pressing one of two keys as quickly and as accurately as possible. In one version of the task, they had to indicate whether the arrow pointed to a proximal or distal location. In another version, they had to identify the word printed in the arrow [Stroop task (7)]. In both versions, participants responded faster to (i.e., processed more efficiently) distance-congruent stimuli (in which the spatially distant arrow contained a word that denoted large temporal distance, large social distance, or low likelihood and the spatially proximal arrow contained words that denoted temporal proximity, social proximity or high likelihood) than to distance-incongruent stimuli (in which spatially distal arrows contained



words denoting proximity and spatially proximal arrows contained words denoting remoteness).

These results suggest that spatial distance, temporal distance, social distance, and hypotheticality have a common meaning—psychological distance—and that people access this meaning spontaneously, even when it is not directly related to their current task. This view is consistent with research in neuroscience. Thinking about the future, remembering the past, and taking another person's perspective activate a common brain network involving the prefrontal cortex and the medial temporal lobe (8–10). Thus, the same neural substrate is activated by different forms of transcending the present.

### Psychological Distance and Level of Mental Construal

Our second hypothesis states that more distal objects in any dimension will be construed at a higher level. It may seem intuitive that from far away we see the forest, and, as we get closer, we see trees. It is also intuitive that to see the forest we need to step back, whereas to see the trees we need to get closer. These should apply, however, not only to spatial distance but also to other distance dimensions and not only to visual input, where it might seem a natural constraint of our perceptual system, but also to conceptual abstraction. We do not literally see either tomorrow or next year. Yet, we may think about tomorrow in terms of trees and about next year in terms of the forest. Moreover, thinking of trees may prompt us to think of tomorrow, whereas thinking of the forest may prompt us to think of next year. The link between distance and construal has important implications for perception, categorization, and inference.

**Perception.** In a series of studies, participants completed what they believed to be sample items of a task that required abstraction of coherent images from fragmented or noisy visual input [the Gestalt Completion Test (11) (Fig. 3)]. Participants' performance improved from 74% correct to 86% correct when they anticipated working on the actual task in the more distant future (12). Performance in the task also improved when participants thought the actual task was less likely to take place (13) and when social distance was enhanced by priming of high social status (14). A psychologically distant perspective thus seems to enable people to see the “big picture” better.

Although abstraction improves the ability to perceive the gestalt in a visual array, it has an opposite ef-

fect when the task requires attention to minute details. Distance should therefore have a detrimental effect on the ability to identify a missing element within a coherent whole. Indeed, participants did worse (57% correct versus 65% correct) on sample items of a task in which they had to find differences between two pictures when they believed they were less likely to complete the task later (13).

**Categorization.** We examined the effects of temporal distance on category breadth (15) by asking individuals to imagine an event (e.g., a camping trip) occurring in either the near or the distant future. For each event, participants grouped a set of related objects (e.g., tent, ball, snorkel) into as many groups as they deemed appropriate. Consistent with the idea that distance promotes the use of more abstract concepts, participants who thought of a more distant event created fewer, broader groups of objects.

Reduced likelihood and social distance had the same effect (13, 14). For example, objects that pertained to less likely events (e.g., a trip that had a high probability of being cancelled) were grouped into broader categories.

Actions, like objects, may be construed in high-level terms, which link them to a superordinate purpose (why one performs them), or in low-level terms, which link them to subordinate means (how one performs them). Here, too, greater psychological distance promotes higher levels of construal (16): Participants tended to describe more distant future activities (e.g., studying) in high-level terms (e.g., “doing well in school”) rather than in low-level terms (e.g., “reading a textbook”). Similar effects emerged when actions were to take place in a spatially distant location (17), when the actions were framed as unlikely to actually take place (13), and when the actor was described as dissimilar to the perceiver (18).

**Inference.** We can explain others' behavior in terms of abstract dispositions of the actor (traits, values, and attitudes) or in terms of specific situational factors. If someone steps on your foot in an elevator, for example, you might say to yourself, “she is clumsy” or “the elevator is too crowded.” In terms of CLT, the former constitutes a high-level construal, whereas the latter constitutes a low-level construal. Social psychological research has shown that various forms of social distance are associated with emphasizing high-level personal dispositions and underweighting low-level situational factors. For example, people's explanation of their own behavior emphasizes concrete situational factors that operate at the moment of action, whereas their explanation of others' behavior emphasizes stable and personal dispositions (19, 20). In a related vein, personal memories that are recalled from a third-person perspective rather than from a first-person perspective (e.g., “try to remember your first day at school, as if you are a kid again” versus “... as if you are now watching the kid you were”) tend to employ dispositional (as opposed to situational) terms (21, 22). Similarly, group perception research shows that compared with in-groups, out-groups are described in more abstract terms and believed to possess more global and stable traits [e.g. (23, 24, 25)].

In accordance with the predictions of CLT, research has found



**Fig. 3.** Items from the Gestalt Completion Test (11). Identifying the pictures (from top-right to bottom left: a boat, a rider on a horse, a rabbit, a baby) requires visual abstraction. Participants were better at identifying pictures that they believed were sample items of a more distant future task (12) or a less likely task (13).

that other psychological distances produce similar effects. Behavior that is expected to occur in the more distant future is more likely to be explained in dispositional rather than in situational terms (26). Another study (27) extended this finding to spatial distance. Participants drew stronger inferences about others' personality from behaviors that took place in spatially distal, as compared with spatially proximal locations. These findings suggest that we believe that personality is reflected in what people do in distant times and places rather than in proximal ones.

*Reciprocal relation between construal level and distance.* If high-level construals serve to represent psychologically distant events, then activating high-level construals should lead people to think of events in psychologically more distant situations. For example, if social and temporal remoteness enhance the tendency to think of a person's abstract traits, then thinking of a person's traits should bring to mind socially and temporally remote situations. Indeed, we found that thinking about an activity in high level, "why," terms rather than low level, "how," terms led participants to think of the activity as taking place in more distant points in time (28).

The associations between distance and level of construal was also demonstrated with an Implicit Associations Test (29, 30). Participants in these studies were presented with words from four categories: high-level construal (e.g., category names such as "drinks"); low-level construal (e.g., exemplar names such as "Coke"); small psychological distance (e.g., socially proximal words such as "ours" or "friend"); and large psychological distance (e.g., socially distant words such as "theirs" or "stranger"). Participants mapped words from these four categories on two responses, pressing either a left key or a right key on the computer keyboard. On congruent trials, high-level stimuli were paired with distant stimuli and low-level stimuli were paired with proximal stimuli, whereas on incongruent trials, high-level stimuli were paired with proximal stimuli and low-level stimuli were paired with distal stimuli. With all four dimensions of psychological distance, participants were faster with congruent than with incongruent pairings, which suggested that they implicitly associated large psychological distances with high-level construal and small psychological distances with low-level construal.

In sum, research shows that as psychological distance increases, construals become more abstract, and as level of abstraction increases, so too do the psychological distances people imagine. These findings suggest that abstract thinking is used to transcend the present and expand one's mental horizon by thinking farther into time and space and considering remote social targets and unlikely possibilities. It is noteworthy that neuropsychological research has shown that the brain is hierarchically organized with higher points in the cortical hierarchy representing increasingly more abstract aspects of stimuli (31, 32). For

example, progressively anterior subregions of the prefrontal cortex have been found to be associated with more abstract representations (33–35). Possibly, this organization of information in the brain might be related to distance from stimuli, such that activation systematically progresses to higher points in the hierarchy as psychological distance from the stimuli increases.

### The Effect of Psychological Distance on Prediction, Evaluation, and Behavior

We make predictions, evaluations, and choices with respect to our construal of objects rather than the objects themselves. These construals depend not only on the actual attributes of the objects, but also on their psychological distance. It follows that distance in time and space, social distance, and probability should similarly affect prediction, evaluation, and behavior inasmuch as they all lead people to rely on higher-level construals.

*Psychological distance and prediction.* Normatively, distant events should be predicted with less certainty than near events. Because we know less about the more distant future, for example, we should be less confident when making predictions about temporally distal events. According to CLT, however, higher-level construals should actually make people more certain in predicting more distant outcomes. As suggested earlier, the very function of high-level construals is to enable individuals to transcend mentally the "here and now" by forming a structured representation of the invariant features of the available information and projecting it onto distal objects. Consequently, predictions of future experiences would be more schematic than the actual experiences, giving rise to a variety of prediction biases that stem from underweighting contextual and incidental features (36–38). In accordance with this reasoning, students were more confident that an experiment would yield theory-confirming results when they expected the experiment to take place in a more distant point in time (39). Apparently, when making predictions for the more distant experiment, participants gave more weight to the theory (high-level construal) and less weight to incidental noise factors (low-level construal).

In a study that investigated the effect of spatial distance on the tendency to base predictions on global versus local information (27), New York University (NYU) participants viewed a series of graphs depicting information from the years 1999 to 2004 (e.g., average number of photocopies per student). The information was said to pertain to the NYU campus in Manhattan (spatially near condition) or to the NYU campus in Florence, Italy (spatially distant condition). Each graph showed either an upward or a downward trend, with the final year (2004) always deviating from that global trend. Participants estimated the likelihood that the year 2005 would be consistent with the general trend or with the more recent local deviation. In terms

of CLT, global trends convey a high-level construal, whereas deviations, being local exceptions, should receive more weight in low-level construals. Consistent with this reasoning, spatial distance enhanced the tendency to predict on the basis of the global trend rather than on the basis of local deviation.

*Psychological distance and evaluation.* A common assumption in the behavioral sciences is that the value of an outcome diminishes as temporal distance from the outcome increases (40–42)—positive outcomes seem less positive when removed in time (intertemporal discounting). The prediction from CLT, however, is that increased temporal distance, as with any psychological distance, should shift the overall attractiveness of an outcome closer to its high-level construal value and away from its low-level construal value. When the low-level value of an outcome is more positive than its high-level value, temporal discounting would obtain, so that the outcome would be less attractive in the more distant future. When the high-level value of an outcome is more positive, however, the outcome should be more attractive in the distant future.

According to CLT, central, goal-related features of outcomes constitute a high-level construal of these outcomes, whereas peripheral, goal-irrelevant features of outcomes constitute a low-level construal. Distancing an outcome should therefore increase the weight of central features relative to peripheral features. Support for this prediction was found in a study in which participants imagined buying a radio set in order to listen to morning programs either the next day or in one year (43). In one version, participants were informed that the sound quality of the radio set was good, but that the built-in clock was relatively useless. In a different version, participants were informed that the sound quality of the radio set was poor, but that the clock turned out to be quite useful. Participants had to rate their satisfaction from the imagined purchase of the radio set. As predicted, thinking about the radio set in the more distant future increased satisfaction when the sound quality was good and the clock was useless, but decreased satisfaction when the sound quality was poor and the clock was good, which indicated that time distance increased the weight of central features and decreased the weight of peripheral features. It seems, then, that people's overriding goals are more likely to guide their choices for psychologically distant than for psychologically near situations.

Desirability concerns involve the value of the action's end state (a high-level construal), whereas feasibility concerns involve the means used to reach the end state (a low-level construal). Therefore, desirability concerns should receive greater weight over feasibility concerns as psychological distance increases. Consistent with this prediction, we found that as temporal distance from an activity (e.g., attending a guest lecture) increased, the attractiveness of the activity depended more on its desirability (e.g.,



how interesting the lecture was) and less on its feasibility (e.g., how convenient the timing of the lecture was) (16). As a result, people are more likely to end up overcommitting themselves when planning the distant future than near future, as they would neglect constraints (16). Similar results emerged with probability as a psychological distance dimension (44). These findings suggest that distance increases the attractiveness of alternatives that are desirable but hard to obtain, but decreases the attractiveness of alternatives that are less desirable but easy to obtain. Extending this effect to the realm of risky choice, we found that people take greater risks (i.e., favoring bets with a low probability of winning a high amount over those that offer a high probability to win a small amount) in decisions about temporally more distant bets (45).

**Psychological distance and behavior.** Like predictions and evaluations, behavior should be increasingly based on high-level construal aspects as psychological distance increases. As outcomes seem more temporally, spatially, or socially remote or unlikely to materialize, actions should be guided more by one's central, global concerns and less by one's secondary, local concerns.

Issues within interpersonal negotiation can differ in their centrality and worth. If negotiators can concede on secondary issues in exchange for getting what they want on high-priority issues, a process called logrolling, they are more likely to maximize both individual and joint outcomes. Because negotiators would be expected to focus more on central concerns and less on peripheral concerns as distance increases, this should lead to more logrolling agreements about more distal situations. In line with this prediction, a study of live negotiation (46) found that 91% of dyads with a temporally distant perspective reached a fully logrolling agreement as compared with only 50% of dyads with a temporally near perspective.

Exercising self-control requires acting in line with one's central, superordinate, and global considerations in the presence of more locally tempting alternatives. Because such considerations naturally relate to high-level construals, psychological distance should facilitate self-control. Indeed, people seem to be better able to choose delayed but valuable outcomes for the distant than for the near future (47). As another example, choosing a negative but diagnostic assessment of one's abilities rather than a flattering but non-diagnostic assessment requires prioritizing the long-term benefits of self-improvement over subordinate concerns about feeling good. Consistent with this prediction, participants were more likely to prefer the negative but diagnostic assessment when it was expected in the more distant future (48). A recent series of studies (49) has directly linked construal level to self-control, showing that forming a high-level construal of situations enhanced self-control (e.g., choosing a delayed reward, enduring painful but valuable diagnostic procedures). In the same vein, research on delay of gratification in children showed that

an abstract representation of the temptation increases delay relative to a more concrete representation (50).

In summary, a range of studies suggests that people rely on high-level construals to a greater extent when predicting, evaluating, and taking action with respect to more distant situations. Ironically, the increasing reliance on high-level construals for more distant situations often leads people to make more confident predictions, more polarized evaluations, and clearer choices. This result is counterintuitive if one believes that distant situations should afford less certainty and thus reduce confidence and decisiveness.

## Conclusion

Considerable research across the behavioral sciences has examined how people respond to events in the recent versus distant past and the near versus distant future, to spatially near versus far objects, to themselves versus others, and to real versus hypothetical or probable versus improbable events. Without denying the uniqueness of each distinction, we propose that they all constitute dimensions of psychological distance. Their point of origin is one's direct experience of the "here and now." Transcending this point entails constructing mental models of what is not directly experienced, and the farther removed an object is from direct experience, the higher (more abstract) the level of construal of that object. Lower-level construals enable people to be immersed in the rich details of the immediate situation, whereas higher-level construals enable appraisal of the general meaning that might apply across a wide range of alternatives. Consistent with this proposal, the research reviewed in this article suggests that different distance dimensions are mentally associated, that distancing on any of these dimensions is associated with higher levels of construal, and that they have similar effects on prediction, evaluation, and behavior.

## References and Notes

1. M. Flinn, D. Geary, C. Ward, *Evol. Hum. Behav.* **26**, 10 (2005).
2. T. Suddendorf, M. C. Corballis, *Behav. Brain Sci.* **30**, 335 (2007).
3. N. Liberman, Y. Trope, E. Stephan, in *Social Psychology: A Handbook of Basic Principles*, E. T. Higgins, A. W. Kruglanski, Eds. (Guilford, New York, 2007), pp. 353–381.
4. Y. Trope, N. Liberman, *Psychol. Rev.* **110**, 403 (2003).
5. D. Casasanto, L. Boroditsky, *Cognition* **106**, 579 (2008).
6. Y. Bar-Anan, N. Liberman, Y. Trope, D. Algom, *J. Exp. Psychol. Gen.* **136**, 610 (2007).
7. R. Stoop, *J. Exp. Psychol.* **18**, 643 (1935).
8. D. R. Addis, D. L. Schacter, *Hippocampus* **18**, 227 (2008).
9. R. L. Buckner, D. C. Carroll, *Trends Cogn. Sci.* **11**, 49 (2007).
10. D. L. Schacter, D. R. Addis, R. B. Buckner, *Nat. Rev. Neurosci.* **8**, 657 (2007).
11. R. B. Ekstrom, J. W. French, H. H. Harman, D. Dermen, *Manual for Kit of Factor-Referenced Cognitive Tests* (Educational Testing Service, Princeton, NJ, 1976).
12. J. Förster, R. S. Friedman, N. Liberman, *J. Pers. Soc. Psychol.* **87**, 177 (2004).
13. C. J. Wakslak, Y. Trope, N. Liberman, R. Alony, *J. Exp. Psychol. Gen.* **135**, 641 (2006).
14. P. K. Smith, Y. Trope, *J. Pers. Soc. Psychol.* **90**, 578 (2006).
15. N. Liberman, M. C. Sagristano, Y. Trope, *J. Exp. Soc. Psychol.* **38**, 523 (2002).
16. N. Liberman, Y. Trope, *J. Pers. Soc. Psychol.* **75**, 5 (1998).
17. K. Fujita, M. D. Henderson, J. Eng, Y. Trope, N. Liberman, *Psychol. Sci.* **17**, 278 (2006).
18. I. Liviatan, Y. Trope, N. Liberman, *J. Exp. Soc. Psychol.* **44**, 1256 (2008).
19. E. E. Jones, R. E. Nisbett, in *Attribution: Perceiving the Causes of Behavior*, E. E. Jones et al., Eds. (General Learning Press, Morristown, NJ, 1972), pp. 79–94.
20. D. T. Gilbert, E. C. Pinel, T. D. Wilson, S. J. Blumberg, T. P. Wheatley, *J. Pers. Soc. Psychol.* **75**, 617 (1998).
21. M. G. Frank, T. Gilovich, *J. Pers. Soc. Psychol.* **57**, 399 (1989).
22. G. Nigro, U. Neisser, *Cognit. Psychol.* **15**, 467 (1983).
23. K. Fiedler, G. R. Semin, C. Finkenauer, I. Berkel, *Pers. Soc. Psychol. Bull.* **21**, 525 (1995).
24. B. Park, C. M. Judd, *J. Pers. Soc. Psychol.* **59**, 173 (1990).
25. P. W. Linville, G. W. Fischer, C. Yoon, *J. Pers. Soc. Psychol.* **70**, 421 (1996).
26. S. Nussbaum, Y. Trope, N. Liberman, *J. Pers. Soc. Psychol.* **84**, 485 (2003).
27. M. D. Henderson, K. F. Fujita, Y. Trope, N. Liberman, *J. Pers. Soc. Psychol.* **91**, 845 (2006).
28. N. Liberman, Y. Trope, S. M. McCrae, S. J. Sherman, *J. Exp. Soc. Psychol.* **43**, 143 (2007).
29. A. G. Greenwald et al., *Psychol. Rev.* **109**, 3 (2002).
30. Y. Bar-Anan, N. Liberman, Y. Trope, *J. Exp. Psychol. Gen.* **135**, 609 (2006).
31. K. Grill-Spector, R. Malach, *Annu. Rev. Neurosci.* **27**, 649 (2004).
32. M. D. Liberman, R. Gaunt, D. T. Gilbert, Y. Trope, in *Advances in Experimental Social Psychology*, M. Zanna, Ed. (Academic Press, New York, 2002), vol. 34, pp. 200–249.
33. D. Badre, M. J. D'Esposito, *J. Cogn. Neurosci.* **19**, 2082 (2007).
34. E. Koehlin, C. Summerfield, *Trends Cogn. Sci.* **11**, 229 (2007).
35. N. Ramnani, A. M. Owen, *Nat. Rev. Neurosci.* **5**, 184 (2004).
36. D. T. Gilbert, T. D. Wilson, *Science* **317**, 1351 (2007).
37. T. D. Wilson, D. T. Gilbert, in *Advances in Experimental Social Psychology*, P. Mark, Ed. (Elsevier Academic Press, San Diego, CA, 2003), vol. 35, pp. 345–411.
38. A. Kahneman, A. B. Krueger, D. Shkade, N. Schwarz, D. A. Stone, *Science* **312**, 1908 (2006).
39. S. Nussbaum, N. Liberman, Y. Trope, *J. Exp. Psychol. Gen.* **135**, 152 (2006).
40. G. Ainslie, *Psychol. Bull.* **82**, 463 (1975).
41. T. Schelling, *Am. Econ. Rev.* **74**, 1 (1984).
42. T. O'Donoghue, M. Rabin, *J. Behav. Decis. Making* **13**, 233 (2000).
43. Y. Trope, N. Liberman, *J. Pers. Soc. Psychol.* **79**, 876 (2000).
44. A. Todorov, A. Goren, Y. Trope, *J. Exp. Soc. Psychol.* **43**, 473 (2007).
45. M. Sagristano, Y. Trope, N. Liberman, *J. Exp. Psychol. Gen.* **131**, 364 (2002).
46. M. D. Henderson, Y. Trope, P. J. Carnevale, *J. Pers. Soc. Psychol.* **91**, 712 (2006).
47. D. Read, G. Loewenstein, R. Baumeister, Eds., *Time and Decision* (Russell Sage Foundation, New York, 2003).
48. A. L. Freitas, P. Salovey, N. Liberman, *J. Pers. Soc. Psychol.* **80**, 410 (2001).
49. K. Fujita, Y. Trope, N. Liberman, M. Levin-Sagi, *J. Pers. Soc. Psychol.* **90**, 351 (2006).
50. W. Mischel, Y. Shoda, M. L. Rodriguez, *Science* **244**, 933 (1989).
51. This research was supported by an Israeli Science Foundation grant 1346-2004 to N.L., a Binational Science Foundation grant 2001-057 to N.L. and Y.T., and a National Institute of Mental Health, NIH, grant R01 MH059030 to Y.T.

10.1126/science.1161958

## ERRATUM

*Post date 13 March 2009*

**Reviews:** "The psychology of transcending the present" by N. Liberman and Y. Trope (21 November 2008, p. 1201). On page 1203, the legend to Fig. 3 should read as follows: "Items from the Street Gestalt Completion Test (courtesy of Teachers College, Columbia University)." The text referring to the figure should be changed to "the Gestalt Completion Test (Fig. 3), see also (11)."



# Fossil Pollen as a Guide to Conservation in the Galápagos

Jacqueline F. N. van Leeuwen,<sup>1</sup> Cynthia A. Froyd,<sup>2\*</sup> W. O. van der Knaap,<sup>1</sup> Emily E. Coffey,<sup>2</sup> Alan Tye,<sup>3†</sup> Katherine J. Willis<sup>2,4</sup>

In the Galápagos Islands, one of the greatest current ecological threats is the detrimental impact of nonnative plant species introduced since European contact almost 500 years ago (1); removal of nonnative species has become a key conservation-restoration priority. The situation in the Galápagos is typical of many biodiverse oceanic islands; globally, millions of dollars are spent annually on the control of invasive plant species. Ecologically appropriate restoration, however, requires the accurate determination of species' provenance: Is a species native or introduced to a region? Although this might seem relatively straightforward in well-documented ecosystems, such information is not always readily available for many of the most-biodiverse or unique landscapes. In these, nonnative species status designations frequently have their basis in what can only be termed ecological conjecture, often derived from status determinations in neighboring areas; the date and site of first appearances in herbarium collections; the characteristics of the existing species distribution, including active current changes in distribution; and association of the species with humans.

The study of fossil pollen and plant remains preserved in sedimentary deposits reveals species' distributions over recent millennia. By using these techniques (2), we show that at least six presumed nonnative or doubtfully native species (*Ageratum conyzoides*, *Borreria laevis*/*Diodia radula*-type, *Brickellia diffusa*, *Cuphea carthagenensis*, *Hibiscus diversifolius*, and *Ranunculus flagelliformis*) are in fact native to the Galápagos archipelago (Fig. 1) *B. laevis* and *D. radula* cannot be distinguished palynologically and are combined in one type. Of the six species, *H. diversifolius* has been identified as a possible invasive habitat transformer posing a potential threat to the island ecosystem (3). The others are mostly pantropical weedy species commonly identified as introduced or invasive throughout the Pacific Islands (4). All of these species have been identified as nonnative by at least one of the Galápagos botanical authorities (5, 6) (inferred for the recently discovered *R. flagelliformis*); however, questions

concerning their provenance have led conservationists to regard them as doubtfully native.

The first human presence in Galápagos is believed to have occurred with European contact in 1535 (7). Abundant fossil pollen of the species shown in Fig. 1 has been found in sediment sequences from four sites in the highlands of Santa Cruz Island, in the center of the Galápagos archi-

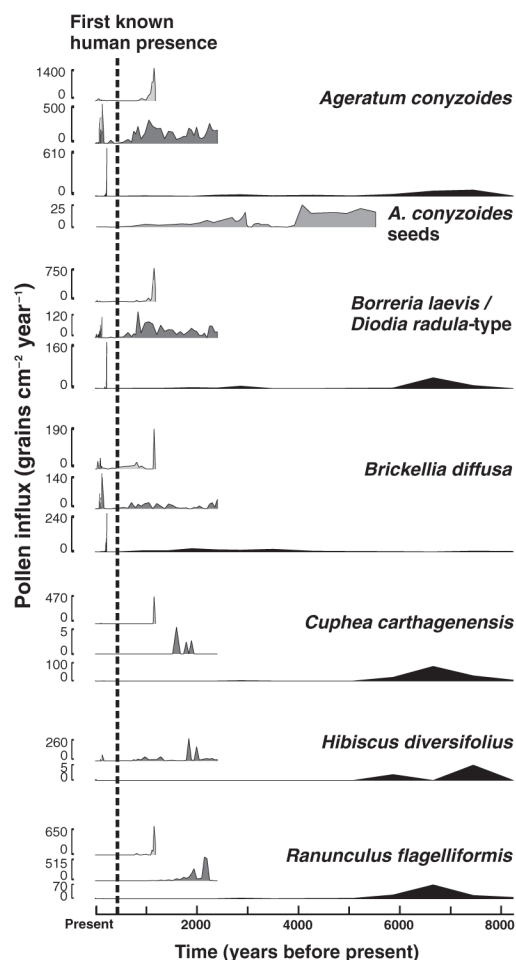


**Fig. 1.** Pollen influx (grains  $\text{cm}^{-2}$  of sediment  $\text{year}^{-1}$ ) and accumulation rate of *A. conyzoides* seed fragments  $>125 \mu\text{m}$  (pieces  $\text{cm}^{-2}$  of sediment  $\text{year}^{-1}$ ) for four sites in the Santa Cruz highlands, Galápagos, Ecuador. Pollen results for Psidium Bog [~1200 calendar years before the present (cal. yr B.P.)] are shown in light gray, Tiny Bog (~2400 cal. yr B.P.) in dark gray, and Inconspicuous Bog (~8200 cal. yr B.P.) in black. *A. conyzoides* seed fragment results are from East Bog (~5500 cal. yr B.P.).

pelago. All six pollen taxa were present thousands of years before the advent of human impact, providing evidence of their native status. Early macrofossil evidence of *A. conyzoides* (from about 5400 years ago) further confirms the palynological results (Fig. 1). All of these species are present in the Santa Cruz highlands today, although some, such as *H. diversifolius* and *R. flagelliformis*, are currently quite rare compared with their much higher abundances in the past. In fact, at present *H. diversifolius* appears to be spreading on Santa Cruz, which had been interpreted as evidence for its invasive status but may be the result of a re-occupation of former habitats. Nonnative species with such limited distributions are often perceived to be more suitable targets for eradication, particularly if believed to be either recent arrivals (for example, *R. flagelliformis* was only first discovered in Galápagos in 1972) or habitat transformers (for example, *H. diversifolius*).

The risk of applying inappropriate management to what are in fact native species is highlighted by these results. Paleoecology also has wider implications for the classification of invasive species throughout the Pacific Islands. It is probable that these six species are native to other regions in the Pacific where they may have been classified as nonnative and also that there may be other presumed invasives that have been incorrectly designated.

## References and Notes

1. J. Magee et al., *Science* **294**, 1279 (2001).
2. Materials and methods are available on Science Online.
3. Database of the Galápagos Flora, Department of Botany, Charles Darwin Research Station, Galápagos, Ecuador.
4. U.S. Forest Service Pacific Island Ecosystems at Risk (PIER), [www.hear.org/pier/](http://www.hear.org/pier/).
5. J. E. Lawesson et al., *Rep. Bot. Inst. Univ. Aarhus* **16**, 1 (1987).
6. D. M. Porter, in *Patterns of Evolution in Galapagos Organisms*, R. I. Bowman, M. Berson, A. E. Leviton, Eds. (American Association for the Advancement of Science, San Francisco, 1983), pp. 33–96.
7. R. C. Suggs, *Z. Ethnol.* **92**, 239 (1967).
8. We thank I. Robertson for helpful comments on the manuscript, the Galápagos National Park Service, and I. Flett and P. Q. Dresser for radiocarbon dates. This research was supported by the UK Natural Environment Research Council (grant NE/C510667/1 awarded to K.J.W. and C.A.F.), the National Geographic Society and the Swiss Association of Friends of the Galápagos Islands (W.O.v.d.K.), and European Commission grant 017008-2.

## Supporting Online Material

[www.sciencemag.org/cgi/content/full/322/5905/1206/DC1](http://www.sciencemag.org/cgi/content/full/322/5905/1206/DC1)  
Materials and Methods  
Tables S1 and S2  
References

18 July 2008; accepted 2 September 2008  
10.1126/science.1163454

<sup>1</sup>Institute of Plant Sciences and Oeschger Centre for Climate Change Research, University of Bern, Altenbergrain 21, CH-3013 Bern, Switzerland. <sup>2</sup>Long-Term Ecology Laboratory, Oxford University Centre for the Environment, South Parks Road, Oxford OX1 3QY, UK. <sup>3</sup>Charles Darwin Research Station, Galápagos, Ecuador. <sup>4</sup>Department of Biology, University of Bergen, N-5007 Bergen, Norway.

\*To whom correspondence should be addressed. E-mail: [cynthia.froyd@ouce.ox.ac.uk](mailto:cynthia.froyd@ouce.ox.ac.uk)

†Present address: Secretariat of the Pacific Regional Environment Programme (SPREP), Post Office Box 240, Apia, Samoa.

# Time-Resolved Dynamics in N<sub>2</sub>O<sub>4</sub> Probed Using High Harmonic Generation

Wen Li,<sup>1\*</sup> Xibin Zhou,<sup>1</sup> Robynne Lock,<sup>1</sup> Serguei Patchkovskii,<sup>2</sup> Albert Stolow,<sup>2</sup> Henry C. Kapteyn,<sup>1</sup> Margaret M. Murnane<sup>1</sup>

The attosecond time-scale electron-recollision process that underlies high harmonic generation has uncovered extremely rapid electronic dynamics in atoms and diatomics. We showed that high harmonic generation can reveal coupled electronic and nuclear dynamics in polyatomic molecules. By exciting large amplitude vibrations in dinitrogen tetroxide, we showed that tunnel ionization accesses the ground state of the ion at the outer turning point of the vibration but populates the first excited state at the inner turning point. This state-switching mechanism is manifested as bursts of high harmonic light that is emitted mostly at the outer turning point. Theoretical calculations attribute the large modulation to suppressed emission from the first excited state of the ion. More broadly, these results show that high harmonic generation and strong-field ionization in polyatomic molecules undergoing bonding or configurational changes involve the participation of multiple molecular orbitals.

In polyatomic molecules, electronic and vibrational excitations can couple and rapidly redistribute both energy and charge during dynamic processes. Because of the importance of these dynamics in chemical and biological systems, the ability to probe dynamics in larger polyatomic molecules ultimately is a requirement for any broadly useful spectroscopy or dynamical imaging technique. As an example, time-resolved photoelectron spectroscopy (TRPES) is a weak-field perturbative method that can probe these dynamics (1–3). In TRPES, the molecule is first excited by a pump pulse. A time-delayed probe pulse then projects the complex evolving wave packet onto the molecular ionization continuum, and the outgoing electron is analyzed as a function of pump-probe delay. The cation electronic states, their associated electronic continua, and the vibrational structure of the ionization continuum are used as “templates” for projecting out the electronic and vibrational components of the complex wave packet. This evolving projection onto multiple electronic continua permits the disentangling of electronic and vibrational dynamics during nonadiabatic processes in polyatomic molecules (4).

High harmonic generation (HHG) is a strong-field nonperturbative process (5, 6) that is closely related to photoelectron spectroscopy, occurring at laser intensities of  $>10^{13}$  W cm<sup>-2</sup>. In atoms, HHG is successfully described by an adiabatic single active electron (SAE) model involving three steps: strong-field tunnel ionization, propagation of the continuum electron in response to

the laser field, and finally, recombination of the electron with its parent ion, which results in the emission of a high-energy photon (7–10). However, in the case of HHG from a polyatomic molecule, the physics is more complex because of the many-body electronic structure of polyatomic molecules and the existence of rovibrational and nonadiabatic dynamics. The recombination matrix element for the HHG process and the photoionization matrix element of the photoabsorption process are the same because these steps are the inverse of each other. Therefore, the multiple electronic continua relevant to probing complex polyatomic dynamics via TRPES must also play a role when HHG is used to probe these dynamics. The use of HHG as a probe has two potential advantages over TRPES: the ability to access attosecond-time-scale processes and the ability of HHG to simultaneously probe with many photon energies. However, until recently (11, 12), only the highest occupied molecular orbital (HOMO) has usually been considered to explain both strong-field ionization and high harmonic emission. This simplification comes from the adiabatic and SAE approximations that underlie theories of tunnel ionization in atoms and molecules [Ammosov-Delone-Krainov (ADK) and molecular ADK (13, 14) models] and are integral to the three-step model of HHG (7–9). In polyatomic molecules, however, both approximations can fail dramatically, particularly so when the molecule is dynamically evolving, as we show here. Strong-field ionization can become nonadiabatic and involve multielectron excitations (15, 16). Theoretical efforts to relax the SAE approximation are being attempted in order to address these issues by introducing multielectron effects in the recombination step of HHG (11, 12, 17, 18).

Prior investigations showed that HHG from rotational axis-aligned molecules is a potential

probe of static molecular structure (19, 20) because the emission strength depends on the molecular orbital nature of the ground electronic state and its alignment with respect to the laser field. Recent related work used the photoelectrons released and rescattered during the strong-field ionization process to recover the static orbital structure of simple diatomic molecules (21). HHG was also used as a probe of simple dynamics in molecules in which, for example, the molecular structure varied slightly without any bond reorganization. Past work showed that the HHG process is sensitive to simple vibrational dynamics in a molecule, even to modes that cannot readily be optically probed (22, 23). The rearrangement of atoms within a molecule during the HHG process can also be inferred by comparing HHG spectra of isotope-substituted molecules (24). Chemical dynamics, however, involve large-amplitude motions. HHG experiments have yet to succeed in observing and understanding large-amplitude structural rearrangements within a polyatomic molecule, in which the simple assumptions are unlikely to remain valid because of dramatic and evolving changes in the ionization/recombination dynamics.

We successfully applied HHG as a time-resolved probe of chemical dynamics in a polyatomic molecule. By exciting a large-amplitude vibrational wave-packet motion in the ground state of a dinitrogen tetroxide (N<sub>2</sub>O<sub>4</sub>) molecule, we observed large modulations in harmonic yield. We discovered that at the outer turning point of the vibration, tunnel ionization populates the ground state of the ion (HOMO<sup>+</sup> A<sub>g</sub> continuum), which has a large recombination dipole and therefore a high probability for harmonic emission. In contrast, at the inner turning point, the first excited state of the ion is populated by tunnel ionization [that is, the (HOMO-1)<sup>+</sup> B<sub>2g</sub> continuum]. This channel has a reduced recombination cross-section and thus suppresses the harmonic emission.

**HHG probing of N<sub>2</sub>O<sub>4</sub> dynamics.** N<sub>2</sub>O<sub>4</sub> is a dimer of NO<sub>2</sub>, with a dissociation energy of ~0.65 eV. N<sub>2</sub>O<sub>4</sub> can be present in dominant quantities (80%) even at room temperature. The molecule has D<sub>2h</sub> symmetry and six Raman-active vibrational modes, the strongest being the low-frequency N-N symmetric stretch (265 cm<sup>-1</sup>, 0.03 eV). By nonresonantly exciting this mode via impulsive stimulated Raman scattering (ISRS), we were able to generate a large-amplitude ground-state vibrational wave packet along the N-N coordinate. This large-amplitude motion correlates upon ionization with a broad range of ionic configurations, leading to the participation of more than one molecular ionization continuum in the HHG process (Fig. 1).

In our experiment, ultrashort laser pulses from a Ti:sapphire laser system (800 nm, ~30 fs, 4 mJ, and 1 kHz) were split into pump and

<sup>1</sup>JILA and Department of Physics, University of Colorado and National Institute of Standards and Technology, Boulder, CO 80309-0440, USA. <sup>2</sup>Steele Institute for Molecular Sciences, National Research Council, Ottawa, ON K1A 0R6, Canada.

\*To whom correspondence should be addressed. E-mail: wli@jila.colorado.edu

probe pulses. The pump pulse was focused onto a  $\text{N}_2\text{O}_4$  gas jet (backing pressure  $\sim 700$  torr) at an incident intensity of  $\sim 2 \times 10^{13} \text{ W cm}^{-2}$  to impulsively excite ground-state vibrations in the molecule. The time-delayed probe pulse was focused to an intensity of  $\sim 2 \times 10^{14} \text{ W cm}^{-2}$  to generate high harmonics from the vibrationally excited molecules. The relative polarizations of the pump and the probe pulses were controlled using a half-wave plate in the pump-beam path. The generated harmonics were then spectrally separated using an extreme ultraviolet (EUV) spectrometer and imaged onto an EUV-sensitive charge-coupled device camera (Andor Technology, South Windsor, CT). The ion signal could also be collected using a mass spectrometer.

In Fig. 2A, we show the experimentally observed high harmonics, from orders 15 to 23, as a function of pump-probe time delay. Lower-order harmonics were not observed because of absorption by the  $0.2\text{-}\mu\text{m}$ -thick aluminum filter that was used to reject the pump laser light. Even in the raw data, a time-dependent oscillation of the harmonic yield is apparent. For all the harmonic orders observed, the time dependence of the HHG emission (Fig. 2C) shows several common characteristics: a sudden drop in HHG yield when the sample is initially excited at time-zero followed by strong oscillations in the HHG yield imposed on a slowly rising baseline. The strong suppression of harmonic generation at time zero is a result of coherent effects due to the overlap of the pump and probe. Strong oscillations in the harmonic yield are present for both parallel and perpendicular polarizations of the pump and probe (Fig. 2).

#### Harmonic modulation by the N-N stretch.

The origin of the strong oscillations in the harmonic yield becomes apparent if we apply a discrete Fourier transform to these data. A single peak at  $255 \pm 10 \text{ cm}^{-1}$  appears in the transform spectra (Fig. 2, C and D, insets). This frequency corresponds unambiguously to the Raman active  $265 \text{ cm}^{-1}$  N-N stretch mode of  $\text{N}_2\text{O}_4$ . Given the ISRS pump mechanism employed here, the initial motion of the vibrational wave packet will be repulsive, with the outer turning point occurring one quarter period after the pump pulse. To verify the exact timing of the emission, we used argon gas in the same setup because HHG from argon exhibits a transient only at time zero because of coherent effects. We thus verified that in  $\text{N}_2\text{O}_4$ , a large peak in HHG yield appears at  $170 \pm 10 \text{ fs}$  in very good agreement with the expected value of  $T + T/4$  where  $T = 130 \text{ fs}$ , which is the vibration period of the N-N stretch mode of  $\text{N}_2\text{O}_4$ . This timing clearly indicates that harmonic yield maximizes at the outer turning point of the N-N stretch vibration. The first peak in emission at  $T/4$  ( $\sim 35 \text{ fs}$ ) is less discernible in the data, probably because of a pump-probe overlap that suppresses the signal.

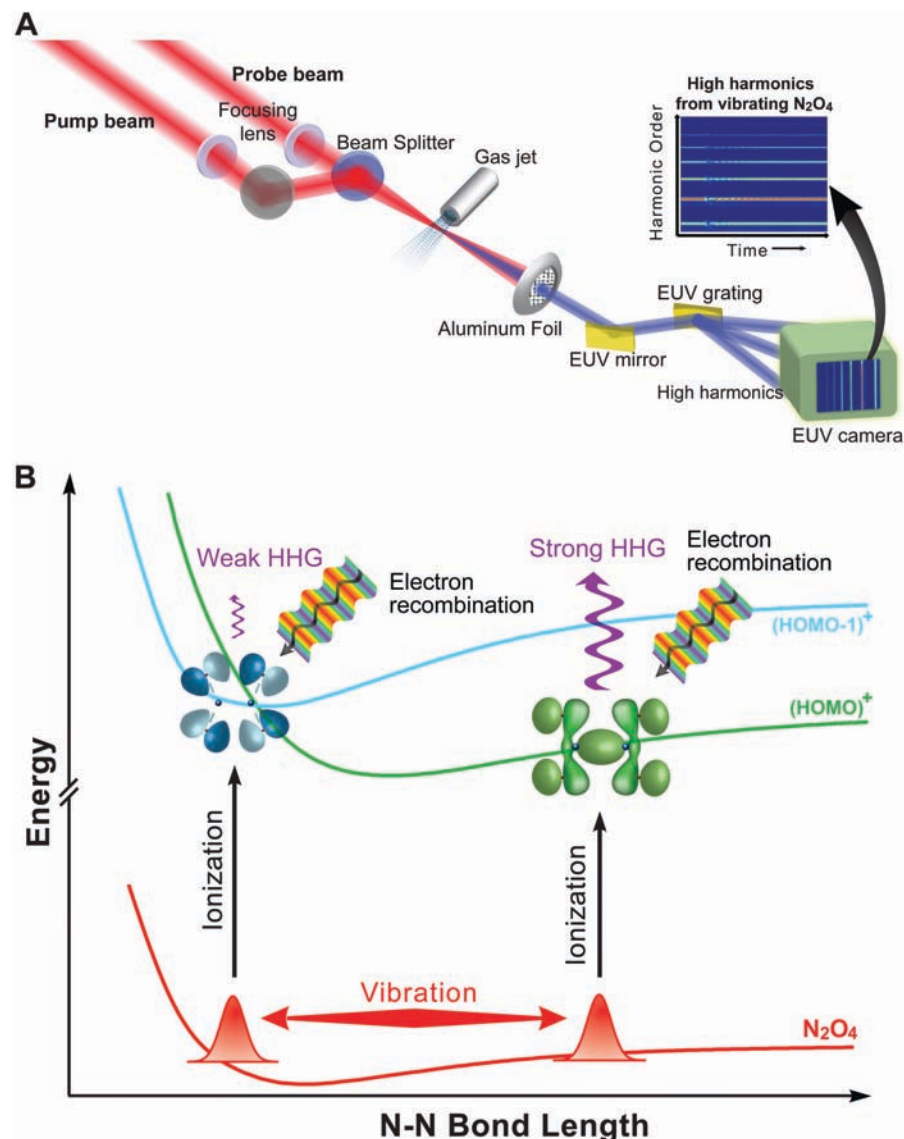


**Fig. 1. (A)** Experimental setup.  $\text{N}_2\text{O}_4$  molecules from an effusive nozzle are excited and probed using ultrafast 800-nm laser pulses. The pump-pulse intensity and duration are chosen to impulsively excite, but not ionize or dissociate,  $\text{N}_2\text{O}_4$ . A more intense collinear probe pulse generates harmonics from the vibrationally excited dimer. **(B)** Schematic of the experiment.

Only those  $\text{N}_2\text{O}_4$  molecules for which the N-N bond axis is closely aligned with the pump-beam polarization are vibrationally excited. This same population of molecules is probed by the HHG probe beam, and exhibit oscillations in high harmonic yield corresponding to the N-N stretch as discussed above. In Fig. 2, the amplitude of the harmonic oscillations diminishes as a function of time following the pump pulse, on a time scale consistent with rotational/vibrational dephasing.

We also measured the ionization yield as a function of pump-probe delay (fig. S1). The yield of  $\text{N}_2\text{O}_4^+$  is approximately the same at the inner and outer turning points. This finding shows that at the inner turning point, the molecule is ionized but harmonic emission is suppressed. Hence, ionization alone (modulation of the ionization

potential or rate due to the vibrational motion) cannot account for the observed large modulation in HHG yield.

The other possibility for the suppression of HHG at the inner turning point of the vibration is a contribution from a different electronic continuum, one that has smaller recombination amplitudes for HHG. We have evidence that this is the case. In Fig. 3, we plot the measured intensity dependence of the HHG peak-to-peak modulation depth of different harmonic orders. The modulation depth increases with increasing laser intensity and decreases with increasing harmonic order. If only a single continuum transition is involved in harmonic emission, then at the relatively high laser intensities that were used in these experiments, ionization will be more saturated at the outer turning point because of



**Fig. 2.** Harmonic yield as a function of delay between the alignment and HHG pulses using (A) parallel (||) and (B) perpendicular (⊥) pump and probe polarizations. The harmonic yield is normalized to the harmonic emission at negative pump-probe delays. Time dependence of the 17th harmonic yield for (C) parallel and (D) perpendicular polarizations. The insets in (C) and (D) show the Fourier transform, dominated by the N-N stretch mode at  $255\text{ cm}^{-1}$ .

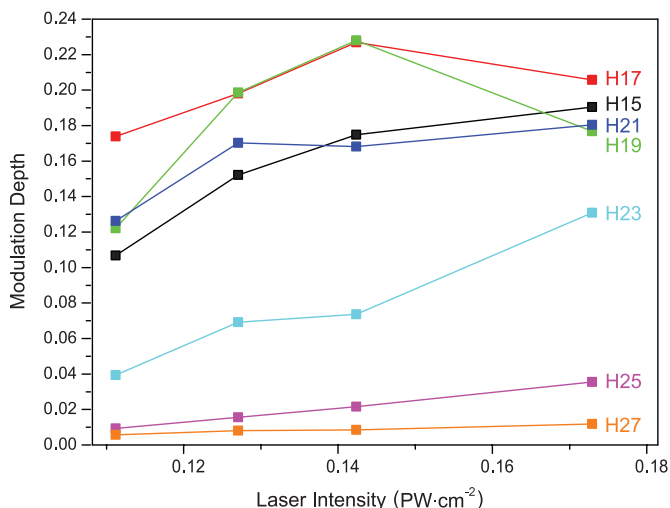
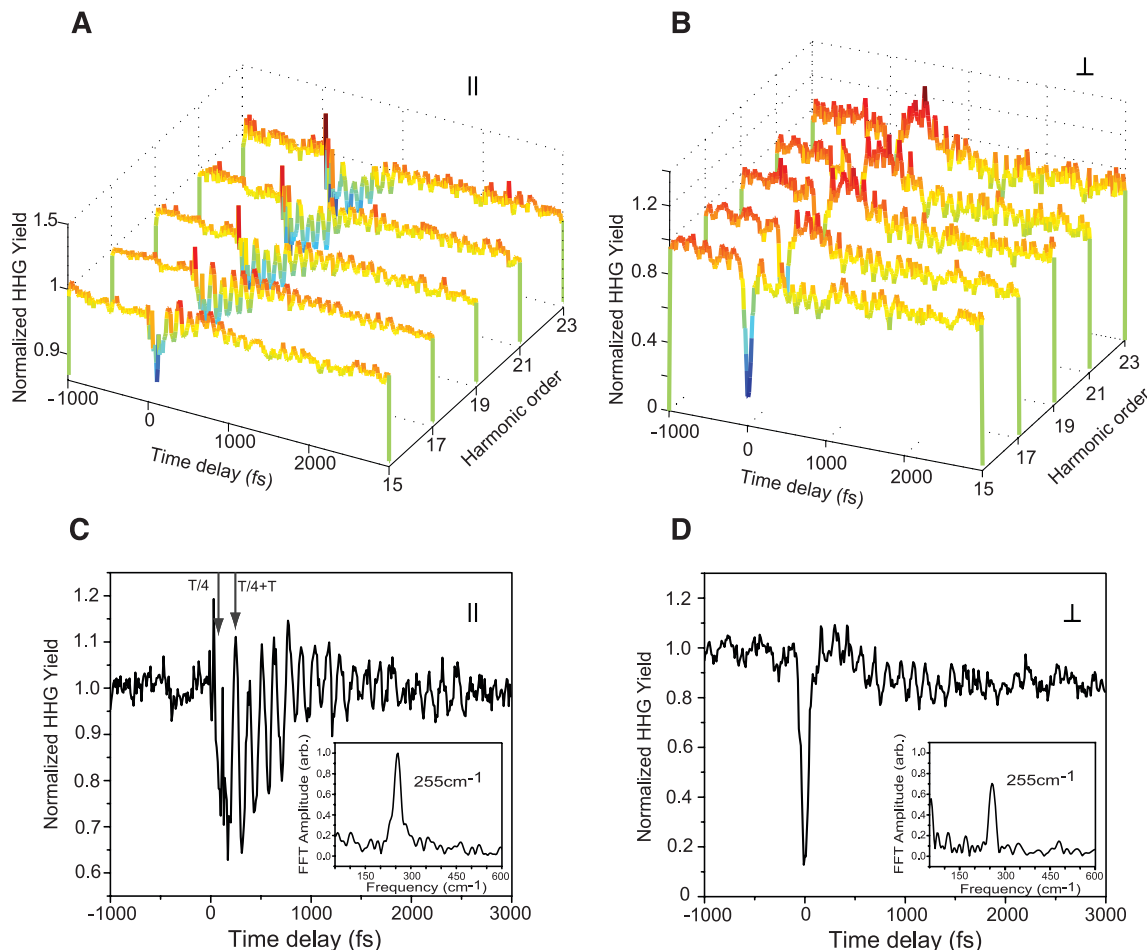


**Fig. 3.** Laser intensity dependence of the vibrational modulation depth for different harmonic orders, showing an increasing modulation depth with increasing laser intensity.

the lower ionization potential at this position relative to the inner turning point. This should lead to a reduced intensity ratio between harmonics emitted at the outer and inner points of the vibration with increasing laser intensity. In contrast, the observed modulation depth increases with increasing laser intensity.

**Ionization of the (HOMO-1) orbital.** To understand the effect of a large excursion on the

HHG process, we performed ab initio calculations of the structure of both the  $\text{N}_2\text{O}_4$  neutral and cation states (25). For  $\text{N}_2\text{O}_4$  molecules, ISRS in the strongly anharmonic ground-state potential results in large vibrational amplitudes of up to  $0.6\text{ \AA}$  (from  $\sim 1.6$  to  $2.2\text{ \AA}$ ). The calculated potential energy curves for the ground state of neutral  $\text{N}_2\text{O}_4$ , the ground state of the cation  $\text{N}_2\text{O}_4^+$  ( $A_g$ ), and the first excited state of the cation ( $B_{2g}$ )

are shown in Fig. 4A. The equilibrium bond length of the  $A_g$  cation has a substantially elongated N-N bond ( $2.21\text{ \AA}$  vertical, elongating to  $2.25\text{ \AA}$  upon complete optimization). This bond lengthening is a consequence of HOMO ionization to the cation ground electronic state, removing a bonding electron. In contrast, ionization of the (HOMO-1) to the  $B_{2g}$  excited state of the cation leaves the N-N bond relatively unchanged ( $1.75\text{ \AA}$  vertical, increasing to  $1.80\text{ \AA}$  upon relaxation). This picture is confirmed by the previously reported He(I) photoelectron spectra of  $\text{N}_2\text{O}_4$ , which show a delayed onset and long progression to the cation ground electronic state as compared with sharp lines and very limited progression to the cation first excited state (26).

The significant difference in bond length for the ground and excited states of the cation implies a strong bond-length dependence of the structural (Franck-Condon) factors for tunnel ionization: The  $A_g$  ground state is expected to be favored at longer N-N distances, whereas the  $B_{2g}$  excited channel benefits when the N-N bond is compressed. To quantify this argument, we performed a model calculation of the energy-dependent contribution to the structural ionization factors using the potential energy surfaces shown in Fig. 4A [supporting online material (SOM) text]. The results (Fig. 4B) show that for

**Fig. 4. (A)** Calculated second-order multiconfigurational quasi-degenerate perturbation theory/complete active space self-consistent field method potential energy curves for neutral  $\text{N}_2\text{O}_4$  (bottom) and the first two cation states (top). **(B)** Structural factors for ionization calculated at different bond lengths. At the short bond length, ionization favors the first excited state of the ion ( $\text{B}_{2g}$  continuum), whereas the ground  $\text{A}_g$  continuum dominates at long bond lengths

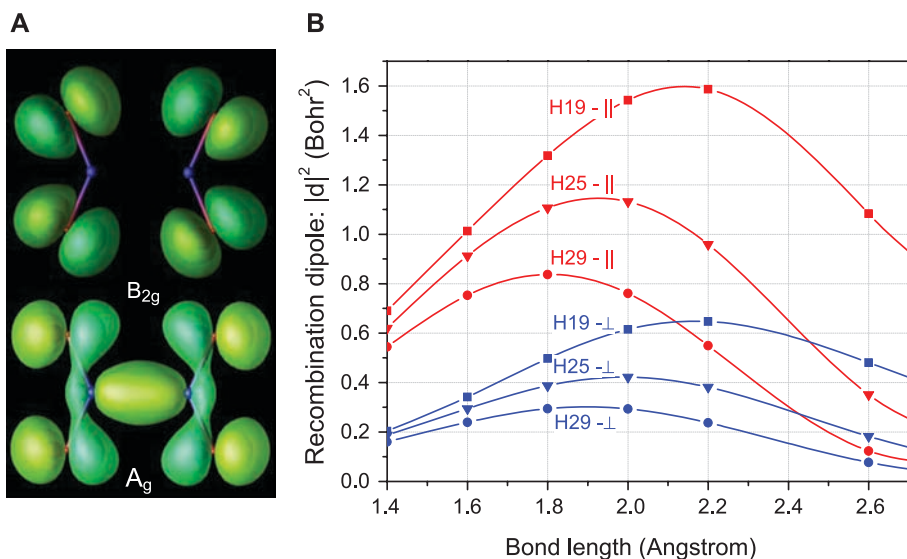
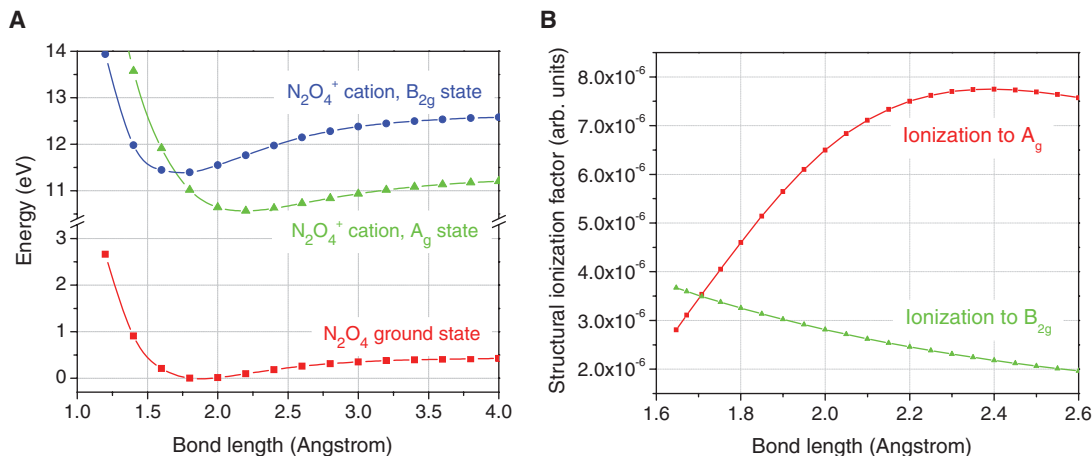


**Fig. 5. (A)** Dyson orbitals corresponding to ionizing to the  $\text{A}_g$  cation state and the  $\text{B}_{2g}$  cation state. The calculated equilibrium bond lengths for the neutral,  $\text{A}_g$ , and  $\text{B}_{2g}$  cation states are 1.808 Å [close to the experimental value of 1.756 Å (27)], 2.248 Å, and 1.8 Å, respectively. **(B)** Recombination dipoles of harmonics for continuum at different bond lengths for parallel (red,  $\parallel$ ) and perpendicular (blue,  $\perp$ ) pump-probe polarization.

N-N bond lengths ( $r_{\text{N-N}}$ ) below 1.7 Å, structural factors favor ionization to the  $\text{B}_{2g}$  excited state. At longer bond lengths, ionization to the  $\text{A}_g$  ground state of the cation is favored, with the corresponding structural factor increasing up to  $r_{\text{N-N}} = 2.3$  Å. Thus, because of the contribution of two ionization channels, the ion yield of  $\text{N}_2\text{O}_4^+$  is not expected to change significantly during the vibration, which is consistent with our experimental findings (fig. S1).

At the relatively high laser intensity used here, saturation due to the depletion of the neutral  $\text{N}_2\text{O}_4$  population may become an important factor. In this regime, the total number of emitters of each type is determined by the ratio of the ionization rates for each species, rather than by the individual rates. The calculated ratio of the  $\text{A}_g/\text{B}_{2g}$  structural factors in  $\text{N}_2\text{O}_4$  increases monotonically with  $r_{\text{N-N}}$ , with the  $\text{B}_{2g}$  state as the preferred channel at short bond lengths,

whereas the  $\text{A}_g$  state dominates when the bond is elongated. Thus, the relative importance of the two channels remains the same, even in the presence of saturation. This result is supported by the observed intensity dependence of the HHG modulation depth (Fig. 3), which increases with increasing laser intensity. As discussed earlier, a decreasing modulation depth with laser intensity is expected if only one electronic continuum is contributing to the harmonic signal.

**Origins of HHG suppression at the inner turning point.** For the propagation of the liberated electron in the continuum, the long-range part of the molecular potential is not substantially influenced by intramolecular vibrations, and no additional modulation of the HHG signal is expected. Therefore, we now consider the electron recombination step. To this end, we calculated the overlap between the N-electron

wave function of the neutral species and the  $(N-1)$ -electron wave function of the ion, the Dyson orbital. This calculation captures the change in the electronic structure of the molecule upon electron removal or recombination. Dyson orbitals for the two main ionization channels, calculated at the equilibrium geometry of the neutral species, are shown in Fig. 5A. The final recombination dipoles for the  $\text{A}_g$  channel as a function of both their N-N bond separations and harmonic order are shown in Fig. 5B. As a result of the presence of nodal planes along all principal directions, the excited ion-state channel ( $\text{B}_{2g}$ ) is suppressed. Nodal planes both decrease recombination matrix elements and reduce the recollision probability (11, 12).

The radial dependence of the calculated recombination dipoles  $\vec{d}$  is sensitive to the harmonic order. At low harmonic orders (H17 to H21), the matrix elements for the parallel pump-probe orientation increase with the N-N bond length, leading to a doubling in harmonic radiation intensity at  $r_{\text{N-N}} = 2.1$  Å ( $|\vec{d}_{\text{H19}}|^2 \approx 1.6 \text{ Bohr}^2$ ) as compared with  $r_{\text{N-N}} = 1.5$  Å ( $|\vec{d}_{\text{H19}}|^2 \approx 0.84 \text{ Bohr}^2$ ). At higher orders (H27, H29), the variation of  $|\vec{d}|^2$  with the bond length does not exceed 15%. This behavior is consistent with the observed decrease in the modulation of harmonic intensity for higher harmonic orders (Fig. 2A). The lower modulation depth observed for perpendicular polarization of the pump and probe pulse is also consistent with the overall  $\sim 60\%$  decrease of the recombination matrix elements for this geometry. For both geometries, the modulation remains in phase for all harmonics, indicating that the observed dependences cannot be explained by the structural dependence of the recombination matrix elements.

Even though the cation excited state (here  $\text{B}_{2g}$ ) does not substantially contribute to HHG emission in  $\text{N}_2\text{O}_4$ , in other molecules emission from different ionization continua will add coherently; thus, observables such as the ellipticity and phase shift of the HHG emission emerge as sensitive diagnostics of dynamics in polyatomic molecules.

**Ruling out NO<sub>2</sub> participation.** Because a small portion (<20%) of NO<sub>2</sub> coexists with N<sub>2</sub>O<sub>4</sub> in our sample, we had to eliminate the possibility that heterodyne mixing of harmonic emission from N<sub>2</sub>O<sub>4</sub> and NO<sub>2</sub> contributed to the observed modulation. If the phase of harmonics emitted from N<sub>2</sub>O<sub>4</sub> at the inner turning and outer turning points were different, interference between emissions from NO<sub>2</sub> and N<sub>2</sub>O<sub>4</sub> could contribute to the modulation observed. Such phase variations could arise from intrinsic phase changes because of the differing ionization potentials at the inner and outer turning points of the vibration or from different generating ion states; that is, A<sub>g</sub> and B<sub>2g</sub>. Only the latter is consistent with our proposed mechanism. Using an interferometry technique demonstrated recently (20), we monitored the fringe pattern generated by interfering HHG from vibrationally excited and unexcited N<sub>2</sub>O<sub>4</sub> molecules (SOM text and fig. S2). No phase change in HHG emission was observed during the vibration within the sensitivity limit of our measurements. This null result is a clear indication that heterodyne mixing does not substantially contribute to our signal.

**Outlook.** This discovery brings both challenges and opportunities to the application of strong-field ionization and HHG to the study of polyatomic structure and dynamics. Although a simple adiabatic picture involving only a single HOMO orbital may be sufficient for some diatomic molecules, generalization to larger molecules undergoing structural changes (for example, chemical reaction) will require consideration of

both many-body and nonadiabatic electronic dynamics (11, 12). However, the sensitivity of strong-field ionization and HHG to the different ionization continua promises that techniques monitoring tunnel ionization, TRPES, and HHG will uncover detailed information on electronic and nuclear structure and dynamics in polyatomic molecules.

#### References and Notes

1. A. Stolow, J. G. Underwood, *Adv. Chem. Phys.* **139**, 497 (2008).
2. A. Stolow, A. E. Bragg, D. M. Neumark, *Chem. Rev.* **104**, 1719 (2004).
3. O. Gessner *et al.*, *Science* **311**, 219 (2006).
4. V. Blanchet, M. Z. Zgierski, T. Seideman, A. Stolow, *Nature* **401**, 52 (1999).
5. M. Ferray *et al.*, *J. Phys. At. Mol. Opt. Phys.* **21**, L31 (1988).
6. A. McPherson *et al.*, *J. Opt. Soc. Am. B* **4**, 595 (1987).
7. K. C. Kulander, K. J. Schafer, J. L. Krause, in *Super-Intense Laser-Atom Physics*, B. Piraux, A. L'Huillier, K. Rzazewski, Eds. (Plenum, NY, 1993), vol. 316, pp. 95–110.
8. M. Lewenstein, P. Balcou, M. Y. Ivanov, P. B. Corkum, *Phys. Rev. A* **49**, 2117 (1994).
9. P. B. Corkum, *Phys. Rev. Lett.* **71**, 1994 (1993).
10. H. Kapteyn, O. Cohen, I. Christov, M. Murnane, *Science* **317**, 775 (2007).
11. O. Smirnova, S. Patchkovskii, Y. Mairesse, N. Dudovich, D. Villeneuve, P. Corkum, M. Ivanov, in *11th International Conference on Multiphoton Processes*, J. Anton, B. Martin, R. Moshhammer, J. Ullrich, Eds. (Max-Planck-Institut für Kernphysik, Heidelberg, Germany, 2008), p. 7.
12. Y. Mairesse, O. Smirnova, N. Dudovich, S. Patchkovskii, M. Yu. Ivanov, D. M. Villeneuve, P. B. Corkum, in *11th International Conference on Multiphoton Processes*, J. Anton, B. Martin, R. Moshhammer, J. Ullrich, Eds. (Max-Planck-Institut für Kernphysik, Heidelberg, Germany, 2008), p. Fr62.
13. M. V. Ammosov, N. B. Delone, V. P. Krainov, *Zhur. Eksp. Teor. Fiz.* **91**, 2008 (1986).
14. X. M. Tong, Z. X. Zhao, C. D. Lin, *Phys. Rev. A* **66**, 033402 (2002).
15. M. Lezius, V. Blanchet, M. Y. Ivanov, A. Stolow, *J. Chem. Phys.* **117**, 1575 (2002).
16. M. Smits, C. A. de Lange, A. Stolow, D. M. Rayner, *Phys. Rev. Lett.* **93**, 203402 (2004).
17. S. Patchkovskii, Z. X. Zhao, T. Brabec, D. M. Villeneuve, *J. Chem. Phys.* **126**, 114306 (2007).
18. R. Santra, A. Gordon, *Phys. Rev. Lett.* **96**, 073906 (2006).
19. J. Itatani *et al.*, *Nature* **432**, 867 (2004).
20. X. B. Zhou *et al.*, *Phys. Rev. Lett.* **100**, 073902 (2008).
21. M. Meckel *et al.*, *Science* **320**, 1478 (2008).
22. N. L. Wagner *et al.*, *Proc. Natl. Acad. Sci. U.S.A.* **103**, 13279 (2006).
23. Z. B. Walters, S. Tonzani, C. H. Greene, *J. Phys. At. Mol. Opt. Phys.* **40**, F277 (2007).
24. S. Baker *et al.*, *Science* **312**, 424 (2006).
25. Computational methods are detailed as supporting material on Science Online.
26. T. H. Gan, J. B. Peel, G. D. Willett, *J. Chem. Soc., Faraday Trans. II* **73**, 1459 (1977).
27. A. Kvick, R. K. McMullan, M. D. Newton, *J. Chem. Phys.* **76**, 3754 (1982).
28. The authors thank M. Ivanov and O. Smirnova for helpful discussions. They also gratefully acknowledge support for this work from the U.S. Department of Energy Office of Basic Energy Sciences and the NSF Physics Frontier Centers and the use of facilities from the NSF Engineering Research Center on EUV Science and Technology.

#### Supporting Online Material

[www.sciencemag.org/cgi/content/full/1163077/DC1](http://www.sciencemag.org/cgi/content/full/1163077/DC1)

SOM Text

Figs. S1 and S2

References

10 July 2008; accepted 24 September 2008  
Published online 30 October 2008;  
10.1126/science.1163077  
Include this information when citing this paper.

## The 2.6 Angstrom Crystal Structure of a Human A<sub>2A</sub> Adenosine Receptor Bound to an Antagonist

Veli-Pekka Jaakola,<sup>1\*</sup> Mark T. Griffith,<sup>1\*</sup> Michael A. Hanson,<sup>1\*</sup> Vadim Cherezov,<sup>1</sup> Ellen Y. T. Chien,<sup>1</sup> J. Robert Lane,<sup>2</sup> Adriaan P. IJzerman,<sup>2</sup> Raymond C. Stevens<sup>1†</sup>

The adenosine class of heterotrimeric guanine nucleotide-binding protein (G protein)-coupled receptors (GPCRs) mediates the important role of extracellular adenosine in many physiological processes and is antagonized by caffeine. We have determined the crystal structure of the human A<sub>2A</sub> adenosine receptor, in complex with a high-affinity subtype-selective antagonist, ZM241385, to 2.6 angstrom resolution. Four disulfide bridges in the extracellular domain, combined with a subtle repacking of the transmembrane helices relative to the adrenergic and rhodopsin receptor structures, define a pocket distinct from that of other structurally determined GPCRs. The arrangement allows for the binding of the antagonist in an extended conformation, perpendicular to the membrane plane. The binding site highlights an integral role for the extracellular loops, together with the helical core, in ligand recognition by this class of GPCRs and suggests a role for ZM241385 in restricting the movement of a tryptophan residue important in the activation mechanism of the class A receptors.

Extracellular adenosine plays an important role in physiology and initiates most of its effects through the activation of four

guanine nucleotide-binding protein (G protein)-coupled receptor (GPCR) subtypes, A<sub>1</sub>, A<sub>2A</sub>, A<sub>2B</sub>, and A<sub>3</sub> (1, 2). Each of these four receptors plays

an essential role in responding to adenosine in the central nervous system (3, 4), regulating pain (5), cerebral blood flow (6), basal ganglia functions (7), respiration (8), and sleep (9). These receptor subtypes are primarily coupled to the cyclic adenosine monophosphate (cAMP) second-messenger system, and each has its own unique pharmacological profile. The A<sub>2A</sub> adenosine subtype is linked to G<sub>s</sub> and G<sub>oif</sub> proteins, and upon receptor activation, the intracellular levels of cAMP increase. At least three of the four adenosine receptor subtypes (A<sub>1</sub>, A<sub>2A</sub>, and A<sub>2B</sub>) are blocked by naturally occurring methylxanthines, such as caffeine, with modest affinity. It is noteworthy that strong epidemiological evidence suggests that coffee drinkers have a lower risk of Parkinson's disease (10). This effect has been linked to caffeine's interaction with the A<sub>2A</sub> adenosine receptor, which controls locomotor behavior in basal ganglia, together with dopamine D<sub>2</sub> and metabotropic glutamate

<sup>1</sup>Department of Molecular Biology, The Scripps Research Institute, La Jolla, CA 92037 USA. <sup>2</sup>Division of Medicinal Chemistry, Leiden/Amsterdam Center for Drug Research, Post Office Box 9502, 2300RA Leiden, Netherlands.

\*These authors contributed equally to this work.

†To whom correspondence should be addressed. E-mail: [stevens@scripps.edu](mailto:stevens@scripps.edu)



receptors (mGluRs) (11, 12). Development of more selective compounds for adenosine receptor subtypes could provide a class of therapeutics for treating numerous human maladies, such as pain (5), Parkinson’s disease (7, 13), Huntington’s disease (14), asthma (15), seizures (16), and many other neurological disorders (14, 17).

We have determined the crystal structure of the human A<sub>2A</sub> adenosine receptor in complex with the subtype-selective high-affinity antagonist 4-(2-[7-amino-2-(2-furyl)-[1,2,4]triazolo-[2,3-a][1,3,5]triazin-5-ylamino]ethyl)-phenol (ZM241385) (18, 19). The basis for this compound’s selectivity over the adenosine A<sub>1</sub> and A<sub>3</sub> receptors can now be analyzed in the context of its molecular interactions with the A<sub>2A</sub> receptor, along with previously reported mutagenesis data. With an additional human GPCR structure, it is now possible to extend the analysis of structural differences as they pertain to receptor pharmacology, ligand recognition, and receptor activation across the members of the class A receptor family.

**Structure determination.** GPCRs have numerous thermodynamic conformations (20, 21), which implies an inherent structural flexibility (22–24). This flexibility manifests itself as thermal instability when extracted by detergent from lipid membranes and is one of the primary challenges in generating crystals of GPCRs (25, 26). In order to overcome this obstacle with the human A<sub>2A</sub> adenosine receptor, we applied the T4-lysozyme (T4L) fusion strategy (24, 27, 28), where most of the third cytoplasmic loop (Leu209<sup>5,70</sup>–Ala221<sup>6,23</sup>) was replaced with lysozyme from T4 bacteriophage and the carboxy-terminal tail (Ala317–Ser412) was deleted to improve the likelihood of crystallization. The resulting recombinant construct (A<sub>2A</sub>-T4L-ΔC) was further stabilized during purification with (i) sodium chloride, which has a beneficial effect on adenosine receptor stability, (ii) a saturating concentration of the nonspecific adenosine receptor antagonist theophylline (ZM241385 was exchanged from theophylline in the last purification step), and (iii) including cholesteryl hemisuccinate (CHS) throughout the purification. Purified A<sub>2A</sub>-T4L-ΔC bound to ZM241385 was crystallized by using the in meso crystallization methodology, in which the lipid phase consisted of a mixture of monoolein and cholesterol (29).

Diffraction data from 13 of the best crystals were combined to yield a 2.6 Å data set (Table 1). Phases were obtained by molecular replacement using the coordinates of the β<sub>2</sub>-adrenergic receptor (β<sub>2</sub>AR) fused to T4L [PDB accession number (PDB ID), 2RH1]. The final refined model includes residues Ile3 to Gln310 of the human A<sub>2A</sub> adenosine receptor, residues 2 to 161 of T4L, five lipid hydrocarbon chains modeled as stearic acid, eight sulfate ions, and the antagonist ZM241385 bound in the ligand-binding cavity (Fig. 1). The experimental elec-

tron density for the amino (Met1 to Pro2) and carboxy (Glu311 to Ala316) termini did not support modeling of these regions. In addition, the tip of the second extracellular loop (Gln148 to Ser156) was not modeled owing to weak experimental electron density. Although cholesterol does have a stabilizing effect on the A<sub>2A</sub> adenosine receptor and was included in the crystallization trials, in contrast to the β<sub>2</sub>AR structure, which has cholesterol bound in a pocket referred to as the cholesterol consensus motif (30), the A<sub>2A</sub> adenosine receptor structure has lipid bound in the same area.

**Biochemical characterization of A<sub>2A</sub>-T4L-ΔC.** We have verified the functionality of A<sub>2A</sub>-T4L-ΔC by comparing its binding properties to A<sub>2A</sub>-T4L and A<sub>2A</sub>-WT (31). The A<sub>2A</sub>-T4L-ΔC, A<sub>2A</sub>-T4L, and A<sub>2A</sub>-WT constructs expressed in Sf9 cells bind [<sup>3</sup>H]ZM241385 with similar affinity as the same constructs transiently expressed in human embryonic kidney (HEK293) cells as judged by radioligand-saturation experiments. This finding was corroborated in competition binding assays, as the two A<sub>2A</sub>-T4L constructs had median inhibitory concentration values sim-

ilar to that of A<sub>2A</sub>-WT for ZM241385 (Fig. 2, and fig. S2 and table S2). However, A<sub>2A</sub>-T4L and A<sub>2A</sub>-T4L-ΔC displayed significantly higher affinity for the subtype-selective agonist CGS21680 as compared with the A<sub>2A</sub>-WT construct, which may indicate a shift toward the activated state induced by the incorporation of the T4L moiety. A comparable construct of the β<sub>2</sub>AR behaved in a similar fashion (24); however, unlike β<sub>2</sub>AR, the A<sub>2A</sub>-WT has no associated basal activity (G protein signaling in the absence of agonist). The inclusion of a high concentration of sodium chloride in the assay medium induced a substantial decrease in the agonist affinity for all of the tested constructs (Fig. 2B), but did not appreciably affect antagonist affinity. Note that the inhibition constant (*K<sub>i</sub>*) values for the agonist in the presence of sodium chloride were virtually identical for all constructs tested (table S2), which suggested that sodium chloride induced a shift in receptor equilibrium to an inactive state (32). In addition, sodium chloride induced a 10°C increase in thermal stability for A<sub>2A</sub>-T4L-ΔC solubilized in *n*-dodecyl-β-D-maltoside (fig. S3).

**Table 1.** Data collection and refinement statistics. Highest resolution shell is shown in parentheses.

A <sub>2A</sub> -T4L-ΔC	
Data collection (APS GM/CA CAT ID-B, 10 μm beam)	
Space group	P2 <sub>1</sub>
Cell dimensions	
<i>a</i> , <i>b</i> , <i>c</i> (Å)	47.7, 76.9, 86.6
(°)	101.3
No. of reflections processed	64,526 (8165)
No. unique reflections	18,465 (356)
Resolution (Å)	20.0–2.6 (2.8–2.6)
<i>R</i> <sub>sym</sub> *	9.8 (38.9)
Mean <i>I</i> /σ( <i>I</i> )	7.0 (2.3)
Completeness (%)	96.8 (93.9)
Multiplicity	3.5 (2.3)
Refinement	
Resolution (Å)	20.0–2.6
No. reflections (reference set)	18,461 (937)
<i>R</i> <sub>crys</sub> / <i>R</i> <sub>free</sub> †	19.6/23.1
No. atoms	3768
Protein	3521
Ions, lipids, ligand and other	165
Water oxygen	82
<i>B</i> -values (Å <sup>2</sup> )	
All atoms	70.6
Protein	69.4
Ligand	66.7
Lipid	94.4
Root mean square deviations from ideality	
Bond lengths (Å)	0.002
Bond angles (°)	0.78
Ramachandran plot statistics (%) (excl. Gly, Pro)	
Most favored regions	92.8
Additionally allowed regions	7.2
Generously allowed regions	0.0
Disallowed regions	0.0

\**R*<sub>sym</sub> = Σ<sub>*hkl*</sub> |*I*(*hkl*) – ⟨*I*(*hkl*)⟩|/Σ<sub>*hkl*</sub> *I*(*hkl*). †*R*<sub>crys</sub> = Σ<sub>*hkl*</sub> |*F*<sub>obs</sub> – *F*<sub>calc</sub>| / Σ<sub>*hkl*</sub> *F*<sub>obs</sub>; *R*<sub>free</sub> = test set 5%.

**Fig. 1.** Crystal structure of  $A_{2A}$ -T4L- $\Delta C$ . **(A)** Overall topology of  $A_{2A}$ -T4L- $\Delta C$ . The transmembrane part of  $A_{2A}$ - $\Delta C$  structure is colored brown (helices I to VIII), and the T4L is in cyan. The structure is viewed perpendicular to the plasma membrane. ZM241385 is colored blue, and the five lipid molecules bound to the receptor are colored red. The four disulfide bonds are yellow. The sulfate ions are omitted. The extracellular loops (ECL1 to 3) are colored green, and the intracellular loops are colored blue. The membrane boundaries are adapted from the OPM database (<http://opm.phar.umich.edu/>) with  $\beta_2$ AR-T4L (2RH1) as a model. **(B)** Rotated 180° around the x axis. The images were created with PyMOL.

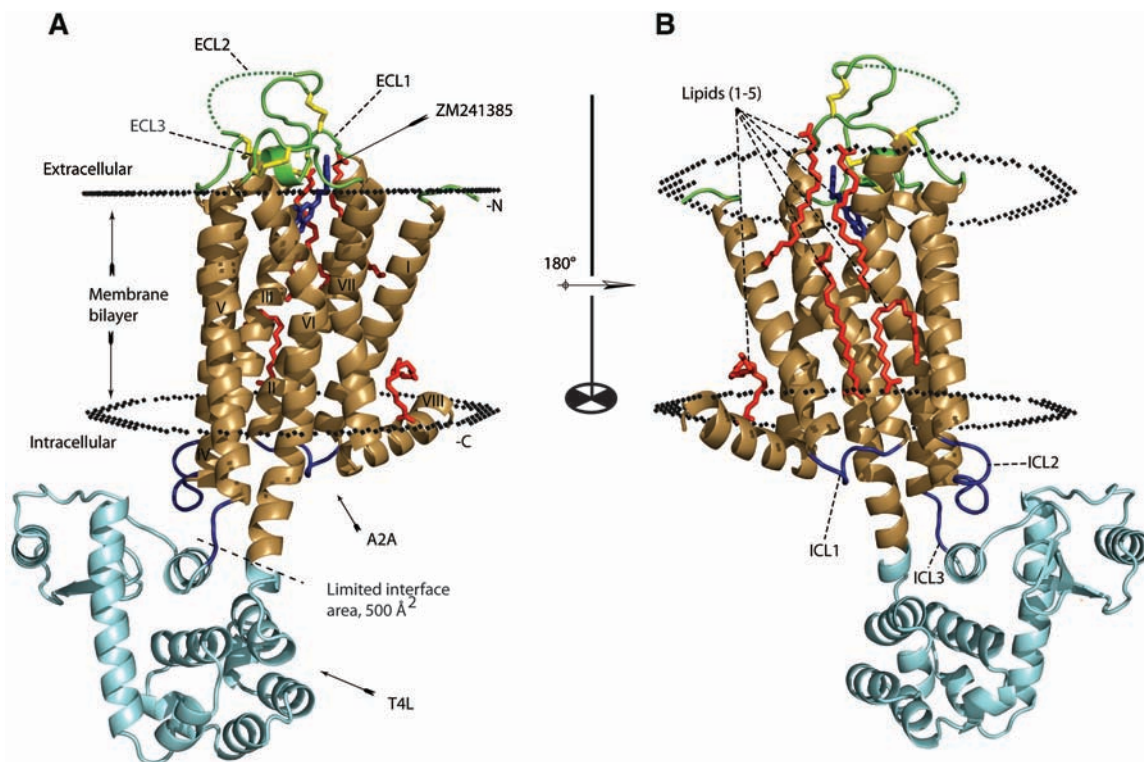
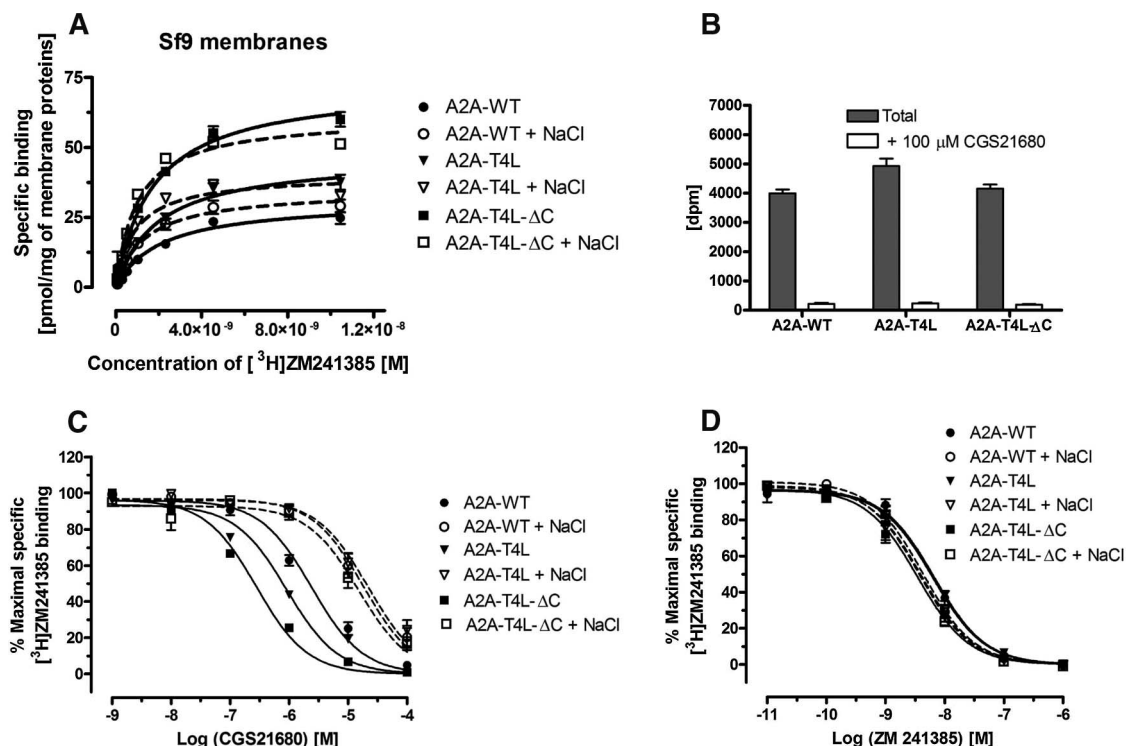


**Fig. 2.** Ligand-binding characteristics of  $A_{2A}$ -WT,  $A_{2A}$ -T4L, and  $A_{2A}$ -T4L- $\Delta C$ . **(A)** Saturation binding isotherm for the binding of [ $^3$ H]ZM241385 to different  $A_{2A}$ -WT,  $A_{2A}$ -T4L, or  $A_{2A}$ -T4L- $\Delta C$  receptors confined in membranes of Sf9 cells. The indicated preparations of  $A_{2A}$  receptors were incubated with different concentrations of [ $^3$ H]ZM241385 in the absence (filled shapes and solid lines) and presence (open shapes and dashed lines) of 1 M NaCl as described in SOM. Figure represents data combined from two separate experiments performed in triplicate. The equilibrium constant ( $K_d$ ) values of [ $^3$ H]ZM241385 in the absence and the presence of 1 M NaCl were  $2.1 \pm 0.7$  nM,  $1.3 \pm 0.2$  nM for  $A_{2A}$ -WT;  $2.0 \pm 0.3$  nM,  $0.9 \pm 0.1$  nM for  $A_{2A}$ -T4L; and  $1.8 \pm 0.2$  nM,  $1.0 \pm 0.1$  nM for  $A_{2A}$ -T4L- $\Delta C$ , respectively. **(B)** One-point binding assay demonstrating the total and nonspecific binding of [ $^3$ H]ZM241385 to membranes (5  $\mu$ g per assay point) of HEK293T cells transfected with  $A_{2A}$ -WT,  $A_{2A}$ -T4L, or  $A_{2A}$ -T4L- $\Delta C$ . [ $^3$ H]ZM241385 was used at a concentration equivalent to the previously observed  $K_d$ . (Bottom) The ability of increasing concentrations of **(C)** the agonist CGS21680 or **(D)** the antagonist ZM241385



to compete with [ $^3$ H]ZM241385 binding at  $A_{2A}$ -WT (circles),  $A_{2A}$ -T4L (triangles),  $A_{2A}$ -T4L- $\Delta C$  (squares) constructs in HEK293T cells was tested in the absence (filled shapes and solid lines) or presence (open shapes and dashed lines) of 1 M NaCl. Figure represents data combined from three separate experiments performed in duplicate.



Thus, radioligand-binding experiments support the conclusion that the construct used for crystallization is a functional receptor with an increased affinity for agonist and wild-type affinity for antagonist.

**Architecture of the human  $A_{2A}$  adenosine receptor.** The residues constituting the transmembrane  $\alpha$  helices are Gly<sup>51,31</sup>–Trp<sup>321,58</sup> (helix I); Thr<sup>41,39</sup>–Ser<sup>67,65</sup> (helix II); His<sup>75,323</sup>–Arg<sup>107,355</sup> (helix III); Thr<sup>119,4,40</sup>–Leu<sup>140,4,61</sup> (helix IV); Asn<sup>175,5,36</sup>–Ala<sup>204,5,65</sup> (helix V); Arg<sup>222,6,24</sup>–Phe<sup>258,6,60</sup> (helix VI); and Leu<sup>269,7,34</sup>–Arg<sup>291,7,56</sup> (helix VII) (33). A small helix that does not cross the cell membrane is located at the membrane-cytoplasm interface and comprises Arg<sup>296,8,47</sup>–Leu<sup>308,8,59</sup> (helix VIII). The  $A_{2A}$  adenosine receptor does not contain the canonical palmitoylation site(s) found in the majority of GPCRs; instead, helix VIII is stabilized by interactions with helix I (34). The residues defining intracellular and extracellular loops (ICLs and ECLs) are Leu<sup>33,1,59</sup>–Val<sup>40,2,38</sup> (ICL1); Ile<sup>108,3,56</sup>–Gly<sup>118,4,39</sup> (ICL2); Leu<sup>208,5,69</sup>–Ala<sup>221,6,23</sup> (ICL3); Thr<sup>68,2,66</sup>–Cys<sup>74,3,22</sup> (ECL1); Leu<sup>141,4,62</sup>–Met<sup>174,5,35</sup> (ECL2); and Cys<sup>259,6,61</sup>–Trp<sup>268,7,33</sup> (ECL3). In the structure, ICL3 has been replaced by 160 residues from T4L (see fig. S1). In addition, the N-linked glycan associated with Asn<sup>154,4,75</sup> has been removed enzymatically to improve crystallization.

Our crystallographic model of  $A_{2A}$ -T4L- $\Delta C$  bound to ZM241385 reveals three features distinct from the previously reported GPCR structures. First, the organization of the extracellular loops is markedly different from  $\beta_1$ AR,  $\beta_2$ AR, and bovine and squid rhodopsins (23, 24, 30, 35–37). Second, ZM241385 binds in an extended conformation perpendicular to the plane of the membrane and colinear with transmembrane helix VII, while interacting with both ECL2 and ECL3. This is somewhat incongruous with earlier molecular modeling studies based on  $\beta_2$ AR and rhodopsin homology models in which ZM241385 and other antagonists were docked into a binding site emulating that of  $\beta_2$ AR and rhodopsin [for examples, see (38, 39), and references therein]. Finally, a subtle divergence in the helical positions and orientations relative to rhodopsin and  $\beta_2$ AR redefines the antagonist-binding cavity so that it is located closer to helices VI and VII and allows only limited interactions with helices III and V.

**Helical position and binding-pocket diversity.** Among the class A GPCRs, the sequence identity is highest within the  $\alpha$ -helical transmembrane regions and ranges from 20 to 50% (40, 41). Not surprisingly, the helical arrangement is similar among the human  $\beta_2$ AR, turkey  $\beta_1$ AR, and squid and bovine rhodopsin structures determined to date. However, shifts in the relative positions of the various helices results in root mean square deviations between 2.0 and 2.5 Å (depending on how the alignment is carried out and which structures are being compared) that has structural and biochemical implications. Most of the structural divergence arises in the

extracellular portions of helices I, II, III, and V, where the variation in the positions of helices II, III, and V appears to redefine the location of the ligand-binding pocket (42). However, comparisons between ground-state rhodopsin bound to retinal and  $\beta_2$ AR bound to carazolol show minimal differences, because the relative helical shifts are smaller (Fig. 3, A and B) (27). The position of the retinal and carazolol-binding pocket is very similar and makes most contact

with helices III, V, and VI (Figs. 3A and 4). The binding pocket of the  $A_{2A}$  adenosine receptor is shifted closer to helices VI and VII, which contribute the majority of the binding interactions associated with helical regions, as judged by occluded surface area calculations (43, 44) (Figs. 3B and 4). A concomitant shift of helices II and V (7 Å and 3 Å, respectively) toward the binding pocket, as well as a lateral shift of helix III toward helix V by 3 Å, compensates for the

**Fig. 3.** Slight changes in helical positions alter the orientation of the ligand-binding pocket. (A) A surface rendering of the binding pocket for ZM241385 in the  $A_{2A}$  adenosine receptor. Helical positions for  $A_{2A}$  adenosine (tan),  $\beta_2$ AR (PDB ID: 2RH1) (blue), and rhodopsin (PDB ID: 1U19) (green) are shown after alignment with the FatCat server (38). Ligands for each receptor are shown to illustrate the differences in binding orientation and the differences in the adenosine  $A_{2A}$ -binding pocket. (B) A top view of the helical bundle illustrating the maximal helical positional shifts of  $A_{2A}$  relative to  $\beta_2$ AR.

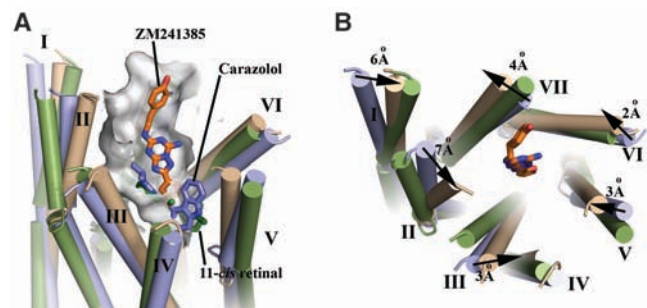
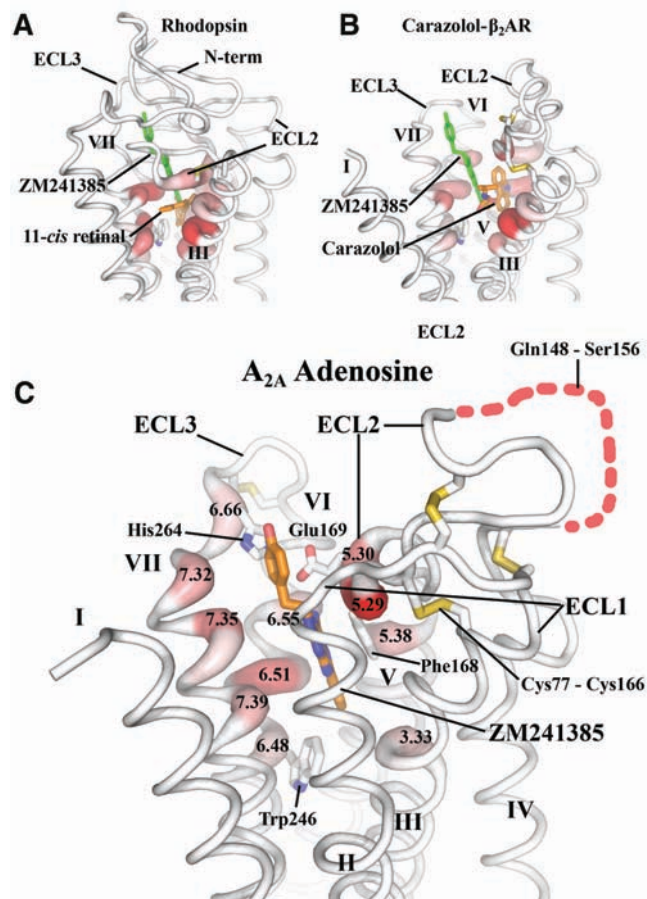


**Fig. 4.** Normalized occluded surface (NOS) area changes due to ligand binding. Increases in occluded surface area are represented as thickened red areas of the protein backbone chain (38). (A) Rhodopsin (PDB ID: 1U19) with retinal (orange) is shown along with the position of ZM241385 (green) for comparison. Retinal makes extensive contact with helices III, V, VI, and VII deep in the binding pocket. (B)  $\beta_2$ AR bound to carazolol (orange) (PDB ID: 2RH1) is shown along with the position of ZM241385 (green) for comparison. Carazolol also makes extensive contacts with helices III, V, VI, and VII deep in the binding pocket but is responsible for minimal changes in NOS of Trp<sup>286,6,48</sup> the canonical “toggle switch.” (C)  $A_{2A}$  adenosine receptor bound to ZM241385 (orange carbon) has a very different ligand binding orientation relative to rhodopsin and  $\beta_2$ AR, resulting in minimal interaction of ligand and with helices III and V, but extensive interactions with helices VI and VII, as well as residues in ECL2 and ECL3. ZM241385 also forms significant contacts with Trp<sup>246,6,48</sup>. All interacting positions on the receptor are displayed as thick red areas and labeled by their corresponding Ballesteros-Weinstein designation (33).





absence of ligand interactions in this region by increasing protein-packing interactions (Fig. 3, A and B).

**Conformational equilibrium and receptor activation.** A common feature of the class A

GPCRs is the presence of a tryptophan residue (at position 6.48) on helix VI whose rotameric position is thought to control the equilibrium between the active and inactive states of each receptor (45). On the basis of the position of

retinal in the rhodopsin structure, it was proposed that ligand interactions with this key residue could modulate receptor equilibrium (46). It is noteworthy that the contact area between the ligand and the “toggle switch” tryptophan residue at position 6.48 varies considerably among the solved receptor structures. For instance, rhodopsin and  $\beta_2$ AR have a similar binding mode as noted; however, retinal in rhodopsin has a contact area of  $36 \text{ \AA}^2$ , whereas carazolol bound to  $\beta_2$ AR lacks any direct contact with Trp286<sup>6.48</sup> (27). Ground-state rhodopsin has virtually no basal activity, whereas  $\beta_2$ AR has a relatively high basal activity that is suppressed somewhat by carazolol as a partial inverse agonist (23, 47). The observed increase in contact area may have direct implications for inverse agonist efficacy or suppressed basal activity by limiting the range of motion of the “toggle switch” tryptophan. The competitive antagonist ZM241385 has a  $14 \text{ \AA}^2$  contact area with Trp246<sup>6.48</sup> despite an altered binding mode relative to rhodopsin (Fig. 4C). Although it remains to be established biochemically, this finding suggests that this ligand may stabilize the  $A_{2A}$  adenosine receptor in an inactive state.

Interactions between the cytoplasmic end of helix III (Asp<sup>3.49</sup>-Arg<sup>3.50</sup>-Tyr<sup>3.51</sup>) forming the conserved sequence motif Asp/Glu-Arg-Tyr (D/ERY) and helix VI (Glu<sup>6.30</sup>) have been proposed to constitute an “ionic lock” that may play a role in restraining the fully in-

**Fig. 5.** Comparison of interactions between helix III (E/DRY motif) and ICL2 for human  $A_{2A}$ -T4L- $\Delta C$ , human  $\beta_2$ AR-T4L (PDB ID: 2RH1), turkey  $\beta_1$ AR (PDB ID 2VT4) and Rhodopsin (PDB ID 1U19). **(A)**  $A_{2A}$ -T4L- $\Delta C$  interactions. The DRY motif does not participate in any stabilizing ionic interactions, similarly to  $\beta_2$ AR and  $\beta_1$ AR. Instead, Arg102<sup>3.50</sup> may play a role in stabilizing the deprotonated state of the adjacent Asp101<sup>3.49</sup> to allow this residue to make stronger hydrogen-bonding interactions with helix II and ICL2. **(B)** Turkey  $\beta_1$ AR participates in interactions similar to those of  $A_{2A}$ -T4L- $\Delta C$  without the hydrogen bond to helix II. **(C)**  $\beta_2$ AR-T4L does not contain a helical segment in ICL2 and has a modified set of interactions. **(D)** The canonical ionic lock in rhodopsin.

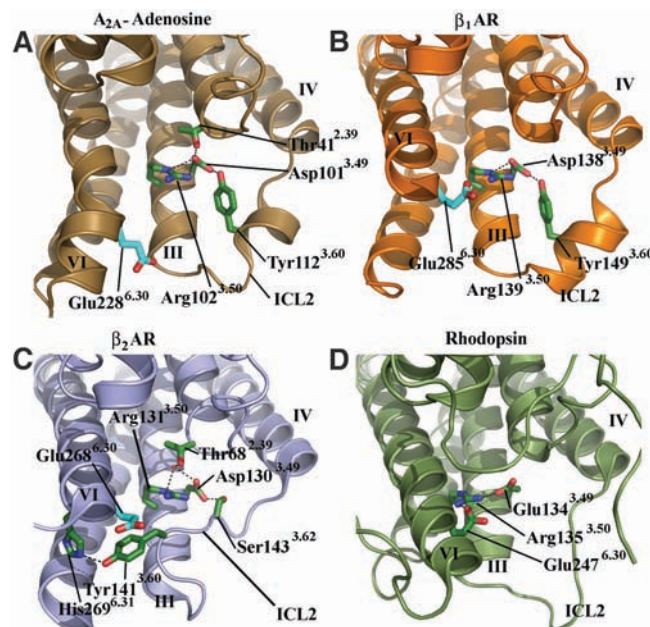
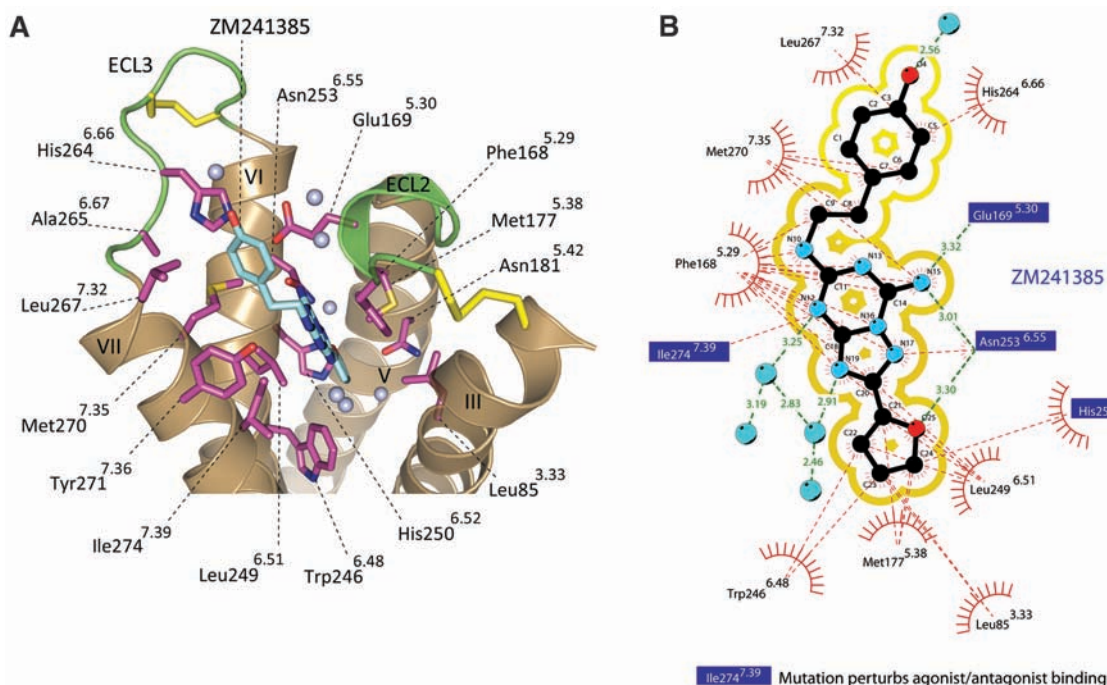


**Fig. 6.** Ligand-binding cavity of  $A_{2A}$ -T4L- $\Delta C$  with ZM241385 bound. **(A)** Residues within 5 Å of the ZM241385 are shown in stick representation. Nitrogen atoms are colored blue; oxygen atoms, red; and sulfur atoms, yellow. Only the interacting helices, ECL3 and the interacting part of ECL2 are shown. The two disulfide bridges in close proximity to the binding cavity are shown as yellow sticks. ZM241385 is positioned colinear with respect to the transmembrane helices V, VI, and VII, and the binding cavity is elongated to the ECL3 and ends of transmembrane helices VI and VII. For comparison with retinal chromophore or  $\beta$ -blockers-binding site, see (Fig. 3) for details. The Phe168<sup>5.29</sup> from ECL2 forms various aromatic stacking interactions with the bicyclic core of ZM241385. Trp246<sup>6.48</sup> associated with stabilizing the antagonist structure is 3 Å from the furan ring of ZM241385. The binding cavity includes seven ordered water molecules shown as light blue dots. **(B)** Schematic representation of the inter-



actions between  $A_{2A}$ -T4L- $\Delta C$  and ZM241385 at the ligand-binding cavity combined with mutation analysis for adenosine agonist and/or antagonist interactions. Mutations that are reported to disrupt antagonist and/or agonist binding are within blue squares: Glu169<sup>5.30</sup>, His250<sup>6.52</sup>, Asn253<sup>6.55</sup>, and Ile274<sup>7.39</sup>.

actions between  $A_{2A}$ -T4L- $\Delta C$  and ZM241385 at the ligand-binding cavity combined with mutation analysis for adenosine agonist and/or antagonist interactions. Mutations that are reported to disrupt antagonist and/or agonist binding are within blue squares: Glu169<sup>5.30</sup>, His250<sup>6.52</sup>, Asn253<sup>6.55</sup>, and Ile274<sup>7.39</sup>.

active conformation of rhodopsin and other class A receptors (36, 48, 49). Of particular note is that, with the exception of the rhodopsins, none of the GPCR structures solved to date have the ionic-lock interaction, including the A<sub>2A</sub> adenosine receptor. Instead, as in  $\beta_1$ AR and  $\beta_2$ AR, the D/ERY motif in the A<sub>2A</sub> adenosine receptor participates in interactions that restrain the conformation of ICL2. In the A<sub>2A</sub> adenosine receptor, Asp101<sup>3,49</sup> forms a hydrogen bond with Tyr112<sup>3,60</sup> in ICL2 and Thr41<sup>2,39</sup> at the base of helix II (Fig. 5A). Similar hydrogen-bonding interactions were reported in the turkey  $\beta_1$ AR structure (37), but not in any of the  $\beta_2$ AR structures where Asp130<sup>3,49</sup> forms a hydrogen bond with Ser143<sup>3,62</sup>, although there is a tyrosine at the 3.60 position (Fig. 5, B and C) (23, 27, 30). This discrepancy is caused by a short helical section in the ICL2 of both  $\beta_1$ AR and the A<sub>2A</sub> adenosine receptor that is not present in any of the  $\beta_2$ AR structures (Fig. 5). It has been proposed that ICL2 serves as a control switch facilitating G protein activation through a select set of interactions (50). Note that the basal activity profile among the  $\beta_1$ AR,  $\beta_2$ AR, and the A<sub>2A</sub> adenosine receptors correlates with the presence of this short helix in ICL2 and the presence of hydrogen-bonding interactions between tyrosine at position 3.60 in ICL2 and Asp at position 3.49. In  $\beta_1$ AR and A<sub>2A</sub> adenosine receptor, both of which have low basal activity, this interaction is present (51, 52). In contrast,  $\beta_2$ AR exhibits high basal activity and lacks helical structure within its ICL2, which results in altered interactions with the DRY motif (51). Instead of participating in an ionic lock, as in rhodopsin, the arginine residue in the D/ERY motif may play a role in stabilizing the deprotonated state of the adjacent aspartate or glutamate residue, which would strengthen the polar interactions between the D/ERY motif and both ICL2 and helix II. This set of interactions may have direct implications in G-protein activation (48).

**Extracellular loops' mediation of ligand entry and binding.** The extracellular surface properties of the A<sub>2A</sub> adenosine receptor are largely dictated by its second extracellular loop (ECL2), which is considerably different from that of  $\beta_1$ AR,  $\beta_2$ AR, and rhodopsin (Fig. 1 and Fig. 4). The ECL2 of the A<sub>2A</sub> adenosine receptor lacks the prominent secondary structural elements, such as  $\beta$  sheet and  $\alpha$  helix, which were observed in the rhodopsin and  $\beta$ ARs, respectively. Instead, the ECL2 of the A<sub>2A</sub> adenosine receptor is mainly a spatially constrained random coil having three disulfide linkages with ECL1 (Fig. 4C). Two of the three disulfide bonds (Cys71<sup>2,69</sup>–Cys159<sup>5,20</sup> and Cys74<sup>3,22</sup>–Cys146<sup>4,67</sup>) are unique to the A<sub>2A</sub> adenosine receptor; the third (Cys77<sup>3,25</sup>–Cys166<sup>5,27</sup>) is conserved among many class A GPCRs. In addition, a fourth intraloop disulfide bond is formed in ECL3 between Cys259<sup>6,61</sup>

and Cys262<sup>6,64</sup> with the sequence Cys-Pro-Asp-Cys (CPDC), which creates a kink in the loop that constrains the position of ECL3 and orients His264<sup>6,66</sup> at the top of the ligand-binding site. It is interesting that the extensive disulfide bond network forms a rigid, open structure exposing the ligand-binding cavity to solvent, possibly allowing free access for small molecule ligands. In addition, the family-conserved disulfide bridge (Cys77<sup>3,25</sup>–Cys166<sup>5,27</sup>) is adjacent to a short helical segment that presents two crucial residues for ligand-binding interactions (Phe168<sup>5,29</sup> and Glu169<sup>5,30</sup>). The missing tip of the loop (Gln148 to Ser156) is spatially distinct from the ligand-binding site and probably does not directly interact with the binding cavity. Mutation of Cys262<sup>6,64</sup> to Gly did not affect binding to radioligand agonist or antagonist, which indicated that the kink in ECL3 may not be a prerequisite for receptor function or that the other disulfide bonds are sufficient to constrain extracellular loop architecture (53). Mutational studies on the A<sub>1</sub> adenosine receptor indicate that these cysteine residues (Cys80<sup>3,25</sup>–Cys169<sup>5,27</sup> in the A<sub>1</sub> receptor) (see fig. S1) are critical for expression because of a complete loss of radiolabeled-antagonist binding in the absence of this disulfide bond.

**Analysis of the ligand-binding cavity.** To date, structural and biophysical data on the class A GPCRs with diffusible ligands has been dominated by the biogenic amine receptors, such as the adrenergic, dopamine, and serotonin families. These amine ligands are all positively charged at physiologic pH and are known to interact with a key negatively charged aspartate residue (Asp<sup>3,32</sup>) on helix III. Indeed, in all three of the available  $\beta$ -adrenergic structures, each cocrystallized ligand interacts with this residue and binds in a pocket quite similar to that of retinal in rhodopsin. Analysis of the binding sites of the three available GPCR structures indicates two possibilities for the other members of the class A family: (i) Other ligands will bind in a spatially similar binding site, with the ligand specificity dictated by sequence differences within the binding pocket, or (ii) ligands for other receptors may bind in a completely different fashion by interacting with other positions on the receptor. In contrast to the  $\beta$ -adrenergic ligands and retinal, ZM241385 occupies a significantly different position in the transmembrane network (Fig. 4), where its orientation is almost perpendicular to the membrane plane (Figs. 4C and 6). The bicyclic triazolotriazine core of ZM241385 is anchored by an aromatic stacking interaction with Phe168<sup>5,29</sup>, an aliphatic hydrophobic interaction with Ile274<sup>7,39</sup> and a hydrogen-bonding interaction with Asn253<sup>6,55</sup> (Fig. 6). Adjacent to Phe168<sup>5,29</sup>, a polar residue (Glu169<sup>5,30</sup>) interacts with the exocyclic amino group (N15 atom) linked to the bicyclic core of ZM241385 (Fig. 6B). Mu-

tation of Glu169<sup>5,30</sup> to alanine reduces the affinity for both antagonists and agonists and causes a reduction in agonist efficacy by three orders of magnitude (54). However, mutating this position to glutamine did not have a substantial impact on antagonist-binding affinity, which suggested hydrogen bonding as the predominant means of interacting with N15 of ZM241385, as opposed to Coulombic interactions (Fig. 6B). Early studies indicate that mutation of Asn253<sup>6,55</sup> to alanine, which would disrupt an important polar contact with the exocyclic N15 atom of ZM241385, results in a complete loss of both agonist and antagonist binding (55). The structure also shows that Ile274<sup>7,39</sup> forms a hydrophobic contact with the C12 atom of ZM241385; accordingly, mutation of Ile274<sup>7,39</sup> to alanine results in negligible antagonist binding and an order of magnitude reduction in agonist potency (55). No mutagenesis data are available for Phe168<sup>5,29</sup> or Leu249, both of which anchor the bicyclic ring of ZM241385 through  $\pi$  stacking and hydrophobic interactions, respectively, although their involvement in ligand binding has been proposed (56). The phenolic hydroxyl group extending from the ethylamine chain of ZM241385 forms a hydrogen bond with an ordered water molecule. The phenyl ring forms hydrophobic interactions with Leu267<sup>7,32</sup> and Met270<sup>7,35</sup> that would suggest hydrophobicity rather than aromaticity as means of interaction with the phenolic substituent. Indeed, a ZM241385 derivative, with a cycloalkyl substituent (LUF5477) instead of phenylmethylene, also has high affinity for the A<sub>2A</sub> adenosine receptor (57). In a recent study on new antagonists for the A<sub>2A</sub> adenosine receptor, it was demonstrated that tremendous substituent flexibility exists in this area of the pharmacophore (58). This observation correlates well with the directionality of the phenylethylamine substituent in ZM241385, because it is directed toward the more-solvent-exposed extracellular region (ECL2 and ECL3) rather than toward the transmembrane domain of the receptor, as was previously proposed (38, 39). The other substituent in ZM241385 is the furan ring, a feature that occurs in many A<sub>2A</sub> adenosine receptor antagonists. This moiety is located deep in the ligand-binding cavity and directed toward helices V and VII, where it hydrogen-bonds to Asn253<sup>6,55</sup> and forms a water-mediated interaction with His250<sup>6,52</sup> (Fig. 6A). Hydrophobic interactions of the furan ring system include His250<sup>6,52</sup> with C23 and Leu249<sup>6,51</sup> with the C22 and C21 atoms of ZM241385. Mutation of His250<sup>6,52</sup> to alanine completely abolishes ligand binding, whereas mutation to phenylalanine or tyrosine residues modestly affects agonist binding but not antagonist binding (55, 59); replacement with an asparagine slightly increases ligand affinity (59). The furan ring is  $\sim 3$  Å away from the highly conserved Trp246<sup>6,48</sup>, an important residue in



receptor activation as discussed above (60). We speculate that the hydrophobic interactions between ZM241385's furan ring and this residue will hinder the structural rearrangements necessary for activation and so constrain the receptor in an inactive state.

The A<sub>2A</sub> adenosine ligand-bound structure suggests that there is no general, family-conserved receptor-binding pocket in which selectivity is achieved through different amino acid side chains. Rather, the pocket itself can vary in position and orientation and so offer more opportunity for receptor diversity and ligand selectivity. Perhaps as a result of this shift, the empirically determined positions of the substituents (phenyl and furanyl) extending from the aromatic core of ZM241385 deviate substantially from what was suggested in molecular modeling studies in which the ligand-binding site of retinal and/or  $\beta$ -blockers was used as the starting point (38, 39). The position of these substituents can be seen as the rationale for A<sub>2A</sub> receptor selectivity, and this may help in the design of new chemical entities with increased selectivity for this important drug target.

## References and Notes

- B. B. Fredholm, J. F. Chen, S. A. Masino, J. M. Vaugeois, *Annu. Rev. Pharmacol. Toxicol.* **45**, 385 (2005).
- B. B. Fredholm, A. P. Ijzerman, K. A. Jacobson, K. N. Klotz, J. Linden, *Pharmacol. Rev.* **53**, 527 (2001).
- T. V. Dunwiddie, S. A. Masino, *Annu. Rev. Neurosci.* **24**, 31 (2001).
- K. A. Jacobson, Z. G. Gao, *Nat. Rev. Drug Discov.* **5**, 247 (2006).
- J. Sawynok, X. J. Liu, *Prog. Neurobiol.* **69**, 313 (2003).
- Y. Shi *et al.*, *J. Cereb. Blood Flow Metab.* **28**, 111 (2008).
- M. A. Schwarzschild, L. Agnati, K. Fuxe, J. F. Chen, M. Morelli, *Trends Neurosci.* **29**, 647 (2006).
- S. Lahiri, C. H. Mitchell, D. Reigada, A. Roy, N. S. Cherniack, *Respir. Physiol. Neurobiol.* **157**, 123 (2007).
- R. Basheer, R. E. Strecker, M. M. Thakkar, R. W. McCarley, *Prog. Neurobiol.* **73**, 379 (2004).
- M. A. Hernan, B. Takkouche, F. Caamano-Isorna, J. J. Gestal-Otero, *Ann. Neurol.* **52**, 276 (2002).
- S. Ferre, *J. Neurochem.* **105**, 1067 (2008).
- S. Ferre *et al.*, *Front. Biosci.* **13**, 2391 (2008).
- A. H. Schapira *et al.*, *Nat. Rev. Drug Discov.* **5**, 845 (2006).
- D. Blum, R. Hourez, M. C. Galas, P. Popoli, S. N. Schiffmann, *Lancet Neurol.* **2**, 366 (2003).
- R. A. Brown, D. Spina, C. P. Page, *Br. J. Pharmacol.* **153**, (Suppl. 1), S446 (2008).
- M. J. During, D. D. Spencer, *Ann. Neurol.* **32**, 618 (1992).
- E. E. Benarroch, *Neurology* **70**, 231 (2008).
- E. Ongini, S. Dionisotti, S. Gessi, E. Irenius, B. B. Fredholm, *Naunyn-Schmiedeberg's Arch. Pharmacol.* **359**, 7 (1999).
- S. M. Poucher *et al.*, *Br. J. Pharmacol.* **115**, 1096 (1995).
- B. E. Cohen *et al.*, *Proc. Natl. Acad. Sci. U.S.A.* **102**, 965 (2005).
- B. K. Kobilka, X. Deupi, *Trends Pharmacol. Sci.* **28**, 397 (2007).
- V. P. Jaakola, J. Prilusky, J. L. Sussman, A. Goldman, *Protein Eng. Des. Sel.* **18**, 103 (2005).
- S. G. Rasmussen *et al.*, *Nature* **450**, 383 (2007).
- D. M. Rosenbaum *et al.*, *Science* **318**, 1266 (2007).
- F. Magnani, Y. Shibata, M. J. Serrano-Vega, C. G. Tate, *Proc. Natl. Acad. Sci. U.S.A.* **105**, 10744 (2008).
- M. J. Serrano-Vega, F. Magnani, Y. Shibata, C. G. Tate, *Proc. Natl. Acad. Sci. U.S.A.* **105**, 877 (2008).
- V. Cherezov *et al.*, *Science* **318**, 1258 (2007).
- C. K. Engel, L. Chen, G. G. Prive, *Biochim. Biophys. Acta* **1564**, 38 (2002).
- Materials and methods are available as supporting material on Science Online.
- M. A. Hanson *et al.*, *Structure* **16**, 897 (2008).
- A<sub>2A</sub>-T4L refers to a construct in which the third cytoplasmic loop (residues Leu208<sup>5,69</sup> to Ala221<sup>6,23</sup>) was replaced with T4L, and the full carboxy terminus was intact (Ala317 to Ser412). A<sub>2A</sub>-WT refers to the wild-type construct without T4L. All constructs have a FLAG purification tag in the amino terminus and 10 histidine residues in the carboxy terminus.
- Z. G. Gao, A. P. Ijzerman, *Biochem. Pharmacol.* **60**, 669 (2000).
- Amino acid numbering is based on the human adenosine A<sub>2A</sub> primary sequence (accession number P29274). Note: In addition to numbering residue positions in the primary amino acid sequence, the residues have numbers in superscripts (X.YY) that indicate their position in each transmembrane helix (X, helix number, from 1 to 8), relative to the most conserved reference residue in that helix (YY). This residue is arbitrarily assigned the number 50; numbers decrease toward the N terminus and increase toward the C terminus. However, the numbering is not used in loop regions beyond residues X.20 and/or X.80 or T4L.
- In this crystal form, the crystallographic contacts are mostly driven by the T4L protein where receptor-to-lysozyme and lysozyme-to-lysozyme mainly form the lattice contacts. A relatively large receptor-to-receptor crystallographic interface (~520 Å<sup>2</sup>) forms antiparallel receptor dimers (fig. S4). The total surface interface between receptor and T4L moieties is ~1300 Å<sup>2</sup>, whereas lysozyme-to-lysozyme is ~200 Å<sup>2</sup>. The largest contact interface (~500 Å<sup>2</sup>) between receptor and T4L is noncrystallographic and is located in the cytoplasmic site, where receptor is fused to the T4L. The other receptor-to-lysozyme surface interfaces are crystallographic (260 Å<sup>2</sup>). In comparison with the previously solved  $\beta_2$ AR-T4L fusion proteins, the T4L domain is tilted from the membrane plane and creates more surface interactions than seen in human  $\beta_2$ AR-T4L constructs that were solved in different space groups.
- M. Murakami, T. Kouyama, *Nature* **453**, 363 (2008).
- K. Palczewski *et al.*, *Science* **289**, 739 (2000).
- T. Warne *et al.*, *Nature* **454**, 486 (2008).
- A. Martinielli, T. Tuccinardi, *Med. Res. Rev.* **28**, 247 (2008).
- O. Yuzlenko, K. Kiec-Kononowicz, *J. Comput. Chem.*, 21 May 2008, 10.1002/jcc.21001, in press.
- P. Joost, A. Methner, *Genome Biol.* **3**, RESEARCH0063 (2002).
- D. K. Vassiliadis *et al.*, *Proc. Natl. Acad. Sci. U.S.A.* **100**, 4903 (2003).
- The FatCat server (<http://fatcat.burnham.org/>) was used for structural alignment of the transmembrane helices with the rhodopsin structure 1U19 as a reference taken directly from that server: "It simultaneously addresses the two major goals of flexible structure alignment; optimizing the alignment and minimizing the number of rigid-body movements (twists) around pivot points (hinges) introduced in the reference structure."
- G. S. Ratnaparkhi, R. Varadarajan, *Biochemistry* **39**, 12365 (2000).
- We used the program Occluded Surface (OS) that calculates the occluded surface and atomic packing of protein model structures: [www.csb.yale.edu/userguides/datamanip/os/](http://www.csb.yale.edu/userguides/datamanip/os/).
- It has been speculated that the general activation mechanism include following changes 6.47 (gauche + conformer) / 6.48 (trans - conformer) / 6.52 (trans - conformer) represent the active state (R\*) and 6.47 (trans - conformer) / 6.48 (gauche + conformer) / 6.52 (gauche + conformer) represent inactive state (R).
- D. L. Farrens, C. Altenbach, K. Yang, W. L. Hubbell, H. G. Khorana, *Science* **274**, 768 (1996).
- Basal or constitutive activity is the spontaneous production of cellular response in the absence of a ligand. An inverse agonist shifts the equilibrium toward the inactive state. An agonist shifts the conformation toward the active state. A (neutral) antagonist binds to receptors and blocks the active site but does not shift the equilibrium. A typical GPCR can "dial" almost any conformational equilibrium between fully inactive and fully active; therefore, an agonist or inverse agonist can be classified as partial to full. Depending on receptor and cellular environment, the nature of an inverse agonist and a truly neutral antagonist can be difficult to detect.
- R. Vogel *et al.*, *J. Mol. Biol.* **380**, 648 (2008).
- T. Okada *et al.*, *J. Mol. Biol.* **342**, 571 (2004).
- E. S. Burstein, T. A. Spalding, M. R. Brann, *J. Biol. Chem.* **273**, 24322 (1998).
- L. Birnbaumer, F. O. Levy, X. Zhu, A. J. Kaumann, *Tex. Heart Inst. J.* **21**, 16 (1994).
- J. Zezula, M. Freissmuth, *Br. J. Pharmacol.* **153** (suppl. 1), S184 (2008).
- D. J. Scholl, J. N. Wells, *Biochem. Pharmacol.* **60**, 1647 (2000).
- J. Kim *et al.*, *Mol. Pharmacol.* **49**, 683 (1996).
- J. Kim, J. Wess, A. M. van Rhee, T. Schoneberg, K. A. Jacobson, *J. Biol. Chem.* **270**, 13987 (1995).
- S. Moro *et al.*, *Chem. Commun. (Camb.)* 2949 (2003).
- M. De Zwart *et al.*, *Drug Dev. Res.* **48**, 95 (1999).
- M. Mantri *et al.*, *J. Med. Chem.* **51**, 4449 (2008).
- Q. Jiang, B. X. Lee, M. Glashofer, A. M. van Rhee, K. A. Jacobson, *J. Med. Chem.* **40**, 2588 (1997).
- M. Audet, M. Bouvier, *Nat. Chem. Biol.* **4**, 397 (2008).
- This work was supported by the NIH Roadmap Initiative grant P50 GM073197 for technology development, Protein Structure Initiative grant U54 GM074961 for target processing, and Pfizer (R.C.S.). A.P.I.J. and J.R.L. thank the Dutch Top Institute Pharma for financial support through the GPCR forum program (D1-105). The authors thank P. Kuhn for encouragement and support, J. Velasquez for help on molecular biology, T. Trinh and K. Allin for help on baculoviral expression, Q. Li and T. Mulder for biochemical and pharmacological characterization of the receptor constructs, A. Walker for assistance with manuscript preparation, and I. Wilson for scientific feedback and discussions. The authors acknowledge Y. Zheng, The Ohio State University, and M. Caffrey, University of Limerick, for the generous loan of the in meso robot [built with support from the National Institutes of Health (GM075915), the National Science Foundation (IIS0308078), and Science Foundation Ireland (02-IN1-B266)]; and J. Smith, R. Fischetti, and N. Sanishvili at the GM/CA-CAT beamline at the Advanced Photon Source, for assistance in development and use of the minibeam and beamtime. The GM/CA-CAT beamline (23-ID) is supported by the National Cancer Institute (Y1-CO-1020) and the National Institute of General Medical Sciences (Y1-GM-1104). Atomic coordinates and structure factors have been deposited in the Protein Data Bank with identification code 3EML. The authors, R.C.S., V.-P.J., M.T.G., M.A.H., and V.C. have filed a patent related to the crystals of human adenosine A<sub>2A</sub> receptor.

## Supporting Online Material

[www.sciencemag.org/cgi/content/full/1164772/DC1](http://www.sciencemag.org/cgi/content/full/1164772/DC1)  
Materials and Methods  
Tables S1 to S3  
Figs. S1 to S6  
References

18 August 2008; accepted 25 September 2008  
Published online 2 October 2008;  
10.1126/science.1164772  
Include this information when citing this paper.



# The Fermi Gamma-Ray Space Telescope Discovers the Pulsar in the Young Galactic Supernova Remnant CTA 1

A. A. Abdo,<sup>1,2</sup> M. Ackermann,<sup>3</sup> W. B. Atwood,<sup>4</sup> L. Baldini,<sup>5</sup> J. Ballet,<sup>6</sup> G. Barbiellini,<sup>7,8</sup> M. G. Baring,<sup>9</sup> D. Bastieri,<sup>10,11</sup> B. M. Baughman,<sup>12</sup> K. Bechtol,<sup>3</sup> R. Bellazzini,<sup>5</sup> B. Berenji,<sup>3</sup> R. D. Blandford,<sup>3</sup> E. D. Bloom,<sup>3</sup> G. Bogaert,<sup>13</sup> E. Bonamente,<sup>14,15</sup> A. W. Borgland,<sup>3</sup> J. Bregeon,<sup>5</sup> A. Brez,<sup>5</sup> M. Brigida,<sup>16,17</sup> P. Bruel,<sup>13</sup> T. H. Burnett,<sup>18</sup> G. A. Caliendo,<sup>16,17</sup> R. A. Cameron,<sup>3</sup> P. A. Caraveo,<sup>19</sup> P. Carlson,<sup>20</sup> J. M. Casandjian,<sup>6</sup> C. Cecchi,<sup>14,15</sup> E. Charles,<sup>3</sup> A. Chekhtman,<sup>2,21</sup> C. C. Cheung,<sup>22</sup> J. Chiang,<sup>3</sup> S. Ciprini,<sup>14,15</sup> R. Claus,<sup>3</sup> J. Cohen-Tanugi,<sup>23</sup> L. R. Cominsky,<sup>24</sup> J. Conrad,<sup>20,25</sup> S. Cutini,<sup>26</sup> D. S. Davis,<sup>2,27</sup> C. D. Dermer,<sup>2</sup> A. de Angelis,<sup>28</sup> F. de Palma,<sup>16,17</sup> S. W. Digel,<sup>3</sup> M. Dormody,<sup>4</sup> E. do Couto e Silva,<sup>3</sup> P. S. Drell,<sup>3</sup> R. Dubois,<sup>3</sup> D. Dumora,<sup>29,30</sup> Y. Edmonds,<sup>3</sup> C. Farnier,<sup>23</sup> W. B. Focke,<sup>3</sup> Y. Fukazawa,<sup>31</sup> S. Funk,<sup>3</sup> P. Fusco,<sup>16,17</sup> F. Gargano,<sup>17</sup> D. Gasparrini,<sup>26</sup> N. Gehrels,<sup>22,32</sup> S. Germani,<sup>14,15</sup> B. Giebels,<sup>13</sup> N. Giglietto,<sup>16,17</sup> F. Giordano,<sup>16,17</sup> T. Glanzman,<sup>3</sup> G. Godfrey,<sup>3</sup> I. A. Grenier,<sup>6</sup> M.-H. Grondin,<sup>29,30</sup> J. E. Grove,<sup>2</sup> L. Guillemot,<sup>29,30</sup> S. Guiriec,<sup>23</sup> A. K. Harding,<sup>22</sup> R. C. Hartman,<sup>22</sup> E. Hays,<sup>22</sup> R. E. Hughes,<sup>12</sup> G. Jóhannesson,<sup>3</sup> A. S. Johnson,<sup>3</sup> R. P. Johnson,<sup>4</sup> T. J. Johnson,<sup>22,32</sup> W. N. Johnson,<sup>2</sup> T. Kamae,<sup>3</sup> Y. Kanai,<sup>33</sup> G. Kanbach,<sup>34</sup> H. Katagiri,<sup>31</sup> N. Kawai,<sup>33,35</sup> M. Kerr,<sup>18</sup> T. Kishishita,<sup>36</sup> B. Kiziltan,<sup>37</sup> J. Knödseder,<sup>38</sup> M. L. Kocian,<sup>3</sup> N. Komin,<sup>6,23</sup> F. Kuehn,<sup>12</sup> M. Kuss,<sup>5</sup> L. Latronico,<sup>5</sup> M. Lemoine-Goumard,<sup>29,30</sup> F. Longo,<sup>7,8</sup> V. Lonjou,<sup>29,30</sup> F. Loparco,<sup>16,17</sup> B. Lott,<sup>29,30</sup> M. N. Lovellette,<sup>2</sup> P. Lubrano,<sup>14,15</sup> A. Makeev,<sup>21</sup> M. Marelli,<sup>19</sup> M. N. Mazziotta,<sup>17</sup> J. E. McEnery,<sup>22</sup> S. McGlynn,<sup>20</sup> C. Meurer,<sup>25</sup> P. F. Michelson,<sup>3</sup> T. Mineo,<sup>39</sup> W. Mitthumsiri,<sup>3</sup> T. Mizuno,<sup>31</sup> A. A. Moiseev,<sup>40</sup> C. Monte,<sup>16,17</sup> M. E. Monzani,<sup>3</sup> A. Morselli,<sup>41</sup> I. V. Moskalenko,<sup>3</sup> S. Murgia,<sup>3</sup> T. Nakamori,<sup>33</sup> P. L. Nolan,<sup>3</sup> E. Nuss,<sup>23</sup> M. Ohno,<sup>36</sup> T. Ohsugi,<sup>31</sup> A. Okumura,<sup>42</sup> N. Omodei,<sup>5</sup> E. Orlando,<sup>34</sup> J. F. Ormes,<sup>43</sup> M. Ozaki,<sup>36</sup> D. Paneque,<sup>3</sup> J. H. Panetta,<sup>3</sup> D. Parent,<sup>29,30</sup> V. Pelassa,<sup>23</sup> M. Pepe,<sup>14,15</sup> M. Pesce-Rollins,<sup>5</sup> G. Piano,<sup>41</sup> L. Pieri,<sup>10</sup> F. Piron,<sup>23</sup> T. A. Porter,<sup>4</sup> S. Rainò,<sup>16,17</sup> R. Rando,<sup>10,11</sup> P. S. Ray,<sup>2</sup> M. Razzano,<sup>5</sup> A. Reimer,<sup>3</sup> O. Reimer,<sup>3</sup> T. Reposeur,<sup>29,30</sup> S. Ritz,<sup>22,32</sup> L. S. Rochester,<sup>3</sup> A. Y. Rodriguez,<sup>44</sup> R. W. Romani,<sup>3</sup> M. Roth,<sup>18</sup> F. Ryde,<sup>20</sup> H. F.-W. Sadrozinski,<sup>4</sup> D. Sanchez,<sup>13</sup> A. Sander,<sup>12</sup> P. M. Saz Parkinson,<sup>4</sup> T. L. Schalk,<sup>4</sup> A. Sellerholm,<sup>25</sup> C. Sgrò,<sup>5</sup> E. J. Siskind,<sup>45</sup> D. A. Smith,<sup>29,30</sup> P. D. Smith,<sup>12</sup> G. Spandre,<sup>5</sup> P. Spinelli,<sup>16,17</sup> J.-L. Starck,<sup>6</sup> M. S. Strickman,<sup>2</sup> D. J. Suson,<sup>46</sup> H. Tajima,<sup>3</sup> H. Takahashi,<sup>31</sup> T. Takahashi,<sup>36</sup> T. Tanaka,<sup>3</sup> J. B. Thayer,<sup>3</sup> J. G. Thayer,<sup>3</sup> D. J. Thompson,<sup>22</sup> S. E. Thorsett,<sup>4</sup> L. Tibaldo,<sup>10,11</sup> D. F. Torres,<sup>44,47</sup> G. Tosti,<sup>14,15</sup> A. Tramacere,<sup>3,48</sup> T. L. Usher,<sup>3</sup> A. Van Etten,<sup>3</sup> N. Vilchez,<sup>38</sup> V. Vitale,<sup>41</sup> P. Wang,<sup>3</sup> K. Watters,<sup>3</sup> B. L. Winer,<sup>12</sup> K. S. Wood,<sup>2\*</sup> H. Yasuda,<sup>31</sup> T. Ylinen,<sup>20,49</sup> M. Ziegler<sup>4\*</sup>

Energetic young pulsars and expanding blast waves [supernova remnants (SNRs)] are the most visible remains after massive stars, ending their lives, explode in core-collapse supernovae. The Fermi Gamma-Ray Space Telescope has unveiled a radio quiet pulsar located near the center of the compact synchrotron nebula inside the supernova remnant CTA 1. The pulsar, discovered through its gamma-ray pulsations, has a period of 316.86 milliseconds and a period derivative of  $3.614 \times 10^{-13}$  seconds per second. Its characteristic age of  $10^4$  years is comparable to that estimated for the SNR. We speculate that most unidentified Galactic gamma-ray sources associated with star-forming regions and SNRs are such young pulsars.

After the discovery of radio pulsars in the late 1960s, some clear supernova remnant (SNR)–pulsar associations were discovered (most notably the Crab and Vela systems). Observations in the radio, x-ray, and gamma-ray bands with increasing sensitivity during the past 30 years have added many more SNR/pulsar associations. Yet we are still far from the complete census of these products of massive star deaths, which is needed to study a major population of stellar and Galactic astronomy. Here we report the discovery of a gamma-ray pulsar with a spin period of 316 ms, coinciding with the previously known gamma-ray source 3EG J0010+7309, thus confirming the identification of the neutron star (NS) powering the pulsar wind nebula (PWN) and the gamma-ray source. This pulsar detection im-

plies that many of the yet-unidentified low-latitude Galactic gamma-ray sources also could be pulsars.

A survey of radio sources conducted at 960 MHz with the Owens Valley Radio Observatory in the 1960s led to the discovery of a previously uncataloged extended source (1), designated CTA 1, as the first object in Caltech's catalog A. Follow-up radio surveys (2–7) with increased sensitivity and angular resolution showed that CTA 1 has the typical morphology of a shell-type SNR with an incomplete shell of filaments and extended emission from a broken shell roughly circular and  $\sim 90$  arc min in diameter (Fig. 1). The excitation of atomic lines in the shocked interstellar medium with well-defined optical filaments (8) lends further support to the identification of CTA 1 as a young SNR in the Sedov phase of expansion.

The radio and x-ray characteristics of CTA 1 imply that it is  $1.4 \pm 0.3$  kpc away (6) and that it exploded 5000 to 15,000 years ago (6, 9, 10).

Imaging and spectroscopy of CTA 1 with *ROSAT* (11), *ASCA* (9), *XMM* (10), and *Chandra* (12) revealed a typical center-filled or composite SNR with a central point source, RXJ0007.0+7303, embedded in a compact nebula, and a jetlike extension (12). The offset of the x-ray source from the geometrical center of the SNR suggested that it has a transverse velocity (11) of  $\sim 450$  km s<sup>-1</sup>. The natural interpretation of these data are that of a young NS, visible both in thermal surface and nonthermal magnetospheric emission (12), powering a synchrotron PWN. The thermal spectrum from the NS (11, 12) is not easily interpreted: The temperature is too high and the required emission area is too small if the NS has no atmosphere. A particle-heated polar cap could be a possibility. Alternatively, if the NS has a light element atmosphere and cools through a direct Urca process, a cooling age of  $(1 \text{ to } 2) \times 10^4$  years is also possible (11). Although no signs of periodicity could be found in the x-ray data (11), the energetics of the PWN lead to typical requirements for the time-averaged spin-down power of the putative pulsar of  $10^{36}$  to  $10^{37}$  erg s<sup>-1</sup>. Very deep searches (12) for a counterpart of the x-ray source in radio and optical wavebands resulted only in upper limits. If RX J0007.0+7303 is indeed a radio pulsar, its radio luminosity is an order of magnitude below the faintest radio pulsars known (12). It is likely that the radio beam does not intersect the Earth.

High-energy emission ( $>100$  MeV) from the *EGRET* source 3EG J0010+7309 matches RX J0007.0+7303 spatially, although the *EGRET* position uncertainty is very large (13). The position derived from *EGRET* photons above 1 GeV (14) at galactic longitude  $l$  and latitude  $b = 119.87, 10.52$  with an error radius of 11 arc min (95% confidence) overlaps even better with the *ROSAT* source ( $l, b = 119.6602, 10.4629$ ). It has thus been suggested that the 3EG source is an unresolved source in CTA 1 (14), or, more generally, that several unidentified gamma-ray sources are associated with SNRs (15). However, confirmation of such SNR associations based on imaging was not possible with the *EGRET* angular resolution. The CTA 1 gamma-ray source shows all indications of being a young pulsar: The gamma-ray flux was constant through the epochs of *EGRET* observations (1991 to 1995), and the spectrum showed a hard power law with an index of  $-1.6 \pm 0.2$  and a spectral steepening above  $\sim 2$  GeV (14), which is similar to other *EGRET* pulsars like Geminga and Vela. For an assumed pulsar beam of 1 sr (and taking into account the uncertainty in distance), the observed gamma-ray flux corresponds to a luminosity of  $(4 \pm 2) \times 10^{33}$  erg s<sup>-1</sup>, which is well within the range of the luminosities of Geminga [ $9 \times 10^{32}$  erg s<sup>-1</sup>,  $P \sim 237$  ms (where  $P$  is the spin period)] and Crab ( $4 \times 10^{34}$  erg s<sup>-1</sup>,  $P \sim 33$  ms).

On 11 June 2008, the Fermi Gamma-Ray Space Telescope was launched into a low Earth

orbit (16). The imaging gamma-ray telescope LAT (Large Area Telescope), Fermi's main instrument, covers the energy range from 20 MeV up to >300 GeV with a sensitivity that exceeds that of *EGRET*. The first exposures of the region of CTA 1 were made during the commissioning phase of Fermi LAT (30 June to 30 July 2008) and in the initial days (5 to 20 August 2008) of routine operations. Although the telescope was not yet fully tuned and calibrated during commissioning, >900 gamma-ray photons above 100 MeV from 3EG J0010+7309 were recorded during these exposures [see supporting online material (SOM)], which amounts to ~2.6 times the number collected with *EGRET* from this source over its entire mission.

A bright gamma-ray source is detected at  $l, b = 119^\circ.652, 10^\circ.468$  with a 95% (statistical) error circle radius of  $0^\circ.038$  (a systematic error of  $\sim 0^\circ.02$  is not included). Figure 1 shows the LAT source and the x-ray source RX J00070+7302, which is located central to the PWN, superimposed on the radio map at 1420 MHz (7). These fall on the edge of 3EG J0010+7309 ( $l, b = 119.92, 10.54$ ) and its 95% error circle of radius  $0.24^\circ$ . The measured flux of the LAT source is  $(3.8 \pm 0.2) \times 10^{-7}$  photons ( $>100$  MeV)  $\text{cm}^{-2} \text{s}^{-1}$ , with an additional systematic uncertainty of 30%, owing to the ongoing calibration of the instrument, which is consistent with the *EGRET* measured flux of  $(4.2 \pm 0.5) \times 10^{-7}$  ph  $\text{cm}^{-2} \text{s}^{-1}$  (13).

The arrival times of the LAT photons, which are recorded with 300-ns accuracy and referenced to the Fermi satellite Global Positioning System clock, were corrected to the solar system barycenter (SSB) using the JPL DE405 solar system ephemeris and the Chandra x-ray position (Table 1). Photons with energy >100 MeV were selected within a radius of  $1^\circ$  around the source position and searched for periodicity. The results described here are not altered substantially if photons within selection radii between  $0.7^\circ$  and  $2.5^\circ$  are used.

Application of a new search technique based on photon arrival-time differencing (17)—which is highly efficient for sparse photon data—and refining and fitting the detections with the pulsar analysis packages PRESTO (18) and Tempo2 (19) resulted in the detection of strong pulsations in the selected photons (see SOM). Figure S1 shows that the pulsations are markedly present over the complete time interval of observation. The pulsar rotational ephemeris is given in Table 1.

By extracting photons around the Vela pulsar from the same set of observations and applying the same analysis procedures, we found the rotational ephemeris for the Vela pulsar to be in good agreement with the values obtained by the LAT radio pulsar timing collaboration (20).

A contour plot of period-period derivative search space reveals the pulsar (Fig. 2), as does the resulting gamma-ray light curve above 100 MeV (Fig. 3).

A NS with a moment of inertia of  $I = 1.0 \times 10^{45}$  g  $\text{cm}^2$  and angular frequency  $\omega$  is assumed to lose its rotational energy through magnetic dipole radiation and follow a braking law of  $\dot{\omega} \propto -\omega^3$ . This can be integrated to yield the characteristic age  $\tau = \omega/2\dot{\omega}$ , which is a coarse estimate of the true age of a pulsar. The spin-down power  $\dot{E}_{\text{rot}} = I\omega\dot{\omega}$  and the dipole magnetic field strength,  $B = 3.2 \times 10^{19} \sqrt{P\dot{P}}$  G, also follow from the parameters of rotation.

For the CTA 1 pulsar, we derive a characteristic age of  $\sim 1.4 \times 10^4$  years, a spin-down power of  $\sim 4.5 \times 10^{35}$  erg  $\text{s}^{-1}$ , and a surface magnetic field strength of  $1.1 \times 10^{13}$  G. This field strength is higher than any of the *EGRET* detected pulsars and second highest among known gamma-ray pulsars. PSR J1509-58, with an inferred field of  $1.54 \times 10^{13}$  G, shows emission only up to  $\sim 30$  MeV, whereas emission from the CTA 1 pulsar is present to at least 5 GeV.

We searched archival data of exposures by *XMM*, *ASCA*, Chandra, and *EGRET* for periods near that extrapolated from the LAT ephemeris. The pulsar was not strongly detected in these data (21).

<sup>1</sup>National Research Council Research Associate, National Academy of Sciences, Washington, DC 20001, USA. <sup>2</sup>Space Science Division, Naval Research Laboratory, Washington, DC 20375, USA. <sup>3</sup>W. W. Hansen Experimental Physics Laboratory, Kavli Institute for Particle Astrophysics and Cosmology, Department of Physics and Stanford Linear Accelerator Center, Stanford University, Stanford, CA 94305, USA. <sup>4</sup>Santa Cruz Institute for Particle Physics, Department of Physics and Department of Astronomy and Astrophysics, University of California at Santa Cruz, Santa Cruz, CA 95064, USA. <sup>5</sup>Istituto Nazionale di Fisica Nucleare, Sezione di Pisa, I-56127 Pisa, Italy. <sup>6</sup>Laboratoire Astrophysique, Interactions, Multi-échelles—Commissariat à l'Énergie Atomique (CEA)—CNRS—Université Paris Diderot, Service d'Astrophysique, CEA Saclay, F-91191 Gif sur Yvette, France. <sup>7</sup>Istituto Nazionale di Fisica Nucleare, Sezione di Trieste, I-34127 Trieste, Italy. <sup>8</sup>Dipartimento di Fisica, Università di Trieste, I-34127 Trieste, Italy. <sup>9</sup>Rice University, Department of Physics and Astronomy, MS-108, Post Office Box 1892, Houston, TX 77251, USA. <sup>10</sup>Istituto Nazionale di Fisica Nucleare, Sezione di Padova, I-35131 Padova, Italy. <sup>11</sup>Dipartimento di Fisica "G. Galilei," Università di Padova, I-35131 Padova, Italy. <sup>12</sup>Department of Physics, Center for Cosmology and Astro-Particle Physics, The Ohio State University, Columbus, OH 43210, USA. <sup>13</sup>Laboratoire Leprince-Ringuet, École Polytechnique, CNRS/IN2P3, Palaiseau, France. <sup>14</sup>Istituto Nazionale di Fisica Nucleare, Sezione di Perugia, I-06123 Perugia, Italy. <sup>15</sup>Dipartimento di Fisica, Università degli Studi di Perugia, I-06123 Perugia, Italy. <sup>16</sup>Dipartimento di Fisica "M. Merlin" dell'Università e del Politecnico di Bari, I-70126 Bari, Italy. <sup>17</sup>Istituto Nazionale di Fisica Nucleare, Sezione di Bari, 70126 Bari, Italy. <sup>18</sup>Department of Physics, University of Washington, Seattle, WA 98195–1560, USA. <sup>19</sup>Istituto Nazionale di Astrofisica—Istituto di Astrofisica Spaziale e Fisica Cosmica, I-20133 Milano, Italy. <sup>20</sup>Department of Physics, Royal Institute of Technology (Kungliga Tekniska Högskolan), AlbaNova, SE-106 91 Stockholm, Sweden. <sup>21</sup>George Mason University, Fairfax, VA 22030, USA. <sup>22</sup>NASA Goddard Space Flight Center, Greenbelt, MD 20771, USA. <sup>23</sup>Laboratoire de Physique Théorique et Astroparticules, Université Montpellier 2, CNRS/IN2P3, Montpellier, France. <sup>24</sup>Department of Physics and Astronomy, Sonoma State University, Rohnert Park, CA 94928–3609, USA. <sup>25</sup>Department of Physics, Stockholm University, AlbaNova, SE-106 91 Stockholm, Sweden. <sup>26</sup>Agenzia Spaziale Italiana Science Data Center, I-00044 Frascati (Roma), Italy. <sup>27</sup>Center for Space Sciences and Technology, University of Maryland, Baltimore County, Baltimore, MD 21250, USA. <sup>28</sup>Dipartimento di Fisica, Università di Udine and Istituto Nazionale di Fisica Nucleare, Sezione di Trieste,

Gruppo Collegato di Udine, I-33100 Udine, Italy. <sup>29</sup>CNRS/IN2P3, Centre d'Études Nucléaires Bordeaux Gradignan, UMR 5797, Gradignan, 33175, France. <sup>30</sup>Université de Bordeaux, Centre d'Études Nucléaires Bordeaux Gradignan, UMR 5797, Gradignan, 33175, France. <sup>31</sup>Department of Physical Science and Hiroshima Astrophysical Science Center, Hiroshima University, Higashi-Hiroshima 739-8526, Japan. <sup>32</sup>University of Maryland, College Park, MD 20742, USA. <sup>33</sup>Department of Physics, Tokyo Institute of Technology, Meguro-ku, Tokyo 152-8551, Japan. <sup>34</sup>Max-Planck-Institut für Extraterrestrische Physik, Giessenbachstraße, 85748 Garching, Germany. <sup>35</sup>Cosmic Radiation Laboratory, Institute of Physical and Chemical Research (RIKEN), Wako, Saitama 351-0198, Japan. <sup>36</sup>Institute of Space and Astronautical Science, Japan Aerospace Exploration Agency (JAXA), 3-1-1 Yoshinodai, Sagami-hara, Kanagawa 229-8510, Japan. <sup>37</sup>University of California Observatories/Lick Observatories, 1156 High Street, Santa Cruz, CA 95064, USA. <sup>38</sup>Centre d'Étude Spatiale des Rayonnements, CNRS/UPS, BP 44346, F-30128 Toulouse Cedex 4, France. <sup>39</sup>Istituto di Astrofisica Spaziale e Fisica Cosmica Palermo, 90146 Palermo, Italy. <sup>40</sup>Center for Research and Exploration in Space Science and Technology, NASA Goddard Space Flight Center, Greenbelt, MD 20771, USA. <sup>41</sup>Istituto Nazionale di Fisica Nucleare, Sezione di Roma "Tor Vergata" and Dipartimento di Fisica, Università di Roma "Tor Vergata," I-00133 Roma, Italy. <sup>42</sup>Department of Physics, Graduate School of Science, University of Tokyo, 7-3-1 Hongo, Bunkyo-ku, Tokyo 113-0033, Japan. <sup>43</sup>Department of Physics and Astronomy, University of Denver, Denver, CO 80208, USA. <sup>44</sup>Institut de Ciències de l'Espai (Institut d'Estudis Espacials de Catalunya—Consejo Superior de Investigaciones Científicas), Campus Universitat Autònoma de Barcelona, 08193 Barcelona, Spain. <sup>45</sup>NYCB Real-Time Computing Inc., 18 Meudon Drive, Lattinotown, NY 11560–1025, USA. <sup>46</sup>Department of Chemistry and Physics, Purdue University Calumet, Hammond, IN 46323–2094, USA. <sup>47</sup>Institució Catalana de Recerca i Estudis Avançats, Barcelona, Spain. <sup>48</sup>Consorzio Interuniversitario per la Fisica Spaziale, I-10133 Torino, Italy. <sup>49</sup>School of Pure and Applied Natural Sciences, University of Kalmar, SE-391 82 Kalmar, Sweden.

\*To whom correspondence should be addressed. E-mail: gok@mpe.mpg.de (G.K.); kent.wood@nrl.navy.mil (K.S.W.); ziegler@scipp.ucsc.edu (M.Z.)

†Present address: Laboratoire Astrophysique, Interactions, Multi-échelles—Commissariat à l'Énergie Atomique (CEA)—CNRS—Université Paris Diderot, Service d'Astrophysique, CEA Saclay, F-91191 Gif sur Yvette, France.

**Table 1.** Rotational ephemeris for the pulsar in CTA 1. The numbers in parentheses indicate the error in the last decimal digit. For the SSB correction, the position of the Chandra x-ray source (12) was assumed.

Frequency (Hz)	Frequency derivative ( $\text{s}^{-2}$ )	Period (ms)	Period derivative ( $\text{s s}^{-1}$ )	Epoch [MJD (TDB)]	R.A. [J2000.0]	DEC. [J2000.0]	Galactic longitude	Galactic latitude
3.165922467(9)	$-3.623(4) \times 10^{-12}$	315.8637050(9)	$3.615(4) \times 10^{-13}$	54647.440 938	00 <sup>h</sup> 07 <sup>m</sup> 01 <sup>s</sup> .56	+73° 03' 08".1	119°.65947(3)	+10°.463348(3)



The new pulsar in CTA 1 exhibits all of the characteristics of a young high-energy pulsar, which powers a synchrotron PWN embedded in a larger SNR. The spin-down power of the CTA 1 pulsar of  $\sim 4.5 \times 10^{35}$  erg s $^{-1}$  is sufficient to supply the PWN with magnetic fields and energetic electrons at the required rate of  $10^{35}$  to  $10^{36}$  erg s $^{-1}$  (10), and the pulsar age is consistent with the inferred age for the SNR. With its spin-down power of  $\sim 4.5 \times 10^{38}$  erg s $^{-1}$ , the Crab pulsar supplies the Crab nebula with its requirement of  $\sim 10^{38}$  erg s $^{-1}$  with a similar efficiency (22). Comparing the total luminosity from

the CTA 1 pulsar inferred from the LAT flux measured for 3EG J0010+7309 to the pulsar spin-down power, we estimate an efficiency of converting spin-down power into pulsed gamma rays that is  $\sim 1\%$ , if the emission is beamed into a solid angle of 1 sr. The Vela pulsar, which is of similar age, has a gamma-ray efficiency of 0.1%; however, PSR B1706-44 (23) (with an age of  $1.7 \times 10^4$  years) has an efficiency of 1.9%, and the much older Geminga pulsar ( $3.4 \times 10^5$  years) converts its spin-down into energetic gamma-rays with an efficiency of  $\sim 3\%$ .

**Fig. 1.** The Fermi LAT gamma-ray source, central PWN x-ray source, and corresponding *EGRET* source superimposed on a 1420-MHz map (7) of CTA 1. The LAT source and its 95% error region (small red circle) is displayed on the map, together with the central PWN source RX J00070+7302 (black cross) and the position and error of the corresponding *EGRET* source 3EG J0010+7309 (large blue circle). The coincidence of the pulsed gamma-ray source and the x-ray point source embedded in the off-center PWN is notable. The offset of the pulsar from the center of the radio SNR, which is thought to be the place of origin, is quite visible. The inferred transverse speed of the pulsar is  $\sim 450$  km s $^{-1}$ , which is a reasonable speed of a pulsar (30).

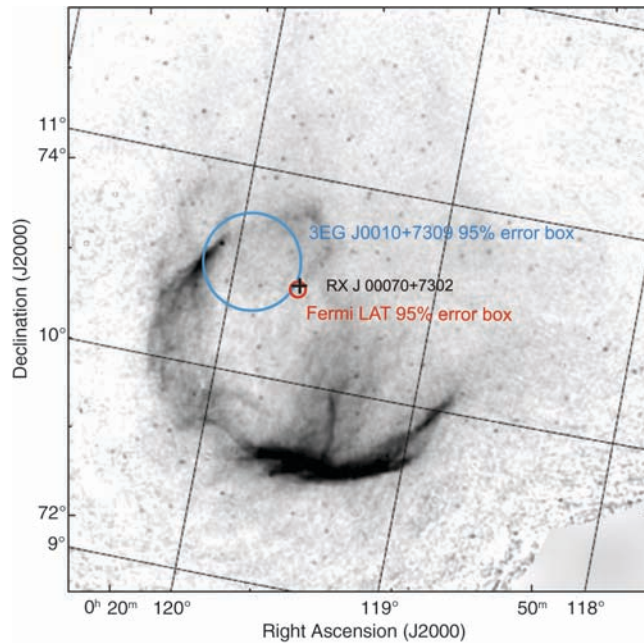
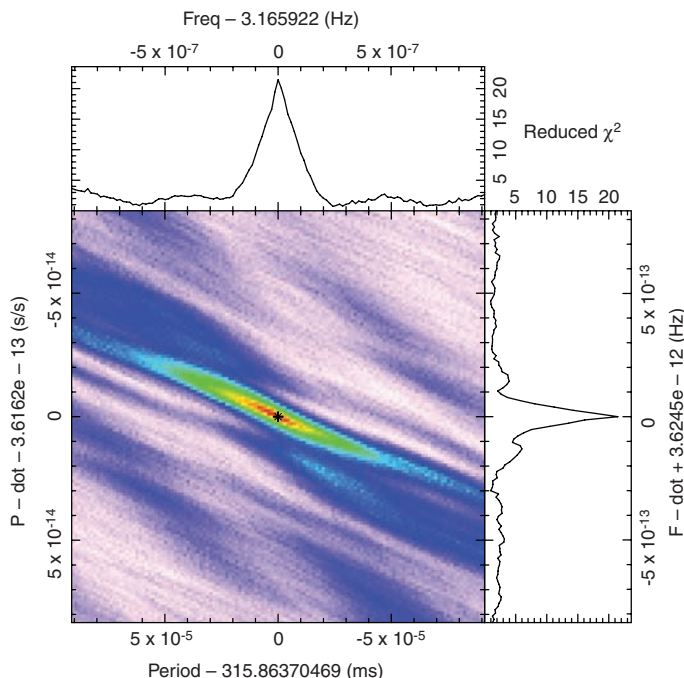


**Fig. 2.** Contours of detection significance over a range of period and period derivative using photons within a radius of  $1^\circ$  around RXJ0007.0+7303. The initial indication of a signal in this  $P, \dot{P}$  region was found with a search technique that uses photon arrival-time differencing (17), whereas the determination of the exact ephemeris makes use of the tools PRESTO and Tempo2 (18, 19).



The gamma-ray characteristics and the absence of a radio signal (12) from the CTA 1 pulsar are suggestive of the family of outer-gap or slot-gap model descriptions for energetic pulsars (24–26). These outer-magnetosphere models naturally generate gamma-ray emission over a broad range of phase, with superposed sharp peaks resulting from caustics in the pattern of the emitted radiation. Because the emission is predicted to cover such a large area of the sky ( $\gg 1$  sr) in such models, the total radiated luminosity as inferred from the observed pulsed flux could result in an efficiency as high as 10%, depending on the magnetic inclination angle. The absence of the radio signal is readily explained by misalignment of a narrow radio beam and our line of sight. Both conditions can be met if we see the pulsar at a large angle with respect to the spin and magnetic field axes, but only a detailed model can quantify the viewing geometry of the CTA 1 pulsar. Spectral cut-offs at energies of 1 to 10 GeV that would be indicative of a polar cap mechanism with attenuation of outgoing photons via magnetic pair creation (27) or curvature radiation-reaction limited acceleration in an outer gap (28) are not yet discernible.

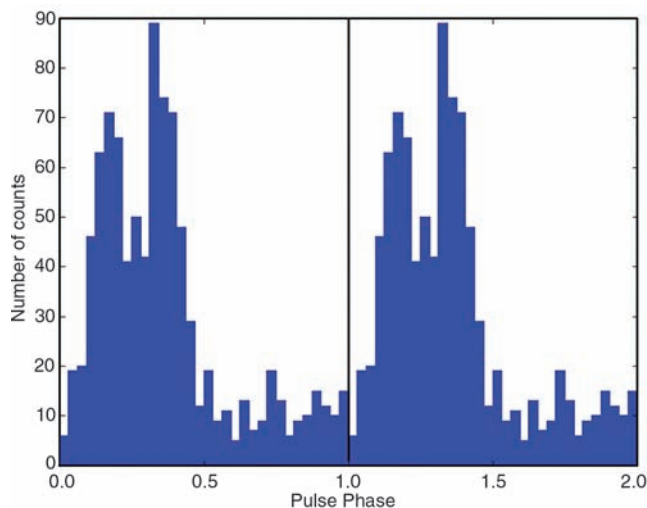
Our detection of a new gamma-ray pulsar during the initial operation of the Fermi LAT implies that there may be many gamma-ray-loud but x-ray- and radio-quiet pulsars.

Although 3EG J0010+7309 was long suspected to be a gamma-ray pulsar because of its clear association with a SNR at  $\sim 10^\circ$  Galactic latitude, it is also fairly typical of many unidentified *EGRET* sources. If the radio remnant CTA 1 was located at low Galactic latitudes, it could have been more difficult to recognize because of the higher and structured radio background of the Galactic disk. About 75% of the low Galactic latitude *EGRET* sources ( $|b| < 10^\circ$ ,  $\sim 100$  objects in the 3EG catalog and CTA 1 just on the edge of this region) are still unidentified, although several are associated with SNRs.

The unidentified low Galactic latitude *EGRET* sources represent the closer and brighter objects of a Galaxy-wide population of gamma-ray sources. *EGRET* was not sensitive enough to discern the more distant sources, which blurred into the diffuse Galactic emission. A model Galactic population conforming to the *EGRET* measurements (29), distributed in galacto-centric distance and height above the disk, yields several thousand sources of typical  $>100$ -MeV luminosities in the range of  $6 \times 10^{34}$  to  $4 \times 10^{35}$  erg s $^{-1}$ . The CTA 1 pulsar with an isotropic luminosity above 100 MeV of  $\sim 6 \times 10^{34}$  erg s $^{-1}$  falls in the range required for these sources. The CTA 1 pulsar detection implies that gamma-loud but radio- and x-ray-faint pulsars are likely to be detectable in a fair fraction of the remnants of massive star deaths. Topics as diverse as the SN rate in the Galaxy, the development of young (including historical) SNRs, and the physics of pulsar emission can then be studied.



**Fig. 3.** Gamma-ray ( $>100$  MeV) light-curve of the pulsar in CTA 1 shown over two periods of rotation with a resolution of 32 phase bins per period (corresponding to  $\sim 10$  ms per bin). The two maxima in the broad emission feature each have a full width at half maximum of  $\sim 0.12$  and are separated by  $\sim 0.2$  in phase. Overall, the LAT pulsar light-curve is similar to the gamma-ray light-curve of the EGRET pulsar PSR B1706-44 (23).



#### References and Notes

- D. E. Harris, J. A. Roberts, *Publ. Astron. Soc. Pac.* **72**, 237 (1960).
- D. E. Harris, *Astrophys. J.* **135**, 661 (1962).
- J. L. Caswell, *Mon. Not. R. Astron. Soc.* **136**, 11 (1967).
- W. Sieber, C. G. T. Haslam, C. J. Salter, *Astron. Astrophys.* **74**, 361 (1979).
- W. Sieber, C. J. Salter, C. J. Mayer, *Astron. Astrophys.* **103**, 393 (1981).
- S. Pineault et al., *Astron. J.* **105**, 1060 (1993).
- S. Pineault et al., *Astron. Astrophys.* **324**, 1152 (1997).
- F. Mavromatakis et al., *Astron. Astrophys.* **353**, 371 (2000).
- P. Slane et al., *Astrophys. J.* **485**, 221 (1997).
- P. Slane et al., *Astrophys. J.* **601**, 1045 (2004).
- F. D. Seward, B. Schmidt, P. Slane, *Astrophys. J.* **453**, 284 (1995).
- J. P. Halpern et al., *Astrophys. J.* **612**, 398 (2004).
- R. C. Hartman et al., *Astrophys. J.* **123** (suppl.), 79 (1999).
- K. T. S. Brazier et al., *Mon. Not. R. Astron. Soc.* **295**, 819 (1998).
- S. J. Sturmer, C. D. Dermer, J. Mattox, *Astron. Astrophys.* **120** (suppl.), 445 (1996).
- P. F. Michelson et al., *Proceedings of 1st GLAST Symposium*, S. Ritz, P. Michelson, C. Meegan, Eds. (American Institute of Physics, New York, 2007).
- W. B. Atwood et al., *Astrophys. J.* **652**, L49 (2006).
- S. M. Ransom, thesis, Harvard University (2001), available at <http://www.cv.nrao.edu/~sransom/presto/>.
- G. B. Hobbs, R. T. Edwards, R. N. Manchester, *Not. R. Astron. Soc.* **369**, 655 (2006).
- D. A. Smith et al., *Astron. Astrophys.*, in press; preprint available at <http://adsabs.harvard.edu/abs/2008arXiv0810.16375>.

- Extrapolation of the present pulsar ephemeris back to the archival epochs results in a large range of uncertainty for the period. Searches in *XMM* data by members of the Fermi LAT collaboration are not yet conclusive.
- T. Gold, *Nature* **221**, 25 (1969).
- D. J. Thompson et al., *Astrophys. J.* **465**, 385 (1996).
- K. Hirotani, preprint available at <http://arxiv.org/abs/0809.1283v1> (2008).
- A. K. Harding, J. V. Stern, J. Dyks, M. Frackowiak, *Astrophys. J.* **680**, 1378 (2008).
- R. W. Romani, I. A. Yadigaroglu, *Astrophys. J.* **438**, 314 (1995).
- M. G. Baring, *Adv. Space Res.* **33**, 552 (2004).
- R. W. Romani, *Astrophys. J.* **470**, 469 (1996).
- G. Kanbach et al., *Astron. Astrophys.* **120** (suppl.), 461 (1996).
- G. Hobbs et al., *Mon. Not. R. Astron. Soc.* **360**, 974 (2005).
- The Fermi LAT Collaboration acknowledges the generous support of a number of agencies and institutes, including NASA and the U.S. Department of Energy in the United States; the Commissariat l'Energie Atomique and the Centre National de la Recherche Scientifique/Institut National de Physique Nucléaire et de Physique des Particules in France; the Agenzia Spaziale Italiana and the Istituto Nazionale di Fisica Nucleare in Italy; the Ministry of Education, Culture, Sports, Science and Technology, the High Energy Accelerator Research Organization, and JAXA in Japan, and the K. A. Wallenberg Foundation and the Swedish National Space Board in Sweden.

#### Supporting Online Material

[www.sciencemag.org/cgi/content/full/1165572/DC1](http://www.sciencemag.org/cgi/content/full/1165572/DC1)  
Fig. S1

5 September 2008; accepted 8 October 2008

Published online 16 October 2008;

10.1126/science.1165572

Include this information when citing this paper.

## Observation of Pulsed $\gamma$ -Rays Above 25 GeV from the Crab Pulsar with MAGIC

The MAGIC Collaboration\*

One fundamental question about pulsars concerns the mechanism of their pulsed electromagnetic emission. Measuring the high-end region of a pulsar's spectrum would shed light on this question. By developing a new electronic trigger, we lowered the threshold of the Major Atmospheric  $\gamma$ -ray Imaging Cherenkov (MAGIC) telescope to 25 giga-electron volts. In this configuration, we detected pulsed  $\gamma$ -rays from the Crab pulsar that were greater than 25 giga-electron volts, revealing a relatively high cutoff energy in the phase-averaged spectrum. This indicates that the emission occurs far out in the magnetosphere, hence excluding the polar-cap scenario as a possible explanation of our measurement. The high cutoff energy also challenges the slot-gap scenario.

It is generally accepted that the primary radiation mechanism in pulsar magnetospheres is synchrotron-curvature radiation. This occurs when relativistic electrons are trapped along the magnetic field lines in the extremely strong field of the pulsar. Secondary mechanisms include ordinary synchrotron and inverse Compton scattering. It is not known whether the emission of electromagnetic radiation takes place closer to the neutron star (NS)

[the polar-cap scenario (1–3)] or farther out in the magnetosphere [the slot-gap (4–6) or outer-gap (7–9) scenario (Fig. 1)]. The high end of the  $\gamma$ -ray spectrum differs substantially between the near and the far case. Moreover, current models of the slot gap (6) and the outer gap (8, 9) differ in their predicted  $\gamma$ -ray spectra, even though both gaps extend over similar regions in the magnetosphere. Therefore, detection of  $\gamma$ -rays above 10 GeV would allow one to discriminate between different pulsar emission models.

At gamma-ray energies ( $E$ ) of  $\sim 1$  GeV, some pulsars such as the Crab (PSR B0531+21) are

among the brightest  $\gamma$ -ray sources in the sky. The Energetic  $\gamma$ -ray Experiment Telescope (EGRET) detector, aboard the Compton  $\gamma$ -ray Observatory (CGRO), measured the  $\gamma$ -ray spectra of different pulsars only up to  $E \approx 5$  GeV because of its small detector area ( $\sim 0.1$  m<sup>2</sup>) and the steeply falling  $\gamma$ -ray fluxes at higher energies. At  $E > 60$  GeV, Cherenkov telescopes (10) are the most sensitive instruments because of their large detection areas of  $\geq 10^4$  m<sup>2</sup>. But, in spite of several attempts, no pulsar has yet been detected at such energies (11–16). This suggests a spectral cutoff; that is, that the pulsar's emission drops off sharply, between a few giga-electron volts and a few tens of giga-electron volts.

The Crab pulsar is one of the best candidates for studying such a cutoff. Its spectrum has been measured by EGRET (17) up to  $E \approx 5$  GeV without a clear cutoff being seen. Earlier observations with the 17-m-diameter Major Atmospheric  $\gamma$ -ray Imaging Cherenkov (MAGIC) (18) telescope (Canary Island of La Palma, 2200 m above sea level) revealed a hint of pulsed emission at the 2.9 standard deviation ( $\sigma$ ) level above 60 GeV (19, 20). To verify this result, we developed and installed a new trigger system that lowered the threshold of MAGIC from  $\sim 50$  GeV to 25 GeV [supporting online material (SOM) text] (21).

We observed the Crab pulsar between October 2007 and February 2008, obtained 22.3 hours of good-quality data, and detected pulsed emission above 25 GeV. The pulsed signal (Fig. 2) has an

\*The full list of authors and affiliations is presented at the end of this paper.

overall significance of  $6.4\sigma$  with  $8500 \pm 1330$  signal events. Phase zero ( $\phi = 0$ ) is defined as the position of the main radio pulse (22). Our  $E > 25$  GeV data show pronounced pulses at  $\phi = 0$  (main pulse, P1) and at  $\phi = 0.3$  to  $0.4$  (interpulse, P2). These pulses are coincident with those measured by EGRET at  $E > 100$  MeV and those coming from our own optical measurement. P1 and P2 have similar amplitudes at  $E = 25$  GeV, in contrast to measurements at lower energies of  $E > 100$  MeV, at which P1 is dominant. The present data show a small excess ( $3.4\sigma$ ) above 60 GeV for P2, which is consistent with our previous Crab observation (19, 20).

For the Crab pulsar, EGRET measured a power-law spectrum [ $F(E) \propto E^{-\alpha}$  with a spectral index  $\alpha = 2.022 \pm 0.014$  and  $F$  is the flux] in the energy range from  $E = 0.1$  GeV to 5 GeV (17). At  $E = 25$  GeV we measured a flux that was several times lower than a straightforward extrapolation of the EGRET spectrum, which would require a spectral cutoff of somewhere between 5 and 25 GeV. Pulsar emission scenarios predict a generalized exponential shape for the cutoff that may be described as  $F(E) = AE^{-\alpha} \exp[-(E/E_0)^\beta]$ , where  $A$  is a normalized constant,  $E_0$  is the cutoff energy, and  $\beta$  measures the steepness of the cutoff. To determine the relevant parameters, we performed a joint fit to the Imaging Compton Telescope (COMPTEL) ( $\approx 1$  to 30 MeV), EGRET ( $\approx 30$  MeV to 10 GeV), and MAGIC ( $> 25$  GeV) data. For the conventional cases of  $\beta = 1$  (exponential) and  $\beta = 2$  (super-exponential), we found  $E_0 = 17.7 \pm 2.8_{\text{stat}} \pm 5.0_{\text{syst}}$  GeV (stat, statistical error; syst, systematic error) and  $E_0 = 23.2 \pm 2.9_{\text{stat}} \pm 6.6_{\text{syst}}$  GeV, respectively (Fig. 3). When  $\beta$  is left as a free parameter, the best fit yields  $E_0 = 20.4 \pm 3.9_{\text{stat}} \pm 7.4_{\text{syst}}$  GeV and  $\beta = 1.2$ . The systematic error is dominated by a possible mismatch between the energy calibrations of EGRET and MAGIC (SOM text).

From a theoretical point of view, the spectral cutoff is explained as a combination of the maximum energies that electrons ( $e^-$ ) can reach (because of the balance between acceleration and radiation losses) and the absorption of the emitted  $\gamma$ -rays in the magnetosphere. Absorption is controlled by two mechanisms: (i) magnetic  $e^+e^-$  pair production in the extremely strong magnetic field close to the pulsar surface and (ii) photon-photon  $e^+e^-$  pair production in dense photon fields. If, for a young pulsar like the Crab with a magnetic field  $B \sim 10^{12}$  to  $10^{13}$  G, emission occurs close to the NS surface [as in classical polar-cap models (1–3)], then magnetic pair-production attenuation provides a characteristic super-exponential cutoff at relatively low energies; that is, a few giga-electron volts at most (3). If, on the other hand, emission occurs farther out in the magnetosphere, at several stellar radii or close to the light cylinder [as in slot-gap (4–6) and outer-gap (7–9, 23) models], then absorption mainly arising from photon-photon collisions sets in at higher energies and produces a shallower cutoff (roughly exponential in shape). In either case, however, the measured  $E_0$  could be intrinsic to the emitted spectrum and hence would only provide an upper limit to the absorption strength.

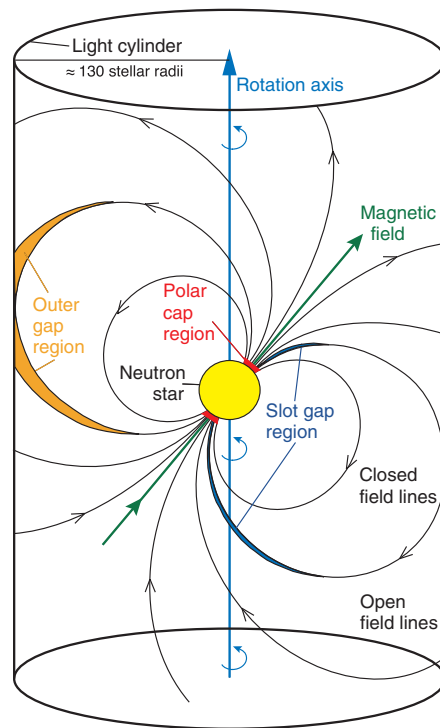


**Fig. 1.** A sketch of the Crab pulsar's magnetosphere. Electrons are trapped and accelerated along the magnetic field lines of the pulsar and emit electromagnetic radiation via the synchrotron-curvature mechanism. Vacuum gaps or vacuum regions occur at the polar cap (1–3) very close to the neutron star surface in a thin layer extending for several stellar radii along the boundary of the closed magnetosphere, the so-called slot gap (4–6), and in the outer region (7–9) close to the light cylinder (the outer gap). Vacuum gaps are filled with plasma, but its density is lower than the critical Goldreich-Julian density (24), in which the magnetically induced electric field is saturated, and therefore electrons can be accelerated to very high energies. Absorption of high-energy  $\gamma$ -rays occurs by interaction with the magnetic field (magnetic pair production) as well as with the photon field (photon-photon pair production). The former dominates close to the surface of the neutron star where the magnetic field is strongest; it leads to a superexponential cutoff at relatively low energies (few giga-electron volts). Photon-photon collisions prevail farther out in the magnetosphere close to the light cylinder, where the magnetic field is lower, and lead to a roughly exponential cutoff at higher ( $> 10$  GeV) energies.

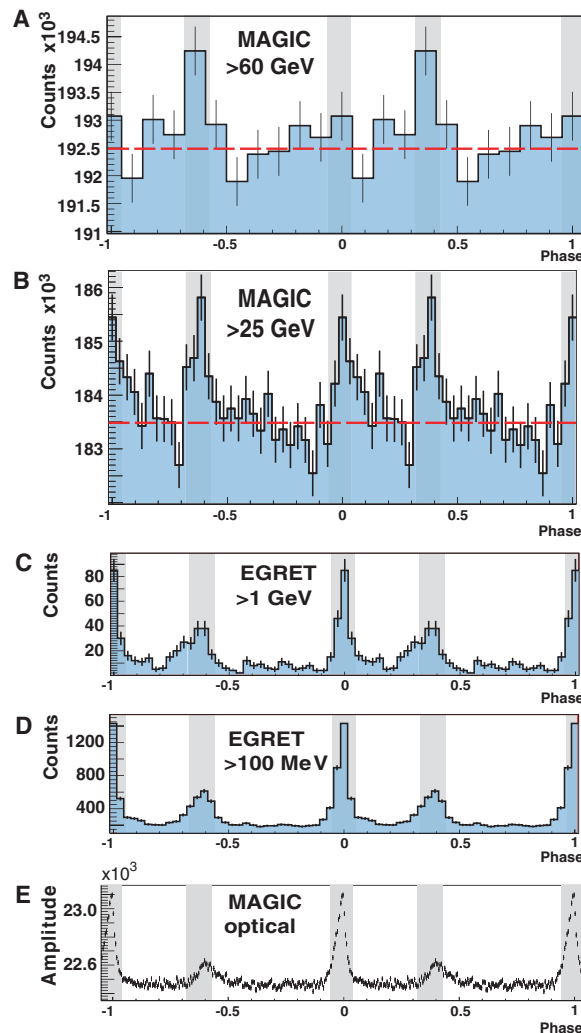


**Fig. 2.** Pulsed emission in different energy bands. The shaded areas show the signal regions for P1 and P2. (A) Evidence of an emission ( $3.4\sigma$ ) greater than 60 GeV for P2, measured by MAGIC. (B) Emission  $\geq 25$  GeV, measured by MAGIC. (C) Emission  $\geq 1$  GeV, measured by EGRET (17). (D) Emission  $\geq 100$  MeV, measured by EGRET (25). (E) Optical emission measured by MAGIC with the central pixel (26) of the camera. The optical signal has been recorded simultaneously with the  $\gamma$ -rays. P1 and P2 are in phase for all shown energies. The ratio of P2/P1 increases with energy from (B) to (D). In the search for a pulsed emission, the arrival time of each event, after correcting for the solar system barycenter, was transformed into the phase of the rotational period of the neutron star. The significance of the  $\gamma$ -ray pulsation greater than 25 GeV was evaluated by a single-hypothesis test (SOM text), in which the  $\gamma$ -ray emission was assumed to be coming from the two fixed phase intervals (shaded regions): P1 (phase 0.94 to 0.04) and P2 (phase 0.32 to 0.43), as defined in (19, 20). The signal results in  $8500 \pm 1330$  signal events ( $6.4\sigma$ ).



Equation 1 of (3) (a largely model-independent relation derived from simulations of  $\gamma$ -ray absorption by magnetic-pair production in rotating magnetic dipoles) relates the pair-creation cutoff energy,  $E_{\max}$ , with the location of the emission region  $r/R_0$  ( $R_0$  is the NS radius;  $r$  is the distance of the

emission region from the center of the NS) for a NS with surface magnetic field  $B_0$  and period  $P$ :

$$E_{\max} \approx 0.4 \sqrt{P \frac{r}{R_0}} \max \left\{ 1, \frac{0.1 B_{\text{crit}}}{B_0} \left( \frac{r}{R_0} \right)^3 \right\} \text{ GeV} \quad (1)$$

**Fig. 3.** Model fits to the signal-event distribution. Shown is the measured distribution of excess events in bins of *SIZE* integrated over P1 and P2. *SIZE* is a main image parameter that measures the total intensity of the Cherenkov flash in the camera in units of photoelectrons (phe). In this analysis, it was used as a rough estimate of the  $\gamma$ -ray energy. To determine the cutoff energy, we folded the power law function with the generalized exponential shape function  $F(E) = AE^{1\alpha} \exp[-(E/E_0)^\beta]$  with the MAGIC telescope's effective area to calculate the expected signal in each *SIZE* bin (forward unfolding). The expected signal was compared with the measured excess events by calculating a  $\chi^2$  test. We obtained the best fit by minimizing the joint  $\chi^2$  between real data (from COMPTEL, EGRET, and MAGIC) and the generalized function  $F(E) = AE^{1\alpha} \exp[-(E/E_0)^\beta]$ . In the conventional cases of  $\beta = 1$  (exponential) and  $\beta = 2$  (superexponential), we found  $E_0 = 17.7 \pm 2.8_{\text{stat}} \pm 5.0_{\text{syst}}$  GeV and  $E_0 = 23.2 \pm 2.9_{\text{stat}} \pm 6.6_{\text{syst}}$  GeV, respectively. If instead we leave  $\beta$  as a free parameter, the best fit yields  $E_0 = 20.4 \pm 3.9_{\text{stat}} \pm 7.4_{\text{syst}}$  GeV and  $\beta = 1.2$ .

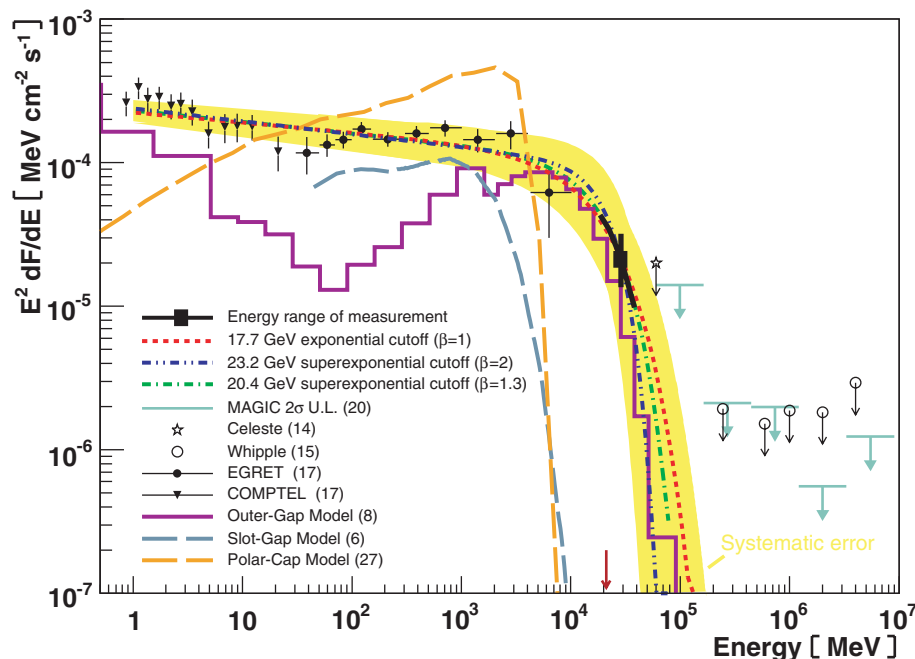
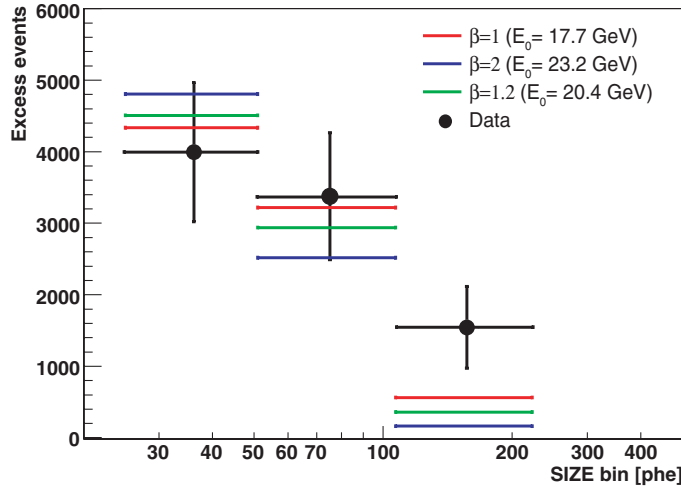


**Fig. 4.** Crab pulsar spectral cutoff. The solid circles and triangles on the left represent flux measurements from EGRET and COMPTEL (17). The arrows on the right denote upper limits from various previous experiments. We performed a joint fit of a generalized function  $\{F(E) = A E^{-\alpha} \exp[-(E/E_0)^\beta]\}$  to the MAGIC, EGRET, and COMPTEL data. The figure shows all three fitted functions for  $\beta = 1$  (red line),  $\beta = 2$  (blue line), and the best-fit,  $\beta = 1.2$  (green line). The black line indicates the energy range, the flux, and the statistical error of our measurement. The yellow band illustrates the joint systematic error of all three solutions. The measurement is compared with three current pulsar models, a polar-cap model, a slot-gap model, and an outer-gap model. The sharp cutoff of the polar-cap (27) model is due to magnetic-pair production close to the surface of the neutron star. The slot-gap model (6) does not reach the observed cutoff energy, whereas the outer-gap (8) model can explain the high energy cutoff. The numbers in parentheses refer to the list of references.

The appropriate values for the Crab pulsar are  $B_0 = 8 \times 10^{12}$  G (8), natural constant  $B_{\text{crit}} = 4.4 \times 10^{13}$  G (3), and  $P = 0.033$  s ( $B_{\text{crit}} = 4.4 \times 10^{13}$  G is the critical field that marks the onset of quantum effects in a magnetized plasma). Using for  $E_{\max}$  the superexponential cutoff energy  $E_0 = 23.2 \pm 2.9_{\text{stat}} \pm 6.6_{\text{syst}}$  GeV, derived above for  $\beta = 2$  as appropriate for the polar-cap scenario, one obtains  $r/R_0 > 6.2 \pm 0.2_{\text{stat}} \pm 0.4_{\text{syst}}$ ; that is, the emitting region is located well above the NS surface. This result, however, contradicts the basic tenet of the polar-cap scenario (1–3) that particle acceleration and radiation emission do occur very close to the pulsar surface. This inconsistency rules out the polar-cap scenario for the Crab pulsar.

Our results therefore favor an outer-gap or slot-gap scenario for the Crab pulsar. For example, using in Eq. 1 the value of  $E_0$  that corresponds to  $\beta = 1$  (approximately consistent with the outer-gap picture), a high-altitude emitting region is inferred, which is fully consistent with the assumed scenario. Specific recent outer-gap (8, 9) and slot-gap (6) predictions are compared with our data in Fig. 4. Although the former can provide emission of photons of energies as high as 25 GeV and hence explain our  $\gamma$ -ray data, the latter cannot. Thus, current outer-gap models seem preferred in explaining our measurement.

Lastly, our present measurements reveal a trend of P2/P1 increasing with energy: It is  $<0.5$  at 100 MeV,  $\approx 1$  at 25 GeV, and  $>1$  at 60 GeV (Fig. 2). This trend provides valuable information for theoretical studies that will further constrain the location of the emission region in the Crab pulsar's magnetosphere [for example, (9)].

#### References and Notes

1. M. A. Ruderman, P. G. Sutherland, *Astrophys. J.* **196**, 51 (1975).
2. J. K. Daugherty, A. K. Harding, *Astrophys. J.* **252**, 337 (1982).
3. M. G. Baring, *Adv. Space Res.* **33**, 552 (2004).
4. J. Arons, E. T. Scharlemann, *Astrophys. J.* **231**, 854 (1979).
5. A. G. Muslimov, A. K. Harding, *Astrophys. J.* **606**, 1143 (2004).
6. A. K. Harding, J. V. Stern, J. Dyks, F. Frackowiak, *Astrophys. J.* **680**, 1378 (2008).
7. K. S. Cheng, C. Ho, M. Ruderman, *Astrophys. J.* **300**, 500 (1986).
8. K. Hirotani, *arXiv:0809.1283*, (2008).
9. A. P. S. Tang, J. Takata, J. Jia, K. S. Cheng, *Astrophys. J.* **676**, 562 (2008).
10.  $\gamma$ -rays induce particle air showers in the atmosphere that emit Cherenkov light. The detection of this light allows measuring the energy and the direction of the incident  $\gamma$ -ray.
11. P. Chadwick *et al.*, *Astropart. Phys.* **9**, 131 (1998).
12. P. G. Edwards *et al.*, *Astron. Astrophys.* **291**, 468 (1994).
13. F. Aharonian *et al.*, *Astrophys. J.* **614**, 897 (2004).
14. M. de Naurois *et al.*, *Astrophys. J.* **566**, 343 (2002).
15. R. W. Lessard *et al.*, *Astrophys. J.* **531**, 942 (2000).
16. F. Aharonian *et al.*, *Astron. Astrophys.* **466**, 543 (2007).
17. L. Kuiper *et al.*, *Astron. Astrophys.* **378**, 918 (2001).
18. See the MAGIC telescope Web site; <http://www.magic.mppmu.mpg.de>.
19. A. N. Otte, thesis, Technical University, Munich (2007); available online at <http://mediatum2.ub.tum.de/doc/620881/document.pdf>.
20. J. Albert *et al.*, *Astrophys. J.* **674**, 1037 (2008).
21. The threshold of a Cherenkov telescope is usually defined as the peak in the energy distribution of triggered  $\gamma$ -ray events for a  $\gamma$ -ray source with an  $E^{-2.6}$  power-law photon energy spectrum.
22. A. G. Lyne, R. S. Pritchard, F. Smith, *Mon. Not. R. Astron. Soc.* **265**, 1003 (1993).

23. R. W. Romani, *Astrophys. J.* **470**, 469 (1996).
24. P. Goldreich, W. H. Julian, *Astrophys. J.* **157**, 869 (1969).
25. Data provided by EGRET; <http://legacy.gsfc.nasa.gov/compton/data/egret/>.
26. F. Lucarelli *et al.*, *Nucl. Instr. Meth. A* **589**, 415 (2008).
27. A. K. Harding, private communication.
28. We thank the electronics division at the Max-Planck-Institut, Munich, for their work in developing and producing the analog sum trigger system, especially O. Reimann, R. Maier, S. Tran, and T. Dettlaff. We also thank L. Stodolsky for comments. We acknowledge the Instituto de Astrofísica for providing all infrastructure on the Roque de los Muchachos in La Palma. The support of the German Bundesministerium für Bildung, Wissenschaft, Forschung und Technologie and Max-Planck-Gesellschaft, the Italian INFN and INAF, the Swiss Schweizerische Nationalfonds, and Spanish Ministerio de Ciencia e Innovación is acknowledged. This work was also supported by ETH research grant TH 34/043, by the Polish Ministertwo Nauki i Szkolnictwa Wyzszego grant N N203 390834, and by the Young Investigators Program of the Helmholtz Gemeinschaft.

#### Supporting Online Material

[www.sciencemag.org/cgi/content/full/1164718/DC1](http://www.sciencemag.org/cgi/content/full/1164718/DC1)  
SOM Text  
Figs. S1 to S11  
References

15 August 2008; accepted 8 October 2008  
Published online 16 October 2008;  
10.1126/science.1164718  
Include this information when citing this paper.

#### List of authors and affiliations:

E. Aliu,<sup>1</sup> H. Anderhub,<sup>2</sup> L. A. Antonelli,<sup>3</sup> P. Antoranz,<sup>4</sup> M. Backes,<sup>5</sup> C. Baixeras,<sup>6</sup> J. A. Barrio,<sup>4</sup> H. Bartko,<sup>7</sup> D. Bastieri,<sup>8</sup> J. K. Becker,<sup>5</sup> W. Bednarek,<sup>9</sup> K. Berger,<sup>10</sup> E. Bernardini,<sup>11</sup> C. Bigongiari,<sup>8</sup>†

A. Biland,<sup>2</sup> R. K. Bock,<sup>7,8</sup> G. Bonnoli,<sup>12</sup> P. Bordes,<sup>13</sup> V. Bosch-Ramon,<sup>13</sup> T. Bretz,<sup>10</sup> I. Britvitch,<sup>2</sup> M. Camara,<sup>4</sup> E. Carmona,<sup>7</sup> A. Chilingarian,<sup>14</sup> S. Commichau,<sup>2</sup> J. L. Contreras,<sup>4</sup> J. Cortina,<sup>1</sup> M. T. Costado,<sup>15,16</sup> S. Covino,<sup>3</sup> V. Cufet,<sup>5</sup> F. Dazzi,<sup>5</sup> A. De Angelis,<sup>17</sup> E. De Cea del Pozo,<sup>18</sup> R. de los Reyes,<sup>4</sup> B. De Lotto,<sup>17</sup> M. De Maria,<sup>17</sup> F. De Sabata,<sup>17</sup> C. Delgado Mendez,<sup>15</sup> A. Dominguez,<sup>19</sup> D. Dorner,<sup>10</sup> M. Doro,<sup>8</sup> D. Elsässer,<sup>10</sup> M. Errando,<sup>1</sup> M. Fagioli,<sup>12</sup> D. Ferenc,<sup>20</sup> E. Fernandez,<sup>1</sup> R. Firpo,<sup>1</sup> M. V. Fonseca,<sup>4</sup> L. Font,<sup>6</sup> N. Galante,<sup>7</sup> R. J. Garcia Lopez,<sup>15,16</sup> M. Garzarczyk,<sup>7</sup> M. Gaug,<sup>15</sup> F. Goebel,<sup>7</sup> D. Hadash,<sup>5</sup> M. Hayashida,<sup>7</sup> A. Herrero,<sup>15,16</sup> D. Höhne,<sup>10</sup> J. Hose,<sup>7</sup> C. C. Hsu,<sup>7</sup> S. Huber,<sup>10</sup> T. Jogler,<sup>7</sup> D. Kranich,<sup>2</sup> A. La Barbera,<sup>3</sup> A. Laille,<sup>20</sup> E. Leonardo,<sup>12</sup> E. Lindfors,<sup>21</sup> S. Lombardi,<sup>8</sup> F. Longo,<sup>17</sup> M. Lopez,<sup>8</sup>† E. Lorenz,<sup>27</sup> P. Majumdar,<sup>7</sup> G. Maneva,<sup>18</sup> N. Mankuzhiyil,<sup>17</sup> K. Mannheim,<sup>10</sup> L. Maraschi,<sup>3</sup> M. Mariotti,<sup>9</sup> M. Martinez,<sup>2</sup> D. Mazin,<sup>1</sup> M. Meucci,<sup>12</sup> M. Meyer,<sup>10</sup> J. M. Miranda,<sup>4</sup> R. Mirzoyan,<sup>7</sup> M. Moles,<sup>19</sup> A. Moralejo,<sup>1</sup> D. Nieto,<sup>4</sup> K. Nilsson,<sup>21</sup> J. Ninkovic,<sup>7</sup> N. Otte,<sup>23,7</sup>†§ I. Oya,<sup>4</sup> R. Paoletti,<sup>12</sup> J. M. Paredes,<sup>13</sup> M. Pasanen,<sup>21</sup> D. Pascoli,<sup>8</sup> F. Pauss,<sup>2</sup> R. G. Pegna,<sup>12</sup> M. A. Perez-Torres,<sup>19</sup> M. Persic,<sup>24</sup> L. Peruzzo,<sup>8</sup> A. Piccioli,<sup>12</sup> F. Prada,<sup>19</sup> E. Prandini,<sup>8</sup> N. Puchades,<sup>1</sup> A. Raymers,<sup>14</sup> W. Rhode,<sup>5</sup> M. Ribó,<sup>13</sup> J. Rico,<sup>1,25</sup> M. Rissi,<sup>2</sup>† A. Robert,<sup>6</sup> S. Rügamer,<sup>10</sup> A. Saggion,<sup>8</sup> T. Y. Saito,<sup>7</sup> M. Salvati,<sup>3</sup> M. Sanchez-Conde,<sup>19</sup> P. Sartori,<sup>8</sup> K. Satalecka,<sup>11</sup> V. Scalzotto,<sup>8</sup> V. Scapin,<sup>17</sup> T. Schweizer,<sup>7</sup>†‡ M. Shayduk,<sup>7</sup>† K. Shinozaki,<sup>7</sup> S. N. Shore,<sup>26</sup> N. Sidro,<sup>1</sup> A. Sierpowska-Bartosik,<sup>18</sup> A. Sillanpää,<sup>21</sup> D. Sobczynska,<sup>9</sup> F. Spanier,<sup>10</sup> A. Stamerra,<sup>12</sup> L. S. Stark,<sup>2</sup> L. Takalo,<sup>21</sup> F. Tavecchio,<sup>3</sup> P. Temnikov,<sup>22</sup> D. Tescaro,<sup>1</sup> M. Teshima,<sup>7</sup> M. Tluczykont,<sup>11</sup> D. F. Torres,<sup>18,25</sup> N. Turini,<sup>12</sup> H. Vankov,<sup>22</sup> A. Venturini,<sup>8</sup> V. Vitale,<sup>17</sup> R. M. Wagner,<sup>7</sup> W. Witte,<sup>7</sup> V. Zabalza,<sup>13</sup> F. Zandanel,<sup>19</sup> R. Zanin,<sup>1</sup> J. Zapatero,<sup>5</sup> O. C. de Jager,<sup>27</sup>|| E. de Ona Wilhelmi<sup>1</sup>||¶

<sup>1</sup>Institut de Física d'Altes Energies, Edifici Cn, Campus Universitat Autònoma de Barcelona E-08193 Bellaterra, Spain. <sup>2</sup>Eidgenössische Technische Hochschule (ETH), Zürich CH-8093, Switzerland. <sup>3</sup>L'Istituto Nazionale di Astrofisica (INAF), I-00136 Rome, Italy. <sup>4</sup>Universidad Complutense, E-28040 Madrid, Spain. <sup>5</sup>Technische Universität Dortmund, D-44221 Dortmund, Germany. <sup>6</sup>Universitat Autònoma de Barcelona, E-08193 Bellaterra,

Spain. <sup>7</sup>Max-Planck-Institut für Physik, D-80805 München, Germany. <sup>8</sup>Università di Padova and Istituto Nazionale di Fisica Nucleare (INFN), I-35131 Padova, Italy. <sup>9</sup>University of Lodz, PL-90236 Lodz, Poland. <sup>10</sup>Universität Würzburg, D-97074 Würzburg, Germany. <sup>11</sup>Deutsches Elektronen Synchrotron, D-15738 Zeuthen, Germany. <sup>12</sup>Università di Siena and INFN Pisa, I-53100 Siena, Italy. <sup>13</sup>Universitat de Barcelona, Institut de Ciències del Cosmos (ICC)/Institut d'Estudis Espacials de Catalunya (IEEC), E-08028 Barcelona, Spain. <sup>14</sup>Yerevan Physics Institute, AM-375036 Yerevan, Armenia. <sup>15</sup>Instituto de Astrofísica de Canarias, E-38200, La Laguna, Tenerife, Spain. <sup>16</sup>Departamento de Astrofísica, Universidad, E-38206 La Laguna, Tenerife, Spain. <sup>17</sup>Università di Udine and INFN Trieste, I-33100 Udine, Italy. <sup>18</sup>IEEC-Consejo Superior de Investigaciones Científicas (CSIC), E-08193 Bellaterra, Spain. <sup>19</sup>Instituto de Astrofísica de Andalucía (CSIC), E-18080 Granada, Spain. <sup>20</sup>University of California at Davis, Davis, CA 95616-8677, USA. <sup>21</sup>Tuorla Observatory, Turku University, FI-21500 Piikkiö, Finland. <sup>22</sup>Institute for Nuclear Research and Nuclear Energy, BG-1784 Sofia, Bulgaria. <sup>23</sup>Humboldt-Universität zu Berlin, D-12489 Berlin, Germany. <sup>24</sup>INAF/Osservatorio Astronomico and INFN, I-34143 Trieste, Italy. <sup>25</sup>Institució Catalana de Recerca i Estudis Avançats, E-08010 Barcelona, Spain. <sup>26</sup>Università di Pisa and INFN Pisa, I-56126 Pisa, Italy. <sup>27</sup>Unit for Space Physics, Northwest University, Potchefstroom 2520, South Africa.

†Present address: Instituto de Física Corpuscular, CSIC-Universitat de València, E-46101 Valencia, Spain.

‡To whom correspondence should be addressed. E-mail: tschweiz@mppmu.mpg.de (T.S.); nepomake@scipp.ucsb.edu (N.O.); Michael.Rissi@phys.ethz.ch (M.R.); shayduk@mppmu.mpg.de (M.S.); marcos.lopezmoya@pd.infn.it (M.L.M.)

§Present address: Santa Cruz Institute for Particle Physics, University of California, Santa Cruz, CA 95064, USA.

||These authors are not members of the MAGIC Collaboration.

¶Present address: Astroparticule et Cosmologie, CNRS, Université Paris, F-75205 Paris Cedex 13, France.

# Ab Initio Determination of Light Hadron Masses

S. Dürr,<sup>1</sup> Z. Fodor,<sup>1,2,3</sup> J. Frison,<sup>4</sup> C. Hoelbling,<sup>2,3,4</sup> R. Hoffmann,<sup>2</sup> S. D. Katz,<sup>2,3</sup> S. Krieg,<sup>2</sup> T. Kurth,<sup>2</sup> L. Lellouch,<sup>4</sup> T. Lippert,<sup>2,5</sup> K. K. Szabo,<sup>2</sup> G. Vulvert<sup>4</sup>

More than 99% of the mass of the visible universe is made up of protons and neutrons. Both particles are much heavier than their quark and gluon constituents, and the Standard Model of particle physics should explain this difference. We present a full ab initio calculation of the masses of protons, neutrons, and other light hadrons, using lattice quantum chromodynamics. Pion masses down to 190 mega-electron volts are used to extrapolate to the physical point, with lattice sizes of approximately four times the inverse pion mass. Three lattice spacings are used for a continuum extrapolation. Our results completely agree with experimental observations and represent a quantitative confirmation of this aspect of the Standard Model with fully controlled uncertainties.

The Standard Model of particle physics predicts a cosmological, quantum chromodynamics (QCD)-related smooth transition between a high-temperature phase dominated by quarks and gluons and a low-temperature phase dominated by hadrons. The very large energy densities at the high temperatures of the early universe have essentially disappeared through expansion and cooling. Nevertheless, a fraction of this energy is carried today by quarks and gluons, which are confined into protons and neutrons. According to the mass-energy equivalence  $E = mc^2$ , we experience this energy as mass. Because more than 99% of the mass of ordinary matter comes from protons and neutrons, and in turn about 95% of

their mass comes from this confined energy, it is of fundamental interest to perform a controlled ab initio calculation based on QCD to determine the hadron masses.

QCD is a generalized version of quantum electrodynamics (QED), which describes the electromagnetic interactions. The Euclidean Lagrangian with gauge coupling  $g$  and a quark mass of  $m$  can be written as  $\mathcal{L} = -1/(2g^2) \text{Tr} F_{\mu\nu} F_{\mu\nu} + \bar{\psi} [\gamma_\mu (\partial_\mu + A_\mu) + m] \psi$ , where  $F_{\mu\nu} = \partial_\mu A_\nu - \partial_\nu A_\mu + [A_\mu, A_\nu]$ . In electrodynamics, the gauge potential  $A_\mu$  is a real valued field, whereas in QCD it is a  $3 \times 3$  matrix field. Consequently, the commutator in  $F_{\mu\nu}$  vanishes in QED but not in QCD. The  $\psi$  fields also have an additional "color" index in

QCD, which runs from 1 to 3. Different "flavors" of quarks are represented by independent fermionic fields, with possibly different masses. In the work presented here, a full calculation of the light hadron spectrum in QCD, only three input parameters are required: the light and strange quark masses and the coupling  $g$ .

The action  $S$  of QCD is defined as the four-volume integral of  $\mathcal{L}$ . Green's functions are averages of products of fields over all field configurations, weighted by the Boltzmann factor  $\exp(-S)$ . A remarkable feature of QCD is asymptotic freedom, which means that for high energies (that is, for energies at least 10 to 100 times higher than that of a proton at rest), the interaction gets weaker and weaker ( $1, 2$ ), enabling perturbative calculations based on a small coupling parameter. Much less is known about the other side, where the coupling gets large, and the physics describing the interactions becomes nonperturbative. To explore the predictions of QCD in this nonperturbative regime, the most systematic approach is to discretize ( $3$ ) the above Lagrangian

<sup>1</sup>John von Neumann-Institut für Computing, Deutsches Elektronen-Synchrotron Zeuthen, D-15738 Zeuthen and Forschungszentrum Jülich, D-52425 Jülich, Germany. <sup>2</sup>Bergische Universität Wuppertal, Gausstrasse 20, D-42119 Wuppertal, Germany. <sup>3</sup>Institute for Theoretical Physics, Eötvös University, H-1117 Budapest, Hungary. <sup>4</sup>Centre de Physique Théorique (UMR 6207 du CNRS et des Universités d'Aix-Marseille I, d'Aix-Marseille II et du Sud Toulon-Var, affiliée à la FRUMAM), Case 907, Campus de Luminy, F-13288, Marseille Cedex 9, France. <sup>5</sup>Jülich Supercomputing Centre, FZ Jülich, D-52425 Jülich, Germany.

on a hypercubic space-time lattice with spacing  $a$ , to evaluate its Green's functions numerically and to extrapolate the resulting observables to the continuum ( $a \rightarrow 0$ ). A convenient way to carry out this discretization is to place the fermionic variables on the sites of the lattice, whereas the gauge fields are treated as  $3 \times 3$  matrices connecting these sites. In this sense, lattice QCD is a classical four-dimensional statistical physics system.

Calculations have been performed using the quenched approximation, which assumes that the fermion determinant (obtained after integrating over the  $\psi$  fields) is independent of the gauge field. Although this approach omits the most computationally demanding part of a full QCD calculation, a thorough determination of the quenched spectrum took almost 20 years. It

was shown (4) that the quenched theory agreed with the experimental spectrum to approximately 10% for typical hadron masses and demonstrated that systematic differences were observed between quenched and two-flavor QCD beyond that level of precision (4, 5).

Including the effects of the light sea quarks has dramatically improved the agreement between experiment and lattice QCD results. Five years ago, a collaboration of collaborations (6) produced results for many physical quantities that agreed well with experimental results. Thanks to continuous progress since then, lattice QCD calculations can now be performed with light sea quarks whose masses are very close to their physical values (7) (though in quite small volumes). Other calculations, which include these sea-quark

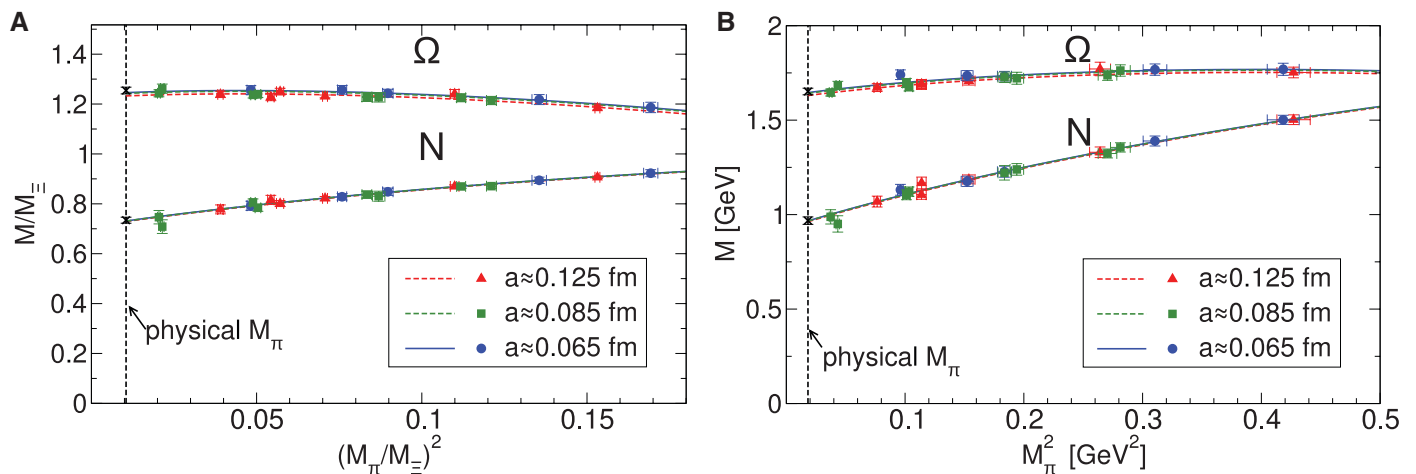
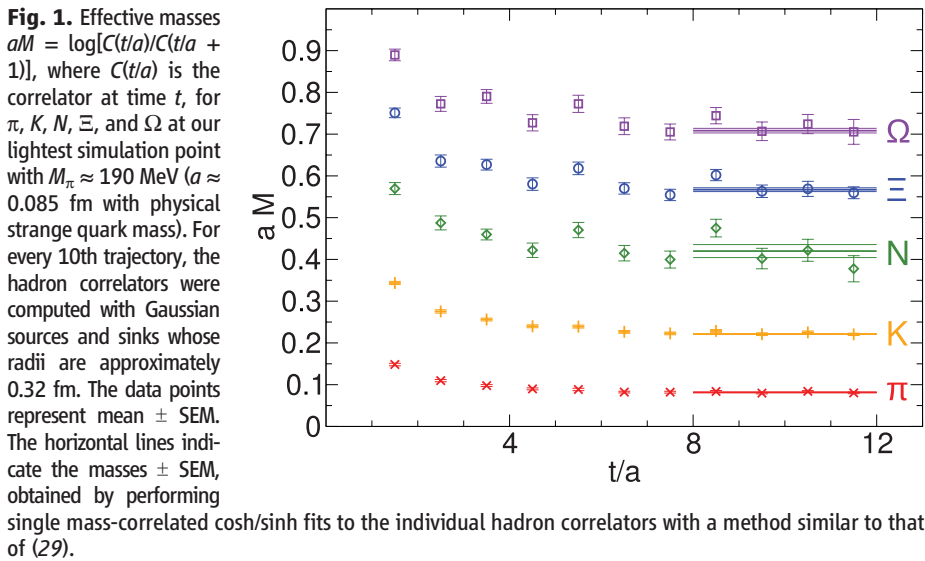
effects in the light hadron spectrum, have also appeared in the literature (8–16). However, all of these studies have neglected one or more of the ingredients required for a full and controlled calculation. The five most important of those are, in the order that they will be addressed below:

1) The inclusion of the up ( $u$ ), down ( $d$ ), and strange ( $s$ ) quarks in the fermion determinant with an exact algorithm and with an action whose universality class is QCD. For the light hadron spectrum, the effects of the heavier charm, bottom, and top quarks are included in the coupling constant and light quark masses.

2) A complete determination of the masses of the light ground-state, flavor nonsinglet mesons and octet and decuplet baryons. Three of these are used to fix the masses of the isospin-averaged light ( $m_{ud}$ ) and strange ( $m_s$ ) quark masses and the overall scale in physical units.

3) Large volumes to guarantee small finite-size effects and at least one data point at a significantly larger volume to confirm the smallness of these effects. In large volumes, finite-size corrections to the spectrum are exponentially small (17, 18). As a conservative rule of thumb,  $M_\pi L \gtrsim 4$ , with  $M_\pi$  the pion mass and  $L$  the lattice size, guarantees that finite-volume errors in the spectrum are around or below the percent level (19). Resonances require special care. Their finite volume behavior is more involved. The literature provides a conceptually satisfactory framework for these effects (20, 21), which should be included in the analysis.

4) Controlled interpolations and extrapolations of the results to physical  $m_{ud}$  and  $m_s$  (or eventually directly simulating at these mass values). Although interpolations to physical  $m_s$ , corresponding to  $M_K \cong 495$  MeV, are straightforward, the extrapolations to the physical value of



The curves are the corresponding fits. The crosses are the continuum extrapolated values in the physical pion mass limit. The lattice-spacing dependence of the results is barely significant statistically despite the factor of 3.7 separating the squares of the largest ( $a \approx 0.125$  fm) and smallest ( $a \approx 0.065$  fm) lattice spacings. The  $\chi^2/\text{degrees of freedom}$  values of the fits in (A) are 9.46/14 ( $\Omega$ ) and 7.10/14 ( $N$ ), whereas those of the fits in (B) are 10.6/14 ( $\Omega$ ) and 9.33/14 ( $N$ ). All data points represent the mean  $\pm$  SEM.

The curves are the corresponding fits. The crosses are the continuum extrapolated values in the physical pion mass limit. The lattice-spacing dependence of the results is barely significant statistically despite the factor of 3.7 separating the squares of the largest ( $a \approx 0.125$  fm) and smallest ( $a \approx 0.065$  fm) lattice spacings. The  $\chi^2/\text{degrees of freedom}$  values of the fits in (A) are 9.46/14 ( $\Omega$ ) and 7.10/14 ( $N$ ), whereas those of the fits in (B) are 10.6/14 ( $\Omega$ ) and 9.33/14 ( $N$ ). All data points represent the mean  $\pm$  SEM.



$m_{ud}$ , corresponding to  $M_\pi \approx 135$  MeV, are difficult. They need computationally intensive calculations, with  $M_\pi$  reaching down to 200 MeV or less.

5) Controlled extrapolations to the continuum limit, requiring that the calculations be performed at no less than three values of the lattice spacing, in order to guarantee that the scaling region is reached.

Our analysis includes all five ingredients listed above, thus providing a calculation of the light hadron spectrum with fully controlled systematics as follows.

1) Owing to the key statement from renormalization group theory that higher-dimension, local operators in the action are irrelevant in the continuum limit, there is, in principle, an unlimited freedom in choosing a lattice action. There is no consensus regarding which action would offer the most cost-effective approach to the continuum limit and to physical  $m_{ud}$ . We use an action that improves both the gauge and fermionic sectors and heavily suppresses non-physical, ultraviolet modes (19). We perform a series of  $2 + 1$  flavor calculations; that is, we include degenerate  $u$  and  $d$  sea quarks and an additional  $s$  sea quark. We fix  $m_s$  to its approximate physical value. To interpolate to the physical value, four of our simulations were repeated with a slightly different  $m_s$ . We vary  $m_{ud}$  in a range that extends down to  $M_\pi \approx 190$  MeV.

2) QCD does not predict hadron masses in physical units: Only dimensionless combinations (such as mass ratios) can be calculated. To set the overall physical scale, any dimensionful observable can be used. However, practical issues influence this choice. First of all, it should be a quantity that can be calculated precisely and whose experimental value is well known. Second, it should have a weak dependence on  $m_{ud}$ , so that its chiral behavior does not interfere with that of other observables. Because we are considering spectral quantities here, these two conditions should guide our choice of the particle whose mass will set the scale. Furthermore, the particle should not decay under the strong interaction. On the one hand, the larger the strange content of the particle, the more precise the mass determination and the weaker the dependence on  $m_{ud}$ . These facts support the use of the  $\Omega$  baryon, the particle with the highest strange content. On the other hand, the determination of baryon decuplet masses is usually less precise than those of the octet. This observation would suggest that the  $\Xi$  baryon is appropriate. Because both the  $\Omega$  and  $\Xi$  baryon are reasonable choices, we carry out two analyses, one with  $M_\Omega$  (the  $\Omega$  set) and one with  $M_\Xi$  (the  $\Xi$  set). We find that for all three gauge couplings,  $6/g^2 = 3.3, 3.57$ , and  $3.7$ , both quantities give consistent results, namely  $a \approx 0.125, 0.085$ , and  $0.065$  fm, respectively. To fix the bare quark masses, we use the mass ratio pairs  $M_\pi/M_\Omega, M_K/M_\Omega$  or  $M_\pi/M_\Xi, M_K/M_\Xi$ . We determine the masses of the baryon octet ( $N, \Sigma, \Lambda, \Xi$ ) and decuplet ( $\Delta, \Sigma^*, \Xi^*, \Omega$ ) and those members of the light pseudoscalar ( $\pi, K$ ) and

vector meson ( $\rho, K^*$ ) octets that do not require the calculation of disconnected propagators. Typical effective masses are shown in Fig. 1.

3) Shifts in hadron masses due to the finite size of the lattice are systematic effects. There are two different effects, and we took both of them into account. The first type of volume dependence is related to virtual pion exchange between the different copies of our periodic system, and it decreases exponentially with  $M_\pi L$ . Using  $M_\pi L \gtrsim 4$  results in masses which coincide, for all practical purposes, with the infinite volume results [see results, for example, for pions (22) and for baryons (23, 24)]. Nevertheless, for one of our simulation points, we used several volumes and determined the volume dependence, which was included as a (negligible) correction at all points (19). The second type of volume dependence exists only for resonances. The coupling between the resonance state and its decay products leads to a nontrivial-level structure in finite volume. Based on (20, 21), we calculated the corrections necessary to reconstruct the resonance masses from the finite volume ground-state energy and included them in the analysis (19).

4) Though important algorithmic developments have taken place recently [for example

(25, 26) and for our setup (27)], simulating directly at physical  $m_{ud}$  in large enough volumes, which would be an obvious choice, is still extremely challenging numerically. Thus, the standard strategy consists of performing calculations at a number of larger  $m_{ud}$  and extrapolating the results to the physical point. To that end, we use chiral perturbation theory and/or a Taylor expansion around any of our mass points (19).

5) Our three-flavor scaling study (27) showed that hadron masses deviate from their continuum values by less than approximately 1% for lattice spacings up to  $a \approx 0.125$  fm. Because the statistical errors of the hadron masses calculated in the present paper are similar in size, we do not expect significant scaling violations here. This is confirmed by Fig. 2. Nevertheless, we quantified and removed possible discretization errors by a combined analysis using results obtained at three lattice spacings (19).

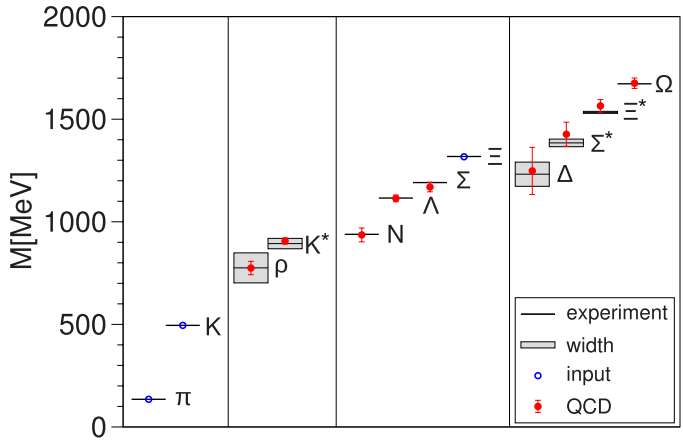
We performed two separate analyses, setting the scale with  $M_\Xi$  and  $M_\Omega$ . The results of these two sets are summarized in Table 1. The  $\Xi$  set is shown in Fig. 3. With both scale-setting procedures, we find that the masses agree with the hadron spectrum observed in nature (28).

Thus, our study strongly suggests that QCD is the theory of the strong interaction, at low

**Table 1.** Spectrum results in giga-electron volts. The statistical (SEM) and systematic uncertainties on the last digits are given in the first and second set of parentheses, respectively. Experimental masses are isospin-averaged (19). For each of the isospin multiplets considered, this average is within at most 3.5 MeV of the masses of all of its members. As expected, the octet masses are more accurate than the decuplet masses, and the larger the strange content, the more precise is the result. As a consequence, the  $\Delta$  mass determination is the least precise.

$X$	Experimental (28)	$M_X$ ( $\Xi$ set)	$M_X$ ( $\Omega$ set)
$\rho$	0.775	0.775 (29) (13)	0.778 (30) (33)
$K^*$	0.894	0.906 (14) (4)	0.907 (15) (8)
$N$	0.939	0.936 (25) (22)	0.953 (29) (19)
$\Lambda$	1.116	1.114 (15) (5)	1.103 (23) (10)
$\Sigma$	1.191	1.169 (18) (15)	1.157 (25) (15)
$\Xi$	1.318	1.318	1.317 (16) (13)
$\Delta$	1.232	1.248 (97) (61)	1.234 (82) (81)
$\Sigma^*$	1.385	1.427 (46) (35)	1.404 (38) (27)
$\Xi^*$	1.533	1.565 (26) (15)	1.561 (15) (15)
$\Omega$	1.672	1.676 (20) (15)	1.672

**Fig. 3.** The light hadron spectrum of QCD. Horizontal lines and bands are the experimental values with their decay widths. Our results are shown by solid circles. Vertical error bars represent our combined statistical (SEM) and systematic error estimates.  $\pi, K$ , and  $\Xi$  have no error bars, because they are used to set the light quark mass, the strange quark mass and the overall scale, respectively.



energies as well, and furthermore that lattice studies have reached the stage where all systematic errors can be fully controlled. This will prove important in the forthcoming era in which lattice calculations will play a vital role in unraveling possible new physics from processes that are interlaced with QCD effects.

## References and Notes

1. D. J. Gross, F. Wilczek, *Phys. Rev. Lett.* **30**, 1343 (1973).
2. H. D. Politzer, *Phys. Rev. Lett.* **30**, 1346 (1973).
3. K. G. Wilson, *Phys. Rev. D Part. Fields* **10**, 2445 (1974).
4. S. Aoki et al., *Phys. Rev. Lett.* **84**, 238 (2000).
5. S. Aoki et al., *Phys. Rev. D Part. Fields* **67**, 034503 (2003).
6. C. T. H. Davies et al., *Phys. Rev. Lett.* **92**, 022001 (2004).
7. S. Aoki et al., <http://arxiv.org/abs/0807.1661> (2008).
8. C. W. Bernard et al., *Phys. Rev. D Part. Fields* **64**, 054506 (2001).
9. C. Aubin et al., *Phys. Rev. D Part. Fields Gravit. Cosmol.* **70**, 094505 (2004).
10. N. Ukita et al., *Proc. Sci. LAT2007*, 138 (2007).
11. M. Gockeler et al., *Proc. Sci. LAT2007*, 129 (2007).
12. D. J. Antonio et al., *Phys. Rev. D Part. Fields Gravit. Cosmol.* **75**, 114501 (2007).
13. A. Walker-Loud et al., <http://arxiv.org/abs/0806.4549> (2008).
14. L. Del Debbio, L. Giusti, M. Luscher, R. Petronzio, N. Tantalo, *J. High Energy Phys.* **02**, 056 (2007).
15. C. Alexandrou et al., <http://arxiv.org/abs/0803.3190> (2008).
16. J. Noaki et al., *Proc. Sci. LAT2007*, 126 (2007).
17. M. Luscher, *Commun. Math. Phys.* **104**, 177 (1986).
18. M. Luscher, *Commun. Math. Phys.* **105**, 153 (1986).
19. See supporting material on Science Online.
20. M. Luscher, *Nucl. Phys. B* **354**, 531 (1991).
21. M. Luscher, *Nucl. Phys. B* **364**, 237 (1991).
22. G. Colangelo, S. Durr, *Eur. Phys. J. C* **33**, 543 (2004).
23. A. Ali Khan et al., *Nucl. Phys. B* **689**, 175 (2004).
24. B. Orth, T. Lippert, K. Schilling, *Phys. Rev. D Part. Fields Gravit. Cosmol.* **72**, 014503 (2005).
25. M. A. Clark, *Proc. Sci. LAT2006*, 004 (2006).
26. W. M. Wilcox, *Proc. Sci. LAT2007*, 025 (2007).
27. S. Durr et al., <http://arxiv.org/abs/0802.2706> (2008).
28. W. M. Yao et al., *J. Phys.* **G33**, 1 (2006).
29. C. Michael, A. McKerrell, *Phys. Rev. D Part. Fields* **51**, 3745 (1995).
30. Computations were performed on the Blue Gene supercomputers at FZ Jülich and at IDRIS and on clusters at Wuppertal and CPT. This work is supported in part by European Union (EU) grant I3HP; Országos Tudományos Kutatási Alapprogramok grant AT049652; Deutsche Forschungsgemeinschaft grants FO 502/1-2 and SFB-TR 55; EU grants RTN contract MRTN-CT-2006-035482 (FLAVIANet) and (FP7/2007-2013)/ERC no. 208740; and the CNRS's GDR grant 2921. Useful discussions with J. Charles and M. Knecht are acknowledged.

## Supporting Online Material

[www.sciencemag.org/cgi/content/full/322/5905/1224/DC1](http://www.sciencemag.org/cgi/content/full/322/5905/1224/DC1)

SOM Text

Figs. S1 to S5

Tables S1 and S2

References

14 July 2008; accepted 1 October 2008

10.1126/science.1163233

# 4D Imaging of Transient Structures and Morphologies in Ultrafast Electron Microscopy

Brett Barwick, Hyun Soon Park, Oh-Hoon Kwon, J. Spencer Baskin, Ahmed H. Zewail\*

With advances in spatial resolution reaching the atomic scale, two-dimensional (2D) and 3D imaging in electron microscopy has become an essential methodology in various fields of study. Here, we report 4D imaging, with in situ spatiotemporal resolutions, in ultrafast electron microscopy (UEM). The ability to capture selected-area-image dynamics with pixel resolution and to control the time separation between pulses for temporal cooling of the specimen made possible studies of fleeting structures and morphologies. We demonstrate the potential for applications with two examples, gold and graphite. For gold, after thermally induced stress, we determined the atomic structural expansion, the nonthermal lattice temperature, and the ultrafast transients of warping/bulging. In contrast, in graphite, striking coherent transients of the structure were observed in both image and diffraction, directly measuring, on the nanoscale, the longitudinal resonance period governed by Young's elastic modulus. The success of these studies demonstrates the promise of UEM in real-space imaging of dynamics.

Electrons, because of their wave-particle duality, can be accelerated to have picometer wavelength and focused to image in real space (*1*). With the impressive advances made in transmission electron microscopy (TEM), augmented by scanning and aberration-correction features, it is now possible to image with high resolution (2–7), reaching the sub-angstrom scale. Together with the progress made in electron crystallography, tomography, and single-particle imaging (8–13), today the electron microscope in different variants of two-dimensional (2D) and 3D recordings has become a central tool in many fields, from materials science to biology (14–16). For all conventional microscopes, the electrons are generated either thermally by heating the

cathode or by field emission, and as such the electron beam is made of random single-electron bursts with no control over the temporal behavior. In these microscopes, time resolution of milliseconds or longer, being limited by the video rate of the detector, can be achieved, while maintaining the high spatial resolution, as demonstrated in environmental-TEM studies (17).

Ultrafast imaging, using pulsed photoelectron packets, provides opportunities for studying, in real space, the elementary processes of structural and morphological changes. In electron diffraction, ultrashort time resolution is possible (18), but the data are recorded in reciprocal space. With nanosecond and submicron image resolutions (19, 20) limited by space charge, ultrashort processes cannot be observed. To achieve ultrafast resolution in microscopy, the concept of single-electron pulse imaging (18) was realized as a key to the elimination of the Coulomb repulsion between electrons while maintaining the high temporal and spatial resolutions. As long

as the number of electrons in each pulse is below the space-charge limit, the packet can have a few or tens of electrons, and the temporal resolution is still determined by the femtosecond (fs) optical pulse duration and the energy uncertainty, which is also on the fs time scale (21), and the spatial resolution is atomic scale (22). However, the goal of full-scale dynamic imaging can be attained only when, in the microscope, the problems of in situ high-spatiotemporal resolution for selected image areas and of heat dissipation (for reversible processes) are overcome.

Here, we present the methodology of ultrafast imaging with applications in studies of structural and morphological changes in single-crystal gold and graphite films, which exhibit entirely different dynamics. For both, the changes were initiated by in situ fs impulsive heating, while image frames and diffraction patterns were recorded in the microscope at well-defined times after the temperature jump. The time axis in the microscope is independent of the response time of the detector, and it is established using a variable delay-line arrangement; a 1- $\mu\text{m}$  change in optical path of the initiating (clocking) pulse corresponds to a time step of 3.3 fs.

Shown in Fig. 1 is a picture of the second-generation ultrafast electron microscope (UEM-2) built at the California Institute of Technology (Caltech). The integration of two laser systems to a modified electron microscope is indicated in the figure, together with a representative image showing the resolution of a 3.4 Å lattice spacing obtained in UEM without the field-emission-gun (FEG) arrangement of conventional TEM. In the figure, the fs laser system is used to generate the single-electron packets, whereas the ns laser system was used for both single-shot and stroboscopic recordings (23). In the single-electron mode of operation, as in UEM-1 (24), the coherence volume is well defined and appropriate for image formation in repetitive events (25). The dynamics are fully reversible, retracing an identical evolution after each initiating laser pulse; each image is constructed stroboscopically, in seconds,

Physical Biology Center for Ultrafast Science and Technology, Arthur Amos Noyes Laboratory of Chemical Physics, California Institute of Technology, Pasadena, CA 91125, USA.

\*To whom correspondence should be addressed. E-mail: zewail@caltech.edu

from typically  $10^6$  pulses, and all time frames are processed to make a movie. The time separation between pulses can be varied to allow complete heat dissipation in the specimen.

In the hundreds of images collected for each time scan, the dynamics was followed for area-specific changes, giving rise to selected-area-image dynamics (SAID) and selected-area-diffraction dynamics (SADD); for the former, in real space, from contrast change, and for the latter, in Fourier space, from changes of the Bragg peak separations, amplitudes, and widths. It is the advantage of microscopy that allows us to perform this “parallel-imaging” dynamics with pixel resolution, when compared with diffraction, in this case up to one part in 4 million ( $2048 \times 2048$  pixels). As shown below, it would not have been possible to observe the selected temporal changes if the total image were to be averaged over all pixels. Neither could we have resolved the ultrafast dynamics if the time resolution were nanoseconds or longer.

In Fig. 2, A and B, we display representative time-framed images of the gold nanocrystal using the fs excitation pulses at a repetition rate of 200 kHz and peak excitation fluence of  $\sim 1.7$  mJ/cm<sup>2</sup> with an estimated spot diameter of 60  $\mu$ m. In the first image, taken at  $-84$  ps, before the clocking pulse ( $t = 0$ ), typical characteristic features, such as bend contours, of the single crystal gold are observed in the image. Bend contours, which appear as broad fuzzy dark lines in the image, are diffraction contrast effects occurring in warped or buckled samples of constant thickness (26). In the dark regions, the zone axis (the crystal [100]) is well aligned with the incident electron beam and electrons are scattered efficiently, whereas in the lighter regions, the alignment of the zone axis deviates more and the scattering efficiency is lower. Because bend contours generally move when deformation causes tilting of the local crystal lattice, they provide in images a sensitive visual indicator of the occurrence of such deformations.

At positive times, after  $t = 0$ , visual dynamical changes are observed in the bend contours (Fig. 2B). A series of such image frames with equal time steps provides a movie of the morphological dynamics (Movie S1). To more clearly display the temporal evolution, image-difference frames were constructed. Depicted as insets in Fig. 2B are those obtained when referencing to the  $-84$  ps frame for  $t = +66$  ps and  $+151$  ps. In the difference images, the regions of white or black indicate locations of surface morphology change (bend contour movement), whereas gray regions are areas where the contrast is unchanged from that of the reference frame. The white and black features in the difference images are nanometer-scale, reflecting the local dynamics of deformations. Care was taken to ensure the absence of long-term specimen drifts because they can cause apparent contrast change.

To quantify the changes in the image, we used the following method of cross-correlation. The

normalized cross-correlation of an image at time  $t$  with respect to that at time  $t'$  is expressed as

$$\gamma(t'; t) = \frac{\sum_{x,y} C_{x,y}(t) C_{x,y}(t')}{\sqrt{\sum_{x,y} C_{x,y}(t)^2 \sum_{x,y} C_{x,y}(t')^2}} \quad (1)$$

where the contrast  $C_{x,y}(t) = [I_{x,y}(t) - \bar{I}(t)]/\bar{I}(t)$ ;  $I_{x,y}(t)$  is the intensity of the pixel at the position of  $(x,y)$  at time  $t$ , and  $\bar{I}(t)$  is the mean of  $I_{x,y}(t)$ . This correlation coefficient  $\gamma(t'; t)$  is a measure of the temporal change in “relief pattern” between the two images being compared, which can be used as a guide to image dynamics as a function of time. Two types of cross-correlation plots were made, those referenced to a fixed-image frame before  $t = 0$  and those that show correlation between adjacent time points. (Another quantity that shows time dependence qualitatively similar to that of the image cross-correlation is the standard deviation of pixel intensity in difference images).

Shown in Fig. 2, C and D, are the cross-correlation values between the image at each measured time point and a reference image recorded before the arrival of the clocking pulse. The experiments were repeated (for different time-delay steps of 500 fs, 1 ps, 5 ps, and 50 ps), and similar results were obtained (Fig. 2C), showing that morphology changes are completely reversible and reproducible over each 5- $\mu$ s interpulse interval. The adjacent-time cross-correlations reveal the time scales for intrinsic changes in the images, which disappear for time steps below 5 ps, consistent with full-image rise in time (27). Over all pixels, the time scale for

image change covers the full range of time delay, from picoseconds to nanoseconds, indicating the collective averaging over sites of the specimen; as shown in Fig. 2C, the overall response can be fit to two time constants of 90 ps and 1 ns.

The power of SAID is illustrated when the dynamics of the bend contours are followed in different selected areas of the image, noted in the micrographs as SAI #1, #2, and #3. The corresponding image cross-correlations (Fig. 2D) have different shape and amplitude from each other and from the full-image correlation. The large differences observed here and for other data sets, including onsets delayed in time (Fig. 2, G to L) and sign reversals, indicate the variation in local deformation dynamics. In Fig. 2, G to K, a time-resolved SAI at higher magnification is depicted. A broad and black “penguin-like” contour is observed as the dominant feature of this area. As shown in the frames, a colossal response to the fs heating is noted. The gray region inside the black contour appears and broadens with time. Also, a new black contour above the large central white hole begins to be evident at 1200 ps and gains substantial intensity over the following 50 ps; all frames taken construct a movie of SAID (Movie S2).

The observed SAID changes correspond to diffraction contrast (bright-field) effects in bend contours, as mentioned above. It is known that the shape of bend contours can be easily altered by sample tilting or heating inside the microscope. However, here in the UEM measurements, the changes in local tilt are transient in nature, reflecting the temporal changes of morphology and structure. Indeed, when the experiments were repeated in the TEM mode of operation, that is,

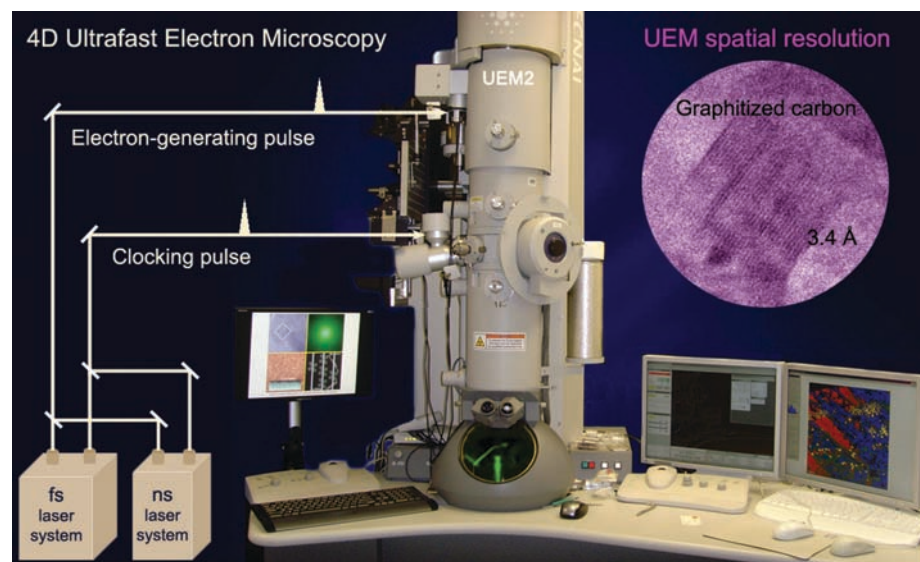


**Fig. 1.** Photograph of the UEM-2 microscope at Caltech, together with a high-resolution image of a graphitized carbon sample showing 3.4 Å lattice fringes. Displayed is the interface of two laser systems (fs and ns) to a modified, hybrid 200-kV TEM designed with two ports for optical access. It is straightforward to switch (by flipping two mirrors) between the laser systems to permit both fs and ns operation. The optical pulses are directed to the photocathode to generate electron packets, as well as to the specimen to initiate (clock) the change in images with a well-defined delay time  $\Delta t$ . The time axis is defined by variable delay between the electron generating and clocking pulses.



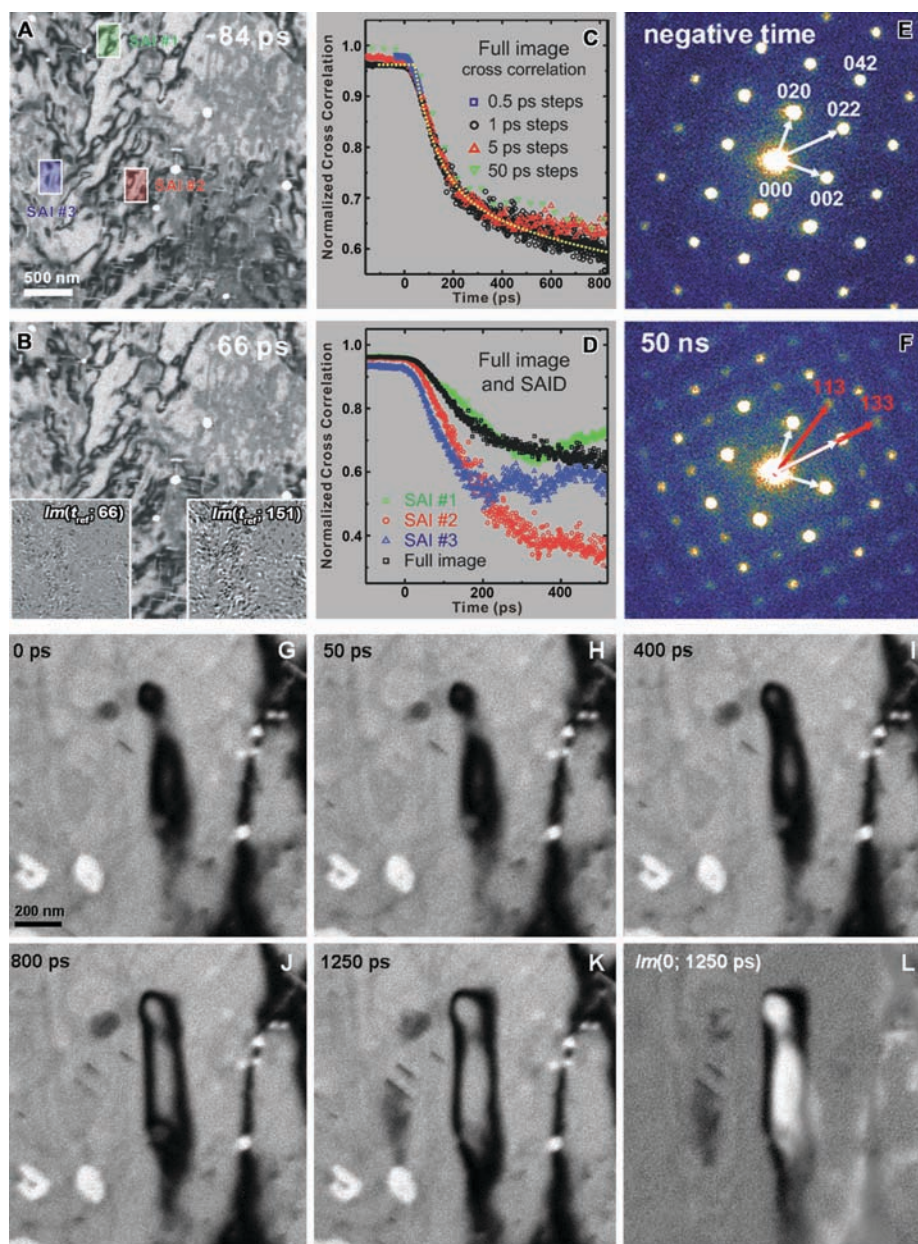


**Fig. 2.** Time-resolved images and diffraction. (A and B) Images obtained stroboscopically at two typical time delays after heating with the fs pulse (fluence of  $1.7 \text{ mJ/cm}^2$ ). The gold specimen, 11 nm thick, was obtained from Ted Pella Inc.; the single-crystal film was mounted on a standard 3-mm 400-mesh grid. Shown are the bend contours (dark bands), and holes in the sample (bright white circles). The insets are image-difference frames  $Im(t_{\text{ref}}, t)$  with respect to the image taken at  $-84 \text{ ps}$ . The thickness was checked by EELS in our UEM-2. (C) Time dependence of image cross-correlations of the full image from four independent scans taken with different time steps. A fit to biexponential rise of the 1-ps step scan is drawn, yielding time constants of 90 ps and 1 ns. (D) The time dependence of image cross-correlations at 1-ps time steps for the full image and for selected areas of interest SAI #1, #2, and #3, as shown in the  $-84 \text{ ps}$  image (A). (E and F) Diffraction patterns obtained using a single pulse of  $\approx 10^6$  electrons with high peak heating fluence ( $40 \text{ mJ/cm}^2$ ) and selected-area aperture of  $25\text{-}\mu\text{m}$  diameter; two frames are given to indicate the change. Diffraction spots were indexed and representative indices are shown. (G to L) High-magnification nanoscale image change with time. The sample normal is tilted at a  $10^\circ$  angle to the microscope axis. In these bright-field images (also in Fig. 2), the boundaries are assigned to the  $\{111\}$  twins of gold (36). Note the large change in the penguin-like contrast with time. The bright regions in the field of view correspond to holes locally damaged by laser heating above the threshold in previous experiments. (L) is a difference image,  $Im(0; 1250 \text{ ps})$ , which properly eliminates reference and unchanged (with time) features, including holes.

for the same heating laser pulse and same scanning time but with continuous electron probe beam, no image change was observed. This is further supported by the change in diffraction observed at high fluences and shown in Fig. 2, E and F, for two frames, at negative time and at  $+50 \text{ ns}$ ; in the latter, additional Bragg spots are visible, a direct evidence of the transient structural change due to bulging at longer times.

Whereas real-space imaging shows the time-dependent morphology, the SADD provides structural changes on the ultrashort time scale. Because the surface normal of the film is parallel to the  $[100]$  zone axis, the diffraction pattern of the sample was properly indexed by the face-centered-cubic (fcc) structure projected along the  $[100]$  zone axis at zero tilt angle (see the single-pulse diffraction pattern of Fig. 2E). From the positions of the transient spots in Fig. 2F, which are reflections from the  $\{113\}$  and  $\{133\}$  planes, forbidden in the  $[100]$  zone-axis viewing, we measured the interplanar spacings to be  $1.248$  and  $0.951 \text{ \AA}$ , respectively. To reproduce the appearance of those peaks, we need to tilt the sample by an angle of more than  $10^\circ$  without laser heating. From stroboscopic SAD patterns, Bragg peak separations, amplitudes, and widths were obtained as a function of time. The results indicate different time scales from those of image dynamics.

The average amplitude of  $\{042\}$  diffraction peaks drops significantly; the rise time is  $12.9 \text{ ps}$ , whereas the change in average separation of all planes observed in the  $[100]$  zone axis is delayed by  $31 \text{ ps}$  and rises in  $60 \text{ ps}$  (Fig. 3A) (28). The delay in the onset of separation change with respect to amplitude change is similar to the time scale for the amplitude to reach its plateau value of 15% reduction in the case of the  $\{042\}$  amplitude shown. These structural dynamics are consistent with the electron and lattice temperature obtained by optical reflectivity (29). To determine the recovery time of the structure, we carried out stroboscopic (and also single-pulse) experiments over the time scale of microseconds. The recovery transient in the inset of Fig. 3A (at  $7 \text{ mJ/cm}^2$ ) gives a time constant of  $2.2 \text{ }\mu\text{s}$ ; we made calculations of 2D lateral heat transport with thermal conductivity  $\lambda = 3.17 \text{ W/(cm}\cdot\text{K)}$  at  $300 \text{ K}$  and laser spot diameter of  $60 \text{ }\mu\text{m}$ , and reproduced the observed time scale.

The atomic-scale motions, which lead to structural and morphological changes, can now be visualized. Because the specimen is nanoscale in thickness, the initial temperature induced is essentially uniform across the atomic layers and heat can only dissipate laterally. It is known that for metals the lattice temperature is acquired after the large increase in electron temperature (30). The results in Fig. 3A give the temperature rise as  $13 \text{ ps}$ ; from the known electron and lattice heat-capacity constants [ $C_1 = 70 \text{ J/(m}^3\cdot\text{K}^2)$  and  $C_2 = 2.5 \times 10^6 \text{ J/(m}^3\cdot\text{K)}$ , respectively] and the electron-phonon coupling [ $g = 2 \times 10^{16} \text{ W/(m}^3\cdot\text{K)}$ ], we obtained the initial heating time of  $\sim 10 \text{ ps}$  for electron temperature  $T_1 = 2500 \text{ K}$ , in good



agreement with the observed rise (29). Reflectivity measurements do not provide structural information, but they give the temperature rise (29). For bulk material, the time scale for heating ( $\sim 1$  ps) is shorter than that of the nanoscale specimen ( $\sim 10$  ps), due to confinement in the latter, which limits the ballistic motion of electrons in the specimen (29), and this is evident in the UEM studies. Because the plane separation is 0.4078 nm, the change of the average peak separation (0.043%), at the fluence of 1.7 mJ/cm<sup>2</sup> of the fs pulse, gives a lateral lattice constant change of 0.17 pm.

Up to 30 ps, the lattice is hot but, because of macroscopic lattice constraint, the atomic stress cannot lead to changes in lateral separations, which are the only separations visible for the [100] zone-axis probing. However, the morphology warping change is correlated with atomic (lateral) displacements in the structure as it relieves the structural constraint. Indeed, the time scale of the initial image change is comparable to that of plane separations in diffraction (60 to 90 ps). This initial warping, which changes image contrast, is followed by longer time (nanosecond) minimization of surface energy and bulging, as shown in Fig. 2D. If the picometer-scale lateral structural change (0.17 pm) were applied to the thickness, the stress over the 11-nm specimen would give a total expansion of 4.7 pm. Considering the influence of the measured lateral expansion, the maximum bulge reaches 1 to 10 nm, depending on the lateral scale (31). Finally, the calculated Debye-Waller factor for structural changes gives a temperature of 420 K ( $\Delta T = 125$  K), in agreement with the lattice temperature derived under similar conditions, noting that for the nanoscale material the temperature is higher than in the bulk (29, 31).

Graphite, with its unique 2D structure and physical properties, was the second specimen studied in the application of the UEM methodology reported here. In contrast to the observations made for gold, in graphite, by off-axis selected-area recording, coherent resonance modulations in the image, and also in diffraction, were directly resolved in real time. The damped resonance of very high frequency, as shown below, has its origin in the nanoscale dimension of the specimen and its elasticity. The initial fs pulse induces an impulsive stress in the film and the ultrafast electron tracks the change of the transient structure, both in SAID and SADD. In Fig. 3, B and C, we display the diffraction pattern and the results obtained by measuring changes of the diffraction spot ( $1\bar{2}2$ ) and, in Fig. 4 those obtained by dark-field (DF) imaging with the same diffraction spot being selected by the objective aperture. The specimen was tilted at a 21° angle to the microscope axis, and the diffraction pattern was indexed along the [011] zone axis. With different magnifications, Moiré (fig. S1) and buckling fringes are observed in the images (Fig. 4).

For both the image and the diffraction, a strong oscillatory behavior is evident, with a well-defined period and decaying envelope. When the

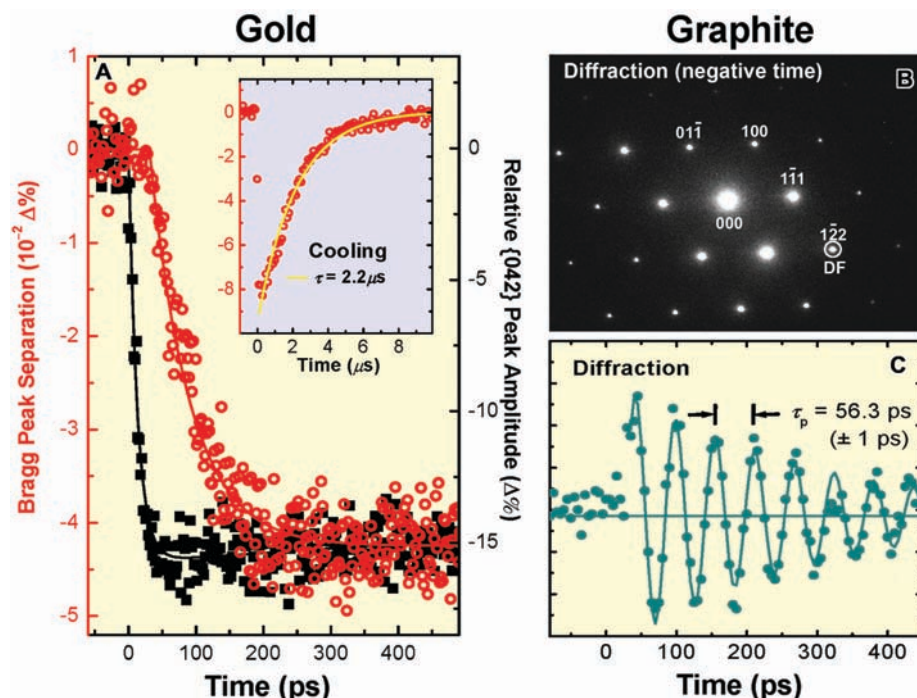


**Fig. 3.** Structural dynamics and heat dissipation in gold, and coherent resonance of graphite. (A) SADD for fs excitation at 1.7 mJ/cm<sup>2</sup> peak fluence (519 nm). The Bragg separation for all peaks and the amplitude of the {042} peaks are shown in the main panel; the inset gives the 2.2-μs recovery (by cooling) of the structure obtained by stroboscopic ns excitation at 7 mJ/cm<sup>2</sup>. The peak amplitude has been normalized to the transmitted beam amplitude, and the time dependence of amplitude and separation is fit as an exponential rise, and a delay with rise, respectively. (B) The diffraction pattern of graphite taken at negative time, that is, before the arrival of the clocking pulse. The experiments were carried out with a natural single crystal of graphite on a grid. To prepare the specimen, a graphite crystal was glued to the grid and repeatedly cleaved. The glue was subsequently dissolved in acetone, and graphite flakes with varying dimensions were left on the grid, covering some of the grid squares completely. The graphite thickness for the data shown is 103 nm as determined by EELS in UEM-2. The specimen was tilted at a 21° angle to the microscope axis, and the diffraction pattern was obtained by using a SAD aperture of 6-μm diameter. The diffraction spots were indexed according to the hexagonal structure of graphite along the [011] zone axis, and representative indices are shown. The circled diffraction ( $1\bar{2}2$ ) spot is the one used for the DF imaging of Fig. 4. (C) Resonance oscillations observed for the Bragg ( $1\bar{2}2$ ) peak in the diffraction pattern of (B); the oscillation period ( $\tau_p$ ) is measured to be 56.3 ps. For a thickness of 64 nm, the period is 35.4 ps.

diffraction transient was fitted to a damped resonance function  $[(\cos 2\pi t/\tau_p)\exp(-t/\tau_{\text{decay}})]$ , we obtained  $\tau_p = 56.3 \pm 1$  ps for the period. The decay of the envelope for this particular resonance is significantly longer;  $\tau_{\text{decay}} = 280$  ps. This coherent transient decay, when Fourier transformed, indicates that the thickness variation of the film is only  $\pm 3$  nm (Eq 2.). The thickness of the film was determined ( $d = 103$  nm) using electron energy loss spectroscopy (EELS) in our UEM (mean-free path of inelastic scattering of 150 nm).

To test the validity of this resonance behavior, we repeated the experiments for another thickness,  $d = 64$  nm. The period indeed scaled with  $d$ , giving  $\tau_p = 35.4$  ps. These hitherto unobserved, in real time, very-high-frequency resonances (30 gigahertz range) are unique to the nanoscale thickness of graphite. They also reflect the (harmonic) motions due to strain along the  $c$ -axis direction, because they were not observed when we repeated the experiment for the electron incident along the [001] zone axis. The fact that the period of the diffraction is the

same as that of the image suggests the direct correlation between local atomic structure and macroscopic elastic behavior.

After a femtosecond pulse of stress on an ideal freely vibrating nanofilm, oscillations are expected which are related to the velocity ( $v$ ) of acoustic waves between specimen boundaries, which in turn can be related to Young's modulus ( $Y$ ) of the  $c$  axis ( $c_{33}$  elastic modulus):

$$\frac{1}{\tau_p} = \frac{nv}{2d} = \frac{n}{2d} \left( \frac{Y}{\rho} \right)^{1/2} \quad (2)$$

where  $n$  is a positive integer, with  $n = 1$  being the fundamental resonance frequency (higher  $n$ 's are for overtones). Knowing the measured  $\tau_p$ 's and  $d$ 's, we obtained  $v = 3.6 \times 10^5$  cm/s. For a graphite density  $\rho = 2.26$  g/cm<sup>3</sup>,  $Y$  equals 30 GPa for the  $c$  axis strain in the natural specimen examined, a value that is certainly in the range of the reported 20 to 47 GPa for  $c_{33}$  (32, 33). Pyrolytic graphite has  $Y$  values that range from about 10 to 1000 GPa, depending on the orien-

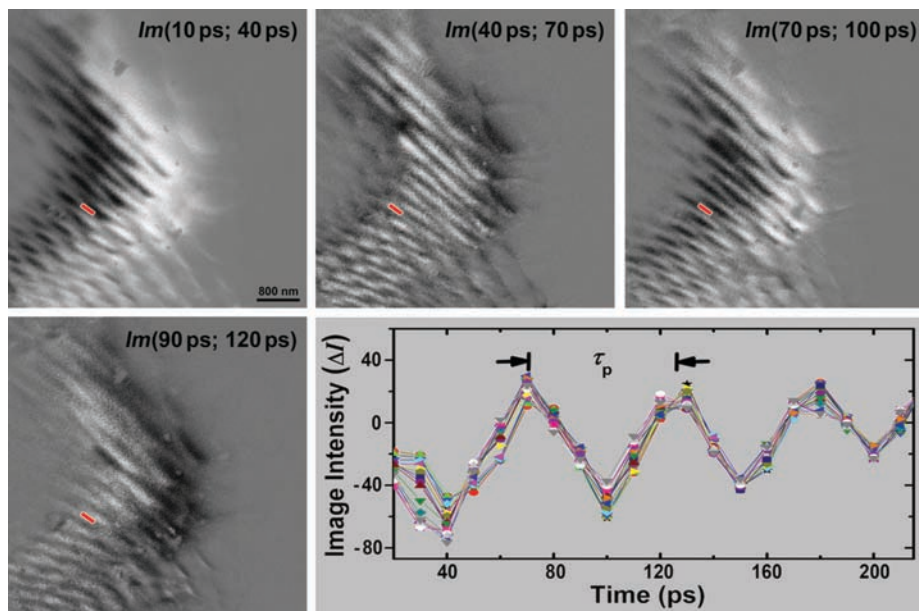


**Fig. 4.** Image, selected areas, and time dependence of intensity difference (DF) for graphite. Moiré fringes (37) were observed at high resolution (fig. S1), and their separations vary from 2.6 nm to 36.6 nm depending on the angle between two layers. The buckling fringes here are separated by  $\sim 300$  nm but vary with location; the scanning tunneling microscopy-observed fringes (38) are on the scale of 150 nm, reflecting differences in (zone-axis) scattering (39, 40). Shown are several difference images,  $Im(t - 30 \text{ ps}; t)$ , and a plot of SAI intensities. The difference images were constructed from a series of DF images obtained by selecting the Bragg ( $1\bar{2}2$ ) spot circled in Fig. 3B. The selected areas for the intensity plot are indicated by the red box. The temporal evolution of the DF difference images clearly shows the resonance behavior, with time steps corresponding to the peak and trough in the intensity oscillations. Note the direct change in contrast with time and its recurrences at longer time. Each color in the intensity plot corresponds to a selected area of a  $1 \times 100$ -pixel slice parallel to contrast fringes in the DF image. The image change displays the oscillatory behavior with the same  $\tau_p$  as that of diffraction in Fig. 3C.

tation, reaching the lowest value in bulk graphite and the highest one for graphene (32, 34). Extension of these real-time measurements to different length scales, specimens of different density of dislocations, orientations, and the like would allow further exploration of their influences, at the nanoscale, on  $v$ ,  $Y$ , and other properties. We note that selected-area imaging was critical because different regions have temporally different amplitudes and phases across the image. The presence of inhomogeneity on the micrometer scale of the thermoelastic properties of grains in polycrystalline materials is a motif of time-integrated imaging in scanning electron acoustic microscopy (35).

Uniting the power of the spatial resolution of EM with the ultrafast electron timing of UEM enables the unraveling of the elementary dynamics of structures and morphologies in the four dimensions of time and space. With total dissipation of specimen heat between pulses, selected-area dynamics make it possible to study the changes in seconds of recording and for selected pixels of the image. The applications given here, for both gold and graphite in the nonequilibrium state (temperature rate reaching  $10^{13}$  K/s), display a wide range of time and length scales of structure and morphology, as well as ultrafast coherent (resonance) behavior. These examples illustrate the potential for other applications, including nanomechanical

systems (41), especially when incorporating the different and valuable variants of EM that we have in our UEM for physical and biological imaging.

#### References and Notes

- M. Knoll, E. Ruska, *Z. Phys.* **78**, 318 (1932).
- A. V. Crewe, J. Wall, *J. Langmore, Science* **168**, 1338 (1970).
- M. Haider *et al.*, *Nature* **392**, 768 (1998).
- D. A. Muller *et al.*, *Science* **319**, 1073 (2008).
- P. E. Batson, N. Dellby, O. L. Krivanek, *Nature* **418**, 617 (2002).
- K. Kimoto *et al.*, *Nature* **450**, 702 (2007).
- M. A. O'Keefe, *Ultramicroscopy* **108**, 196 (2008) and references therein.
- D. J. De Rosier, A. Klug, *Nature* **217**, 130 (1968).
- R. Henderson, *Q. Rev. Biophys.* **37**, 3 (2004).
- V. Lucic, F. Förster, W. Baumeister, *Annu. Rev. Biochem.* **74**, 833 (2005).
- A. Komeili, Z. Li, D. K. Newman, G. J. Jensen, *Science* **311**, 242 (2006).
- W. Jiang *et al.*, *Nature* **439**, 612 (2006).
- X. D. Zou, S. Hovmöller, *Acta Crystallogr. A* **64**, 149 (2008).
- P. W. Hawkes, J. C. H. Spence, Eds., *Science of Microscopy* (Springer, New York, 2006), vol. 1.
- J. M. Thomas, in *Physical Biology: From Atom to Medicine* A. H. Zewail, Ed. (Imperial College Press, London, 2008).
- A. Howie, P. M. Midgley, C. J. Humphreys, O. Terasaki, in *Turning Points in Solid-State, Materials and Surface Science* K. D. M. Harris, P. P. Edwards, Eds. (Royal Society of Chemistry, Cambridge, 2008).
- E. D. Boyes, P. L. Gai, *Ultramicroscopy* **67**, 219 (1997).
- A. H. Zewail, *Annu. Rev. Phys. Chem.* **57**, 65 (2006) and references therein.
- H. Dömer, O. Bostanjoglo, *Rev. Sci. Instrum.* **74**, 4369 (2003).
- T. Lagrange *et al.*, *Acta Mater.* **55**, 5211 (2007).

- A. Gahlmann, S. T. Park, A. H. Zewail, *Phys. Chem. Chem. Phys.* **10**, 2894 (2008).
- H. S. Park, J. S. Baskin, O.-H. Kwon, A. H. Zewail, *Nano Lett.* **7**, 2545 (2007).
- O.-H. Kwon *et al.*, *Proc. Natl. Acad. Sci. U.S.A.* **105**, 8519 (2008).
- A. H. Zewail, V. A. Lobastov, Method and system for ultrafast photo-electron microscope, US Patent 7,154,091 B2, 20050401 (2006).
- A. H. Zewail, in *Visions of Discovery: Shedding New Light on Physics and Cosmology*, R. Chiao, W. Phillips, A. Leggett, M. Cohen, G. Ellis, D. York, R. Bishop, C. Harper, Eds. (Cambridge University Press, Cambridge, 2008), chap. 2.
- B. Fultz, J. M. Howe, *Transmission Electron Microscopy and Diffractometry of Materials* (Springer, New York, 2002).
- The deviation from 1 in the correlation of independent measurements for the same real image pattern is a measure of the overall scale of image relief relative to the random noise contribution in the frames. Thus, a flatter image, relative to the noise, will have a smaller  $\gamma$  value for independently recorded frames; see, for example, the slight difference in baseline values in Fig. 2C.
- The width rises because of the induced structural inhomogeneity, as expected, and near  $t = 0$  an initial decrease is noted, which indicates that the overall temporal response is much faster than that of the amplitude or separation rise.
- J. Hohlfield *et al.*, *Chem. Phys.* **251**, 237 (2000).
- G. Ertl, *Adv. Catal.* **45**, 1 (2000).
- We have calculated the maximum strain-induced tilt angle of the surface normal and found it to be  $\phi \cong \sqrt{6\Delta L/L}$ . For  $\Delta L/L = 0.043\%$ ,  $\phi = 2.9^\circ$ , and the corresponding bulge reaches 1 to 10 nm when the local (lateral) deformation scale is 0.08 to 0.8  $\mu\text{m}$ . For the nanosecond heating at a fluence of 40 mJ/cm<sup>2</sup> (Fig. 2F), the Bragg spot separation change is  $\sim 1\%$ , giving  $\phi = 14^\circ$ . The calculated angles correspond well to the angles of microscope specimen tilt needed to produce diffraction and contrast changes similar to those caused by heating. The lateral expansion of  $\Delta L/L = 0.043\%$  after fs heating gives, at equilibrium, a temperature change of 30 K, using  $\alpha = 14.2 \times 10^{-6} \text{ K}^{-1}$ . A higher  $\Delta T$  derived from the intensity changes (Debye-Waller factor) may have some contribution from zone-axis tilt. Because the zone axis was along the [100] direction before the arrival of the heat impulse, the influence of tilting would make the derived  $\Delta T$  a maximum value.
- O. L. Blakslee, D. G. Proctor, E. J. Seldin, G. B. Spence, T. Weng, *J. Appl. Phys.* **41**, 3373 (1970).
- W. N. Reynolds, *Physical Properties of Graphite* (Elsevier, Amsterdam, 1968).
- C. Lee, X. Wei, J. W. Kysar, J. Hone, *Science* **321**, 385 (2008).
- D. G. Davies, *Philos. Trans. R. Soc. Lond. A* **320**, 243 (1986).
- P. B. Hirsch, A. Howie, R. B. Nicholson, D. W. Pashley, M. J. Whelan, *Electron Microscopy of Thin Crystals* (Butterworths, London, 1965).
- F. E. Fujita, K. Izui, *J. Phys. Soc. Jpn.* **16**, 214 (1961).
- S. K. Choudhary, A. K. Gupta, *Jpn. J. Appl. Phys.* **46**, 7450 (2007).
- Z. L. Wang, *Elastic and Inelastic Scattering in Electron Diffraction and Imaging* (Plenum, New York, 1995).
- D. Shindo, K. Hiraga, *High-Resolution Electron Microscopy for Materials Science* (Springer-Verlag, Tokyo, 1998).
- O.-H. Kwon *et al.*, *Nano Lett.* **8**, 3557 (2008).
- We thank F. Carbone for his handling of the graphite film and for helpful discussion. This work was supported by the National Science Foundation and Air Force Office of Scientific Research in the Gordon and Betty Moore Center for Physical Biology at Caltech. Research on biological UEM imaging was supported by the National Institutes of Health. Caltech has filed a provisional patent application for the microscope described here.

#### Supporting Online Material

www.sciencemag.org/cgi/content/full/322/5905/1227/DC1  
Fig. S1  
Movies S1 and S2

30 July 2008; accepted 22 October 2008  
10.1126/science.1164000



# High Harmonic Generation from Multiple Orbitals in N<sub>2</sub>

Brian K. McFarland, Joseph P. Farrell, Philip H. Bucksbaum, Markus Gühr\*

Molecular electronic states energetically below the highest occupied molecular orbital (HOMO) should contribute to laser-driven high harmonic generation (HHG), but this behavior has not been observed previously. Our measurements of the HHG spectrum of N<sub>2</sub> molecules aligned perpendicular to the laser polarization showed a maximum at the rotational half-revival. This feature indicates the influence of electrons occupying the orbital just below the N<sub>2</sub> HOMO, referred to as the HOMO-1. Such observations of lower-lying orbitals are essential to understanding subfemtosecond/subangstrom electronic motion in laser-excited molecules.

Tomographic imaging of molecules by means of high harmonic generation (HHG) has attracted wide interest (1). The method can be easily described in the framework of a strong-field three-step model (2, 3). In this model, a portion of the electron wave function corresponding to the highest occupied molecular orbital (HOMO) tunnels into the continuum and is accelerated in a strong oscillating optical field. This continuum part of the wave function is treated as a free electron wave packet that interferes coherently with the bound part of the HOMO when it returns to the molecule. Recombination dipole radiation is emitted on every half-cycle of the driving field, and the coherent superposition of this radiation over multiple cycles forms a discrete spectrum of odd-order high harmonics. These harmonics typically have an approximately constant amplitude over a broad spectral range called the plateau region. The plateau is followed by a sharp decrease in amplitude known as the cutoff region located near the energy given by  $3.17 U_p + \text{IP}$ , where  $U_p$  is the ponderomotive energy and IP is the ionization potential. The spectrum contains information about the HOMO structure. Tomographic reconstruction achieves subangstrom spatial resolution determined by the shortest de Broglie wavelength of the recombining electrons. The harmonics also carry subfemtosecond timing information as a result of the subcycle electron recombination. This high temporal and spatial resolution can enable ultrafast movies of molecular orbital dynamics; however, to date, only the stationary HOMO has been imaged. Electron dynamics result from the coherent superposition of multiple electronic stationary states. Observing subfemtosecond electron dynamics therefore requires the participation of multiple orbitals in HHG.

Here, we report simultaneous HHG from two molecular electronic orbitals, the HOMO and the next lower bound HOMO-1, in N<sub>2</sub>. The

HOMO-1 participation emerges through enhancements in the HHG signal at characteristic alignment angles of the molecular axis to the polarization of the harmonic generating pulse. The angular alignment is accomplished by impulsive rotational excitation of a cold (40 K) and dense N<sub>2</sub> jet by a nonresonant femtosecond laser pulse (4). In the vicinity of a rotational revival, the molecules undergo a rapid change in alignment, which modulates the HHG.

In our experiment, low-order harmonics (i.e., harmonics 15 to 25) show a weakening of the harmonic signal if the molecular axis is perpendicular to the harmonic generation laser polarization. However, at higher harmonic orders, a

peak appears that is highly pronounced in this configuration. We attribute the minimum amplitude in the low harmonics to HHG derived predominantly from the HOMO; the peak at higher harmonics is characteristic of HHG from the HOMO-1. The prominent peak at higher harmonics shows three important features of the HOMO-1 that are predicted by semiclassical simulations and simple ionization arguments: The cutoff extends to shorter wavelengths relative to an isotropic ensemble; it is strongest when the molecular axes are near 90° to the harmonic generation polarization; and it presents itself most clearly near the cutoff.

Past studies of HHG from aligned N<sub>2</sub> concentrated on the plateau region for orbital reconstruction (1) and not on the cutoff region where the HOMO-1 signal is most pronounced. We observe that the HOMO-1 signal is very sensitive to the molecular alignment, and we tune our alignment parameters to optimize the signal.

The preferential field ionization of a more deeply bound state over a less deeply bound state is possible because of the different geometries of the corresponding wave functions in the molecular frame. This scenario is analogous to the field ionization of Stark states in atoms, where states with a magnetic quantum number  $m_l = 0$  ionize more easily than  $m_l > 0$  states because the  $m_l = 0$  states overlap the saddle point in the potential (5). Field ionization is most sensitive to the outer

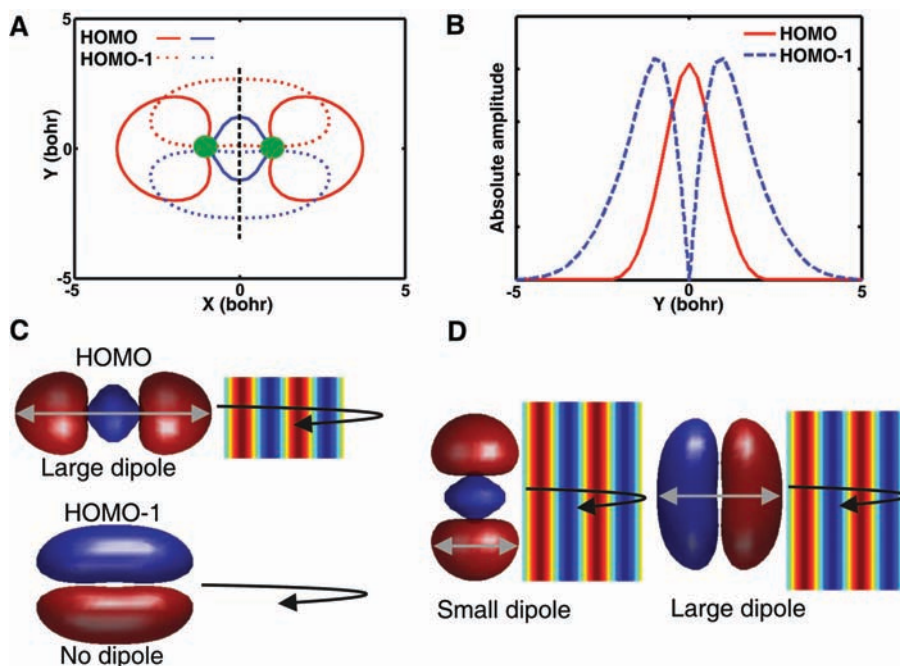


**Fig. 1.** (A) Isoamplitude lines of the N<sub>2</sub> HOMO (solid lines) and HOMO-1 (dashed lines). The color indicates the sign of the wave function. The green disks indicate the position of the nuclei. (B) Absolute amplitude of the HOMO (solid red line) and the HOMO-1 (dashed blue line) along a direction perpendicular to the internuclear axis, indicated by the black dashed line in (A). (C) Sketch of the recombining free electron wave for the electric field creating the high harmonics polarized along the internuclear axis. A strong dipole is induced in the HOMO, whereas no dipole is induced in the HOMO-1 (see text). (D) Same sketch as in (C) for a harmonic generating field polarized perpendicular to the internuclear axis. Relative to (C), the dipole for the HOMO is weakened, whereas the HOMO-1 dipole is strengthened.

PULSE Institute, SLAC, Menlo Park, CA 94025, USA, and Departments of Physics and Applied Physics, Stanford University, Stanford, CA 94305, USA.

\*To whom correspondence should be addressed. E-mail: mguehr@stanford.edu

parts of the electron wave function near this saddle point (6). Figure 1A illustrates this point with cuts through isoprobability density surfaces of the HOMO and HOMO-1 of  $N_2$ . The orbitals are obtained by ab initio calculations using an STO-3G basis set in the Gaussian software package (7). The  $N_2$  HOMO and HOMO-1 exhibit  $\sigma_g$  and  $\pi_u$  symmetries, respectively. The cuts through the HOMO and HOMO-1 orbitals show that the HOMO extends farther than the HOMO-1 along the direction parallel to the internuclear axis. Therefore, the HOMO will preferentially ionize when the electric field is parallel to the internuclear axis. The situation is reversed in the direction perpendicular to the internuclear axis, where the HOMO-1 protrudes farther than the HOMO. This property is further demonstrated in Fig. 1B, which gives one-dimensional cuts through the orbitals along the black dashed line in Fig. 1A. We conclude that the HOMO-1 ionizes more easily than the HOMO when the laser field is polarized  $90^\circ$  with respect to the internuclear axis. This conclusion is supported by a strong-field ionization calculation for the HOMO and HOMO-1 orbitals (8).

After strong-field ionization of a particular orbital, the acceleration of the electron in the laser field results in an energy-dispersed (chirped) electron wave packet. The recombining electron wave packet is therefore a de Broglie wave,  $\Phi_{\text{free}}$ , whose instantaneous wavelength  $\lambda_{\text{dB}}$  changes as a function of recombination time. The returning electron wave forms a superposition with the  $N_2$  orbital, inducing a time-dependent dipole moment described by  $\langle \text{HOMO} | ez | \Phi_{\text{free}} \rangle$  or  $\langle \text{HOMO-1} | ez | \Phi_{\text{free}} \rangle$  for the respective orbital (where  $z$  is along the  $\mathbf{k}$ -vector of the returning electron) as it moves across the  $N_2$  molecule. Figure 1C shows the recombination step for molecules standing parallel to the harmonic generation polarization. Recombination to the HOMO gives rise to a large dipole because the expectation value of  $z$  can

vary all along the long axis of the HOMO (1). The HOMO-1, however, will not produce any signal because the nodal structure reduces the recombination probability (9) and, in addition, the opposite parity of the two HOMO-1 lobes produces two dipoles that cancel because of a  $\pi$  phase shift.

For recombination with the generation laser polarization perpendicular to the internuclear axis (Fig. 1D), the electron distribution of the HOMO is considerably more confined and yields a diminished dipole moment relative to the parallel case. The HOMO-1, on the other hand, is less confined than the HOMO and will give rise to a correspondingly stronger time-dependent dipole moment. We neglect dipoles perpendicular to the harmonic generation polarization because they are not phase-matched for alignment ensembles with mirror symmetry around the plane formed by the harmonic generation polarization and the propagation vector of the laser pulse (10).

To optimize the HOMO-1 signal, it is necessary to align the molecular axes perpendicular to the generation field. We can achieve this through impulsive alignment in two different ways. The alignment and generation polarizations can be set parallel, which leads to an anti-aligned ensemble just past the half-revival (4.4 ps) where the molecules are perpendicular to the laser polarization. Alternatively, the laser polarizations can be perpendicular, in which case a prolate (Fig. 2C) ensemble with the desired alignment occurs at the half-revival (4.1 ps). We found that an alignment scheme with perpendicular polarizations enhances the contrast of the HOMO-1 with respect to the HOMO. The HOMO-1 has a characteristic spectral signature. Because of the larger IP of the HOMO-1, we expect the HOMO-1 to have a higher cutoff than the HOMO.

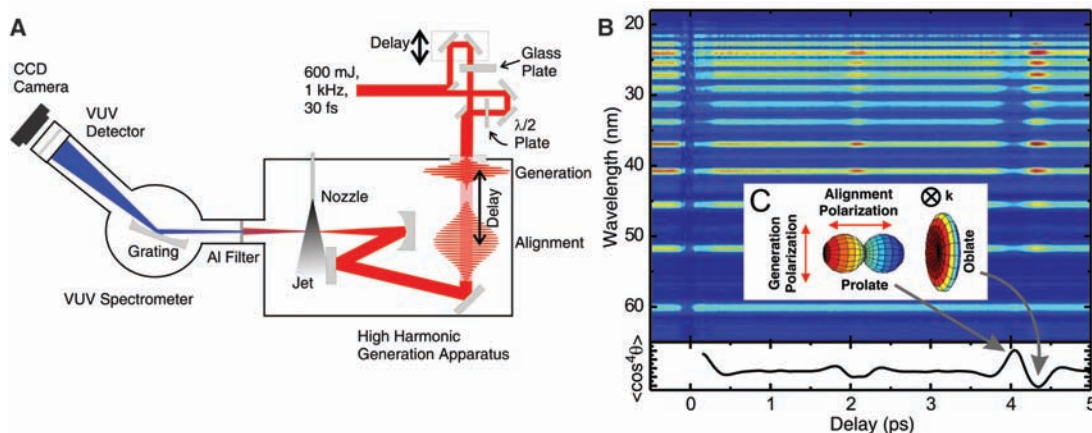
Figure 2A shows a diagram of the experiment. A wavefront beam splitter divides the output of a 1-kHz, 30-fs Ti:sapphire laser sys-

tem into two time-delayed pulses. The first pulse (alignment pulse, 90 fs for optimal alignment, intensity  $I_{\text{align}} = 2.5 \times 10^{13}$  W/cm $^2$ ) aligns the molecules; the second pulse (generation pulse, 30 fs, intensity  $I_G = 1.7 \times 10^{14}$  to  $2.3 \times 10^{14}$  W/cm $^2$ ) generates harmonics from the aligned molecules. The pulses are focused with a spherical mirror ( $R = 800$  mm) into a supersonically cooled gas jet of  $N_2$  molecules in vacuum. The jet is positioned about 2 mm beyond the focus for optimal phase matching (11). The long alignment pulse excites a rotational wave packet in the molecules, leading to periodic field-free alignment (4). We examine the high harmonics generated near the half-revival, around 4.1 ps, where constructive interference of the rotational coherence for  $N_2$  leads to a strong modulation of the alignment parameter  $\langle \cos^4 \theta \rangle$  (12), where  $\theta$  is the angle between the alignment laser polarization and the internuclear axis. The lower panel of Fig. 2B shows the calculated value of  $\langle \cos^4 \theta \rangle$  for a rotational temperature of  $T = 40$  K and an alignment laser intensity of  $I_{\text{align}} = 2.5 \times 10^{13}$  W/cm $^2$ . The harmonics between 20 and 70 eV pass through an Al filter (thickness 100 nm) into an imaging spectrometer, where the harmonics that are phase-matched on axis ("short" trajectories) are selected by an aperture (13).

Figure 2B shows a false-color plot of harmonic spectra collected for different delays between the perpendicularly polarized alignment pulse and the harmonic generation pulse. The odd harmonics of the fundamental radiation from the 15th to the 39th (cutoff) harmonic are modulated along the time axis by the rotational revivals. The character of this modulation is similar for the lower harmonics but changes for harmonics in the cutoff region. Specifically, the signal suppression in the plateau harmonics (near 0.25 ps and 4.1 ps) becomes an enhancement for cutoff harmonics.

We integrate over the center portion of each harmonic peak and normalize to the baseline

**Fig. 2. (A)** Experimental setup. The 600- $\mu$ J, 30-fs pulse is split into alignment and generating pulses with variable relative delay. The alignment pulse is chirped by a glass plate to 90 fs. The relative polarization can be set to  $90^\circ$  by a  $\lambda/2$  plate. The alignment pulse excites a rotational wave packet in the molecules in a supersonic gas jet, and the delayed generation pulse produces high harmonics from the molecules. An aluminum filter blocks the fundamental and passes the harmonics. The vacuum ultraviolet (VUV) light is dispersed by a flat-field toroidal grating (300 lines/mm) and collected by a microchannel plate phosphor screen detector viewed by a charge-coupled device camera. **(B)** Upper panel: Harmonic spectrum as a function of alignment-generation delay in a false-color plot (blue, low signal; red, high signal). Lower panel: Calculated expectation value  $\langle \cos^4 \theta \rangle$ , where  $\theta$  is the angle between the alignment laser polarization and



the internuclear axis. **(C)** Angular distributions at the rotational half-revival, which has axial symmetry around the alignment polarization. At 4.1 ps, the molecular axis distribution has a prolate shape around the alignment polarization; at 4.4 ps after the alignment pulse, it has an oblate shape. The polarizations of the alignment and generation pulses are indicated by the arrows. The  $\mathbf{k}$ -vectors of the pulses point into the page.



alignment signal. The resulting integrated harmonic signals are plotted for a range of time delays (3.5 to 4.7 ps) in Fig. 3A for three values of the generation intensity  $I_G$ . Concentrating on  $I_G = 2.3 \times 10^{14}$  W/cm<sup>2</sup>, revival traces are plotted for harmonic 15 and for harmonics 25 to 39, with the cutoff at harmonic 39. Harmonics 15 to 23 have the same shape, and we plot harmonic 15 as a representative of these curves. Starting at harmonic 25, the minimum at 4.1 ps begins to flatten, and harmonics 31 and above show a peak superimposed on the minimum. At harmonic 39, the temporal structure is completely inverted relative to the trend seen for harmonic 15.

A comparison with the  $\langle \cos^4 \theta \rangle$  characteristics in Fig. 2B shows that the harmonic signal is modulated by the molecular revival structure induced by the alignment pulse. The 15th to 25th harmonics have a minimum at 4.1 ps, when a prolate alignment distribution appears in the direction perpendicular to the generation polarization. A maximum in this harmonic range occurs at 4.4 ps, when an oblate distribution appears in the plane orthogonal to the alignment polarization (Fig. 2C). The alignment distribution and the ionization and recombination characteristics of the N<sub>2</sub> HOMO explain these revival signals. The minimum in the revival signal at 4.1 ps occurs when alignment is perpendicular to the generation laser polarization. As explained above, we expect low ionization and a small recombination dipole for the HOMO under these conditions. At 4.4 ps, the alignment is parallel to the HHG laser polarization, resulting in more ionization, a larger recombination dipole, and thus a maximum in the HHG from the HOMO. These observations connect the revival signal in harmonics 15 to 25 to HHG from the HOMO.

A different phenomenon is revealed for harmonics 25 and greater. As described above, a peak grows out of the minimum at 4.1 ps, lead-

ing to the inverted structure at harmonic 39. This peak is indicative of HHG from the HOMO-1. We expect ionization and recombination to be stronger for the HOMO-1 relative to the HOMO when the molecular ensemble is oriented 90° to the generation laser polarization. Furthermore, the HOMO-1 signal should dominate at harmonic 39 because of the extended cutoff. We show below that the evolution of this feature with harmonic number is also consistent with high harmonics from the HOMO-1. The revival structures in harmonics 25 to 35 show attributes of both HOMO and HOMO-1 harmonic generation where the HOMO contribution is strongest for the low harmonics and the HOMO-1 contribution becomes prominent in the high harmonics.

We studied the dependence of the HOMO-1 peak on  $I_G$  by introducing pellicle beam splitters without changing the alignment intensity or any other parameter. The temporal modulation of each harmonic changes with  $I_G$ . For example, the 33rd harmonic for the highest  $I_G$  shows a valley at 4.1 ps and a peak at 4.4 ps attributed to the HOMO, superimposed on the peak at 4.1 ps attributed to the HOMO-1. At  $I_G = 1.9 \times 10^{14}$  W/cm<sup>2</sup>, the same harmonic shows only the HOMO-1 peak; the HOMO features are absent.

Our results bear some similarities to previous reports of inversions of the alignment-dependent signal in CO<sub>2</sub>, which were attributed either to interference effects (14) or to ionization depletion (15, 16). The aspects of the present work that allow us to eliminate these explanations cleanly are the perpendicular geometry and the dependence of our spectra on the intensity of the generating pulse. The interference model proposed in (14) explains their observations for CO<sub>2</sub> consistently and does not predict a change of the revival structure with  $I_G$ . In contrast, we observe that the revival structure of N<sub>2</sub> depends on  $I_G$ , which strongly suggests the involvement of dif-

ferent orbitals that we propose. Furthermore, ionization depletion effects that have been observed and analyzed in (15, 16) lead to specific predictions for the harmonic intensity dependence on  $I_G$ . In our geometry of a prolate ensemble aligned perpendicular to the generation polarization, the ionization depletion model predicts an increasing harmonic signal for increasing  $I_G$ . This is opposite to the trend we observe at 4.1 ps in Fig. 3A (for example, harmonic 29). Therefore, we rule out either of these alternative explanations for our data.

These simple arguments for multiple orbital contributions are supported by semiclassical simulations of the recombination process in HHG. Details of our simulation procedures can be found in (17). The phase of a free electron wave  $\Phi_{\text{free}}$  is calculated by integrating the Lagrangian of an electron in the electric field, neglecting the shape of the molecular potential (strong-field approximation). We calculate the dipole  $\langle \text{HOMO} | e z | \Phi_{\text{free}} \rangle$  or  $\langle \text{HOMO-1} | e z | \Phi_{\text{free}} \rangle$  for multiple angles  $\alpha$  between the molecular axis and the propagation vector of the recombining wave ( $z$  axis) and superimpose them according to the calculated prolate molecular distribution at 4.1 ps (18). The dipoles are Fourier-transformed and multiplied by  $\omega^4$  (19). Because we take only one ionization-recombination event into account, we obtain the envelope of the harmonics in Fig. 3B.

We estimate that ionization and electron dispersion have a small effect on the relative HHG amplitudes of the HOMO and HOMO-1, according to the following argument. The dependence of the N<sub>2</sub> ionization on the angle between the ionizing laser polarization and the alignment distribution has been studied (20). A comparison of this experimental result with the angular ionization dependence of the HOMO calculated with the MO-ADK method (6, 20) allows us to estimate that the HOMO-1 has 2 to 3.5 times the ionization rate of the HOMO when the ionizing field is perpendicular to the alignment distribution. In addition, the dispersion of the free electron wave in the direction perpendicular to its propagation is greater for the HOMO-1 than for the HOMO, because the HOMO-1 is more compact (i.e., contains higher-momentum components). The trends of ionization and dispersion are opposite, and we do not expect their product to change the ratio of the HOMO to HOMO-1 HHG signal considerably.

The HHG spectrum for the HOMO (Fig. 3B) has a clearly visible plateau and a cutoff at 60 eV, matching the prediction of the cutoff law at  $I_G = 2.3 \times 10^{14}$  W/cm<sup>2</sup>; in the HOMO-1 spectrum, the plateau region is reduced. The HOMO-1 spectral amplitude is small for low photon energies but increases in the cutoff region, in agreement with the experiment. The HHG cutoff for the HOMO-1 extends beyond that of the HOMO by more than can be explained by the 1.3-eV difference in IP. It is now well established that the shape of a molecular wave function has a strong effect on

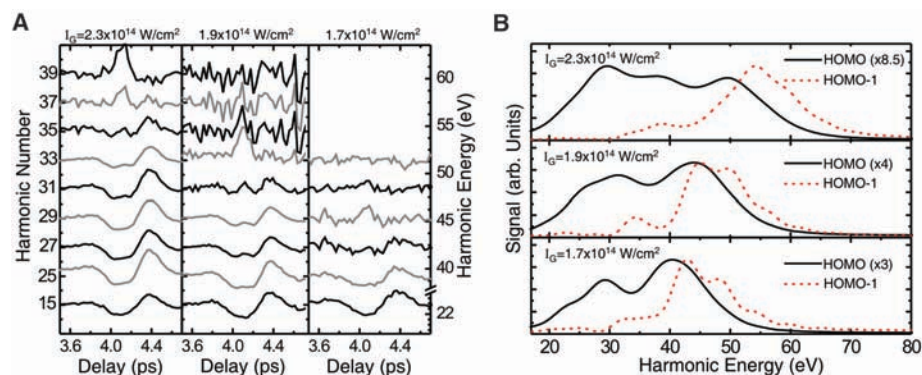


**Fig. 3.** (A) Experimental harmonic signals for three different generation intensities  $I_G$ . The signals are normalized to the harmonic signal of an isotropic ensemble. Therefore, the weak signals in the cutoff are magnified. The cutoffs are located at harmonics 39, 35, and 31 for the three intensities shown. For harmonic 15, a minimum at 4.1 ps is followed by a maximum at 4.4 ps. At higher harmonics, a peak grows out of the minimum at 4.1 ps because of ionization from and recombination to the HOMO-1 (see text). (B) Simulations of the experimental harmonic spectral envelope for the three different generation intensities of (A), considering only the recombination step. We performed the simulations for the prolate molecular distribution used in the experiment. The HOMO-1 spectrum (red dashed curves) has a larger amplitude than that of the HOMO (black curves) in the cutoff region. The HOMO HHG signal is scaled by the factors shown in the figure.

the HHG spectrum (14, 21–23). This is the primary reason for the relative enhancement of the HOMO-1 component of the HHG signal in our experiment. The model in (21) applied to the antisymmetric HOMO-1 predicts an HHG enhancement for the condition  $\Delta = \lambda_{dB}/2$ , where  $\Delta$  is the separation between the two antinodes in the wave function along the direction of the returning electron  $\mathbf{k}$ -vector. For a prolate molecular distribution, the prominent direction is  $\alpha = 90^\circ$ , which results in  $\Delta = 1.74$  bohr. The electron recombines, releasing a photon whose energy is equal to the sum of the electron kinetic energy and the ionization potential, and so this  $\lambda_{dB}$  of 3.48 bohr leads to a maximum at 60 eV in the emitted spectrum. For molecules with smaller  $\alpha$ , which are also present in the prolate distribution,  $\Delta$  becomes larger. This results in a shift of the constructive interference to larger  $\lambda_{dB}$  and smaller photon energies. Therefore, we expect a strong contribution from the HOMO-1 in the energy range around and below 60 eV, as seen in Fig. 3B. The cutoff for our intensities lies in this energy range, and we observe an agreement between the calculation and the data in Fig. 3. The full width at half maximum of the HOMO-1 spectrum in the constructive interference region is 20 eV for the highest  $I_G$  and about 10 eV for

the lowest  $I_G$ . This trend agrees with the experiment: The HOMO-1 feature is prominent from harmonic 25 to harmonic 39, corresponding to a width of 22 eV for the highest  $I_G$ ; for the lowest  $I_G$ , the peak appears from harmonic 25 to harmonic 31, corresponding to a width of 9 eV.

**Note added in proof:** We expect that the multiorbital contributions in HHG are general, which is supported by recent conference reports on HHG in  $\text{CO}_2$  (24, 25).

#### References and Notes

1. J. Itatani *et al.*, *Nature* **432**, 867 (2004).
2. P. B. Corkum, *Phys. Rev. Lett.* **71**, 1994 (1993).
3. K. C. Kulander, K. J. Schafer, J. L. Krause, *Laser Phys.* **3**, 359 (1993).
4. H. Stapelfeldt, T. Seideman, *Rev. Mod. Phys.* **75**, 543 (2003).
5. Th. F. Gallagher, *Rydberg Atoms* (Cambridge Univ. Press, Cambridge, 1994).
6. X. M. Tong, Z. X. Zhao, C. D. Lin, *Phys. Rev. A* **66**, 033402 (2002).
7. M. J. Frisch *et al.*, Gaussian 03, Revision C.02 (Gaussian Inc., Wallingford, CT, 2004).
8. V. I. Usachenko, S. I. Chu, *Phys. Rev. A* **71**, 063410 (2005).
9. M. Spanner, O. Smirnova, P. B. Corkum, M. Y. Ivanov, *J. Phys. B* **37**, L243 (2004).
10. J. Levesque *et al.*, *Phys. Rev. Lett.* **99**, 243001 (2007).
11. P. Balcou, P. Salières, A. L'Huillier, M. Lewenstein, *Phys. Rev. A* **55**, 3204 (1997).
12. S. Ramakrishna, T. Seideman, *Phys. Rev. Lett.* **99**, 113901 (2007).

13. P. Salières, A. L'Huillier, M. Lewenstein, *Phys. Rev. Lett.* **74**, 3776 (1995).
14. X. Zhou *et al.*, *Phys. Rev. Lett.* **100**, 073902 (2008).
15. A. T. Le, X.-M. Tong, C. D. Lin, *Phys. Rev. A* **73**, 041402 (2006).
16. P. Liu *et al.*, *Phys. Rev. A* **78**, 015802 (2008).
17. M. Gühr, B. K. McFarland, J. P. Farrell, P. H. Bucksbaum, *J. Phys. B* **40**, 3745 (2007).
18. J. Ortigoso, M. Rodríguez, M. Gupta, B. Friedrich, *J. Chem. Phys.* **110**, 3870 (1999).
19. J. Levesque, D. Zeidler, J. P. Marangos, P. B. Corkum, D. M. Villeneuve, *Phys. Rev. Lett.* **98**, 183903 (2007).
20. D. Pavičić, K. F. Lee, D. M. Rayner, P. B. Corkum, D. M. Villeneuve, *Phys. Rev. Lett.* **98**, 243001 (2007).
21. M. Lein, N. Hay, R. Velotta, J. P. Marangos, P. L. Knight, *Phys. Rev. A* **66**, 023805 (2002).
22. T. Kanai, S. Minemoto, H. Sakai, *Nature* **435**, 470 (2005).
23. C. Vozzi *et al.*, *Phys. Rev. Lett.* **95**, 153902 (2005).
24. O. Smirnova *et al.*, in *11th International Conference on Multiphoton Processes*, J. Anton *et al.*, Eds. (MPI für Kernphysik, Heidelberg, 2008), p. 7.
25. Y. Mairesse *et al.*, in *11th International Conference on Multiphoton Processes*, J. Anton *et al.*, Eds. (MPI für Kernphysik, Heidelberg, 2008), p. Fr62.
26. We thank H. Merdji and O. Smirnova for insightful discussions. Supported by the U.S. Department of Energy Division of Basic Energy Sciences through the Stanford Linear Accelerator Center, and by a Humboldt Foundation fellowship (M.G.).

7 July 2008; accepted 16 September 2008

Published online 30 October 2008;

10.1126/science.1162780

Include this information when citing this paper.

## Radar Sounding Evidence for Buried Glaciers in the Southern Mid-Latitudes of Mars

John W. Holt,<sup>1\*</sup> Ali Safaeinili,<sup>2</sup> Jeffrey J. Plaut,<sup>2</sup> James W. Head,<sup>3</sup> Roger J. Phillips,<sup>4</sup> Roberto Seu,<sup>5</sup> Scott D. Kempf,<sup>1</sup> Prateek Choudhary,<sup>1</sup> Duncan A. Young,<sup>1</sup> Nathaniel E. Putzig,<sup>4</sup> Daniela Biccari,<sup>5</sup> Yonggyu Gim<sup>2</sup>

Lobate features abutting massifs and escarpments in the middle latitudes of Mars have been recognized in images for decades, but their true nature has been controversial, with hypotheses of origin such as ice-lubricated debris flows or glaciers covered by a layer of surface debris. These models imply an ice content ranging from minor and interstitial to massive and relatively pure. Soundings of these deposits in the eastern Hellas region by the Shallow Radar on the Mars Reconnaissance Orbiter reveal radar properties entirely consistent with massive water ice, supporting the debris-covered glacier hypothesis. The results imply that these glaciers formed in a previous climate conducive to glaciation at middle latitudes. Such features may collectively represent the most extensive nonpolar ice yet recognized on Mars.

In equatorial regions of Mars, steep slopes (e.g., massifs and channel walls) typically exhibit talus fans and cones at their bases. In the martian mid-latitudes, however, many massifs are instead accompanied by broad, lobate aprons extending up to ~20 km away from their bases (1). They are characterized by gently sloping surfaces with convex-upward margins, relatively steep outer edges, and both radial and concentric ridge-and-furrow lineations (2); these features all indicate flow of a viscous material. Such “lobate debris aprons” (LDAs) occur in the 30° to 60° latitude belts in both hemispheres

(Fig. 1A), concentrated in the north along the topographic dichotomy and in the south around massifs on the rims of the Hellas and Argyre basins (2). These latitudinal bands correlate with the shallow-subsurface stability field for water ice (i.e., ice could exist just below the surface but would sublimate at the surface) (3, 4). Additionally, the flow-like morphology of the lobes suggests the presence of a viscosity-lowering agent such as ice (2, 4).

Opinions differ, however, on the origin and amount of such ice and its mode of emplacement. Some propose that ancient ground ice was mo-

bilized during LDA formation (5); others suggest that frost deposited from the atmosphere diffused into pore spaces (2), lubricating the debris deposits derived from nearby steep slopes and forming something akin to terrestrial rock glaciers (6). Different approaches have been used to estimate the amount of ice within LDAs. At a minimum, ice volumes on the order of ~10 to 15% are required to mobilize talus (2). However, surface pitting and structures suggest that the ice content is more than 50% for some LDAs (7). This estimate is also consistent with those based on detailed topographic profiles (8, 9) and rheological arguments (10). Some terrestrial analogs (11–13) suggest that LDAs might be debris-covered glaciers, essentially pure glacial ice below a protective layer of debris. Superposed rimless craters with broad central peaks and moat-shaped borders indicate formation on an ice-rich substrate (14). However, the presence of massive ice (or very ice-rich mixtures) is impossible to confirm or reject on the basis of optical imagery or surface morphology alone.

We used the Shallow Radar (SHARAD) (15) on the Mars Reconnaissance Orbiter (MRO) to probe the internal structure of several LDAs sur-

<sup>1</sup>Institute for Geophysics, Jackson School of Geosciences, University of Texas, Austin, TX 78758, USA. <sup>2</sup>Jet Propulsion Laboratory, California Institute of Technology, Pasadena, CA 91109, USA. <sup>3</sup>Department of Geological Sciences, Brown University, Box 1846, Providence, RI 02912, USA. <sup>4</sup>Southwest Research Institute, Boulder, CO 80302, USA. <sup>5</sup>INFOCOM Research, University of Rome “La Sapienza,” 00184 Rome, Italy.

\*To whom correspondence should be addressed. E-mail: jack@ig.utexas.edu



rounding massifs on the eastern rim of the Hellas impact basin (Fig. 1) where more than 90 LDA complexes flank steep topography (2, 6, 16). The southernmost LDA we studied (LDA-2, Fig. 1B) has multiple lobes that coalesce to form a continuous deposit extending more than 20 km outward from a massif along ~170 km of its margins. Surface features indicating viscous flow are numerous, including both longitudinal and transverse lineations (16) (Fig. 2).

Radar waves penetrate the surface and pass through materials that do not severely attenuate or scatter them. Reflections arise from interfaces with dielectric contrasts. SHARAD has penetrated the ~2-km-thick polar layered deposits in both the north and south, detecting many internal reflectors (17, 18). Smaller targets can be more challenging because SHARAD's antenna pattern is broad, resulting in surface reflections up to a few tens of kilometers away from the suborbital point in rugged areas, versus only a few kilometers in smooth, flat areas. These off-nadir echoes can appear at time delays similar to those arising from subsurface interfaces, so steps are required to avoid misinterpreting this surface clutter as subsurface echoes. Synthetic-aperture data pro-

cessing is used to improve along-track resolution to ~300 m, greatly reducing along-track clutter and focusing the surface and subsurface features. We used the known topography of the surface and the radar geometry to model cross-track clutter together with nadir surface echoes (see supporting online text). Comparisons of radar sounding data with these synthetic surface echoes and the examination of possible surface echo sources in imagery (19) were undertaken for all cases shown here; such a procedure is a necessary part of radar sounding data interpretation in high-relief environments.

Examination of radar data from SHARAD orbit 6830 where it crosses multiple LDAs in the eastern Hellas region (a-a', Fig. 1B) shows that the only radar reflections not matching simulated surface echoes occur where the spacecraft passes over each LDA (Fig. 3, A and B); therefore, these echoes are interpreted as arising from within or beneath the LDAs. In one case (LDA-2A), surface clutter is predicted near the terminus of the LDA, where it may obscure portions of a subsurface reflector that clearly extends farther inward below the LDA. LDA-2A and LDA-2B show evidence for multiple, closely spaced sub-

surface reflectors indicating the presence of at least one thin (~70 m assuming a water-ice composition), distinct deposit below thicker deposits (up to 800 m).

Another criterion for the interpretation of subsurface echoes is consistency between multiple tracks. Orbit 7219 (Fig. 1B, b-b') crosses LDA-2A and LDA-2B near orbit 6830 (Fig. 1B, a-a') but at a different angle. The secondary echoes in orbit 7219 (Fig. 4, A to C) are nearly identical to those observed for orbit 6830 (Fig. 3, right side). The nearby crossing of LDA-2C by orbit 3672 (Fig. 1B, c-c') shows overall consistency across different lobes of this LDA complex while exhibiting slightly varying details of the subsurface. LDA-2C is characterized by what appears to be a more extensive basal deposit relative to LDA-2B. This was observed in additional nearby crossings.

SHARAD is capable of resolving reflections separated by ~0.1  $\mu$ s in time (i.e., ~10 m in ice or ~5 m in rock), yet there are no indications of structure within the LDAs apart from thin deposits near the base. Hints of potential internal reflectors within the LDAs can all be correlated with surface clutter in the simulated data (e.g., LDA-1 and LDA-2B; Fig. 3). There is also an apparent lack of volume scattering (i.e., radar reflectors dispersed throughout the material) at SHARAD frequencies. Although some dispersed energy follows LDA surface echoes, we attribute this to small-scale surface roughness such as that visible in imagery (Fig. 2), as it is not noticeably different in the radar data from nearby LDA-free

**Fig. 1. (A)** Topography of Mars (24). Major features are identified, and latitude bands exhibiting lobate debris aprons (LDAs) and lineated valley fill are highlighted (1, 2). The location of our study area along the eastern rim of the Hellas impact basin is also denoted. **(B)** Topography of study area, with MRO/SHARAD ground tracks shown for orbits 6830 (a-a'), 7219 (b-b'), and 3672 (c-c'). LDAs crossed by these tracks are labeled.

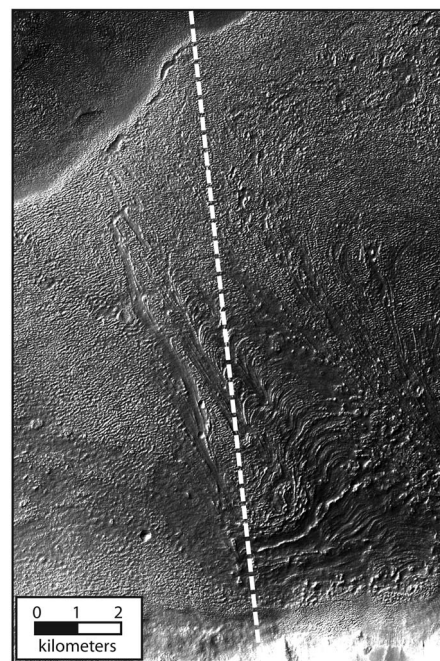
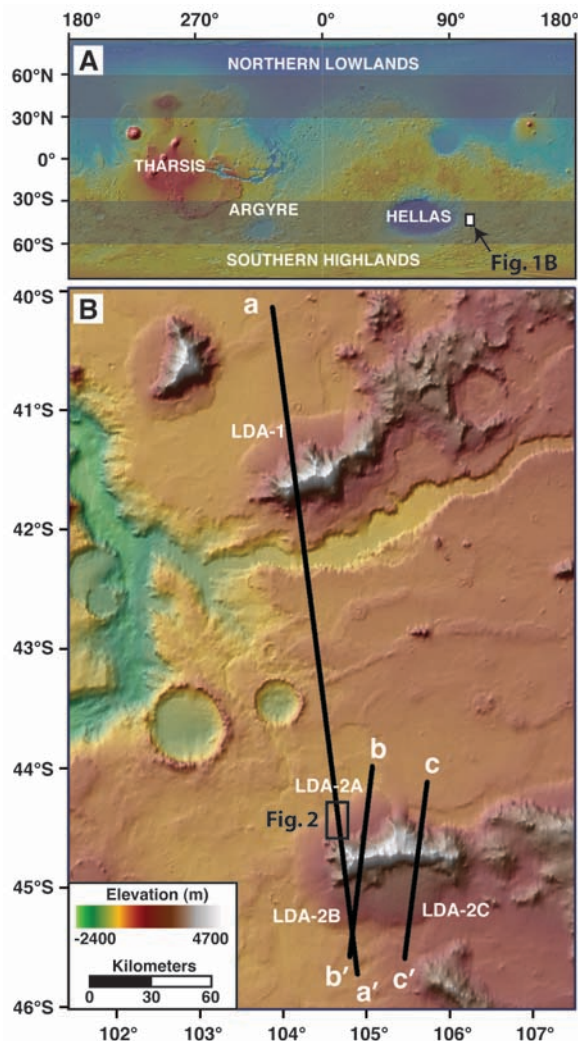


**Fig. 2.** Image showing surface of LDA-2A where it is crossed by orbit 6830 (see Fig. 1B for location). Textures visible include transverse and longitudinal ridge-and-furrow lineations indicative of viscous flow. [From MRO Context Camera image P01\_002294\_1349]

areas (Fig. 1 and Fig. 3B) and is supported by simulations (Fig. 3A and Fig. 4, A and D). These properties of the radar data indicate that (i) the material is largely homogeneous, and (ii) it lacks a significant fraction of large (i.e., several meters across or larger) rock fragments. Both characteristics support the debris-covered glacier hypothesis.

A further constraint on composition comes from the measured loss of radar energy through the material. We measured the correlation between the strength of the subsurface echo and the delay between the upper and lower echo (or, equivalently, the thickness of the medium). It is expected that there will be a proportional drop in the subsurface echo strength as the depth to the bed increases. The radar attenuation had an upper bound of  $\sim 10$  dB/km (fig. S1). This is consistent

with radar attenuation by relatively pure water ice, rather than by a rock-dominated composition (20), and is supported by Mars-analog laboratory studies of water-ice mixtures with basaltic dust indicating that a dust fraction higher than 10% is unlikely for losses of this magnitude (21).

As a check on this interpretation, we used the velocity of electromagnetic waves in water ice (real dielectric constant of 3.2) to convert the time-delay data into depth. The resulting basal geometries (Fig. 3C and Fig. 4, C and F) show a lower interface that smoothly continues the general trend of the nearby surface, with a slight slope in some cases (up to  $1.5^\circ$ ) toward the adjacent massif. Some increased slope relative to the surroundings is consistent with the proximal buildup of colluvium from high topography before the

deposition of the ice-rich material, or a sublimation lag from an older ice-rich deposit. The combination of a low radar attenuation and an implied water-ice radar velocity is similar to the findings for the polar layered deposits by the Mars Advanced Radar for Subsurface and Ionospheric Sounding (MARSIS) radar sounder on the Mars Express orbiter (22, 23). As in those cases, our results point to a composition dominated by ice with perhaps a small fraction of dust or rock, rather than typical rock-dominated deposits or rock-ice mixtures with a roughly equal distribution.

All of these radar-based observations indicate that LDAs consist of massive ice covered by a relatively thin debris layer. The thickness of the surface debris layer cannot be observed because the vertical resolution of the radar is too limited

**Fig. 3.** Results for SHARAD orbit 6830 (line a-a' in Fig. 1B). (A) Simulated surface echoes (clutter) in one-way travel time. (B) SHARAD data in one-way travel time. Vertical arrows identify echoes not consistent with surface clutter simulation and also confirmed in adjacent tracks. These echoes are interpreted to result from the subsurface. Radar returns are weak to nonexistent over steep massif slopes because of the scattering of energy away from the spacecraft. (C) Radar data converted to depth assuming a water-ice composition. All echoes appearing after the surface echo have new positions in this representation, including clutter.

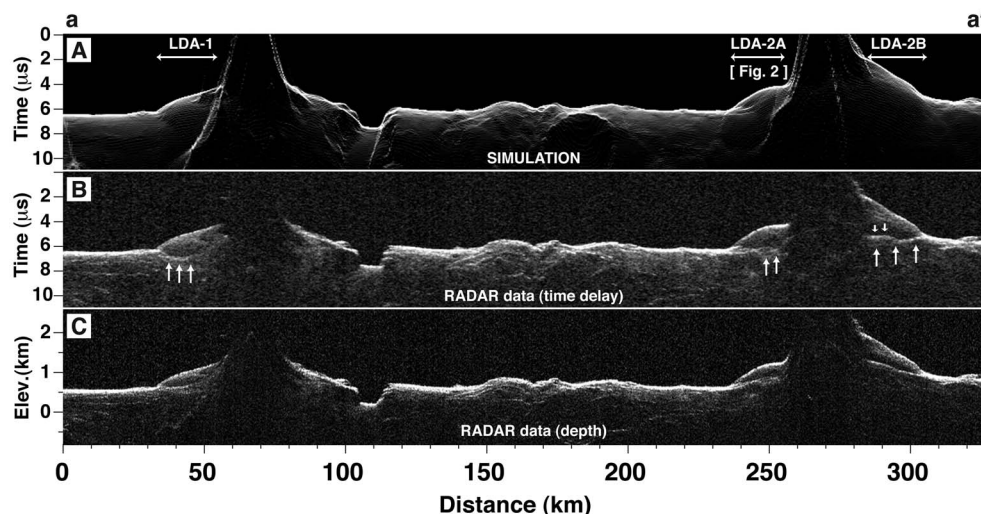
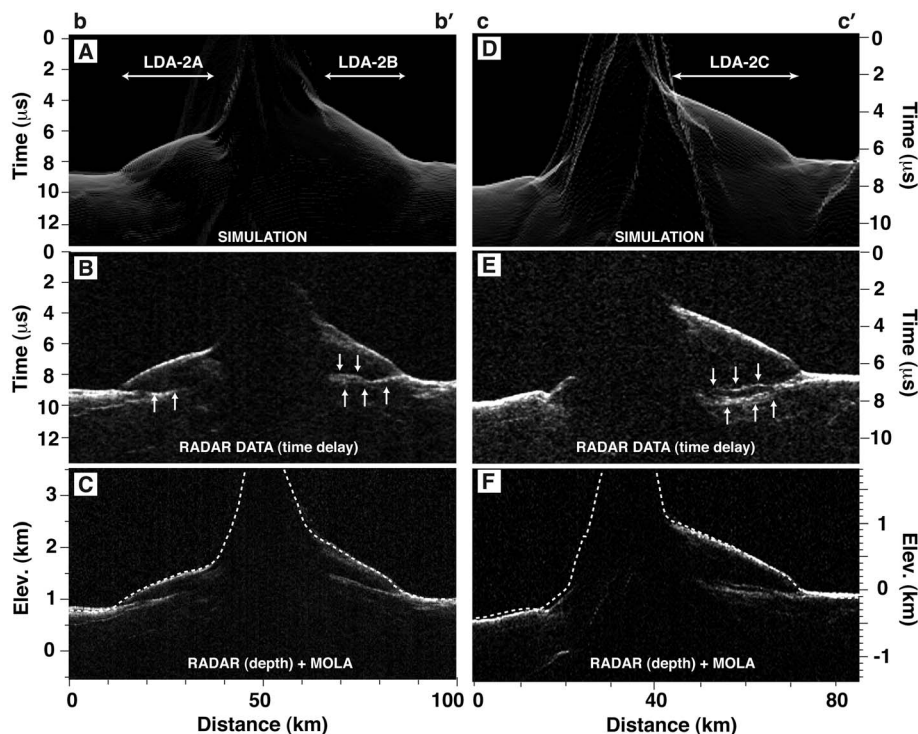


**Fig. 4.** Results for SHARAD orbits 7219 (left) and 3672 (right). Locations are indicated as b-b' and c-c' (Fig. 1B), respectively. (A and D) Simulated surface clutter. (B and E) SHARAD data with interpreted subsurface echoes denoted by vertical arrows. Both simulated and real data are shown in one-way travel time. (C and F) Radar data converted to depth using a wave velocity in water ice, with Mars Orbiter Laser Altimeter-derived surface elevations (24) superimposed (dashed white line). Note multiple reflectors near the base of LDA-2B and LDA-2C, confirmed by additional adjacent orbits, indicating thin basal deposits.





or the lower interface is too gradual to produce a detectable reflection. For the former case, we estimate the layer to be <10 m thick. The reflectors seen near the base of some deposits (Fig. 3B and Fig. 4, B and E) may be the result of thin layers of ice covered with debris similar to that seen at the upper surface.

With sufficient coverage, it will be possible to derive accurate regional estimates of total ice volume. On the basis of our findings and previous volume estimates from surface morphology (6), there may be up to ~28,000 km<sup>3</sup> of water ice sequestered in the eastern Hellas LDAs alone. This is ~1% of the total water volume contained in the polar caps (24) and is equivalent to a global water layer ~20 cm thick. For comparison, a much younger, meters-thick surface-mantling layer over much of the 30° to 60° latitude bands may contain an approximately equivalent volume of water in the form of interstitial ground ice (25). Subtle morphological differences observed among LDAs may be due to variations in ice content (9), and although the extension of radar studies to more LDAs is required to fully evaluate their potential range of compositions, preliminary results from Deuteronilus Mensae in the northern hemisphere corroborate our findings for eastern Hellas (26). Collectively, LDAs may therefore represent the largest reservoir of nonpolar water ice recognized on Mars.

Why would such large quantities of snow and ice accumulate in the eastern Hellas region in particular? Over time scales of millions of years, Mars undergoes large changes in spin-axis obliquity (27), forcing changes in insolation, and hence in climate (28) and the subsequent distribution of ice (29). Climate simulations (30) performed with a model that includes the current water cycle but

assumes an obliquity of 45° predict snow accumulation in the eastern Hellas region from a south polar water source that operates efficiently at the southern summer solstice, when the southern polar cap releases large amounts of water vapor. This vapor moves northward and is deflected by cold air moving southward from the Hellas basin; the subsequent cooling causes strong condensation and precipitation in the area of the LDAs (30), which we have shown to contain primarily water ice. We therefore conclude that these deposits harbor large quantities of water ice derived from high-obliquity epochs, now concealed beneath a thin protective layer. This ice survives from climatic conditions markedly different from today's and is potentially accessible to future landed missions, not only for scientific study but as a resource to support exploration.

#### References and Notes

- M. H. Carr, G. G. Schaber, *J. Geophys. Res.* **82**, 4039 (1977).
- S. W. Squyres, *J. Geophys. Res.* **84**, 8087 (1979).
- F. P. Fanale, J. R. Salvail, A. P. Zent, S. E. Postawko, *Icarus* **67**, 1 (1986).
- M. H. Carr, *Water on Mars* (Oxford Univ. Press, New York, 1996).
- B. K. Lucchitta, *J. Geophys. Res.* **89**, B409 (1984).
- T. L. Pierce, D. A. Crown, *Icarus* **163**, 46 (2003).
- J. W. Head *et al.*, *Nature* **434**, 346 (2005).
- A. Colaprete, B. M. Jakosky, *J. Geophys. Res.* **103**, 5897 (1998).
- H. Li, M. S. Robinson, D. M. Jurdy, *Icarus* **176**, 382 (2005).
- N. Mangold, P. Allemand, *Geophys. Res. Lett.* **28**, 407 (2001).
- J. W. Head *et al.*, *Earth Planet. Sci. Lett.* **241**, 663 (2006).
- D. R. Marchant, J. W. Head III, *Icarus* **192**, 187 (2007).
- J. W. Head, A. L. Nahm, D. R. Marchant, G. Neukum, *Geophys. Res. Lett.* **33**, L08503 (2006).
- A. M. Kress, J. W. Head III, D. R. Marchant, *Lunar Planet. Sci. Conf.* **39**, 1293 (2008).
- R. Seu *et al.*, *J. Geophys. Res.* **112**, E05505 (2007).
- S. C. Mest, D. A. Crown, *Icarus* **153**, 89 (2001).
- R. Seu *et al.*, *Science* **317**, 1715 (2007).
- R. J. Phillips *et al.*, *Science* **320**, 1182 (2008); published online 13 May 2008 (10.1126/science.1157546).
- J. W. Holt *et al.*, *J. Geophys. Res.* **111**, E06524 (2006).
- P. Gudmundsen, in *Electromagnetic Probing in Geophysics*, J. R. Wait, Ed. (Golem, Boulder, CO, 1971), pp. 329–333.
- E. Heggy *et al.*, *Lunar Planet. Sci. Conf.* **38**, 1756 (2007).
- G. Picardi *et al.*, *Science* **310**, 1925 (2005); published online 29 November 2005 (10.1126/science.1122165).
- J. J. Plaut *et al.*, *Science* **316**, 92 (2007); published online 14 March 2007 (10.1126/science.1139672).
- D. E. Smith *et al.*, *J. Geophys. Res.* **106**, 23689 (2001).
- J. F. Mustard, C. D. Cooper, M. K. Rifkin, *Nature* **412**, 411 (2001).
- J. J. Plaut *et al.*, *Lunar Planet. Sci. Conf.* **39**, 2290 (2008).
- J. Laskar, P. Robutel, *Nature* **361**, 608 (1993).
- J. Laskar *et al.*, *Icarus* **170**, 343 (2004).
- J. W. Head *et al.*, *Nature* **426**, 797 (2003).
- F. Forget, R. M. Haberle, F. Montmessin, B. Levrard, J. W. Head, *Science* **311**, 368 (2006).
- We thank F. Russo, M. Cutigni, O. Fuga, and E. Giacomoni of the SHARAD Operations Center for their role in acquiring the data over these targets; F. Bernardini for his assistance in the U.S. data processing effort; and two anonymous reviewers for their comments and suggestions. Work at the University of Texas was supported by the Institute for Geophysics of the Jackson School of Geosciences and NASA grant NAG5-12693 (J.W.H.). MRO is operated for NASA by Caltech's Jet Propulsion Laboratory. SHARAD was provided to MRO by the Italian Space Agency through a contract with Thales Alenia Space Italia and is operated by the INFOCOM Department, University of Rome. This is UTIG contribution 2006.

#### Supporting Online Material

www.sciencemag.org/cgi/content/full/322/5905/1235/DC1

SOM Text

Fig. S1

References

5 August 2008; accepted 3 October 2008

10.1126/science.1164246

## Variation in Evolutionary Patterns Across the Geographic Range of a Fossil Bivalve

Melissa Grey,<sup>1\*</sup> James W. Haggart,<sup>2,1</sup> Paul L. Smith<sup>1</sup>

The fossil record is the only direct source of data for studying modes (patterns) and rates of morphological change over long periods of time. Determining modes and rates is important for understanding macroevolutionary processes, but just how modes and rates vary within a taxon, and why, remain largely unaddressed. We examined patterns of morphological change in the shell of the Mesozoic marine bivalve genus *Buchia* over its geographic and temporal range. Most modes conformed to either random walks or stasis, and both modes and rates showed variability between locations. For example, stasis was more common in deeper marine environments, whereas random walks occurred more often at the highest paleolatitudes studied. These results indicate that the environment can play an important role in shaping patterns of evolution.

**D**ocumenting patterns of morphological change (modes) and the speed at which they occur (rates) are fundamental to our understanding of macroevolutionary processes

over geologic time. The fossil record has provided examples of three principal modes of evolution, namely: random walks; directional change (gradualism); and stasis, which is often interrupted by

punctuated change. The ability to quantify rates and classify modes of evolution in the fossil record has improved over recent decades with the advent of quantitative model-based tests [e.g., (1–4)]. However, it remains virtually unknown whether modes and rates of evolution vary within a taxon, but this is difficult to assess because it requires large samples spanning both the geographic and temporal range of the taxon. *Buchia*, a marine bivalve distantly related to mussels, meets these requirements. The genus existed for ~25 million years, arising during the early Late Jurassic (155.6 million years ago) and becoming extinct in the Early Cretaceous (130.0 million years ago) (5), and includes numerous species that lived in a variety of sedimentary environments across the Northern Hemisphere (figs. S1 and S2). Most *Buchia* species are cosmopolitan

<sup>1</sup>Department of Earth and Ocean Sciences, University of British Columbia, Vancouver, British Columbia V6T 1Z4, Canada.

<sup>2</sup>Geological Survey of Canada, 625 Robson Street, Vancouver, British Columbia V6B 5J3, Canada.

\*To whom correspondence should be addressed. E-mail: mgrey@eos.ubc.ca

and their dispersal was geologically instantaneous; the genus is thus particularly useful for the study of evolutionary patterns. These features also contribute to the value and importance of *Buchia* species as time-diagnostic index fossils for biostratigraphic correlations in the Northern Hemisphere [e.g., (5–8)].

Of the three principal modes of evolution, random walks are nondirectional over time, oscillating around a mean morphology (2). A random-walk pattern does not imply that the role of evolutionary processes, such as natural selection, is negligible for a particular taxon, only that sustained directionality or stasis is not observed (2). When observed in the fossil record, directional changes usually imply that evolution is gradual (2). Punctuations can also be directional, but because they take place over geologically rapid time periods (e.g., thousands to millions of years), they are less likely to be preserved in the fossil record [but see (9) for examples of punctuations]. There is no widely accepted definition of stasis, although it is often described as representing either a constrained change (1) or no net change (10). A recent survey of more than 100 fossil sequences comprising a variety of taxa, all analyzed by the same method for determining mode, has shown that directional evolution is rare and/or brief and most fossil lineages exhibit evolutionary patterns that conform to random walks or stasis (11). It remains unclear, however, whether evolutionary patterns differ within the history and geographic range of a taxon. To examine this issue, we studied evolutionary modes and rates over much of *Buchia*'s temporal and geographic range.

Fossil material used for this study was obtained from previously published and temporally well-resolved stratigraphic sections [supporting online material (SOM)] (12). We observed morphological change in the shape and size of buchiid shells over time by measuring six traits, defined by linear and angular measurements (fig. S3), on more than 1500 shells whose relative geologic ages were known. The traits measured have been used in other buchiid studies to differentiate between species (13). Fossil specimens were taken from previously collected and published material from six locations, including the Canadian Arctic; Grassy Island and Taseko Lakes, British Columbia, Canada; eastern Heilongjiang Province, China; East Greenland; and Southern Primorye, Far East Russia (12). Study locations are essentially coeval (fig. S2), represent a reflective sample of the geographical range of *Buchia* (paleolatitudes ranged from 47° to 81°N; Table 1 and fig. S1), and span much of the genus's temporal range (fig. S2), within which a number of ancestor-descendant relationships have been proposed (5) (SOM). The locations also represent a variety of marine depositional environments, from shallow-water, inner-shelf settings to deep-water deposits (Table 1 and table S1).

The data used to determine mode of evolution include the six individual morphological traits and the primary and secondary canonical variates from

canonical variate analyses (14). These canonical variates (CV1 and CV2, respectively) are a linear combination of the measured traits and represent the most important variables for morphological distinction of buchiid specimens through time (i.e., they are the traits that exhibit the most change) (Fig. 1 and Table 1). We explored evolutionary mode using two quantitative methods: the program Enigma 2.4 (1, 12) uses a random walk model for a stratophenetic series and the program PaleoTS (2, 12) uses a likelihood-based procedure that chooses among models of different modes. The random walk method calculates Hurst estimates ( $h$ ) and  $P$  values. Hurst estimates range from 0 to 1, where high values of  $h$  (i.e.,  $h > 0.9$ ) indicate strong directional change, and low values indicate stasis ( $h < 0.2$ ) or random walks ( $0.25 < h < 0.55$ ) (1, 12).  $P$  values indicate the probability of a random walk; low  $P$  values ( $P < 0.5$ ) suggest a small probability that the pattern was generated by a random process, whereas high  $P$  values ( $P \geq 0.9$ ) indicate random walks or stasis (1, 12). The likelihood-based procedure chooses the best fit of the data among three models: directional, unbiased random walk, and stasis. Support for the models was assessed with two metrics, Akaike information criterion ( $AIC_C$ ) and Akaike weights; the model with the lowest  $AIC_C$  and highest Akaike weight is the best supported (2, 12). Results in Fig. 1 and Table 1 illustrate the need for using quantitative versus qualitative classification of evolutionary mode because visual inspection of data plots cannot always distinguish the patterns that can be delineated with model-based tests [(1) and figure 1, A to C, of (2)].

Results from both mode tests were equivalent and show that the mode of evolution varied between locations (Table 1 and table S2, A to F). For the six locations studied, we found that stasis occurs more often in deeper-water environments and random walks occur more often at the highest paleolatitudes (Table 1). For ease of display, we provide results from both mode tests only for the primary canonical variable [CV1, from the canonical variate analysis (14)] (Table 1), and results for the other morphological traits are shown from the likelihood-based tests (table S2, A to F). For CV1, five of the six locations show either stasis or random walks, with only one identified case of directionality (Table 1). Hurst estimates (fig. S4, A to D) indicate weak directionality for Grassy Island ( $h = 0.7$ ,  $P = 0.4$ ) (fig. S4B), stasis for Greenland (average  $h = 0.14$ , average  $P = 0.99$ ) (fig. S4D), and random walks for both the Arctic (average  $h = 0.2$ , average  $P = 0.91$ ) (fig. S4A) and Taseko Lakes (average  $h = 0.33$ , average  $P = 0.85$ ) (fig. S4C) locations. The likelihood tests supported all of these findings (table S2, A to C and E). The mode for the localities in China and Russia could not be assessed reliably with Hurst estimates due to low numbers of stratigraphic intervals (1) (table S1); however, the number of samples was not an issue for the likelihood-based test, which supports stasis and random modes, respectively (table S2, D and F). All other traits studied, including the secondary canonical variable (CV2) and the six individual traits, show similar results in their distribution of modes. Out of 42 mode tests with the likelihood-based procedure, only 5% were directional, whereas 43% con-

**Table 1.** Modes and rates for all geographical locations studied for the primary canonical variate (CV1).

Location	Paleolatitude (°N)	Depositional marine environment (from primary reference, table S1)	Mode from Hurst estimate and maximum likelihood	Average rate	CV1 Components*
Arctic Canada	81	Shallow	Random walk	$1.8 \times 10^{-5}$	Dorsal angle, ventral angle (57%)
Grassy Island, BC	49 <sup>†</sup>	Shallow	Weakly directional	$2.2 \times 10^{-5}$	Dorsal angle, ventral angle (67%)
Taseko Lakes, BC	51 <sup>†</sup>	Shallow	Random walk	$7.3 \times 10^{-5}$	Dorsal angle, ventral angle (60%)
Eastern Heilongjiang, China	47 <sup>†</sup>	Deep	Stasis <sup>‡</sup>	$3.6 \times 10^{-5}$	Length (34%)
East Greenland	49.5	Deep, with some shallow-water deposits	Stasis	$1.8 \times 10^{-5}$	Dorsal angle (33%)
Southern Primorye, Far East Russia	71	Shallow	Random walk <sup>‡</sup>	$8.8 \times 10^{-7}$	Height, length (40%)

\*Refer to fig. S3 for a description of traits measured and (12, 14) for canonical variate procedure. <sup>†</sup>The paleolatitudes for China, Grassy Island, and Taseko Lakes are approximate because there is no consensus on the geographic position of these areas in the Late Jurassic–Early Cretaceous. <sup>‡</sup>The mode for these localities could not be assessed with Hurst estimates (12).



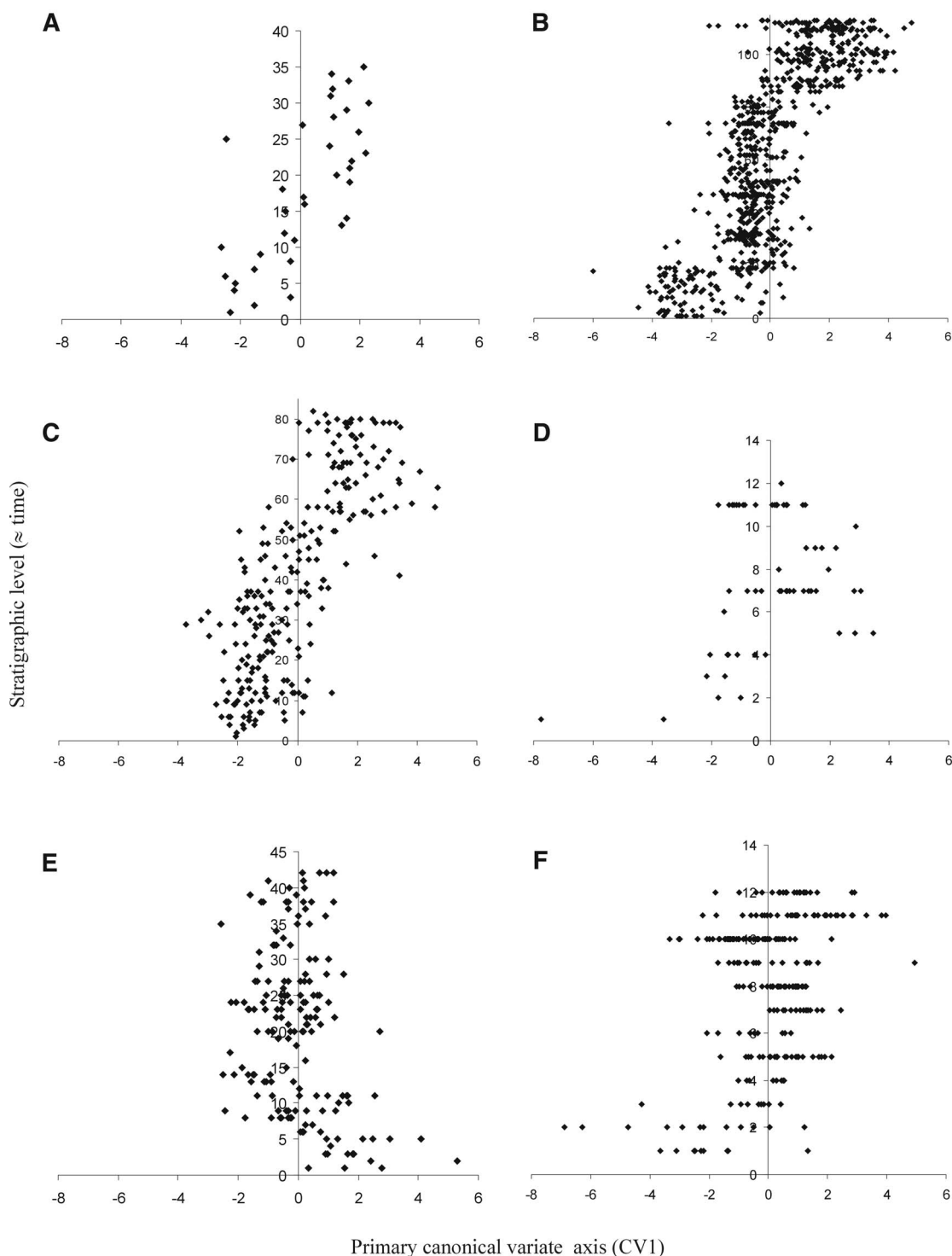
formed to stasis and 52% to random walks (table S2, A to F). These frequencies are similar to those reported in a recent survey that examined a variety of macro- and microfossil lineages and traits (11).

Research addressing the distribution and variability of evolutionary rates during a species' existence is critical for exploring the relation between mode and rate (15). A variety of metrics are used to calculate rates. The common Darwin metric has an inverse relation with time (16), meaning that

neontological studies will inherently have higher rates because they sample a much shorter period of time [e.g., (17)]. We used a method based on trait variances and generation time (time needed to complete one generation) to minimize any dependence on absolute time scales (3). Rates less than  $1 \times 10^{-4}$  represent stabilizing selection; those less than  $5 \times 10^{-2}$  represent genetic drift; and rates greater than  $5 \times 10^{-2}$  are indicative of directional selection (3).

The average rates for all geographical locations range from  $8.8 \times 10^{-7}$  to  $1.8 \times 10^{-5}$  (Table 1). All rates for all locations range from  $9 \times 10^{-9}$  to  $1.2 \times 10^{-2}$  and most are in the realm of stabilizing selection, although some suggest the occurrence of genetic drift (fig. S5, A to F). There are no examples of rates above  $5 \times 10^{-2}$ , and therefore directional selection was not detected. The same method applied to fossil stickleback fish found that, despite other types of evidence supporting

**Fig. 1. (A to F)** Morphological change in the primary canonical axis (CV1) over relative time for each of the six locations studied: (A) Canadian Arctic; (B) Grassy Island, Canada; (C) Taseko Lakes, Canada; (D) eastern Heilongjiang Province, China; (E) East Greenland; and (F) Far East Russia (Southern Primorye). CV1 represents the linear combination of variables that best separates between stratigraphic intervals (i.e., shows the most change).



directional selection in the lineage, selection did not appear to affect the observed morphological changes, suggesting that this method is biased against finding evidence for directional change (18). For fossils, the number of generations between successive samples is generally so high that the amount of morphological change would have to be unrealistically high for directional selection to be detected with current methods.

Our research compared trends for the same taxon in different geographical locations and identified a possible environmental influence on evolutionary modes and rates. We found that the two current quantitative methods used for delineating evolutionary mode provide equivalent results but that the likelihood-based test can be more useful when comparing sequences with fewer time (stratigraphic) intervals. Our analysis demonstrates that, for the same suite of characters over similar time periods, all three modes of evolution (directional, random, and stasis) are found within the genus *Buchia* throughout its geographic range, indicating that there is an environmental component to mode. More specifically, we found that there may be a relation between mode and paleolatitude, because random evolutionary trajectories were all found at the highest paleolatitudes

(Table 1), but this must be confirmed by studying buchiids at a wider range of paleolatitudes. Our results also suggest that, in *Buchia*, stasis occurs more frequently in deep-water marine environments.

#### References and Notes

1. P. D. Roopnarine, *Paleobiology* **27**, 446 (2001).
2. G. Hunt, *Paleobiology* **32**, 578 (2006).
3. M. Lynch, *Am. Nat.* **136**, 727 (1990).
4. B. Hannisdal, *Paleobiology* **33**, 98 (2007).
5. J. A. Jeletzky, *Geol. Surv. Can. Bull.* **103** (1965).
6. J. Sha *et al.*, *Cretac. Res.* **24**, 715 (2003).
7. F. Surlyk, V. A. Zakharov, *Palaeontology* **25**, 727 (1982).
8. I. I. Sey, E. D. Kalacheva, *Palaeogeogr. Palaeoclimatol. Palaeoecol.* **150**, 49 (1999).
9. J. B. C. Jackson, A. H. Cheetham, *Trends Ecol. Evol.* **14**, 72 (1999).
10. H. D. Sheets, C. E. Mitchell, *Genetica* **112-113**, 105 (2001).
11. G. Hunt, *Proc. Natl. Acad. Sci. U.S.A.* **104**, 18404 (2007).
12. Materials and methods are available as supporting material on Science Online.
13. M. Grey, J. W. Haggart, P. L. Smith, *Palaeontology* **51**, 583 (2008).
14. Canonical variate analysis (CVA) determines which variables discriminate between groups of previously identified specimens and is also used for predictive classification. A priori grouping for the CVA was based on the stratigraphy (a proxy for time) of each specimen; this allowed changes in morphology to be tracked through relative time (e.g., a specimen found in a higher part of

the geologic section is geologically "younger" than one found in the lower part of the section).

15. P. D. Roopnarine, *Annu. Rev. Ecol. Syst.* **34**, 605 (2003).
16. P. D. Gingerich, *Science* **222**, 159 (1983).
17. D. N. Reznick, F. H. Shaw, H. Rodd, R. G. Shaw, *Science* **275**, 1934 (1997).
18. M. A. Bell, M. P. Travis, D. M. Blouw, *Paleobiology* **58**, 814 (2006).
19. Supported by a Natural Sciences and Engineering Research of Canada (NSERC) grant (to P.L.S.) and an NSERC PGS-A scholarship (to M.G.). We are grateful to P. Alsen, T. Bogdanova, A. Crame, J. S. Crampton, J. Dougherty, J. Grant-Mackie, D. A. T. Harper, D. Hikuroa, N. Hudson, E. Kalacheva, J. Rassmussen, J. Sha, I. Sey, and F. Surlyk for use of their collections and hospitality; to P.G. Lelièvre for creating the MatLab morphometrics program (MorphLab 1.0); and to G. Hunt and P. Roopnarine for help and program codes for analyzing mode. This manuscript was substantially improved by the comments and suggestions of three reviewers.

#### Supporting Online Material

www.sciencemag.org/cgi/content/full/1162046/DC1

Materials and Methods

SOM Text

Figs. S1 to S5

Tables S1 and S2

References

19 June 2008; accepted 14 October 2008

Published online 23 October 2008;

10.1126/science.1162046

Include this information when citing this paper.

## Selfish Genetic Elements Promote Polyandry in a Fly

T. A. R. Price,<sup>1</sup> D. J. Hodgson,<sup>1</sup> Z. Lewis,<sup>2</sup> G. D. D. Hurst,<sup>3</sup> N. Wedell<sup>1\*</sup>

It is unknown why females mate with multiple males when mating is frequently costly and a single copulation often provides enough sperm to fertilize all a female's eggs. One possibility is that remating increases the fitness of offspring, because fertilization success is biased toward the sperm of high-fitness males. We show that female *Drosophila pseudoobscura* evolved increased remating rates when exposed to the risk of mating with males carrying a deleterious sex ratio-distorting gene that also reduces sperm competitive ability. Because selfish genetic elements that reduce sperm competitive ability are generally associated with low genetic fitness, they may represent a common driver of the evolution of polyandry.

Why females of nearly all animals tend to mate with more than one male (polyandry) remains a pressing question for evolutionary biology (1, 2). However, the driving forces behind the origin and maintenance of polyandry are uncertain, because for many species, the costs of mating multiply often appear to outweigh the benefits (3–5). Polyandry may benefit females by increasing the fitness of their offspring (6, 7). For example, in polyandrous systems, females could remate with more attractive males, increasing their likelihood of

producing sons with higher mating success (8). Polyandry also allows females control over paternity through sperm competition [the competition for fertilization of ova that occurs between sperm from more than one male (2)]. If paternity is biased toward the sperm of males of higher viability, then a multiply mating female will on average have higher-fitness offspring than a monogamous female (7, 9). In crickets, for example, polyandrous females have a higher hatching success when they bias paternity against more closely related males (10). It is also possible that selfish genetic elements promote polyandry by creating a correlation between male fitness and sperm competitive ability (11, 12).

Selfish genetic elements spread through populations because they subvert normal patterns of inheritance in ways that increase their representation in the next generation, often at a cost to

the bearer. They are ubiquitous in living organisms, where they can make up a large part of the genome (11). Several selfish genetic elements, such as meiotic drive elements, B chromosomes, and endosymbionts, are associated with reduced male fertility, often due to direct manipulation of spermatogenesis (13), and female fitness is frequently reduced when females mate with males that carry these elements (11). Where males harboring such selfish genes suffer reduced paternity in sperm competition, theory predicts that this will favor increased polyandry in females, because remating will reduce exposure through biased fertilization against gametes carrying these elements (12).

To test the hypothesis that the presence of selfish genetic elements may select for increased rates of female remating, we examined the evolutionary response of remating rate to the presence of the selfish gene SR (sex ratio), an X-chromosome meiotic driver in the fruit fly *Drosophila pseudoobscura* (14, 15). This gene is common in populations of *D. pseudoobscura*. It has little consistent effect in females, but in males it causes the developmental failure of all sperm bearing a Y chromosome. Consequently, male carriers produce fewer sperm and sire only daughters (14), frequently resulting in female-biased population sex ratios (16). There is no genetic resistance to sex ratio drive in *D. pseudoobscura* (17). Females have higher fitness if they avoid mating with SR males due to higher sperm numbers in non-SR males, which sire offspring of both sexes and whose male offspring have a full complement of sperm. Yet, females cannot distinguish between SR and non-SR males before

<sup>1</sup>School of Biosciences, University of Exeter, Cornwall Campus, Penryn TR10 9EZ, UK. <sup>2</sup>Graduate School of Environmental Science, Okayama University, Okayama 700-8530, Japan. <sup>3</sup>School of Biological Sciences, University of Liverpool, Liverpool L69 7ZB, UK.

\*To whom correspondence should be addressed. E-mail: n.wedell@exeter.ac.uk



mating (15). However, the loss of half of the developing sperm (Y-chromosome that do not carry SR) reduces the number of sperm that SR males transfer to females (18), which makes them poor sperm competitors relative to unaffected males (18). Given the poor performance of SR males in sperm competition, we predict that in populations containing SR sperm, females should evolve high rates of remating to promote sperm competition and thus reduce the average paternity of SR males.

Female *D. pseudoobscura* flies collected from Arizona showed significant variation in remating rate between isofemale lines (descendants of a single wild-caught female) (see supporting online methods; median test for remating day differences between  $F_2$  daughters of isofemale lines:  $N = 100$ ,  $\chi^2_{20} = 31.8$ ,  $P = 0.045$ ; range of mean day of remating: 2 to 5 days), demonstrating that this population contained variation in remating rates that selection could act upon. Four selection lines carried SR at an initial frequency of 30% and were maintained at a 2:1 female-to-male sex ratio, as observed in many natural SR-carrying populations (16). Four lines lacked a SR element and had a 1:1 sex ratio, representing natural non-SR populations. An additional four lines lacked SR but were experimentally maintained at a 2:1 sex ratio, to control for any potential effect of sex ratio on the evolution of female remating rate. Before setting up the populations, we examined the remating propensities of the SR and non-SR isolines and found that they did not differ significantly ( $N = 28$ ,  $\chi^2_1 = 0.015$ ,  $P = 0.902$ ), thus ensuring there was no initial difference in female remating rate between the SR and non-SR flies from which the selection lines were formed. We also used simulations to confirm that the experimental setup produced an unbiased sample of female mating rates between treatments in the first experimental generation [supporting online material (SOM)].

After 10 generations of experimental evolution, we assayed remating rates within the selection lines by counting the number of females that mated on their second exposure to males (SOM) (Fig. 1). In a second assay at generation 11, we individually mated virgin females from each line to standard, stock non-SR males and then recorded the time until remating occurred (SOM) (Figs. 2 and 3). Both methods of assessment showed that females from SR-carrying lines were more likely to remate at the first opportunity than females from the other treatments (first assay:  $\chi^2_2 = 15.279$ ,  $P = 0.0005$ ; second assay:  $\chi^2_2 = 6.524$ ,  $P = 0.0383$ ), and that there was a shorter overall time to remating (second assay  $\chi^2_2 = 17.731$ ,  $P = 0.0001$ ). Thus, evolution of increased remating rates in the presence of SR was both rapid and dramatic, with females doubling their likelihood of remating at the first opportunity compared to females from non-SR lines, and reducing the mean number of days to remating from 3.25 to 2.75 in only 10 generations of experimental evolution.

The presence of SR chromosomes was associated with an increased willingness of females to remate, as predicted by theory (12). Three alternative explanations for the increase in remating—a male effect, phenotypic effect, and inbreeding—were rejected. First, the increase in female remating rates could not be due to differences in the ability of males from different lines to acquire copulations and prevent female remating (either

randomly or due to the presence of the SR chromosome) because the effect was still observed when females were exposed to tester males from an unselected non-SR stock population. Second, it is unlikely that increased female remating rates were caused by a phenotypic effect of the SR chromosome when expressed in females, because the frequency of SR was less than 5% in each line when the assays were conducted. Ad-

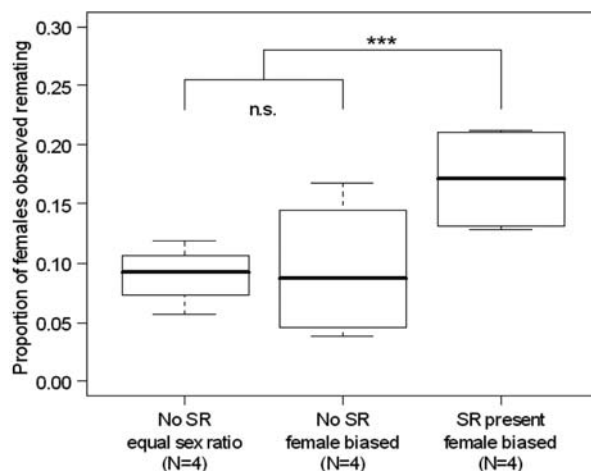


**Fig. 1.** The proportion of females observed remating at generation 10, for each selection regime ( $N = 12$  lines), showing median, interquartile range, and range. \*\*\* $P$ , 0.0005; n.s., not significant.

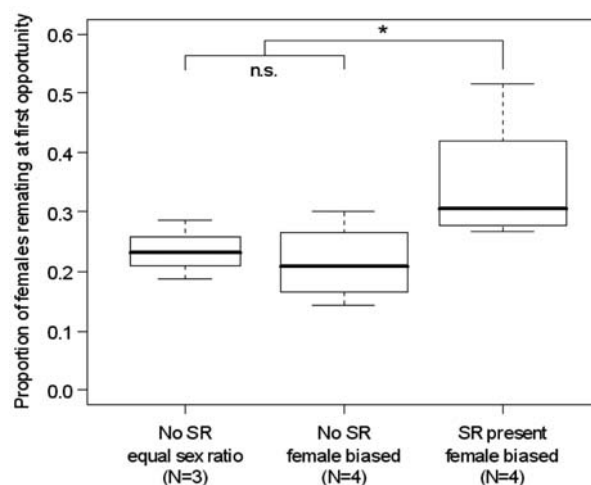


**Fig. 2.** The proportion of selection line females remating at their first opportunity, for each selection regime ( $N = 11$  lines), when offered standardized stock males, showing median, interquartile range, and range. \* $P$ , 0.0383; n.s., not significant.

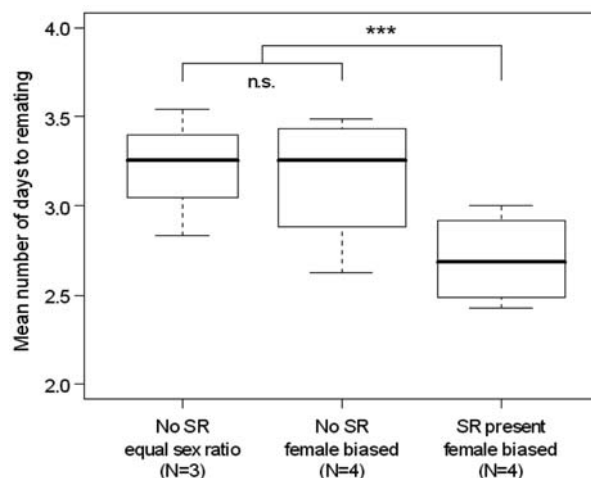


**Fig. 3.** The mean number of days to remating, for each selection regime ( $N = 11$  lines), when females mated to standardized stock males, showing median, interquartile range, and range. \*\*\* $P$ , 0.0001; n.s., not significant.

ditionally, no influence of SR alleles on female remating behavior has been shown (15). Third, we doubt that the remating rate increase was driven by SR populations being more inbred and females avoiding inbreeding depression (10), because our experimental populations of 120 adults per generation were large enough to avoid appreciable inbreeding (19). There also was no *a priori* reason to expect a greater inbreeding effect in the female-biased SR populations compared to the non-SR female-biased populations.

The most parsimonious explanation for the evolution of increased female remating rates in the presence of SR is therefore that the direct benefits of decreased risk of sperm limitation due to mating with SR males, combined with the benefit of reduced exposure of the progeny of polyandrous females to SR, has driven the spread of alleles for increased remating rates through the populations. The observed increases in female remating rates (2.75 versus 3.25 days) are well within the natural variation of the source population (2 to 5 days). Thus, we conclude that increased female remating rates evolved through selection for alleles that promote polyandry in SR populations.

Avoidance of selfish genetic elements is likely to promote the evolution of polyandry, wherever a selfish genetic element reduces both the sperm competitive ability of carrier males and the fitness of progeny that inherit the gene (7, 12). Sex chromosome meiotic drive elements are likely to considerably reduce male fertility

because their transmission mode involves a substantial failure of spermatogenesis (13, 14). They also impose serious costs because they destroy sperm and distort brood sex ratios (14). Sex chromosome drive is widespread (20) and may be common (21, 22). Most segregation distorters are active in males (23), and reduced sperm production associated with both X- and Y-chromosome drive has been observed (13). Similarly, males may suffer reduced fertility from other selfish genes, such as autosomal drive genes, B chromosomes (24), intracellular parasites (25), and possibly some transposons (26). Thus, a wide range of selfish genetic elements potentially provide the critical combination of low sperm competitive ability and low fitness that could favor polyandry. Because such selfish elements are ubiquitous in living organisms and frequently compromise male fertility, they may provide a generally overlooked explanation for why polyandry is very widespread.

#### References and Notes

1. T. R. Birkhead, A. P. Møller, *Sperm Competition and Sexual Selection* (Academic Press, London, 1998).
2. L. W. Simmons, *Sperm Competition and Its Evolutionary Consequences in the Insects* (Princeton Univ. Press, Princeton, NJ, 2001).
3. G. Arnqvist, L. Rowe, *Sexual Conflict* (Princeton Univ. Press, Princeton, NJ, 2005).
4. T. Chapman, L. F. Liddle, J. M. Kalb, M. F. Wolfner, L. Partridge, *Nature* **373**, 241 (1995).
5. H. Crudgington, M. Siva-Jothy, *Nature* **407**, 855 (2000).
6. M. D. Jennions, M. Petri, *Biol. Rev. Camb. Philos. Soc.* **75**, 21 (2000).

7. J. A. Zeh, D. W. Zeh, *Proc. R. Soc. London Ser. B* **264**, 69 (1997).
8. M. Olsson, R. Shine, T. Madsen, A. Gullberg, H. Tegelström, *Nature* **383**, 585 (1996).
9. D. J. Hosken, T. W. J. Garner, T. Tregenza, N. Wedell, P. I. Ward, *Proc. R. Soc. London Ser. B* **270**, 1933 (1993).
10. T. Tregenza, N. Wedell, *Nature* **415**, 71 (2002).
11. A. Burt, R. Trivers, *Genes in Conflict: The Biology of Selfish Genetic Elements* (Harvard Univ. Press, Cambridge, MA, 2006).
12. D. Haig, C. T. Bergstrom, *J. Evol. Biol.* **8**, 265 (1995).
13. T. A. R. Price, N. Wedell, *Genetica* **132**, 295 (2008).
14. J. Jaenike, *Annu. Rev. Ecol. Syst.* **32**, 25 (2001).
15. J. Powell, *Progress and Prospects in Evolutionary Biology: The Drosophila Model* (Oxford Univ. Press, Oxford, 1997).
16. S. H. Bryant, A. T. Beckenbach, G. Cobbs, *Evolution* **36**, 27 (1982).
17. D. Policansky, B. Dempsey, *Evolution* **32**, 922 (1978).
18. T. A. R. Price *et al.*, *Evolution* **62**, 1644 (2008).
19. W. Rice, B. Holland, *Evolution* **59**, 682 (2005).
20. L. D. Hurst, A. Pomiankowski, *Genetics* **128**, 841 (1991).
21. J. Jaenike, *Am. Nat.* **148**, 237 (1996).
22. F. Jiggins, G. Hurst, M. Majerus, *Am. Nat.* **154**, 481 (1999).
23. D. R. Taylor, P. K. Ingvarsson, *Genetica* **117**, 27 (2003).
24. L. W. Beukeboom, *Evol. Ecol.* **8**, 1 (1994).
25. F. E. Champion de Crespigny, N. Wedell, *Proc. R. Soc. London Ser. B* **273**, 1455 (2006).
26. T. K. Rajendra, K. V. Prasanth, S. C. Lakhota, *J. Genet.* **80**, 97 (2001).
27. Isofemale lines were collected with assistance from T. Markow. We thank J. Blount, F. E. Champion de Crespigny, D. J. Hosken, and T. Tregenza for discussion. Funded by a Natural Environment Research Council grant (N.W. and G.H.).

#### Supporting Online Material

www.sciencemag.org/cgi/content/full/322/5905/1241/DC1  
Materials and Methods  
References

25 July 2008; accepted 15 October 2008  
10.1126/science.1163766

## Regulation of Microtubule Dynamics by Reaction Cascades Around Chromosomes

Chaitanya A. Athale, Ana Dinarina, Maria Mora-Coral, Céline Pugieux, François Nedelec, Eric Karsenti\*

During spindle assembly, chromosomes generate gradients of microtubule stabilization through a reaction-diffusion process, but how this is achieved is not well understood. We measured the spatial distribution of microtubule aster asymmetry around chromosomes by incubating centrosomes and micropatterned chromatin patches in frog egg extracts. We then screened for microtubule stabilization gradient shapes that would generate such spatial distributions with the use of computer simulations. Only a long-range, sharply decaying microtubule stabilization gradient could generate aster asymmetries fitting the experimental data. We propose a reaction-diffusion model that combines the chromosome generated Ran-guanosine triphosphate-Importin reaction network to a secondary phosphorylation network as a potential mechanism for the generation of such gradients.

In eukaryotic cells, chromosomes regulate spindle assembly by generating a gradient of Ran-guanosine triphosphate (RanGTP) in their vicinity (1–5). In frog eggs and egg extracts, it has been shown that this gradient triggers the nucleation of spindle microtubules (MTs) by activating the protein TPX2 (6) and stabilizes the plus ends of centrosomal MTs by activating the kinase CDK11

(7). When centrosomes are incubated together with chromatin stripes or beads in those extracts, the centrosomal asters are asymmetric, sending longer microtubules preferentially toward chromatin, presumably because of their increased stability in this region (8, 9). However, the exact distribution of the CDK11-dependent MT stabilization activity and how this could translate into a defined asym-

metry of centrosomal asters in the vicinity of chromosomes has remained unclear.

To visualize the shape of the stabilization gradient, we designed an experimental system allowing the precise measurement of centrosomal MT asymmetry as a function of centrosome distance from chromatin (10). We immobilized chromatin beads on patches of defined sizes and distributions and incubated them in *Xenopus* egg extracts containing purified human centrosomes (Fig. 1, A and B). The chromatin patches nucleated MTs actively, and spindles assembled robustly on practically all patches. In the experiments designed to assay aster asymmetry, we added anti-TPX2 antibodies to the extract to prevent chromatin mediated MT nucleation around the beads and their interaction with centrosome-nucleated MTs (7). In this assay, centrosomal MTs displayed a radial symmetric distribution when far away from chromatin patches and became asymmetric when closer, whereas no obvious interactions between astral microtubules and the beads could be detected (Fig. 1B).

In parallel to this experimental setup, we developed a simple generic model to carry out com-

Cell Biology and Biophysics Unit, European Molecular Biology Laboratory (EMBL), Meyerhofstrasse 1, Heidelberg, Germany.

\*To whom correspondence should be addressed. E-mail: karsenti@embl.de



puter simulations. It includes a centrosome with dynamic MTs, circular chromatin, and a MT stabilization gradient (Fig. 1, C and D). The centrosome nucleates a finite number of MTs from equally spaced points on its periphery. According to the MT dynamic instability model, MTs are allowed to grow and shrink with parameter values  $v_g$  and  $v_s$  (velocities of growth and shrinkage, respectively) and  $f_{cat}$  and  $f_{res}$  (frequencies of catastrophe and rescue, respectively), derived from measurements in mitotic *Xenopus* extracts (table S1) (Fig. 1C). In the absence of a gradient, the average MT length ( $\langle L \rangle$ ) rises rapidly and achieves a symmetric steady-state value of 4.23  $\mu\text{m}$  within 100 s. This matches the value obtained from an analytical solution (4.25  $\mu\text{m}$ ) (11). The stabilization gradient is modeled as a two-dimensional spatial change in  $f_{cat}$  and  $f_{res}$  scaled between values measured in mitotic extracts and extracts containing RanQ69L (12) (Fig. 1D and table S1). The RanQ69L values are assumed to correspond to the situation around chromatin. For a gradient with a range of  $\sim 20 \mu\text{m}$  and an aster located at 20  $\mu\text{m}$  from the surface of chromatin, mean MT lengths also achieve a steady state within 100 s. These asters are, however, asymmetric and polarized toward chromatin with MT mean lengths of  $\sim 7 \mu\text{m}$  toward chromatin and 5  $\mu\text{m}$  away from it (Fig. 1D).

Using the experimental setup, we measured the maximal aster asymmetry ( $C_a$ ) as a function of centrosome position relative to chromatin (Fig. 2A).  $C_a$  reached a maximum value ( $\sim 2$ ) when centrosomes were  $\sim 20 \mu\text{m}$  from chromatin, in agreement with previous results (8). When centrosomes were further away (between 50 and 100  $\mu\text{m}$ ),  $C_a$  was close to 1 (symmetric asters). We found a linear correlation between the  $C_a$  value of each aster and the length of its longest MT pointing toward chromatin (Fig. 2B), indicating that the change in  $C_a$  was due to a lengthening of MTs toward chromatin and not to a possible shortening of MTs away from it. A few astral MTs were longer than the chromatin-centrosome distance (Fig. 2C). Although we do not rule out that they physically contact the chromatin, we can explain the MT lengthening simply by the stabilizing effects of diffusible factors generated by chromatin. Such weak asymmetries were generated by a highly stochastic process involving MT dynamic instability (movies S1 and S2).

We thus screened for  $f_{cat}$  and  $f_{res}$  gradient shapes that would generate the aster asymmetry observed experimentally. A long-range shallow gradient, a short exponential, and a long-range step gradient were tested (Fig. 2, D to F). Of these, only the step gradient with a cutoff distance of  $R_c = 22 \mu\text{m}$  reproduced the asymmetry measured in the experiments (Fig. 2F). The long-range step gradient reproduced the experimental values better than any other tested model because the asymmetry is expected to be maximal at the edge of the decaying stabilization gradient. On either side of this edge, asymmetry should tend toward the minimum; i.e.,  $C_a \sim 1$ .

We then simulated the functional consequence of the astral asymmetry caused by a long-range step gradient on the first capture time ( $t_c$ ) of a single microtubule by chromatin. Previous models such as random (13) or biased (14) “search and capture” have predicted biologically unreasonable  $t_c$  values ( $>30 \text{ min}$ ) for centrosomes located farther than  $\sim 30 \mu\text{m}$  from chromatin. In the presence of the step gradient described here,  $t_c$  remains on the order of a few minutes for centrosome-chromatin distances as large as 45  $\mu\text{m}$  (fig. S2). In addition, the capture-time values appear less variable in the presence of a step gradient. This is consistent with the previous finding that  $t_c$  is sensitive to location of the centro-

some with respect to the edge of a sharply decaying stabilization gradient (14). Thus, long-range, abruptly decaying stabilization gradients efficiently reduce  $t_c$  and increase the robustness of the search and capture mechanism.

What kind of molecular mechanism could produce a long-range, sharp decaying gradient of  $f_{res}$  and  $f_{cat}$  values around chromatin in the cytoplasm? In developmental biology (15–17), eukaryotic cells (18), and bacteria (19), step gradients (boundaries) are modeled by zero-order (15, 20) ultrasensitive reaction networks, but other possibilities could be thought of (such as cooperativity or positive feedback) (17). In frog egg extracts, the

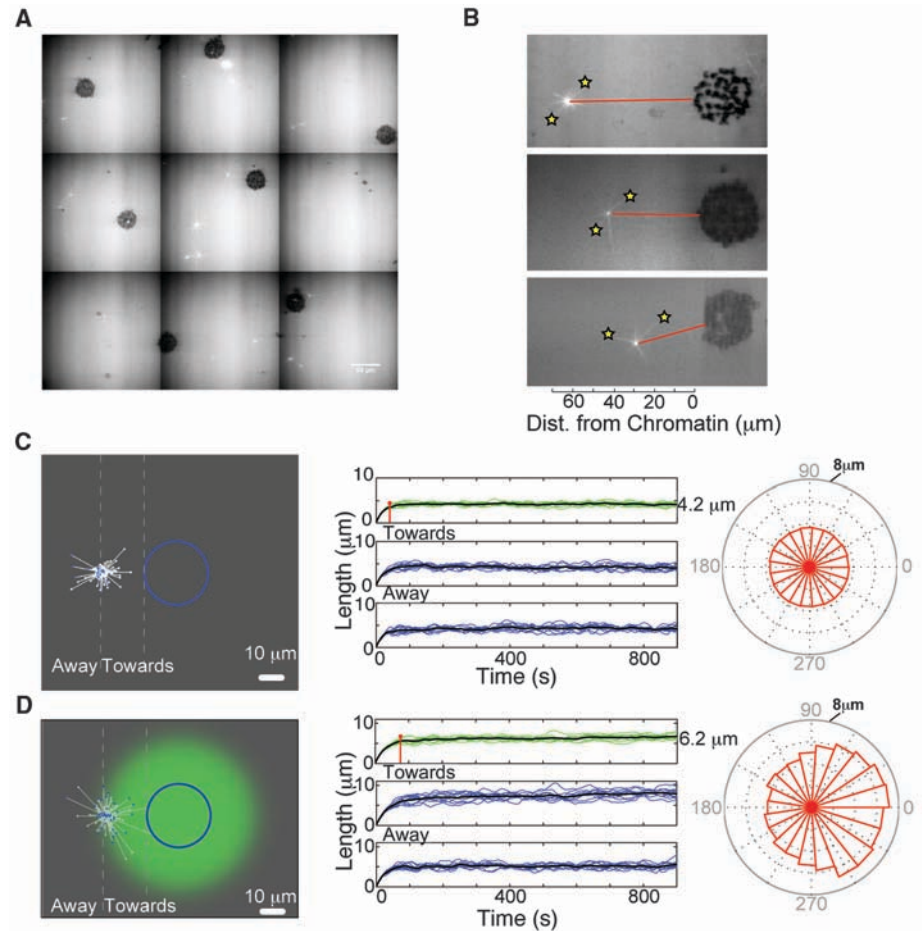


**Fig. 1.** Experimental and simulation of centrosomal aster asymmetry in the vicinity of chromatin. (A) *Xenopus* egg extracts with centrosomes and fluorescent tubulin were flowed into a chamber over a glass surface containing immobilized chromatin-bead patches and imaged with confocal microscopy. Centrosomes are shown in white, and the round chromatin patches are in dark gray. (B) Still images of three asters located at different distances from DNA indicate increasing asymmetry closer to the DNA surface. Stars indicate the longest microtubules in the toward and away directions, and the red line denotes the axis between the centrosome and nearest DNA patch. (C and D) Snapshot of a simulation with a centrosome near a DNA patch (blue) (C) without and (D) with the MT stabilization gradient. The  $f_{res}$  values are displayed on a scale from green to gray. The MTs ends are represented as white in a growing state and blue in a shrinking state. In the middle column, the uppermost panels indicate the MT lengths evolution in time, averaged (black lines) over 10 different runs (green lines). The two lower panels depict the time-dependent mean distribution of MT lengths pointing toward and away from the chromatin, respectively. The rightmost rose plots describe the steady-state angular distribution of the MT length (radial extent indicates length in microns) with respect to chromatin at zero degrees. The aster without a gradient is symmetric, whereas in the presence of a stabilization gradient it is asymmetric.

stabilization effect around chromosomes involves the local activation of a kinase (CDK11), which dissociates from importins in response to high RanGTP concentration (17). We therefore built a reaction-diffusion model downstream of the previously modeled Ran gradient (2), which involves a protein kinase ( $E1$ ) and a phosphatase ( $E2$ ) (Fig. 3A). The locally activated kinase ( $E1$ ) converts the substrate ( $W$ ) into a phosphorylated form ( $Wp$ ) locally, whereas the phosphatase ( $E2$ ), free to diffuse in the cytoplasmic space, dephosphorylates  $Wp$  globally (Fig. 3A and fig. S3). We modeled  $Wp$  as stabilizing MTs directly while  $W$  is inactive. The reaction parameters are given in table S1 and were chosen to reflect realistic kinetic constants and diffusion rates for proteins. We tested the following scenarios (Fig. 3B): (i) a linear network where  $[W]$  is not saturating, (ii) a network where  $WE1$  interaction is cooperative, (iii) a positive feedback network where  $Wp$  inhibits the phosphatase, and (iv) a zero-order ultrasensitive network where  $[W]$  is saturating for both enzymes (15, 20). The reactions between the components are

described by the following partial differential equations

$$\frac{\partial[E1]}{\partial t} = S + (d_1 + k_1) \cdot [WE1] - a_1 \cdot [W] \cdot [E1]^n + D_1 \cdot \Delta[E1] \quad (1)$$

$$\frac{\partial[E2]}{\partial t} = (d_2 + k_2) \cdot [WpE2] - a_2 \cdot [Wp] \cdot [E2] + D_2 \cdot \Delta[E2] \quad (2)$$

$$\frac{\partial[W]}{\partial t} = -a_1 \cdot [W] \cdot [E1]^n + d_1 \cdot [WE1] + k_2 \cdot [WpE2] + D_3 \cdot \Delta[W] \quad (3)$$

$$\frac{\partial[WE1]}{\partial t} = a_1 \cdot [W] \cdot [E1]^n - (d_1 + k_1) \cdot [WE1] + D_4 \cdot \Delta[WE1] \quad (4)$$

$$\frac{\partial[Wp]}{\partial t} = -a_2 \cdot [Wp] \cdot [E2] + d_2 \cdot [WpE2] + k_1 \cdot [WE1] + D_5 \cdot \Delta[Wp] \quad (5)$$

$$\frac{\partial[WpE2]}{\partial t} = a_2 \cdot [Wp] \cdot [E2] - (d_2 + k_2) \cdot [WpE2] + D_6 \cdot \Delta[WpE2] \quad (6)$$

The term  $S$  in Eq. 1 connects this network to the RanGTP-Importin gradient-forming reaction system (supporting online material text). Also, in the above equations,  $d$  is the dissociation rate,  $k$  is the rate of product formation,  $a$  is the association rate,  $n$  is the Hill coefficient, and  $D$  is the diffusion coefficient of each species (1–6). In the positive feedback network, the parameter  $k_2$  is replaced by a variable  $k'_2$ , such that  $k'_2 = k_2 \cdot K_f / (K_f + [Wp])$ , where  $K_f$  is the feedback strength (17).  $Wp$  reaches steady-state concentration within 150 s for all models (Fig. 3C). Gradients of RanGTP and Importin- $E1$  complexes extend over 4 to 10  $\mu\text{m}$  away from chromosomes with amplitudes between 0.5 and 1  $\mu\text{M}$ . Gradients of  $E1$ ,  $WE1$ , and  $WpE2$  extend over similar distances away from chromosomes but have lower amplitudes on the order of 0.05 to 0.1  $\mu\text{M}$ . Both gradient extents and amplitudes vary somewhat according to network topology. All networks generated gradients of  $Wp$  extending over 20 to 25  $\mu\text{m}$  with amplitudes ranging from 0.2 to 0.8  $\mu\text{M}$ , depending on the topology of the network. Only the zero order network produced a relatively long-range, sharply decaying gradient.

To examine whether some of these gradients could generate distributions of aster asymmetries as a function of chromatin distance similar to those observed experimentally, we made  $Wp$  stabilize MT plus ends by affecting MT dynamics transition frequencies as a function of chromatin distance ( $r$ ) as follows

$$f_{\text{cat}}(r) = ([Wp(r)]/[Wp]^{\text{max}}) \cdot (f_{\text{cat}}^{\text{min}} - f_{\text{cat}}^{\text{max}}) + f_{\text{cat}}^{\text{max}} \quad (7)$$

$$f_{\text{res}}(r) = ([Wp(r)]/[Wp]^{\text{max}}) \cdot (f_{\text{res}}^{\text{max}} - f_{\text{res}}^{\text{min}}) + f_{\text{res}}^{\text{min}} \quad (8)$$

The gradients of MT dynamic instability parameters generated by the linear network produced an asymmetry pattern that is a poor fit to the experimental results (Fig. 4). The positive feedback network did not generate any asymmetry pattern, as expected from the shape of the  $Wp$  gradient that is too shallow (Fig. 4, A and B). The Hill cooperative and the zero-order ultrasensitive networks generated asymmetry patterns that were best fit to the experimental results, both for the amplitude and extent of the gradients (Fig. 4). The distance from chromatin at which asters showed half maximum asymmetry was on the order of 20  $\mu\text{m}$  in both cases. The fit of the asymmetry generated by the ultrasensitive or Hill-cooperative networks is not as good as with the pure step gradient (compare Figs. 2C and 4B). It is possible that alternative, additional, or more complex mechanisms are at work or that we did not find the exact parameters combination. However, the present results demonstrate that it is possible to generate gradients of microtubule dynamic instability around chromosomes having

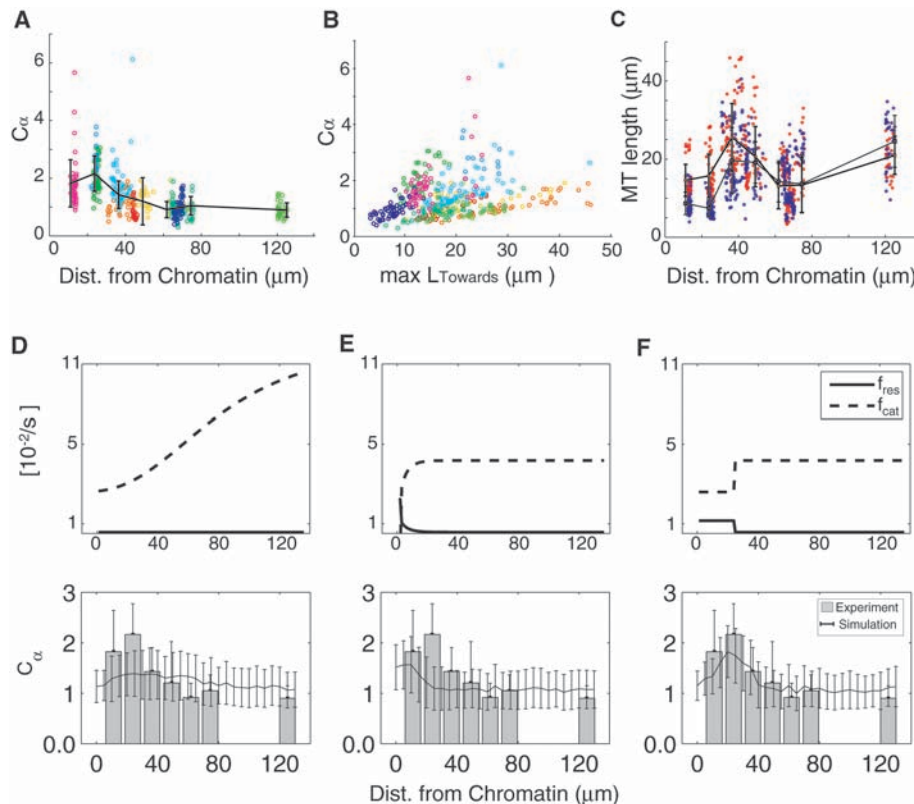


**Fig. 2.** Experimental measures of aster asymmetry around chromatin beads and comparison with simulations. (A) Distance of each aster from the chromatin patch in each time frame plotted against maximal asymmetry ( $C_\alpha$ ). The different colors represent individual asters, and the line plot indicates the trend of the average  $C_\alpha$  distribution (black line) with error bars representing SD. (B)  $C_\alpha$  plotted as a function of the length of the longest MT toward DNA. (C) Absolute lengths of MTs toward (red) and away (blue) from DNA plotted as a function of the DNA-aster distance and overlaid with mean trend lines. (D to F)  $f_{\text{cat}}$  and  $f_{\text{res}}$  values around chromatin chosen between those measured in M phase extracts and in M phase extracts treated with RanQ69L (mimicking the situation around chromatin) plotted as a long-range shallow gradient (D), a short-range exponential gradient (E), and a long-range step gradient (F). In the lower panels, the simulated  $C_\alpha$  distributions generated by these gradients (lines) are compared with the experimental data (histograms).

an extent of ~20  $\mu\text{m}$  with enzymatic networks composed of proteins having realistic diffusivity and kinetic constants.

Our hypothetical network consists of a kinase-phosphatase-substrate system regulated by RanGTP. Small heterotrimeric GTP-binding

protein systems are involved in various processes, ranging from signal transduction (21) to cell polarity (22) and membrane trafficking (23). In

**Fig. 3.** RanGTP-based hypothetical reaction networks generate long-range gradients in the cytoplasm. **(A)** Inter-conversion between Ran-guanosine diphosphate (RanGDP) and RanGTP by the chromatin-bound Ran-guanine nucleotide exchange factor (RCC1) opposed by the cytoplasmic Ran-GTPase activating protein (RanGAP) generates a short-range RanGTP gradient around chromatin. RanGTP binding to Importin $\beta$  releases a hypothetical cargo protein E1 (a kinase that distributes over a longer-range gradient). E1 in turn catalyzes the formation of Wp, assumed to regulate MT dynamics. The part of the network that has previously been modeled (5) is displayed in gray; the hypothesized components are in black. The parameters and initial values of the reaction are described in table S1. **(B)** Different hypothetical reaction scheme for W and Wp. **(C)** (Top) A steady state is reached in a few minutes in all models. (Bottom) Each model predicts a specific steady-state concentration profile of W and Wp (left y axis) and of E1, E2, WE1, and WpE2 (right y axis). **(D)** Comparison of the free Wp gradient shapes generated by these different network topologies.

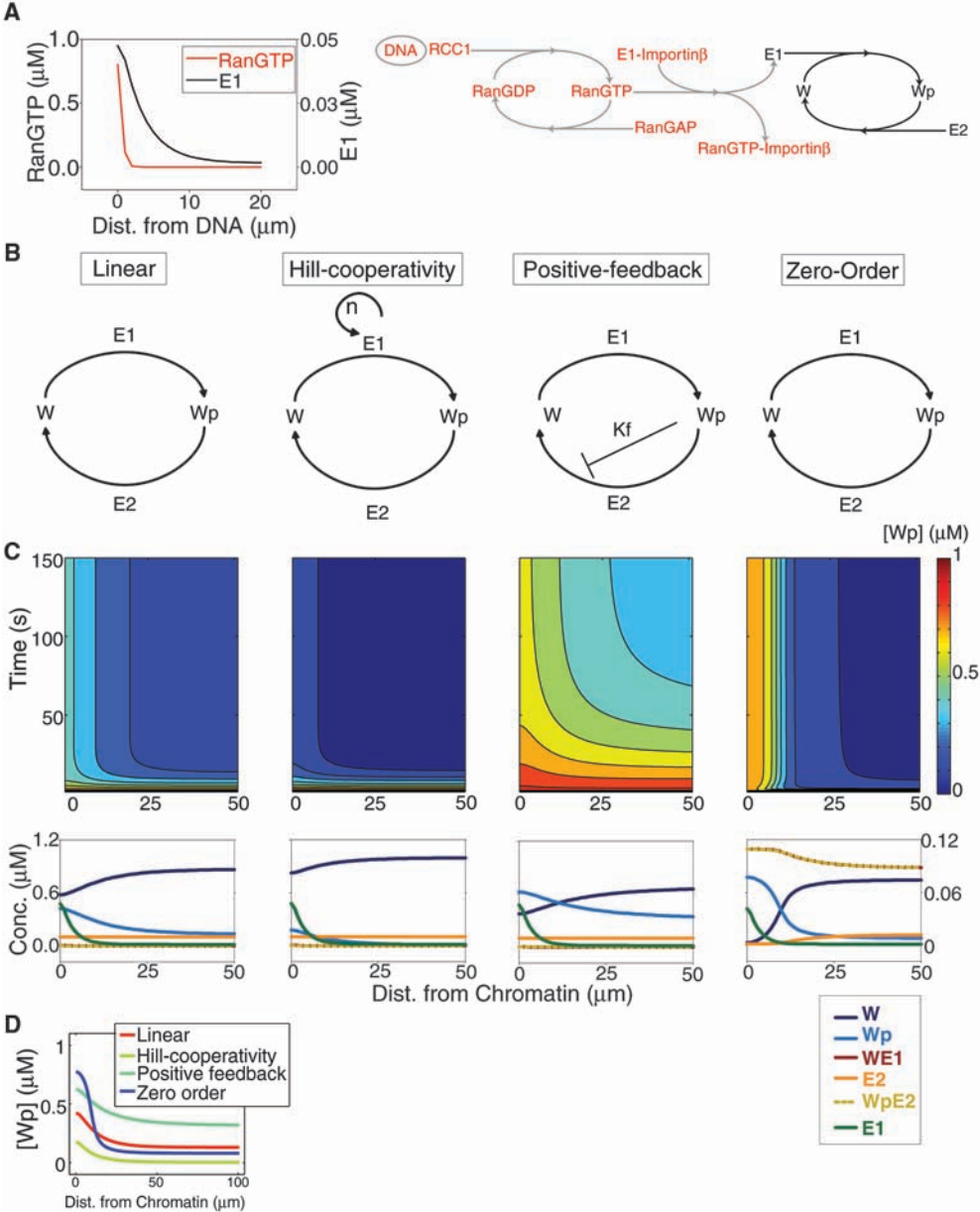
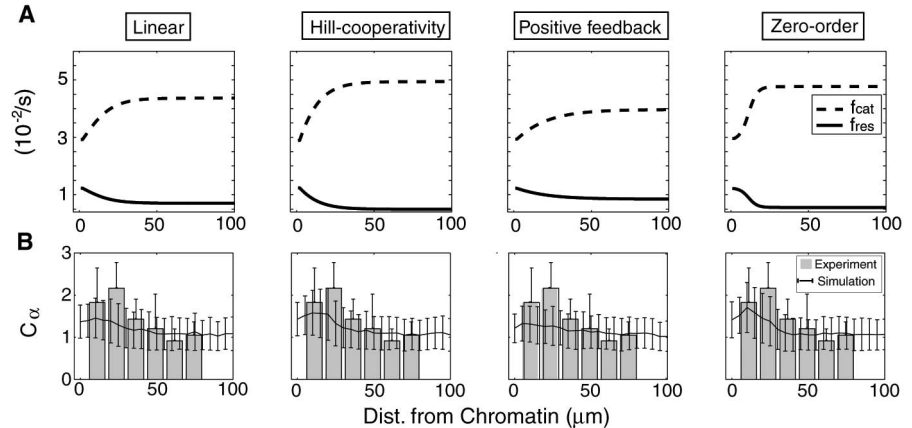


**Fig. 4.** The RanGTP-dependent ultrasensitive reaction-diffusion system reproduces the experimentally measured aster asymmetry. **(A)** Wp gradients obtained from the linear unsaturated, Hill-cooperative, positive feedback and zero-order ultrasensitive models are used to derive gradients of  $f_{cat}$  and  $f_{res}$ . **(B)** Simulated mean  $C_\alpha$  obtained for the above gradients acquired for asters positioned at different distances from chromatin for the four models (lines) overlaid on the experimental data (histograms). Error bars indicate SD of the mean for both experiments and simulations. The Hill-cooperativity and zero-order ultrasensitive models fit the experimental data best.





almost all cases, they are coupled to the downstream modulation of kinase activities (24–26). Such systems may also generate local gradients involved in a variety of morphogenetic processes at the subcellular level.

## References and Notes

- P. Bastiaens, M. Caudron, P. Niethammer, E. Karsenti, *Trends Cell Biol.* **16**, 125 (2006).
- M. Caudron, G. Bunt, P. Bastiaens, E. Karsenti, *Science* **309**, 1373 (2005).
- P. Kalab, R. Heald, *J. Cell Sci.* **121**, 1577 (2008).
- P. Kalab, A. Pralle, E. Y. Isacoff, R. Heald, K. Weis, *Nature* **440**, 697 (2006).
- P. Kalab, K. Weis, R. Heald, *Science* **295**, 2452 (2002).
- O. J. Gruss *et al.*, *Nat. Cell Biol.* **4**, 871 (2002).
- H. Yokoyama *et al.*, *J. Cell Biol.* **180**, 867 (2008).
- R. E. Carazo-Salas, E. Karsenti, *Curr. Biol.* **13**, 1728 (2003).
- M. Dogterom, M. A. Felix, C. C. Guet, S. Leibler, *J. Cell Biol.* **133**, 125 (1996).
- Materials and methods are available as supporting material on Science Online.
- F. Verde, M. Dogterom, E. Stelzer, E. Karsenti, S. Leibler, *J. Cell Biol.* **118**, 1097 (1992).
- R. E. Carazo-Salas, O. J. Gruss, I. W. Mattaj, E. Karsenti, *Nat. Cell Biol.* **3**, 228 (2001).
- T. E. Holy, S. Leibler, *Proc. Natl. Acad. Sci. U.S.A.* **91**, 5682 (1994).
- R. Wollman *et al.*, *Curr. Biol.* **15**, 828 (2005).
- A. Goldbeter, D. E. Koshland Jr., *Proc. Natl. Acad. Sci. U.S.A.* **78**, 6840 (1981).
- M. Howard, P. R. ten Wolde, *Phys. Rev. Lett.* **95**, 208103 (2005).
- G. J. Meleu, S. Levy, N. Barkai, B.-Z. Shilo, *Mol. Syst. Biol.* **1**, 2005.0028 (2005).
- J. Stelling, B. N. Kholodenko, *J. Math. Biol.*, published online 19 February 2008, 10.1007/s00285-008-0162-6.
- S. B. van Albada, P. R. ten Wolde, *PLoS Comput. Biol.* **3**, 1925 (2007).
- E. R. Stadman, P. B. Chock, *Proc. Natl. Acad. Sci. U.S.A.* **74**, 2761 (1977).
- S. Etienne-Manneville, A. Hall, *Nature* **420**, 629 (2002).
- P. G. Charest, R. A. Firtel, *Biochem. J.* **401**, 377 (2007).
- P. Del Conte-Zerial *et al.*, *Mol. Syst. Biol.* **4**, 206 (2008).
- V. Delorme *et al.*, *Dev. Cell* **13**, 646 (2007).
- H. Katoh, M. Negishi, *Nature* **424**, 461 (2003).
- C. I. Maeder *et al.*, *Nat. Cell Biol.* **9**, 1319 (2007).
- We thank D. Foethke for inputs about the Cytosim code, M. Caudron and R. Carazo-Salas for sharing data, M. Loose for help in the initial set up of chromatin bead patterns, and the EMBL Advanced Light Microscopy Facility for invaluable help with microscopy. We acknowledge the center for Modeling and Simulation the Bioscience (BIOMS) for funding F.N. and C.A.A., the Spanish ministry of education for funding M.M.-C., European Union Specific Targeted Research Project BioMics for funding A.D., and support from Human Frontier Science Program grant RGY85.

## Supporting Online Material

www.sciencemag.org/cgi/content/full/1161820/DC1

Materials and Methods

SOM Text

Figs. S1 to S4

Tables S1 and S2

References

Movies S1 and S2

16 June 2008; accepted 6 October 2008

Published online 23 October 2008;

10.1126/science.1161820

Include this information when citing this paper.

# Canonical Wnt Signaling Regulates Organ-Specific Assembly and Differentiation of CNS Vasculature

Jan M. Stenman,<sup>1\*</sup> Jay Rajagopal,<sup>1,2</sup> Thomas J. Carroll,<sup>1†</sup> Makoto Ishibashi,<sup>1‡</sup> Jill McMahon,<sup>1</sup> Andrew P. McMahon<sup>1,3§</sup>

Every organ depends on blood vessels for oxygen and nutrients, but the vasculature associated with individual organs can be structurally and molecularly diverse. The central nervous system (CNS) vasculature consists of a tightly sealed endothelium that forms the blood-brain barrier, whereas blood vessels of other organs are more porous. *Wnt7a* and *Wnt7b* encode two Wnt ligands produced by the neuroepithelium of the developing CNS coincident with vascular invasion. Using genetic mouse models, we found that these ligands directly target the vascular endothelium and that the CNS uses the canonical Wnt signaling pathway to promote formation and CNS-specific differentiation of the organ's vasculature.

Several signaling pathways have been defined that generally regulate vascular development [e.g., (1)]. However, much less is known about the control of organ-specific vascularization and endothelial cell differentiation. The endothelium of the central nervous system (CNS) differs from most other organ systems in that the vascular cells establish a blood-brain barrier (BBB) that serves a critical

neuroprotective role in preventing the free flow of substances between the blood and CNS [e.g., (2)]. Consequently, the BBB also presents a physical block to the passage of potentially therapeutic agents. Diseases of the brain's vasculature are the third leading cause of death in the United States (3). Thus, defining the signaling pathways that promote the formation and differentiation of the CNS vasculature has important clinical ramifications.

At embryonic day 8.5 (E8.5) in the mouse, migrating paraxial mesoderm-derived angioblasts form a perineural vascular plexus (PNVP) surrounding the neural tube, the CNS anlagen. Endothelial cell sprouting from the PNVP initiates intraneural vascular plexus (INVP) formation at E9.5. Several Wnt family members, including *Wnt7a* and *Wnt7b*, are expressed in the neural tube coincident with neural tube angiogenesis (4). By E10.5, *Wnt7a* and *Wnt7b* are expressed in broad overlapping domains along the dorsal-ventral axis in the presumptive spinal cord and complementary patterns in the future forebrain

(fig. S1). Because single null mutants for either *Wnt7a* or *Wnt7b* (5, 6) do not exhibit an early neural tube phenotype, we derived *Wnt7a/b* double mutant embryonic stem cell lines and used tetraploid aggregations to demonstrate a neural tube-specific hemorrhaging phenotype in embryos lacking both signaling activities.

To examine the role of these Wnts in detail, we generated a more tractable genetic system in which the embryo-specific removal of *Wnt7a* and *Wnt7b* function avoided an early lethality due to *Wnt7b* function in placental development (7). In this model, all *Wnt7a/b* double mutants die around E12.5, displaying a severe CNS-specific hemorrhaging phenotype and disorganization of neural tissue (Fig. 1, A and E, and figs. S2 and S3). These data indicated that Wnt signaling is essential for CNS vascular development. In most instances, when a single active *Wnt7a* or *Wnt7b* allele remained, no phenotype was observed (figs. S2 and S3).

A detailed molecular analysis of CNS vascular development was performed using antibodies to several general endothelial markers, including fetal liver kinase 1 (FLK1) and the pericyte marker platelet-derived growth factor receptor- $\beta$  (PDGFR $\beta$ ) (Fig. 1, B to D and F to H, and figs. S3 and S4). Consistent with normal vascular endothelial growth factor (VEGF) signaling (8), a PNVP surrounded the neural tube in *Wnt7a/b* double mutants at E12.5. However, endothelial cells and pericytes were absent from all ventral neural regions of the presumptive spinal cord except the floor plate (Fig. 1, F to H). In the dorsal neural tube, endothelial cells and pericytes were present but clustered abnormally and formed vessels with expanded lumens, most noticeably where the expression of dorsal Wnts intersects with that of *Wnt7a* and *Wnt7b* (Fig. 1F and fig. S5). Thus, whereas *Wnt7a* and *Wnt7b* are critical for ventral CNS vascularization, other Wnts may also participate in this process in more dorsal domains of the presumptive spinal cord. When

<sup>1</sup>Department of Molecular and Cellular Biology, Harvard University, Cambridge, MA 02138, USA. <sup>2</sup>Department of Internal Medicine, Massachusetts General Hospital, Boston, MA 02114, USA. <sup>3</sup>Harvard Stem Cell Institute, Harvard University, Cambridge, MA 02138, USA.

\*Present address: Ludwig Institute for Cancer Research, Karolinska Institute, Box 240, SE-171 77 Stockholm, Sweden.

†Present address: Department of Internal Medicine (Nephrology) and Molecular Biology, University of Texas Southwestern Medical Center, Dallas, TX 75390, USA.

‡Present address: Graduate School of Medicine, Kyoto University, Yoshida Sakyo-ku, Kyoto 606-8501, Japan.

§To whom correspondence should be addressed. E-mail: mcmahon@mcb.harvard.edu

embryos were examined at E10.5, ventral vasculature was clearly already defective (fig. S6). In contrast, no obvious differences could be observed in neural tube patterning, neural proliferation, cell death, neural tube organization, or localization of the general angiogenic factor VEGF when control embryos were compared with *Wnt7a/b* double mutants (figs. S7 to S9).

To confirm that the *Wnt7a/b* double mutant phenotype was specific to *Wnt7a/b* action in the neuroepithelium, we used a *NestinCre* allele to conditionally remove *Wnt7b* activity from neuroepithelial cells on a *Wnt7a* mutant background (figs. S10 and S11) (9, 10). Although only partial recombination occurred by E10.5 in this

model (fig. S10) (11), we observed CNS-specific hemorrhaging in the *NestinCre;Wnt7a/b* double mutants at E12.5 (Fig. 1I and fig. S2). A molecular analysis revealed the presence of a PNVP and an INVP (Fig. 1, J to L, and fig. S4); however, the numbers of endothelial cells and pericytes in the INVP were greatly reduced and the morphology of blood vessels was abnormal.

We next examined the cellular target and signaling mechanisms underlying *Wnt7a/b* action. Canonical Wnt signaling produces a transcriptional activation complex between  $\beta$ -catenin ( $\beta$ Cat) and its DNA binding partners, LEF/TCF factors. Analysis of a mouse carrying a  $\beta$ -catenin-activated nuclear  $\beta$ -galactosidase transgene (a BAT-Gal reporter

mouse) revealed sites of canonical Wnt signaling (12).  $\beta$ -Galactosidase was observed in FLK1/friend leukemia integration 1 (FLI1)-positive endothelial cells (13) in the PNVP and INVP at E10.5 (Fig. 2, A to D) (12). Several members of the Frizzled Wnt receptor family (fig. S12) and lymphoid enhancer binding factor 1 (LEF1), a critical component and direct feedforward target of canonical Wnt signaling, showed similar endothelial distribution (Fig. 2, E to H). Together these data suggest that *Wnt7a* and *Wnt7b* produced by the pseudostratified neuroepithelium may directly target endothelial cells in the basally positioned PNVP, thereby triggering angiogenesis through a canonical Wnt signaling pathway.

**Fig. 1.** (A to L) Neuroepithelial *Wnt7a* and *Wnt7b* expression is critical for CNS vascularization. *Wnt7a*<sup>+/+</sup>;*Wnt7b*<sup>c3/+</sup> [(A) to (D)] mutants appeared phenotypically normal at E12.5. In contrast, *Sox2Cre*<sup>+/+</sup>;*Wnt7a*<sup>-/-</sup>;*Wnt7b*<sup>c3/d3</sup> [(E) to (H)] and *NestinCre*<sup>+/+</sup>;*Wnt7a*<sup>-/-</sup>;*Wnt7b*<sup>c3/d3</sup> [(I) to (L)] mutants exhibited severe hemorrhaging restricted to the CNS [arrowheads in (E) and (I) point to hemorrhaging in the CNS]. Furthermore, FLK1 [(B), (D), (F), (H), (J), and (L)] and PDGFR $\beta$  [(C), (G), and (K)] immunodetection of endothelial cells and pericytes, respectively, demonstrated that CNS vascularization was normal in *Wnt7a*<sup>+/+</sup>;*Wnt7b*<sup>c3/+</sup> [(B) to (D)] mutants but was perturbed ventrally in *Sox2Cre*<sup>+/+</sup>;*Wnt7a*<sup>-/-</sup>;*Wnt7b*<sup>c3/d3</sup> [brackets, (F) and (G)] and to a lesser extent in *NestinCre*<sup>+/+</sup>;*Wnt7a*<sup>-/-</sup>;*Wnt7b*<sup>c3/d3</sup> mutants [(J) to (L)]. In the dorsal neural tube of *Sox2Cre*<sup>+/+</sup>;*Wnt7a*<sup>-/-</sup>;*Wnt7b*<sup>c3/d3</sup> embryos, endothelial cells and pericytes formed abnormal clusters and enlarged lumens in vascular structures [e.g., arrowhead in (F)]. Boxes in (B), (F), and (J) show the approximate region of (D), (H), and (L), respectively. tel, telencephalon; sc, spinal cord; d, dorsal; v, ventral; NT, neural tube.

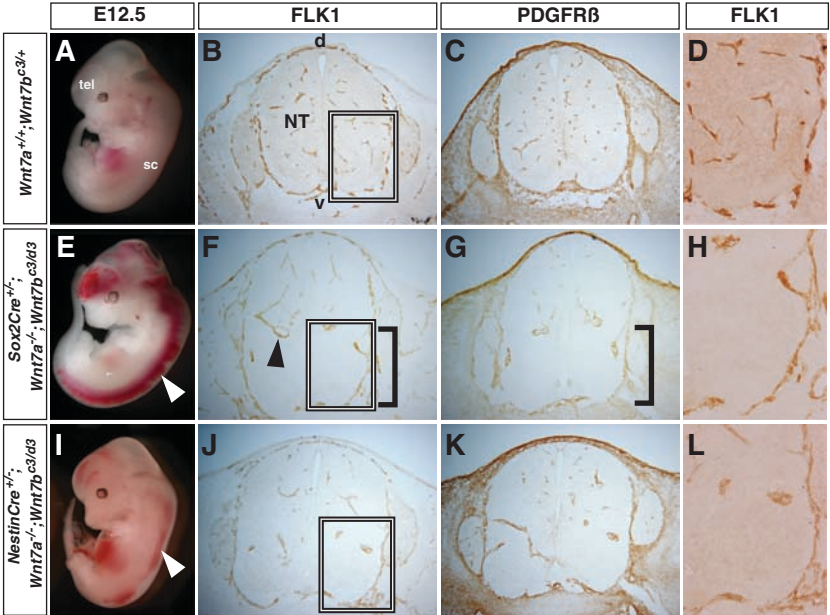
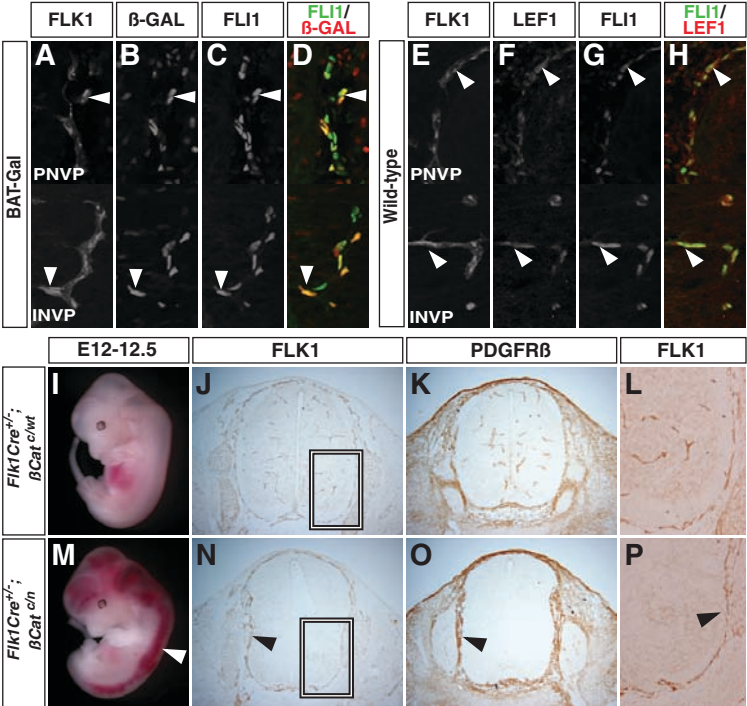


**Fig. 2.** (A to H) Canonical Wnt signaling in endothelial cells is critical for CNS vascularization. In BAT-Gal mice,  $\beta$ -galactosidase was observed in FLI1/FLK1-positive endothelial cells in the PNVP and INVP of the E10.5 spinal cord [arrowheads, (A) to (D)]. The Wnt target LEF1 showed a similar endothelial cell distribution [arrowheads, (E) to (H)]. (I to P) Endothelial-specific removal of  $\beta$ Cat function in *Flk1Cre*<sup>+/+</sup>; $\beta$ Cat<sup>c/n</sup> embryos resulted in a severe CNS-specific hemorrhaging phenotype in mice that survived to E12 [(I) and (M); arrowhead in (M) points to hemorrhaging in the CNS]. FLK1 [(J), (L), (N), and (P)] and PDGFR $\beta$  [(K) and (O)] immunodetection of endothelial cells and pericytes, respectively, demonstrated that a PNVP formed in *Flk1Cre*<sup>+/+</sup>; $\beta$ Cat<sup>c/n</sup> embryos [arrowheads in (N) to (P)], but there was an almost complete failure of angiogenesis into the adjacent neural tube [(N) to (P)]. Boxes in (J) and (N) show the approximate region of (L) and (P), respectively.





To examine this possibility, we removed  $\beta$ Cat from vascular precursors combining a *Flk1Cre* driver line (14) with a conditional  $\beta$ Cat allele (figs. S13 and S14) (15). In those embryos that survived until E12, the vascular phenotype was enhanced (Fig. 2, I and M, and fig. S15); the PNVP was present, but endothelial cells and pericytes were entirely absent from the neuroepithelium (Fig. 2, J to L and N to P). In contrast, when  $\beta$ Cat activity was removed from neural progenitors, no vascular phenotype was observed (fig. S16). Thus,  $\beta$ Cat plays a neural tube-specific role in regulating vascular development. The more severe phenotype in the *Flk1Cre*;  $\beta$ Cat model is consistent with a broad role extending to other Wnt expression domains in the developing CNS.

Another report of  $\beta$ Cat removal using a different vascular Cre driver (*Tie2Cre*) suggested an enhanced vascular fragility through destabilization of adherens junctions (16). However, our observations, including normal VE-cadherin in the *Flk1Cre*;  $\beta$ Cat model (fig. S17), argue against a broad structural role for  $\beta$ Cat in regulating vascular integrity and are more consistent with a localized signaling function. An up-regulation in  $\gamma$ -catenin in endothelial cells deficient in  $\beta$ Cat (fig. S14) may functionally substitute for  $\beta$ Cat's structural role, as in other systems (17, 18).

The development of a mature BBB results from activation of a CNS-specific endothelial cell differentiation program, the trigger for which is unclear. The first molecular changes are apparent within the PNVP coincident with vascular inva-

sion of the neural tube; formation of a full BBB occurs over a prolonged period of development (2). The glucose transporter GLUT-1 is present in neuroepithelial cells before vascular invasion but is down-regulated in the neuroepithelium and up-regulated in the developing vascular endothelium as angiogenesis occurs; high levels of GLUT-1 are a hallmark of the adult BBB (fig. S18) (2). At E12.5, *Wnt7a/b* double mutants showed reduced levels of GLUT-1 in the PNVP and INVP (Fig. 3, A and E), and persistent GLUT-1 expression was observed in the ventral neuroepithelium in the absence of angiogenesis (Fig. 3, A to H). In *Flk1Cre*;  $\beta$ Cat mutant embryos, GLUT-1 was also markedly down-regulated in the PNVP and persisted throughout the neuroepithelium (Fig. 3, I to P). Unlike the developing CNS vasculature, GLUT-1 levels were unaltered in other regions of *Flk1Cre*;  $\beta$ Cat mutants where GLUT-1 levels were high, such as the limb vasculature. Taken together, these findings support a direct role for canonical Wnt signaling in organ-specific endothelial cell differentiation.

To determine whether *Wnt7* subfamily signaling is sufficient to induce GLUT-1 in endothelial cells, we targeted the *Rosa26* locus with a construct enabling Cre-mediated control of the expression of a bicistronic message encoding *Wnt7a* and *lacZ* (fig. S19). In addition to driving Cre expression in the developing neuroepithelium, *NestinCre* showed low-level sporadic recombination in scattered cells outside the CNS (Fig. 4, A and E). *NestinCre*-driven ectopic *Wnt7a* expression in these regions enhanced GLUT-1 synthesis in endothelial cells (Fig. 4, B to D and F to H). Thus, *Wnt7* signaling regulates an early feature of a CNS-specific vascular program.

Previous *in vivo* studies have suggested roles for various Wnts in specific aspects of vascular development. *Wnt7b* action has been linked to regression of the hyaloid vasculature by triggering apoptosis, as well as development of the lung vasculature via an indirect mechanism (19, 20). In addition, *Wnt2* is thought to play a role in placental vasculature (21) and the putative Wnt receptor *Fzd5* in vascular development of the yolk sac (22). *In vitro* studies have also suggested roles for Wnt signaling in the proliferation, survival, and formation of capillary-like networks (23–27). Our study provides direct *in vivo* evidence for *Wnt7a*- and *Wnt7b*-mediated regulation of organ-specific vascular development. Their

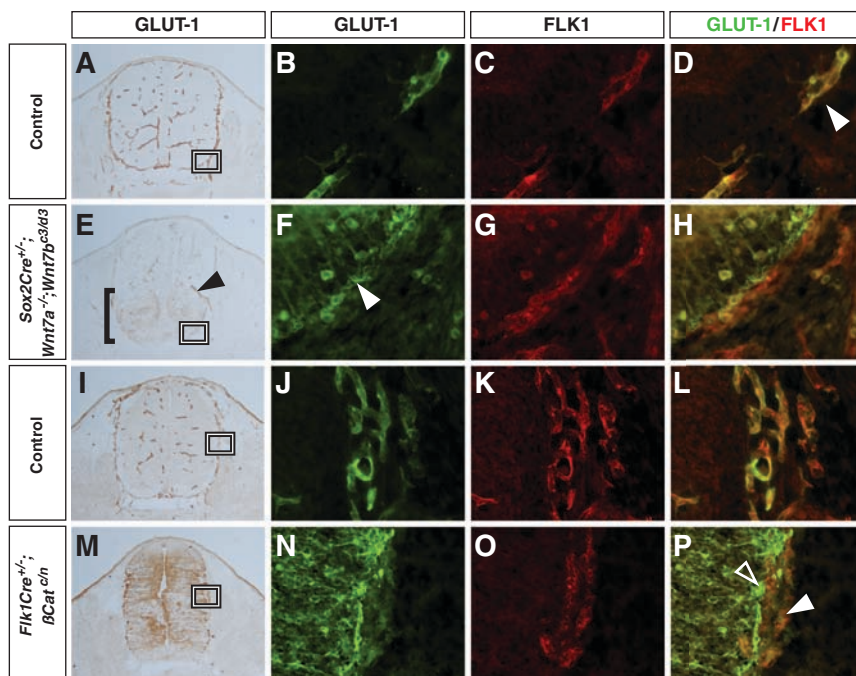
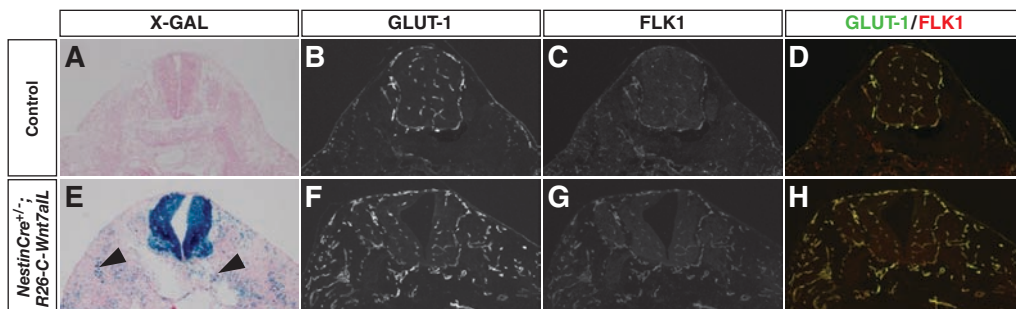


**Fig. 3.** Canonical Wnt signaling is necessary for differentiation of the CNS vasculature. (A to H) The BBB marker GLUT-1 was severely down-regulated at E12 to E12.5 in the PNVP and INVP in *Sox2Cre*<sup>+/-</sup>; *Wnt7a*<sup>-/-</sup>; *Wnt7b*<sup>c3/d3</sup> double mutants [(E) to (H)] relative to control embryos [(A) to (D)]; arrowhead in (D) points to a GLUT-1-positive vessel. Some vascular segments expressed low levels of GLUT-1 in the mutants [arrowhead in (E)]. Weak GLUT-1 activity remained in the ventral neuroepithelium when vascular invasion failed [bracket in (E), arrowhead in (F)]. (I to P) In *Flk1Cre*<sup>+/-</sup>;  $\beta$ Cat<sup>en</sup> embryos, at E12 a reduction of GLUT-1 in the PNVP relative to control embryos was evident [(I) to (L), (M) to (P); solid arrowhead in (P)]. However, strong GLUT-1 was detected in the neuroepithelium [(M) to (P); open arrowhead in (P)]. Boxes in (A), (E), (I), and (M) show the approximate region of (B) to (D), (F) to (H), (J) to (L), and (N) to (P) in separate sections, respectively.

**Fig. 4.** Ectopic *Wnt7a* expression is sufficient to induce GLUT-1 in endothelial cells outside the CNS. (A to H) *NestinCre*-mediated ectopic activation of a bicistronic message encoding *Wnt7a* and *E. coli* nuclear  $\beta$ -galactosidase in scattered cells outside the neural tube [(A), arrowheads in (E)] resulted in up-regulation of GLUT-1 in vascular endothelium outside the CNS [compare (F) to (H) with control embryos in (B) to (D)].





cellular target is the nascent endothelial network of the neural tube. These, and likely other Wnt family members, act through a canonical Wnt signaling pathway to promote formation and differentiation of the CNS vasculature. Whether this pathway also plays a later role in vascularization of other organ systems remains to be determined.

Our findings may have important clinical ramifications. For example, local reductions in Wnt signaling levels could potentially lead to malformation of CNS vasculature. In addition, if BBB properties in the adult are regulated by Wnt, altering Wnt activity may be a fruitful strategy for delivery of pharmacological agents to the CNS. Interestingly, there is a correlation between neoangiogenesis and  $\beta$ Cat accumulation in the endothelium of brain tumors such as gliomas and human glioblastoma multiforme (28, 29). This raises the possibility that canonical Wnt signaling may not only support vascular development but also promote tumor pathogenesis in the CNS.

#### References and Notes

1. A. M. Suburo, P. A. D'Amore, *Handb. Exp. Pharmacol.* **176**, 71 (2006).
2. B. Engelhardt, *Cell Tissue Res.* **314**, 119 (2003).
3. A. M. Miniño, M. P. Heron, B. L. Smith, *Deaths: Preliminary Data for 2004* (National Center for Health Statistics, Hyattsville, MD, 2006).
4. B. A. Parr, M. J. Shea, G. Vassileva, A. P. McMahon, *Development* **119**, 247 (1993).
5. B. A. Parr, A. P. McMahon, *Nature* **395**, 707 (1998).
6. B. A. Parr, V. A. Cornish, M. I. Cybulsky, A. P. McMahon, *Dev. Biol.* **237**, 324 (2001).
7. See supporting material on Science Online. The conditional Wnt7b allele is referred to as "c3" and the recombined allele as "d3."
8. K. A. Hogan, C. A. Ambler, D. L. Chapman, V. L. Bautch, *Development* **131**, 1503 (2004).
9. F. Tronche *et al.*, *Nat. Genet.* **23**, 99 (1999).
10. D. Graus-Porta *et al.*, *Neuron* **31**, 367 (2001).
11. M. Backman *et al.*, *Dev. Biol.* **279**, 155 (2005).
12. S. Maretto *et al.*, *Proc. Natl. Acad. Sci. U.S.A.* **100**, 3299 (2003).
13. L. A. Brown *et al.*, *Mech. Dev.* **90**, 237 (2000).
14. T. Motoike, D. W. Markham, J. Rossant, T. N. Sato, *Genesis* **35**, 153 (2003).
15. V. Brault *et al.*, *Development* **128**, 1253 (2001).
16. A. Cattelino *et al.*, *J. Cell Biol.* **162**, 1111 (2003).
17. H. Haegel *et al.*, *Development* **121**, 3529 (1995).
18. J. Huelsken *et al.*, *J. Cell Biol.* **148**, 567 (2000).
19. I. B. Lobov *et al.*, *Nature* **437**, 417 (2005).
20. W. Shu, Y. Q. Jiang, M. M. Lu, E. E. Morrisey, *Development* **129**, 4831 (2002).
21. S. J. Monkley, S. J. Delaney, D. J. Pennisi, J. H. Christiansen, B. J. Wainwright, *Development* **122**, 3343 (1996).
22. T. Ishikawa *et al.*, *Development* **128**, 25 (2001).
23. A. M. Goodwin, J. Kitajewski, P. A. D'Amore, *Growth Factors* **25**, 25 (2007).
24. K. Venkiteswaran *et al.*, *Am. J. Physiol. Cell Physiol.* **283**, C811 (2002).
25. M. Wright, M. Aikawa, W. Szeto, J. Papkoff, *Biochem. Biophys. Res. Commun.* **263**, 384 (1999).
26. T. N. Masckauchan *et al.*, *Mol. Biol. Cell* **17**, 5163 (2006).
27. T. N. Masckauchan, C. J. Shawber, Y. Funahashi, C. M. Li, J. Kitajewski, *Angiogenesis* **8**, 43 (2005).
28. H. Yano *et al.*, *Neurol. Res.* **22**, 527 (2000).
29. H. Yano *et al.*, *Neurol. Res.* **22**, 650 (2000).
30. We thank P. D'Amore for helpful discussions. Supported by a Wenner-Gren Foundations (Sweden) postdoctoral fellowship (J.M.S.), National Heart, Lung, and Blood Institute grant HL076393 (J.R.), and NIH grant DK054364 (A.P.M.). The authors have a patent pending on the basis of the results reported in this paper. A.P.M. has been a paid consultant for Merck, Genentech, and Wythe in the past 3 years.

#### Supporting Online Material

www.sciencemag.org/cgi/content/full/322/5905/1247/DC1  
Materials and Methods  
Figs. S1 to S19  
References

13 August 2008; accepted 6 October 2008  
10.1126/science.1164594

## Regulation of Pancreatic $\beta$ Cell Mass by Neuronal Signals from the Liver

Junta Imai,<sup>1</sup> Hideki Katagiri,<sup>2\*</sup> Tetsuya Yamada,<sup>1</sup> Yasushi Ishigaki,<sup>1</sup> Toshinobu Suzuki,<sup>1,2</sup> Hirohito Kudo,<sup>1,2</sup> Kenji Uno,<sup>2</sup> Yutaka Hasegawa,<sup>1</sup> Junhong Gao,<sup>2</sup> Keizo Kaneko,<sup>1,2</sup> Hisamitsu Ishihara,<sup>1</sup> Akira Niiijima,<sup>3</sup> Masamitsu Nakazato,<sup>4</sup> Tomoichiro Asano,<sup>5</sup> Yasuhiko Minokoshi,<sup>6</sup> Yoshitomo Oka<sup>1</sup>

Metabolic regulation in mammals requires communication between multiple organs and tissues. The rise in the incidence of obesity and associated metabolic disorders, including type 2 diabetes, has renewed interest in interorgan communication. We used mouse models to explore the mechanism whereby obesity enhances pancreatic  $\beta$  cell mass, pathophysiological compensation for insulin resistance. We found that hepatic activation of extracellular regulated kinase (ERK) signaling induced pancreatic  $\beta$  cell proliferation through a neuronal-mediated relay of metabolic signals. This metabolic relay from the liver to the pancreas is involved in obesity-induced islet expansion. In mouse models of insulin-deficient diabetes, liver-selective activation of ERK signaling increased  $\beta$  cell mass and normalized serum glucose levels. Thus, interorgan metabolic relay systems may serve as valuable targets in regenerative treatments for diabetes.

Obesity is a major public health concern in most industrialized countries (1). The development of insulin resistance in obese individuals can promote pancreatic  $\beta$  cell proliferation, a compensatory response that leads to increased insulin secretion (2). This in turn can lead to hyperinsulinemia, often observed in type 2 diabetes and metabolic syndrome. The mechanism(s) by which obesity-induced insulin resistance alters pancreatic  $\beta$  cell mass are poorly understood.

Metabolic communication between organs is essential for maintaining systemic glucose and energy homeostasis. In addition to humoral factors such as hormones and cytokines (3, 4), neuronal signals, both afferent (5, 6) and efferent (7), play important roles in such interorgan metabolic communication (8). Disruption of insulin signaling in the liver (9),

but not in muscle (10) or adipose tissue (11), induces pancreatic  $\beta$  cell hyperplasia and hyperinsulinemia, which suggests that the liver plays important roles in regulating pancreatic  $\beta$  cell mass.

To identify possible mechanisms underlying the compensatory responses of pancreatic  $\beta$  cells to obesity-induced insulin resistance, we studied proteins that are up-regulated or activated in the livers of mouse obesity models. One of these proteins is extracellular regulated kinase (ERK). We confirmed that ERK phosphorylation is enhanced in the livers of leptin-deficient (ob/ob) and high-fat-diet-induced obese (HF) mice (fig. S1A) (12), two murine obesity models that exhibit islet hyperplasia in response to insulin resistance.

Activation of mitogen-activated protein kinase/ERK kinase (MEK) results in ERK phosphoryl-

ation (13). To elucidate the metabolic roles of hepatic ERK activation, we expressed the constitutively active mutant of MEK-1 (CAM) in the liver (14). To distinguish endogenous from exogenous MEK1, we expressed the *Xenopus* homolog of MEK1. Mice administered an adenovirus encoding the LacZ gene were used as controls. Systemic infusion of recombinant adenoviruses resulted in expression of transgenes primarily in the liver, particularly hepatocytes (6) (fig. S1B), with no detectable expression in other organs, including the gastrointestinal tract (fig. S1C). Hepatic ERK phosphorylation, which is dependent on adenoviral titers (fig. S1D), was strongly enhanced on day 3 but had returned to the control level by day 9 after adenoviral administration (Fig. 1A). Hepatic ERK phosphorylation levels of CAM mice on day 3 were at most 2.1 times as high as those in the murine obesity model (fig. S1A). Hepatic lipid accumulation was markedly enhanced on day 3 but had also returned to the control level by day 14 (fig. S1E). No tumor formation was observed in the livers of CAM mice on day 44 (fig. S1F).

<sup>1</sup>Division of Molecular Metabolism and Diabetes, Tohoku University Graduate School of Medicine, Sendai 980-8575, Japan.

<sup>2</sup>Division of Advanced Therapeutics for Metabolic Diseases, Center for Translational and Advanced Animal Research, Tohoku University Graduate School of Medicine, Sendai 980-8575, Japan.

<sup>3</sup>Niigata University School of Medicine, Niigata 951-8510, Japan.

<sup>4</sup>Third Department of Internal Medicine, Miyazaki Medical College, University of Miyazaki, Miyazaki, Miyazaki 889-1692, Japan.

<sup>5</sup>Department of Medical Science, Graduate School of Medicine, University of Hiroshima, Hiroshima, Japan.

<sup>6</sup>Division of Endocrinology and Metabolism, Department of Developmental Physiology, National Institute for Physiological Sciences, Okazaki, Japan.

\*To whom correspondence should be addressed. E-mail: katagiri@mail.tains.tohoku.ac.jp

Notably, CAM-adenovirus administration induced insulin hypersecretion. CAM mice exhibited better glucose tolerance, with markedly higher serum insulin levels at 15 min after a glucose load during glucose tolerance testing (Fig. 1B) but no significant alterations in insulin sensitivity (Fig. 1C). Enhanced glucose-stimulated insulin

secretion was also observed in isolated pancreatic islets from CAM mice (fig. S2A). Hepatic expression levels of gluconeogenic enzymes were decreased in CAM mice (fig. S2B), which may account for the lowering of fasting blood glucose levels. In addition, pancreatic islet masses in CAM mice increased gradually, by a factor of 1.9 on day

15 (Fig. 1D and fig. S2C), with no significant differences in the body weights of LacZ and CAM mice (fig. S2D). The pancreatic insulin content of CAM mice also increased, rising to more than double the control level on day 16 (Fig. 1E), although these insulinotropic effects were attenuated after about 6 weeks (fig. S3, A and B). Hepatic activation of the p38 MAPK pathway—another MAPK pathway induced by administration of adenovirus encoding the constitutively active mutant of MAPK kinase 6 (CAMKK6) (fig. S4A)—did not cause insulin hypersecretion (fig. S4B) or increase pancreatic insulin content (fig. S4C).

To examine the mechanisms underlying the increased pancreatic insulin content in CAM mice, we performed bromodeoxyuridine (BrdU) staining. BrdU-positive cells were dramatically increased specifically in pancreatic islets in CAM mice, by a factor of 4.7, on day 3 after adenoviral treatment (Fig. 1F). Furthermore, nearly all (97.6%) BrdU-positive islet cells were also positive for insulin (Fig. 1G), indicating selective proliferation of pancreatic  $\beta$  cells in CAM mice.

The ERK pathway in pancreatic  $\beta$  cells is required for mitogenic responses (15); however, exogenous *Xenopus* MEK1 expression was undetectable in CAM mouse islets (Fig. 1H), making it unlikely that the  $\beta$  cell proliferation observed in CAM mice is due to direct infection of pancreatic  $\beta$  cells by the CAM-adenovirus.

We hypothesized that interorgan metabolic communication from the liver to pancreatic islets is the mechanism underlying insulin hypersecretion and selective proliferation of pancreatic  $\beta$  cells in CAM mice. Efferent vagal signals to the pancreas modulate insulin secretion (16) and pancreatic islet mass (17, 18). To examine the possible role of efferent vagal signals, we performed pancreatic vagotomy (PV) or a sham operation on the mice, followed by adenoviral administration 7 days later. PV almost completely abolished the CAM-induced glucose-lowering effects (Fig. 2A) and enhancement of glucose-stimulated insulin secretion (Fig. 2B), as well as the increases in pancreatic insulin content (Fig. 2C) and BrdU-positive islet cells (Fig. 2D) with no significant body weight alterations (fig. S5A). PV did not decrease glucose-stimulated insulin secretion, pancreatic insulin contents, or BrdU-positive islet cell numbers in LacZ mice (Fig. 2, B to D). These results strongly suggest that vagal nerves innervating the pancreas are involved in insulin hypersecretion and pancreatic  $\beta$  cell proliferation in CAM mice.

Thus, hepatic ERK activation is likely to transmit signals from the liver to the central nervous system (CNS), resulting in activation of the efferent vagus to the pancreas. To explore afferent signals from the liver to the CNS, we first performed hepatic vagotomy (HV). Contrary to the PV results, however, HV did not affect blood glucose levels (Fig. 2A), glucose-stimulated insulin secretion (Fig. 2B), or pancreatic insulin content (Fig. 2C) in CAM mice. Next, we blocked another type of afferent neuronal signal originating in the liver, the splanchnic nerve, which contains

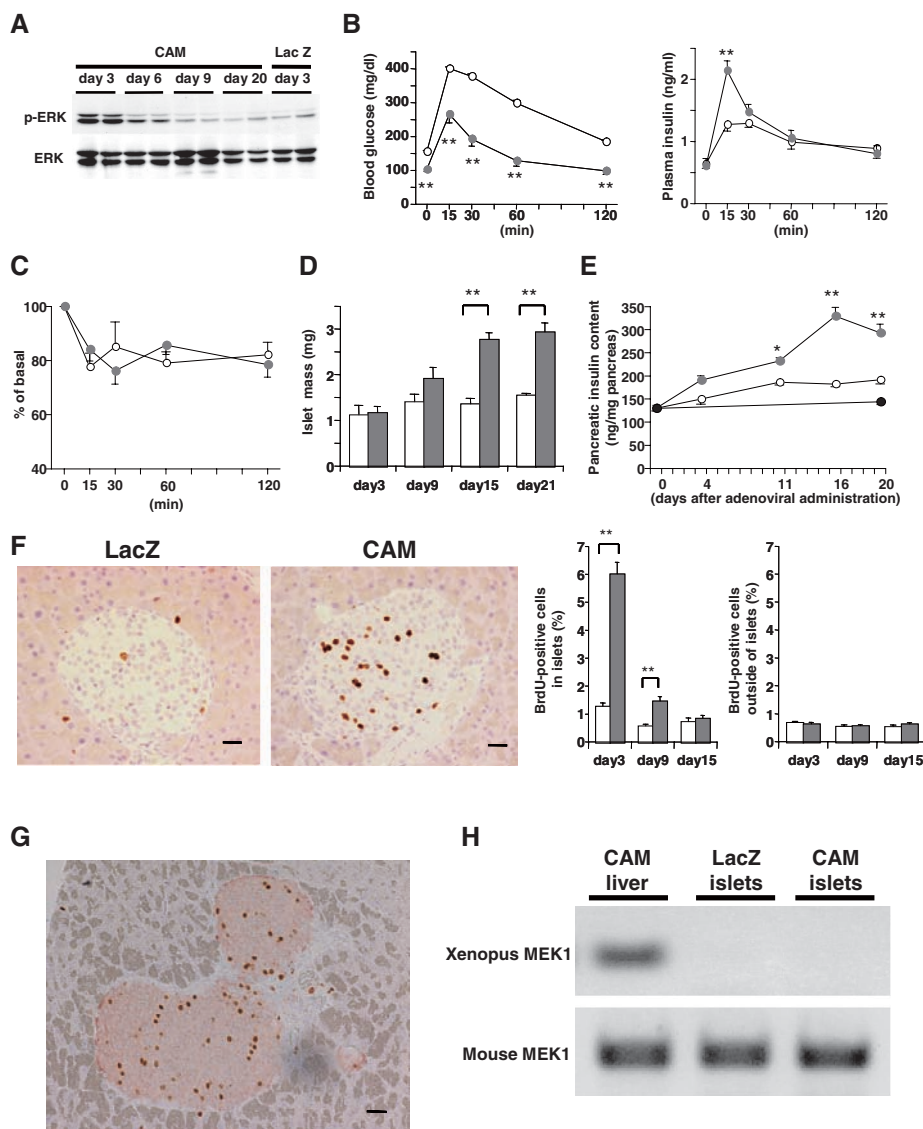


**Fig. 1.** Activation of hepatic ERK pathway in mice enhances glucose-stimulated insulin secretion and pancreatic  $\beta$  cell proliferation.

(A) Time courses of hepatic ERK phosphorylation after injection of  $1 \times 10^8$  plaque-forming units (PFU) per mouse of recombinant adenovirus containing CAM. (B) Blood glucose (left) and plasma insulin (right) levels during glucose tolerance tests performed on day 3 after adenoviral administration. (C) Blood glucose levels after intraperitoneal insulin injection on day 3 after adenoviral administration. Data are presented as percentages of the blood glucose levels immediately before insulin loading. In (B) and (C), open and closed circles indicate LacZ and CAM mice, respectively. (D and E) Time course of islet masses (D) and pancreatic insulin content (E). In (E), white, gray, and black circles indicate LacZ, CAM and untreated mice, respectively. (F) BrdU staining of pancreases. Representative images on day 3 after adenoviral administration are shown in the two left panels. Scale bar, 100  $\mu$ m. Time course of BrdU-positive cell ratios within (left) and outside of (right) the islets. In (D) and (F), open and closed bars indicate LacZ and CAM mice, respectively. (G) Double staining of pancreases from CAM mice with BrdU (brown) and insulin (red) on day 3 after adenoviral administration. A representative image is shown. Scale bar, 100  $\mu$ m. (H) Expression of exogenous (*Xenopus*) MEK1 (upper panel) and endogenous (mouse) MEK1 (lower panel) in pancreatic islets of LacZ and CAM mice on day 3 after adenoviral treatments. After 40 polymerase chain reaction cycles, the samples were subjected to gel electrophoresis. Data are presented as means  $\pm$  SEM. \*,  $P < 0.05$ , \*\*,  $P < 0.01$  versus LacZ mice, assessed by unpaired  $t$  test.

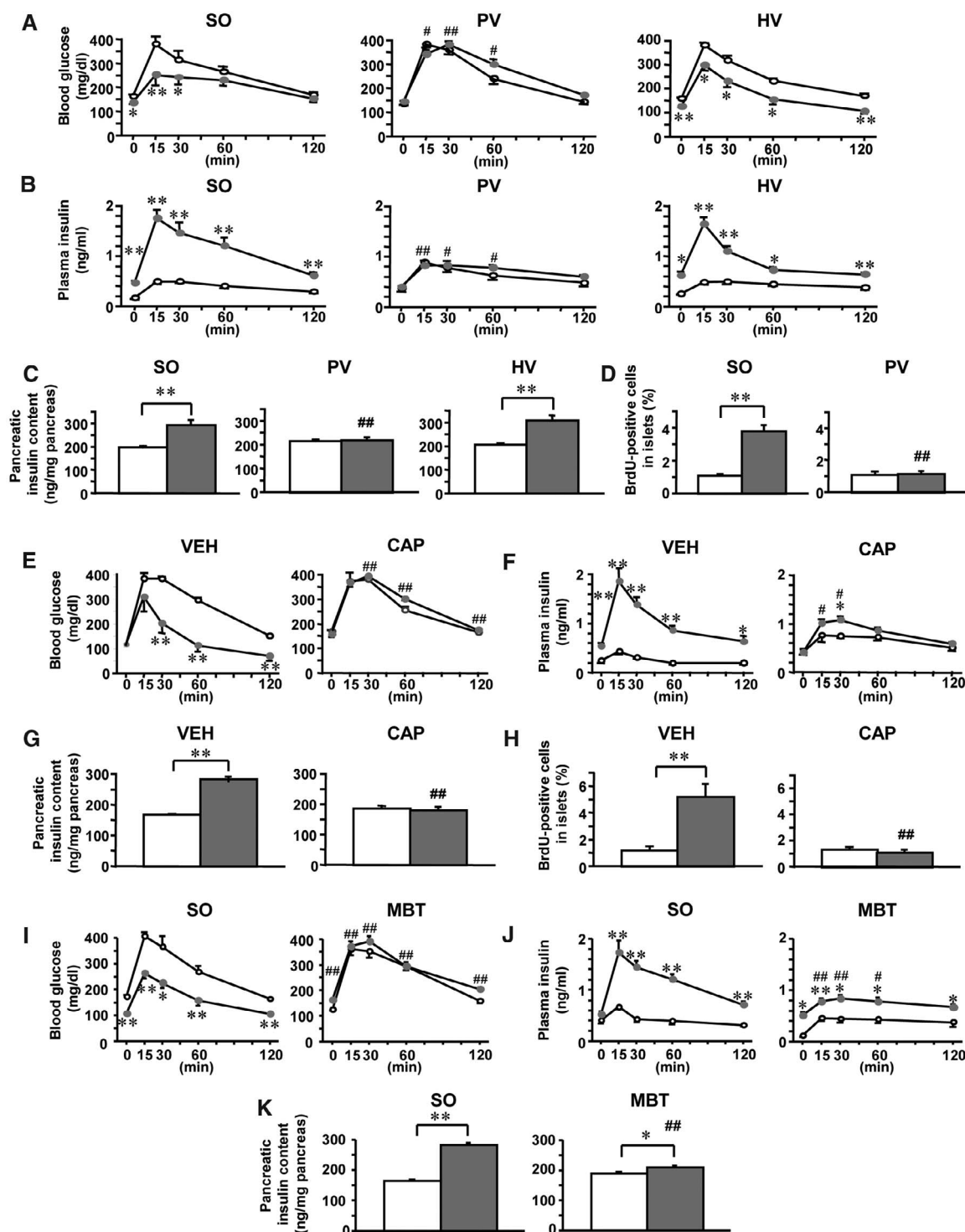


afferent fibers from the hepatobiliary system (19). Capsaicin application to the splanchnic nerve caused selective pharmacological deafferentation with no apparent effects on other nerves, including subdiaphragmatic vagal trunks (fig. S5B), and markedly blunted the glucose-lowering effects (Fig. 2E), glucose-stimulated insulin secretion (Fig. 2F), and increases in pancreatic insulin content (Fig. 2G) and BrdU-positive islet cells (Fig. 2H) in CAM mice. To exclude the possi-

bility that these capsaicin effects are mediated by blockade of the celiac branch of the vagal nerve, we performed denervation of the celiac branch in CAM mice. After celiac vagus dissection, CAM-adenovirus administration still increased glucose-stimulated insulin secretion during glucose tolerance testing (fig. S6A) and pancreatic insulin content (fig. S6B). Collectively, these results suggest afferent signals from the liver to the CNS to be at least partially mediated by afferent splanchnic nerves.

To evaluate CNS involvement, we performed bilateral midbrain transection (MBT), which was confirmed by functional (fig. S7A) and histological (fig. S7B) analyses. MBT markedly blunted the glucose-lowering effects (Fig. 2I), glucose-stimulated insulin secretion (Fig. 2J), and increase in pancreatic insulin content (Fig. 2K) in CAM mice, suggesting CNS involvement in this neuronal pathway. Thus, the mechanism underlying these selective islet responses observed in CAM

**Fig. 2.** Dissection of the pancreatic vagus, afferent blockade of the hepatic splanchnic nerve, or midbrain transection inhibits pancreatic  $\beta$  cell proliferation and insulin hypersecretion in CAM mice. (A and B, E and F, and I and J) Blood glucose [(A), (E), and (I)] and plasma insulin [(B), (F), and (J)] levels during glucose tolerance tests performed on day 3 after adenoviral administration, after sham operation (SO), pancreatic vagotomy (PV), and hepatic vagotomy (HV) [(A) and (B)], vehicle (VEH) and capsaicin (CAP) treatments [(E) and (F)], and SO and midbrain transection (MBT) [(I) and (J)]. (C, G, and K) Pancreatic insulin content of SO, PV and HV mice (C), VEH and CAP mice (G), and SO and MBT mice (K) on day 16 after adenoviral administration. (D and H) BrdU-positive cell ratios in whole islet cells in SO and PV mice (D) and VEH and CAP mice (H) on day 3 after adenoviral administration. Open bars/circles, LacZ mice; closed bars/circles, CAM mice. Data are presented as means  $\pm$  SEM. \*,  $P < 0.05$ ; \*\*,  $P < 0.01$  versus LacZ mice; #,  $P < 0.05$ ; ##,  $P < 0.01$  versus SO-CAM [(A) to (D) and (I) to (K)] or VEH-CAM [(E) to (H)] mice, assessed by unpaired  $t$  test.



mice involves interorgan communication mediated by the peripheral and the central nervous system.

To determine whether this neuronal interorgan communication is involved in islet hyperplasia in obesity-induced insulin resistance, we inhibited

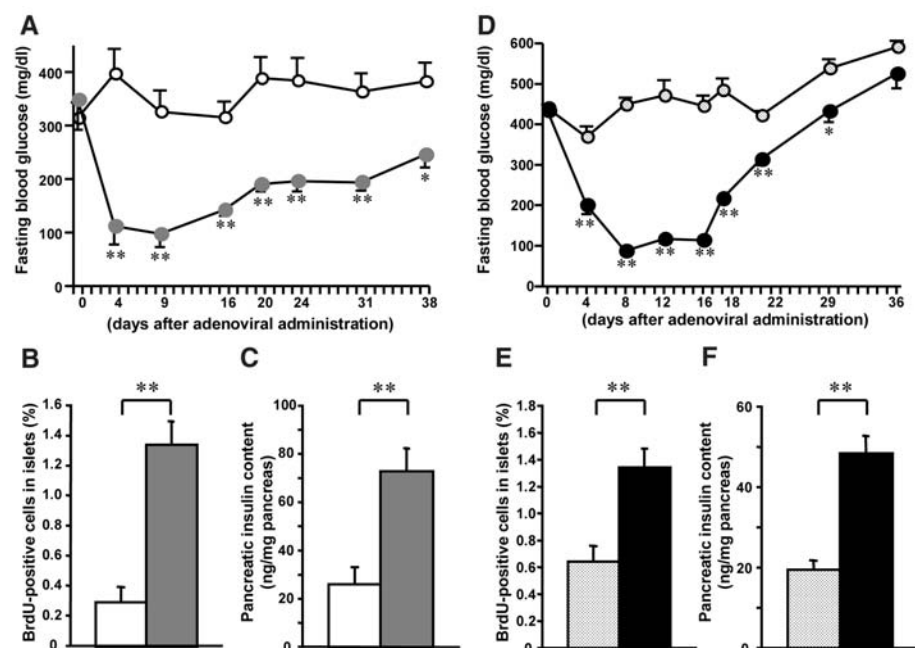
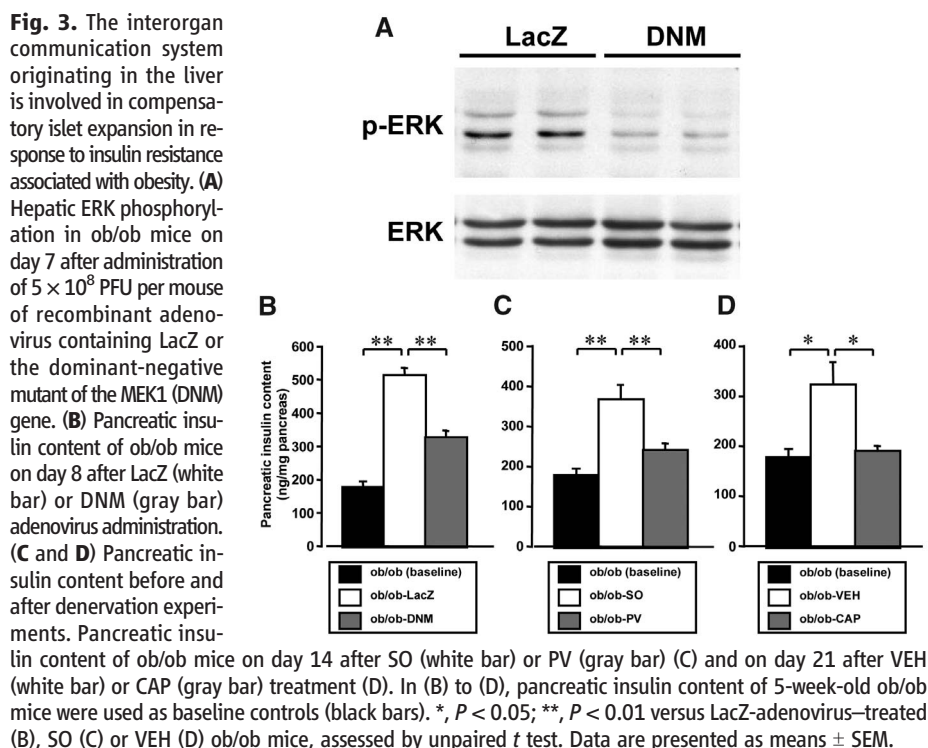


**Fig. 4.** Hepatic ERK activation induces pancreatic  $\beta$  cell proliferation and normalizes blood glucose levels in murine models of insulin-deficient diabetes. **(A and D)** Time course of fasting blood glucose levels in  $1.5 \times 10^8$  PFU per mouse of LacZ- and CAM-adenovirus-treated STZ (A) and Akita (D) mice. **(B and E)** BrdU-positive cell ratios in whole islet cells in STZ-LacZ and STZ-CAM mice (B) and Akita-LacZ and Akita-CAM mice (E) on day 3 after adenoviral administration. **(C and F)** Pancreatic insulin content of STZ-LacZ and STZ-CAM mice (C) and Akita-LacZ and Akita-CAM mice (F) on day 16 after adenoviral administration. (A) to (C): white bars/circles, STZ-LacZ mice; gray bars/circles, STZ-CAM mice. (D) to (F): dotted bars/circles, Akita-LacZ-mice; black bars/circles, Akita-CAM-mice. Data are presented as means  $\pm$  SEM. \*,  $P < 0.05$ ; \*\*,  $P < 0.01$  versus [(A) to (C)] STZ-LacZ mice or [(D) to (F)] Akita-LacZ mice, assessed by unpaired *t* test.

hepatic hyperactivation of ERK signaling (fig. S1A) by expressing the dominant-negative mutant of MEK1 (DNM) in the livers of ob/ob and HF obesity mice. DNM-adenovirus administration suppressed hepatic ERK phosphorylation (Fig. 3A and fig. S8A) without affecting hepatic p38 MAPK phosphorylation (fig. S4D). In LacZ-adenovirus-treated control ob/ob and HF mice, pancreatic insulin content rose significantly, paralleling obesity development. In contrast, DNM-adenovirus administration blunted these rises in pancreatic insulin content in ob/ob (Fig. 3B) and HF mice (fig. S8B). These findings suggest that activation of the hepatic ERK pathway is involved in pancreatic islet expansion during obesity development.

Next, we examined the involvement of afferent splanchnic and efferent pancreatic vagal nerves in pancreatic islet expansion during obesity development. In pair-fed ob/ob mice, blockade of these neuronal signals blunted the normal rise in pancreatic insulin content (Fig. 3, C and D). Furthermore, pancreatic vagotomy suppressed glucose-stimulated insulin secretion in ob/ob mice, resulting in impairment of glucose tolerance (fig. S8C). Taken together, these results suggest that this interorgan communication system is physiologically involved in compensatory islet responses to insulin resistance associated with obesity.

To determine whether targeting of this interorgan communication system affects insulin-deficient (type 1) diabetes, we administered CAM-adenovirus to streptozotocin (STZ)-induced diabetic mice, a murine model of pharmacological  $\beta$  cell loss. Fasting blood glucose levels of CAM-adenovirus-treated STZ mice were dramatically improved (Fig. 4A). This was associated with an increase in the number of BrdU-positive islet cells (Fig. 4B) and an increase in pancreatic insulin content (Fig. 4C). We then administered CAM-adenovirus to Akita mice (20), a murine model of endoplasmic reticulum (ER) stress-induced  $\beta$  cell loss (21), because ER stress in  $\beta$  cells is involved in diabetes development (22–24). In these mice as well, CAM-adenovirus treatment lowered blood glucose levels (Fig. 4D), enhanced proliferation of pancreatic islet cells (Fig. 4E), and increased pancreatic insulin content (Fig. 4F). In both these mouse models of insulin-deficient diabetes, CAM-adenovirus treatment greatly improved glucose tolerance by raising serum insulin levels (fig. S9, A and C) but did not significantly alter insulin sensitivity (fig. S9, B and D). In STZ-induced diabetic mice, the glucose-lowering effect induced by CAM persisted for at least 38 days (Fig. 4A), although in Akita mice it was gradually attenuated and was no longer significant by day 36 (Fig. 4D), possibly due to ER stress-induced apoptosis of regenerated  $\beta$  cells. Thus, manipulation of this interorgan communication system may lead to the development of novel therapeutic strategies for insulin-deficient diabetes.

We have identified a neuronal relay that induces proliferation of pancreatic  $\beta$  cells in response to insulin resistance, indicating that the CNS obtains information from peripheral organs and mod-



ulates pancreatic islet mass. Hepatic ERK activation is likely to play an important role in compensatory islet hyperplasia, although it is not yet clear how ERK signaling affects the neuronal pathway. The therapeutic effects we observed in two mouse models of insulin-deficient diabetes are especially noteworthy. Type 1 diabetes mellitus is characterized by progressive loss of pancreatic  $\beta$  cells, leading to a life-long insulin dependency. Recently, it was reported that  $\beta$  cell mass is also decreased in type 2 diabetes (25). Although substantial progress has been made with therapies that are based on transplantation of pancreatic islets (26), immune rejection and donor supply are still major challenges. In this context, therapeutic manipulation of the interorgan signaling mechanism described here may merit investigation as a potential strategy for regeneration of a patient's own  $\beta$  cells. Our results may open a new paradigm for regenerative medicine: regeneration of damaged tissues by targeting of interorgan communication systems, especially neural pathways.

References and Notes

1. J. P. Despres, I. Lemieux, *Nature* **444**, 881 (2006).  
2. M. Prentki, C. J. Nolan, *J. Clin. Invest.* **116**, 1802 (2006).  
3. J. M. Friedman, J. L. Halaas, *Nature* **395**, 763 (1998).  
4. E. D. Rosen, B. M. Spiegelman, *Nature* **444**, 847 (2006).  
5. T. Yamada *et al.*, *Cell Metab.* **3**, 223 (2006).  
6. K. Uno *et al.*, *Science* **312**, 1656 (2006).  
7. T. K. Lam, G. J. Schwartz, L. Rossetti, *Nat. Neurosci.* **8**, 579 (2005).  
8. H. Katagiri, T. Yamada, Y. Oka, *Circ. Res.* **101**, 27 (2007).  
9. M. D. Michael *et al.*, *Mol. Cell* **6**, 87 (2000).  
10. J. C. Bruning *et al.*, *Mol. Cell* **2**, 559 (1998).  
11. M. Bluher *et al.*, *Dev. Cell* **3**, 25 (2002).  
12. S. Yang, H. Z. Lin, J. Hwang, V. P. Chacko, A. M. Diehl, *Cancer Res.* **61**, 5016 (2001).  
13. L. Chang, M. Karin, *Nature* **410**, 37 (2001).  
14. Materials and methods are available as supporting material on Science Online.  
15. R. K. Gupta *et al.*, *Genes Dev.* **21**, 756 (2007).  
16. D. Gautam *et al.*, *Cell Metab.* **3**, 449 (2006).  
17. T. Kiba *et al.*, *Gastroenterology* **110**, 885 (1996).  
18. A. Edvell, P. Lindstrom, *Am. J. Physiol.* **274**, E1034 (1998).  
19. H. R. Berthoud, *Anat. Rec. A Discov. Mol. Cell. Evol. Biol.* **280**, 827 (2004).  
20. J. Wang *et al.*, *J. Clin. Invest.* **103**, 27 (1999).

21. S. Oyadomari *et al.*, *J. Clin. Invest.* **109**, 525 (2002).  
22. H. P. Harding, D. Ron, *Diabetes* **51** (suppl. 3), S455 (2002).  
23. R. J. Kaufman, *J. Clin. Invest.* **110**, 1389 (2002).  
24. H. Ishihara *et al.*, *Hum. Mol. Genet.* **13**, 1159 (2004).  
25. A. E. Butler *et al.*, *Diabetes* **52**, 102 (2003).  
26. A. M. Shapiro *et al.*, *New Engl. J. Med.* **355**, 1318 (2006).  
27. We thank M. Yokoyama for the generous gift of recombinant adenoviruses. This work was supported by Grants-in Aid (H.K., Y.O., and J.I.); the 21st Center of Excellence (COE) (H.K.) and Global-COE (Y.O.) programs from the Ministry of Education, Culture, Sports, Science and Technology of Japan; and a Grant-in Aid (Y. O.) from the Ministry of Health, Labor and Welfare of Japan. Tohoku University, J. I., H.K., and Y.O. have applied for patents related to this work in the United States and Japan.

**Supporting Online Material**  
[www.sciencemag.org/cgi/content/full/322/5905/1250/DC1](http://www.sciencemag.org/cgi/content/full/322/5905/1250/DC1)  
Materials and Methods  
Figs. S1 to S9  
References

5 February 2008; accepted 15 October 2008  
10.1126/science.1163971

# Control of Toxic Marine Dinoflagellate Blooms by Serial Parasitic Killers

Aurelie Chambouvet, Pascal Morin, Dominique Marie, Laure Guillou\*

The marine dinoflagellates commonly responsible for toxic red tides are parasitized by other dinoflagellate species. Using culture-independent environmental ribosomal RNA sequences and fluorescence markers, we identified host-specific infections among several species. Each parasitoid produces 60 to 400 offspring, leading to extraordinarily rapid control of the host's population. During 3 consecutive years of observation in a natural estuary, all dinoflagellates observed were chronically infected, and a given host species was infected by a single genetically distinct parasite year after year. Our observations in natural ecosystems suggest that although bloom-forming dinoflagellates may escape control by grazing organisms, they eventually succumb to parasite attack.

Although photosynthetic dinoflagellates are important primary producers in marine ecosystems, some bloom-forming species produce toxins that can cause illness and even death in humans (1). These harmful algal blooming (HAB) species are particularly prevalent in warm, stratified, and nutrient-enriched coastal waters (2, 3). Documented HAB events have increased substantially during recent decades as a result of extensive coastal eutrophication and, possibly, global climate change (4).

In 1968, Taylor proposed using specific dinoflagellate parasites, such as the Syndiniales *Amoebophrya* spp. (5), as biological control agents for HAB organisms. This idea was rejected because of the apparent lack of specificity of the parasites; however, the homogeneous

morphology of these parasites masks extensive genetic diversity (6). Recently, the widespread existence of *Amoebophrya* spp. was "redis-

covered" by culture-independent methods, and they were renamed "novel alveolate group II" (7–9). This eukaryotic lineage frequently forms 10 to 50% of sequences retrieved within coastal environmental clone libraries (10, 11). Indeed, up to 44 distinct clusters have been detected, with extensive intraclade genetic diversity (12); the genetic diversity of the parasites appears to be comparable to the species richness of their hosts.

We sampled a marine coastal estuary (the Penzé River, northern Brittany, France) for 3 consecutive years (2004 to 2006), using catalyzed reporter deposition fluorescent in situ hybridization (CARD-FISH; tables S1 and S2) with probes specifically designed to detect group II alveolates. Our aim was to examine how the abundance and diversity of the parasites influenced their host populations in natural environments. In May and June of each year, we observed a rapid succession of four major species of photosynthetic

**Table 1.** Specificity of Syndiniales group II in the Penzé estuary in 2005 and 2006. Prevalences (percentage of infected cells) when a general oligonucleotide probe (ALV01) and clade-specific probes were used are shown (results for clades 1, 2, and 14; for description of clades see Fig. 3). Observations of a mature trophont inside the host cell are indicated by an asterisk. ND, not done. Numbers in parentheses show the percentage of the signal obtained when the general probe was used, explained by the clade-specific probes.

Host species	Dates (day/month/year)	Syndiniales group II, all clades	Syndiniales group II, clade 1	Syndiniales group II, clade 2	Syndiniales group II, clade 14
<i>H. rotundata</i>	03/06/2005	26*	26* (100%)	ND	ND
	29/05/2006	29*	23* (79%)	0	2 (<1%)
<i>S. trochoidea</i>	14/06/2005	23*	ND	11* (48%)	ND
	16/06/2006	33*	0	18* (55%)	3 (<1%)
	18/06/2006	26*	0	29* (>100%)	9 (3%)
<i>A. minutum</i>	14/06/2005	40*	0	0	0
	22/06/2006	19*	6 (3%)	0	0
<i>H. triquetra</i>	20/06/2005	10*	ND	0	11* (>100%)
	22/06/2006	14*	0	0	14* (100%)

Station Biologique, CNRS, UMR 7144, Place Georges Teissier, 29682 Roscoff Cedex, France; and Laboratoire Adaptation et Diversité en Milieu Marin, Université Pierre et Marie Curie, Paris 6, Paris, France.

\*To whom correspondence should be addressed. E-mail: lguillou@sb-roscoff.fr

dinoflagellates (the dominant species changed every week; Fig. 1), namely *Heterocapsa rotundata* at the end of May, followed by *Scrippsiella trochoidea*, *Alexandrium minutum*, and *H. triquetra*. These species all have a worldwide distribution in marine coastal ecosystems, and one of them, *A. minutum*, produces paralytic shellfish poison.

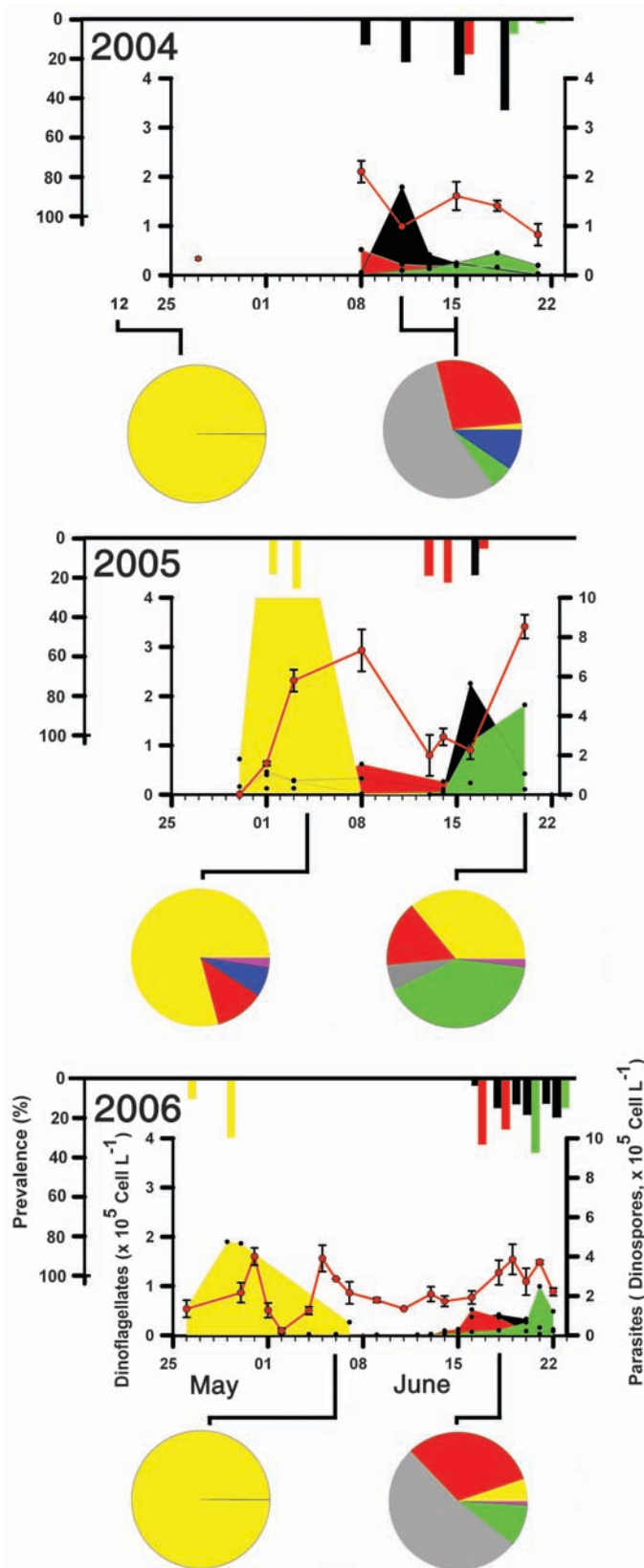
No significant correlation was observed between the decline of the individual dinoflagellate species and the physicochemical environmental variables (nitrate, nitrite, phosphate, silicate, salinity, temperature, or tidal amplitude), which remained relatively constant during the 3-year study period (figs. S1 and S2). There was pervasive chronic infection of all the observed dinoflagellate species by Syndiniales; the infections occurred every year, even when host species abundance was low (Fig. 2). The prevalence of parasitized dinoflagellate cells reached 46%, with a mean value of 21% (Fig. 1) during summer. Similar values were obtained for all the species observed, including the toxic algae *A. minutum*, and are consistent with previously published data from a variety of coastal settings and several dinoflagellate host taxa (13–18). A similar average prevalence (28%) was observed for *Dinophysis norvegica* from the North Sea when a specific FISH detection approach was used (19). The sensitivity of the CARD-FISH analysis permitted the detection of early-stage infections as well as all the life-cycle stages of the parasite, including the very small free-living stage (3 to 5  $\mu\text{m}$  in diameter). In all cases, the parasites closely corresponded to the description of *Amoebophrya* spp. provided by Cachon in 1964 (20).

Infections were initiated by the invasion of host cells by one or several very small infective cells called dinospores (20) (Fig. 2A). After several rounds of active nuclear replication, a large multinucleated trophont (the endoparasitic stage, Fig. 2, B to D) characteristic of the genus *Amoebophrya* is produced. Cultures and field observations show that this trophont matures in 2 days (13, 21). The pressure of the trophont during the final stages of maturation distorts and enlarges the dinoflagellate cells (compare Fig. 2, B and C). Ultimately, the trophont ruptures the host cell wall and is elongated by a final evagination to form a swimming structure, the vermiform stage (20) (Fig. 2, D and E). Within a few hours, the vermiform structure fragments into 60 to 400 dinospores (13, 20, 21), each of which is able to reinfect a new host.

The amplification of newly infective parasite cells has the capacity to rapidly counter the growth rate of the host. Accordingly, the decline of the dinoflagellate populations correlated with the release of the free-living form of the parasite in the ecosystem; the dinospores were detectable in the ecosystem within 10 days of their release (a phenomenon illustrated by *H. rotundata* at the beginning of June 2005 and by *A. minutum* in 2004, Fig. 1). Although large numbers of dinospores were produced during the population

decline of one dinoflagellate species, they did not prevent the growth of any other species, strongly suggesting that the parasites are host-specific. Each year, four main clades of group II Syndiniales were always detected (Fig. 1):

**Fig. 1.** Dinoflagellate-parasitoid successions and abundances in the Penzé estuary (northern Brittany, France) and the genetic clades of parasites occurring during May and June during 3 consecutive years (2004, 2005, and 2006). Dinoflagellate species are shown in the colored solid curves and by the left axis. Yellow, *H. rotundata*; red, *S. trochoidea*; black, *A. minutum*; green, *H. triquetra*. The free-living stage (dinospore) of group II Syndiniales is shown by the red line and the right axis. Prevalences (percentage of infected host) are shown in the inverted histogram at the top of each panel with the same color code as used for the host. Dinoflagellates were counted by microscopy, and dinospores and prevalence were detected with the general probe ALV01 by FISH. Error bars indicate SDs between triplicates. The pie charts represent the relative contribution, in percentages, of clones belonging to group II Syndiniales obtained from biased polymerase chain reaction amplifications made at two different dates during the monitored period. Yellow, clade 1; red, clade 2; gray, clade 3; green, clade 14; blue, clade 32; pink, clade 42.





separated from each other by at least 44 point mutations (Fig. 3).

Significant intraclade genetic microdiversity was found within environmental sequences (from the 238 sequences analyzed, 170 haplotypes were different). Clades 1 and 3 both have a starlike

distribution, with an excess of rare haplotypes (Fig. 3). Furthermore, the results of Tajima's D test were significantly negative (table S3), suggesting a recent evolutionary origin and/or a rapid evolutionary divergence resulting from strong selection pressure. Clades 2 and 14 are more complex,

probably indicating a more ancient evolutionary history and cryptic species (fig. S3).

The specificity of the four main parasite clades detected was assessed by FISH, using specific oligonucleotide probes (tables S1 and S2). Clades 1, 2, and 14 each infected a single dinoflagellate species: *H. rotundata*, *S. trochoidea*, and *H. triquetra*, respectively (Table 1). This specificity is very stable over time; the same parasite clade infected the same species year after year. In all cases, for a given host/parasite pair, the prevalence threshold detected for a given host species when the general probe for group II Syndiniales was used was similar to the value obtained when the clade-specific probe was used (Table 1). Occasionally, parasites attacked non-optimal host species, but mature trophonts were not observed (Table 1). Similar nonspecific and unproductive infections have been also observed in cultured strains of *Amoebophrya* (21, 22). Unfortunately, we were not able to detect any cells targeted by clade 3 using the FISH technique, and none of the major clades (1, 2, 3, and 14) detected in our genetic clone libraries seemed to be specific to the toxic dinoflagellate *A. minutum*.

HABs occur when dinoflagellates escape not only predation but also parasitic infection. *A. minutum* had been suspected to be invasive after being introduced along the Atlantic coast of France, where blooms were first observed in the late 1980s (22). Blooms of *A. minutum* in the Penzé estuary were recorded for the first time in 1994 (fig. S4). Cell densities were reported to exceed  $10 \times 10^6$  cells/liter (22). Over the ensuing 9 years, toxic blooms occurred with remarkable regularity in the Penzé (22), but although this species is still present in the ecosystem, blooms no longer occur (fig. S5). The population of *A. minutum* is now regulated by the parasitoids.

Environmental sequences belonging to Syndiniales have been detected in almost every marine ecosystem (12). Their host ranges are extremely diverse, extending from dinoflagellates to ciliates, radiolarians, cercozoans, chaetognaths, copepods, cnidarians, appendicularians, crabs, and even fish eggs. Thus, most marine planktonic groups are potentially affected by these parasites, which like the viruses that control bacterial populations, play a top-down control role in their host populations. However, the dinoflagellate parasites have a different impact on organic carbon transfer: In contrast to viruses, dinospores can be directly grazed by larger predators and thus are implicated in carbon transfer to higher trophic levels.

The capacity of these parasitoids to control their hosts is highly dependent on the parasitic fitness and mechanisms underlying the parasitic specificity. This also means that these natural biological controls are potentially less efficient when an exotic species is newly imported into an ecosystem (the enemy release hypothesis) (23) or when a rare species is promoted into abundance by substantial environmental change (such as coastal eutrophication or climate change).

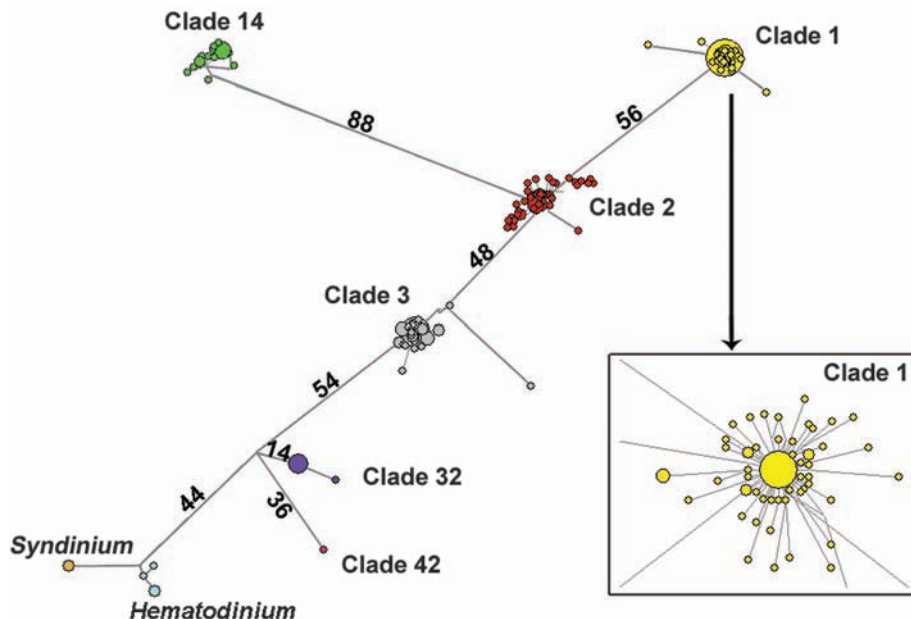
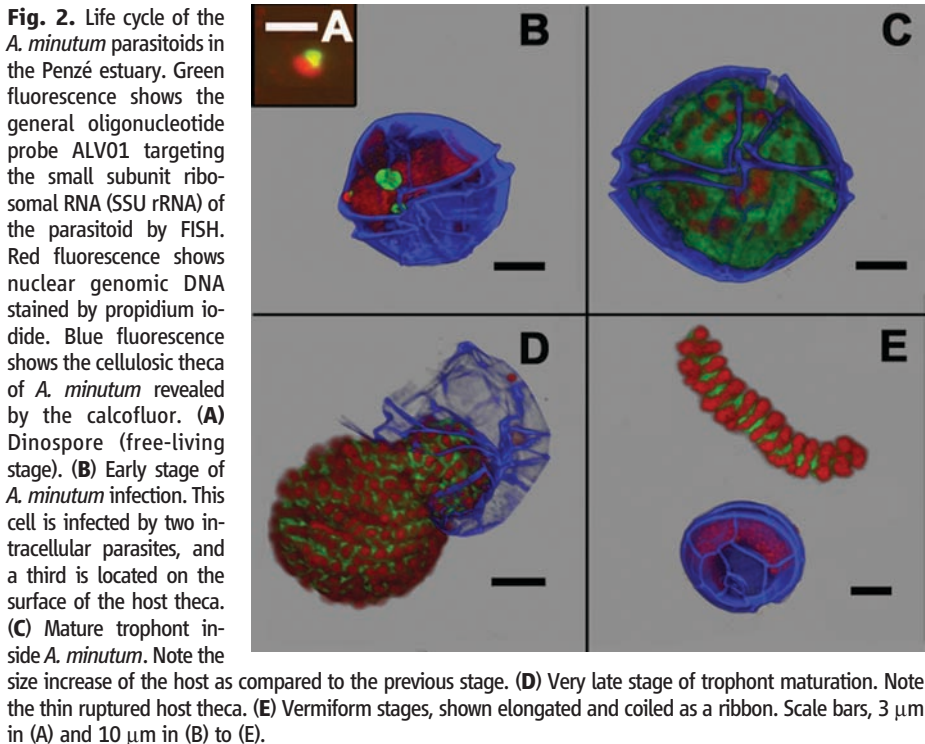


**Fig. 3.** Median-joining network depicting the phylogenetic relationship among environmental Syndiniales group II SSU rRNA gene sequences obtained from the Penzé estuary over 3 years (238 sequences in total). The solid colored circles follow the same color code as in Fig. 1. The size of each circle is proportional to the corresponding haplotype frequency. Each branch length is proportional to the number of mutational steps (the number of mutations between major clades is written above the branch). Four sequences of *Hematodinium* sp. and four of *Syndinium* sp. (group IV Syndiniales that are parasites of decapods and copepods, respectively) were used as outgroups.

Thus, the recent increase of inshore HAB events may originate in geographical and temporary disruptions between these dinoflagellates and their natural parasites.

### References and Notes

1. A. Zingone, H. O. Enevoldsen, *Ocean Coast. Manage.* **43**, 725 (2000).
2. T. J. Smayda, C. S. Reynolds, *J. Plankton Res.* **23**, 447 (2001).
3. T. J. Smayda, C. S. Reynolds, *J. Sea Res.* **49**, 95 (2003).
4. D. M. Anderson, *Nature* **388**, 513 (1997).
5. F. J. R. Taylor, *J. Fish. Res. Board Can.* **25**, 2241 (1968).
6. J. H. Gunderson, S. A. John, W. C. Boman, D. W. Coats, *J. Eukaryot. Microbiol.* **49**, 469 (2002).
7. P. López-García, F. Rodríguez-Valera, C. Pedrós-Alió, D. Moreira, *Nature* **409**, 603 (2001).
8. S. Y. Moon-van der Staay, R. De Wachter, D. Vaulot, *Nature* **409**, 607 (2001).
9. B. Díez, C. Pedrós-Alió, R. Massana, *Appl. Environ. Microbiol.* **67**, 2932 (2001).
10. K. Romari, D. Vaulot, *Limnol. Oceanogr.* **43**, 784 (2004).
11. L. K. Medlin, K. Metfies, H. Mehl, K. Wiltshire, K. Valentin, *Microb. Ecol.* **52**, 53 (2006).
12. L. Guillou *et al.*, *Environ. Microbiol.* **10**, 3349 (2008).
13. D. W. Coats, K. R. Bockstahler, *J. Eukaryot. Microbiol.* **41**, 586 (1994).
14. D. W. Coats, E. J. Adam, C. L. Gallegos, S. Hedrick, *Aquat. Microb. Ecol.* **11**, 1 (1996).
15. E. Chatton, *Arch. Zool. Exp. Gen.* **59**, 1 (1920).
16. P. Lopez-Garcia, H. Philippe, F. Gail, D. Moreira, *Proc. Natl. Acad. Sci. U.S.A.* **100**, 697 (2003).
17. I. G. Lizarraga, D. A. S. Beltrones, *Acta Bot. Mex.* **65**, 1 (2003).
18. L. Nishitani, G. Erickson, K. K. Chew, in *Toxic Dinoflagellates*, D. M. Anderson, A. W. White, D. G. Baden, Eds. (Elsevier, New York, 1985), pp. 225–232.
19. P. S. Salomon, S. Janson, E. Graneli, *Environ. Microbiol.* **5**, 1046 (2003).
20. J. Cachon, *Ann. Sci. Nat. Zool. Paris.* **VI**, 1 (1964).
21. D. W. Coats, M. G. Park, *J. Phycol.* **38**, 520 (2002).
22. J. F. Maguer, M. Wafar, C. Madec, P. Morin, E. Erard-Le Denn, *Limnol. Oceanogr.* **49**, 1108 (2004).
23. R. M. Keane, M. J. Crawley, *Trends Ecol. Evol.* **17**, 164 (2002).
24. We thank A. Carlier, D. Charruau, A. Groisillier, and S. Maury for their earlier contributions to this work; D. Vaulot, P. von Dassow, and A. Worden for critically reading this manuscript; P. Falkowski for his help with corrections and discussions; W. Coats for cultures of *Amoebophrya* spp. that greatly helped us to test the oligonucleotide probes and for constructive discussions; D. Jollivet for his help with genetic population analysis; The Service Mer et Observation of the Roscoff Biological Station; and E. Macé for sample collections and nutrient acquisition parameters. This work was financially supported by the Groupement d'Intérêt Scientifique Génomique Marine and the French Agence Nationale de la Recherche project Aquapadox. We also thank Zeiss for help in the acquisition of the confocal micrographs. Sequences have been deposited in GenBank under accession numbers FJ356776 to FJ357007. The authors declare no competing financial interests.

### Supporting Online Material

www.sciencemag.org/cgi/content/full/322/5905/[page]/DC1  
Materials and Methods  
SOM Text  
Figs. S1 to S5  
Tables S1 to S3  
References

7 August 2008; accepted 14 October 2008  
10.1126/science.1164387

## Antimicrobial Defense and Persistent Infection in Insects

Eleanor R. Haine,<sup>1</sup> Yannick Moret,<sup>2</sup> Michael T. Siva-Jothy,<sup>1</sup> Jens Rolff<sup>1\*</sup>

During 400 million years of existence, insects have rarely succumbed to the evolution of microbial resistance against their potent antimicrobial immune defenses. We found that microbial clearance after infection is extremely fast and that induced antimicrobial activity starts to increase only when most of the bacteria (99.5%) have been removed. Our experiments showed that those bacteria that survived exposure to the insect's constitutive immune response were subsequently more resistant to it. These results imply that induced antimicrobial compounds function primarily to protect the insect against the bacteria that persist within their body, rather than to clear microbial infections. These findings suggest that understanding of the management of antimicrobial peptides in natural systems might inform medical treatment strategies that avoid the risk of drug resistance.

By contrast with the clinical use of antibiotics, resistance to natural antibiotics appears to be rare (1, 2). Possibly, natural antibiotics play a different role in the wild than in medical applications (3), and our lack of understanding of

their natural role results in unforeseen problems when they are used therapeutically, such as the rapid emergence of antibiotic-resistant pathogens.

Insects rely on a suite of systemic responses to combat infection (4) that can be classified into

two main types. "Constitutive" defenses are always present and ready to act; they rely on the response of insect immune cells (haemocytes) and several rapidly activated enzyme cascades such as phenoloxidase (5, 6) to defend against pathogens. Coupled with this line of defense is the "induced" response, which consists mainly of a suite of antimicrobial peptides (7). This component of the antimicrobial response takes at least 1 to 3 hours to generate (8) and 12 to 48 hours to reach peak levels (9). The induced response persists for weeks in a variety of insects: for example, at least 14 days in bumble bees (10) and mealworm beetles (9), and up to 44 days in dragonflies (11). Because immune responses bear costs [e.g., antagonistic pleiotropy (12), metabolic costs (13), and self-harm (14)], these slow and long-lasting antimicrobial responses, which are

<sup>1</sup>Department of Animal and Plant Sciences, University of Sheffield, Sheffield S10 2TN, UK. <sup>2</sup>Équipe Ecologie Évolutive, UMR CNRS 5561 Biogéosciences, Université de Bourgogne, 6 boulevard Gabriel, 21000 Dijon, France.

\*To whom correspondence should be addressed. E-mail: jor@sheffield.ac.uk

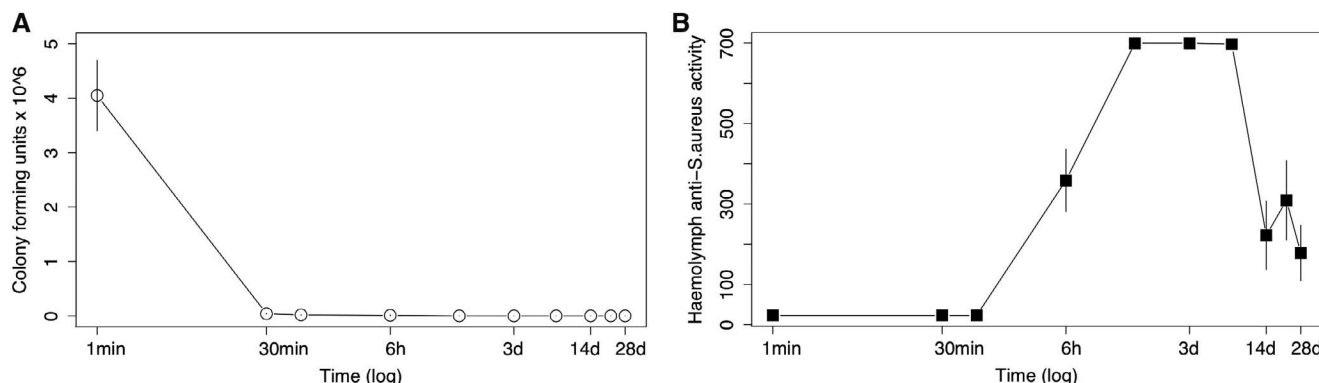


**Fig. 1.** The number of colony-forming units (CFU) recovered from *T. molitor* haemolymph over 28 days (A), and the haemolymph anti-*S. aureus* activity from the same individuals (B). Induced haemolymph anti-*S. aureus* activity

was measured as the number of *S. aureus* CFUs killed during 2 hours of exposure to *T. molitor* haemolymph and is shown as CFU  $\times 10^3$ . Each point represents the mean number of CFUs from 7 to 10 beetles ( $\pm 1$  SEM).



under selection in the wild (15), must have an as yet undetermined adaptive benefit. Insects may maintain heightened defenses after an insult to deal with reinfection by the same agent (16, 17). However, recent work on *Drosophila melanogaster* showed that haemocytes, rather than antimicrobial peptides, are responsible for the protection against secondary infection (18).

Alternatively, we propose that long-lasting antimicrobial responses serve to “mop up” bacteria that survive the constitutive immune response and eliminate or control these potentially resistant bacteria from the haemocoel. At the level of an individual host, this would prevent the reappearance of infection that is refractory to the host’s constitutive defenses. A consequence of this process would be a reduction in the emergence of resistant bacteria that at least provides a means of managing persistent infections, especially because most insects use a variety of antimicrobial peptides (7).

We made three predictions from this basis. (i) Most bacteria will be eliminated before the induced antimicrobial response occurs. (ii) Some bacteria will survive the initial haemocyte-mediated immune response and persist in the haemolymph for at least as long as the induced antimicrobial response persists. (iii) When exposed to a naïve insect, these surviving bacteria will be more resistant to the insect’s constitutive immune response than the original pathogen strain.

We conducted two studies to test our predictions. First, we examined how quickly a dose of bacteria is cleared from insect haemolymph by the constitutive immune system, while measuring

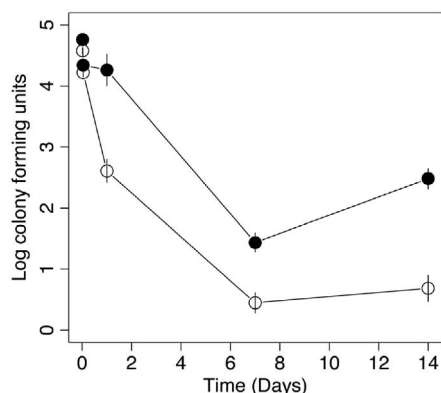


**Fig. 2.** The  $\log_{10}$  of CFUs recovered from *T. molitor* haemolymph after injection of the host-naïve strain of *S. aureus* (open circles) and after injection of surviving bacteria into naïve individuals (closed circles). Briefly, glycerol stocks were made from bacterial colonies recovered at five different time points after injection of the original *S. aureus* strain; these were then used to immunize naïve beetles, and the number of surviving CFUs was counted at the same time points, i.e., bacteria recovered after 1 day of exposure to the beetle immune response were injected into naïve individuals, and the number of CFUs surviving was counted after 1 day. Each data point represents the mean log CFUs counted from 10 individuals  $\pm$  1 SEM.

induced haemolymph antimicrobial activity in the same insects [Supporting Online Material (SOM)]. Second, we conducted a selection experiment in which we compared the survivorship of bacteria within hosts that had been exposed to insect immune responses for different times with the naïve population from which they were drawn.

We measured the ability of the beetle *Tenebrio molitor* immune system to clear bacteria from its hemocoel by injecting a large dose [ $4 \times 10^6$  colony-forming units (CFUs)] of *Staphylococcus aureus* (19, 20) into the body cavity of individual adult female beetles. We used stationary-phase bacteria to ensure that there was sufficient genetic variation in the overnight culture for our selection experiment and because naturally acquired bacteria in an insect’s environment are likely to be in stationary phase. We used a high dose to maximize the likelihood of detecting downstream effects in the experiment. Haemolymph was harvested at 10 time points (between 0 and 28 days) after injection and used to determine the number of surviving bacteria and the induced antimicrobial activity against *S. aureus* in the haemolymph. There was very rapid clearance of *S. aureus* from naïve host haemolymph. More than 99.5% of injected *S. aureus* had been cleared in less than an hour (Fig. 1). Recovery of live bacteria continued to fall until 14 days after injection, after which ~50 CFUs per host remained. It is possible that rather than being killed, bacteria were inaccessible to our sampling technique. Although our data showed that bacteria were attached to insect tissues (SOM), they also revealed that the pattern of *S. aureus* clearance from tissue homogenates was identical to that from the haemolymph samples (SOM), indicating that these bacteria were still attacked by the host’s immune system.

Cell-free haemolymph was tested for its ability to kill *S. aureus* by means of an in vitro killing reaction (SOM). Induced antimicrobial activity only started to increase in the haemolymph 30 min after most bacteria were cleared (Fig. 1). This activity peaked at 24 hours after challenge, long after most bacterial clearance had occurred, and remained elevated until 28 days after challenge, when there were few recovered CFUs (Fig. 1).

Constitutive defenses, including haemocytes and cytotoxic enzyme cascades, are responsible for “frontline” physiological defense against microbial insults (21). Our observations imply that induced antimicrobial effectors do not function to clear bacteria, but rather “mop up” those that have survived selection via the host’s constitutive defenses (22). We propose that “surviving” bacteria exhibit some resistance to the initial beetle immune response and that the function of the late, and prolonged, peak in induced antimicrobial peptide activity is to prevent the enrichment of resistant bacteria. This argument relies on the assumption that the surviving bacteria are more resistant to the host’s defenses than were those bacteria that were killed. We tested this assumption by harvesting surviving bacteria from

beetles after five different periods of immune exposure within the host (30 min, 1 hour, 1 day, 7 days, and 14 days). Surviving bacteria were then grown overnight in vitro, after which we compared survival of persisting bacteria against the survival of naïve bacteria within naïve beetle hosts. The results are shown in Fig. 2. Separate analyses of covariance testing for the effects of “strain” (“survivors” versus “naïve”) and beetle size on  $\log_{10}$  CFUs recovered at each time point revealed significant effects of strain at 30 min ( $F_{1,18} = 9.97$ ,  $P = 0.0054$ ), 1 day ( $F_{1,15} = 58.63$ ,  $P < 0.0001$ ), 7 days ( $F_{1,17} = 12.62$ ,  $P = 0.0025$ ), and 14 days ( $F_{1,24} = 23.33$ ,  $P < 0.0001$ ). Host size had no effect. Significantly more “survivor” *S. aureus* survived after injection into naïve beetles compared with “naïve” bacteria (Fig. 2). Bacteria that survived longer exposure to a beetle’s immune system were better survivors upon exposure to a naïve beetle’s immune system.

Two arguments favor our idea that long-lasting antimicrobial activity has evolved as part of a two-stage process, preventing resistance evolution in bacteria and/or managing persistent infections. First, bacteria readily evolve resistance against individual antimicrobial peptides in isolation (23), and recent work (18) suggests that phagocytic haemocytes are responsible for the immune reaction against secondary infections in insects. Moreover, our explanation for long-lasting induced immunity functions in the context of a single infection, whereas the prophylactic explanation requires at least two infections.

Our results have two important implications. First, antimicrobial peptides could well be the last line of defense dealing with persistent infections and the prevention of the evolution of resistant mutants. Second, at the functional level, our interpretation is analogous to human antibiotic therapies. The current focus on the development of insect and other natural antimicrobial peptide-based drugs (2) should take into account functional studies of these compounds in their ecological context (3).

## References and Notes

1. M. Zasloff, *Nature* **415**, 389 (2002).
2. R. E. W. Hancock, H.-G. Sahl, *Nat. Biotechnol.* **24**, 1551 (2006).
3. J. L. Martinez, *Science* **321**, 365 (2008).
4. S. Cherry, N. Silverman, *Nat. Immunol.* **7**, 911 (2006).
5. L. Cerenius, B. L. Lee, K. Söderhäll, *Trends Immunol.* **29**, 263 (2008).
6. M. T. Siva-Jothy, Y. Moret, J. Rolff, *Adv. Insect Physiol.* **32**, 1 (2005).
7. S. Iwanaga, B. Lee, *J. Biochem. Mol. Biol.* **38**, 128 (2005).
8. M. D. Lavine, G. Chen, M. R. Strand, *Insect Biochem. Mol. Biol.* **35**, 1335 (2005).
9. E. R. Haine, L. C. Pollitt, Y. Moret, M. T. Siva-Jothy, J. Rolff, *J. Insect Physiol.* **54**, 1090 (2008).
10. P. Korner, P. Schmid-Hempel, *J. Invertebr. Pathol.* **87**, 59 (2004).
11. P. Bulet et al., *Eur. J. Biochem.* **209**, 977 (1992).
12. A. R. Kraaijeveld, H. C. Godfray, *Nature* **389**, 278 (1997).
13. M. Poulsen, A. N. M. Bot, M. G. Nielsen, J. J. Boomsma, *Behav. Ecol. Sociobiol.* **52**, 151 (2002).
14. B. M. Sadd, M. T. Siva-Jothy, *Proc. Biol. Sci.* **273**, 2571 (2006).

15. B. P. Lazzaro, *Curr. Opin. Microbiol.* **11**, 284 (2008).
16. Y. Moret, M. T. Siva-Jothy, *Proc. R. Soc. Lond. B. Biol. Sci.* **270**, 2475 (2003).
17. B. M. Sadd, P. Schmid-Hempel, *Curr. Biol.* **16**, 1206 (2006).
18. L. N. Pham, M. S. Dionne, M. Shirasu-Hiza, D. S. Schneider, *PLoS Pathog.* **3**, e26 (2007).
19. A. J. Needham, M. Kibart, H. Crossley, P. W. Ingham, S. J. Foster, *Microbiology* **150**, 2347 (2004).
20. J. Garcia-Lara, A. J. Needham, S. J. Foster, *FEMS Immunol. Med. Microbiol.* **43**, 311 (2005).
21. N. Matova, K. V. Anderson, *Proc. Natl. Acad. Sci. U.S.A.* **103**, 16424 (2006).
22. P. E. Dunn, *Annu. Rev. Entomol.* **31**, 321 (1986).
23. G. G. Perron, M. Zasloff, G. Bell, *Proc. R. Soc. Lond. B. Biol. Sci.* **273**, 251 (2006).
24. We thank R. Clare, A. Dobson, S. Webster, and A. Williams for laboratory assistance. P. Brakefield, S. Foster, and M. Osborn made valuable comments that improved the

manuscript. This research was funded by The Leverhulme Trust, and E.R.H. was also supported by The Wellcome Trust.

#### Supporting Online Material

[www.sciencemag.org/cgi/content/full/322/5905/1257/DC1](http://www.sciencemag.org/cgi/content/full/322/5905/1257/DC1)

Materials and Methods

Fig. S1

References

28 August 2008; accepted 17 October 2008  
10.1126/science.1165265

# Multi-University Research Teams: Shifting Impact, Geography, and Stratification in Science

Benjamin F. Jones,<sup>1,2\*</sup> Stefan Wuchty,<sup>3\*†</sup> Brian Uzzi<sup>1,3,4,\*‡</sup>

This paper demonstrates that teamwork in science increasingly spans university boundaries, a dramatic shift in knowledge production that generalizes across virtually all fields of science, engineering, and social science. Moreover, elite universities play a dominant role in this shift. By examining 4.2 million papers published over three decades, we found that multi-university collaborations (i) are the fastest growing type of authorship structure, (ii) produce the highest-impact papers when they include a top-tier university, and (iii) are increasingly stratified by in-group university rank. Despite the rising frequency of research that crosses university boundaries, the intensification of social stratification in multi-university collaborations suggests a concentration of the production of scientific knowledge in fewer rather than more centers of high-impact science.

In May 1845, Samuel F. B. Morse telegraphed the first electronic message, “What hath God wrought?” from Washington, DC, to Baltimore and declared an end to “the tyranny of distance.” Yet, in the 150 years since Morse’s breakthrough, the production of science has had a reputation for geographic localization. Early 20th-century German universities singularly led in chemistry and physics, creating the first commercial dyes and nuclear and rocket programs (1). Silicon Valley became a renowned incubator for excellence in technology (2), and the University of Chicago has been a persistent center for Nobel Prize winners in economics.

Nonetheless, recent observers have suggested a weakening link between location and scientific research—a “death of distance,” in popular coinage (3). In this view, technology is inevitably removing the last barriers of distance, widening access to geographically distant collaborators with potential implications for the location, research quality, and social stratification of science (4, 5). Researchers report, for example, a modest

rise in collaborations between research institutions in a limited sample of fields (6–8), although other authors conclude that face-to-face contact and the “30-feet collaboration rule” nonetheless continue to encourage collaboration at home universities (9–11).

Although these studies suggest a possible trend toward collaboration between authors at different universities, the generalizability of the shift remains unclear, as does the association with research impact and the geographic and social structure of collaboration. With an eye toward understanding the role that multi-university collaborations play in the production of science, we examined (i) trends in multi-university collaborations across the full spectrum of academic fields, (ii) the association of these changes with research impact, and (iii) the role of elite and nonelite universities in these trends. Our sample focuses on a set of 662 major U.S. universities and includes 4.2 million research papers in the Web of Science database, covering 172 fields of science and engineering (SE), 54 fields of social sciences (SS), and 27 fields of arts and humanities (AH) from 1975 to 2005 [the supporting online material (SOM) further defines the sample design, and table S1 lists the universities].

Our analysis indicates a remarkable and nearly universal rise since 1975 in the frequency of collaborations between authors located at different universities. Figure 1 shows the share of research papers published by solo authors, collaborators at the same university, and collaborators between schools. In SE, between-school collab-

orations were rare in 1975, which suggests that this type of collaboration is a relatively modern phenomenon (Fig. 1A). Moreover, among all three authorship arrangements, between-school collaboration is the fastest- and only steadily growing segment, quadrupling its share in SE between 1975 and 2005 to 32.8%. Figure 1B shows that SS have experienced similar trends; the share of SS papers written in multi-university collaborations rose even more rapidly over the 30-year period to a peak share of 34.4%. These upward trends appear even stronger upon further including publications with collaborators outside the sample of major U.S. universities (fig. S1).

Although the rate of increase in multi-university collaborations is essentially constant over our entire period, we found an unusual jump of 3.4% in SE, which is large ( $P < 0.0001$ ) compared to the typical year-on-year increase of 0.8%. Although this single event occurred in 1998, a period when the Internet and other information and computing technologies were spreading widely, multi-university collaborations in SE continued at the pre-1998 rate of growth thereafter. SS show little unusual acceleration in this period. These findings suggest that, although communication technologies may be generally important, multi-university collaborations were largely driven by factors that predated recent communication technologies.

Table 1 demonstrates the generality of these patterns across individual fields. It indicates that 98% (168 of 172) of the SE subfields increased their share of between-school collaborations. In SS, 100% (54 of 54) of the subfields increased their share of research written by coauthors at multiple schools. AH showed little disposition for teamwork in general (Fig. 1C); a more modest majority of fields (67%, 18 of 27) demonstrated a rise in multi-school collaboration. Our analyses further show that the trend toward multi-university collaboration in SE and SS is present for teams of any size (fig. S2) (12).

Although the incidence of between-school collaboration has grown rapidly, the average distance between collaborators has risen only slightly (fig. S3). In 1975, the mean distance between collaborators in SE was 750 miles, whereas it was 800 miles in 2005 (13). The mean distance between collaborators in SS increased from 725 to 800 miles over the same period. Median distances rose from 510 to 560 miles (SE) and 530 to 580 miles (SS). Spatially, this suggests that the death of distance in U.S. science is not primarily

<sup>1</sup>Kellogg School of Management, Northwestern University, Evanston, IL 60208, USA. <sup>2</sup>National Bureau of Economic Research, Cambridge, MA 02138, USA. <sup>3</sup>Northwestern Institute on Complexity (NICO), Northwestern University, Evanston, IL 60208, USA. <sup>4</sup>Haas School of Business, University of California at Berkeley, Berkeley, CA 94720, USA.

\*These authors contributed equally to this work.

†Present address: National Institutes of Health, Bethesda, MD 20982, USA.

‡To whom correspondence should be addressed. E-mail: [uzzi@northwestern.edu](mailto:uzzi@northwestern.edu)

driven by an increase in the distance between long-range collaborators but by an increase in the frequency of collaborations both near and far. It is not the length of a scientist's reach that has changed but rather the incidence of reaching across university boundaries.

To analyze and compare the citation impact of between-school collaborations and within-school collaborations, we estimated the probability that papers written with these two different authorship structures receive above-average citations. We focused on papers published from 1995 to 2005 and on between-school collaborations with two university affiliations, using regression analysis to account for subfield, team size, and publication year differences (13).

Figure 2 presents three primary findings. In both SE and SS, between-school collaborations have a citation-impact advantage over within-school collaborations. Averaging over all schools in our sample (Fig. 2A), within-school collaborations have a baseline probability of producing papers with above-average citations of 32.7% in SE and 34.1% in SS. For between-school collaborations, the marginal probability is 2.9% higher in SE ( $P < 0.0001$ ) or 8.8% above the baseline rate (0.029/0.327). In SS, the marginal gains of between-school collaborations are larger at 5.8% ( $P < 0.0001$ ) or 16.7% above the baseline rate (0.058/0.341).

In Fig. 2B, we further disaggregated the between-school collaborations based on the ranks of the collaborating schools. Schools were ranked by the total number of citations received by the papers published at the school in the corresponding period. We considered only within-school publications in this ranking method so that the school rankings are independent of each university's performance in between-school collaborations. Tier I schools are those ranked in the top 5%, tier II are in the top 6 to 10%, tier III are in the top 11 to 20%, and tier IV are the remainder. Other ranking methods were considered below as robustness checks (14). We took within-school collaborations as the baseline case for each tier and compared the citation impact of multi-university collaborations with that baseline. These results suggest that collaborations between tier I schools show a substantial impact advantage over tier I within-school collaborations. For example, a team of two authors from an elite school such as Harvard tends to produce lower-impact papers than a team of two authors with one at Harvard and the other at Stanford. This finding may challenge claims that within-school collaboration provides decisive advantages by lowering communication and monitoring costs, conveying tacit information, and enabling impromptu interaction. Specifically, in SE, circa 1995 to 2005, a collaboration between tier I institutions is 6.19% more likely ( $P < 0.0001$ ) to be of high impact than a tier I within-school collaboration, which is a 17% increase in the baseline rate (0.062/0.372). In SS fields, there is an even larger 11.7 percentage-point increase ( $P < 0.0001$ )

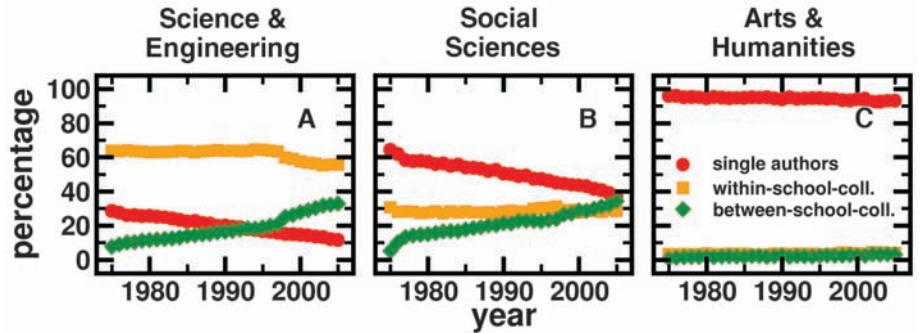
in the probability of being a high-impact paper, which is a 24% increase in the baseline rate (0.117/0.406). We also observe that the advantage of intra-tier partnerships exists for tier II and tier III partnerships and declines as the rank of schools decreases. For partnerships between tier IV schools, the advantage disappears in SS and is slightly negative for SE fields, which suggests that the advantage found in partnerships between similar-quality schools is dominated by, and most pronounced among, elite institutions.

Table S2 considers cross-tier collaborations and shows that their citation impact tends to lie between the impact of the upper and lower tiers' within-school collaborations. The between-school impact tends to lie closer to the upper-tier baseline than the lower-tier baseline. This finding suggests that cross-tier between-school collaboration may follow a "strongest-partner" rather than a "weakest-partner" model, with tier I pulling up tier IV more than tier IV pulls down tier I. Tables S3 and S4 substantiate all the results for alternative school-ranking methods (14), and fig. S5 presents the raw citation impact data, unconditional on field or team size, and shows similar findings.

Further exploring the special role of elite universities in the production of multi-school research, Table 2 decomposes the intensity of multi-university collaboration by university. Con-

sidering papers with two university affiliations, the table cells above the diagonal show the actual share of multi-university collaborations for 2001 to 2005 for each tier pairing, which indicates that elite schools dominate multi-university collaborations in the 2001–2005 period. Just 5% of schools (tier I) hold places in 59.7% of multi-university collaborations in SE (tier I row sum, above the diagonal). In SS, the corresponding fraction is 56.2%. Conversely, only 18.4% of SE multi-university collaborations were formed solely among authors from tier III and IV universities, even though these universities are 90% of the schools in the sample.

We further examined the intensity of stratification in multi-university partnerships by comparing actual collaboration rates between tier pairings with a baseline model of random matching across tiers. Defining  $P_j$  as the fraction of multi-university papers that include tier  $j$ , the probability that a multi-university paper includes tiers  $j$  and  $k$  under random matching is  $2P_jP_k$  if  $j \neq k$  and  $P_jP_k$  if  $j = k$ . The cells of Table 2, below the diagonals, show the ratio of the actual frequency of a given tier-pairing to the expected frequency under random matching. Ratios  $>1$  indicate a greater propensity for tier pairings than expected by random matching and ratios  $<1$  indicate a lesser propensity for tier pairings.



**Fig. 1.** The rise in multi-university collaboration. By comparing the incidence of papers produced by different authorship structures, we see that the share of multi-university collaborations strongly increases from 1975 to 2005. This rise is especially strong in SE (A) and SS (B), whereas it appears weakly in AH (C), in which collaboration of any kind is rare. The share of single-university collaborations remains roughly constant with time, whereas the share of solo-authored papers strongly declines in SE and SS.

**Table 1.** Patterns by subfield. For each subfield, we calculated the fractions of papers written as within-school collaborations and between-school collaborations in 1975–1979 and 2001–2005. Comparing the incidence of these authorship structures between the early and late periods, we determined the number of subfields ( $N$ ) and the fraction of subfields (%) for which the share of each type of collaboration is increasing.

Fields	Total subfields ( $N$ )	Increasing collaborations			
		Within-school		Between schools	
		Subfields ( $N$ )	Subfields (%)	Subfields ( $N$ )	Subfields (%)
SE	172	114	66.3	168	97.7
SS	54	47	87.0	54	100.0
AH	27	16	59.3	18	66.7




We found that tier I–tier I collaborations in SE were 14% more common ( $P < 0.001$ ) than expected under random matching, whereas tier I–tier IV collaborations were 19% less common ( $P < 0.001$ ) than expected. In SS, this inequality is even stronger, for which tier I–tier I collaborations were 27% more common than expected ( $P < 0.001$ ), and tier I–tier IV collaborations were 32% less common ( $P < 0.001$ ). Meanwhile, both SE and SS show that collaborations limited to lower-tier

schools were substantially more common than expected. Lower-tier schools did reach across university boundaries, but they tended to interact within their own tier, echoing the in-group status-matching behavior of elite schools. However, recalling the results in Fig. 2, the tendency to favor in-group matching was an advantage for tier I schools but a disadvantage for those of tier IV. Other ranking methods (14) demonstrated the robustness of these stratification tendencies (tables S6 and S7).

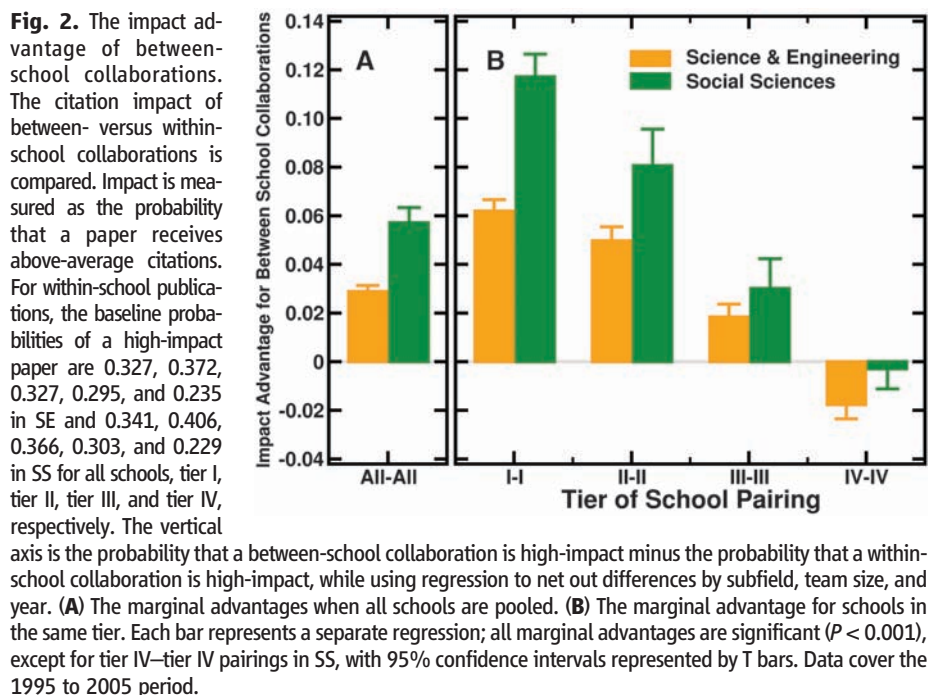


**Table 2.** Who collaborates with whom? For teams that span two different institutions, we calculated the frequency of pairings by school ranks for the period 2001–2005. For each school tier pairing, we show the actual percentage of two-school collaborations above the diagonal. Below the diagonal, we show the ratio of the actual frequency to the expected frequency under random matching. A ratio greater than 1 indicates that such tier pairings are more common than expected, and a ratio less than 1 indicates that such tier pairings are less common than expected. All quantities are statistically significant with  $P < 0.001$  unless marked by a †. Statistical significance was determined by bootstrapping.

Science and Engineering					Social Sciences				
Tier	I	II	III	IV	Tier	I	II	III	IV
I	16.6% 1.14	17.8% 0.98	15.5% 0.91	9.8% 0.81	I	16.2% 1.27	15.0% 1.10	13.7% 0.86	11.2% 0.68
II		4.9% 0.90	9.9% 0.94	7.1% 0.97	II		4.1% 0.97†	9.2% 1.05	7.9% 0.91
III			5.6% 1.03	8.4% 1.19	III			5.1% 0.95	10.9% 1.14
IV				4.4% 1.89	IV				6.7% 1.35


**P:** Frequency of tier combination (in %)   
**R:** Ratio of frequency to expected frequency

The SOM further considers the evolution of social and geographic stratification over time. Table S5 demonstrates that tier I–tier I collaborations rose with time as compared with the expected rate, whereas tier I–tier IV collaborations fell. Thus elite schools have been increasingly likely to capture the impact advantages of their collaborations, whereas tier IV schools appear to lose ground in accessing top-tier collaborations. Finally, figs. S6 to S9 illustrate the intersection of social and geographic distance for the Boston, Chicago, Los Angeles, New York, North Carolina, and San Francisco research centers. Top schools in these regions increasingly collaborated with geographically distant top schools, whereas their other partnerships declined. Partnership choice increasingly appears to be based on who the collaborators are rather than where they are, with an emphasis on in-group status matching.

The shift toward cross-institutional collaboration suggests a fundamental transformation in the production of high-impact science. Prior work established that teamwork has become ubiquitous across scientific fields and supplanted solo-authored work in the production of the highest-impact research (15, 16). We demonstrate that the rising collaboration in science is increasingly composed of collaborations that span university boundaries. Moreover, elite universities play a dominant role in this shift. We found that multi-university partnerships (i) are the fastest growing type of authorship structure, (ii) produce the highest-impact papers when they include a top-tier university, and (iii) are increasingly stratified by in-group university rank. Thus, although geographic distance is of decreasing importance, social distance is of increasing importance in research collaborations. Elite universities are more intensely interdependent, playing a higher-impact and increasingly visible role in SE and SS.

Consistent with some claims, we observed that rapid technology advances in the 1990s may have modestly accelerated between-school collaboration, but our results more generally indicate a smooth growth in multi-school collaboration that substantially predated this period. These findings suggest a more complex relationship between social relations and technology in science, with collaboration technologies and social networks potentially being an endogenous outcome of the burgeoning interest in research partnerships (8, 17–19). Others have argued that increasing specialization drives collaboration (20), which, coupled with the limited capacity of academic departments to encapsulate more than a fraction of a field's specializations, may promote institutionally boundaryless collaborations in the search for high-impact science. However, whereas the greater geographic interconnectedness of universities would appear to make geography less important, the corresponding intensification of social stratification in multi-university collaboration tends to embed the production of outstanding scientific knowledge in fewer rather than more centers of high-impact science. The dominant role

of elite universities suggests several ideas for future research, including scale and resource advantages, social networks, journal leadership, and other factors such as matching based on status or quality, that promote a widening rather than a narrowing of stratification in science through the vehicle of multi-university partnerships.

## References and Notes

1. J. P. Murmann, *Knowledge and Competitive Advantage* (Cambridge Univ. Press, Cambridge, 2003).
2. A. L. Saxenian, *Regional Advantage: Culture and Competition in Silicon Valley and Route 128* (Harvard Univ. Press, Cambridge, MA, 1994).
3. F. Cairncross, *The Death of Distance* (Harvard Univ. Press, Cambridge, MA, 1997).
4. S. Teasley, S. Wolinsky, *Science* **292**, 2254 (2001).
5. A. Finholt, M. Gary, Olson, *Psychol. Sci.* **8**, 28 (1997).
6. F. Havemann, M. Heinz, H. Kretschmer, *J. Biomed. Discov. Collab.* **1**, 6 (2006).
7. T. S. Rosenblat, M. M. Mobius, *Q. J. Econ.* **119**, 971 (2004).
8. A. Agrawal, A. Goldfarb, *Am. Econ. Rev.* **98**, 1578 (2008).
9. G. M. Olson, J. S. Olson, *Hum. Comp. Interact.* **15**, 139 (2000).
10. E. Bradner, G. Mark, in *Proceedings of the 2002 ACM Conference on Computer Supported Cooperative Work* (ACM, New York, 2002), pp. 226–235.
11. J. Cummings, S. Keisler, *Res. Policy*, in press.
12. We also found (fig. S2) that social scientists have a substantially higher propensity to engage in multi-university collaboration for any given team size. For example, a team of size 2 in SS operated across universities nearly 40% of the time in the year 2000, whereas the corresponding propensity in SE was 18%, a 2-to-1 ratio that holds approximately over time. This difference may follow from conditions such as the relative capital intensity of lab sciences, which particularly favor colocation in SE. The relative tendency toward multi-university collaboration in SS is offset by the greater incidence of large teams in SE and the fact that larger teams are more likely to be assembled from multiple universities. Hence, the absolute fraction of multi-university work turns out to be similar in both SE and SS (Fig. 1).
13. We focused on cases with two university affiliations, which allowed us to categorize multi-university collaborations into explicit tier pairings, as seen in Fig. 2. Two-university collaborations represent over 90% of multi-university collaborations (fig. S4). The regressions are linear probability models (ordinary least squares), in which an indicator for whether the paper is above the mean impact in its field and year is regressed on indicator variables for authorship structure (solo-authored, within-school collaboration, or between-school collaboration), publication year, team size, and subfield, with standard errors clustered by subfield.
14. To determine the ranking of each school, we pooled all papers that have been published entirely by a given school in each year by using only within-school collaborations and papers of single authors. We then counted the number of citations those papers received and ranked the schools according to their total citation count. This ranking method is equivalently described as the average citation impact (a quality measure) times the number of publications (a quantity measure). Between-school papers were omitted from the measure of school ranking to ensure that the papers used to assign tiers were independent of the papers used to assess between-school impact. Alternative measures are average citation impact, as a pure quality measure, and the university Hirsch index (21), which emphasizes very-high-impact papers. A university's Hirsch index for a given publication period is the largest number  $H$  such that  $H$  of its papers received at least  $H$  citations. As noted in the text and detailed in tables S2, S4, S6, and S7, the patterns of impact and stratification are consistent across these alternative ranking approaches. Table S8 lists the top 50 universities under different ranking methods.
15. S. Wuchty, B. Jones, B. Uzzi, *Science* **316**, 1036 (2007).
16. S. Wuchty, B. Jones, B. Uzzi, *Science* **317**, 1496 (2007).
17. V. Gurbaxani, *Commun. ACM* **33**, 65 (1990).
18. R. K. Merton, *On Social Structure and Science* (Univ. Chicago Press, Chicago, IL, 1996).
19. R. Guimera, B. Uzzi, J. Spiro, L. A. N. Amaral, *Science* **308**, 697 (2005).
20. B. F. Jones, *Rev. Econ. Studies*, in press.
21. J. E. Hirsch, *Proc. Natl. Acad. Sci. U.S.A.* **102**, 16569 (2005).
22. We thank K. Murnighan, K. Williams Phillips, S. Stern, S. S. Sanchez, and two anonymous referees for helpful comments. The Northwestern Institute on Complex Systems provided financial support.

## Supporting Online Material

[www.sciencemag.org/cgi/content/full/1158357/DC1](http://www.sciencemag.org/cgi/content/full/1158357/DC1)

Materials and Methods

Figs. S1 to S9

Tables S1 to S8

27 March 2008; accepted 25 September 2008

Published online 9 October 2008;

10.1126/science.1158357

Include this information when citing this paper.

## Sample Storage System

Traxis is a sample storage coding system designed to enhance compound traceability and retrieval. The Traxis system includes a uniquely identified tube, a polypropylene tube, a multipierceable resealing cap, and a range of specially designed readers and tube sorters to allow accurate identification and fast manipulation of the Traxis tubes. Traxis tubes can be encrypted with up to 8.5 billion different combinations of a numerical code that provide a unique identification and enhanced sample storage traceability. The Traxis reader can simultaneously scan all 96 tubes in a rack without the need for any tube removal. The caps are hydrophobic and can be pierced at least 12 times without risk of sample evaporation or contamination.

[Micronic](#)

For information 724-941-6411

[www.micronic.com](http://www.micronic.com)



## Comet Assay Electrophoresis System

A novel complete system is available for the comet assay, the only direct method for the detection of DNA damage in cells. The comet assay is used in cancer research, in genotoxicity studies on environmental mutagens, and for screening compounds for cancer therapeutics. Based on single-cell gel electrophoresis in a controlled pH environment, the assay allows the integrity of stained nuclear DNA to be examined and measured. The new assay includes CometSlides, reagents, control cells, and an electrophoresis unit that retains test cells in a uniquely configured electrophoretic field permitting consistent DNA migration patterns, which are critical for standardization of the assay.

[Trevigen](#)

For information 800-873-8443

[www.trevigen.com](http://www.trevigen.com)

## Fusion Cloning System

The Stargate Fusion Cloning System allows the construction of artificial operons for multiple gene expression in bacterial or mammalian cells or the generation of fusion proteins. Stargate enables the systematic combination of promoters (that is, hosts), purification tags, or other genetic elements with any gene of interest in a convenient cloning system. Three different versions of the cloning sets are available.

[IBA](#)

For information +49-551-50672-114

[www.stargate-cloning.com](http://www.stargate-cloning.com)

## Fluorescent Conjugates

The Dylight fluorescent conjugates are designed to fill the need for probes with high fluorescence and photostability that allow sensitive detection of low-abundant proteins. They combine the sensitivity and reproducibility of KPL's affinity-purified antibodies and streptavidin with a series of intense fluorescent DyLight dyes for brilliant analysis in fluorescence microscopy, flow cytometry, protein immunoblotting, enzyme-linked immunosorbent assays, and other fluorescent applications. The conjugates are available with three dyes with well-differentiated emission spectra suitable for sensitive multicolor analysis.

[KPL](#)

For information 800-638-3167

[www.kpl.com](http://www.kpl.com)

## X-Ray Diffraction System

The Rapid II is a compact, high-resolution X-ray diffraction system. The latest member of a family of large area curved imaging plate detectors, the Rapid II includes every component needed to deliver no-compromise performance for applications ranging from applied to chemical crystallography. Typical applications include high-resolution charge density measurement, microdiffraction, diffuse scattering, measurement of weakly diffracting disordered materials, small molecule crystallography, wide-angle X-ray scattering, stress and texture measurements, and general purpose powder diffraction. The new 2DP software allows simultaneous manipulation of multiple images with various analytical protocols. In addition to general, two-dimensional intensity image processing, the software provides for display and automatic calculation of stress and texture data. The Rapid II's curved imaging plate detector has numerous advantages over other types of X-ray detectors, the most obvious being an extremely large active area, low noise, and wide dynamic range.

[Rigaku Americas](#)

For information 281-362-2300

[www.rigakuMSC.com](http://www.rigakuMSC.com)

## CYP450 Antibody Panel

A new panel of human and rodent cytochrome P450 (CYP450) antibodies is available for use in drug discovery. These antibodies bind to most human isoforms of CYP450, as well as rat and mouse antibodies. They can be used to develop assays for the pharmaceutical, cosmetic, agricultural, and industrial sectors.

[Millipore](#)

For information 800-548-7853

[www.millipore.com](http://www.millipore.com)

## Tracking Moving Specimens

Designed to solve the problem of tracking a moving specimen, PhotoTrack can be combined with closed-loop DC servo motor stages to keep free-moving samples in the field of view, wherever they go. PhotoTrack makes use of a low-light-level rapid position-sensing quadrant photomultiplier tube sensor to monitor a bright reference spot on the target. It then commands an automated XY stage to maintain that spot in the center of a microscope's field of view.

[ASI/Applied Scientific Instrumentation](#)

For information 800-706-2284

[www.ASIimaging.com](http://www.ASIimaging.com)

Electronically submit your new product description or product literature information! Go to [www.sciencemag.org/products/newproducts.dtl](http://www.sciencemag.org/products/newproducts.dtl) for more information.

Newly offered instrumentation, apparatus, and laboratory materials of interest to researchers in all disciplines in academic, industrial, and governmental organizations are featured in this space. Emphasis is given to purpose, chief characteristics, and availability of products and materials. Endorsement by *Science* or AAAS of any products or materials mentioned is not implied. Additional information may be obtained from the manufacturer or supplier.



# Finance's Quant(um) Mechanics

One of the earliest “alternative” science careers, quantitative finance is now deeply embedded in the world’s finance industry

**SAY YOU’RE A PHYSICIST WITH A STRONG MATHEMATICAL** background, eager for intellectual stimulation and pining for some challenging problems to solve. You could seek a faculty gig and spend the next couple of decades developing a theory of everything. Or you could become a “quant” (short for “quantitative analyst”) and use advanced mathematics to help move mountains—of cash—through the world’s financial systems.

For anyone with a choice, Wall Street might not seem like an obvious employment destination at a time when the industry is crashing and burning. But quantitative analysis has a long history as an “alternative” career for scientists. In the past couple of decades, quants, in fact, have made themselves essential to the success—or failure—of financial-sector companies. It follows that despite the mortgage meltdown and the resulting credit calamity, exciting opportunities still exist for scientists with serious quantitative chops to work in finance—albeit, experts say, to a somewhat lesser extent in the near term. As scientific historian George Dyson says, in this time of crisis “we need more scientists in the banking system, not less.”



**Fast turnaround.** David Armet likes the fast-paced problem solving.

## What quants do

The sexiest quant careers, says Mark Joshi, a professor of actuarial studies at the University of Melbourne in Australia, are in derivatives pricing and statistical arbitrage—buying and selling to take advantage of market inefficiencies. Other quants perform portfolio analysis, and still others assess the models built by other quants. Wherever there’s a need for serious quantitative analysis in the financial industry—

and that’s pretty much everywhere—you’ll find a quant.

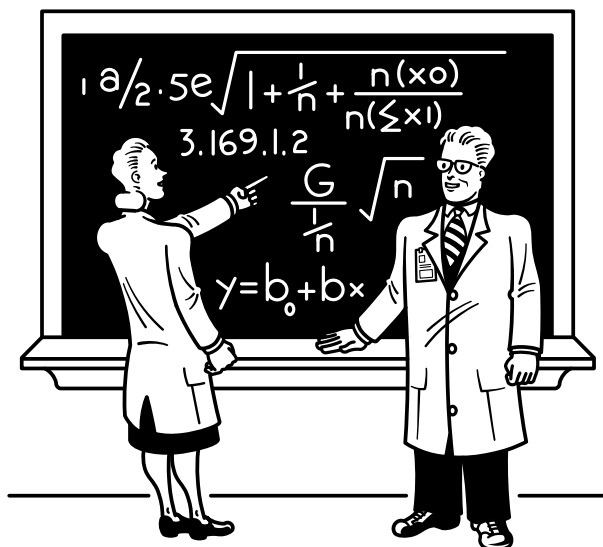
Quants engage in a common activity: creating a wide variety of mathematical methods and applying them, via computer algorithms, to the solution of a particular financial problem. “If you look at the behavior of financial markets and try to describe that behavior using math, you very quickly end up in things like stochastic processes,” says Leif Andersen, a managing director and senior trading strategist at Bank of America based in Charlotte, North Carolina, with more than 10 years’ experience as a quant. Andersen, who has a master’s degree in mechanical engineering, another in electrical engineering, an MBA, and a Ph.D. in mathematical sciences, leads a team of 20 quants in the bank’s investment business. Andersen’s team works in a wide range of markets, including commodities, interest rates, and credit, computing prices and devising hedging strategies for the bank’s activities in capital markets. “When we have a good understanding of the markets and have a model for it, we try to use the model for certain applications like pricing instruments in the market, and that requires computer algorithms,” Andersen says. “So you have a mathematical model which you implement on the computer. That’s pretty much the exercise.”

## Quant qualifications

Bank of America employs several thousand quantitative analysts, says Sam Murray, global executive quantitative recruiter for the company. About a third of the bank’s quants have Ph.D.s. Murray’s typical hire comes straight from academia with a master’s degree or a Ph.D. in physics, mathematics, statistics, or a related field. “People who come from a theoretical physics background do quite well with this,” Andersen says. “The problems we face are very similar to the problems they face.”

One unique aspect of the quant field is that work experience is sometimes considered a liability. Jim Varriale, publisher of QUANTster.com, a job Web site for quants, says that “the most sought-after quants are the fresh-out Ph.D.s in physics, math, and computer science” with no formal background in finance. “Companies want to train them themselves,” he says. “I don’t want to hire people with a financial background—they come with preconceived notions about how markets behave,” asserts Pierre P. Villeneuve, managing director of Mapleridge Capital Corp. in Toronto, Canada. “We would have to unbrainwash

CREDITS: (BANNER IMAGES) JASON SZENES/EPA/CORBIS; PHOTOS.COM; (BOTTOM) ALICIA REEVES



Does G stand for force due to gravity or greenbacks?

them, and that's a lot of work." Villeneuve says he prefers to "hire raw scientists to bring quant skills and the strong intuition to marry the science with the business."

Another route into the field is a master's degree program in quantitative finance. Several such programs have sprung up recently. Many students already have advanced education in a scientific discipline when they enter the programs.

#### Quant communication

Hiring managers in quantitative finance may not seek financial experience, but they do look for the same "soft skills" sought by hiring managers in almost every industry—especially communication skills. "You have to be able to translate business problems into 'quantspeak' that teams of quants can work on," says Ivan Marcotte, senior vice president and global portfolio strategies executive at Bank of America and a 20-year-veteran quant. "You have to then take those results and translate them back into 'businessspeak' so that the business leaders know how to use the results and the efforts of our quantitative associates to get the most lift for our company."

Christine Jerritts, 31, senior mathematician at Quantitative Equity Strategies, a quant research and service company in Highlands Ranch, Colorado—and, incidentally, a race car driver for Team QuantSPEED in Denver—agrees. "Translation is number one," she says.

#### Complexity, with less waiting

Quantitative analysis, practitioners say, provides many of the advantages of scientific work with fewer disadvantages. "The complexity is as rich as in physics," Andersen says, "and you have a lot of people using your stuff all the time, which is very gratifying, particularly for people like myself coming out of an engineering background." Also, "you have a certain amount of instant gratification in this line of work," he continues, "where in many other fields, it takes you 15 years to get involved in some project with 15 co-collaborators." David Armet, 26, who works in quantitative and algorithmic trading on the currency desk at a global investment bank in London,

describes his work as "reactionary." He loves his job partly, he says, because of the very fast turnaround in solving a problem.

The field also pays well, especially in good times. Rita Raz, president of Analytic Recruiting Inc. in New York City and a quant recruiter for 29 years, says that an entry-level quant with a doctorate can expect a base salary of at least \$80,000 to \$90,000 and a signing bonus that's just as large. After 5 years in the field, Raz says, quants can expect to earn about \$130,000 in base salary and much larger bonuses—as much as 300% of the base salary in a successful year.

#### Finance's quantitative future

In science, there's commonly a gap between the short-term demand for employees and the needs perceived by high-minded experts. Everyone agrees that we need more researchers to solve many of the world's problems, but that rarely translates directly into jobs. Such a gap exists right now in quantitative finance. The recent financial crisis—which was global in scope but especially acute in the United States and a few other countries—has damaged short-term prospects for anyone seeking to enter the finance industry. Quants are no exception. Some even believe that, due to the role they played in some of the industry's more vulnerable areas, such as derivatives and hedge funds, quants may be affected more by the slowdown than most.

Emanuel Derman, a professor at Columbia University and one of the giants of quantitative analysis, believes that the recent crisis will make the job market for quants "obviously worse. There will be less appetite for complex products, less need for models, less money to hire, and less demand for quants in the short and intermediate run. ... It's hard to see out a long way with so many structural changes and government intervention." Still, he believes that the long-term outlook is solid because "derivatives and electronic markets and algorithmic trading are



**Fast money.** Christine Jerritts says that for "quants" working in finance, "translation is number one."

here to stay." Like Dyson, he believes that "in the long run, markets need more analytical and computer skills, not less." One possible bright spot even in the short term: The demand for quants in the regulatory area is likely to increase, Derman says.

In the decades since they first prowled Wall Street, quants have insinuated themselves deep into the fabric of the finance industry. So, though there will be ups and downs, quant careers aren't likely to disappear, even in a down market. "Nothing works if we're not there," Armet says. "The lights don't turn on if we're not there. ... We are essential to keeping the bank running." As long as banks keep running, there will be a demand for fresh talent.

—ALAINA G. LEVINE

Alaina G. Levine writes from Tucson, Arizona.



# Analyzing Scientific Investments

A background in science can be an advantage for analysts charged with determining the value of science-based companies

**HOW DO FINANCIAL SERVICES COMPANIES KNOW WHICH HIGH-tech sectors are likely to pay off and which companies rest on a solid scientific base?** Many of them employ a small coterie of scientists who combine strong analytical skills with deep scientific knowledge to advise on investments in science-based businesses. These scientifically trained financial analysts fulfill an important function: assessing the economic value and predicting the future performance of products, companies, and industries.

Unlike quantitative analysts—physicists and mathematicians who work on the mathematical models behind high-volume trading (see p. 1264)—financial analysts tend to move into high finance later in their careers and rely heavily on their intimate knowledge of a scientific field. Meet some financial analysts who have made that transition:

» **Stefan Hamill's** intellectual curiosity led him to a Ph.D. at the Cambridge Centre for Protein Engineering just as biotech was becoming the latest buzzword and the tech boom was building steam. Later, that same curiosity led him down a new path, to a career as a financial analyst. "Today, I provide investment advice across the whole health care sector, including biotech, pharmaceutical, and services firms," says Hamill, who is now head of health care at Noble, a U.K.-based investment bank.

Hamill says his scientific background is central to his work. It allows him to judge the fundamentals of a health care business without being intimidated by the science. Also key: the ability to speak two languages—the language of finance and the language of science. "I have always found my strong quantitative skill set to be an advantage throughout my finance career and often find myself translating the language of science into the language of investment," he says.

» **Paul Cornelius**, a corporate adviser for London-based FinnCap, is an engineer with a doctorate from the University of Wales. He did an apprenticeship at the U.K. government's Atomic Weapons Establishment. A stint at British Steel during the company's merger with Hoogovens in 1999 to form Corus provided his first exposure to the world of finance. He spent some time trading technology stocks during

new technologies and from a mathematical perspective when analyzing capital markets and financial modeling," Cornelius explains. "Confidence when dealing with numbers is key, and the mathematical experience gained through my science degree and engineering work experience gives me an advantage over some of my peers."



**"Forging a scientific career is somewhat similar to forging a career as a financial analyst, as you are essentially building a personal franchise and reputation."**

—STEFAN HAMILL,  
NOBLE INVESTMENTS

because, he says, there were no jobs in industry and proposed changes in university contracts made an academic career less economically appealing. He found his past engineering experience, including a stint as head of research in the Fuels and Energy Research Group at the University of Surrey, useful in his work on the privatization of the U.K. utilities. "I even sold the power station where I had done some of my Ph.D.," he says.

the dot-com boom, then applied for a job at an investment bank. Today, as research director for FinnCap, Cornelius examines business plans and emerging technologies to assess their viability in the market, prepares investment reports and financial models, and advises fund managers on whether to buy or sell stocks.

"I believe my background in science and engineering has helped me immeasurably, in both understanding the technical aspects of

» Asked when he was 5 years old what he wanted to be when he grew up, **Martin Hall** answered "bank manager." Earning a doctorate and doing postdoc work in neurology proved to be just a detour en route to his current position as a corporate financier specializing in life sciences at Eden Financial, a multinational company that advises hedge funds and investment banks. Together, he says, he and a colleague were the first to devise a robust method for valuing biotech companies. "One of the key advantages was my knowledge of the clinical trial process and the regulatory processes, which enabled me to make judgment calls about the likelihood of a product in R&D making it to the market," says Hall. His method is still used by most analysts today.

» After a 6-year course in biology in the Netherlands and a stint as a salesperson, **Anne Marieke Ezendam** moved into finance in 1998. She is now a portfolio manager specializing in biotech and pharma at Credit Suisse. "Science is a great background because it teaches you to ask questions," she says. "You also have to examine all the research in an area to see if a company and its product are viable, so you have to understand the subject."

» **Kevin Lapwood**, who has a Ph.D. in combustion science, was a pioneer as a scientist in the finance industry. Lapwood jumped scientific ship in the 1980s after a lectureship at the University of Surrey in the U.K.



### From the bench to the big board

Hamill says the most important factor in moving from science to finance is desire: You really have to want to do it, as the transition requires a lot of time and commitment. Immerse yourself and read widely, Hamill advises, so you can understand the basics of share prices and company fundamentals. The *Financial Times* and *The Economist* are important periodicals. Useful books range from simple introductions such as Nassim Nicholas Taleb's *Fooled By Randomness* to more technical texts for braver souls. Aspiring analysts might even consider managing a small portfolio of shares, whether as an exercise or for real.

In the research lab, put some energy into understanding the potential commercial aspects of what you are doing, Cornelius advises. Evaluate the technology in the lab for commercial potential. Consider whether the tools you're using—including mathematical techniques, programming languages, and so on—have applications in financial markets. Many job specifications within the financial market now list requirements for programming languages and other sector-specific experience, which can often prove a useful guide.

Indeed, many of the skills scientists pick up in the course of their training—social, programming, presentation, time management—are transferable to careers in finance. Another shared trait: the importance of social capital. “Forging a scientific career is somewhat similar to forging a career as a financial analyst, as you are essentially building a personal franchise and reputation,” Hamill says.

Universities now offer a range of finance courses. There are also self-study courses such as those offered by the Chartered Financial Analyst Institute. Lapwood says he is much more likely now to interview a science or engineering graduate if they have an accountancy or business qualification.

### Making the leap

Eventually, you'll need to acquire some direct financial experience. Getting involved in business networks and enterprise initiatives at your university can lead to the right connections. Younger



“Science is a great background because it teaches you to ask questions.”

—ANNE EZENDAM,  
CREDIT SUISSE

scientists could also investigate internships in financial companies, whereas more seasoned researchers may want to consider consulting work.

Being older is not a disadvantage, some analysts say. “I would personally like to see far more mid-career researchers change to the business world, as the skills and experience they have are valuable in the financial markets,” says Cornelius. Hall agrees. Having experience is a real advantage, he says,

and it is not unreasonable to consider a career change after several years of research or industry experience.

But there can be some downsides in delaying the move. “We see a flow of mid-career candidates looking to make the transition,” Hamill says. “The problem tends to be that with age comes higher expectation, yet the training and experience required take years to amass.” Whatever your age, expect it to take some time, he advises. “If it's a complete change in direction mid-career, be prepared to spend several years learning the ropes alongside younger colleagues.”

### The impact of the credit crunch

The recent market turmoil has made the job market for wannabe financial analysts tougher. But even skeptics believe that a transition to a finance career remains possible for committed and competent scientists. The recent crisis is just part of the boom-and-bust cycle of finance, Lapwood says, although it means that the most likely way in now is through smaller companies, as most of the big banks are cutting back on entry-level personnel and finance companies rarely take a long view on hiring.

Because career transitions—like market recoveries—take time, right now, when others are bailing out, might just be a good time to get started. “I would urge students to prepare for the recovery ... next year or the year after,” Cornelius says.

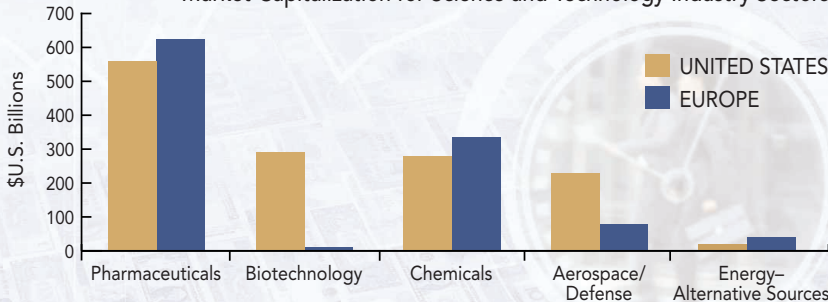
Others are even more bullish. Hamill says businesses like his will always be on the lookout for talent—even if the positions available are fewer and more challenging—and will want to come out of the downturn with strong teams. Exceptional people with drive will find positions, he says, and the rewards are worth the effort. “In my experience, the investment world is a very varied and intellectually stimulating place,” he says. “I will probably stay in this field for the remainder of my career.”

—AMARENDRA SWARUP

Amarendra Swarup is a science writer in London.

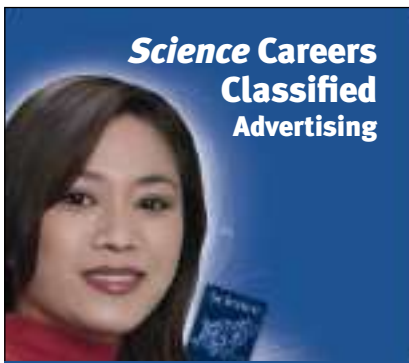
### WHY AND WHERE INVESTMENT COMPANIES NEED INDUSTRY ANALYSTS

Market Capitalization for Science and Technology Industry Sectors



SOURCE: BLOOMBERG, NOVEMBER 2008

**Decisions, decisions.** Analysts with scientific training guide billions in investments in science-based industry.



We've got **Careers** down to a **Science**.

For full advertising details, go to [www.sciencecareers.org](http://www.sciencecareers.org) and click on **For Advertisers**, or call one of our representatives.

## United States & Canada

E-mail: [advertise@sciencecareers.org](mailto:advertise@sciencecareers.org)  
Fax: 202-289-6742

### IAN KING

Associate Director, *Science Careers*  
Phone: 202-326-6528

### JORIBAH ABLE

Industry - US & Canada  
Phone: 202-326-6572

### ALEXIS FLEMING

Northeast Academic  
Phone: 202-326-6578

### TINA BURKS

Southeast Academic  
Phone: 202-326-6577

### DARYL ANDERSON

Midwest/Canada Academic  
Phone: 202-326-6543

### NICHOLAS HINTIBIDZE

West Academic  
Phone: 202-326-6533

## Europe & International

E-mail: [ads@science-int.co.uk](mailto:ads@science-int.co.uk)  
Fax: +44 (0) 1223 326532

### TRACY HOLMES

Associate Director, *Science Careers*  
Phone: +44 (0) 1223 326525

### ALEX PALMER

Phone: +44 (0) 1223 326527

### DAN PENNINGTON

Phone: +44 (0) 1223 326517

### SUSANNE KHARRAZ TAVAKOL

Phone: +44 (0) 1223 326529

### LOUISE MOORE

Phone: +44 (0) 1223 326528

## Japan

### MASHY YOSHIKAWA

Phone: +81 (0) 3 3235 5961  
E-mail: [myoshihawa@aaas.org](mailto:myoshihawa@aaas.org)

### To subscribe to *Science*:

In US/Canada call 202-326-6417 or 1-800-731-4939  
In the rest of the world call +44 (0) 1223-326-515

*Science* makes every effort to screen its ads for offensive and/or discriminatory language in accordance with US and non-US law. Since we are an international journal, you may see ads from non-US countries that request applications from specific demographic groups. Since US law does not apply to other countries we try to accommodate recruiting practices of other countries. However, we encourage our readers to alert us to any ads that they feel are discriminatory or offensive.

**Science Careers**

From the journal *Science*



## POSITIONS OPEN

### ASSISTANT/ASSOCIATE/FULL PROFESSOR (COMPUTATIONAL BIOLOGIST)

Department of Biological Sciences/Center for  
Computation and Technology

The Department of Biological Sciences and the Center for Computation and Technology (CCT) at Louisiana State University (LSU) invite applications for a joint faculty position in computational biology, broadly defined. Required qualifications: Ph.D.; a successful track record of independent research; areas of interest include, but are not limited to: biomolecular structure/function, systems biology modeling, genomics, and computational neuroscience. Responsibilities: maintains and has a vigorous, extramurally funded research program and contributes to undergraduate and graduate teaching; works closely with faculty in biological sciences and other departments at LSU, as well as the CCT faculty to foster the development of a center of excellence in computational biology at LSU. LSU anticipates hiring several additional faculty in computational biology in the future.

The CCT offers an innovative and interdisciplinary research environment for advancing computational sciences, including a highly competitive computing environment with access to 100 TFlops of computing resources in conjunction with the Louisiana Optical Network Initiative (LONI). This position is also offered in conjunction with the LONI Institute ([website: http://institute.loni.org/](http://institute.loni.org/)), a bold new inter-university collaboration aiming to fill a dozen new faculty positions in related areas. LSU is part of the national TeraGrid. For additional information visit our departmental [website: http://www.biology.lsu.edu](http://www.biology.lsu.edu), and the CCT [website: http://www.cct.lsu.edu/home](http://www.cct.lsu.edu/home).

*An offer of employment is contingent on a satisfactory pre-employment background check.* Application deadline is January 30, 2009, or until a candidate is selected. Send curriculum vitae (including e-mail address), statements of research and teaching interests, three letters of recommendation, and no more than three representative publications to:

Charyl Thompson  
Department of Biological Sciences  
202 Life Sciences Building  
Louisiana State University  
Reference: Log #2041  
Baton Rouge, LA 70803

*LSU is an Equal Opportunity/Equal Access Employer. We encourage applications from women and minorities.*

The Biology Department and the Institute for Environmental Science and Sustainability at Wilkes University offers a two-year **TEACHING/RESEARCH POSTDOCTORAL FELLOWSHIP** in ecology funded by the Howard Hughes Medical Institute starting in 2009. Wilkes University, located near the Pocono Mountains, offers low-cost living and numerous outdoor activities within a 2.5-hour drive of New York City and Philadelphia.

The position entails 70 percent research and 30 percent teaching. The research topic is open, but should mesh with faculty interests. Examples of ongoing research include seed dispersal, landscape effects on community structure and function, forest regeneration, and food web reconstruction in natural or human-impacted systems. See [website: http://www.wilkes.edu/wiess](http://www.wilkes.edu/wiess) for more information on research and teaching activities. Desirable skills may include spatial modeling/geographic information system, statistics, or demographic modeling. Fellows will teach a course in their specialty and may help develop a new research-intensive laboratory course. A Ph.D. is required and strong interpersonal and writing skills are essential. Salary and benefits are competitive and commensurate with experience.

Submit curriculum vitae, transcripts, representative publications, research and teaching statements, and contact information for three references to both [e-mail: ecaply@wilkes.edu](mailto:ecaply@wilkes.edu) and [e-mail: jeffrey.stratford@wilkes.edu](mailto:jeffrey.stratford@wilkes.edu). Indicate the reference # GS0182 on the subject line. Review of applications will begin one month after ad publication date. Start date is flexible. *Wilkes University is an Equal Opportunity Employer committed to a diverse faculty, staff, and student body. Applicants from diverse backgrounds are strongly encouraged to apply.*

## POSITIONS OPEN

**MICHIGAN STATE  
UNIVERSITY**

### JOHN A. HANNAH DISTINGUISHED PROFESSORSHIP in GENE REGULATION Department of Biochemistry and Molecular Biology

Michigan State University (MSU) invites applications and seeks nominations for a John A. Hannah Professorship in Gene Regulation. The position is intended to complement a strong gene regulatory research presence in areas of structural, biochemical, genetic, and bioinformatic studies in animal, plant, and microbial systems. The individual selected will bring innovative and multidisciplinary approaches to bear on central questions in gene regulation, including but not restricted to analysis of regulatory networks, structural analysis of higher-order complexes, systems biology, microRNAs, and dynamics of molecular complexes in live cells. It is anticipated that the candidate will contribute to the highly collaborative research atmosphere on campus and take a leadership role in enhancing training and research in the area of gene regulation. The recent MSU Midwest Symposium on Transcriptional Regulation and Systems Biology showcases work in this area. MSU is making significant investments in gene expression in development and disease ([website: http://bmb.msu.edu/gecd/index.html](http://bmb.msu.edu/gecd/index.html)), including four additional faculty positions that the new Hannah Professor will take a lead in recruiting.

This tenured research and teaching position comes with significant operating funds provided annually for program support. The primary appointment will be based in the Department of Biochemistry and Molecular Biology, with possible joint appointments in related departments.

The John A. Hannah Professorships were established in 1969, and are awarded to exceptional scholars to honor Hannah's 25 years as president of the University. Applications will be received until a suitable candidate is identified.

Applications should include cover letter, curriculum vitae, and statement of research interests and future directions. Application materials should be sent electronically to [e-mail: hannahchair@cns.msu.edu](mailto:hannahchair@cns.msu.edu). Questions regarding this position may be sent to [David Arnosti \(e-mail: arnosti@msu.edu\)](mailto:David.Arnosti@msu.edu).

*Women and minorities are encouraged to apply. Michigan State University is an Affirmative Action, Equal Opportunity Employer; MSU is committed to achieving excellence through cultural diversity. The University actively encourages applications and/or nominations of women, persons of color, veterans, and persons with disabilities.*

### FACULTY POSITION in PHARMACOLOGY East Tennessee State University

**ASSISTANT/ASSOCIATE PROFESSOR.** The Department of Pharmacology at the James H. Quillen College of Medicine invites applications for a faculty position. The Department is seeking a candidate with a nationally competitive research program in neuropharmacology and/or psychopharmacology. Applicants must have a Ph.D. and/or M.D. and postdoctoral training, and preferably have a nationally funded research program. Additional responsibilities will include teaching medical and graduate students. Appointments will be tenure or research track commensurate with qualifications and experience. Successful applicants will be provided competitive salaries and startup packages. East Tennessee State University (ETSU), [website: http://www.etsu.edu](http://www.etsu.edu), is located in one of the nation's most beautiful regions, just north of the Great Smoky Mountain National Park. Applicants should submit an ETSU application, curriculum vitae, brief statement of current and future research goals, and names and addresses of three references to: **Ms. Betty Hughes, Department of Pharmacology, James H. Quillen College of Medicine, East Tennessee State University, P.O. Box 70577, Johnson City, TN 37614-1708.** *Affirmative Action/Equal Opportunity Employer.*



WWW.NIH.GOV

# Positions NIH

## THE NATIONAL INSTITUTES OF HEALTH



### Investigator Recruitment in Genetic Disease Research

National Human Genome Research Institute

The Genetic Disease Research Branch (GDRB) of the National Human Genome Research Institute (NHGRI) provides unparalleled opportunities for young investigators to develop world-class research programs in genetics and genomics. The Branch is pleased to announce that it is seeking to recruit a new tenure-track investigator to pursue innovative, independent research as part of this group of highly interactive and supportive investigators.

Current GDRB faculty members use a variety of approaches to study the regulation and function of genes involved in normal and abnormal development, focusing on diseases in both humans and model systems. We are seeking to recruit an individual whose research interests and approaches complement those already found within the Branch. Specifically, the ideal candidate will have an interest in developing a research program that integrates:

- **Clinical or translational research**
- **Molecular and genomic approaches aimed at understanding the mechanisms of normal development and disease**
- **Basic genetic or genomic research**

The Branch strongly supports interdisciplinary research, with NHGRI faculty providing mentoring and guidance to individuals interested in developing research programs involving basic, clinical, and translational approaches.

The successful candidate will be able to take advantage of interactions with a highly collegial group of scientists within NHGRI and on the NIH campus as a whole. In addition, the successful candidate will have access to NHGRI's outstanding core laboratories, as well as the unparalleled resources of the NIH Clinical Center.

Candidates must have a Ph.D., M.D., or equivalent degree, as well as comprehensive, advanced training and a record of accomplishment in one of the targeted areas. This position includes a generous start-up allowance, an ongoing commitment of research space, laboratory resources, and positions for personnel and trainees.

Interested applicants should submit a *curriculum vitae*, a three-page description of proposed research, and three letters of recommendation through our online application system, at <http://research.nhgri.nih.gov/apply>.

**Applications will be reviewed starting Monday, December 15, 2008 and will be accepted until the position is filled.**

For more information on GDRB and NHGRI's Intramural Program, please see <http://genome.gov/DIR>. Specific questions regarding the recruitment may be directed to Dr. William Pavan, the Search Chair, at [bpavan@nhgri.nih.gov](mailto:bpavan@nhgri.nih.gov). Questions may also be directed to Dr. Leslie Biesecker, the GDRB Branch Chief, at [leslieb@nhgri.nih.gov](mailto:leslieb@nhgri.nih.gov).

DHHS and NIH are Equal Opportunity Employers and encourage applications from women and minorities.

**NATIONAL HUMAN GENOME RESEARCH INSTITUTE** Division of Intramural Research

U.S. DEPARTMENT OF HEALTH AND HUMAN SERVICES | NATIONAL INSTITUTES OF HEALTH | [genome.gov/DIR](http://genome.gov/DIR)



#### PROGRAM OFFICER

The National Institute of Mental Health (NIMH), National Institutes of Health (NIH), Department of Health and Human Services, is inviting inquiries from potential candidates for a Program Officer position within the Adult Psychopathology and Psychosocial Intervention Research Branch, Division of Adult Translational Research and Treatment Development (DATR). This Program Officer will provide leadership and direction for a research program of national and international scope in the area of Schizophrenia Spectrum Disorders. The incumbent will be responsible for program leadership and development, project management and administration, and scientific activities. The Branch supports research on the foundations of psychopathology and promotes translational research on the development, onset, and course of adult psychopathology and its fundamental processes, such as emotion, cognition, and motivation. The program encompasses research on modifiable risk and protective factors and modern psychometric techniques, especially via interdisciplinary approaches that integrate biology and psychology. The scientific and technical background appropriate for this position could come from any of a large number of areas, including, but not limited to: psychiatry, psychology, and public health. Candidates must have a relevant doctoral degree and research experience in schizophrenia spectrum disorders. An individual filling this position would work closely with the Branch Chief, Adult Psychopathology and Psychosocial Intervention Research Branch, DATR. The ability to work both independently and collaboratively is required. Strong scientific, analytic, communication, and organizational skills are also required. This is a permanent position. Salary will be commensurate with experience.

To explore interest in potential candidacy for this position, email or fax curriculum vitae to **Michael Kozak, Ph.D.**, at [kozakm@mail.nih.gov](mailto:kozakm@mail.nih.gov) or 301-443-4611 (fax). **Telephone inquiries are welcome at 301-443-6471.** With nationwide responsibility for improving the health and well being of all Americans, the Department of Health & Human Services oversees the research programs of the National Institutes of Health. <http://www.os.dhhs.gov>.



#### National Institute of Mental Health Deputy Director Office of the Director

The National Institute of Mental Health, a major research component of the National Institutes of Health (NIH) and the Department of Health and Human Services (DHHS), is seeking exceptional candidates for the position of Deputy Director, Office of the Director (OD). The Deputy Director serves as the second-in-command for the Institute. Working closely with the Director, the Deputy Director assists in the scientific and administrative management of an organization with a budget of \$1.4 billion and a staff of approximately 1,300. (<http://www.nimh.nih.gov/index.shtml>)

The Deputy Director is primarily responsible for implementation of the Institute's Strategic Plan and management of the daily operations of the Institute. In this sense, the Deputy Director is the chief internal champion and guarantor for the intellectual and administrative environment at the Institute. The Deputy Director is aided in this effort by the Directors of the Institute's divisions and offices. The Deputy Director also serves as an ambassador and spokesperson for the Institute.

Applicants must have a Ph.D., M.D., or equivalent degree in the biomedical sciences, with broad senior-level research experience and experience in direct administration of a research program. Applicants should be known and respected within their profession, both nationally and internationally, as distinguished individuals of outstanding scientific competence and administrative capability. Salary is commensurate with experience and accomplishments. Experience with NIH administrative policies, procedures, and operations is highly desirable but not essential.

Interested candidates should send a letter of interest, including a brief description of research and administrative experience, a curriculum vitae and bibliography, and the names of at least three references to: **Chair, NIMH Deputy Director Search Committee at [NIMHsearch@mail.nih.gov](mailto:NIMHsearch@mail.nih.gov) or at 6001 Executive Blvd, Room 8235, MSC 9669 Bethesda, MD 20892-9669 (for express or courier delivery use Rockville, MD 20852).** Review of applications will begin on **November 3, 2008**, but applications will continue to be accepted and considered until the position is filled. For questions contact **Dr. Thomas Insel, Director, NIMH** at [tinsel@mail.nih.gov](mailto:tinsel@mail.nih.gov).



# MichiganTech

## Endowed Professorships and Faculty Positions in Computational Discovery and Innovation

Michigan Technological University announces a Strategic Faculty Hiring Initiative (SFHI) that will add ten tenure-track positions, including at least two endowed professorships, during 2009. SFHI is an ongoing commitment to substantially expand Michigan Tech's faculty resources in targeted strategic areas of multidisciplinary research and inquiry. This initiative follows on last year's first SFHI which resulted in ten hires in the area of Sustainability.

Michigan Tech seeks to attract exceptional candidates whose interests and capabilities match the following objectives and activities: develop computationally based tools, processes, and environments; extend the boundaries of high-performance computing (HPC); investigate and model complex systems; foster synergies in research methodologies, computational techniques, and innovation.

Michigan Tech seeks a diverse applicant pool from a wide range of disciplines in this strategic initiative. For full consideration, applications should be received by January 30, 2009; review will continue until all positions are filled. Attractive salary, benefit and start-up packages will be provided for successful applicants.

Details about the Michigan Tech Strategic Faculty Hiring Initiative in *Computational Discovery and Innovation* are available at [www.mtu.edu/sfhi](http://www.mtu.edu/sfhi). Applicants should prepare their materials as a single PDF document, and send it as an e-mail attachment to [provost@mtu.edu](mailto:provost@mtu.edu). More general information on Michigan Technological University is available at [www.mtu.edu](http://www.mtu.edu).

Michigan Tech is an internationally renowned doctoral research university located in Michigan's scenic Upper Peninsula, on the south shore of Lake Superior. Houghton provides a unique setting where natural beauty, culture, education, and a diversity of residents from around the world come together to share a superb living and learning experience.

*Michigan Technological University is an Equal Opportunity, Affirmative Action Employer/ Educational Institution. Applications from women and minorities are encouraged.*

**BCM** Baylor College of Medicine®

## CENTER FOR MEMORY AND LEARNING

**Menninger Department of Psychiatry and Behavioral Sciences**

### Tenure Track Faculty Position

The Center for Memory and Learning and the Menninger Department of Psychiatry and Behavioral Sciences at Baylor College of Medicine are recruiting a tenure track Assistant or Associate Professor with expertise and research interests in the genetics of human learning disabilities/psychiatric disease. Candidates should have a Ph.D. and/or M.D. and postdoctoral experience. This is a research position, although M.D. appointees may have a limited amount of clinical activity. The candidate will have a primary faculty appointment in the Department of Psychiatry and will be a member of the Center for Memory and Learning, with opportunities for affiliations with other departments and programs. The position will provide a competitive allowance for laboratory start-up and ongoing support. Please send *curriculum vitae* and statement of research interests electronically as a single PDF to [lyndaa@bcm.tmc.edu](mailto:lyndaa@bcm.tmc.edu). Please have hard copies of at least three letters of reference sent to: CML Search Committee, c/o Lynda Lynch, Department of Molecular and Cellular Biology, Baylor College of Medicine, One Baylor Plaza, BCM130, Houston, TX 77030 by February 15, 2008.

*Baylor College of Medicine is an Equal Opportunity/ Affirmative Action and Equal Access Employer.*

## Head, Electron Microscopy Facility Sloan-Kettering Institute

The Sloan-Kettering Institute (SKI) is seeking to fill a position to lead its Electron Microscopy (EM) Core Facility. SKI offers a highly interactive basic, translational and clinical cancer-focused research environment ([www.ski.edu](http://www.ski.edu)) and is located in a multi-institutional academic community. This is a non-tenure track position, fully supported by the Institution.

In this position, you will oversee all operations of the EM Facility including supervision of staff, operations and troubleshooting of Transmission and Scanning Electron microscopes. You will provide technical consultation to the academic staff to optimize use of the microscopes to support research objectives and provide hands-on training to facility users. Additionally, you will assure that established standards of quality are met and that the facility remains state-of-the art. You will also perform administrative duties that include preparation of reports, budgets and charge backs to facility users.

Applicants must have Ph.D. in Biology or other related areas and several years of experience with Transmission Electron Microscopy in an analytical research and development or academic environment. A record of productivity and management experience is desirable.

Candidates should e-mail their CV and bibliography, a cover letter describing career objectives, and the names of 3 referees in PDF format to: [cbtrack@mskcc.org](mailto:cbtrack@mskcc.org). Inquiries regarding this position should be sent to Diane Tabarini, PhD, Director Core Facility Operations at [tabarind@mskcc.org](mailto:tabarind@mskcc.org) or Alan Hall, PhD, Chairman of Cell Biology at [halla@mskcc.org](mailto:halla@mskcc.org). Deadline: December 1, 2008. Memorial Sloan-Kettering is an affirmative action, equal opportunity employer.



Memorial Sloan-Kettering Cancer Center

[www.mskcc.org](http://www.mskcc.org)



國家衛生研究院  
National Health Research Institutes

## Immunology Research Center National Health Research Institutes (NHRI) Taiwan

The newly established Immunology Research Center at the National Health Research Institutes (NHRI) in Taiwan invites applications for multiple tenure-track/tenured faculty positions at the rank of **Assistant, Associate, or Full Investigator** (the equivalents of Assistant, Associate, and Full Professor). Highly qualified candidates are sought with research interests in all areas of **Immunology and Signal Transduction**, especially in the areas of cell signaling and gene regulation, innate immunity, cancer immunology, hematopoietic/cancer stem cells, Treg/Th17 cells, and gene targeting. Applicants should have a Ph.D. and/or M.D. degree as well as extensive postdoctoral experience. Selection will be based on excellence in research and the potential to maintain an outstanding research program. Investigators will have the opportunity to train graduate students from several affiliated universities. A generous annual intramural support will be provided.

Applicants should send curriculum vitae, description of research accomplishments and future objectives, and three reference letters to:

**Faculty Search Committee  
Immunology Research Center  
National Health Research Institutes  
35 Keyan Road, Zhunan Town  
Miaoli County 35053, Taiwan**

Review of credentials is ongoing and will continue until the positions are filled. Further information can be obtained from **Ms. Yu-Feng Huang** at [kitty01@nhri.org.tw](mailto:kitty01@nhri.org.tw).

# PICTURE YOURSELF AS A AAAS SCIENCE & TECHNOLOGY POLICY FELLOW

## **Make a Difference.**

Help give science a greater voice in Washington, DC! Since 1973, AAAS Fellows have applied their skills to federal decision-making processes that affect people in the U.S. and around the world, while learning first-hand about the government and policymaking.

## **Join the Network.**

Year-long fellowships are available in the U.S. Congress and federal agencies. Applicants must hold a PhD or equivalent doctoral-level degree in any behavioral/social, biological, medical/health, or physical science, or any engineering discipline. Individuals with a master's degree in engineering and three years of post-degree professional experience also may apply. Federal employees are not eligible and U.S. citizenship is required.

## **Apply.**

The application deadline for the 2009-2010 AAAS Fellowships is 15 December 2008. Fellowships are awarded in the spring and begin in September. Stipends range from \$70,000 to \$92,000.

*Note: Additional fellowships are available through approximately 30 scientific society partners. Individuals are encouraged to apply with AAAS as well as with any scientific societies for which they qualify.*

Full details at: **[fellowships.aaas.org](http://fellowships.aaas.org)**



*Enhancing Public Policy,  
Advancing Science Careers*

### **Christina Kakoyannis, PhD**

Forest Resources,  
Oregon State University

2005-2007 AAAS Fellow  
at the U.S. Environmental  
Protection Agency in the  
Office of Environmental  
Policy Innovation,  
Evaluation Support Division

Now an evaluation officer  
at the National Fish and  
Wildlife Foundation in  
Washington, DC



ADVANCING SCIENCE, SERVING SOCIETY



The Science and Technology Foundation of Albacete (STFA), Spain, invites applications for up to sixty research positions in different Research Centers located in the Science and Technology Park of Albacete, or the University of Castilla-La Mancha.

Successful applicants must hold a doctorate in an appropriate field, must have demonstrated an ability to suitably conduct research, and have acquired at least four years of postdoctoral experience. Applicants will be expected to develop and maintain an independent research plan and help to establish interdisciplinary programs in different areas of science or technology. These areas include, but are not limited to, Health and Biomedicine, Agriculture, Mechanical Engineering, Information and Communication Technologies, New materials, Nanoscience, Nanotechnology and Nanobiotechnology, and Robotics. Exceptional candidates in these or in other areas will be given serious consideration. Salary and rank are commensurate with qualifications and experience of the candidates. Selected candidates will be offered an initial three year contract period, after which they will be evaluated according to their scientific productivity and accomplishments. Candidates with a favorable evaluation will be offered a permanent contract as staff researchers.

STFA embraces diversity and seek candidates who will create a climate that attracts students and researchers of all races, nationalities and genders. We strongly encourage women and underrepresented minorities to apply. Located in the renowned region of Castilla-La Mancha, Spain, STFA is an audacious, innovative and inclusive research environment of public service and academic distinction where staff and researchers alike are encouraged to be active citizens of the world.

Qualified candidates are invited to submit their curriculum vitae and a statement of research interests to:

Dr. Jorge Laborda  
Albacete Science and Technology Park  
Centro de Emprendedores. Paseo de la Innovación, 1.  
02006 Albacete, Spain.  
Albacete, Spain  
Job Code: INCRECYT

Candidates should also arrange to have three letters of recommendation sent directly from the referees to the above address.

All required application materials (curriculum vitae, statement of research interests and letters of recommendation) should be received by December 15th.

For informal enquiries please contact increcyt@pcyta.com and visit our website www.pcyta.com for the full application procedure.

Funded by the European Social Fund (ESF INVESTING IN PEOPLE). Operational Programme 2007-2013 Priority Axis 3.



## A FACULTY POSITION IN PLANT BIOLOGY

The Institute of Plant and Microbial Biology, Academia Sinica, Taipei is inviting applications for a research focused faculty position in any area of plant biology. Applicants with experience in bioinformatics/systems biology or plant secondary metabolism will be of special interest. This position can be at the level of Assistant, Associate, or Full Research Fellow (equivalent to Assistant, Associate, and Full Professor in a university) depending on the applicant's experience. Excellent facilities and starter grants will be provided for the position. For details of the Institute and Academia Sinica, please visit the website at <http://ipmb.sinica.edu.tw/>. Applicants are expected to have a Ph.D. degree plus postdoctoral training. Chinese language skills are NOT required and international scientists are encouraged to apply.

The application folder should include curriculum vitae, a statement of research accomplishments, and future research plans. The application folder and at least three letters of recommendation should be sent to: **Dr. Shu-Hsing Wu, Chair of Search Committee, Institute of Plant and Microbial Biology, Academia Sinica, 128, Sec 2, Academia Rd, Nankang, Taipei, Taiwan 11529. e-mail: shuwu@gate.sinica.edu.tw FAX: (+886)2-2782-1605.** The review of applications will start on **February 1, 2009** and continue until the position is filled.



## DEAN, ROSENSTIEL SCHOOL OF MARINE AND ATMOSPHERIC SCIENCE

University of Miami (UM) invites nominations and applications for Dean of the Rosenstiel School of Marine and Atmospheric Science (RSMAS). With a strong institutional foundation, the new Dean will have the unique opportunity to lead the School to greater prominence through the pursuit of excellence in research and education and the continued development of interdisciplinary initiatives.

The new Dean will bring to the position a record of personal excellence in research and scholarship, strong background in post-secondary education, demonstrated skill in resource development and fund raising, extensive experience in management and administration, and earned respect in the national and international communities. S/he must possess a fundamental commitment to scholarly excellence and first-class education. In this deanship, the University seeks an energetic and creative leader—a builder and a collaborator—who is an inclusive and responsive academic administrator with the capacity to inspire and nurture consensus.

RSMAS is one of the premier oceanographic research and education institutions in the world. As the only subtropical institute of its kind in the continental United States, it has a distinguished faculty across a variety of disciplines, a substantial professional staff, and an excellent record of acquiring competitive external funding. Through excellence in applied and basic marine and atmospheric research, the School sheds light on today's most pressing environmental issues, including fisheries, oceans, human health, storms and hurricanes, climate change, and coral reefs. The School's academic role includes strong graduate research programs in Applied Marine Physics, Marine Affairs and Policy, Marine and Atmospheric Chemistry, Marine Biology and Fisheries, Marine Geology and Geophysics, and Meteorology and Physical Oceanography and is also responsible for nationally recognized undergraduate Marine and Atmospheric Science programs.

UM is one of the nation's leading private research universities, serving over 15,600 undergraduate and graduate students and offering 120 undergraduate, 107 masters, 50 doctoral and two professional areas of study. RSMAS, established in 1943, is located on Virginia Key in Biscayne Bay and has some 100 faculty, 250 staff, 250 graduate students, and 100 undergraduates. Additional information about the UM and RSMAS can be found at the University's website: [www.miami.edu](http://www.miami.edu). Applications and nominations should be sent, preferably in electronic form, to: **Vivian Brocard, Vice President and Director, Isaacson, Miller, 3744@imsearch.com.**

The University of Miami is an Equal Opportunity/Affirmative Action Employer



ISAACSON, MILLER  
[www.imsearch.com](http://www.imsearch.com)

## NATIONAL RESEARCH COUNCIL

OF THE NATIONAL ACADEMIES

### Research Associateship Program

#### Postdoctoral Research Awards

#### Senior Research Awards

#### Summer Faculty Fellowships

#### Davies Teaching Fellowships

offered for research at  
US government laboratories

### Opportunities for postdoctoral and senior research in all areas of science and engineering

- Awards for independent research at approximately 100 participating laboratory locations
- 12-month awards renewable for up to 3 years
- Annual stipend \$42,000 to \$72,000 - higher for senior researchers
- Relocation, professional travel, health insurance
- Annual application deadlines Feb. 1, May 1, Aug. 1, Nov. 1
- Many opportunities available to non-US as well as US citizens

Detailed program information, including instructions on how to apply, is available on the NRC Web site at :  
**[www.national-academies.org/rap](http://www.national-academies.org/rap)**

Applicants must initiate dialogue with prospective Advisors at the Lab as early as possible, before their anticipated application deadline.

Questions should be directed to the :

#### National Research Council

TEL: (202) 334-2760

E-MAIL: [rap@nas.edu](mailto:rap@nas.edu)

Qualified applicants will be reviewed without regard to race, religion, color, age, sex or national origin.

#### THE NATIONAL ACADEMIES

Advisers to the Nation on Science, Engineering, and Medicine



# MICHIGAN STATE UNIVERSITY

## Cancer Biologist Endowed Professorship at Michigan State University

Michigan State University, in East Lansing, Michigan, invites applications and nominations to fill an endowed, tenured, faculty position in one or more of the following departments: Biochemistry & Molecular Biology, Microbiology & Molecular Genetics, Pharmacology & Toxicology, or Physiology. The Walter F. Patenge Health Sciences Professorship is a laboratory-based research-oriented position that will be filled by an established cancer biologist with a superior record of peer-reviewed publications and an outstanding record of funded research in the area of human cancer.

MSU has research strengths in a wide array of basic and clinical sciences that promote a highly collegial and interdisciplinary environment with many collaborative opportunities. MSU has established state of the art research support facilities in such areas as genomics, proteomics, and microscopy. The Patenge Professor will have access to graduate students in his/her department(s) as well as graduate students in two interdepartmental programs: Cell & Molecular Biology, and Genetics. The Patenge search is part of a coordinated, well-funded initiative to enhance research on human disease at MSU.

The Patenge Professor will receive: sizeable laboratory space, a substantial setup package, the annual interest from the endowment to further the candidate's research, and an annual salary from the university commensurate with the rank of endowed professor.

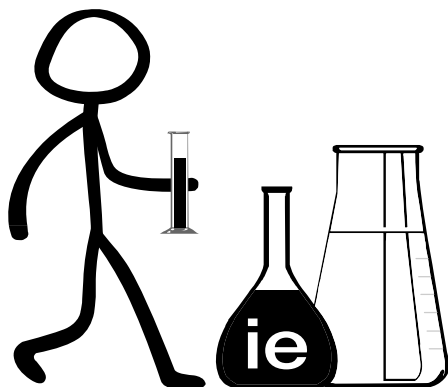
**QUALIFICATIONS:** The Patenge Professor will possess a research and/or medical degree (e.g., Ph.D., Sc.D., D.O., M.D.). Candidates must have a background that demonstrates his/her ability to work synergistically with both scientific and medical colleagues. The candidate will provide energetic leadership and creative direction in building a world-class cancer research program.

**APPLICATIONS:** This position will remain open until filled. Send a letter of application, a detailed curriculum vita and a statement of research goals along with pertinent reprints and contact information for three references (address, e-mail, and phone). These materials should be addressed to: **Chairperson, Patenge Search Committee; A314 East Fee Hall; Michigan State University, East Lansing, MI 48824.** E-mailed submissions in PDF format are welcomed and encouraged at [patenge.search@hc.msu.edu](mailto:patenge.search@hc.msu.edu).

MSU is committed to achieving excellence through cultural diversity. The University actively encourages applications and/or nominations of women, persons of color, veterans and persons with disabilities.

**MSU IS AN AFFIRMATIVE ACTION, EQUAL OPPORTUNITY EMPLOYER.**

## GRADUATE PROGRAM



**Discover the formula for success**

### Master in Biotechnology Management

Recent advances in life sciences have brought about a revolution in the biotechnology industry. To face these new challenges and meet the resulting business opportunities, IE Business School offers an innovative and challenging Master's program in Biotechnology Management, which combines general business knowledge with specialized industry know-how.

The program is aimed at professionals from either a scientific or management background looking to jump-start or further their careers within the biotech industry.

Our program methodology reflects today's international business environment, where cross-cultural teams work on global projects regardless of their geographic location. You will not have to leave your residence or work place for extended periods of time to pursue a truly rewarding learning experience.

For more information about this program, please visit: [www.ie.edu/biotech](http://www.ie.edu/biotech)  
Admissions contact: [biotech@ie.edu](mailto:biotech@ie.edu)

IE Business School, Madrid, Spain • Tel. + 34 91 568 96 10

[www.ie.edu/business](http://www.ie.edu/business)

At Monsanto, our talented employees are contributing to our success as a global leader in agriculture. We are creating solutions that improve productivity in farming while reducing the impact on our environment. We are looking for a talented individual for the following position in **Ankeny, IA:**

### Soy Discovery Breeding Lead

This is an exciting and challenging role to apply molecular genetic technologies to soy breeding for enhancing crop yield and agronomic traits, such as maturity and oil quality. PhD or equivalent experience in Genetics or Plant Breeding and 5 or more years of additional relevant experience are required.

To view a more complete and detailed job description, please visit our website at [www.monsanto.com](http://www.monsanto.com) and select **req # mons-00009860**. We offer very competitive salaries and an extensive benefits package.

*The life of any plant starts with a seed. Within the right environment it grows to become something amazing. At Monsanto, our philosophy is the same – we are committed to helping individuals progress in careers with unlimited potential.*

## The world, re-imagined

Imagine your world at Monsanto by visiting us on our website, [www.monsanto.com/careers](http://www.monsanto.com/careers)

Monsanto is an equal opportunity employer who values diversity.

MONSANTO  
imagine®



Massachusetts Institute of Technology

It takes everyone at MIT to be MIT.

## Faculty Position

### Department of Chemical Engineering

The MIT Department of Chemical Engineering seeks candidates for a tenure-track faculty position to begin July 2009 or thereafter. Appointment would be at the assistant or untenured associate professor level. In special cases, a senior faculty appointment may be possible. Faculty duties include teaching at the graduate and undergraduate levels, research, and supervision of student research. We will consider candidates with backgrounds and interests in chemical engineering or a related field. Candidates should hold a Ph.D. in chemical engineering or a related field by the beginning of the appointment period. The candidate should have demonstrated excellence in original research.

**Interested candidates should submit application materials electronically at <https://chemefacsrch.mit.edu>. Each application should include: a curriculum vitae; the names and addresses of three or more references; a statement of research interests; and a statement of teaching interests. We request that each candidate arrange for reference letters to be uploaded at <https://chemefacsrch.mit.edu/letters/>. Questions should be addressed to [ChemE-Search-Master@chemefacsrch.mit.edu](mailto:ChemE-Search-Master@chemefacsrch.mit.edu). Responses by December 15, 2008 will be given priority.**

*We especially encourage minorities and women to apply because of MIT's strong commitment to diversity in engineering education, research and practice.*

<http://web.mit.edu>



### FACULTY POSITIONS IN PHYSIOLOGY School Of Medicine Louisiana State University Health Sciences Center New Orleans

The Department of Physiology at LSU Health Sciences Center in New Orleans invites established investigators with PhD or equivalent degree, to apply for tenure track faculty positions at the rank of **ASSOCIATE or FULL**

**PROFESSOR** commensurate with experience. Successful candidates will have a strong record of research accomplishments, lead a productive, nationally funded research program, and have the vision and commitment to build a collaborative research program. Expertise in all areas of physiology will be considered, but special consideration will be given to those that complement the existing research strengths of the department which include pathophysiology of the host defense response to inflammation, trauma & infection, renal physiology, cardiovascular physiology, and obesity & diabetes. Candidates with international distinction in cardiovascular research will be considered for the Pfizer-Ardoin Superchair in Cardiovascular Research. LSUHSC-NO School of Medicine has a collaborative research environment to include core laboratory support for research involving genomics, proteomics, imaging, and flow cytometry. Opportunities are available for interaction with the Centers of Excellence in Alcohol and Drug Abuse, Cancer, Cardiovascular Biology, Neuroscience and Oral Biology as well as the Program in Gene Therapy. Faculty are expected to sustain an externally funded research program in a collaborative environment, to mentor graduate students/postdoctoral fellows, and to participate in graduate and professional education programs. Excellent start-up package and competitive salaries are available.

Applicants should send their curriculum vitae that includes funding history, teaching experience, a statement of research plans, and the names of references to: [physiologyrecruit@lsuhsc.edu](mailto:physiologyrecruit@lsuhsc.edu) or **ATTN: Physiology Faculty Recruitment, Department of Physiology, LSU Health Sciences Center, 1901 Perdido Street, New Orleans, LA 70112**. Review of applications will commence immediately and will continue until the positions are filled.

*LSUHSC is an Equal Opportunity/Affirmative Action Employer.*



ILLINOIS

### Faculty Position — Open Rank Antibiotic Research

The Department of Chemistry and the Institute for Genomic Biology at the University of Illinois at Urbana-Champaign seek applications for an open rank faculty position in the field of antibiotic research. The successful candidate will be expected to play a major role in a multi-investigator research program that addresses broadly defined problems relating to the discovery and development of antibiotics. We are particularly interested in candidates conducting research into microbial secondary metabolism, antimicrobial natural products, or antibiotic biosynthesis. However, applicants with expertise in other areas of antibiotic research will also be seriously considered. An endowed chair position is possible for highly qualified senior applicants. The chosen candidate will be appointed in the Department of Chemistry and will join an active research team in the Institute for Genomic Biology. IGB currently includes members of the Departments of Chemistry, Microbiology, Biochemistry and Chemical and Biomolecular Engineering who are engaged in research towards antibiotic discovery, design and development. Salary is negotiable. Ph.D. required.

The Department of Chemistry prefers that applications be submitted online, and include a cover letter, curriculum vitae, detailed research statement, and three letters of recommendation. To submit an application electronically, go to <https://www.scs.uiuc.edu/faculty> applicants. We strongly recommend that you fill out the online application form as soon as you have assembled the names and email addresses of 3 references. This will create your application file, after which you (and your letter writers) will be able to upload application documents and reference letters. If necessary, applications and an email address could be mailed to: Chemistry/IGB Faculty Search Committee, 107 Noyes Lab, Box D-1, 600 S. Mathews Ave., Urbana, IL 61801. All applications received by December 31, 2008, will receive full consideration. Starting date is August 16, 2009. If you have any questions or need help with the online application process, please call (217)-333-5071.

The University of Illinois is an Affirmative Action-Equal Opportunity Employer.



**TWO ASSISTANT PROFESSOR POSITIONS  
DEPARTMENT OF PHYSIOLOGY  
MEMPHIS, TN**

The Department of Physiology at The University of Tennessee Health Science Center (UTHSC) in Memphis invites outstanding scientists with Ph.D., M.D., or equivalent degrees for **two tenure-track faculty positions at the rank of assistant professor to begin July 1, 2009**. We are searching for creative scientists who have or will establish an extramurally funded research program and also excel at teaching medical, dental, and graduate students. UTHSC is the state's flagship academic health center with an annual budget of close to 400 million dollars, and the Department of Physiology is currently ranked seventh based on extramural funding by the American Physiological Society. We will consider applicants in all areas of physiology, but excellence of the candidates supersedes the area of research interest. The positions are part of the expansion of the department; significant new laboratory space, a substantial start up package, and a competitive salary with an additional incentive bonus will be offered.

Candidates should submit their Curriculum Vitae, a description of research interests/goals (not to exceed two pages) as a single PDF document, and arrange to have three letters of reference sent to: **Gabor Tigyi, M.D., Ph.D., Harriett Van Vleet Professor and Chair, Department of Physiology; E-Mail: PhysiologySearch@utmem.edu; Website: <http://physiol1.utmem.edu>**.

Applicants should have their applications complete by **January 15, 2009**, as review will begin upon receipt of the application.

*UTHSC is an Equal Opportunity Employer.*



**Herman B Wells Center for Pediatric Research  
James Whitcomb Riley Hospital for Children  
Molecular Oncology Program  
Assistant/Associate/Full Professor**

The Department of Pediatrics, Section of Pediatric Hematology/Oncology, and Indiana University School of Medicine is recruiting two full-time academic positions at the Assistant/Associate/Full Professor level in the area of molecular oncology. The senior position comes with an endowed Chair in molecular oncology research. Candidates can be PhD, MD or MD/PhD, must have a strong research background and either current or potential for independent funding. Successful candidates will be expected to establish a robust externally funded research program. Laboratory space is in the Herman B Wells Center for Pediatric Research, which has ongoing programs in cancer biology, DNA repair, cardiology, stem cell biology, genetic blood disorders, myeloid biology, leukemogenesis and development. The position comes with a generous start-up package, outstanding laboratory space and protected time for research-related activities.

The search committee will begin evaluating applications as they are received and applications will continue to be reviewed until the positions are filled. Interested applicants should submit a curriculum vitae, summary of research accomplishments and future research plans, and the names of at least three references to:

**Mark R. Kelley, PhD  
Chair, Search Committee  
HB Wells Center for Pediatric Research  
Cancer Research Institute  
1044 W. Walnut, Room 402  
Indianapolis, IN 46202  
[mkelley@iupui.edu](mailto:mkelley@iupui.edu)**

*Indiana University is an EO/AA Educator, Employer and Contractor (M/F/D).*



STANFORD UNIVERSITY  
SCHOOL OF MEDICINE



LUCILE SALTER PACKARD  
CHILDREN'S HOSPITAL AT STANFORD

**DEPARTMENT OF PEDIATRICS  
Division of Stem Cell Transplantation**

THE NEWLY ESTABLISHED DIVISION OF STEM CELL TRANSPLANTATION OF THE DEPARTMENT OF PEDIATRICS AT STANFORD UNIVERSITY SCHOOL OF MEDICINE - is seeking three full- time research scientists with considerable potential and expertise in hematopoietic stem cell transplantation (HSCT) research. The positions are at the Assistant or Associate Professor level in the University Tenure Line (UTL).

The overriding requirement for faculty appointment, reappointment and promotion within the UTL must be distinguished performance, or (in the case of junior faculty) the promise of distinguished performance. There should be a major commitment to research and teaching. There must be outstanding accomplishments in research and excellent overall performance in teaching, as well as in clinical care and institutional service appropriate to the programmatic need the individual is expected to fulfill. Such programmatic need, including financial viability, should be evaluated and must be established for each appointment, reappointment and promotion.

Successful candidates will lead our multi-disciplinary basic and translational projects in research on hematopoietic stem cell transplantation. Research program areas to develop may include studies of stem cell biology; cancer biology, including cancer stem cells; immune development, regulation, function, and immune deficiency; and gene therapy.

The laboratory-based investigators' research will be supported by generous funding by the Lucile Packard Children's Hospital as part of a major Stem Cell Research Program. The candidates are expected to make important contributions to relevant scientific disciplines, e.g., stem cell biology, cancer biology, immunology, and gene therapy. Clinical investigators will be expected to perform research that will address important aspects of HSCT such as the development of novel HSCT protocols or the assessment of outcome.

Contingent on professional accomplishment, the candidate will be appointed as an Assistant or Associate Professor (University Tenure Line) in the Stanford University School of Medicine. Rank and salary will be commensurate with qualifications and experience.

Applications will be reviewed beginning November 2008 and accepted until the positions are filled. Interested candidates should send a copy of their curriculum vitae, a brief letter outlining their interests and the names of three references to:

**Kenneth Weinberg, M.D  
Anne T. and Robert M. Bass  
Professor of Cancer and Blood Diseases  
Chief, Division of Stem Cell Transplantation  
Department of Pediatrics  
Stanford University School of Medicine  
1000 Welch Road, Suite 300, Mail Code 5798  
Palo Alto, CA 94304**

*Stanford University is an Equal Opportunity Employer and is committed to increasing the diversity of its faculty.*

*It welcomes nominations of and applications from women and members of minority groups, as well as others who would bring additional dimensions to the university's research, teaching and clinical missions.*





## CENTER FOR MEMORY AND LEARNING

Department of Molecular & Cellular Biology  
Department of Pharmacology

### Tenure Track Faculty Position

The Center for Memory and Learning, the Department of Molecular and Cellular Biology and the Department of Pharmacology at Baylor College of Medicine are jointly recruiting a tenure track Assistant or Associate Professor who utilizes the tools of contemporary molecular biology and/or pharmacology to investigate the fundamental mechanisms of learning and memory. Candidates who use animal models to study learning and memory and who have a record of accomplishment in the application of molecular/pharmacological and behavioral approaches are encouraged to apply. We encourage applications from candidates who have an interest in the development of pharmacological agents that alter cognition. Candidates should have a Ph.D. and/or M.D. and postdoctoral experience. The candidate will have primary faculty appointments in the two basic science departments and will be a member of the Center for Memory and Learning, with opportunities for affiliations with other departments and programs. The position will provide a competitive allowance for laboratory start-up and ongoing support. Please send *curriculum vitae* and statement of research interests electronically as a single PDF to [lyndaa@bcm.tmc.edu](mailto:lyndaa@bcm.tmc.edu). Please have hard copies of at least three letters of reference sent to: CML Search Committee, c/o Lynda Lynch, Department of Molecular and Cellular Biology, Baylor College of Medicine, One Baylor Plaza, BCM130, Houston, TX 77030 by February 15, 2008.

*Baylor College of Medicine is an Equal Opportunity/Affirmative Action and Equal Access Employer.*



Weill Cornell Medical College

## Faculty Position Director

### Appel Institute for Alzheimer's Research

Weill Cornell Medical College is currently undergoing a major expansion of its research program including the construction of a new research building. As part of this expansion we are seeking a Director to establish a new institute; The Appel Institute for Alzheimer's Research. The goal of the Institute, consistent with the donor's wishes, is to better understand the mechanisms behind this disease and to develop treatments leading to a cure.

Candidates should have an outstanding record of productivity in basic or clinical research with a major program likely to impact Alzheimer's research. The recruited faculty will be provided with generous support and space as part of this initiative. In addition to medical student teaching, candidates will participate in the Graduate School of Medical Sciences Program which includes faculty from the Weill Cornell Medical College and the Sloan-Kettering Institute, and in the Tri-Institutional MD-PhD Program and the Training Program in Chemical Biology, which also include faculty from The Rockefeller University. Applications should include a curriculum vitae and a statement of research interests. Applications should be sent electronically to: [hmlander@med.cornell.edu](mailto:hmlander@med.cornell.edu) (Dr. Harry Lander, Associate Dean for Research Administration, Weill Cornell Medical College, 1300 York Avenue, New York, NY 10021). All applications will be treated confidentially.

*EEO/AA/M/F/D/V*



## Tenure-track Faculty Position

The Medical College of Georgia's **Vascular Biology Center** is recruiting for **tenure-track faculty**. Successful candidates are expected to have biomedical Ph.D., and/or M.D. degrees and an excellent track

record of training and publications in the area of cardiovascular pathophysiology or metabolic disease. Candidates for Associate Professor should also have active research support from a national funding source and a history of successful funding. We are particularly interested in candidates experienced in vascular disease related to metabolic dysfunction associated with obesity and involved in translational research. Ideal areas of expertise include (but are not limited to): insulin or adipokine signaling, CV inflammation, metabolic/diabetic major organ dysfunction or atherosclerosis. Candidates with established expertise in pulmonary or hypertensive vascular/renal disease are also of interest. The candidate will join an active group of extramurally-funded vascular biologists (currently about \$10 million annually) in recently renovated laboratories utilizing state-of-the-art equipment. He/she will have the opportunity to participate in the two institutional pre- and post-doctoral training programs in Integrative Cardiovascular Biology. A detailed description of VBC faculty and facilities is available at <http://www.mcg.edu/centers/vbc/>. Ample opportunities for collaborative basic and translational research are available and encouraged. The candidate is expected to develop an active, extramurally-funded research program, join a collaborative group of vascular biologists studying obesity and metabolic diseases, and contribute to the development of programmatic projects. Highly competitive salary and start-up package is available.

E-mail CV, letter describing career objectives, and the names of three references to: **Dr. David W. Stepp, Chair of the Search Committee** at [dstepp@mcg.edu](mailto:dstepp@mcg.edu). **Application deadline:** Until Filled.

*The Medical College of Georgia is an Equal Opportunity and Equal Access Institution; AA/EEO/Equal Access or AA/EEO/Equal Access/ADA Employer.*



## COLUMBIA UNIVERSITY Faculty Position in Neural Engineering



The Department of Biomedical Engineering in the Fu Foundation School of Engineering and Applied Science at Columbia University invites applications for a tenure-track faculty position at the Assistant, Associate or Full Professor level in Neural Engineering. Level of appointment depends on qualifications. Specific areas of interest include: neuroimaging, neural tissue engineering, neuromorphic engineering, computational neural modeling and brain machine interfaces. Successful candidates must demonstrate an ability to develop a world-class research program, be capable of obtaining competitive external research funding, and participate in and be committed to outstanding teaching at both the undergraduate and graduate levels. The candidate should have a doctorate in Biomedical Engineering or a related discipline.

Applicants should send a complete curriculum vitae, three publication reprints, a statement of research interests, a statement of teaching experience and philosophy, and names and contact information for four references to: <https://academicjobs.columbia.edu> and search position # 0000163.

**The search will close no sooner than February 28, 2009,  
and until the position is filled.**

Columbia University is an affirmative action/  
equal opportunity employer.



ÉCOLE POLYTECHNIQUE  
FÉDÉRALE DE LAUSANNE

## Tenure Track Assistant Professor in Brain Development and Plasticity at Ecole Polytechnique Fédérale de Lausanne (EPFL)

The Brain Mind Institute of EPFL invites applications for a Tenure Track Assistant Professor position in Brain Development and Plasticity (Nestlé Chair). We are interested in candidates focusing on molecular mechanisms of plasticity, particularly as they relate to the development and operation of cognitive functions. A range of research topics within these areas will be considered including the emergence of cognitive functions, social and emotional development, molecular mechanisms of memory. Candidates whose work bridges the cognitive level with underlying molecular and cellular mechanisms relying on multidisciplinary approaches, such as a combination of molecular, behavioral and neuroimaging-based experimentation are particularly sought. Projects may involve human subjects and/or animal models. Research at the Brain Mind Institute spans across several levels of analysis, from molecular to systems, with an underlying interest in mechanisms of nervous system diseases. Therapeutic and preventive approaches, including the study of the effect of nutrients, are part of ongoing projects. Candidates will develop an independent and vigorous research program, will be committed to excellence in undergraduate/graduate teaching, and supervise PhD students.

Start-up resources and state-of-the-art research infrastructure will be available, within the framework of a campus that fosters very strong interactions between life sciences, basic science, informatics

and engineering. Salaries and benefits are internationally competitive.

Applications should be submitted through the Internet <http://bmisearch-cogdev.epfl.ch> and should include the following documents in PDF format: curriculum vitae, publication list, brief statement of research and teaching interests, names and addresses (including e-mail) of 3 references. The Committee will start analyzing applications on **January 15, 2009**.

Further questions can be addressed to:

**Professor Pierre J. Magistretti**  
Director  
Brain Mind Institute  
School of life sciences, EPFL  
[pierre.magistretti@epfl.ch](mailto:pierre.magistretti@epfl.ch)

For additional information on EPFL, its Faculty of Life Sciences and the Brain Mind Institute, please consult <http://www.epfl.ch>, <http://sv.epfl.ch/> and <http://bmi.epfl.ch/>

The EPFL School of life sciences aims for a very strong presence of women amongst its faculty, and qualified female candidates are strongly encouraged to apply.

## UNIVERSITY OF WYOMING

### COLLEGE OF ENGINEERING AND APPLIED SCIENCE CAREER OPPORTUNITY

#### TENURE-TRACK FACULTY POSITION IN CHEMICAL ENGINEERING

The Department of Chemical and Petroleum Engineering at The University of Wyoming invites applications for a tenure-track faculty position at the rank of Assistant or Associate Professor. The position is open for all chemical engineering research interests, including, but not limited to, bioengineering, biomaterials, polymers, nanotechnology, energy sciences, and advanced materials design or characterization. The position entails developing an externally funded research program with peer-reviewed publication activities, and teaching at both the undergraduate and graduate levels. Applicants must hold a Ph.D. in Chemical Engineering or a related field.

The College of Engineering has over 90 faculty, and offers seven ABET-accredited degree programs. The Department has 14 research-active faculty members and an enrollment of over 240 undergraduate and 50 graduate students. The Chemical Engineering program at the University of Wyoming (UW) is a dynamic and growing entity that benefits from the resources provided by the NIH IMBRE program, a health-infrastructure building program; the University's newly established School of Energy Resources (SER), which substantially helps to facilitate energy-related research and education at the University; and, membership in the North central States Nanotechnology Consortium.

UW is a thriving research university located in Laramie, Wyoming (pop. 28,000), 130 miles northwest of Denver. Laramie is a picturesque and friendly town offering a reasonable cost of living and easy access to outdoor activities in the Rocky Mountain region. Additional information on the Department, College, SER, and Laramie is available at: <http://www.eng.uwyo.edu/chemical>, <http://www.eng.uwyo.edu/>, <http://www.uwyo.edu>, <http://uwacadweb.uwyo.edu/SER/>, <http://eori.uwyo.edu/>, and <http://www.laramie.org>.

Applicants must provide a letter of application, a curriculum vitae, a brief discussion of research goals and teaching philosophy, and a minimum of three reference contacts. Send complete applications electronically to: Ms. Heather Warren, [HWarren@uwyo.edu](mailto:HWarren@uwyo.edu). Screening of applications will begin **December 1, 2008** and continue until the position is filled.

*The university adheres to the principles of affirmative action and welcomes applications from qualified individuals, independent of race, color, religion, sex, national origin, disability, age, veteran status, sexual orientation or political belief. We welcome applications from underrepresented groups, including women and people of color.*

## Science Scholarships and Fellowships

### UNCF/MERCK SCIENCE INITIATIVE

The UNCF/Merck Science Initiative is an innovative approach that will create opportunities in the biological and chemical sciences for African American students throughout the country.



#### UNDERGRADUATE

- Science Research  
Scholarship Awards

#### GRADUATE

- Science Research  
Dissertation Fellowships

#### POSTDOCTORAL

- Science Research  
Fellowships

### APPLY ON-LINE

[www.uncf.org/merck](http://www.uncf.org/merck)

Submit by December 15, 2008

T 703 205 3400

F 703 205 3550

E [uncfmerck@uncf.org](mailto:uncfmerck@uncf.org)





**Science Careers** is the window that displays your vision.

Revealing your vision to employers is our job. We're your source for connecting with top employers in industry, academia, and government. We're the experts and entry point to the latest and most relevant career information across the globe.

Whether you're seeking a new job or career advancement in your chosen field, *Science Careers* is your window to a limitless future.

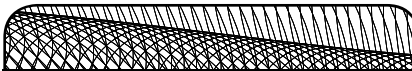
**Improved Website Features:**

- » New design for easier navigation
- » More relevant job search results
- » Automated tools for a more effective search



**Science Careers**  
from the Journal of Science AAAS

[ScienceCareers.org](http://ScienceCareers.org)




**ASSISTANT PROFESSOR/  
ASSOCIATE PROFESSOR,  
IMMUNOLOGY**

The Department of Pathology at The University of Chicago invites applications for tenure track faculty positions at the rank of **ASSISTANT PROFESSOR/ASSOCIATE PROFESSOR** depending on qualifications. We are seeking candidates with exceptional accomplishments in **IMMUNOLOGY** and the ability to lead creative and rigorous research programs in this discipline. This is an outstanding opportunity to join an academically strong and expanding Department, contribute to and enhance the Inter-Departmental Committee on Immunology, and participate in the vibrant scholarly environment at The University of Chicago. Please send curriculum vitae along with a statement of research accomplishments and plans as well as names/contact information of three references to: **The University of Chicago, Department of Pathology, Attn: Immunology Faculty Search Committee, 5841 S. Maryland Ave., MC 3083, Chicago, IL 60637-5420.**



**THE UNIVERSITY  
OF CHICAGO**


The University of Chicago  
is an AA/EEO employer.



**A FACULTY  
POSITION IN  
PLANT-RELATED  
MICROBIOLOGY**

The Institute of Plant and Microbial Biology, Academia Sinica, Taipei is inviting applications for a research focused faculty position in plant-microbe interactions and plant-related microbiology. This position can be at the level of Assistant, Associate, or Full Research Fellow (equivalent to Assistant, Associate, or Full Professor in a university) depending on the applicant's experience. Excellent facilities and starter grants will be provided for the position. For details of the Institute and Academia Sinica, please visit the website at <http://ipmb.sinica.edu.tw/>. Applicants are expected to have a Ph.D. degree plus postdoctoral training. Chinese language skills are NOT required and international scientists are encouraged to apply.

The application folder should include curriculum vitae, a statement of research accomplishments, and future research plans. The application folder and at least three letters of recommendation should be sent to: **Dr. Teng-Yung Feng, Chair of Search Committee, Institute of Plant and Microbial Biology, Academia Sinica, 128, Sec 2, Academia Rd, Nankang, Taipei, Taiwan 11529. e-mail: natfarm@sinica.edu.tw. FAX: (+886)2-2782-1605.** The review of applications will start on **February 1, 2009** and continue until the position is filled.



**RUTGERS**  
THE STATE UNIVERSITY  
OF NEW JERSEY

The Department of Mathematical Sciences invites applications and nominations for the Joseph and Loretta Lopez Endowed Chair in Mathematics. The department seeks a distinguished scholar in mathematics with international reputation, well-established research and teaching record, and demonstrated ability to generate external funding. This endowed chair is the first at the Camden Campus of Rutgers University. It is a tenured faculty position and the chair is for a 5-year renewable term. The holder of this chair will be a senior faculty member and a vigorous participant in the research, instruction and service work of the Department of Mathematical Sciences. The holder will also be expected to play a vital role in the campus' growing program in computational biology and the recently established Center for Computational and Integrative Biology. As such, applicants must demonstrate evidence of research in the areas of mathematical and/or computational biology.

The appointment will commence on September 1, 2009, and is at the rank of associate or full professor. The department will begin reviewing applications on December 17, 2008 and continue its review until the position is filled. Nominations and applications (printed resume with AMS Application Cover Sheet, selected publications, supporting materials), list of publications, should be sent to: **Professor Gabor Toth, Chair, Search Committee, Department of Mathematical Sciences, Rutgers University, Camden, New Jersey, 08102.** Applicants should also arrange for at least four letters of recommendation to be sent.



## FACULTY POSITION Molecular Biologist University of California, Davis

The Entomology Department seeks applicants for a Molecular Biologist at the Assistant Professor level (25% AES research and outreach, 75% instruction and research). We seek an outstanding applicant with a Ph.D. degree in entomology or related disciplines with experience and interest related to basic and applied entomology. The successful candidate will be expected to develop a creative, independent, and productive research program in the area of insect molecular biology. The appointee is required to teach core curriculum courses, supervise graduate students, participate in outreach programs, and perform University service. This appointment is available on or about September 1, 2009. Applicants must submit online at ([http://secure.entomology.ucdavis.edu/fac\\_recruit/login.cfm](http://secure.entomology.ucdavis.edu/fac_recruit/login.cfm)): curriculum vitae; statement of research and teaching interests; official transcripts; publication list, reprints of key publications (up to three), and the names and addresses of at least three references. Inquiries should be addressed to: **Dr. Bruce Hammock, Search Committee Chair, Department of Entomology, 367 Briggs Hall, One Shields Avenue, Davis, CA 95616; (530) 752-0492; [rwveirs@ucdavis.edu](mailto:rwveirs@ucdavis.edu)**. Open until filled but to ensure consideration, applications must be received by **January, 15, 2009**. A more detailed job description can be obtained from the above webpage.

*UC Davis is an Affirmative Action/Equal Employment Opportunity Employer and is dedicated to recruiting a diverse faculty community. We welcome all qualified applicants to apply, including women, minorities, veterans, and individuals with disabilities.*



ÉCOLE POLYTECHNIQUE  
FÉDÉRALE DE LAUSANNE

## Faculty Position in BioMicroengineering at the Ecole polytechnique fédérale de Lausanne (EPFL)

The Institutes of Bioengineering and Microengineering at EPFL are seeking a **tenure track assistant professor** in the field of **biomicro/nanosystems**. Exceptionally qualified candidates may also be considered at a more senior level. Bioengineering at EPFL is well integrated between the Schools of Engineering and Life Sciences. In this search, an appointment is sought within the School of Engineering, in which Microengineering is also situated. The open faculty position is offered in an environment of both theoretical and experimental research, rich for the development of novel basic technologies as well as for seeking deeper understanding of integrative (patho)physiological mechanisms and developing novel technological and biotherapeutic approaches at the levels of genes, biomolecules, cells and tissues.

The Institutes seek to grow at the interface of engineering with biology in the domain of nano- and microtechnologies and integrated systems. We particularly encourage candidates with strong expertise in the areas of bio-MEMS/NEMS, sensing and actuation for in vitro use, for example in basic biological investigation, systems biology, and diagnostics, or in vivo use, for example in diagnostic and sensing systems, integrated systems, and drug delivery. The interface with robotic, surgical and imaging systems is of specific interest. EPFL has strong research facilities, in particular in micro/nanofabrication, imaging, and cytometry.

Successful candidates are expected to initiate independent, creative research programs and participate in undergraduate and graduate teaching. We offer internationally competitive salaries, start-up resources and benefits.

Applications should include a curriculum vitae with a list of publications, a concise statement of research and teaching interests, and the names and addresses (including e-mail) of at least five referees. Applications should be uploaded to <http://biomems-rec.epfl.ch>. The deadline for applications is **15 January 2009**.

Enquiries may be addressed to:

**Prof. Jeffrey A. Hubbell**,  
e-mail: [biomems-rec@epfl.ch](mailto:biomems-rec@epfl.ch)

For additional information on EPFL, School of Engineering, Institute of Bioengineering, and Institute of Microengineering, please consult the web sites: <http://www.epfl.ch>, <http://sti.epfl.ch>, <http://ibi.epfl.ch>, <http://imt.epfl.ch>

EPFL aims to increase the presence of women amongst its faculty, and qualified female candidates are strongly encouraged to apply.

## Head of Biomedical Sciences Department Colorado State University

The Department of Biomedical Sciences has initiated a search for a new Head. We seek a candidate with an internationally recognized research program complementing the existing strengths of the department. Departmental strengths include cardiovascular physiology, neuroscience, and reproduction, all studied at the molecular, cellular, developmental and whole-animal levels. The Head will provide the vision and dynamic leadership requisite for the department's research, teaching, and service missions. Required credentials include a doctoral degree in a field relevant for biomedical science in addition to research, teaching, and service experience commensurate with an appointment as a tenured Professor and Head. Further information about the department can be found at: [www.cvmbs.colostate.edu/bms/](http://www.cvmbs.colostate.edu/bms/).

A letter of application, curriculum vitae, statements of research and service experience, departmental leadership philosophy, vision for education and the names and contact information for three professional references who may be contacted when appropriate should be sent electronically or by post to the chair of the search committee:

**Dr. Edward A. Hoover**  
c/o Carol Dewbre  
CSU, 1680 Campus Delivery  
Fort Collins, CO 80523

[carol.dewbre@colostate.edu](mailto:carol.dewbre@colostate.edu)

Applications should be received by **January 15, 2009**, although applications will be considered until the position is filled.

*CSU is an EO/AA Employer. Colorado State University conducts background checks on all final candidates.*



## Research Group Leader for TSL+ Genetic Control of Crop Disease

The Sainsbury Laboratory (TSL) is evolving its scientific mission so that TSL not only provides fundamental biological insights into plant-pathogen interactions, but also delivers novel, genomics-based, solutions which will significantly reduce losses from major diseases of food crops, especially in developing countries.

TSL seeks an outstanding individual to lead this component of its mission. The successful candidate will have an excellent track record of research leadership and innovation in a relevant area and will be highly skilled and strongly motivated to apply new scientific insights and new technologies to deliver effective disease control in crops.

The appointment comes with generous support from the Gatsby Charitable Foundation and the successful candidate will join four other research group leaders based in the Laboratory's state-of-the-art research facilities on the site of the John Innes Centre in Norwich.

Applications will be accepted until a suitable candidate is found. Informal enquiries should be directed to Sophien Kamoun ([sophien.kamoun@tsl.ac.uk](mailto:sophien.kamoun@tsl.ac.uk)) or Jonathan Jones ([jonathan.jones@tsl.ac.uk](mailto:jonathan.jones@tsl.ac.uk)). Please email formal applications with a CV, names of 3 referees to [HR@tsl.ac.uk](mailto:HR@tsl.ac.uk) quoting the reference number TSL+01/2009. Applications will be reviewed from 01 February 2009.

**Finally...**



a career site that  
**separates itself**  
from the rest.

We've got **Careers** down to a **Science**.

---

*Science* Careers is the “go to” career site for job opportunities and career advice in the science industry. With the best jobs from the industry’s top employers, we’re proud to be No. 1. From job postings, employer profiles, and a resume database to grant information, job alerts, and a careers forum, *Science* Careers really does have it all. And best of all, everything is free! Log on to [www.ScienceCareers.org](http://www.ScienceCareers.org) today and find out why we’re different.

**Science Careers**

From the journal *Science*



[www.ScienceCareers.org](http://www.ScienceCareers.org)



## POSITIONS OPEN

# MICHIGAN STATE UNIVERSITY

## TENURE-TRACK FACULTY POSITION in METABOLIC BIOCHEMISTRY Department of Biochemistry and Molecular Biology

Position: The Department of Biochemistry and Molecular Biology (BMB) at Michigan State University seeks an outstanding **BIOCHEMIST** to establish a strong independent research program in the area of metabolic diseases with emphasis on obesity and diabetes. The position offered is at the **ASSISTANT PROFESSOR** level but, in exceptional cases, the rank of **ASSOCIATE PROFESSOR** will be considered. The research program should employ biochemical or molecular approaches for the study of the regulation of metabolism and attendant changes that lead to obesity, diabetes, or other metabolic syndromes. Studies of adipogenesis, adipokines, regulation of metabolism, or inflammatory responses as they pertain to obesity or diabetes are of interest.

Qualifications: A Ph.D. or Ph.D./M.D. in biochemistry or molecular biology or aligned areas is desired. The successful candidate is expected to develop a productive research program that is externally funded as well as contribute to the teaching of undergraduates, graduates, and medical students. The candidate is also expected to interact with a diverse core of faculty at MSU involved in the study of metabolic diseases which includes translational studies. State-of-the-art facilities that are professionally run are available. Generous startup packages are offered. The BMB website is [website: http://www.bmb.msu.edu](http://www.bmb.msu.edu).

Application: Application materials will be accepted until January 9, 2009, or until a suitable candidate is found. Application materials should include: a cover letter, a description of research interests including future directions, curriculum vitae, and the names of three to five investigators who can provide reference letters. All application materials should be sent electronically to **e-mail: [metabolicbiochem@cns.msu.edu](mailto:metabolicbiochem@cns.msu.edu)** by January 9, 2009. Questions regarding this position may be directed to **Dr. Pam Fraker (e-mail: [fraker@msu.edu](mailto:fraker@msu.edu))**. The Department is highly committed to Affirmative Action and encourages women, persons of color, veterans, or persons with disabilities to apply.

## TWO FACULTY POSITIONS AVAILABLE Department of Dermatology Columbia University

**ASSISTANT/ASSOCIATE PROFESSOR, TENURE TRACK.** Outstanding research scientist working in investigative dermatology or related fields to enhance the existing research programs. Candidates should have research interests in any area of epithelial or skin biology, for example, carcinogenesis, cell cycle, stem cells, melanoma, or molecular genetics. Applicant must have a Ph.D., M.D., or M.D./Ph.D. degree with postdoctoral training and have established a strong independent research program. Candidates are invited to submit curriculum vitae, research plan, and three references.

**PHYSICIAN-SCIENTIST, Veterans Administration System.** M.D. or M.D./Ph.D. candidate for a combined clinician-scientist position jointly with the James Peters Bronx VA Medical Center. Candidates must be Board-certified in dermatology and have research interests in any area of skin biology. Applicant must have undergone postdoctoral training and have established a strong independent research program. Candidates are invited to submit curriculum vitae, research plan, and three references.

Please submit via e-mail to: **Angela M. Christiano, Ph.D., Vice Chair for Research Department of Dermatology, Columbia University, 630 West 168th Street, VC15-202, New York, NY 10032. E-mail: [amc65@columbia.edu](mailto:amc65@columbia.edu)**. Columbia University is an Affirmative Action/Equal Opportunity Employer.

## POSITIONS OPEN

### BIOPHYSICIST

Wilkes University invites applications for a tenure-track joint position in the Department of Biology and Division of Engineering and Physics at the **ASSISTANT PROFESSOR** level, starting August 2009.

We seek a candidate with expertise in biophysics, biomechanics, or bioengineering, with the ability to teach and conduct research in an undergraduate setting, in any area that interfaces biology and physics. Teaching responsibilities will include upper-level courses in area of expertise and introductory physics. A competitive startup package is available. A Ph.D. is required; postdoctoral experience preferred.

The successful candidate will be expected to develop a strong research program involving undergraduates, and participate in a curriculum revision in biology and physics supported by a \$1 million grant from the Howard Hughes Medical Institute.

Applicants should mail their curriculum vitae, statements of teaching and research goals, reprints (PDF), and arrange for three letters of reference to: **Wilkes University, Biophysics Assistant Professor Search, Reference #BIO003, P.O. Box 3924, Scranton, PA 18505-0924**. Indicate the reference number on the envelope. To apply by e-mail, send application materials to **e-mail: [caply@wilkes.edu](mailto:caply@wilkes.edu)** and indicate the reference number in the e-mail subject line. Kindly indicate in your letter where you found out about the position vacancy. Please make sure to include the reference number, or the application will not be processed. Deadline for applications is January 5, 2009.

For further information about this position, please contact the **Chair of the Search Committee, Dr. William Biggers**. E-mail address is **e-mail: [william.biggers@wilkes.edu](mailto:william.biggers@wilkes.edu)**.

*Wilkes University is an Equal Opportunity Employer committed to a diverse faculty, staff, and student body. Applicants from diverse backgrounds are strongly encouraged to apply.*

## FACULTY POSITION University of Pittsburgh Human Genetics

The Department of Human Genetics, University of Pittsburgh, invites applications for two new tenure-track faculty positions at the **ASSISTANT PROFESSOR** level in human genetics. We are seeking outstanding candidates whose research addresses contemporary issues in human genetics. Faculty research interests and academic programs of the Department can be viewed at [website: http://www.hgen.pitt.edu](http://www.hgen.pitt.edu); we will consider excellent applicants with expertise in these or other areas of interest.

These are full-time, tenure-track appointments in the Department of Human Genetics. Appointment at the Assistant Professor level requires a doctoral degree and evidence of outstanding research potential. Appointees at this level will be expected to develop a vigorous, independently funded research program.

Applicants must submit curriculum vitae and names of three references to: **Chairman of the Search Committee, Department of Human Genetics, Graduate School of Public Health, University of Pittsburgh, Pittsburgh, PA 15261**, or electronically to **e-mail: [jnorbut@pitt.edu](mailto:jnorbut@pitt.edu)**. The position will remain open until appropriate candidates have been identified.

*The University of Pittsburgh is an Affirmative Action, Equal Opportunity Employer.*

**FACULTY POSITIONS.** Southern Connecticut State University invites applications for the anticipated vacancies of three tenure-track positions in biology with specialization in anatomy and physiology (#09-003), biology with specialization in bioeducation (#09-002), and biology with specialization in microbiology (#09-004) at the rank of **ASSISTANT/ASSOCIATE PROFESSOR** beginning August 2009.

For full description of the position, application requirements, and submission process, please visit our **website: [http://www.southernct.edu/employment/job\\_openings/](http://www.southernct.edu/employment/job_openings/)**.

*SCSU is an Equal Opportunity Affirmative Action Employer. Women and minorities are strongly encouraged to apply.*

## POSITIONS OPEN



The Department of Plant Pathology at the University of Wisconsin, Madison invites applications for a tenure-track faculty position in plant virology at the **ASSISTANT PROFESSOR** level. Research effort will focus on the biology of plant viruses and their interaction with plants. Possible areas of research include the epidemiology and control of plant virus diseases; the genetics, biochemistry, and cell biology of virus and host functions in virus replication, spread, virulence, and pathogenesis; and virus-vector relationships. The incumbent will be expected to interact with other programs to form a bridge between basic and applied research. Exciting opportunities exist for collaboration with colleagues in virology, plant biology, microbiology, biotechnology, and related disciplines within the Department, College, and University. The incumbent will mentor graduate and undergraduate students and support the teaching and training missions of the University. The position carries a 70 percent research/30 percent teaching distribution of effort, and a nine-month appointment. Requirements include: a Ph.D. in plant pathology, virology, or related discipline; a strong foundation in the principles and concepts of plant pathology and relevant research experience; effective oral and written communication skills; and a positive attitude for teamwork, including the ability to lead and motivate others. The University of Wisconsin attracts excellent graduate students and offers high-quality research and teaching facilities. Madison, the capital of Wisconsin, is a picturesque and progressive city with a strong economy and a vibrant cultural environment. To apply, submit curriculum vitae, a cover letter with a statement of research and teaching interests, a copy of undergraduate and graduate transcripts, and three letters of reference to: **Prof. Amy Charkowski, Department Plant Pathology, 1630 Linden Drive, Madison, WI 53706. Telephone: 608-262-7911, fax: 608-263-2626, e-mail: [amyc@plantpath.wisc.edu](mailto:amyc@plantpath.wisc.edu)**. Applications received by January 9, 2009, will be assured full consideration; review of applications will continue until a suitable candidate is identified. *The University of Wisconsin is an Equal Opportunity/Affirmative Action Employer.*

**NEUROSCIENCE RESEARCH-TRACK or POSTDOCTORAL POSITION**, available immediately to study neurotransmission and synaptic plasticity in the mammalian olfactory bulb. Experience and publications in electrophysiological approaches, particularly patch clamping, or optical imaging required. Position includes highly competitive salary/fringe benefits, grant opportunities, and interaction with neuroscientists in the Department (**website: <http://www.utmem.edu/anatomy-neurobiology/>**) and Neuroscience Institute (**website: <http://www.utmem.edu/neuroscience/>**). Applicants must have a Ph.D. or M.D. Send Word or PDF document application (curriculum vitae and names of three references) via e-mail to: **Matt Ennis (e-mail: [mennis@utmem.edu](mailto:mennis@utmem.edu))**, Department of Anatomy and Neurobiology, University of Tennessee Health Science Center, 855 Monroe Avenue, Suite 515, Memphis, TN 38163. *U. Tennessee is an Affirmative Action Employer, encourages applications from women and underrepresented minorities, and is an Equal Employment Opportunity/Affirmative Action/Title VI/Title IX, Section 504/ADA/ADEA Employer.*

The University of Texas at Brownsville (UTB) invites applications for the position of **DEAN** of the College of Science, Mathematics, and Technology. The College is seeking an individual with vision, enthusiasm, and energy committed to teaching excellence, development of research, and service in a culturally unique and diverse environment. Review of applications will begin January 1, 2009. Please refer to the UTB employment web page at **website: <http://www.utb.edu/ba/hr/employment/pages/staff.aspx>** for a description of the position and application requirements.

# **Science Careers** is the catalyst for your ambition.

Visit our  
**ENHANCED**  
WEBSITE!



Promoting your ambition is what we do. We're your catalyst for connecting with the industry's top employers. We're the experts and source for accessing the latest and most relevant career information across the globe.

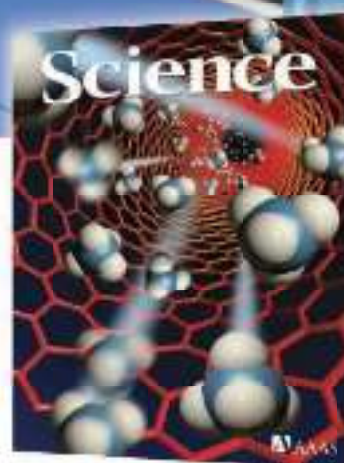
Our newly designed website offers a set of tools that help you discover career opportunities and your personal potential. Whether you're seeking a new job, career advancement in your chosen field, or ways to stay current on industry trends, *Science Careers* is your catalyst for an accelerated future.

#### **Improved Website Features:**

- » Relevant Job E-mail Alerts
- » Improved Resume Uploading
- » Content Specific Multimedia Section
- » Facebook Profile


#### **Job Search Functionality:**

- » Save and Sort Jobs
- » Track Your Activity
- » Search by Geography
- » Enhanced Job Sorting



*Your Future Awaits.*

**Science Careers**

From the journal *Science* 

[ScienceCareers.org](http://ScienceCareers.org)



## POSITIONS OPEN

### LECTURER Biomedical Sciences Division of Biomedical Sciences College of Medicine University of Saskatchewan

The Division of Biomedical Sciences invites applications for a full-time, three-year term Lecturer position. The salary range for this position is established by the current faculty Collective Agreement. We are seeking a highly motivated individual with a strong commitment to teaching. Candidates must have a Ph.D. related to biochemistry, microbiology, or cell biology, and postdoctoral experience in these areas is preferable.

The Division of Biomedical Sciences offers Programs in Anatomy and Cell Biology, Biochemistry, Microbiology, and Immunology, Pharmacology and Physiology. The successful applicant will be responsible for ensuring all students majoring in biomedical sciences receive an enriched laboratory experience. The primary purpose will be to develop and teach the newly established biomedical sciences undergraduate laboratory techniques course (BMS240), one of six common core courses within the Division which serves as a foundation for upper-year specialized courses. The individual in this position will also participate in related program development and delivery within the biomedical core curriculum.

The University of Saskatchewan is a publicly funded institution established in 1907. It has over 19,000 degree students, 4,500 employees, an operating budget of approximately \$200 million, and receives research funds in excess of \$100 million annually. It offers a full range of programs, both academic and professional, in thirteen colleges including seven in the life sciences.

Please send curriculum vitae and the names and e-mail addresses of three references by Saturday, January 31, 2009. A review of applicants will begin immediately with the appointment to begin no later than July 1, 2009.

**Dr. Nick Ovsenek**  
Associate Dean of Biomedical Sciences  
College of Medicine  
University of Saskatchewan  
107 Wiggins Road  
Saskatoon, SK S7N 5E5 Canada  
E-mail: [nick.ovsenek@usask.ca](mailto:nick.ovsenek@usask.ca)  
Fax: 306-966-1460

*The University of Saskatchewan is committed to Employment Equity. Members of designated groups (women, Aboriginal people, people with disabilities, and visible minorities) are encouraged to self-identify on their applications. All qualified candidates are encouraged to apply; however, Canadians and permanent residents will be given priority.*

**SHULL FELLOWSHIP** at the Oak Ridge National Laboratory (ORNL): the Neutron Sciences Directorate of the ORNL invites applications for the Clifford G. Shull Fellowship. The Shull Fellowship provides an exciting opportunity to pursue research applying neutron scattering methods to forefront problems in physics, chemistry, biology, or materials science and engineering. Applications for Shull Fellowships commencing in 2009 are now being accepted. To receive full consideration applications must be submitted by December 12, 2008. For more information, and to apply, go to [website: http://jobs.ornl.gov/index.cfm](http://jobs.ornl.gov/index.cfm). ORNL is an Equal Opportunity Employer, committed to work force diversity. Applicants need not be U.S. citizens.

We seek a **POSTDOCTORAL LIPID BIOCHEMIST** to conduct research on the molecular basis of latency in tuberculosis at the Burnett School of Biomedical Sciences, University of Central Florida, Orlando, Florida. Send curriculum vitae and the contact information of three references by e-mail to **P.E. Kolattukudy**, e-mail: [pk@mail.ucf.edu](mailto:pk@mail.ucf.edu). *The University of Central Florida is an Equal Opportunity, Equal Access, and Affirmative Action Employer. As a member of the Florida State University System, all application materials and selection procedures are available for public review.*

## POSITIONS OPEN



**POSTDOCTORAL POSITIONS.** Projects on epigenetics, homeobox genes, microRNAs, and RNA surveillance in embryonic stem cells and the reproductive system at UCSD (laboratory is moving from University of Texas, M.D. Anderson Center to UCSD in 2009). Recent papers from the laboratory include: *Mol. Cell. Biol.* 28:2138, 2008; *Ann. Review Biochem.* 76:51, 2007; *EMBO J.* 26:1820, 2007; *Cell* 125:1036, 2006; *Genes Dev.* 20:147, 2006; *Cell* 120:369, 2005; and *Nature Struct. Mol. Biol.* 12:801, 2005. Send curriculum vitae and brief cover letter to **Dr. Miles F. Wilkinson** (e-mail: [mwilkins@mdanderson.org](mailto:mwilkins@mdanderson.org)).

### ASSISTANT PROFESSOR POSITIONS Environmental Sciences and Engineering School of Engineering and Applied Sciences Harvard University

The Harvard School of Engineering and Applied Sciences (HSEAS) seeks applicants for openings in environmental sciences and engineering at the level of tenure-track Assistant Professors. Appointments will be made in hydrology and applied chemistry/chemical engineering. The positions require the ability to develop a leading research program and enthusiasm for teaching at both the graduate and undergraduate levels.

An application, assembled as a single PDF file, should include curriculum vitae, separate two-page statements of research and teaching interests, up to three scientific papers, and names and contact information for at least three writers of letters of recommendation. Applications should be sent to e-mail: [esearch@seas.harvard.edu](mailto:esearch@seas.harvard.edu).

Applications will be reviewed beginning 30 November 2008. Later applications are also welcome until the positions are filled. *Harvard University is an Equal Opportunity/Affirmative Action Employer, and applications from women and underrepresented minorities are strongly encouraged.*

### PHYSICIAN SCIENTIST FACULTY POSITIONS in INFECTIOUS DISEASES Virginia Commonwealth University School of Medicine, Richmond, Virginia

The Division of Infectious Diseases and the Department of Microbiology and Immunology are jointly seeking applications from outstanding candidates for two faculty positions in the tenure track at the **ASSISTANT to FULL PROFESSOR** levels. Successful candidates are expected to establish independently funded programs in infectious diseases basic or translational research. Applicants must have an M.D. or M.D./Ph.D. and be Board-certified/Board-eligible in internal medicine and infectious diseases. Attractive salary and startup packages available. Please submit curriculum vitae with a cover letter outlining clinical and research interests and have three letters of reference sent to: **Michael Edmond, M.D., Chair, Division of Infectious Diseases**, at e-mail: [medmond@vcu.edu](mailto:medmond@vcu.edu). *VCU is a culturally diverse, Equal Opportunity Employer. Women, minorities, and persons with disabilities are encouraged to apply.*

### TWO ASSISTANT PROFESSOR TENURE-TRACK FACULTY POSITIONS

These positions are in the Department of Plant Pathology, Physiology, and Weed Science at Virginia Tech. One position will focus on plant metabolomics/metabolic engineering problems; for example in bio-design, bioprocessing, biofuels, production of novel compounds, improved quality or yield of existing plant products, or other value-added traits. The second position will focus on cellular, molecular, or genomic aspects of plant-microbe interactions; for example in cellular biology of plant-viral interactions. Further information and application instructions are available at [website: http://jobs.vt.edu](http://jobs.vt.edu) under posting numbers 081134 and 081133, respectively. *Equal Opportunity/Affirmative Action.*

## POSITIONS OPEN

The Department of Ecology and Evolutionary Biology (EEB; [website: http://www.colorado.edu/ceb/](http://www.colorado.edu/ceb/)) and the Museum of Natural History at the University of Colorado ([website: http://cumuseum.colorado.edu](http://cumuseum.colorado.edu)), Boulder will be filling several positions in phylogenetic biology as part of a broad initiative to enlarge and strengthen comparative and evolutionary biology at the University of Colorado. We are currently inviting applications for the first position to be filled as part of this initiative, a joint tenure-track appointment as **CURATOR of BOTANY and ASSISTANT or ASSOCIATE PROFESSOR**. Primary responsibilities will be to curate and develop the Museum's botany collections, use phylogenetic and systematic approaches as a core part of their research program on any group of plants, and teach in museum and field studies and EEB. The successful individual will be expected to take a leadership position in advancing the role of the Herbarium. Applicants must have a doctoral degree; curatorial experience is important. Apply at [website: http://www.jobsatcu.com/](http://www.jobsatcu.com/), posting# 805528, beginning November 1, 2008. The application package should include curriculum vitae; representative publications; and statements of research, teaching, and curatorial experience and vision; along with names and addresses of four references. Contact e-mail: [robert.guralnick@colorado.edu](mailto:robert.guralnick@colorado.edu). Review of applications begins January 1, 2009, until a successful candidate is identified.

### FACULTY POSITIONS in BIOLOGY University of Colorado Denver

The Department of Biology ([website: http://www.cudenver.edu/biology](http://www.cudenver.edu/biology)) on the University of Colorado (UCD) downtown Denver campus seeks to fill three new tenure-track faculty positions pending final budgetary approval: **ASSISTANT PROFESSOR** in environmental toxicology (job #805315 at [website: http://www.jobsatcu.com](http://www.jobsatcu.com)); **ASSISTANT PROFESSOR** in evolutionary genetics (job #805317 at [website: http://www.jobsatcu.com](http://www.jobsatcu.com)); and **ASSISTANT PROFESSOR** in developmental biology (job #805314 at [website: http://www.jobsatcu.com](http://www.jobsatcu.com)). Review of applications will begin December 10, 2008. *UCD is dedicated to ensuring a safe and secure environment for our faculty, staff, students, and visitors. To achieve this goal, we conduct background investigations for all prospective employees. The University of Colorado is committed to diversity and equality in education and employment.*

We deliver  
customized job alerts.

[www.ScienceCareers.org](http://www.ScienceCareers.org)

## MARKETPLACE

### For COLLAGEN Detection... Connect with Cosmo Bio

**ELISAs to measure COLLAGEN:** Type 1 (hu); Type 2 (hu, ms, rt, +). **ELISAs to measure ANTI-COLLAGEN ANTIBODIES:** Type 1 (hu); Type 2 (hu, ms, rt, +). **SPECIFIC ANTIBODIES:** Types 1, 2, 3, 4, 5, 6, 7, 8, 9, 10, 11, 12, 14. Research Products from Japan [www.cosmobio.com](http://www.cosmobio.com)

## Oligo Labeling Reagents

↓ **BHQ<sup>®</sup>/CAL Fluor<sup>®</sup>/Quasar<sup>®</sup> Amidites**  
↓ **Amidites for 5' & Int. Modifications**  
↓ **Standard and Specialty Amidites**  
**BIOSEARCH TECHNOLOGIES** +1.800.GENOME.1  
[www.btlabelling.com](http://www.btlabelling.com)